Synthesis of Tubulin Inhibitors with Variable Molecular Hinges for the Attachment of Aminopeptidase N Targeting Moieties

Zeeshan Anwar

A thesis presented to the University of Dublin for the degree of
Doctor of Philosophy

Based on research carried out under the supervision of **Dr. John J. Walsh**

School of Pharmacy and Pharmaceutical Sciences

University of Dublin

Trinity College

2019

Declaration

I declare that this thesis has not been submitted as an exercise for a degree at this or any other university and it is entirely my own work. I agree to deposit this thesis in the University's open access institutional repository or allow the Library to do so on my behalf, subject to Irish Copyright Legislation and Trinity College Library conditions of use and acknowledgement.

Zeeshan Anwar

Acknowledgements

First of all, I am thankful to my supervisor, Dr John Walsh for his patience, guidance and dedication throughout the course of my PhD project.

I am grateful to my parents especially my father Saeed Anwar, who have always provided me moral and emotional support in my life. I am also grateful to my wife Hadia Khan for her patience and encouragement.

A special gratitude goes to Abdul Wali Khan University Mardan, Pakistan, for helping and providing funding for my research project.

I wish to say huge thanks to Dr. Manuel Ruether and especially to Dr. John O'Brien for his time and expertise regarding my NMR spectra. I would like to say many thanks to Brian Talbot for running Mass spec and LC-MS samples. Thanks also to Maureen and especially Joe, for always being helpful.

Abstract

This thesis includes synthesis of various tubulin binding agents and their incorporation in to novel dual acting hybrids, which along with the tubulin inhibition also exhibit aminopeptidase N (APN) inhibition activities.

This thesis begins with an overview of the process of angiogenesis, the tumour vasculature network and the differences between tumor and normal vascular systems. The two main therapeutic approaches, by targeting angiogenesis and the newly formed vascular network, are also discussed. Moreover the concept of targeted therapy utilising the multifunctional enzymatic receptor APN is also presented along with various different hybrid drug approaches. The first chapter closes with a brief overview of the principal aims of the project.

The initial focus of chapter 2 was the synthesis of 4-arylcoumarin derivatives having tetramethoxy arrangement. The work described in this chapter then progressed towards thionation of the carbonyl moiety at position 2 as this group can be replaced with a series of incoming nucleophiles unlike its carbonyl counterpart. Having successfully completed this transformation a series of suitable linker units were attached to this position primarily centred around oxime and hydrazone derivatives. Introduction of alcohol, aldehyde, carboxylic acid and amine functionalities at position 3 of the 4-arylcoumarins then follows. Significant emphasis in the later part of the chapter involves the double functionalisation of the 4-arylcoumarin with a phenolic group on the A-ring and an aniline group on the C-ring, as the chapter closes with an evaluation of the newly synthesised compounds as inhibitors of tubulin polymerisation.

The synthesis of the phenstatin series in chapter 3 focuses on introducing additional hinges onto their structure principally based around a catechol structure on the A-ring while the B-ring was represented by a substituted aniline or phenol ring. This chapter also discusses the synthesis of phenstatin-like compounds, having a propanal side chain, an ideal functional group for both derivatisation and for conjugation of APN targeting moieties. These compounds were then evaluated as inhibitors of tubulin polymerisation.

Chapter 4 centres on exploring the concept of hybrid drug therapy and employing it for the targeted delivery of different tubulin binding agents whose synthesis is described in chapters 2 and 3. This chapter involves the incorporation of APN targeting moieties onto the tubulin binding agents for the purpose of creating hybrid drugs that have the capacity to

inhibit both APN and tubulin polymerisation. APN targeting moieties employed include the existing APN inhibitor bestatin and hydroxamates. Compounds are designed in a way either by linking an APN targeting component (bestatin) to tubulin binding agents via ester linkage or in other scenario the APN targeting (hydroxamic acid) and tubulin inhibiting pharmacophoric moieties are merged in a way so that the merged hybrid have both the APN and tubulin polymerisation inhibition activities. In the case of the phenolic ester linked APN targeting moiety, the tubulin binding component is presented in its pro-drug form. The pro-drug will be converted into to its active form by the hydrolysis of the ester linkage at physiological pH. In another hybrid drug approach, the tubulin binding agent consists of an ester linked APN targeting bestatin and an amide linked neutral amino acid thereby presenting the tubulin binding component in its control release form. In order to get converted into its active form, the tubulin binding agent would be dependent on pH mediated hydrolysis of ester linkage as well as APN mediated hydrolysis of the substrate, as APN is known to catalyse the removal of neutral amino acids from *N*-terminus of peptides. Following the synthesis of the hybrid compounds, their evaluation as APN inhibitors is described. Preliminary data is also presented on the release of both the APN inhibitor and substrate from a selection of the hybrids that were synthesised.

Chapter 5 presents the experimental procedures used in the synthesis, characterisation of compounds as well as the procedures utilised for APN inhibition and tubulin polymerisation assay.

Table of Contents

Table of Figures

Table of Schemes

Abbreviations

AAs	Antiangiogenic agents
AcOH	Acetic acid
AHPA	(2S,3R)-3-Amino-2-hydroxy-4-phenylbutyric acid
Anhy.	Anhydrous
APN	Aminopeptidase N
Aq.	Aqueous
Arg	Arginine
Asp	Aspartic acid
BK	Bradykinin
Boc	*tert*-butoxycarbonyl
br	broad
CA-4	Combretastatin A-4
CA-4-P	Combretastatin A-4 Phosphate
$CDCl_3$	Deutrated Chloroform
CD13	Cluster of differentiation 13
CH_3CN	Acetonitrile
CH_3OH	Methanol
COSY	Correlation spectroscopy
Cs_2CO_3	Caesium carbonate
d	doublet
DCM	Dichloromethane
dd	double doublet
DEPT	Distortionless Enhancement by Polarization Transfer
DIPEA	*N*,*N*-Diisopropylethylamine
DMAP	4-Dimethylaminopyridine
DMF	Dimethylformamide

DML	Design Multiple Ligand
DMSO	Dimethyl Sulfoxide
DNA	Deoxyribonucleic acid
Dppf	1,1'-bis(diphenylphosphino)ferrocene
EC	Endothelial cell
ECM	Extracellular matrix
EDC.HCl	N-(3-Dimethylaminopropyl)-N′-ethylcarbodiimide hydrochloride
EPO	Erythropoietin
EPR	Enhanced permeability and retention
Et_3N	Triethylamine
EtOAc	Ethylacetate
EtOH	Ethanol
FDA	Food and Drug administration
GDP	Guanosinediphosphate
Gly	Glycine
GPI	Glycophosphatidylinositol
GTP	Guanosinetriphosphate
H_2O	Water
HCl	Hydrochloric acid
HIFs	Hypoxia induced factors
HIF-1	Hypoxia inducible factor 1
His	Histidine
HMBC	Heteronuclear Multiple-bond Correlation spectroscopy
HREs	Hypoxia responsive elements
HSQC	Heteronuclear Single-Quantum Correlation spectroscopy
IC_{50}	Concentration required for 50% inhibition
IR	Infrared

IFP	Interstitial fluid pressure
K_2CO_3	Potassiumcarbonate
$K_2Cr_2O_7$	Potassiumdichromate
Leu	Leucine
$LiAlH_4$	Lithium aluminium hydride
m	multiplet
mAb	monoclonal antibody
mCPBA	*meta*-Chloroperoxybenzoic Acid
MeOH	Methanol
MLC	Myosin Light chain
MMPs	Matrixmetalloproteinases
MS	Mass spectrometry
N_2	Nitrogen
NaCl	Sodium chloride
Na_2CO_3	Sodium carbonate
$NaHCO_3$	Sodium bicarbonate
NaOH	Sodium hydroxide
NGR	Asparagine-glycine-arginine
NMR	Nuclear Magnetic Resonance
NS	Not soluble
PFP	Pentafluorophenyl
PGs	Prostaglandins
PLGF	Placental growth factor
ppm	Parts per million
PyBrop	Bromotripyrrolidinophosphonium hexafluorophosphate
RNA	Ribonucleic acid
RT	Room Temperature

RTKIs	Receptor tyrosine kinases inhibitors
Rt	Retention time
SC	Stalk Cells
Ser	Serine
TBAF	Tetrabutylamonium Fluoride
TBDMSCl	*tert*-butyldimethylsilyl Chloride
TC	Tip cell
TFA	Trifluoroacetic Acid
THF	Tetrahydrofuran
TKI	Tyrosine Kinase Inhibitors
Trp	Tryptophan
Tyr	Tyrosine
VDAs	Vascular disrupting agents
VEGF	Vascular endothelial growth factor
VEGFRs	Vascular endothelial growth factor receptors
VTAs	Vascular targeting agents
VPF	Vascular permeability factor

Chapter 1

Introduction

1.0 Cancer

Cancer is a defect in the cell division cycle. It is defined as the continuous uncontrolled growth of cells, where cells lose their ability to perform normal physiological functions. It is now the second leading cause of death just behind cardiovascular disease. According to a report in 2012, approximately 14.1 million cancer cases were reported worldwide with an annual death toll of 8.2 million [1, 2].

In 2015, the estimated number of deaths in the US caused by cancer was approximately 589,430 with significantly higher levels due to cancer of the respiratory and digestive systems [3].

In Ireland from 2012-2014, 37,591 cancer and non invasive tumours were diagnosed per year with comparatively higher incidence rate occurring in males [4].

Aggregation of cells into a solid mass results in tumour formation. Tumours can be benign that form locally or it can be malignant with capacity to spread to other organs of the body.

The phenomenon of cancerous cell migration from the site of its origin to the other parts of the bodyis called metastasis. One of the most important factors involved in the migration of cancerous cells and subsequent tumour growth at sites distant from the primary region is the growth of new blood vessels. This process is referred to as angiogenesis [5].

1.1 An insight into angiogenesis

The term angiogenesis describes the birth of new blood vessels from the endothelium of pre-existing vasculature. An illustration of the process is shown in figure 1.1. Judah Folkman was the first to hypothesize the dependence of tumour growth on angiogenesis in 1971 [6]. According to his hypothesis, during normal physiological conditions the process of angiogenesis is accurately regulated. However during cancerous condition, the tumour cells generate chemical signals that shift the endothelial cells from resting phase into a rapid growth phase and causes the release of several different pro-angiogenic factors, including vasculature endothelial growth factors (VEGFs), along with the suppression of different anti-angiogenic factors. The overall result is an imbalance between positive and negative regulators of angiogenesis [7].

In the absence of angiogenesis, a small tumour mass cannot proliferate unless it acquires a new blood supply in order to get oxygen and nutrients. Hypoxia and ischemia are considered to be the main driving forces associated with angiogenesis. The normal

physiological oxygen concentration of cells ranges from 1-13 % depending on the tissue but during pathological conditions the oxygen supply to the cells is highly compromised, resulting in hypoxia. Cancerous cells have the ability to adjust to the hypoxic environment. This hypoxic condition causes the induction of hypoxia induced factors (HIFs) [8]. The hypoxia inducible factor 1 (HIF-1) has a key role under hypoxic condition and is a heterodimer consisting of HIF-1α and HIF-1β subunits. This dimer correlates with hypoxia responsive elements (HREs) to transactivate certain genes that encode different factors involved in the process of angiogenesis, such as vascular endothelial growth factor (VEGF) and erythropoietin (EPO) [9]. VEGF is considered to be the most prominent pro-angiogenic factor. The VEGF family comprises seven members including VEGF-A, VEGF-B, VEGF-C, VEGF-D, VEGF-E, VEGF-F and placental growth factor (PLGF) [10]. VEGFs bind to VEGF-receptors (VEGFRs) found on the surface of endothelial cells, of which there are three subtypes, VEGFR-1, VEGFR-2 and VEGFR-3 [1]. Of all the VEGFs, the VEGF-A is a well-known activator of angiogenesis and acts primarily on endothelial cells. VEGF-A binds to both, the VEGFR-1 and VEGFR-2 but as compared to VEGFR-2 its binding affinity to VEGFR-1 is tenfold higher. However when VEGF-A binds to VEGFR-2 it induces a more potent pro-angiogenic response. In an experiment on mice with no expression of VEGFR-2, no angiogenic response was observed. However proliferation and disorientation of blood vessels have been observed in mice with VEGFR-1 not expressed, that suggest VEGFR-1 is a down regulator of angiogenesis [11, 12].

VEGF on binding to VEGFR-2 causes the activation of endothelial tip cells to release matrix metalloproteinases (MMPs). MMPs cause degradation of proteins of the basement membrane and also cause the detachment of supportive pericytes. This proteolysis induced by MMPs allows the activated endothelial tip cells to migrate towards angiogenic stimuli and starts forming albuminal sprouts [13]. As the albuminal sprouts start migrating towards the angiogenic stimulus, the "stalk cells" evolve that follow the tip cells and proliferate. Unlike tip cells, the endothelial “stalk cells” do not show the same pattern of migration and trail behind the tip cells to form the lumen of new blood vessels [14]. Finally the tip cells converge with the neighbouring sprouts (EC-EC junctions) and anastamose to form a continuous lumen. Once the blood flow starts and oxygen supply is regained, the pro-angiogenic stimuli (VEGF) are deactivated and the newly formed blood vessels are stabilized. Upon stabilization of blood vessels the cells become non-proliferating called phalanx cells. The phalanx cells recruit pericytes and smooth muscle cells that further stabilises the newly formed blood vessels [15]. Angiogenesis is also considered to be a key

component involved in tumour metastases by providing an effective route for the escape of tumour cells from its primary site into the blood circulation [16]. Our focus is mainly on the tumour vasculature that grows around the solid tumours.

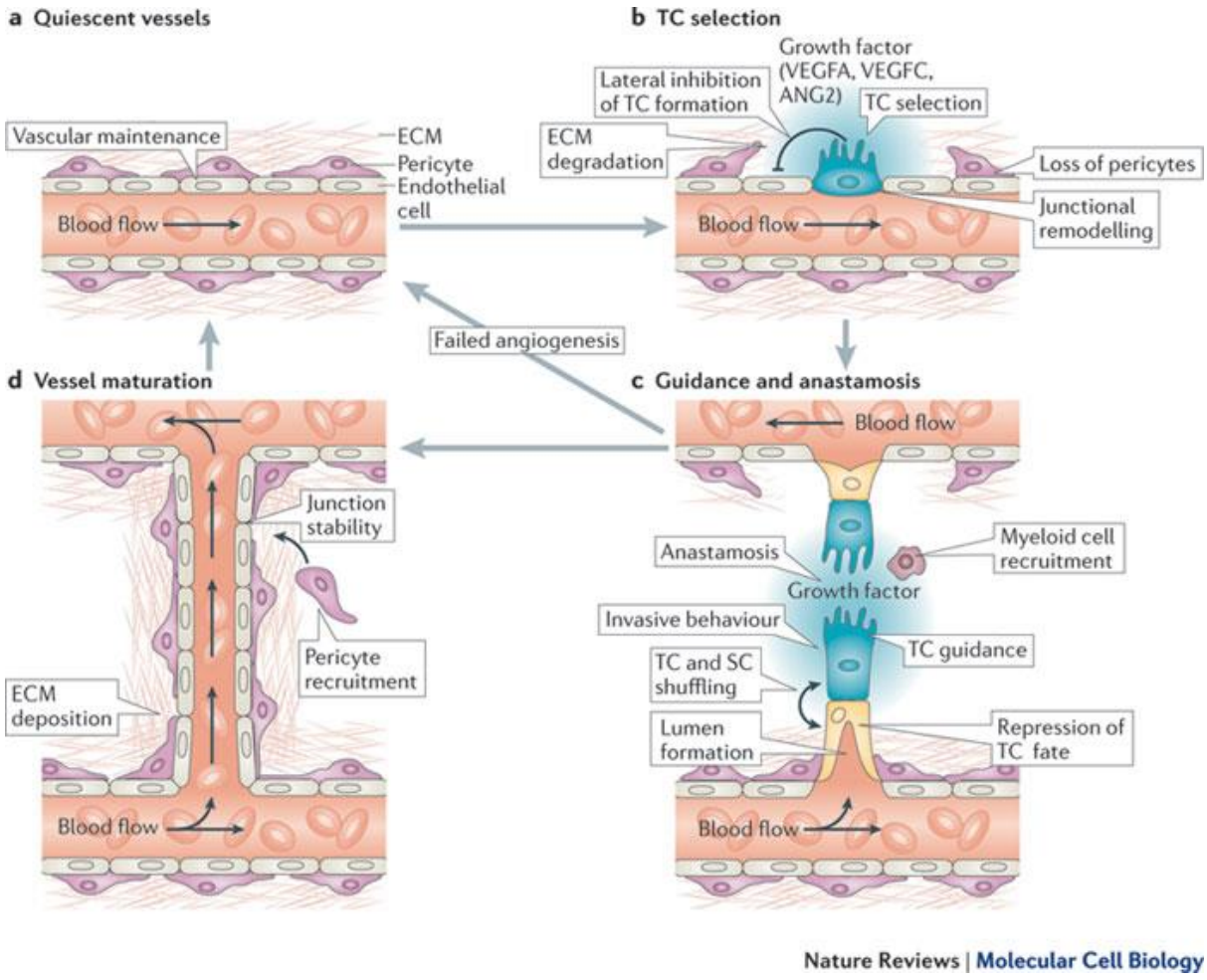

Figure 1.1. Process of Angiogenesis [17].

1.2 Tumour vasculature as a target for anticancer therapy

Targeting of tumour vasculature in anticancer therapy is becoming an area of growing interest. Some anti-vasculature agents have received orphan drug status while others are undergoing clinical trial evaluation at present [18]. The rationale to target tumour vasculature selectively and while leaving the normal vasculature unaffected is mainly based on the differences between the normal and tumour vasculature, (figure 1.2).

The architecture in tumour blood vessels is aberrant with altered blood flow and increased vascular densities [19]. Unlike normal vasculature, tumour blood vessels have enhanced permeability due to the release of different factors including vascular permeability factors, matrix metalloproteinases, bradykinin (BK), nitric oxide, prostaglandins (PGs) and peroxynitrite. Usually the tumour tissue lack effective lymphatic drainage system, vascular

smooth muscles and pericytes. Many of these factors contribute to a phenomenon known as enhanced permeability and retention (EPR) effect that is commonly observed in solid tumours. EPR effect is one of the main characteristic of tumours to be considered in rationalisation of antitumor drug delivery systems. Primarily the result of EPR effect in tumour is that unlike normal vessels, macromolecules can permeate the tumour vasculature and be retained at the tumour site in higher concentration for longer periods of time. While on the other hand, increase in vascular permeability can also lead to an increase in interstitial fluid pressure (IFP) which gradually decreases from the centre of the tumour towards the periphery and this increase in IFP hinders the penetration of anticancer agents to the tumour cells and tends to accumulate at the tumour periphery [20-22]. All of these unique characteristics of tumour vasculature including distinctive microarchitecture containing immature and chaotic vessels, over expression of pro-angiogenic growth factors, dilated and leaky lymphatic vessels, lack of smooth muscles and enhanced permeability present an excellent opportunity for the selective targeting of tumour vasculature [23].

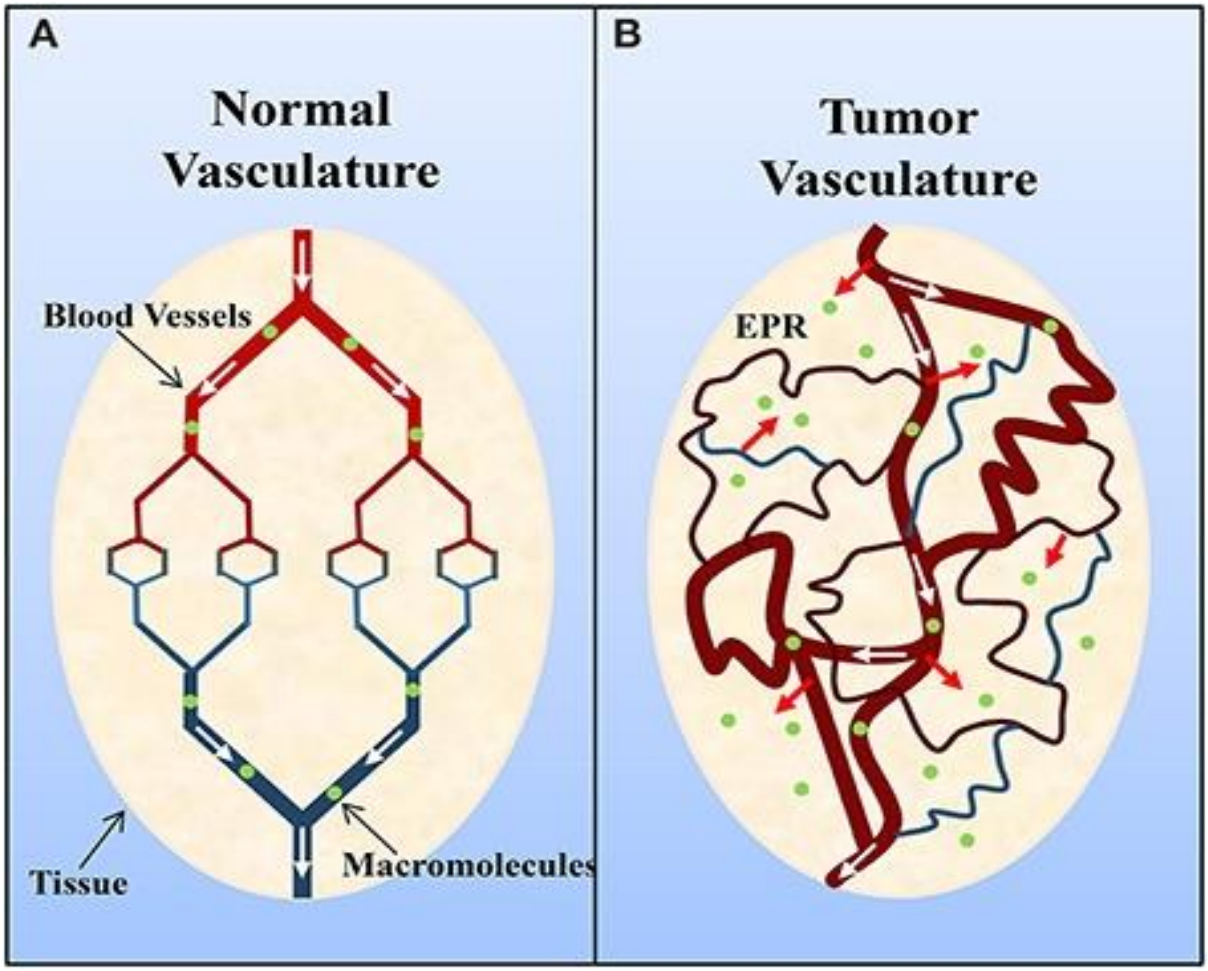

Figure 1.2. Tumour vs Normal vasculature and the EPR effect [24].

1.3 Therapeutic approaches

As far as treatment is concerned, two distinct therapeutic approaches have been evolved, antiangiogenic agents (AAs) and vascular disrupting agents (VDAs). AAs act mainly by preventing the formation of new blood vessels through interference with the signalling pathways, growth factors and other aspects related to the process of angiogenesis. However, VDAs act directly on the established network of tumour blood vessels and causes their destruction, thus depriving the central tumour of blood supply, resulting in hypoxia and necrosis in tumour mass [25].

1.3.1 Anti angiogenic therapy

The rationale behind antiangiogenic therapy is to deprive the tumour from excessive blood vessels that supply nutrients and other components required for its growth. VEGF is the key factor involved in activation of the pro-angiogenic response. Most antiangiogenic therapies target VEGF signalling pathways while some act by inhibiting two or more pro-angiogenic signalling pathways to produce a synergistic effect. Bevacizumab (Avastin®, Genetech), a VEGF inhibiting monoclonal antibody was the first antiangiogenic agent approved by the FDA (Food and Drug administration) in 2004. It was initially approved for metastatic colon cancer in combination with standard chemotherapy and now also finds use for certain other types of cancers. The studies on the use of bevacizumab in breast cancer have shown no effectiveness and that was the reason for its withdrawal from use in breast cancer by the FDA in 2011 [26, 27]. Bevacizumab has been used in combination with already established chemotherapeutics, however as a monotherapy it has also shown to prolong the time to progression of disease in metastatic renal cancer [28]. The combination of bevacizumab with oxaliplatin, fluorouracil, and leucovorin has proved to be effective in enhancing the duration of survival in patients with previously treated metastatic colorectal cancer. The common side effects associated with bevacizumab are hypertension, bleeding, and vomiting [29].

Another type of VEGF inhibitor is the VEGF-Trap (R1R2) (Aflibercept, Regeneron), a fusion protein containing ligand binding elements taken from VEGFR1 and VEGFR2 and has the ability to neutralize circulating VEGF. VEGF-Trap (R1R2) inhibits the interaction between VEGF and its receptor and thus their subsequent activation. In addition, another alternate strategy of blocking the VEGF signalling pathways is the direct inhibition of the VEGF receptors. Small molecules called receptor tyrosine kinases inhibitors (RTKIs) have the ability to target VEGF and other signalling pathways by blocking the VEGF receptors

[30]. Some of the most clinically relevant RTKIs include pazopanib (Votrient, GSK), sorafenib (Bay 43-9006, Nexavar), sunitinib (Sutent, Pfizer), cabozantinib (XL184, Exelixis), axitinib (AG013736, Inlyta), tivozatinib (AV-951) and linifanib (ABT-869) [31].

1.3.2 Vascular targeting agents (VTAs)

The concept of the use of vascular targeting agents (VTAs) as cancer therapeutics was introduced by Juliana Denekamp [32]. The rationale behind vascular targeted therapy is to cause a rapid and selective shutdown of blood vessels of the tumour, thus depriving the tumour of oxygen and nutrient supply and inducing tumour cell death [33]. The ability of the VTAs to target selectively the tumour vasculature while leaving the normal vasculature intact is associated with the structural and pathophysiological differences between normal and tumour blood vessels [23]. Vascular disrupting agents are broadly divided into two main groups on the basis of their mode of action: small molecule VTAs and ligand directed VTAs. Small molecule VTAs have no direct selectivity for tumour blood vessels but exploits the pathophysiological differences between the tumour and normal blood vessel to achieve selective destruction of tumour blood vessels. Ligand directed VTAs utilize a tumour specific ligand such as growth factor, antibody or peptides in order to achieve the selectivity for tumour blood vessels. Small molecule VTAs mainly consist of flavonoids and tubulin binding agents such as combretastatin A1/A4 presented for optimal oral delivery in their phosphate pro-drug forms [34, 35].

1.3.2.1 Tubulin binding vascular targeting agents

The major portion of research carried out so far on VTAs is related to the interaction of VTAs with a globular protein known as tubulin. Microtubule is made up of heterodimers consisting of α- and β-tubulin monomers. The heterodimer polymerises to form the basic unit of microtubule called protofilament [36]. Microtubule consists of 13 protofilaments aligned together laterally to form a cylindrical structure, (figure 1.3). Each α- and β-tubulin monomer have a bound guanosine triphosphate (GTP) and each heterodimer has a dipole with a net negative charge at the α- monomer and a net positive charge at the β- monomer. During polymerization, the positive end of one heterodimer combines with the negative end of the other followed by spontaneous hydrolysis of the GTP bound to the β- tubulin to form guanosine diphosphate (GDP) while the GTP linked to the α-tubulin monomer does not hydrolyse. Moreover, when the GTP attached to the preceding β-tubulin monomer hydrolyzes, a new GTP cap is gained by the following β-tubulin monomer and this phenomenon is called RESCUE which facilitates the polymerisation of the protofilament.

The dimers continue polymerizing but when the addition of dimers slows down, the GTP attached to the β- tubulin monomer hydrolyses before the new dimer is added and as a result of that the protofilament starts depolymerising and this phenomenon is called catastrophe. Microtubules are organized at the centrosome and anchor through a γ-tubulin ring complex (γ-TuRC) at the negative end of microtubule [37, 38]. The microtubules can exist in a steady state with a net polymerisation of tubulin dimers going on at the positive end and a net depolymerisation at the negative end, this property is termed as the treadmilling effect [39]. Moreover the microtubules also have the property to switch stochastically between growing and shortening phases, a phenomenon termed as dynamic instability [40].

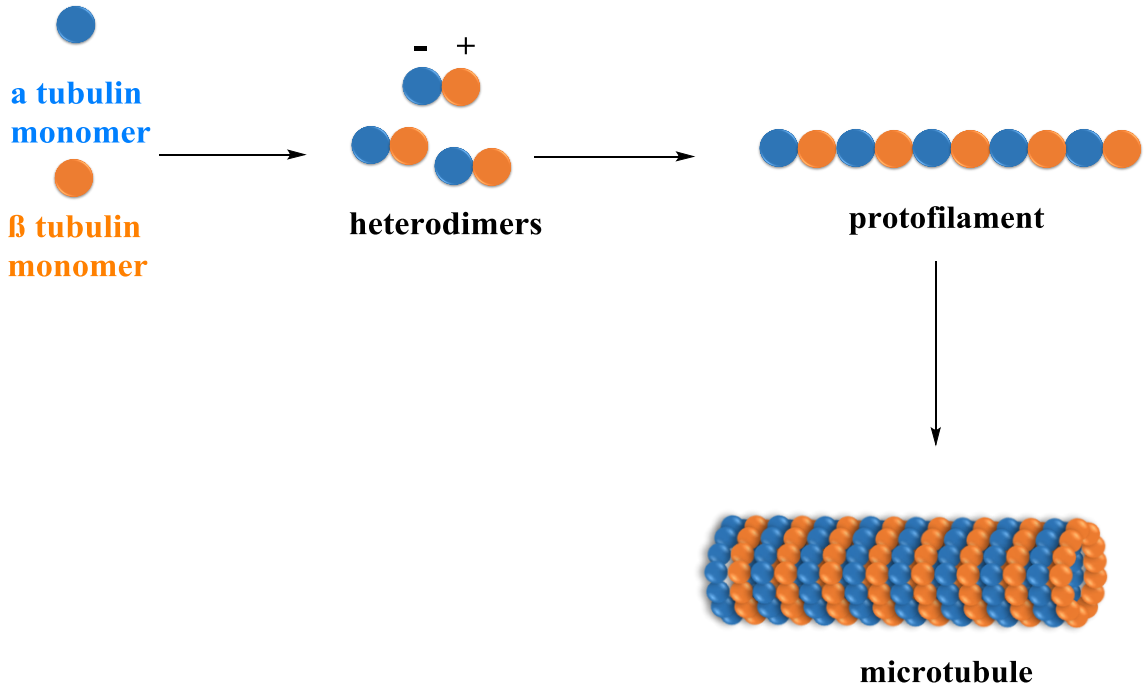

Figure 1.3. Assembling of microtubule

Microtubules have a crucial role in a number of cellular processes and give support and shape to the cell. They are also involved in intracellular transport, and serve as the route by which organelles move through the cell. They are found in almost all eukaryotic cells and have important roles during mitosis and cell division by forming an oval shaped mitotic spindle required for segregation of chromosomes into daughter cells. Microtubules can self-arrange into bundles to form cilia and flagella for cell movement [41-43]. They undergo rapid cycles of polymerization and depolymerisation and a balance between the two is necessary for normal cell cycle progression. The highly dynamic nature of microtubules makes it an ideal target for tubulin binding agents (TBAs) [44].

Several tubulin binding agents have been employed so far as anticancer agents in both haematological malignancies and solid malignant tumors where they act by interfering with microtubule dynamics. Tubulin binding agents exert their effect either by inhibiting microtubule depolymerisation thus stabilizing the microtubule or by inhibiting microtubule polymerization and destabilising the microtubule [45].

Microtubule stabilizing agents can bind to one of the three binding sites including the well-known Taxane binding site located on the luminal surface of the microtubule within β-tubulin [46], epothilones binding site overlaps with the taxane binding site [47] while the laulimalide/peroluside A binding site is located on β-tubulin at the exterior surface of the microtubule [48]. Different microtubule stabilizing agents have been developed including paclitaxel (Taxol) originally isolated from *Taxus brevifolia* (Western yew) by Wani *et al* [49]. Another semi-synthetic and more potent analogue docetaxel (Taxotere) is prepared semi-synthetically from 10-deacetyl baccatin III, isolated from the leaves of *Taxus baccata* [50]. Epothilones constitute another class of compounds that showed potent anticancer activity and among them epothiolone B proved to be 3-20 times more potent than taxanes with low toxicity in adults. Both epothilone A and B are natural products isolated from myxobacterium, *Sorangium cellulosum* [51, 52].

Three distinct binding sites have been identified for the microtubule destabilising agents including the colchicine [53], maytansine [54] and vinca binding sites [55]. Among the molecules interacting with vinca binding site, the most important are naturally and semi-synthetically occurring nitrogenous base compounds called vinca alkaloids, originally extracted from the pink periwinkle plant *Catharanthus roseus* [56]. Many different vinca alkaloids have been isolated and developed but only vincristine, vinblastine and vinorelbine are approved for use in the United States [57]. The chemical structure of vinca alkaloids consists of two basic dimeric multi-ring segments joined together namely catharanthine and vindoline. Vincristine and vinblastine have almost identical structure except for a single substituent on vindoline ring, where vincristine has a formyl substituent while in the case of vinblastine it's a methyl functional group, (figure 1.4).

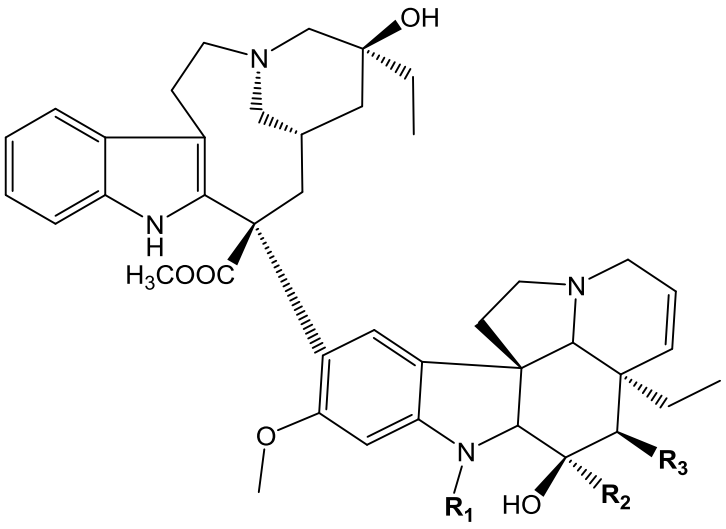

	R_1	R_2	R_3
Vincristine (**1.01**)	CHO	CO_2CH_3	$OCOCH_3$
Vinblastine (**1.02**)	CH_3	CO_2CH_3	$OCOCH_3$
Vindesine (**1.03**)	CH_3	$CONH_2$	OH

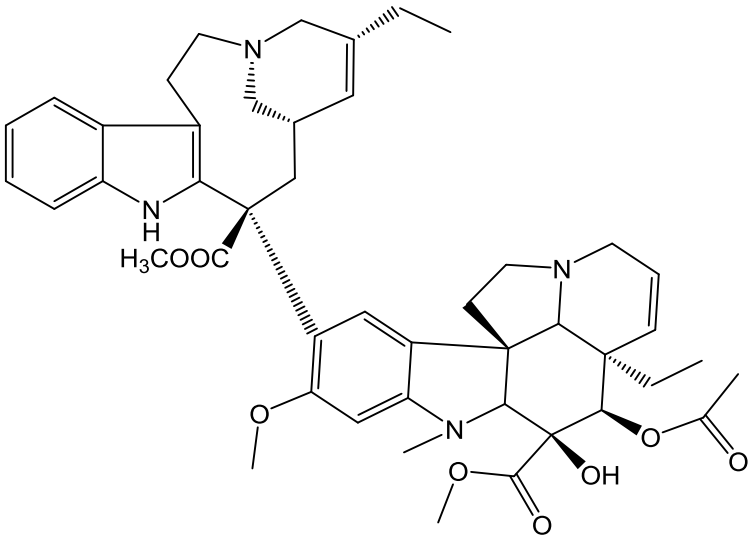

Vinorelbine **(1.04)**

Figure 1.4. Vinca alkaloids

The vinca binding site is mainly constituted by α and β tubulin monomers of two different successive heterodimers [55]. Of all the binding sites available, it is the colchicine binding site that we are interested in as it serves as an excellent target for VTAs and antiangiogenics. The substrate colchicine binds to the colchicine binding site and is effective at inhibiting tumour growth [58] and angiogenesis [59], however its use as an anticancer agent is limited due to its high toxicity [60]. Colchicine is clinically approved as

a first line therapy in the treatment of acute gout arthritis and familial mediterranean fever [61].

1.3.2.2 Combretastatin A-4 and its analogues

Another series of compounds known as combretastatins, first isolated from *Combretum caffrum* in 1988 by Pettit *et al* have structural similarities to colchicine [62]. Combretastatins bind to the colchicines binding site but unlike colchicine, is well tolerated with lower toxicity [63, 64]. The reason for the low toxicity of combretastatins is probably because of their lower exposure to healthy tissues due to their shorter plasma half-lives. Moreover the interaction of combretastatins with its binding site is reversible unlike colchicine, which binds 100 times more strongly to tubulin [65].

Among all the combretastatins the most active are combretastatin A-4 **(1.05)** and A1 **(1.06)**, both having structural similarity to colchicine **(1.07)**, (figure 1.5). CA-4 has been found to induce tumour vascular shutdown at doses less than one tenth of its maximum tolerated dose (MTD) and even a low dose exposure to the proliferating endothelial cells resulted in a profound cytotoxic effect. The main issue with CA-4 is the poor aqueous solubility which has been resolved by the synthesis of water soluble sodium salt of its phosphate pro-drug, combretastatin A-4 phosphate **(1.08)** [66, 67].

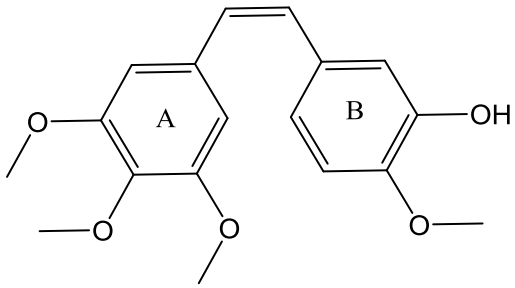

Combretastatin A-4 **(1.05)**

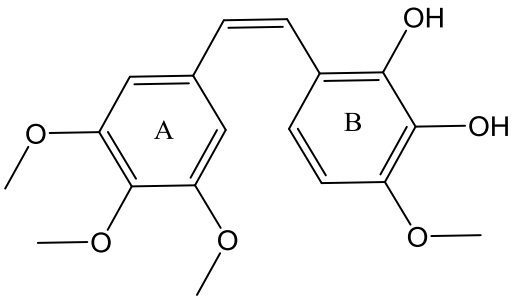

Combretastatin A-1 **(1.06)**

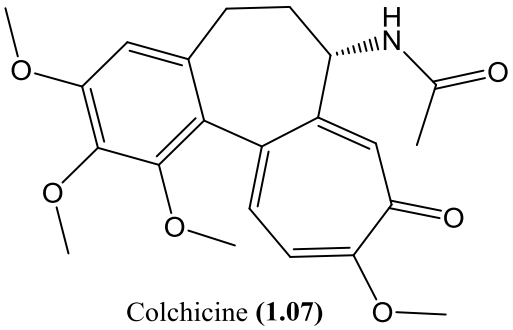

Colchicine **(1.07)**

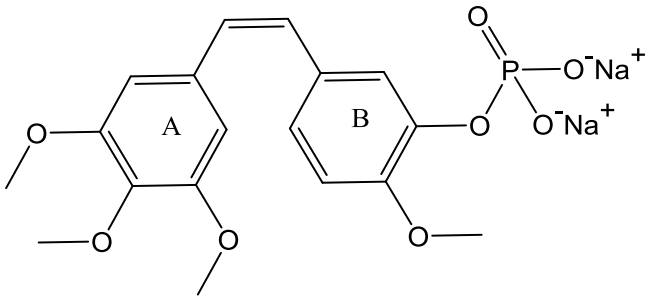

Combretastatin A4 Phosphate Disodium **(1.08)**

Figure 1.5. Structures of colchicine and combretastatins

Unlike traditional anticancer agents the CA-4 phosphate lacks the usual side effects of stomatitis, alopecia and myelosuppression while the most prominent toxic effects reported are hypertension, tumour pain and hematologic toxicities including neutropenia and thrombocytopenia. Other toxicities seen in patients are headache, nausea, fatigue, diarrhoea, vomiting, hypotension, ataxia and dyspnoea [68-70].

The colchicine binding site is mainly located within the intermediate domain of β-tubulin, surrounded by strands S8 and S9, loop T7 and helices H7 and H8; however colchicine is also found to interact with with the loop T5 of the adjacent α-subunit. The T7 loop links the H8 helix to H7. In the absence of ligand, the T7 loop lies in the colchicine binding site but during the entry of colchicine into α-β heterodimer, there is movement of T7 loop and H8 helix, allowing colchicine to enter the binding site, (figure 1.6) [53, 71].

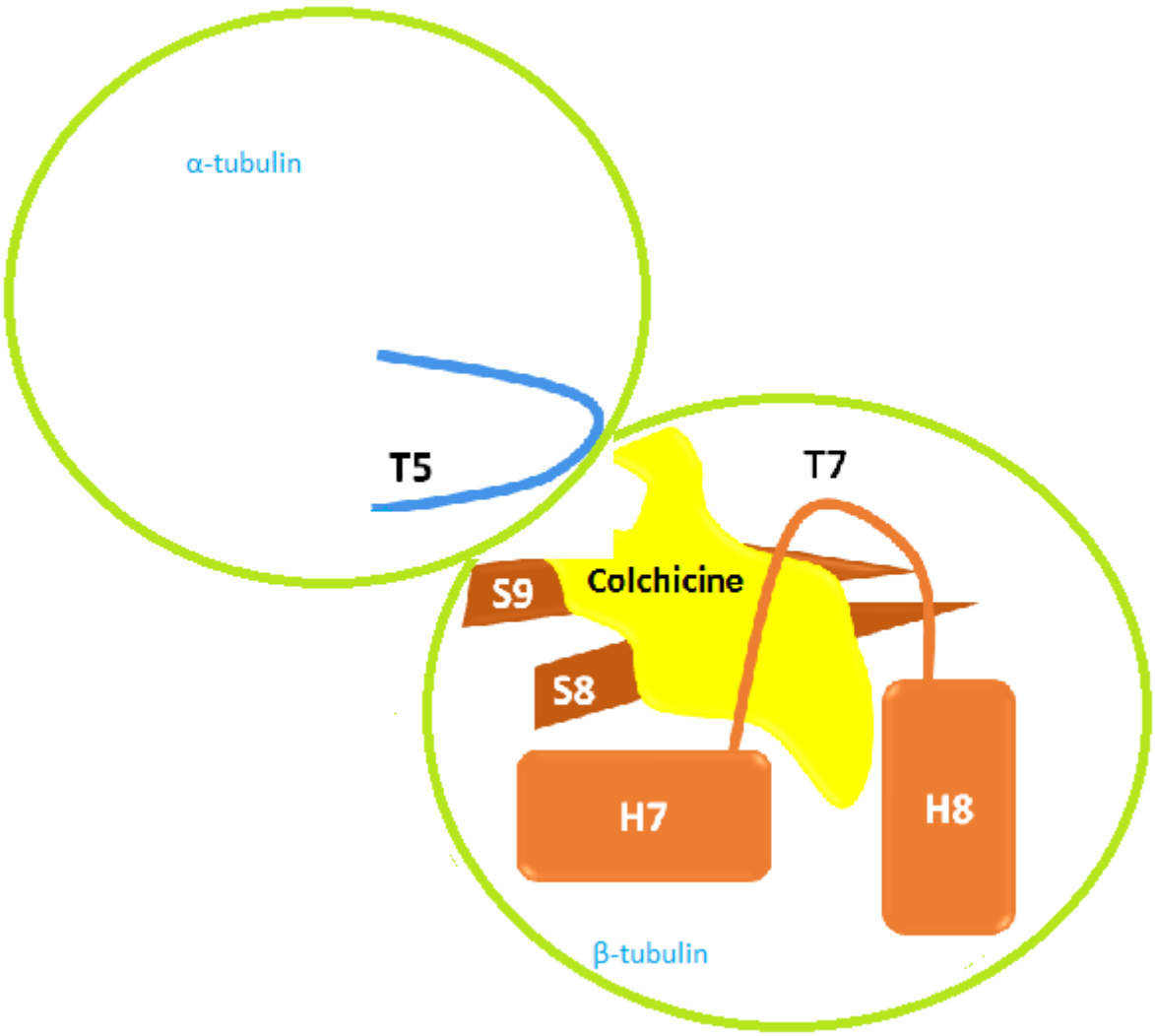

Figure 1.6. Colchicine and its interaction with binding site

The process of vascular disruption by VTAs starts with the activation of RhoA (Ras homolog gene family, member A). The exact mechanism for the activation of RhoA is not clear however it is proposed that VDAs on attachment to its binding site activate a number of different proteins including guanosine nucleotide exchange factors (GEFs). The GEFs then activates Ras homology (RhoA) family of GTPases [72] and was first identified as gene product of Ras homology by Maduale and Axel [73]. The RhoA in turn activates RhoA kinase that phosphorylate the myosin light chain (MLC) resulting in actin-myosin contractility, disruption of cell-cell contact and increased permeability [74].

In case of combretastatin, it has been observed that some cells undergo a blebbing morphology in which the cell detaches its cytoskeleton from the membrane that results in swelling of the membrane and morphological changes to the cells including the increased permeability to macromolecules. The membrane blebbing occurs due to the polymerization of F-actin initiated by the activation of Rho kinases and is regulated by stress activated

protein kinase 2 (SAPK2), extracellular regulated kinases (ERKs) and myosin light chain kinase (MLCK). As a result, F-actin accumulates around the surface of cells causing the membrane to swell into spherical bubbles called blebs. The stress fibers are also disassembled and there is formation of focal adhesions. The net result of this membrane blebbing and endothelial cells contractility is the narrowing of vascular lumen, increased vascular permeability and increase in vascular resistance that leads to haemorrhagic necrosis of the tumour [75].

Many different analogues of combretastatin have been synthesised to date. Common to all of them is the presence of two methoxy substituted aryl rings A and B connected through different length, cyclic or open aliphatic chain bridges, (figure 1.7).

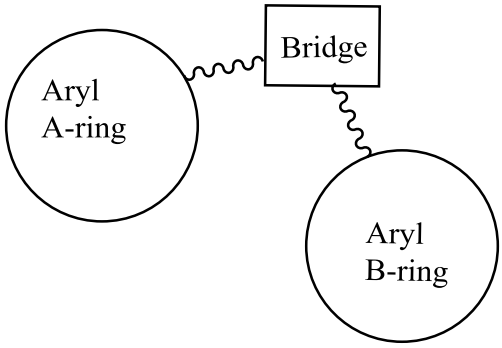

Figure 1.7. General schematic representation of combretastatins structure

Coumarin-based compounds constitute another important class of compounds with a wide variety of different pharmacological effects. These include derivatives with anticoagulant [76], antihypertensive [77], anticonvulsant [78], antiviral [79], antioxidant [80], antibacterial [81] and anti-inflammatory properties [82].

Over the years many different coumarin derivatives have been synthesised and employed successfully as anticancer agents. A series of 3-arylcoumarins has been synthesised by CF Xiao *et al.* and evaluated for their cytotoxic activity against various cancer cell lines. The most active compound among them was **(1.9)** as it has shown reasonable cytotoxic activity in the *in-vitro* analysis [83]. Christian Bailly and co workers have synthesised a series of 4-arylcoumarin analogues of combretastatin. Among them the most active compounds were **(1.10a)** and **(1.10b)** that have shown excellent cytotoxic activity with an IC_{50} value of 0.52 and 0.083 µM in the CEM human leukemia cell line (figure 1.8) [84].

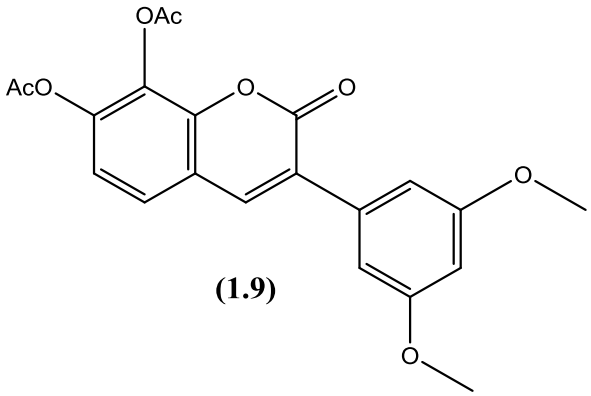

(1.9)

Compounds	Cell lines IC_{50} µM/L			
1.9	KB	KV	MCF-7	MCF-7/ADR
	5.18	13.96	21.43	11.94

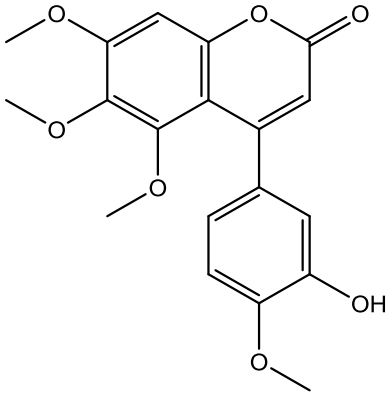

(1.10a)

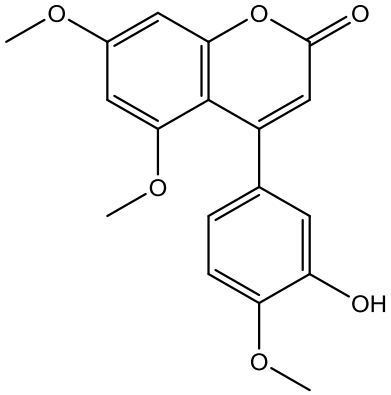

(1.10b)

Figure 1.8. Coumarin derivatives

Phenstatin **(1.11)**, a tetramethoxy substituted benzophenone is another analogue of combretastatin which was originally synthesised serendipitously by Petit *et al.*, while working on structural activity relationship (SAR) based synthesis of the *cis*-isomer of combretastatin A-4. Phenstatin exhibit cytotoxicity and inhibition of tubulin polymerization comparable to that of the combretastatins and overcomes the drawback of the generation of inactive *trans* (*E)* isomer of CA-4 **(1.12)** [85]. Similarly to combretastatin, phenstatin is composed of a trimethoxy substituted A-ring and a monomethoxy substituted B-ring. The only difference is that the alkene of combretastatin is replaced by ketone functional group. Many different SAR studies of combretastatins and their analogues have shown that the presence of two aryl rings linked through a bridge, with cisoidal disposition are crucial for activity. Further studies have shown that a 3,4,5-trimethoxy arrangement at aryl A-ring and a monomethoxy substitution at *para* position of aromatic B-ring are important for tubulin

binding activity of phenstatin. Substitution of 3,4,5-trimethoxy arrangement at A-ring with 2,4,5-trimethoxy reduces the tubulin binding activity of the phenstatin compounds. The presence of a hydroxyl **(1.11)** or amino group **(1.13)** at the *meta*-position of the B-ring increases the tubulin binding activity, (figure 1.9) [85-87].

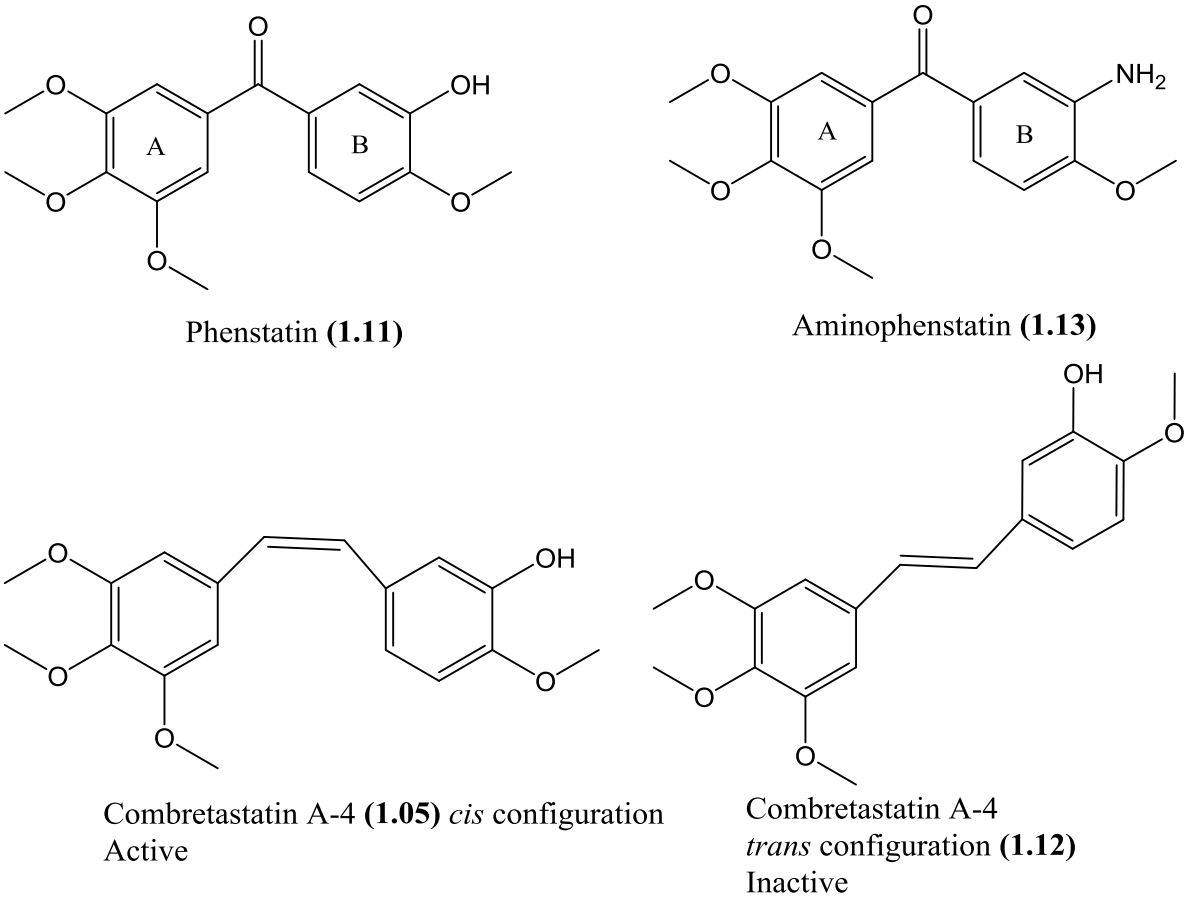

Figure 1.9. Structures of phenstatins and combretastatins

When compared to the A-ring, the B-ring has some flexibility with regard to groups that may constitute this ring. Indeed its replacement with a 5-indolyl ring by Álvarez *et al.* (figure 1.10) resulted in formation of compounds **1.14** and **1.15** that proved to be more potent than CA-4 as tubulin polymerization inhibitors [86, 88]. Other useful modifications to the B-ring without losing cytotoxic and tubulin binding activity includes substitution with benzo[b]furanyl [89], thiophene analogues [90], carbazolyl [91] and indazole analogues [92].

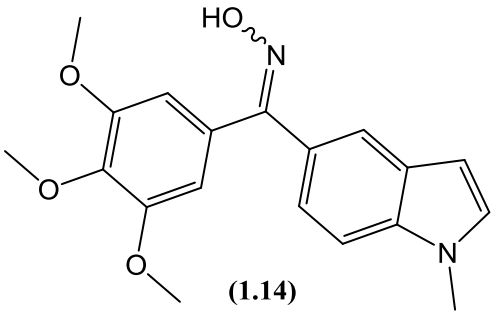

(1.14)

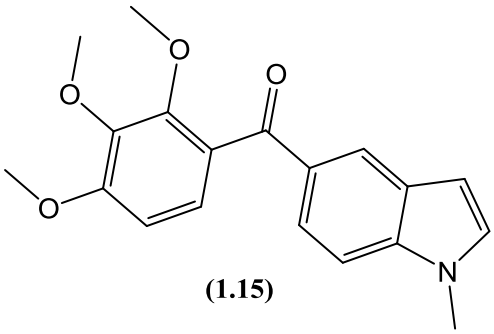

(1.15)

Compounds	Tubulin polymerization inhibition (TPI) and Cell lines (IC_{50} µM)				
	TPI	HeLa	HL-60	A-549	HT-29
(1.14)	1.8	0.36	0.33	>10	0.11
(1.15)	0.4	0.017	_	0.51	0.021
CA-4	3	0.003	0.002	0.003	0.032
phenstatin	2.5	0.03	0.03	0.3	1.8

Figure 1.10. Indolyl derivatives of phenstatin

1.3.2.3 Ligand directed VTAs

Conventional cancer treatments have several limitations including lack of selectivity, inevitable toxicity and drug resistance. With the passage of time the conventional cancer therapies have been improved with the development of new molecular targeting agents [93].

Ligand directed VTAs utilize the concept of targeted therapy which is developed from the idea of "magic bullet", first introduced by Paul Ehrlich. Salvarsan or arsphenamine was the first magic bullet discovered by Ehrlich in 1909 to cure syphilis [94]. With the advancement in molecular biology and biotechnology several small molecules and monoclonal antibodies have been developed which interfere with specific target molecules that appear during malignancy but not under normal physiological conditions. These specific target molecules include different growth factor receptors, regulators of apoptosis, signalling molecules, molecules involved in angiogenesis and metastasis and cell cycle

proteins [95]. Ligand directed VTAs involve the incorporation of such tumour specific pharmacophore(s), growth factor, antibody or peptides on to an active tubulin-based VDA. Among such approaches for selective targeting of tumour blood vessels is the use of hybrid drugs.

1.4 Hybrid drugs

To overcome the drug resistance and toxicities normally associated with monotherapies, a concept of combination therapy was introduced by E Frei III and co-workers in 1965 for treatment of acute leukaemia [96]. In combination therapy, the agents targeting different pathways act synergistically with lower toxicity due to lower therapeutic dosage of each individual candidate [97]. Several different combination have been employed as an anticancer therapy including the combination called POMP that comprises of 6-mercaptopurine (Purinethol), vincristine (Oncovin), methotrexate and prednisone and has proved to be well tolerated with an improved anti-tumour activity in paediatric patients with acute lymphocytic leukemia [96]. Another combination therapy employed is the combretastatin A4 phosphate (CA4P) with bevacizumab that demonstrated improved anticancer activity with good tolerability. This combination synergistically boosts the overall effect of anticancer therapy [98]. Combination therapy exhibits many advantages however its efficacy is sometime compromised by drug-drug interactions [99].

Utilising the concept of combination therapy, a new approach of the hybrid drugs has emerged that comprises the incorporation of two or more entire drugs or just pharmacophores into one single molecule in order to interact with multiple targets and to intensify its effects [100]. The main purpose of designing a hybrid drug is to counteract the side effects associated with one part of the drug, to produce synergistic effect and to lower the risk of drug-drug interaction and drug resistance.

Hybrid anticancer therapy is becoming an area of great interest because of its potential to enhance the biological activity and to overcome the toxicity associated with conventional anticancer therapies. As far as hybrid cancer therapy is concerned, varieties of different designs have been proposed. Among them the main approaches employed are [100]:

i) Hybrid drugs comprising of pharmacophores from two or more drugs

ii) Hybrid drugs comprising of two or more entire drugs

1.4.1 Hybrid drugs comprising of pharmacophores

Hybrid drugs synthesised by incorporating pharmacophores from two or more drugs are of two types: one that have pharmacophores taken from drugs with similar pharmacological targets while other has the pharmacophores from drugs having many different pharmacological targets.

1.4.1.1 Hybrid drugs comprising of pharmacophores with similar pharmacological targets

The synthetic strategy of combining pharmacophores from two or more drugs with similar targets in order to produce a synergistic response has been employed on different anticancer candidates. JK Ryu *et al*. synthesised the hybrid SK-7041 **(1.18)** by merging the hydroxamic acid side chain of trichostatin A (TSA) **(1.16)** and the aryl ring of MS-275 **(1.17)** (figure 1.11), both of which are histone deacetylase (HDAC) inhibitors. The hybrid SK-7041 demonstrated antiproliferative activity and proved to be more potent than vorinostat (SAHA, a histone deacetylase inhibitor) in both lung-derived and breast cancer cell lines [101].

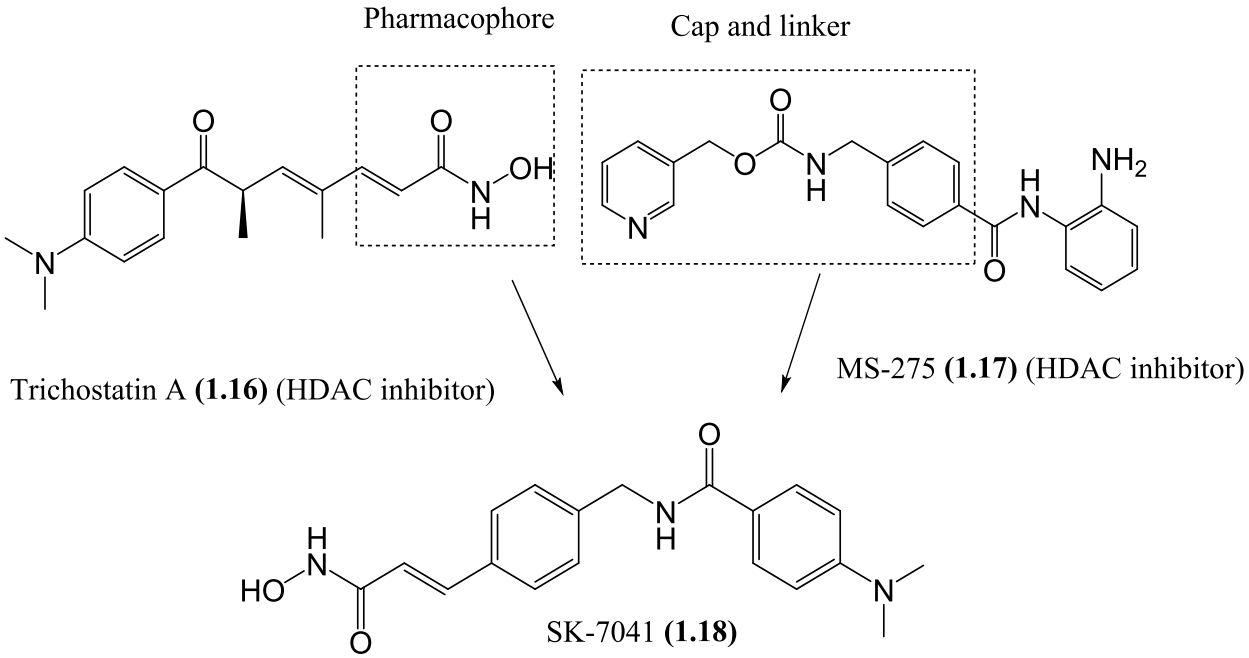

Lung cancer cell lines	**SK7041** IC_{50} µM	**SAHA** IC_{50} µM
A549	0.79±0.06	3.87±0.31
NCI-H23	0.70±0.03	3.45±0.19
NCI-H1299	0.98±0.09	5.23±0.25
Breast cancer cell lines		
MDA-MB-231	1.01±0.28	5.70±0.35
MCF-7	0.72±0.09	2.70±0.36
SK-BR-3	0.26±0.02	1.99±0.12

Figure 1.11. Merging the pharmacophoric moieties of HDAC inhibitors

CJ Andre and co workers synthesised "combretatropones'' hybrids by combining the pharmacophores of two tubulin inhibitors: combretastatin A4 and colchicine (figure 1.12) to produce the combretatropone hybrid **(1.19)** and phenyltropone hybrid **(1.20)**. In their study **(1.20)** was more active than both colchicine and combretastatin A4 in the tubulin polymerisation assay [102].

.

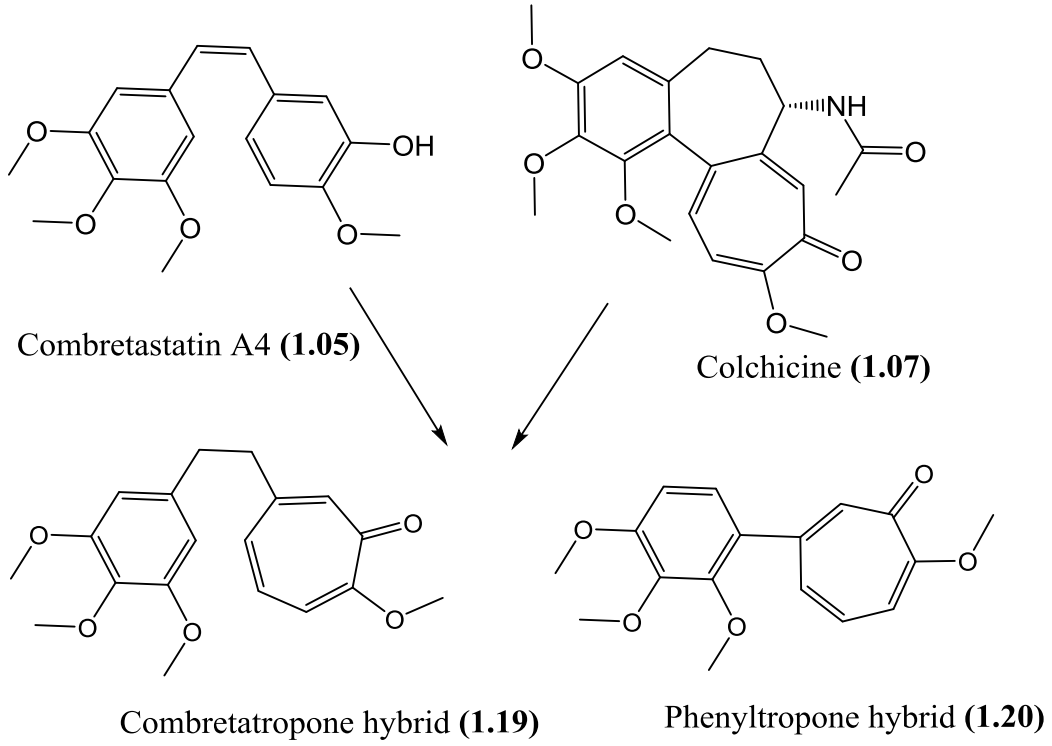

Comp.	IC_{50}(μM) Tubulin polymerization inhibition
Colchicine	3.5
CA-4	2.9
1.19	8.6
1.20	2.5

Figure 1.12. Combretatropone and phenyltropone hybrids

Ojima *et al.* synthesised hybrid **(1.26)** by merging the common pharmacophoric moieties of five microtubule stabilizing agents including paclitaxel **(1.21)**, nonataxel **(1.22)**, discodermolide **(1.23)**, epothilones **(1.24)** and eleutherobin **(1.25)** (figure 1.13). The hybrid demonstrated submicromolar level IC_{50} values (0.39 μM against the human breast cancer cell line MDA-435yLCC6-WT) [103].

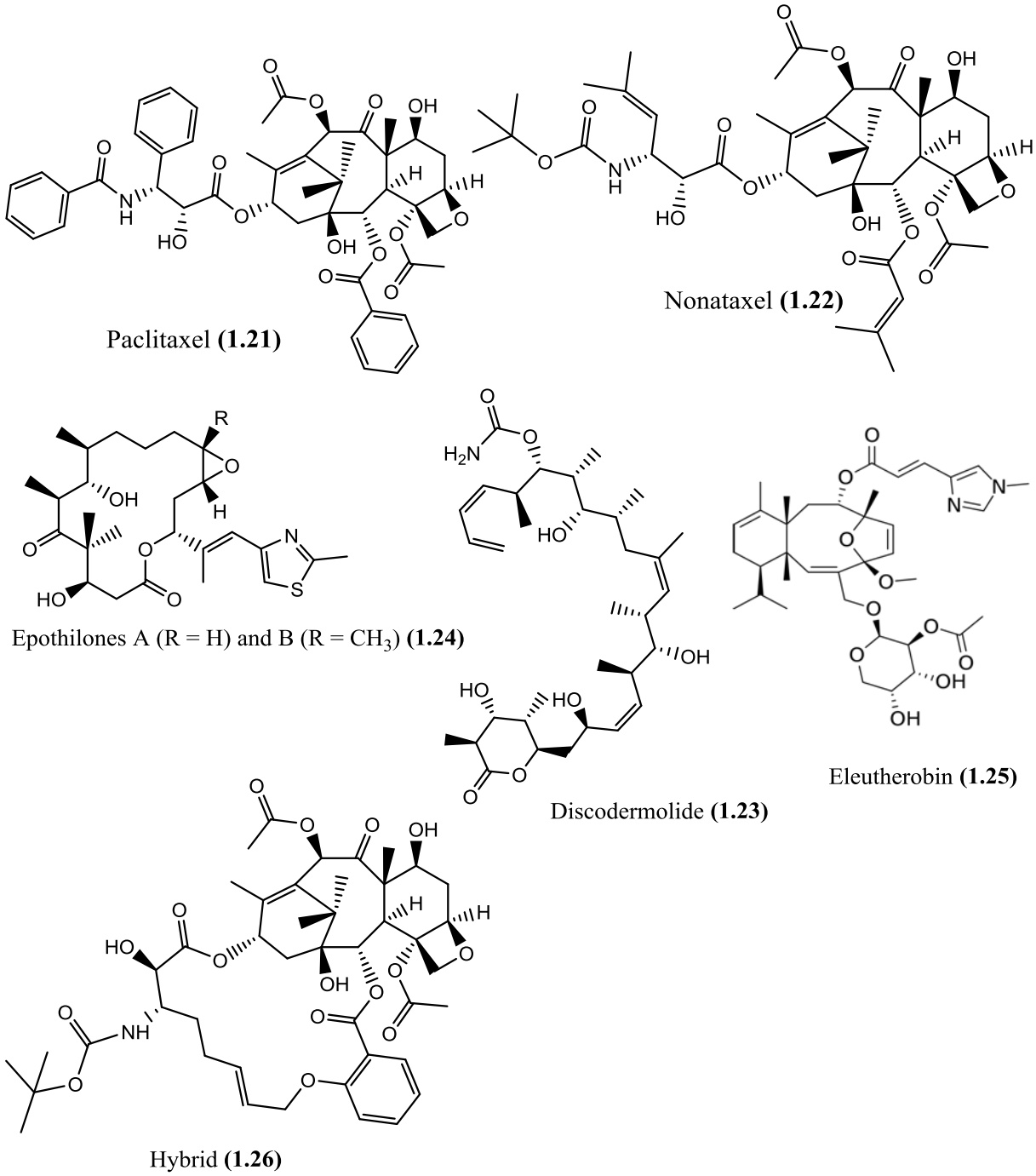

Figure 1.13 Hybrid based on 5 microtubule stabilizing agents.

1.4.1.2 Hybrid drugs comprising of pharmacophores with different pharmacological targets

This strategy is also known as designed multiple ligands and involves the merging of pharmacophores from two or more drugs; each having different pharmacological targets. The strategy is based on the principle that due to the complex nature of the cancer disease the chances of treating this condition with a single mono functional anticancer candidate is

challenging [104]. The main purpose of merging a cocktail of pharmacophores which have different targets is to produce a synergistic response at doses below the maximum tolerated dose and to improve the delivery of the drug to its target site. This approach follows the concept of combination therapy where two or more drugs with different pharmacological targets are used. The combination of two or more drugs acting on different pathways has proven to be highly efficacious. For example, the combination of capecitabine which is a pro-drug of fluorouracil (anti-metabolite), with docetaxel (a tubulin inhibitor) has shown significant efficacy in the survival and time to disease progression in patients with advanced breast cancer during phase III clinical trials. Moreover the combination also resulted in reduction of side effects associated with docetaxel monotherapy [105]. In another example, a combination therapy using histone deacetylase inhibitors (HDACi) along with paclitaxel (a tubulin inhibitor) enhanced the cytotoxic effect of paclitaxel in ovarian cancer cell lines [106].

Zhang *et al* have successfully extended this concept of merging a HADC inhibitor with a tubulin targeting agent by synthesising dual acting hybrids of colchicine **(1.07)** (a tubulin inhibitor) and SAHA **(1.27)** (a histone deacetylase inhibitor). The dual acting hybrids were evaluated as HDAC inhibitors and for their cytotoxic activities in five cancer cell lines. The most potent compound among them was colchicine-SAHA hybrid **(1.28)** (figure 1.14) that demonstrated strongest HDAC inhibition along with significant antiproliferative activity (0.242 μM against A431 cells) [107].

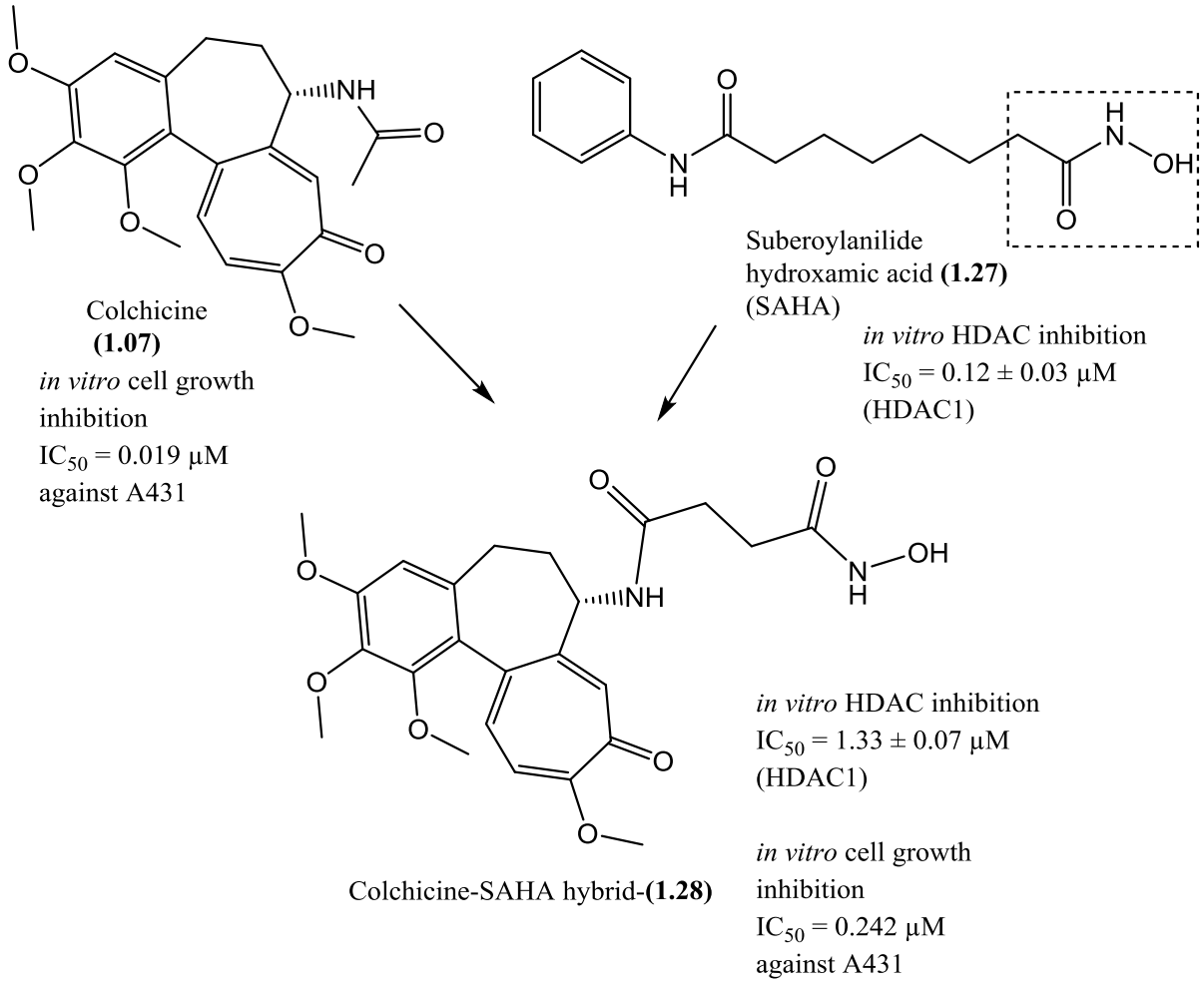

Figure 1.14 colchicine-SAHA hybrid

X Zhang *et al.* have synthesised hybrids in order to demonstrate the potential of combination therapy in one single agent. They have synthesised multi-targeting hybrids by combining the pharmacophoric moieties of a tubulin polymerization inhibitor **(1.29)** and a VEGFR-2 and PDGFR-β inhibitor **(1.30)**. The most potent multi-targeting hybrid was compound **(1.31)** that demonstrated potent inhibition of VEGFR-2 and PDGFR-β along with the inhibition of microtubule (figure 1.15). The hybrid proved to be about 4-fold more potent than sunitinib in inhibiting PDGFR-β and almost equipotent in VEGFR-2 inhibition. Moreover it also showed tubulin polymerization inhibition activity comparable to combretastatin [108].

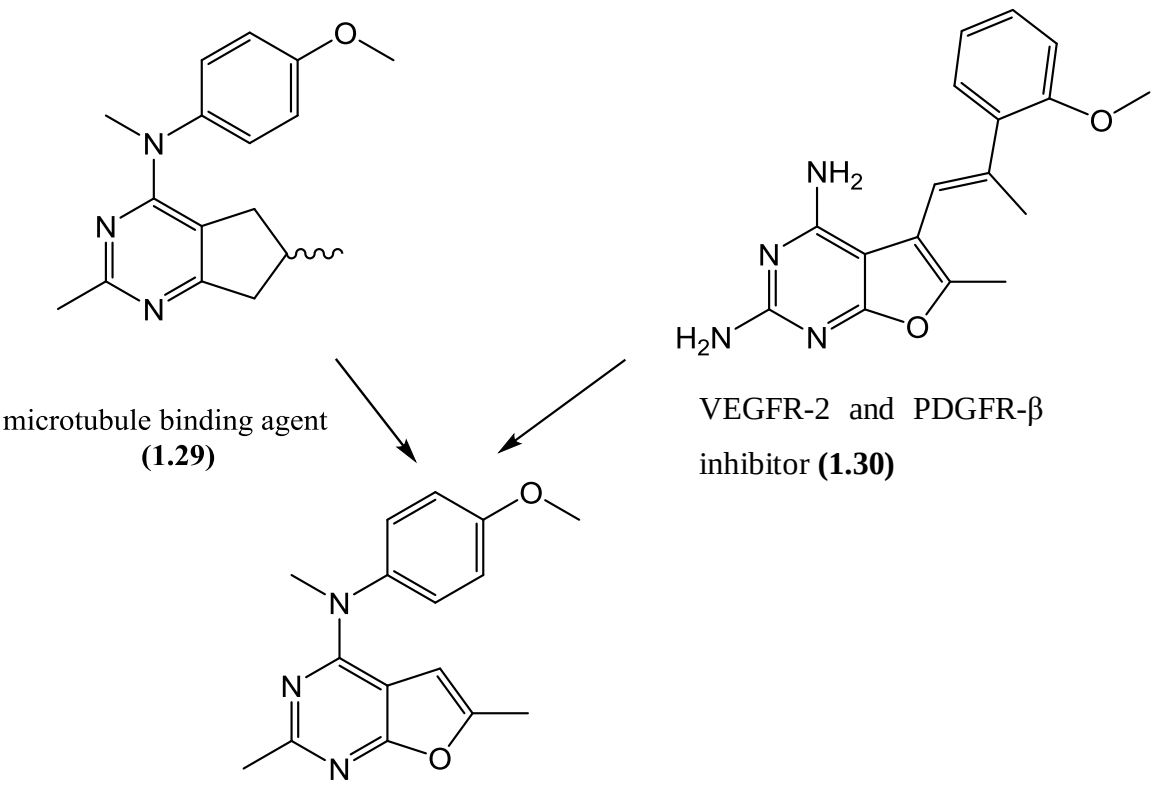

inhibition of tubulin assembly	IC_{50} = 1.9 ± 0.1 µM	(CA-4	IC_{50} = 1.0 ± 0.09 µM)
VEGFR-2 kinase inhibition	IC_{50} = 19.1 ± 3.0 nM	(sunitinib	IC_{50} = 18.9 ± 2.7 nM)
PDGFR-ß kinase inhibition	IC_{50} = 22.8 ± 4.9 nM	(sunitinib	IC_{50} = 83.1± 10.1 nM)

Figure 1.15. Multi-targeting hybrid (1.31)

1.4.2 Hybrid drugs comprising of two or more entire drugs

The hybrid in which two or more entire drugs are linked together is called a drug conjugate. The two drugs can either be linked directly or a linker unit can be used to join them. Again this design can be of two types: one, where the two or more drugs with similar pharmacological targets are linked while the other is where two or more drugs with different pharmacological targets are chemically joined together.

1.4.2.1 Hybrid drugs comprising of two or more entire drugs having similar pharmacological targets

The strategy of hybridizing two or more entire drugs has been utilized on many different cytotoxic agents and the hybrids might consist of either two different drugs with same biological target or only one drug (dimer). This design might be comparatively

advantageous to the hybrids having drugs with distinct targets due to their different cellular localisation of targets as well as the difference in the ligands affinity for the targets [109].

K Bombuwala *et al.* synthesised colchitaxel **(1.32)**, a hybrid consisting of two tubulin inhibitors colchicine **(1.07)** and paclitaxel **(1.21)** in order to compare its activity with the combination of both individual drugs (figure 1.16). The two drugs are linked together by replacing the acetyl group of colchicine with glutamate linker, attached to carbon 7 of paclitaxel. The LogP computed for the colchitaxel was more or less comparable to paclitaxel that indicates the hybrid would have similar cell permeation ability to paclitaxel. For further biological evaluation, the hybrid in various concentrations was evaluated against the IAR20 PC1 rat liver cell line and was compared to the combination of paclitaxel (PTX) and colchicine in varying molar ratio. The alterations caused by the hybrid in the microtubule arrangement were similar to those caused by the combination of PTX and colchicine however bundles of microtubule, a characteristic of the cells treated with the combination of PTX and colchicine were absent in colchitaxel treated cells [110].

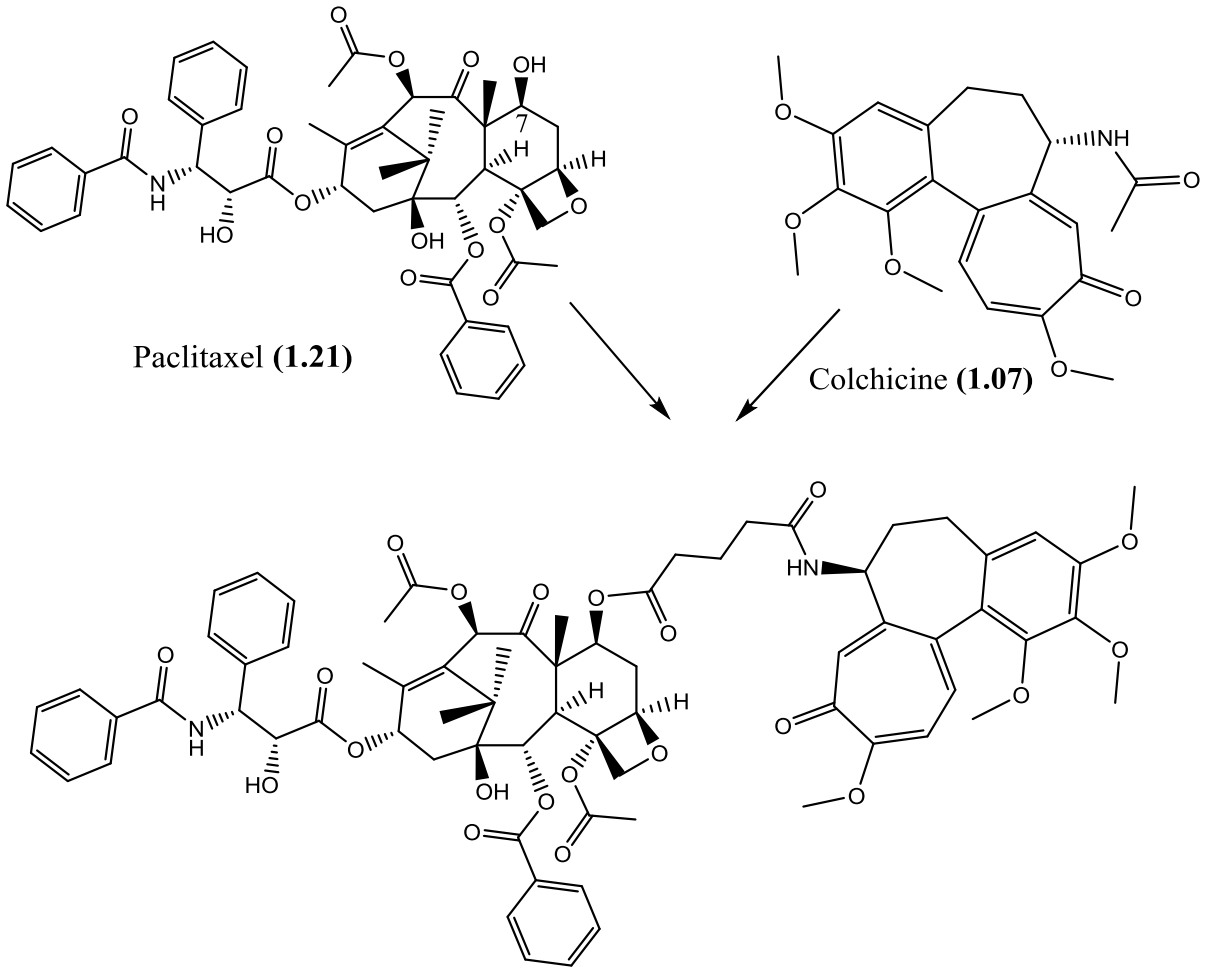

Figure 1.16. Hybrid of colchicine and paclitaxel

Numerous different targets for anticancer drugs including tubulin [111], telomerase [112], receptor tyrosine kinases [113] and matrix metalloproteinases (MMPs) [114] have been utilized to date and many of them pre-exist in dimeric form or require dimerization for their activation. Keeping these dimeric anticancer targets in mind it might be effective to inhibit them using dimeric molecules and the advantages associated to the inhibition of these dimeric targets has been proposed by J Monod *et al* [115].

In keeping with the dimer theme Yamaguchi e*t al.* synthesised and evaluated different aromatase inhibitors and the most potent among them was the diethylaminocoumarin dimer **(1.33)** that demonstrated slightly better aromatase inhibition activity as compared to the current available exemestane **(1.34)** (figure 1.17) [116]. Aromatase enzyme has an important role in the synthesis of estrogen, a hormone involved in development and growth of breast tumors [117].

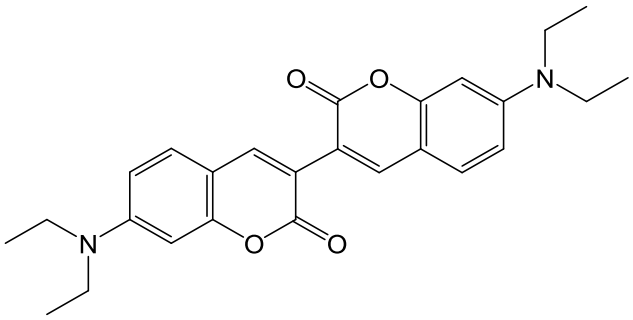

diethylaminocoumarin dimer **(1.33)**
IC_{50} = 28.7 nM

Exemestane **(1.34)**
IC_{50} = 42.5 nM

Figure 1.17. Diethylaminocoumarin dimer

Daunorubicin **(1.35)** is an anticancer agent that exerts its cytotoxic effect by inhibiting the progression of topoisomerase II through DNA intercalation [118]. Daunorubicin dimer **(1.36)** was synthesized by Gary G. Hu *et al*, by linking the two monomers through a xylyl group attached to their amine moieties (figure 1.18). The dimer was shown to intercalate more strongly to DNA than the individual monomers [119].

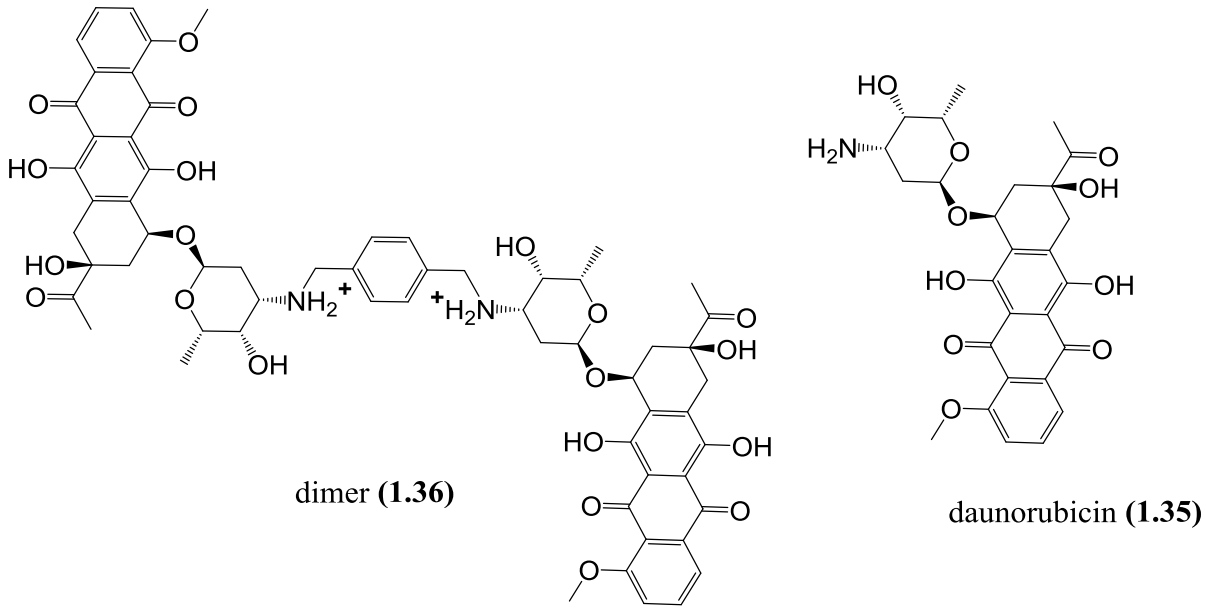

Figure 1.18. Bisdaunomycin (1.36)

1.4.2.2 Hybrid drugs comprising of two or more entire drugs having different pharmacological targets

The strategy of combining two or more entire drugs with different targets is mainly utilized in order to produce a synergistic response or for one drug to act as a tumour homing device for the other in order to improve its targeted delivery. MD Wittman *et al.* synthesised paclitaxel-chlorambucil hybrids **(1.37, 1.38, 1.39, 1.40)** (figure 1.19) in view of synergism demonstrated by paclitaxel in combination with other anticancer agents and the preclinical evidence of *in-vitro* and *in-vivo* sensitivity of paclitaxel resistant cancer cell line to the combination of paclitaxel and an alkylating agent. Paclitaxel is a microtubule stabilizing agent while chlorambucil is a DNA alkylating agent that exerts its cytotoxic effect by interfering with DNA replication. *In-vitro* evaluation of the hybrids as tubulin polymerization inhibitors and cytotoxicity was carried out against the HCT-116 human colon tumor cell line while the *in-vivo* cytotoxicity was determined using the Madison 109 (M109) murine lung carcinoma M109 tumor model. Among the four hybrid molecules synthesised, the hybrid **(1.40)** proved to be the most potent and displayed superior activity to the single agent or combination therapy in the paclitaxel resistant M109/tax1R and paclitaxel sensitive M109 models [120, 121].

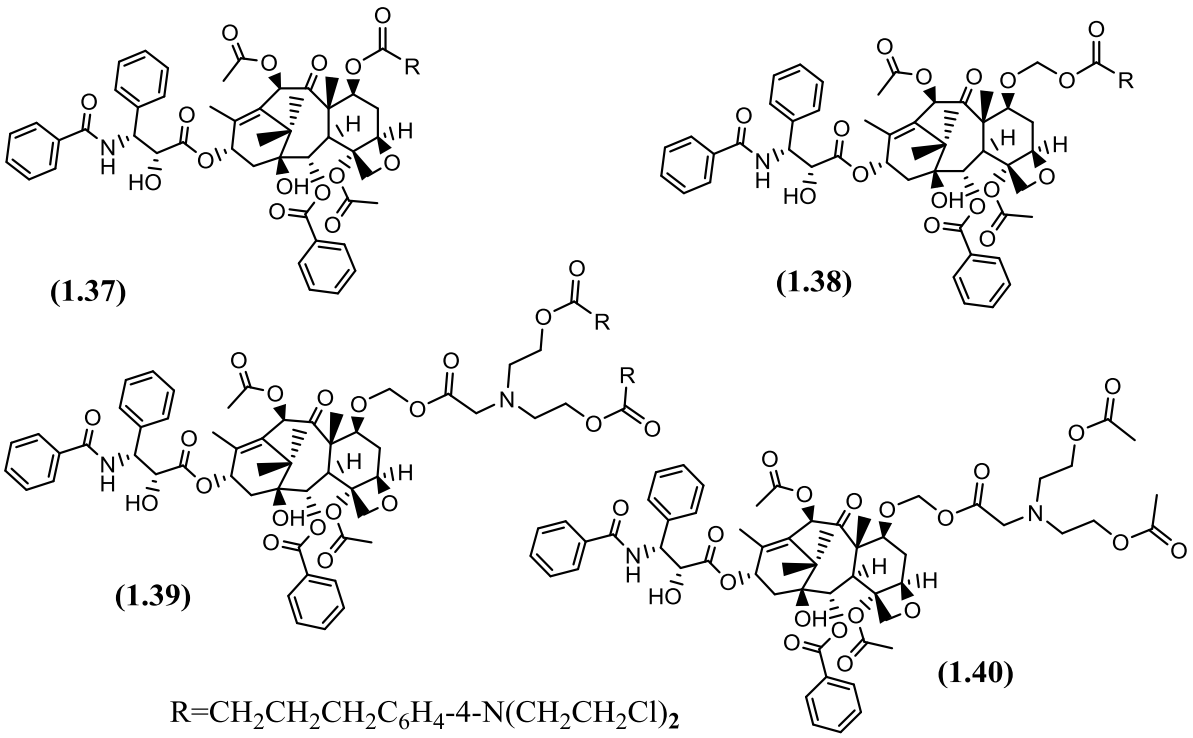

Figure 1.19. Paclitaxel-chlorambucil hybrids

1.4.2.3 Utilisation of homing peptides or monoclonal antibodies as part of the hybrid design

In order to produce the desired therapeutic effects without causing toxicity to the normal cells, an anticancer agent should not only be selectively delivered to the target site but it should also be translocated across the cell membrane. Hybrid drug strategy has also been employed for the targeted delivery of cytotoxic agents. The concept of using peptides, monoclonal antibodies and folic acid as a tumour homing device for an anticancer agent has already been utilized on many different anticancer candidates. Generally two types of peptides have been employed for the delivery of non-specific anticancer drugs to the target sites. Among them are the receptor targeted peptides and cell penetrating peptides (CPPs). As compared to receptor targeted peptides, the CPPs lack cell specificity that reduces the therapeutic effect of the drug attached to it and also enhances the toxic effects due to penetration of CPPs-drug conjugate to the normal tissues. The basic purpose of using peptides for the targeted delivery of anticancer drugs is to reduce the toxicity and multidrug resistance (MDR) associated with them [122-124].

J.W. Kim et al. synthesised a doxorubicin based hybrid utilizing an integrin binding RGD-4C motif for its targeted delivery to the tumour vasculature. Doxorubicin and RGD-4C peptide were linked through succinate bridge. The resultant dox-RGD-4C **(1.41)** conjugate (figure 1.20) demonstrated enhanced *in vivo* anti-tumor effects as compared to free doxorubicin in a mouse hepatoma model [125].

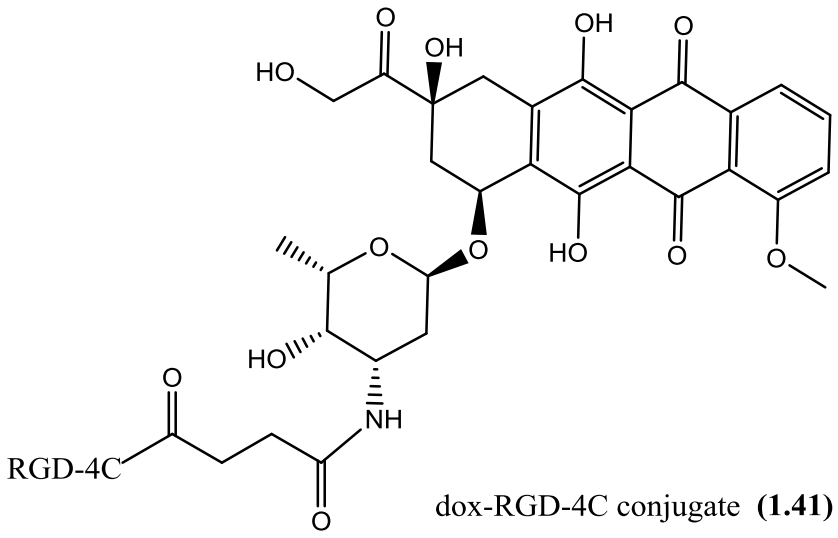

dox-RGD-4C conjugate **(1.41)**

Figure 1.20. Dox-RGD-4C conjugate for targeted delivery

The use of antibody for the selective delivery of cytotoxic agent to the tumour tissue is a growing area of interest. Many different antibody-drug conjugates (ADCs) have been developed, however only four of them have gained market approval. These are gemtuzumab ozogamicin (Mylotarg®), brentuximab vedotin (Adcetris®), trastuzumab emtansine (Kadcyla®) and inotuzumab ozogamicin (Besponsa®).

The successful design of an ADC mainly depends on three main components: the antibody, the cytotoxic payload and the chemistry of the linker unit connecting them [126]. Among the three components another critical factor to be considered while designing ADCs is the target antigen and an ideal target must have copious and uniform expression only on cancerous cells and remain low or absent in healthy cells. It must be accessible to intravascular macromolecules and upon binding of the antibody it should facilitate rapid internalization and trafficking to lysosomes [127].

The linker unit connecting the cytotoxic agent and the monoclonal antibody (mAb) must be stable in systemic circulation in order to avoid undesirable toxicity caused by pre-target release but should get cleaved upon reaching the target site to release the cytotoxic payload. Generally two types of linkers have been utilized in designing ADCs: cleavable linkers having sensitivity to enzymatic or hydrolytic cleavage within the endosomes and non

cleavable linkers that require proteolytic degradation of the antibody peptide in order to effectively release the drug within the lysosomes [128].

Monoclonal antibodies (MAbs) utilized in cancer therapy generally have poor cytotoxic effects but have better solubility so it can also be utilized to overcome the solubility issues associated with some cytotoxic agents [129]. Among more than 60 ADCs in clinical development, the majority (72%) utilize tubulin binding agents as cytotoxic drugs that are also included in two of the four currently approved ADCs [130]. Monoclonal antibodies and ADCs generally target the antigens over-expressed on cancerous cells, however, to a lesser extent they can also bind to the target antigens expressed on healthy cells. Tubulin binding agents serve as an excellent candidate for ADCs because of their low toxicity towards healthy cells [131]. The first marketed ADC was gemtuzumab ozogamicin (Mylotarg®) **(1.42)**, approved by the FDA for the treatment of patients with acute myelogenous leukemia. The ADC consists of an anti-CD33 antibody linked to *N*-acetyl calicheamicin through an acid labile hydrazone linker unit (figure 1.21). The major toxic effect associated with the gemtuzumab ozogamicin was myelosuppression including neutropenia and persistent thrombocytopenia. Other common side effects include fever, chills, rash, nausea and vomiting [132].

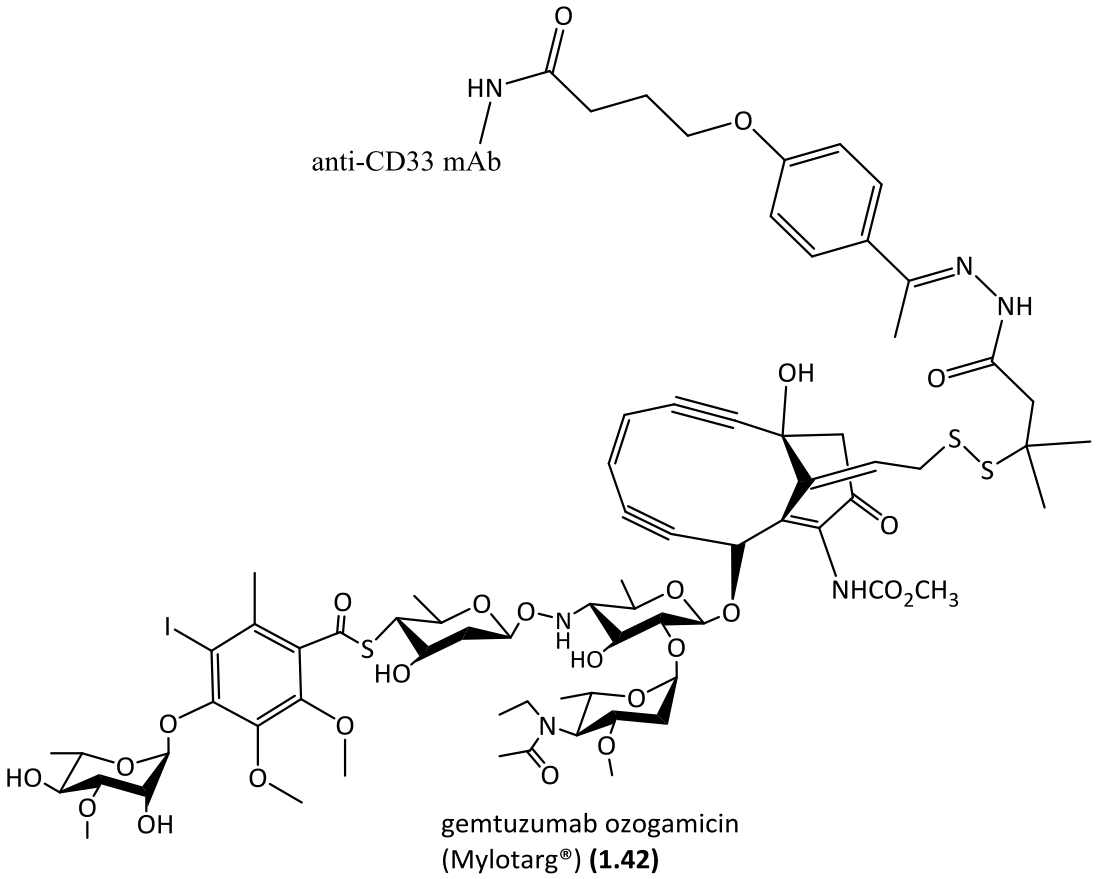

Figure 1.21. First marketed ADC, gemtuzumab ozogamicin (Mylotarg®)

The first ADC for the treatment of solid tumours was trastuzumab emtansine (T-DM1) (Kadcyla®) **(1.43)** that received its market approval by the FDA in 2013 for treating HER2-positive metastatic breast cancer. It consists of monoclonal antibody trastuzumab linked through SMCC, or succinimidyl *trans*-4-(maleimidylmethyl)cyclohexane-1-carboxylate linker unit to the sulfhydryl group of cytotoxic agent, emtansine (DM1) (figure 1.22). Trastuzumab inhibits the growth of cancerous cells by binding to human epidermal growth factor receptor 2 (HER2/neu receptor) while emtansine is a thiol containing derivative of maytansine, an agent that inhibits tubulin polymerization by binding at the rhizoxin binding site. The common adverse effects associated with T-DM1 include fatigue, nausea, thrombocytopenia, increased liver enzyme levels and mucoskeletal pain while hepatotoxicity, heart damage, interstitial lung disease and peripheral neuropath were the severe adverse effects identified during EMILIA trial [130, 133].

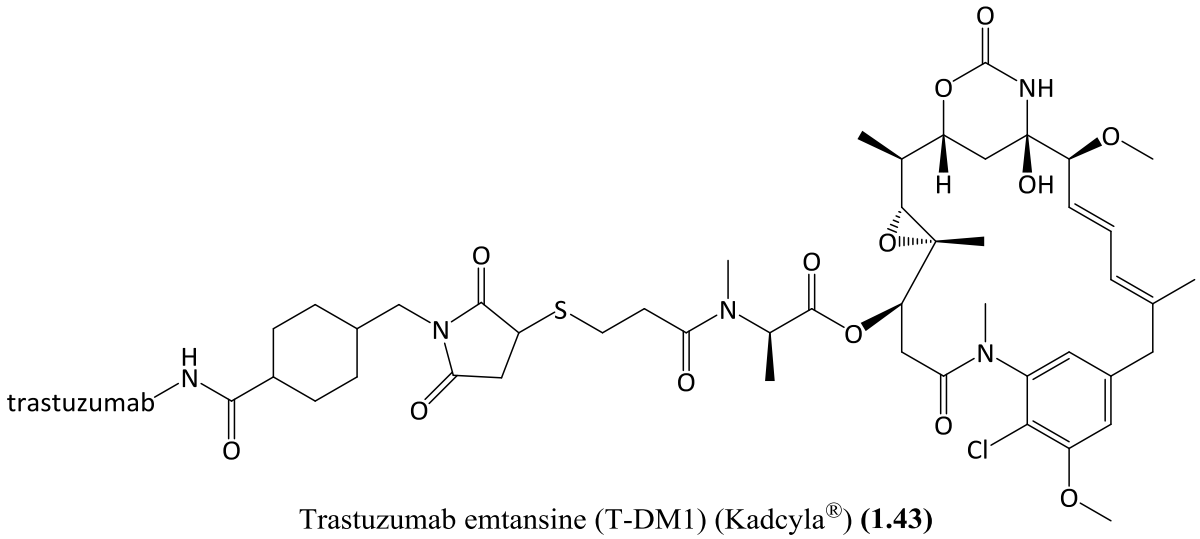

Trastuzumab emtansine (T-DM1) (Kadcyla®) **(1.43)**

Figure 1.22. Trastuzumab emtansine (T-DM1) (Kadcyla®) (1.43)

Our goal of targeted delivery is likewise to implant an active tubulin-based VDA onto a promising hybrid drug candidate having the ability to target Aminopeptidase N (APN). Our strategy was based on the fact that APN is highly expressed on endothelial cells of neoangiogenic but not on normal vasculature, that makes APN an excellent target in hybrid drug therapy [134]. Studies have shown that APN is an essential regulator of angiogenesis and is essential for capillary tube formation. Experimental studies have also demonstrated that treatment of animals with APN inhibitors significantly inhibited the retinal neovacularization, xenograft tumor growth and chorioallantoic membrane angiogenesis indicating APN as a critical regulator of angiogenesis [135]. Furthermore high expression

of APN has been found in a number of different cancers including human uterine cervical cancer [136], pancreatic carcinoma [137] and human colon cancer [138].

1.5 Aminopeptidase N

Aminopeptidase N (APN) also known as CD13 is a zinc dependent membrane-bound ectopeptidase that plays a critical role in angiogenesis and metastasis [139, 140]. The structure of APN is composed of 967 amino acids having a single transmembrane part, a large cellular ectodomain containing the active site and a short *N*-terminal cytoplasmic domain [141]. APN catalyzes the hydrolysis of the *N*-terminal peptide bond in peptides and proteins and has multiple functions, including invasion of tumour cells, proliferation and apoptosis, tumour cell motility, enzymatic regulation of peptides and act as viral receptor and antigen (figure 1.23) [142].

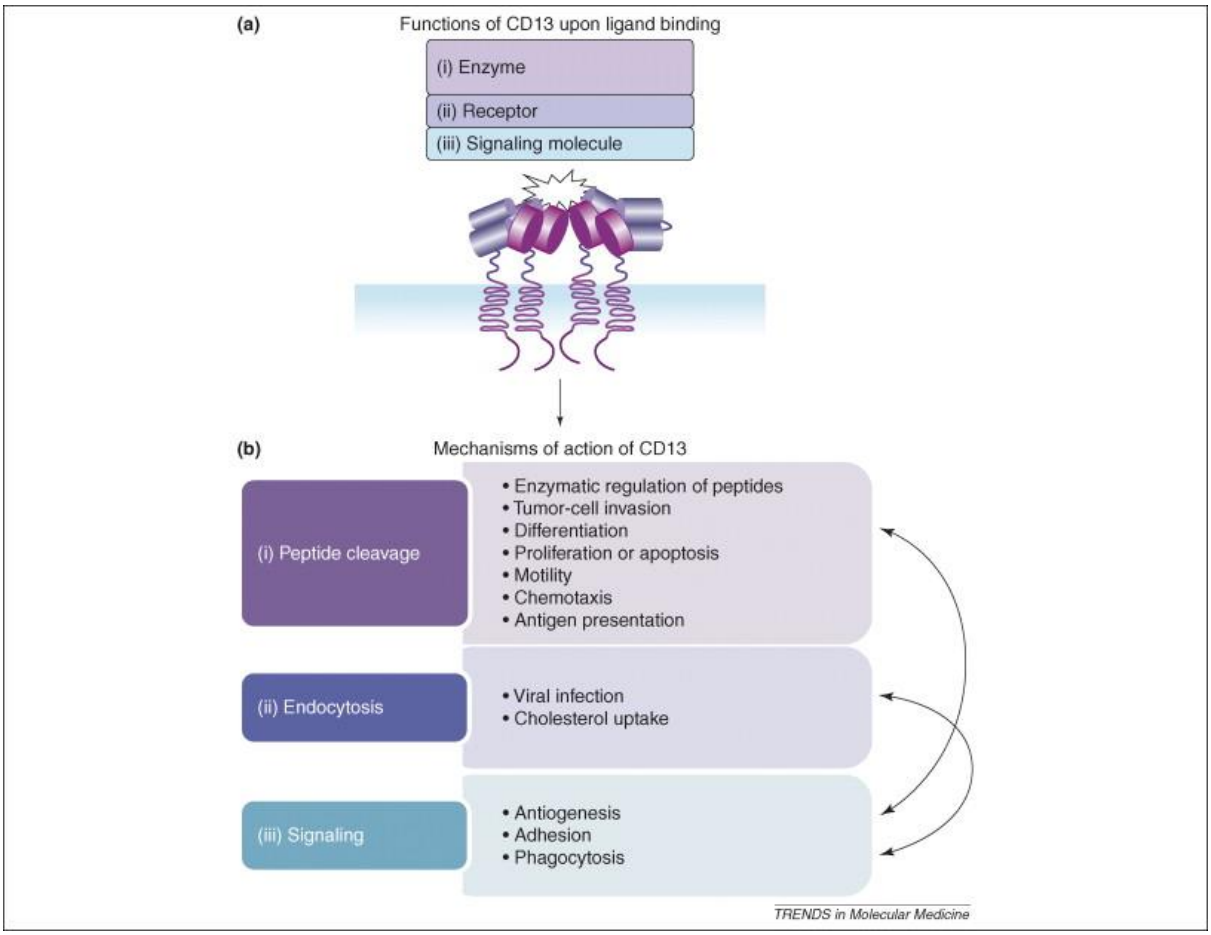

Figure 1.23. The functions and three mechanisms of action of human CD13. As shown in (a), upon ligand binding, CD13 functions: (i) as an enzyme, (ii) as a receptor and/or (iii) as a signaling molecule. Each of these functions depends on at least one of the mechanisms of action listed in (b), namely: (i) peptide cleavage, (ii) endocytosis and (iii) signal transduction. Each of these mechanisms result in the biological phenomena listed on the right side of part (b). Some complex phenomena, such as angiogenesis, invasion and chemotaxis, must occur as a result of the interplay between enzymatic activity and signalling functions. Similarly, upon virus or maybe even cholesterol and NGR-peptide binding (especially NGR-targeted liposomal drugs), the receptor functions could mediate signal transduction required for endocytosis.

The functional interplay between mechanisms of action is represented by the arrows on the right of part (b) [142].

APN is known to be expressed in a number of tissues and cells including renal tubule, breast, intestine, secretory epithelium of bronchial gland, colonal mucosa and synaptic membrane of the central nervous system [143]. Inhibition of APN in different types of cancers could be an effective approach for treatment as well as for the targeted delivery of drugs [144]. Several classes of APN inhibitors have been investigated including sulphonic, boronic and hydroxamic acid peptide analogues [134]. Hydroxamic acid and its derivative have been employed as APN inhibitors in treatment of different types of cancers [145, 146]. Other important APN inhibitors include the first marketed anti-APN drug bestatin **(1.44)** [147], valistatin **(1.45)** and 3-amino-2-hydroxy-4-phenylbutanoylvalylisoleucine **(1.46)** (figure 1.24) [148]. Being the most studied APN inhibitor, bestatin has shown a remarkable cytotoxity and inhibits the growth of leukemic cell lines [149]. It has also shown an increase in survival rate of patients with resected stage I squamous-cell lung carcinoma [150].

R Nishizawa and co workers extensively studied the structure activity relationship of different analogues of bestatin and showed the presence of free amino and carboxyl group to be crucial for APN binding. Furthermore they have demonstrated that the *S* configuration at C2 is crucial for activity while the configuration at C3 isn't absolutely necessary. The presence of leucine residue is also important for activity because the (2*S*,3*R*)-3-Amino-2-hydroxy-4-phenylbutyric acid (AHPA) on its own shows very weak activity. Replacing the leucine of bestatin with amino acids having amino group α to carboxylic acid enhances the activity that indicates the proximity of the amino and carboxylic group of the amino acids has important role and the presence of amino group α to the carboxylic group is crucial for strongest activity, e.g. L-Ile, L-Met, L-Ala and L-Nle. The benzyl group of the bestatin was also substituted with different substituents in order to analyse its effects on enzyme inhibition. It was demonstrated that replacing the benzyl group with hydrogen and aliphatic groups reduces the activity while the maximum activity was observed when the benzyl group of bestatin was replaced with *p*-nitrobenzyl, *p*-chlorobenzyl or *p*-methylbenzyl groups [151].

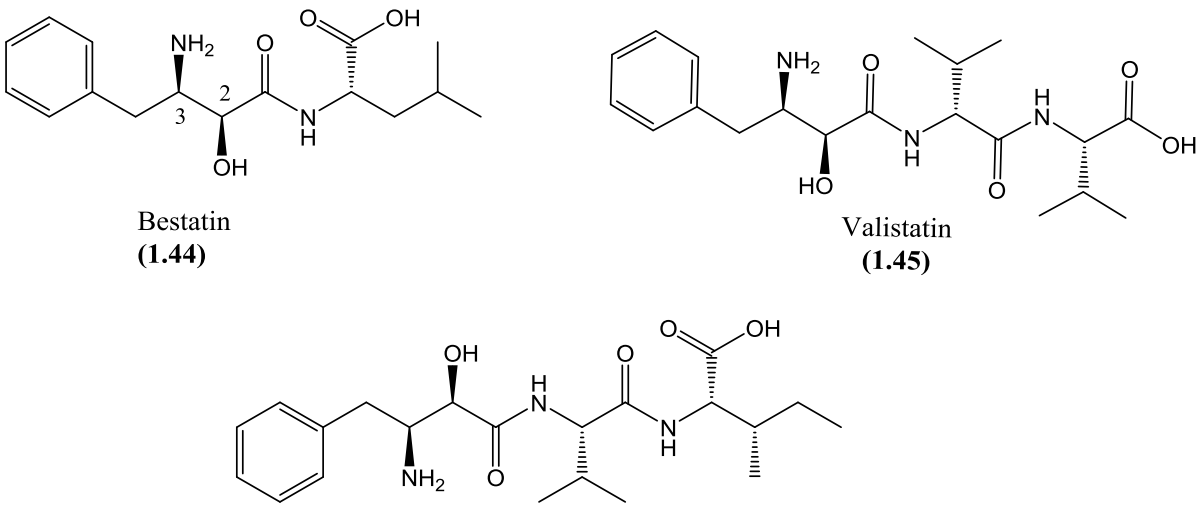

Figure 1.24. Structures of APN inhibitors

1.6 Background and aims of project

The initial research presented in this project followed the work carried out by our former colleagues Hudson and Coogan. Together they synthesised a novel library of 4-phenylcoumarins with promising activity as tubulin polymerization inhibitors. The first 4-phenylcoumarin compound in this series was **GJH140**, synthesised by Hudson [152]. Later on several analogues of 4-phenylcoumarin were also synthesised by Coogan namely **ADR149, ADR084, ADR118** and **ADR116** (figure 1.25) [153]. Common to all these compounds is the trimethoxy substituted aryl ring (A ring), a six membered aliphatic ring (B-ring) and a monomethoxy substituted aryl ring (C ring). The most potent compound in this series was **ADR149** with IC_{50} values of 1.45 ± 1.15 nM against human umbilical vein endothelial cells (HUVECs) and 3.82 ± 1.15 nM against PC-3 cells. Another compound of this series **GJH140** has also shown comparable activity to CA-4 with IC_{50} values of 5.56 ± 1.36 nM against HUVECs and 4.70 ± 1.19 nM against PC-3 cells.

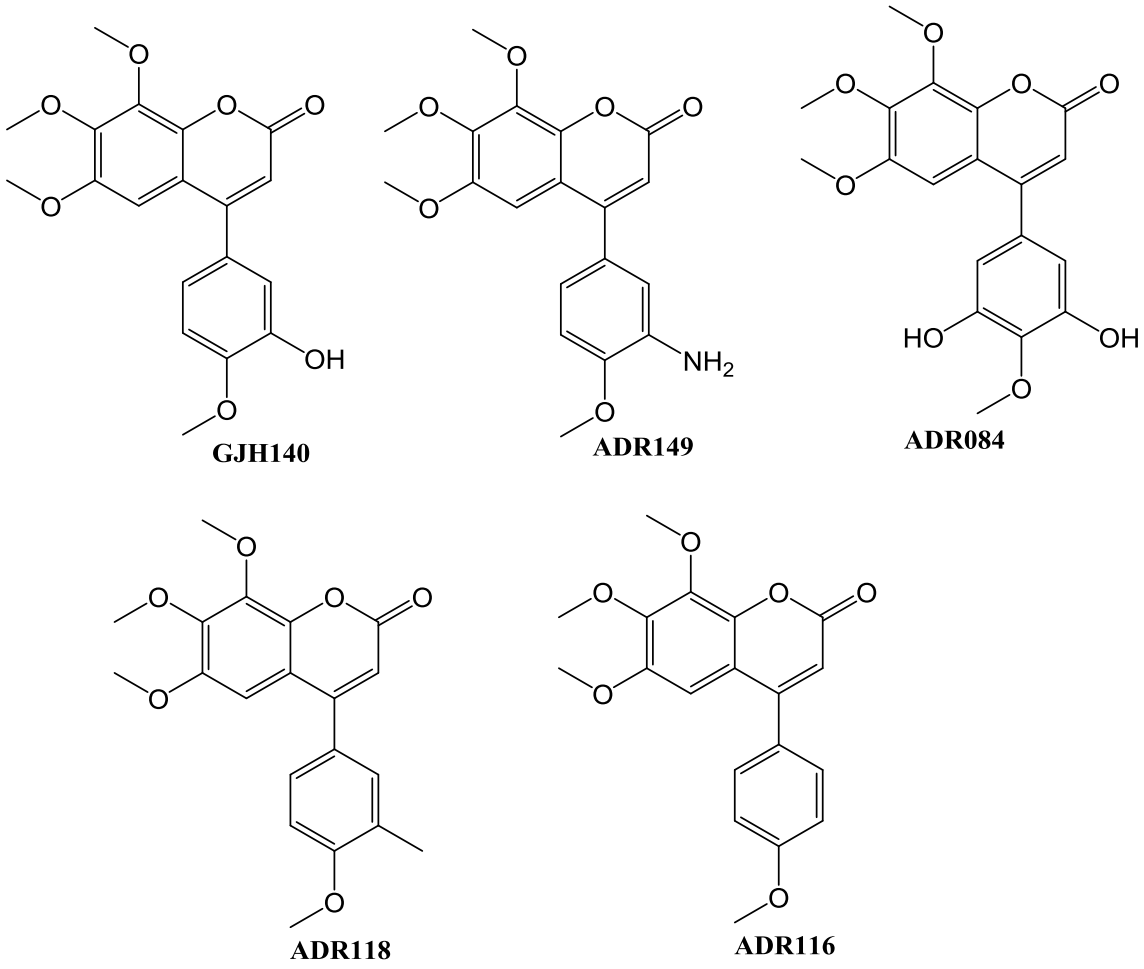

Figure 1.25. Chemical structures of 4-phenylcoumrins

Along with coumarins another library of novel tubulin binding agents has been synthesised by the former PhD students, namely R. Shah, E. McCormack, G Hudson, M White and A Coogan. Common to all these compounds is a trimethoxy substituted A-ring, a seven membered aliphatic B-ring and a monomethoxy substituted aryl C-ring. These compounds have shown comparable biological activity to coumarins. The only disadvantage with these 7-membered ring compounds is their longer synthetic route as compared to coumarins. Among the 7-membered benzoxepinone compounds the most active up to date were **ADR269** and **ADR393**. Another strategy employed by the former colleague Coogan involved the incorporation of hydroxamic acid functionality onto B-ring ketone of 7-membered benzoxepinone compounds to create designed multiple ligands (DMLs). Among the DMLs the most active was **ADR4.26** (IC_{50} = 4.476 ± 1.31 µM), over 7 fold more potent than bestatin (32.55 ± 1.40 µM) in the APN assay while its aniline analogue **ADR4.30** (IC_{50} 33.56 ± 1.22 µM) showed comparable activity to bestatin (figure 1.26).

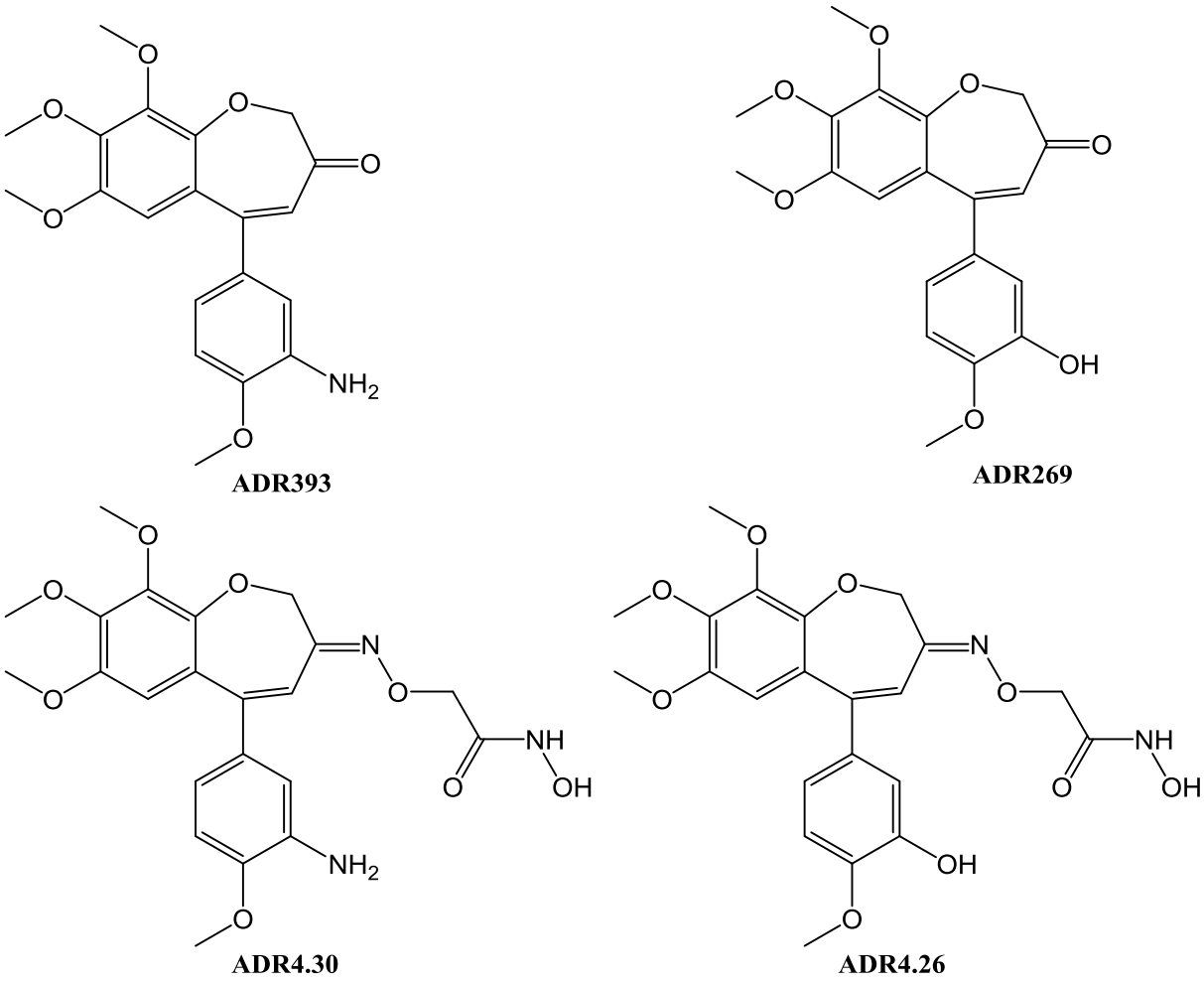

Figure 1.26. Chemical structures of 7-membered ring compounds

Previous attempts to synthesise hydroxamic acid based DMLs of 4-arylcoumarins ended in failure. Despite many attempts to incorporate the hydroxamic acid functionality onto B-ring carbonyl group of 4-arylcoumarins, no success was achieved. The most probable reason was the low polarity of carbonyl group (C=O) towards attack by a range of amine based nucleophiles.

The objectives of our research project were to:

- Scale up the synthesis of 4-arylcoumarins **(ADR084)** and (**ADR149)** employing a new synthetic strategy.
- Explore the effects of different substituents at C2 of 4-arylcoumarins on inhibition of tubulin polymerization.
- Incorporate the hydroxamic functionality onto compounds **ADR084** and **ADR149** to create hydroxamic acid based design multiple ligands and to evaluate theses as APN and tubulin polymerization inhibitors.

- Synthesise bestatin based hybrids of the compounds **ADR084** and **ADR149.**
- Synthesise 4-arylcoumarins having dimethoxy substituted A ring and to evaluate them as tubulin polymerization inhibitors.
- Synthesise dual acting hybrids based on 4-arylcoumarins.
- Synthesise different derivatives of 4-arylcoumarins with reference to C3 and to investigate the effect of different substituents on the tubulin binding activity.
- Synthesise different phenstatin analogues and to assess their activity as tubulin polymerization inhibitors.
- To incorporate the phenstatin based compound into hybrids with the ability to target APN.
- To generate controlled release hybrids by incorporating both a substrate and inhibitor of APN into a potent tubulin binding agent.

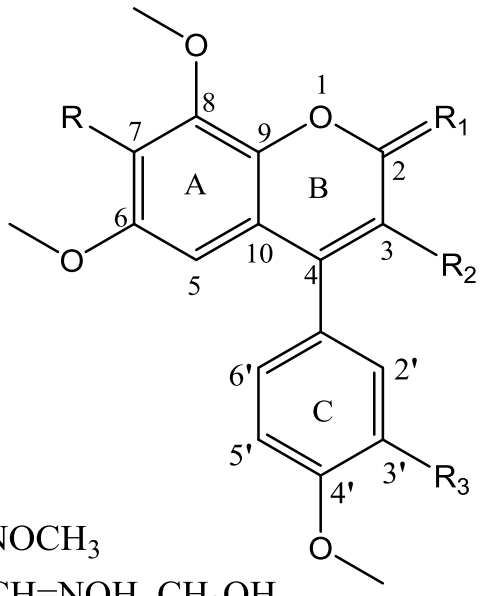

R= OH or OCH_3

R_1 = O, S, NOH, $NOCH_3$

R_2=COOH, CHO,CH=NOH, CH_2OH

R_3= OH or NH_2

Figure 1.27. General structure of 4-phenylcoumarin compounds

1.7 Hybrid drugs design

Hybrid drug therapy is a growing area of intrest, particularly in the field of cancer. The aim of the hybrid drug approach in cancer therapy is either to incorporate two drugs into one molecule in such away to produce a synergistic response or in another scenario one drug to act as a tumor homing device for the selctive delivery of the cytotoxic agent. A series of

novel tubulin binding agents (TBAs) have been synthesised by our lab group that demonstrated potent *in vitro* tubulin polymerisation inhibition however their has been generally a disadvantage of undesirable toxicity and lack of selectivity associated with these agents. In order to produce the desired cytotoxic effects without causing toxicity to the healthy cells an ideal anticancer agent should be selective in its targetting abilities. For the targetted delivery of cytotoxic agents to the tumor tissue various different concepts have been utilised involving the use of peptides, monoclonal antibodies and folic acid. Our concept of targetted therapy is mainly based on the fact that APN is selectively expressed on neoangiogenic but not on normal blood vessels so its serves as an excellent target for the selective delivery of cytotoxic agents. Bestatin and hydroxamic acids have been evaluated as APN inhibitors in various different cancers including lung carcinoma, hepatocellular carcinoma and leukemic cancer cell lines [145, 149, 150]. The aim of our hybrid drug design is to incorporate our promising tubulin binding agents onto an APN targetting motif (bestatin or hydroxamic acids), that will serve as means to deliver them selectively to the target tissue (figure 1.27). The phenolic functional group present on our TBAs could be utilised for the attachment targetting peptide and will form an ester linkage to the peptide and would most likely be cleaved by hydrolysis at physiological pH or through esterase enzymes present in blood.

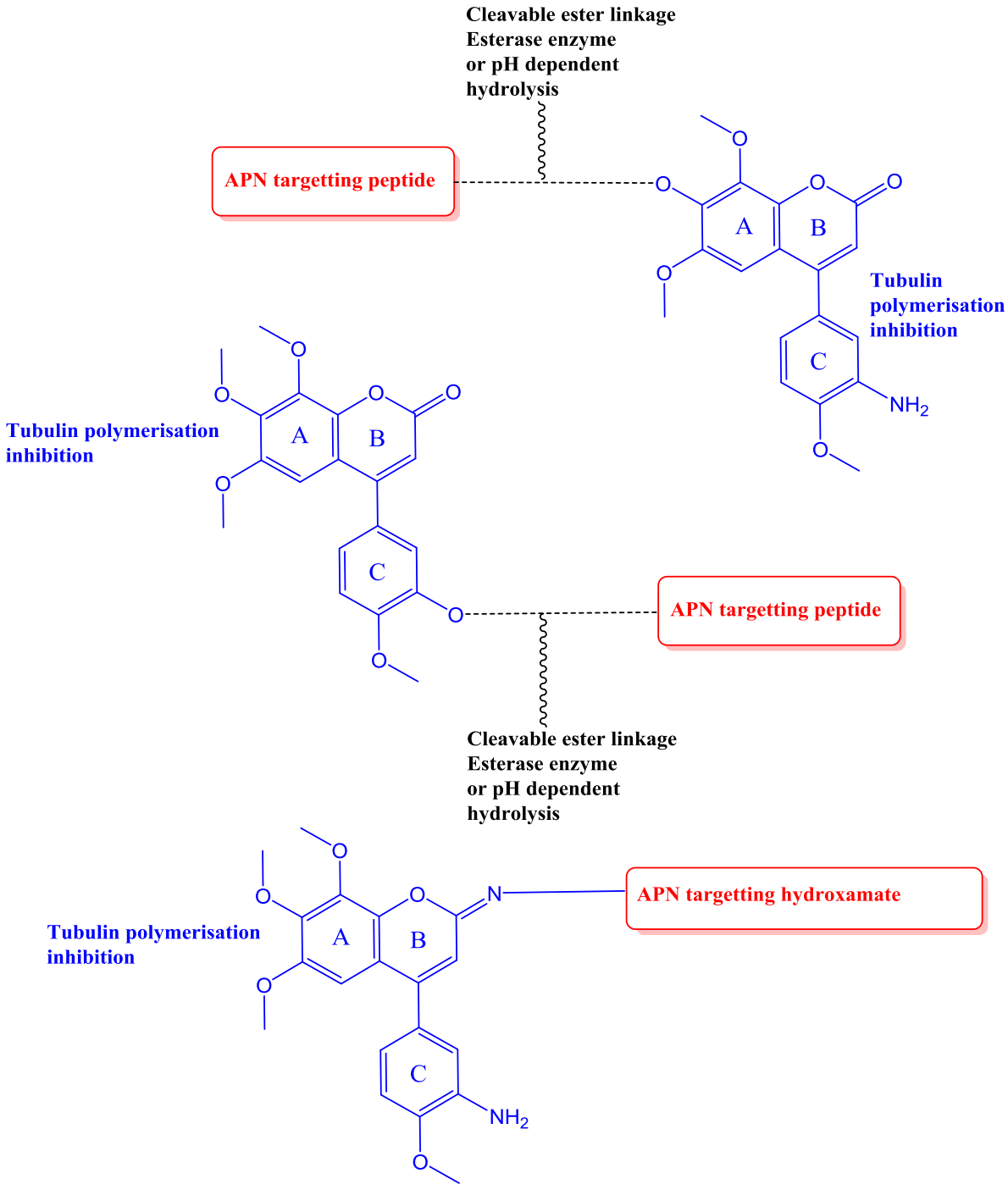

Figure 1.28. Design of peptides and hydroxamic acid based simple hybrid drugs

Along with the synthesis of simple hybrids, it has been hypothesised that by having an amino acid substrate at the aniline functionality of the C-ring would present the tubulin binding component in its prodrug form. Once the drug is delivered to the tumor vasculature, the amino acid residue at the C-ring will be cleaved off due to the high expression of APN, as it is known to catalyse the removal of neutral amino acids from N

terminal of peptides thereby releasing the drug back in to its active form (figure 1.28) [142].

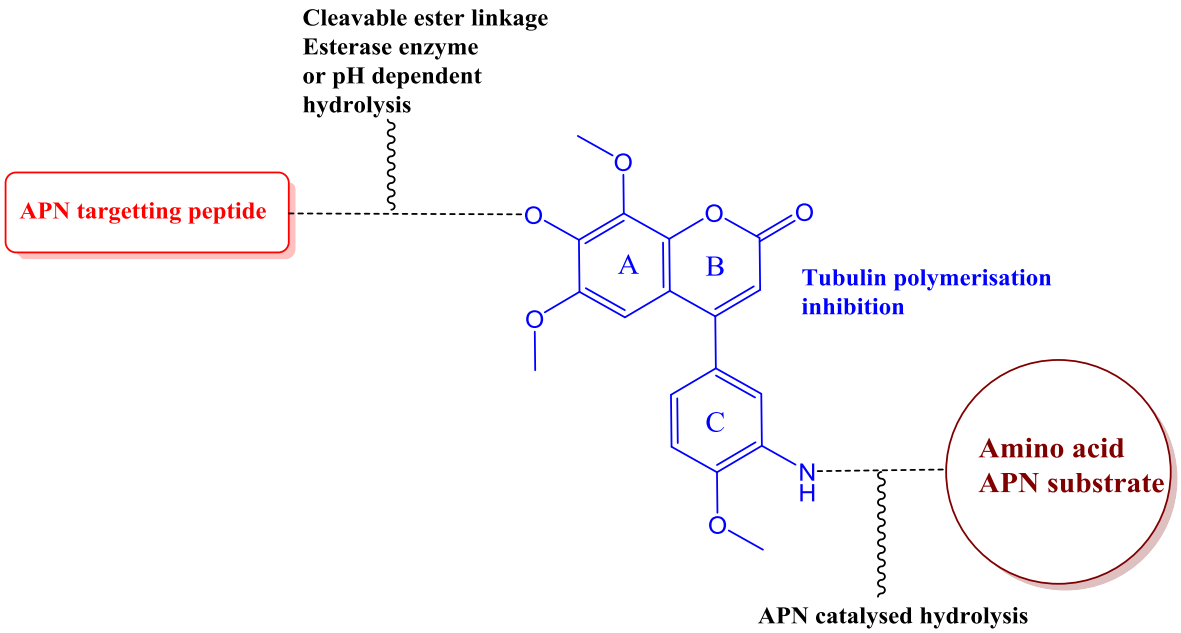

Figure 1.29. Control release hybrid drug design

Chapter 2
Synthesis of 4-arylcoumarin derivatives

2.0 Introduction

The main objective of the work described in this chapter was to synthesise a series of potent tubulin inhibitors with additional linkers for the attachment of APN targeting moieties. A series of novel 4-phenylcoumarin compounds has been already synthesised and evaluated as tubulin polymerisation inhibitors by the former research students of this lab, including Hudson and Coogan. The compound shared structural resemblance to colchicine and combretastatin A-4 by having two aryl rings (A and C) connected in a non-coplanar arrangement through an aliphatic B-ring. These compounds demonstrated potent inhibition of tubulin polymerisation and the most active among them were **GJH140**, having a phenolic and **ADR149**, having an aniline functionality at C-ring (figure 2.0).

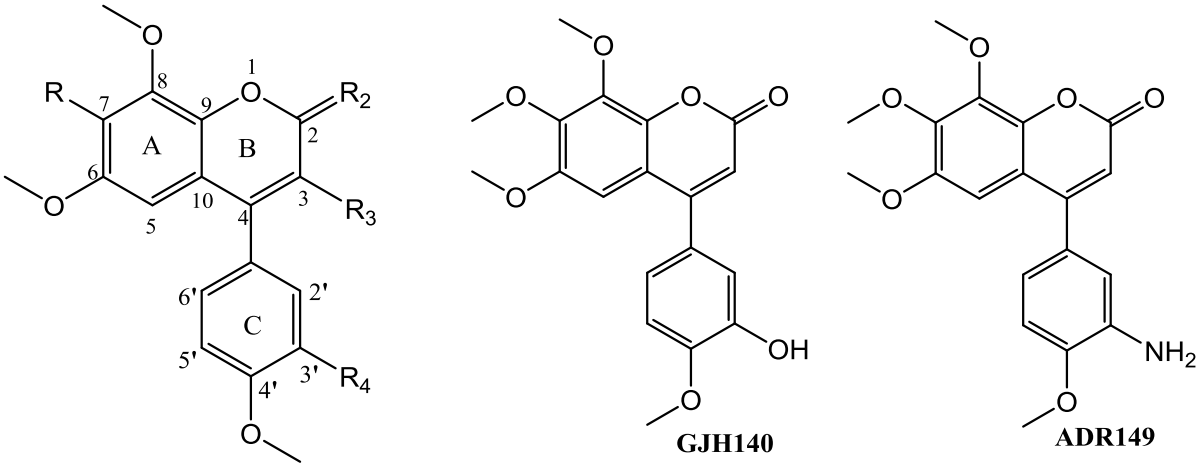

General structure of our desired 4-phenylcoumarins

R= OH, OCH_3, OBn, O-prenyl

R_2 = O, S, NOH, $NOCH_3$

R_3=COOH, CHO,CH=NOH, CH_2OH

R_4= OH or NH_2

Figure. 2.0. General structure of 4-phenylcoumarins along with GJH140 and ADR149

2.1 Synthesis of 4-hydroxycoumarin AB-ring

The initial objective of our project was the synthesis of the target compound 4-hydroxy-6,7,8-trimethoxychromen-2-one **(2.04)** in sufficient quantity for further modification. For the synthesis of this compound initially the shorter synthetic route established by a former colleague A. Coogan was utilised. To ensure the presence of 2,3,4-trimethoxy configuration on the A-ring, the commercially available starting material of the same structural

arrangement i.e. 2,3,4-trimethoxybenzaldehyde was used. The first step of our synthesis involved the oxidation of 2,3,4-trimethoxybenzaldehyde to phenol **(2.01)**. For this purpose we employed Dakin oxidation, which uses hydrogen peroxide and concentrated sulphuric acid in methanol to successfully produce the phenol in one pot with 82% yield (Scheme 2.1). The key approach to obtain this product in high yield was continuous and proper mixing of the reaction contents as the addition of reagents proceeded. The structural identity of the phenol **(2.01)** was confirmed by the ^{1}H NMR spectrum (figure 2.1) that shows the presence of phenolic OH resonating as broad singlet at 5.43 ppm. Moreover the presence of 2 *ortho* coupling protons and the expected 3 methoxy groups were also evident in the spectrum.

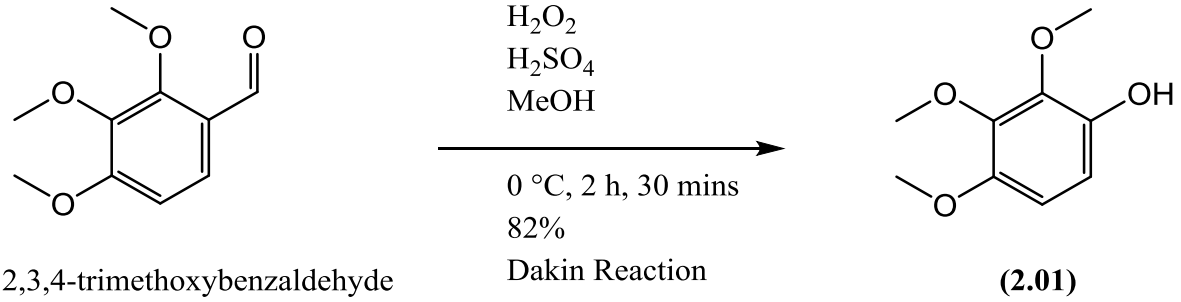

2,3,4-trimethoxybenzaldehyde **(2.01)**

Scheme 2.1. Oxidation of benzaldehyde to phenol **(2.01)** by employing Dakin reaction

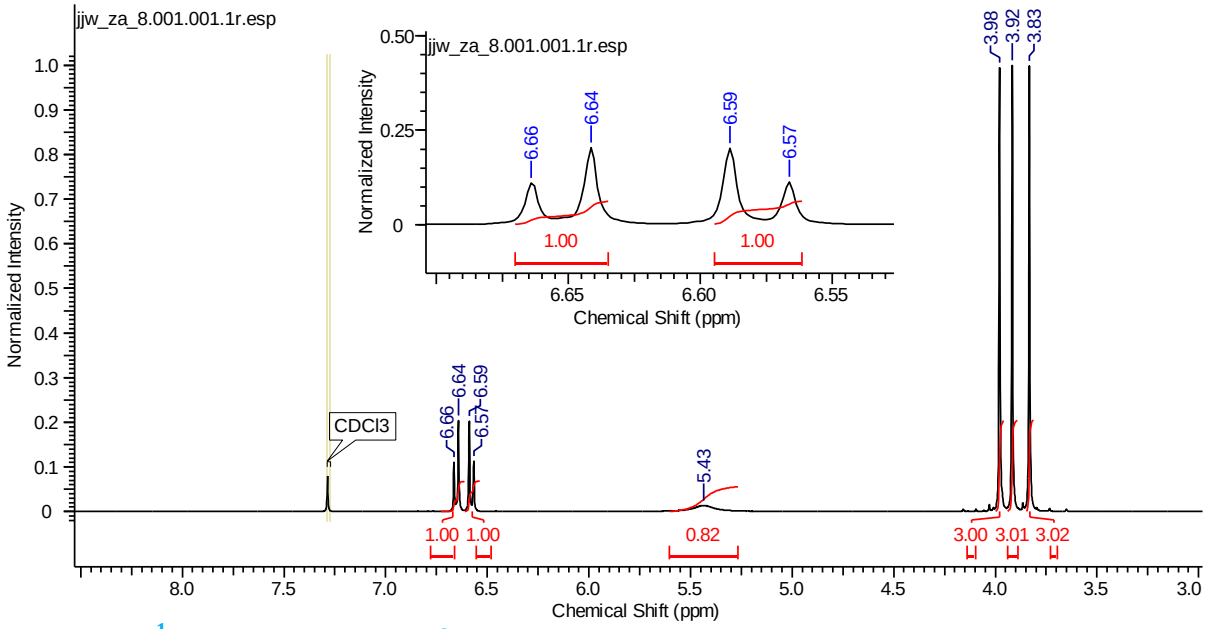

Figure 2.1. ^{1}H NMR spectrum of phenol (2.01)

In the next step, the phenol **(2.01)** was *O*-acetylated by refluxing with acetic anhydride and sodium acetate for 4 hours. Upon completion of the reaction an aqueous work-up was

performed to afford the acetate ester **(2.02)** with a yield of 78% (Scheme 2.2). The structural identity of the compound was confirmed by the presence of methyl group of the ester at 2.33 ppm, in the ^{1}H NMR spectrum (figure 2.2).

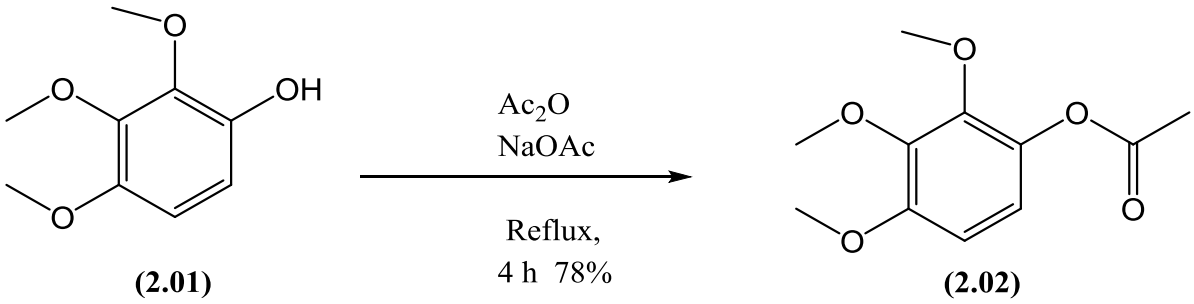

Scheme 2.2. Acetylation of phenol **(2.01)** to give ester **(2.02)**

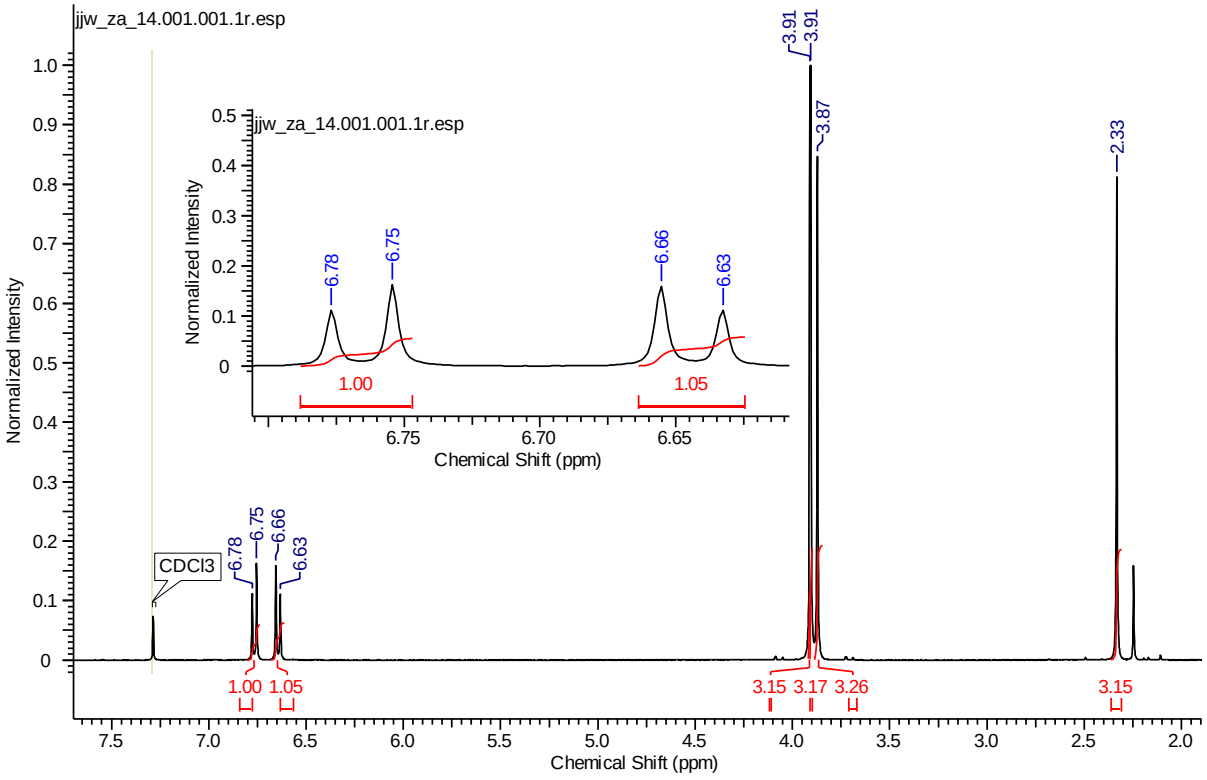

Figure 2.2. ^{1}H NMR spectrum of Ester (2.02)

Migration of the acetyl group to the *ortho*-position was achieved under Fries rearrangement conditions to give keto-phenol **(2.03).** Acetyl migration favours *ortho* position at high temperature while the *para* position is favoured at room temperature. The exact mechanism

of Fries rearrangement has to be determined yet but the proposed mechanism involved the co-ordination of Lewis acid boron trifluoride to the carbonyl oxygen of the acyl group to form a polarised complex (BF_3^----O^+), that causes the rearrangement of BF_3 onto the phenolic oxygen atom. This generates a highly reactive acylium carbocation which reacts in a classical electrophilic aromatic substitution with the aromatic ring at *ortho*/*para* position but as in our case only *ortho* position is available so exclusive *ortho* acetylation occurred (Scheme 2.3). Basic work-up using aqueous sodium hydroxide (2.5 M) hydrolyses the boron complex and neutralises any hydrofluoric acid generated from the loss of aromatic proton. The loss of one aryl proton was evident in the ^1H NMR spectrum (figure 2.3) that confirmed the migration of acetyl group to the *ortho* position. Furthermore, the remaining one aryl proton was now a singlet as expected.

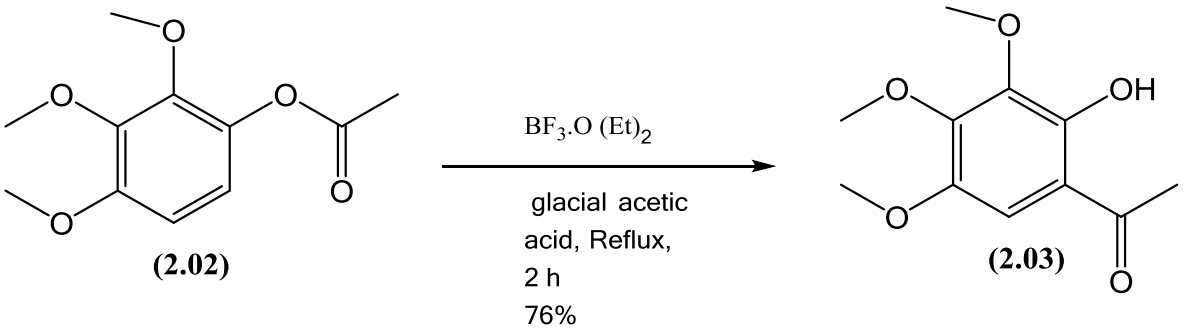

Scheme 2.3. Fries rearrangement of ester **(2.02)** to Keto phenol **(2.03)**

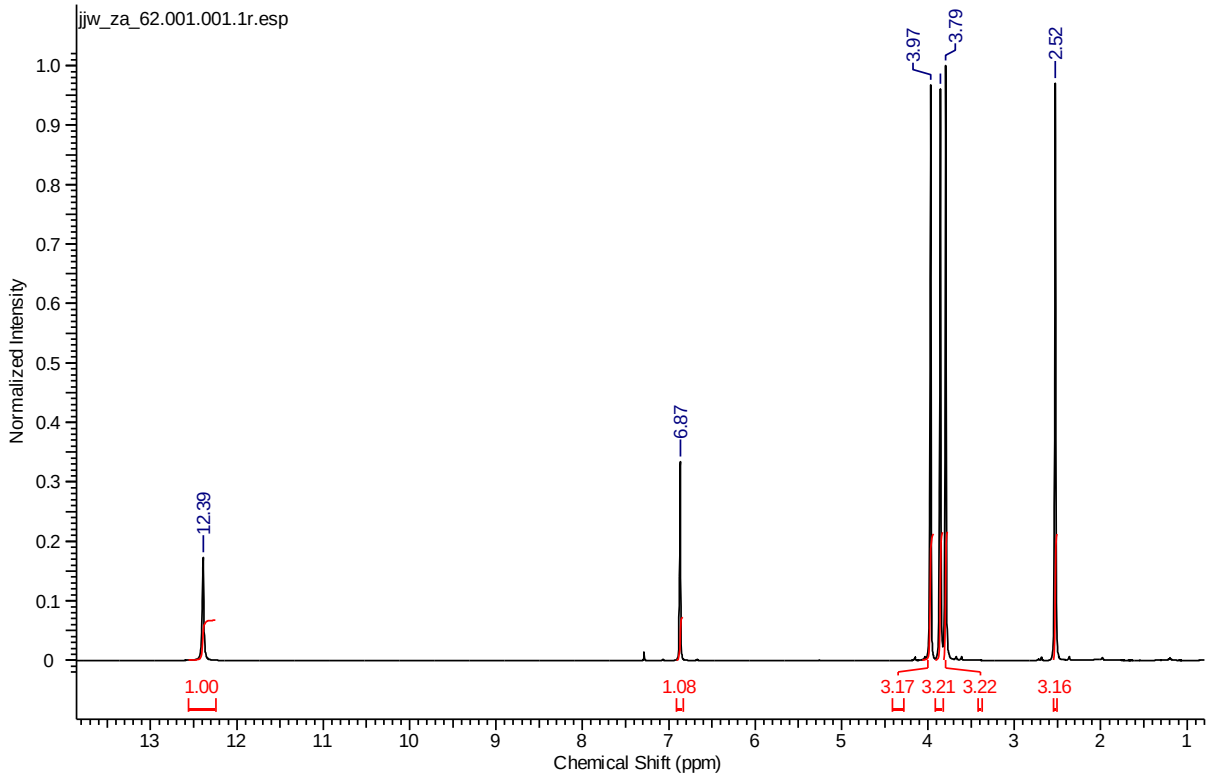

Figure 2.3. ^{1}H NMR spectrum of keto phenol (2.03)

The keto-phenol then underwent Claisen condensation with diethyl carbonate to give the desired coumarin (**2.04**) (Scheme 2.4). The compound was highly insoluble and so was purified by just washing with diethyl ether and the NMR spectra were obtained in deuterated dimethyl sulfoxide. Structural identity of (**2.04**) was confirmed by ^{1}H NMR spectrum (figure 2.4) and mass spectroscopy. A cursory inspection of the ^{1}H NMR spectrum indicated the presence of alkene proton (5.5 ppm) as well as hydroxy proton (12.56 ppm) and the HRMS found the de-protonated mass of 251.0571 ($M\text{-}H^{+}$).

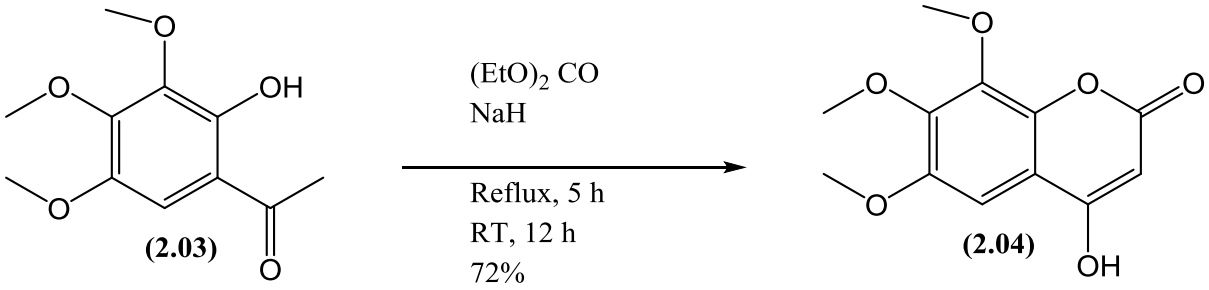

Scheme 2.4. Formation of 4-hydroxycoumarin **(2.04)**

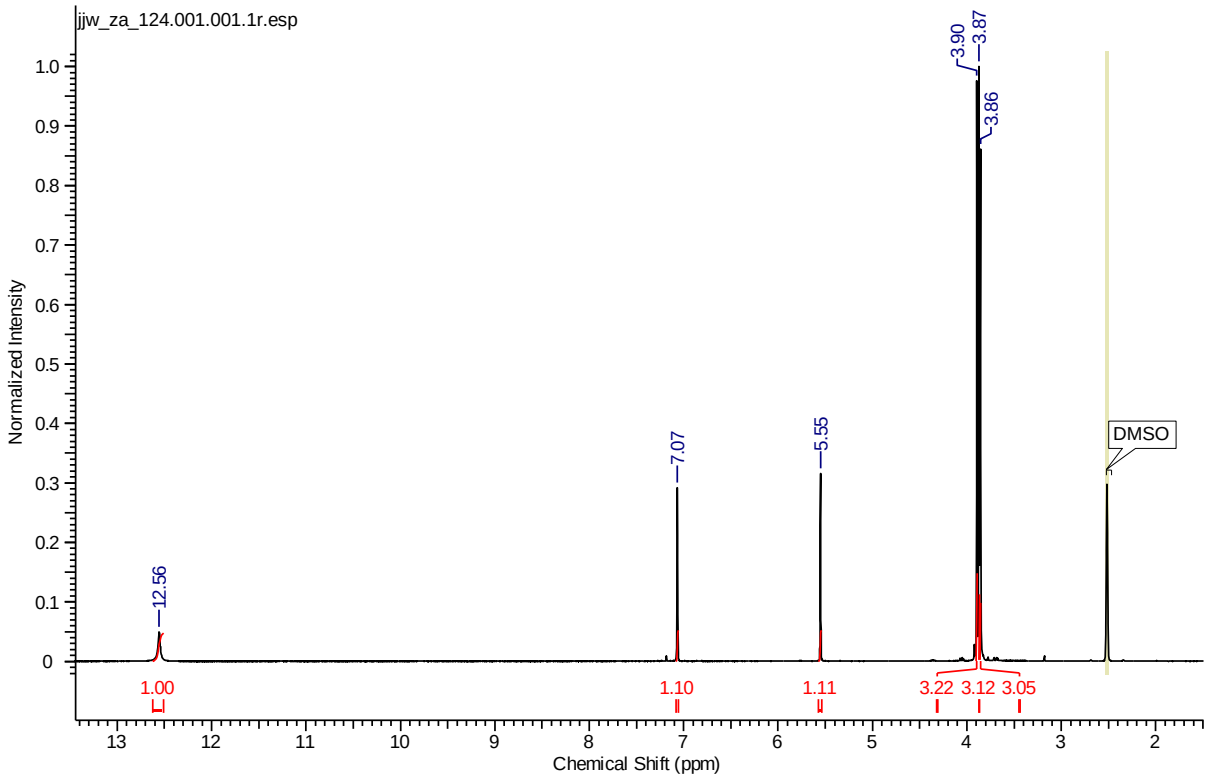

Figure 2.4. ^{1}H NMR spectrum of 4-hydroxycoumarin (2.04)

In order to couple the C-ring onto 4-hydroxycoumarin (**2.04**), it was first converted into its triflate derivative which is a suitable substrate for Suzuki coupling using triflic anhydride, triethylamine as base in anhydrous DCM (Scheme 2.5). The HRMS found the protonated molecular ion of mass 385.0198 ($M + H^{+}$).

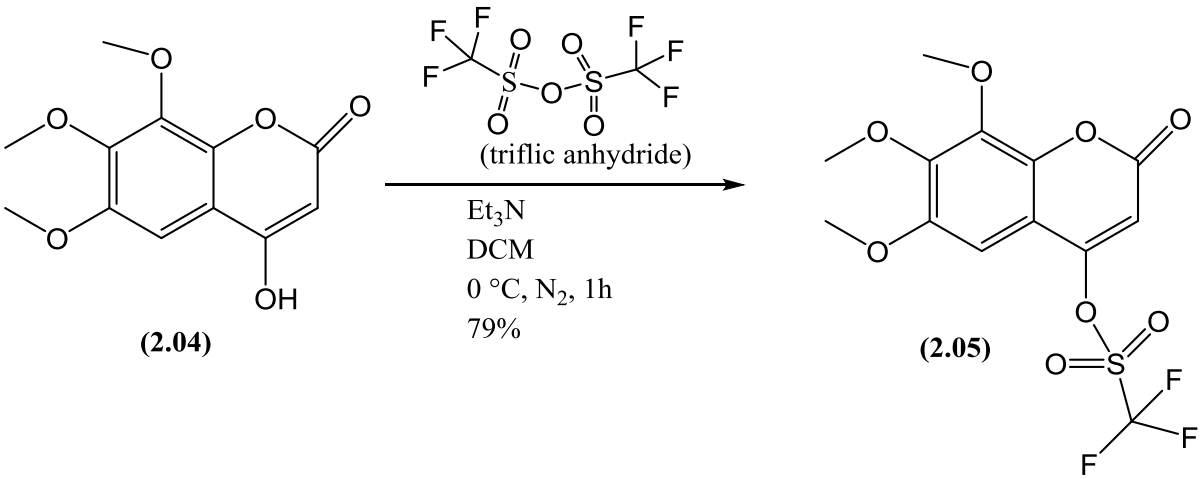

Scheme 2.5. Triflation of 4-hydroxycoumarin **(2.04)** with triflic anhydride

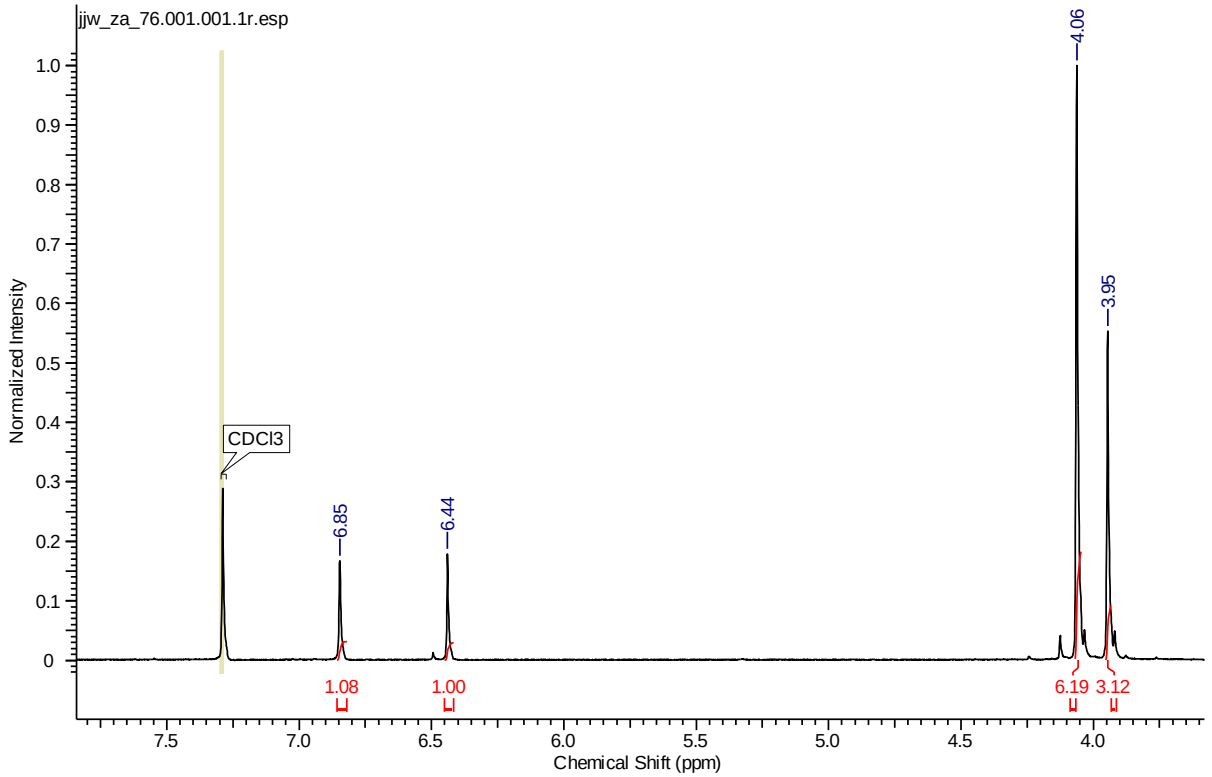

Figure 2.5. ^{1}H NMR spectrum of triflate (2.05)

2.2 Alternate synthetic route for synthesis of coumarin backbone (2.04)

In the later stages of our research we found another effective synthetic route for the synthesis of coumarin **(2.04)**. Likewise to our previous synthetic route, the starting point was again 2,3,4-trimethoxybenzaldehyde. In the first step 2,3,4-trimethoxybenzaldehyde underwent Dakin oxidation to phenol **(2.01),** followed by treatment with meldrum's acid to give acid **(2.06)** (Scheme 2.6). The identity of the meldrum's acid coupled product was confirmed by the inspection of its ^{1}H NMR spectrum (figure 2.6) where the presence of the methylene protons was evident at 3.66 ppm.

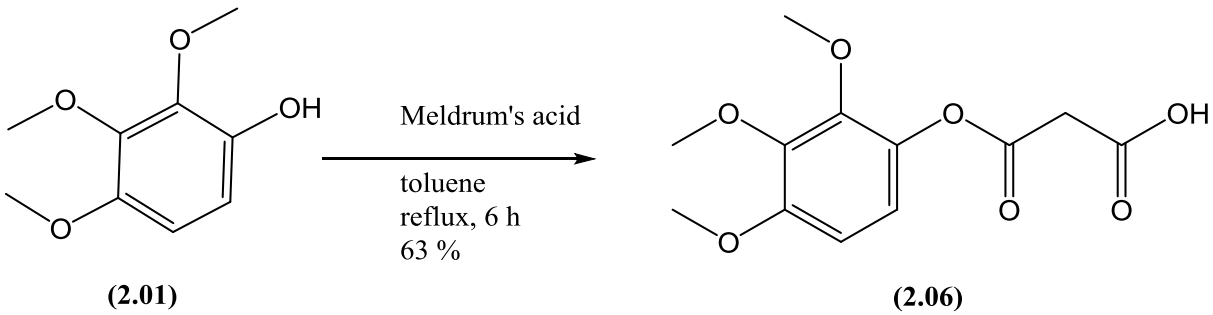

(2.01) **(2.06)**

Scheme 2.6. Synthesis of 3-oxo-3-(2,3,4-trimethoxyphenoxy)propanoic acid **(2.06)**

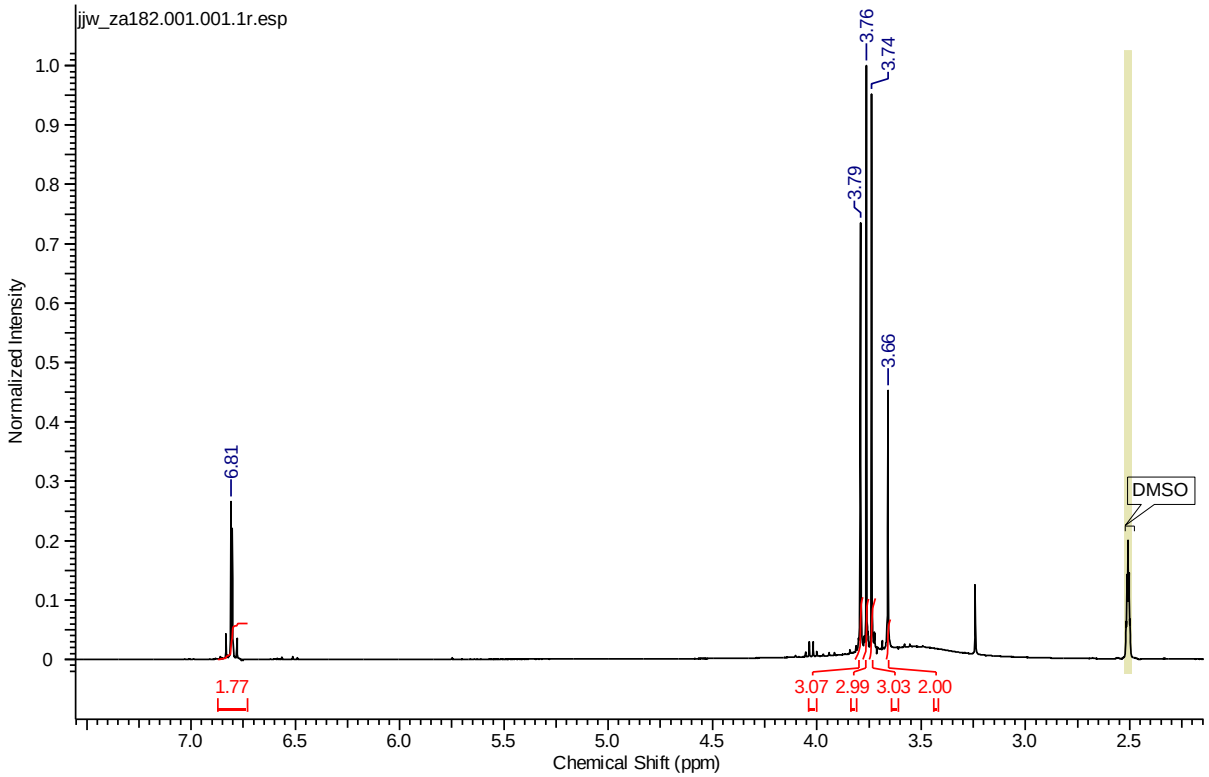

Figure 2.6. ^{1}H NMR spectrum of Acid (2.06)

The resultant acid was then cyclised using Eaton's reagent to give 4- hydroxy coumarin **(2.04)** (scheme 2.7).

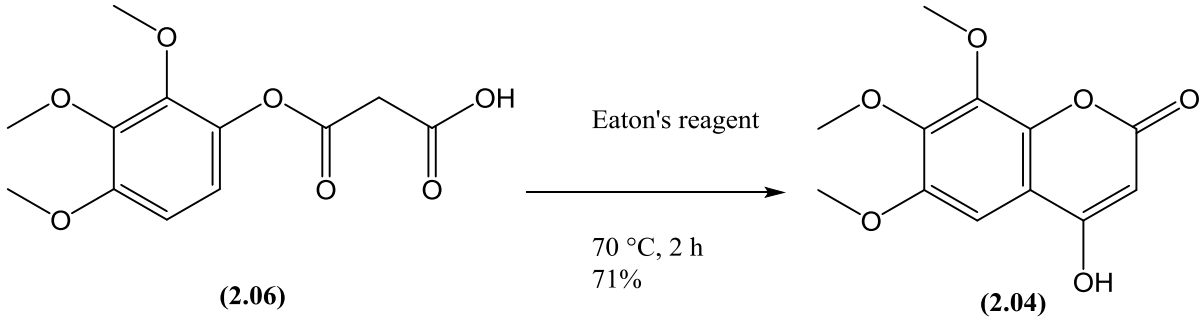

Scheme 2.7. Cyclization of Acid **(2.06)**

2.3 Synthesis of C-ring analogues

2.3.1 Synthesis of Phenolic C-ring analogue

Both the phenolic and aniline C-rings were synthesized separately. For the phenolic C-ring (**2.10**), commercially available 5-bromo-2-methoxybenzaldehyde was used as starting material. In the first step, 5-bromo-2-methoxybenzaldehyde was subjected to Baeyer-Villiger oxidation to afford the formate ester (**2.07**), which was then hydrolysed using 2.5 M aqueous NaOH to the corresponding phenol (**2.08**) (Scheme 2.8).

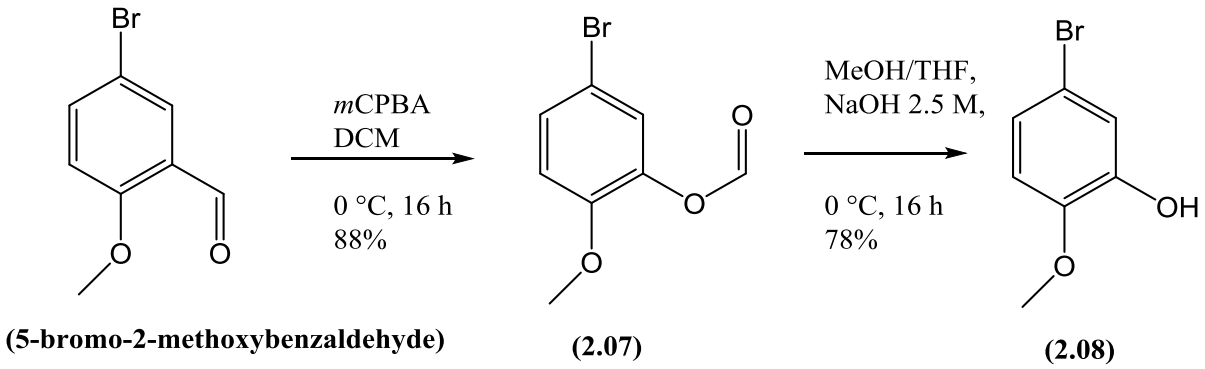

(5-bromo-2-methoxybenzaldehyde) **(2.07)** **(2.08)**

Scheme 2.8. Baeyer-Villiger oxidation of benzaldehyde and subsequent hydrolysis

Silyl protection of phenol (**2.08**) was carried out at room temperature using *tert*-butyldimethyl silyl chloride and imidazole in DMF (Scheme 2.9). The progress of the reaction was monitored by TLC using aqueous potassium permanganate solution as visualizing reagent. After completion, the reaction was quenched with concentrated aqueous NaCl solution, extracted with diethyl ether and dried with $MgSO_4$. Following the evaporation of the organic solvent the remainder was purified by flash column chromatography. The presence of dimethyl (0.18 ppm) and one *tert*-butyl (1.02 ppm) group in the ^1H NMR spectrum of **(2.09)** (figure 2.7) confirmed the silyl protection of the phenol group.

(2.08) **(2.09)**

Scheme 2.9. Silyl protection of phenol **(2.08)**

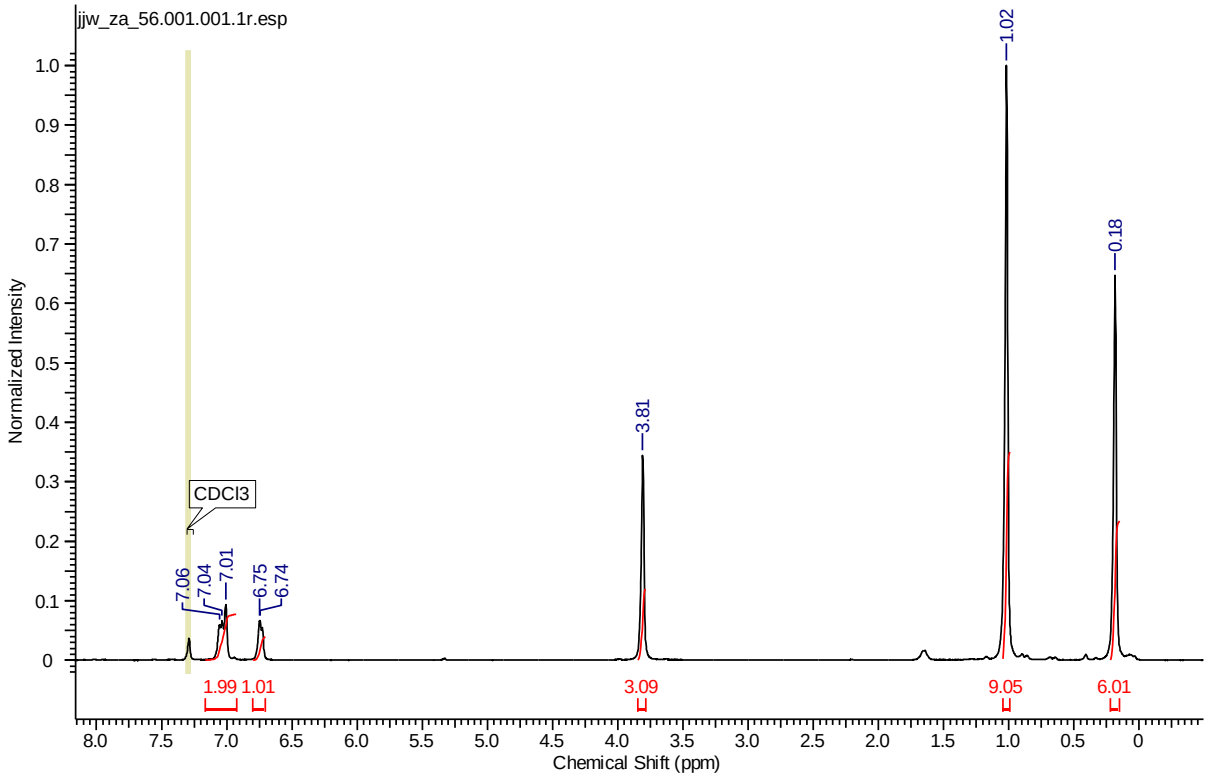

Figure 2.7. ^{1}H NMR spectrum of silyl protected phenol (2.09)

Before the Suzuki reaction could be attempted the silyl protected phenol (**2.09**) was converted into the boronic acid (**2.10**) using *n*-BuLi and triisopropylborate (Scheme 2.10). After the work-up and purification by flash column chromatography, boronic acid **(2.10)** was obtained with a yield of 62%. The structural confirmation was mainly achieved through NMR and mass spectrometry. The HRMS found the boronic acid **(2.10)** as a de-protonated molecular ion with mass of 281.1370 (M- H^{+}).

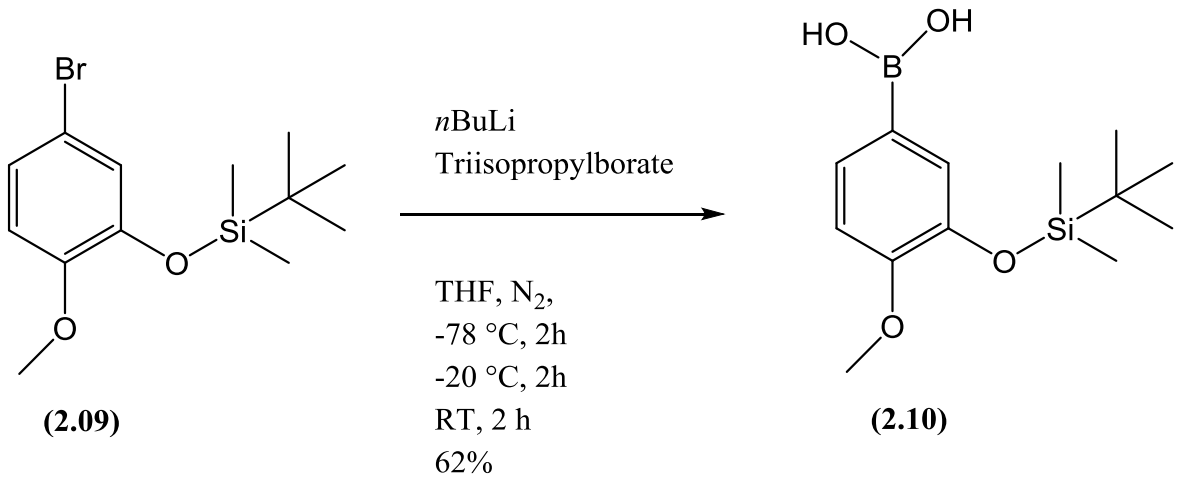

Scheme 2.10. Conversion of aryl bromide **(2.09)** to boronic acid **(2.10)**

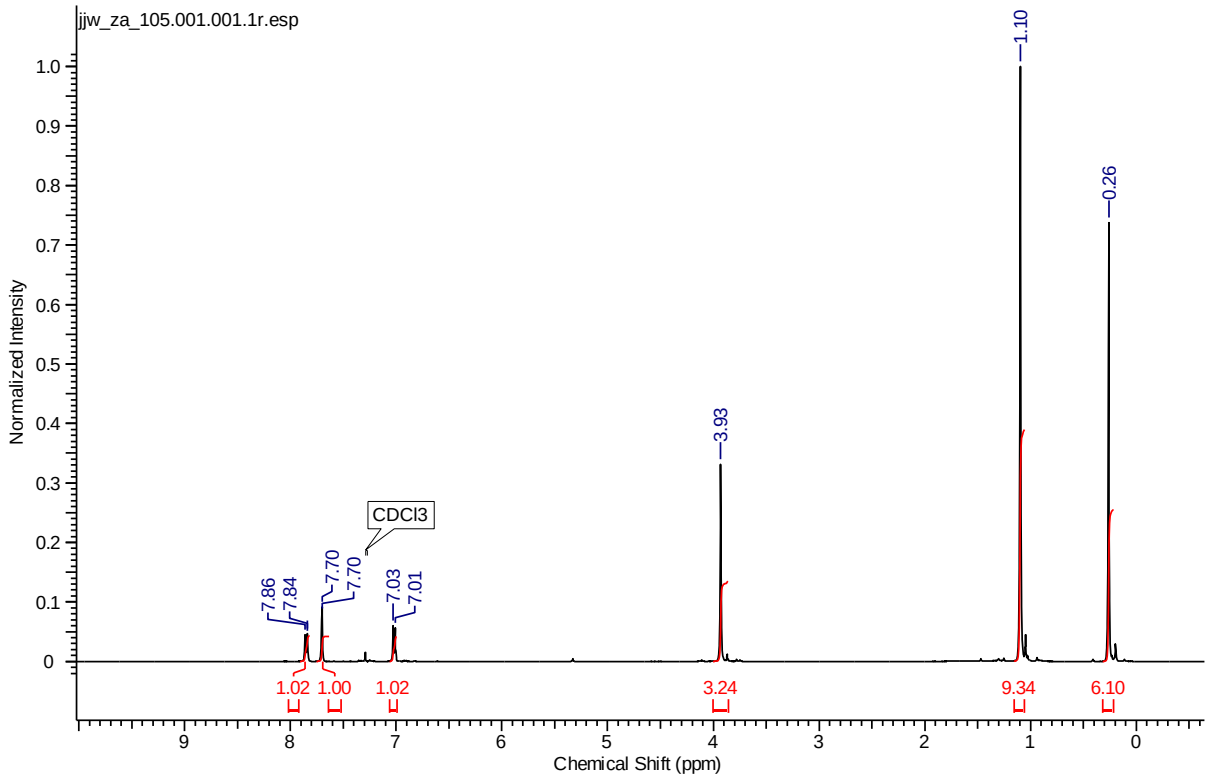

Figure 2.8. ^{1}H NMR spectrum of boronic acid (2.10)

2.3.2 Synthesis of aniline C-ring analogue

For the synthesis of the aniline C-ring, commercially available 4-bromo-2-nitrophenol was used as a starting material. In the first step, the hydroxyl group of 4-bromo-2-nitrophenol was alkylated with iodomethane under basic conditions to give anisole (**2.11**), followed by the reduction of the nitro group, using Sn/HCl to give the aniline (**2.12**) (Scheme 2.11). The work-up procedure was carefully conducted by quenching the acidic mixture with aqueous NaOH (2.5 M) at 0 °C. The structure of the aniline **(2.12)** was confirmed by the ^{1}H NMR spectrum (figure 2.9). The methoxy group was found to resonate at 3.84 ppm while the NH_2 was resonating as a broad singlet at 3.88 ppm (figure 2.10). Along with these resonances, the presence of three aryl protons was also confirmed.

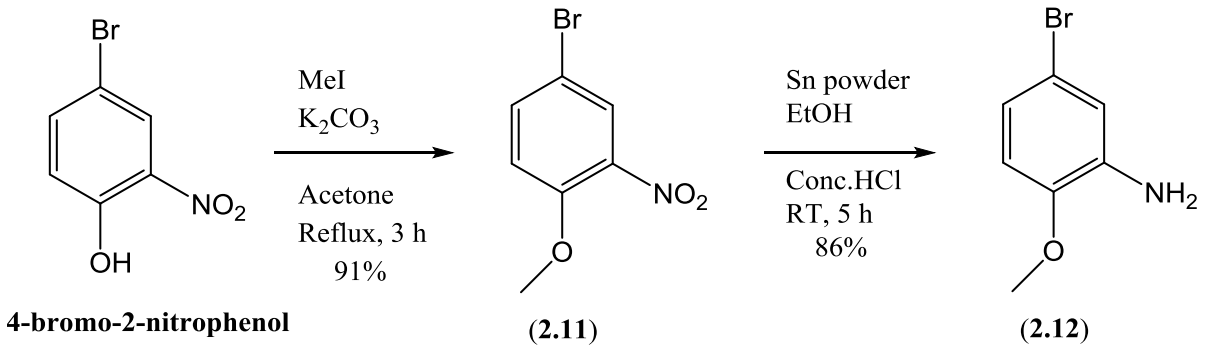

4-bromo-2-nitrophenol (**2.11**) (**2.12**)

Scheme 2.11. Synthesis of aniline C-ring **(2.12)**

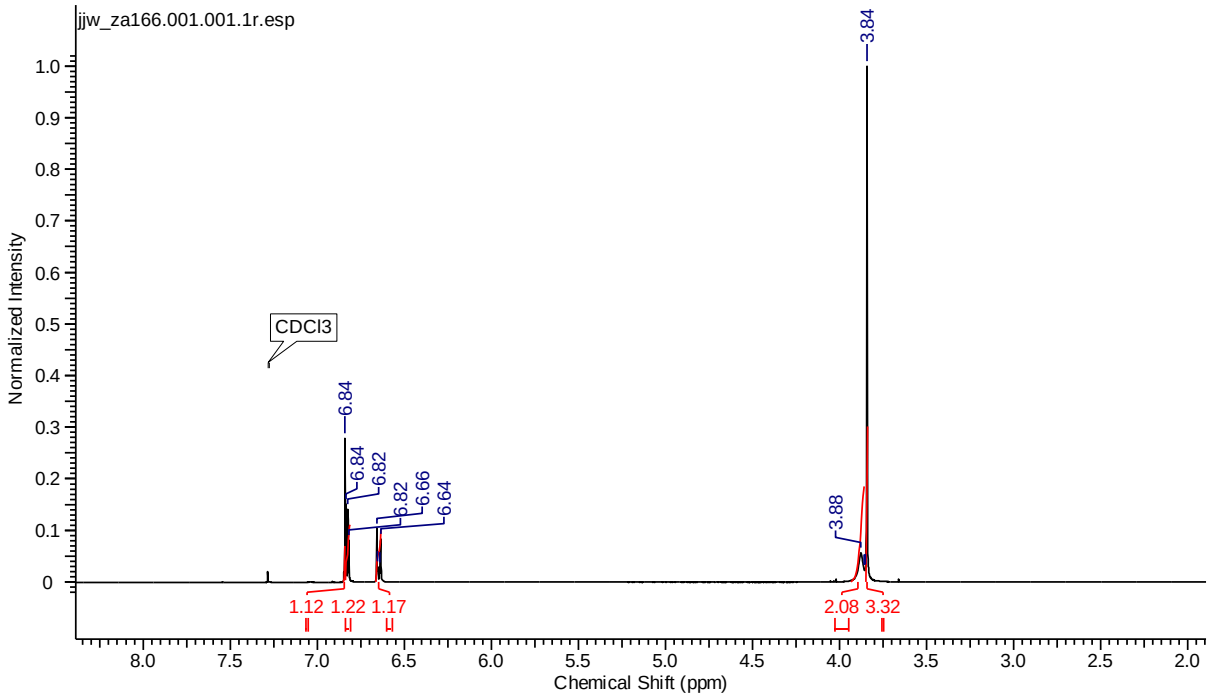

Figure 2.9. ^{1}H NMR spectrum of aniline (2.12)

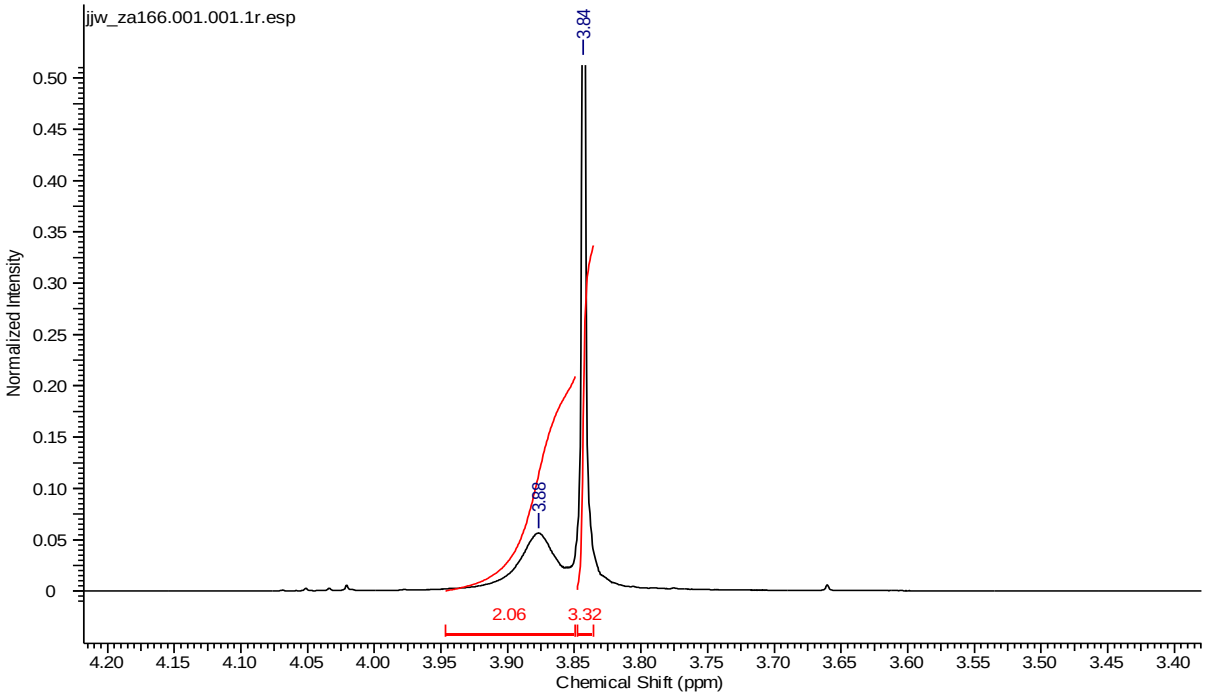

Figure 2.10. Expansion of ^{1}H NMR spectrum of aniline (2.12)

The aniline was than protected by reaction with di-*tert*-butyl dicarbonate to form *N*-*tert* butoxycarbonyl (*N*-*t*Boc) protected aniline **(2.13)**. The reaction was carried out using anhydrous THF under an atmosphere of nitrogen and refluxing at gentle heat over the period of two working days (Scheme 2.12). Aniline protection was confirmed by the presence of *t*-Boc group in the ^{1}H NMR spectrum (figure 2.11) resonating at 1.55 ppm with an integral value of 9 protons.

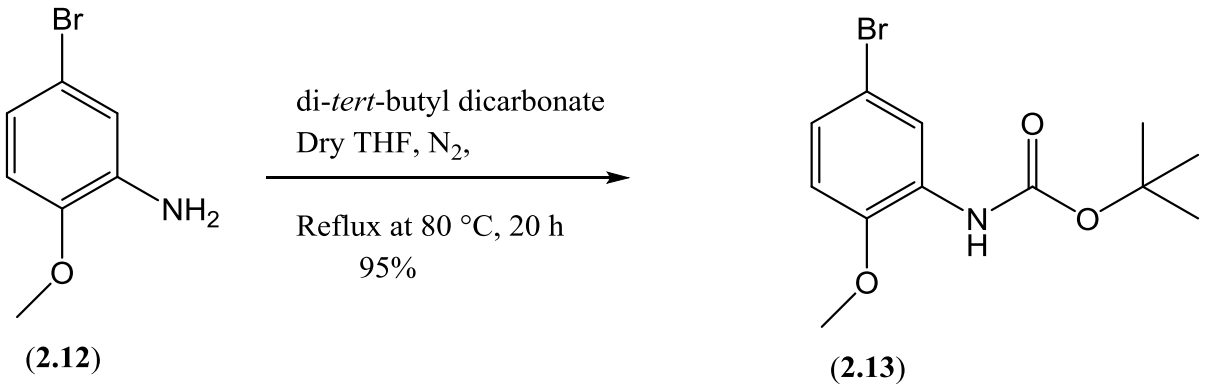

(**2.12**) (**2.13**)

Scheme 2.12. Boc protection of aniline C-ring **(2.13)**

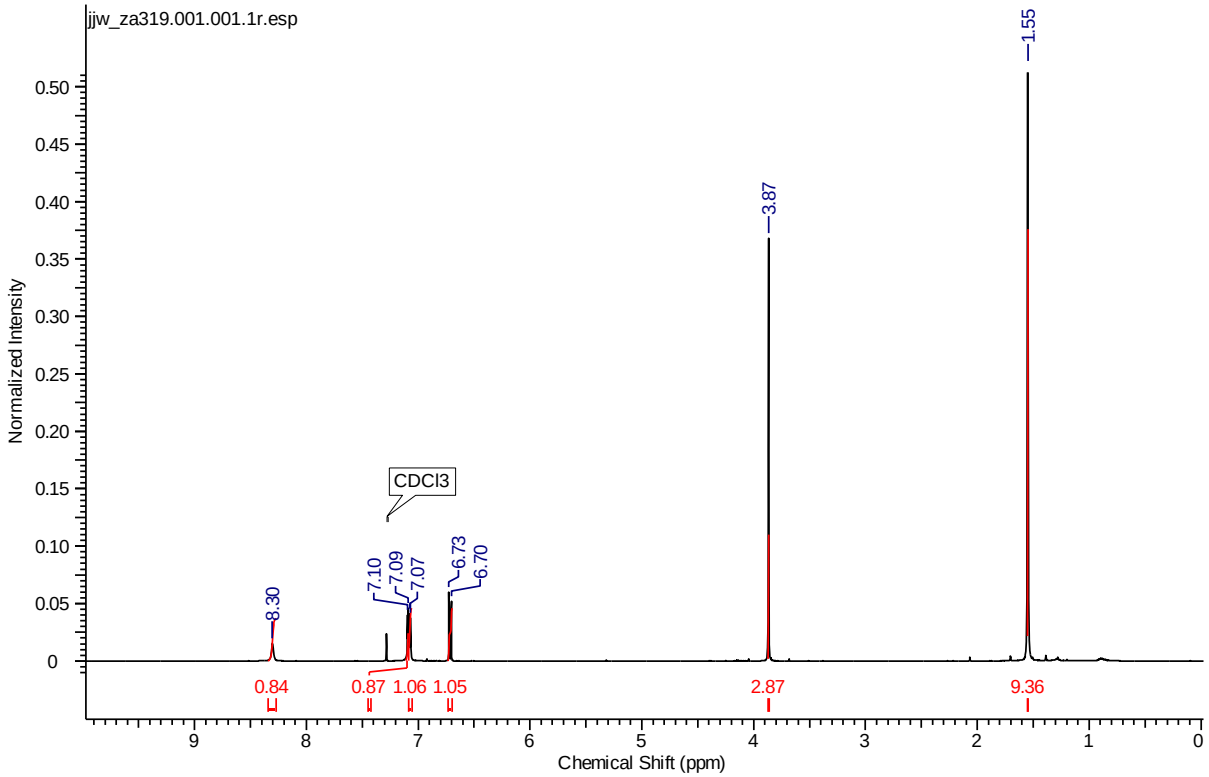

Figure 2.11. ^{1}H NMR spectrum of *N*-Boc aniline (2.13)

To effect the Suzuki coupling of our *N*-Boc protected aniline **(2.13)** with triflate **(2.05)**, the compound **(2.13)** was first converted into the boronic ester **(2.14)** using Miyaura borylation reaction conditions [154] (Scheme 2.13). Generally the Suzuki coupling with boronic acids gives better yield but it was avoided as previous attempts showed it to result in poor yields of product. The reaction was effected by refluxing the mixture at 80 °C for 6 hours followed by 12 hours stirring at room temperature. Finally the structural confirmation of the product was done by NMR spectroscopy. The ^{1}H NMR spectrum (figure 2.12) showed a characteristic peak of two dimethyl groups of boronic ester resonating at 1.34 ppm with an integral value of 12 while the HRMS found the de-protonated molecular ion of mass 348.1989 ($M\text{-}H^{+}$).

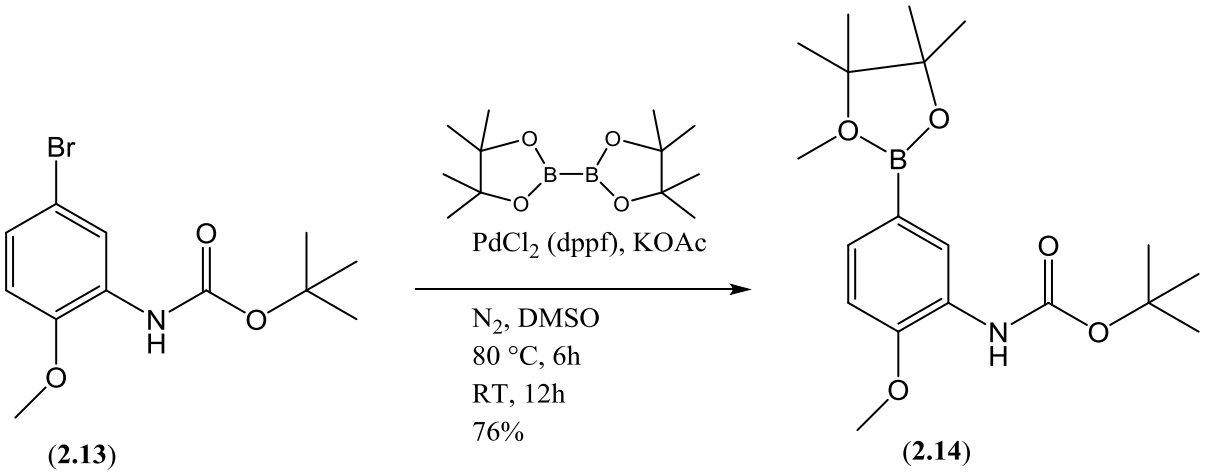

Scheme 2.13. Miyaura borylation of *N*-Boc protected aniline **(2.13)**

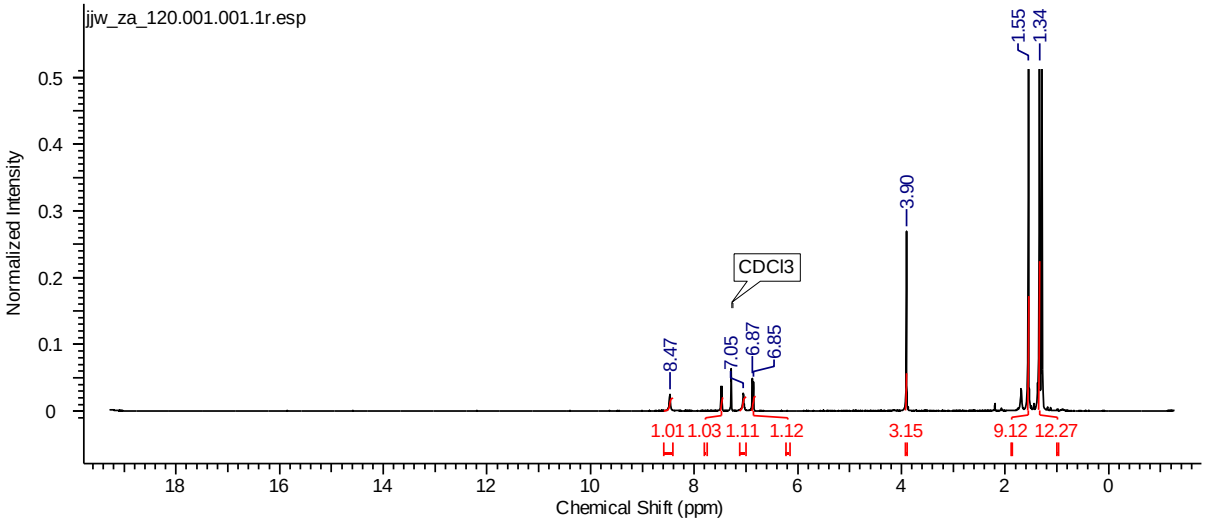

Figure 2.12. ^{1}H NMR spectrum of boronic ester (2.14)

2.4 Aniline C-ring analogue-triflate coupling

After securing the AB-ring **(2.05)** and C-ring analogues we were in a position to go for the Suzuki coupling reaction. Aryl boronic ester **(2.14)** was coupled with triflate **(2.05)** using tetrakis (triphenylphosphine) palladium (0) as catalyst and potassium carbonate as a base (Scheme 2.14). The coupling of boronic ester **(2.14)** was confirmed by ^{1}H NMR spectrum (figure 2.13). The additional feature in the ^{1}H NMR spectrum as compared to 4-hydroxy coumarin **(2.04)** included the presence of characteristic *t*-Boc group at 1.51 ppm. An additional methoxy group was confirmed in the region 3.5-4.5 ppm and finally the aromatic region also had the expected 3 additional protons for the aromatic ring.

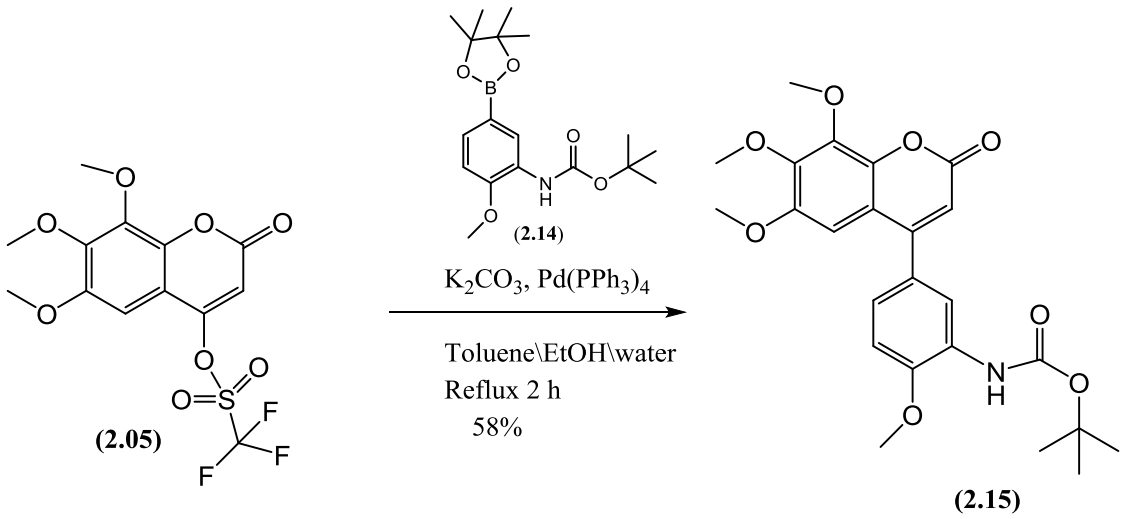

Scheme 2.14. Suzuki coupling of triflate **(2.05)** with boronic ester **(2.14)** to give 4-arylcoumarin intermediate **(2.15)**

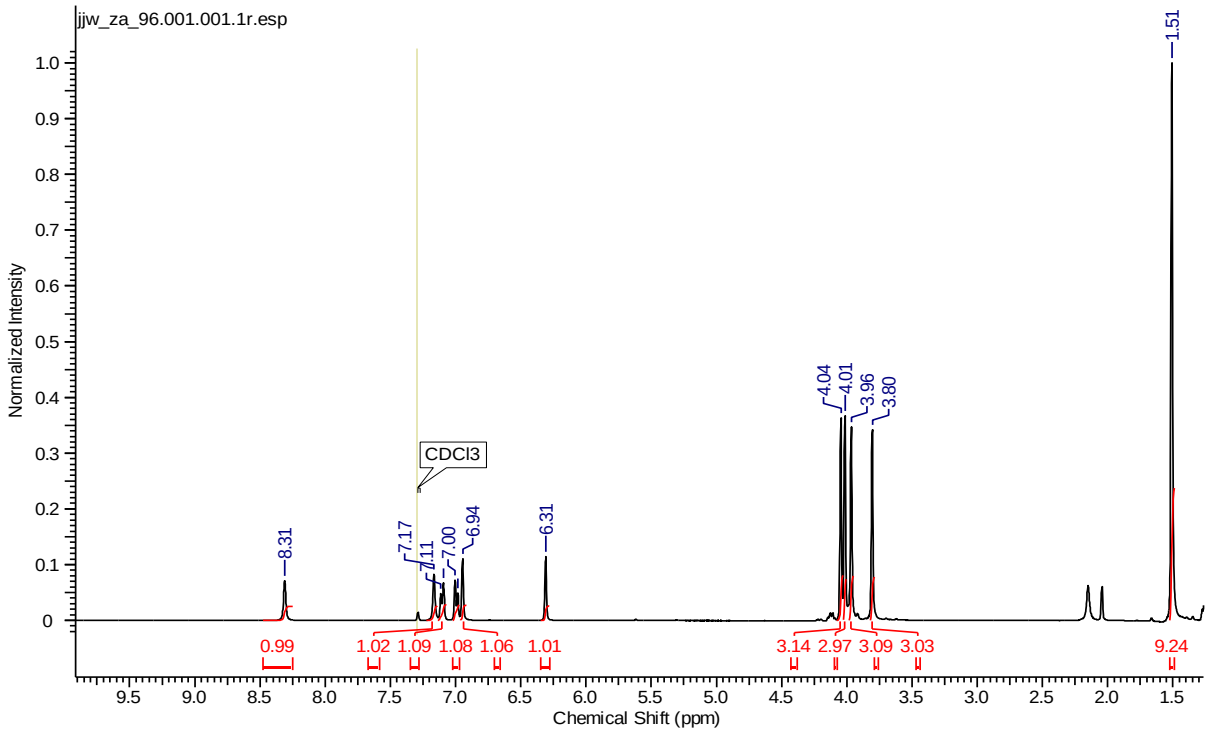

Figure 2.13. ^{1}H NMR spectrum of 4-aryl coumarin intermediate (2.15)

The resultant 4-arylcoumarin **(2.15)** was deprotected with 33% TFA in DCM (Scheme 2.15) to give aniline **(2.16)**. For the structural identification of aniline **(2.16)**, NMR spectroscopy was used. The ^{1}H NMR spectrum (figure 2.14) shows a total of 17 protons while the ^{13}C spectrum (figure 2.15) represents a total carbon count of 19. In the ^{1}H NMR spectrum the NH_2 signal did not appear most probably due to deuterium exchange. The deprotection was confirmed due to the disappearance of signal for *t*-Boc group in the ^{1}H

NMR spectrum. Moreover, the HRMS also found the relevant protonated molecular ion of mass 358.2184.

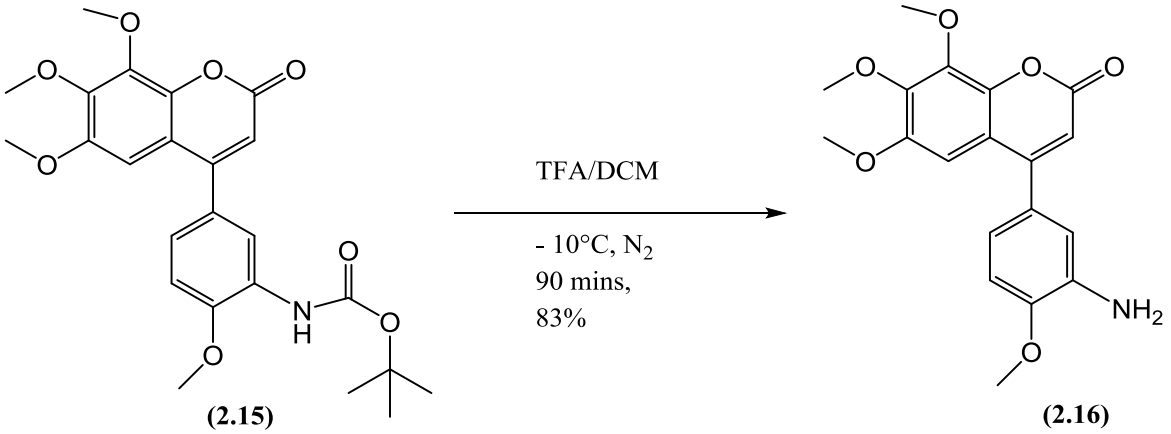

Scheme 2.15. Deprotection of **(2.15)** to give aniline **(2.16)**

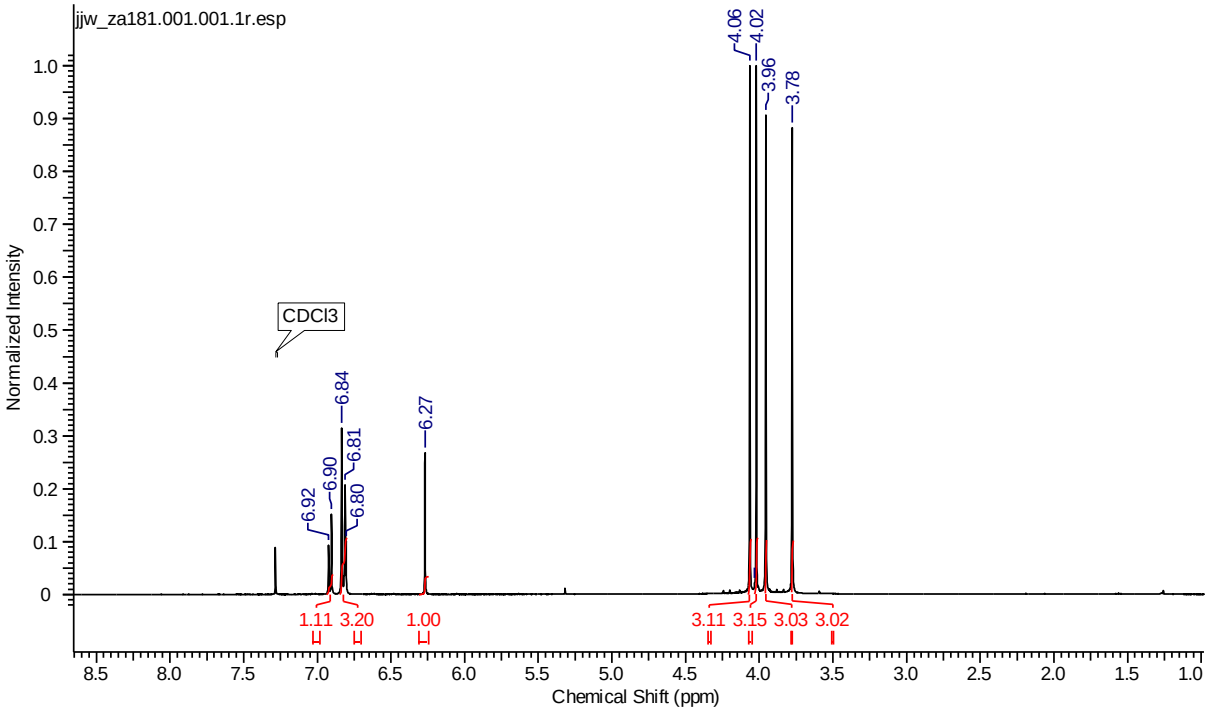

Figure 2.14. ^{1}H NMR spectrum of aniline (2.16)

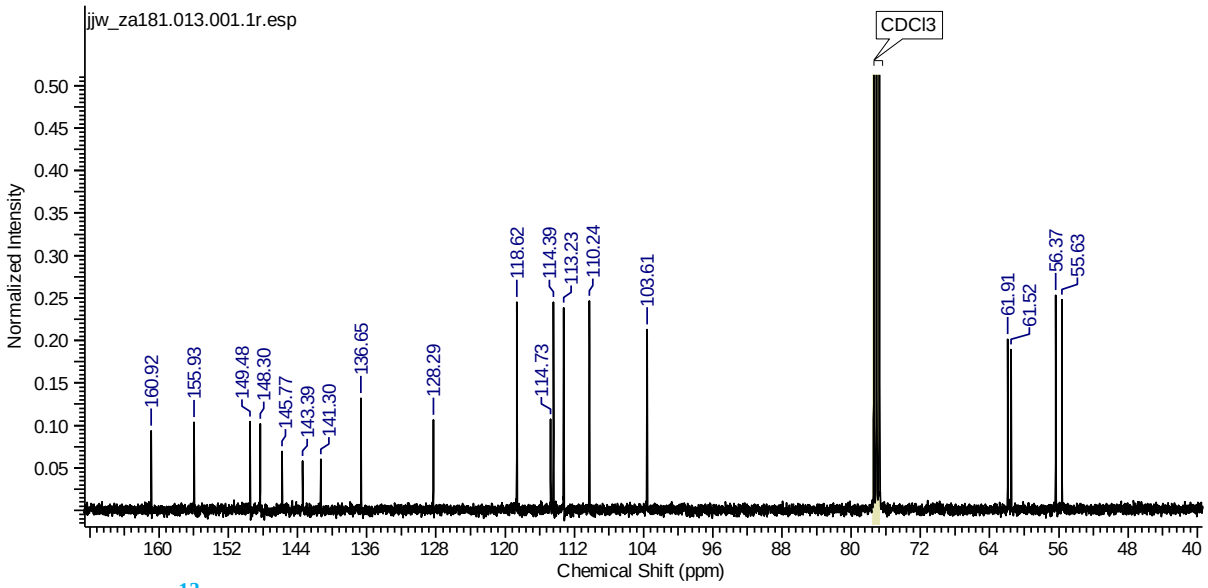

Figure 2.15. ^{13}C NMR spectrum of aniline (2.16)

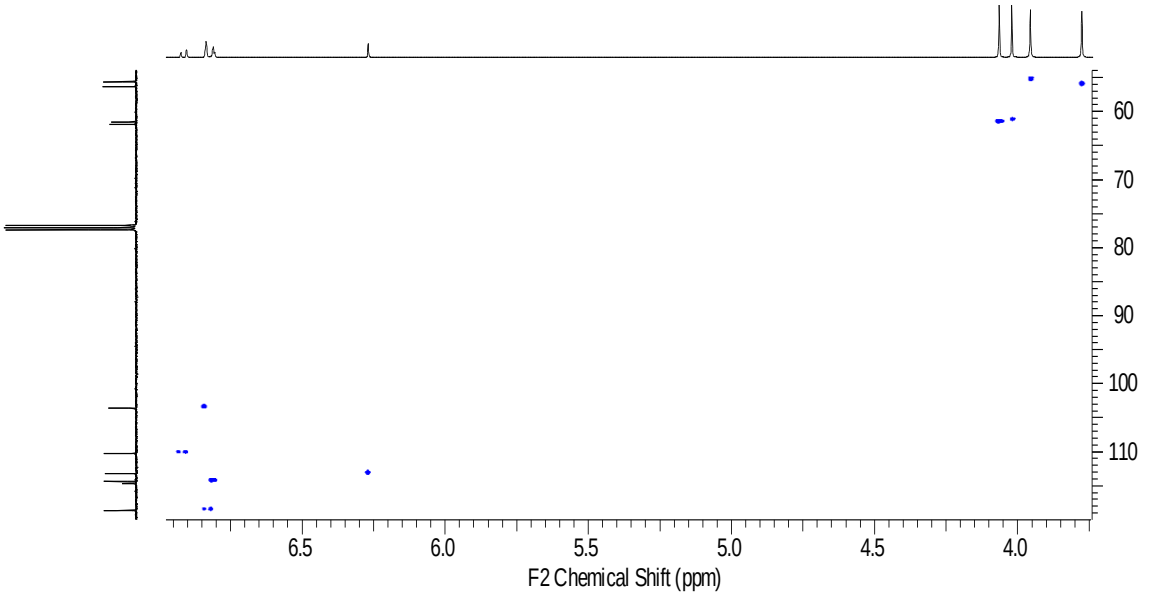

Figure 2.16. HSQC spectrum of aniline (2.16)

2.4.1 Thione derivative of coumarin compound (2.16)

Thione derivatives are more susceptible to nucleophiles than the corresponding carbonyl precursors. The most probable reason for the higher reactivity of thione as compared to ketone is the lower electronegativity of sulphur and the higher polarizability of the C=S bond [155] which can be explained with the help of Hard and Soft Acid and Base (HSAB) theory. According to this theory all the chemical species are assigned as hard or soft and acid or base. Sulphur is grouped as a soft base while oxygen is grouped along with hard

bases. Furthermore according to this theory, the chemical species with soft nucleophile like sulphur will be highly polarized while chemical species with hard nucleophile like oxygen has low polarizability so the thione is strongly electrophilic while the carbonyl of the ketone is a poor electrophile. To covert the carbonyl functionality of **(2.15)** into thione **(2.17)**, Lawesson's reagent was used. For this purpose **(2.15)** was refluxed with Lawesson's reagent using toluene as solvent. The only problem during this reaction was that at low temperature the reaction proceeded very slowly but with good yield while at high temperatures the reaction went to completion within 2 hours but with low yield. The *N*-Boc deprotection step was effected by treating thione **(2.17)** with a 33% solution of trifluoroacetic acid in anhydrous DCM at -10 °C under an atmosphere of nitrogen to afford the free amine (**2.18)** after basic work-up **(**Scheme 2.16). The ^{1}H NMR spectrum (figure 2.17) of compound (2.18) shows the presence of all expected 19 protons while the ^{13}C spectrum (figure 2.18) also confirmed the presence of 19 carbons. The characteristic peaks present in the ^{1}H NMR spectrum include the presence of NH_2 signal (5.06 ppm), 4 methoxy groups (3.5-4.5 ppm), 4 aryl and 1 alkene proton. Moreover the ^{13}C spectrum also confirmed the presence of thiocarbonyl peak resonating at 195.2 ppm. For further confirmation mass spectroscopy was used where the HRMS found the protonated molecular ion of mass 374.1073 ($M+H^+$).

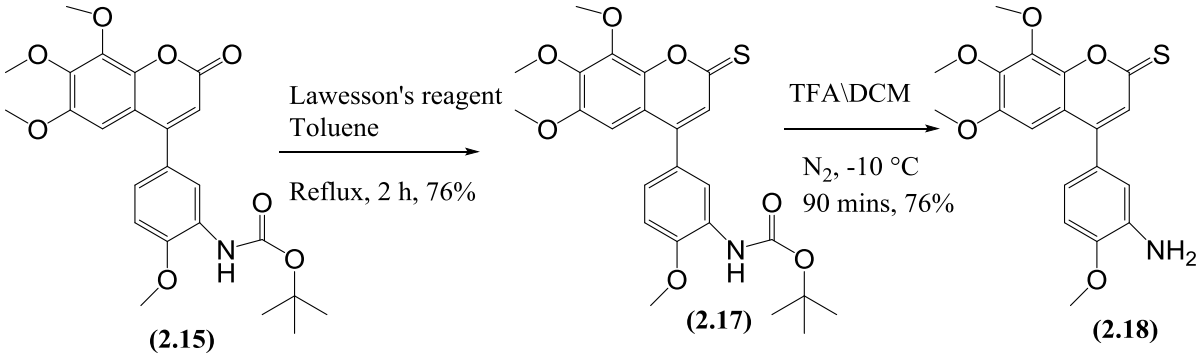

Scheme 2.16. Thionation of ketone **(2.15)**, followed by subsequent deprotection to free amine **(2.18)**

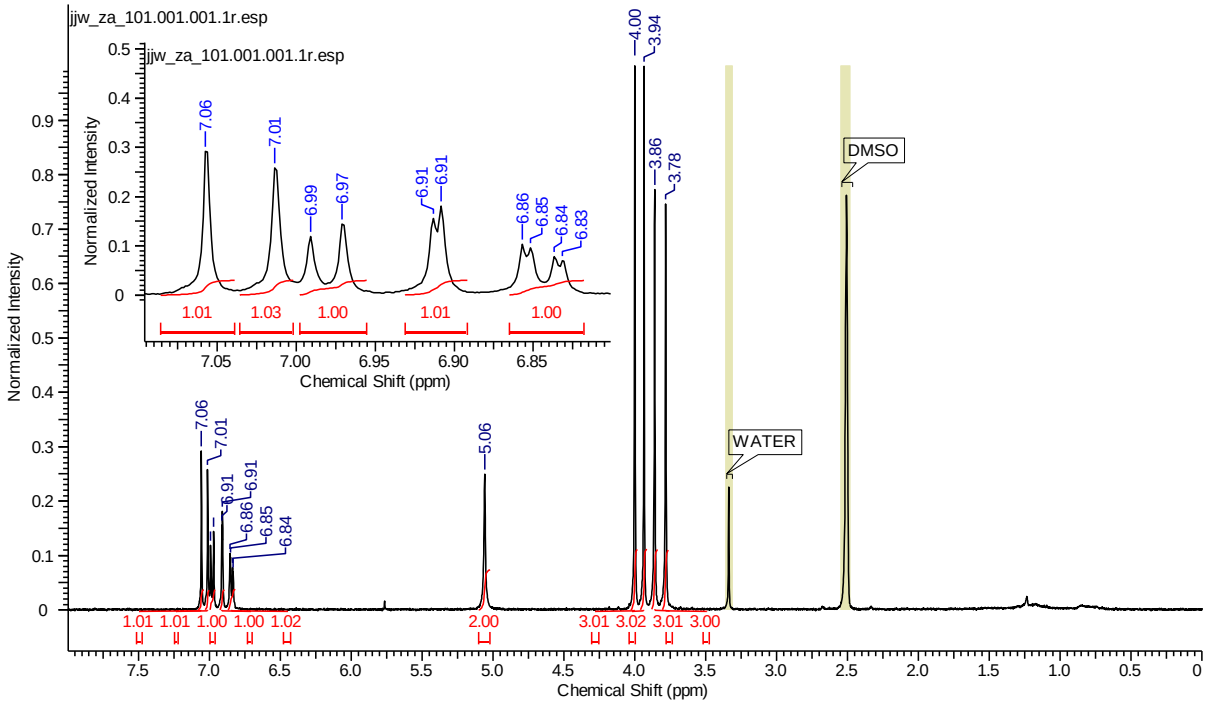

Figure 2.17. ^{1}H NMR spectrum of aniline (2.18)

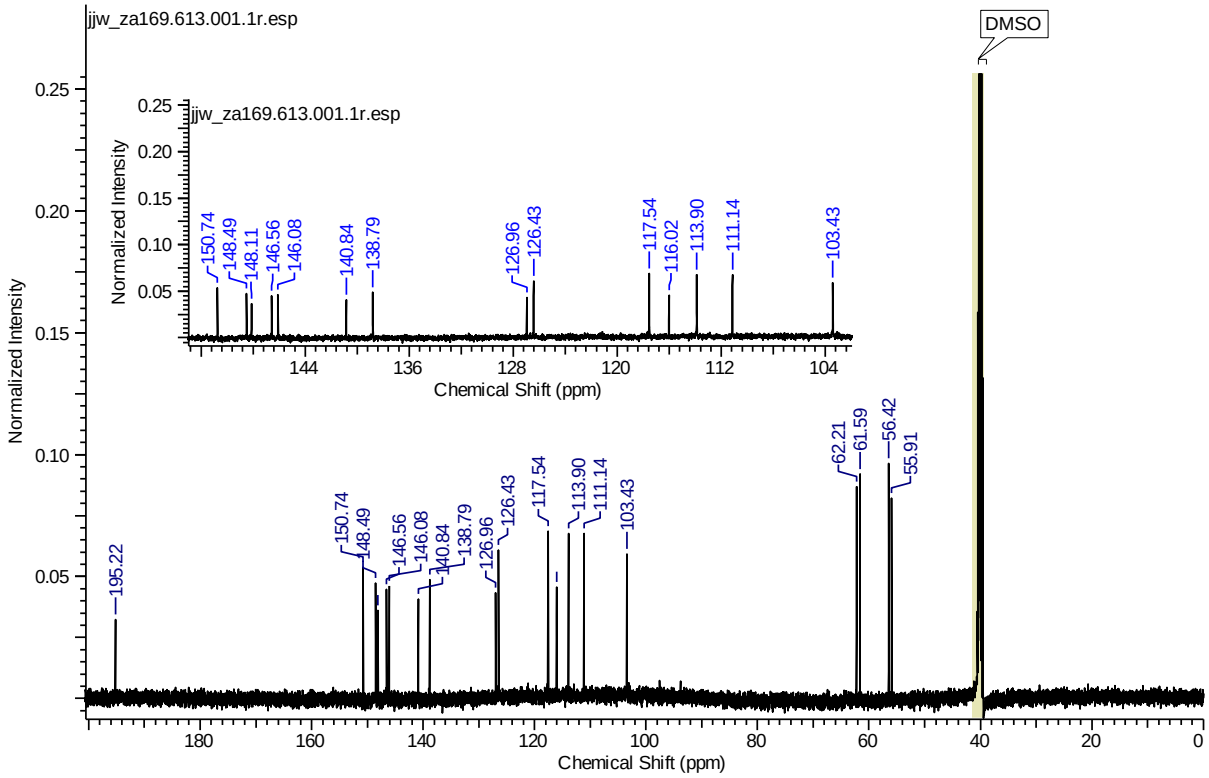

Figure 2.18. ^{13}C NMR spectrum of aniline (2.18)

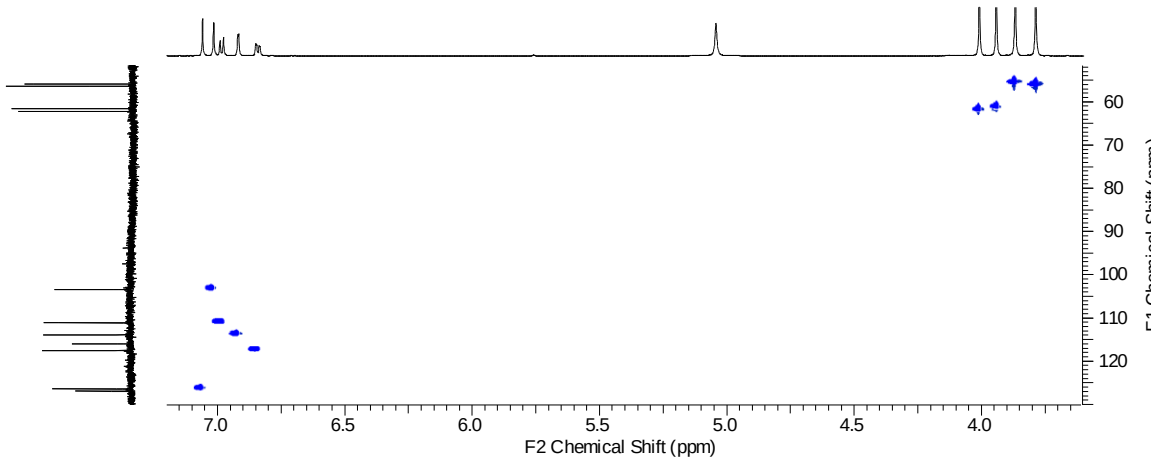

Figure 2.19. HSQC spectrum of aniline (2.18)

2.4.2 Oxime derivative of coumarin compound (2.18)

Having secured a suitable substrate (thione) for a range of different amine based nucleophiles the first step was to prepare the oxime derivative **(2.19)**. For this purpose **(2.17)** was stirred with hydroxylamine hydrochloride using diisopropylethylamine as base and DMF as solvent (Scheme 2.17). In the next step, the *t*-Boc- protecting group was removed to give the final oxime derivative **(2.20)**. For the structural confirmation a combination of NMR and mass spectrometry was used. The ^{1}H NMR spectrum (figure 2.20) represents a count of 20 protons while the ^{13}C spectrum (figure 2.21) confirmed the presence of all expected 19 carbons. The OH of the oxime functionality was found to be resonating as a singlet at 10.25 ppm while the NH_2 appear as a broad singlet at 4.92 ppm in the ^{1}H NMR spectrum.

HRMS analysis gave the relevant protonated molecular ion of mass 373.1383. IR absorption found O-H and N-H band at 3405.19 and 3317.90 cm^{-1}, alkane absorptions at 2941.38 cm^{-1} and 2834.01 cm^{-1} and the C=N absorption at 1636.55 cm^{-1}.

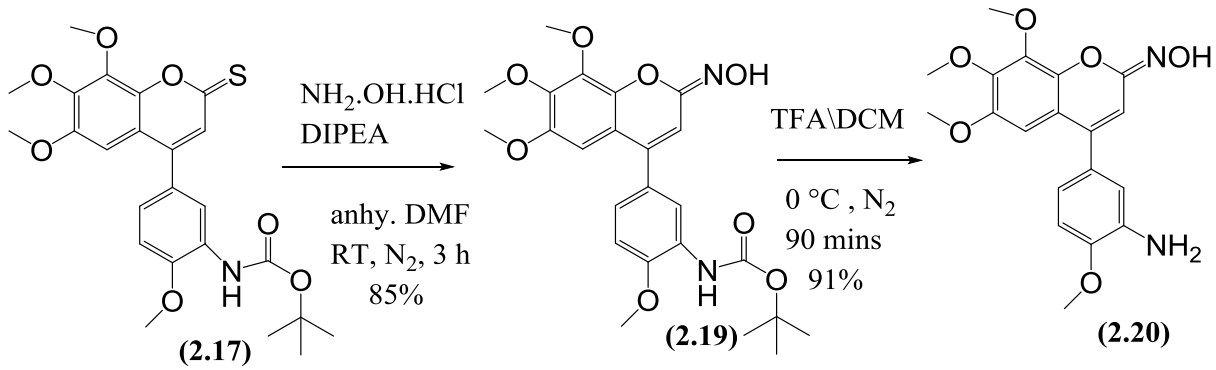

Scheme 2.17. Synthesis of oxime and subsequent removal of *t*-Boc-group to give **(2.20)**.

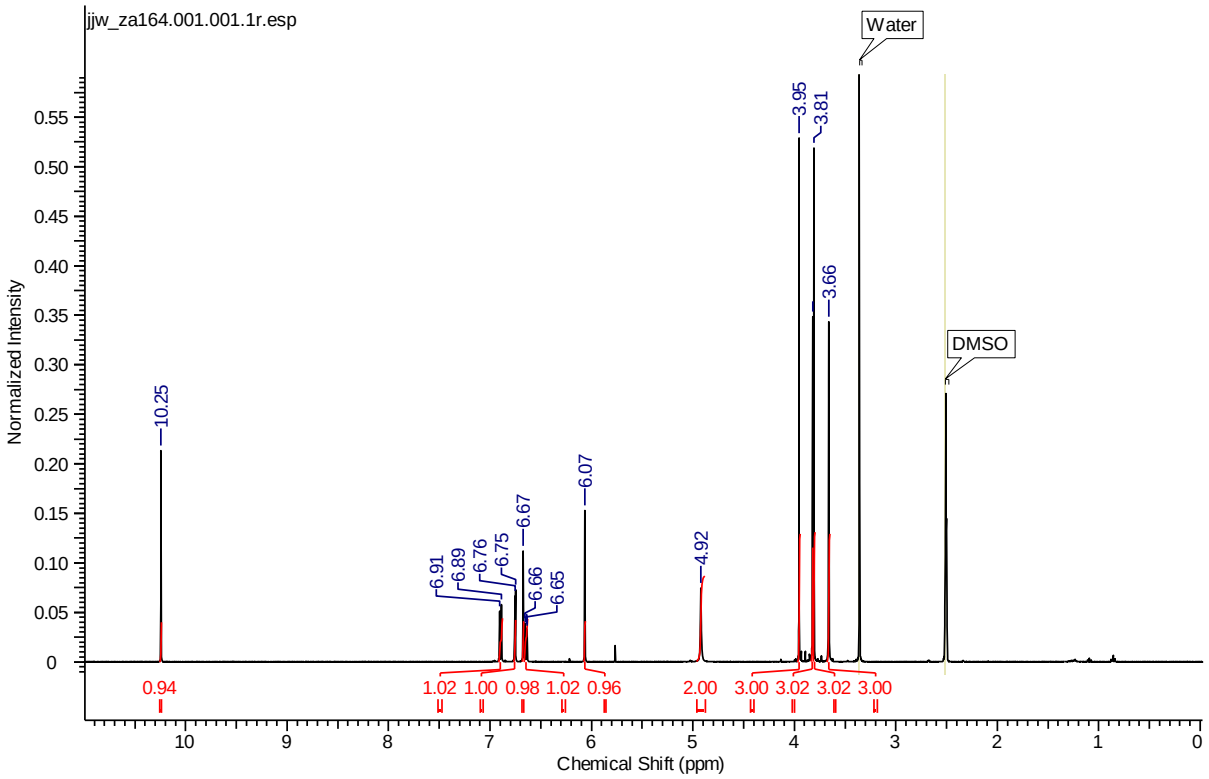

Figure 2.20. ^{1}H NMR spectrum of oxime (2.20)

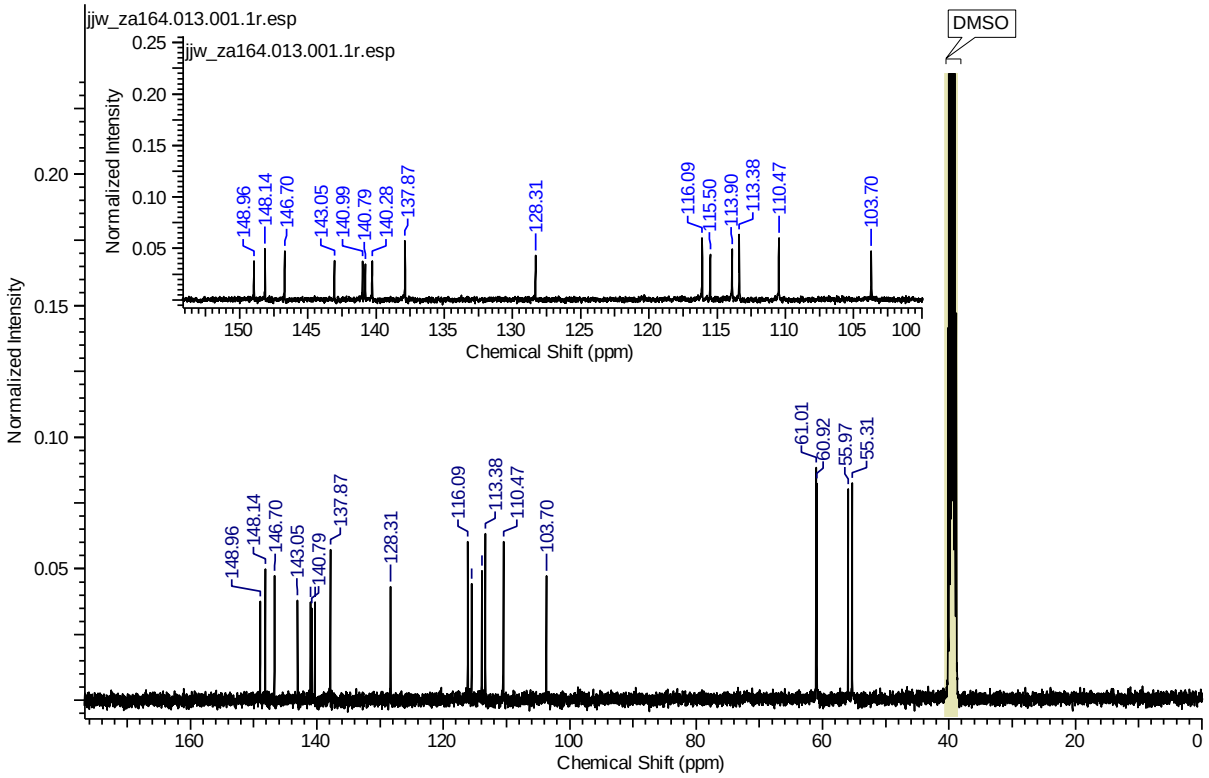

Figure 2.21. ^{13}C NMR spectrum of oxime (2.20)

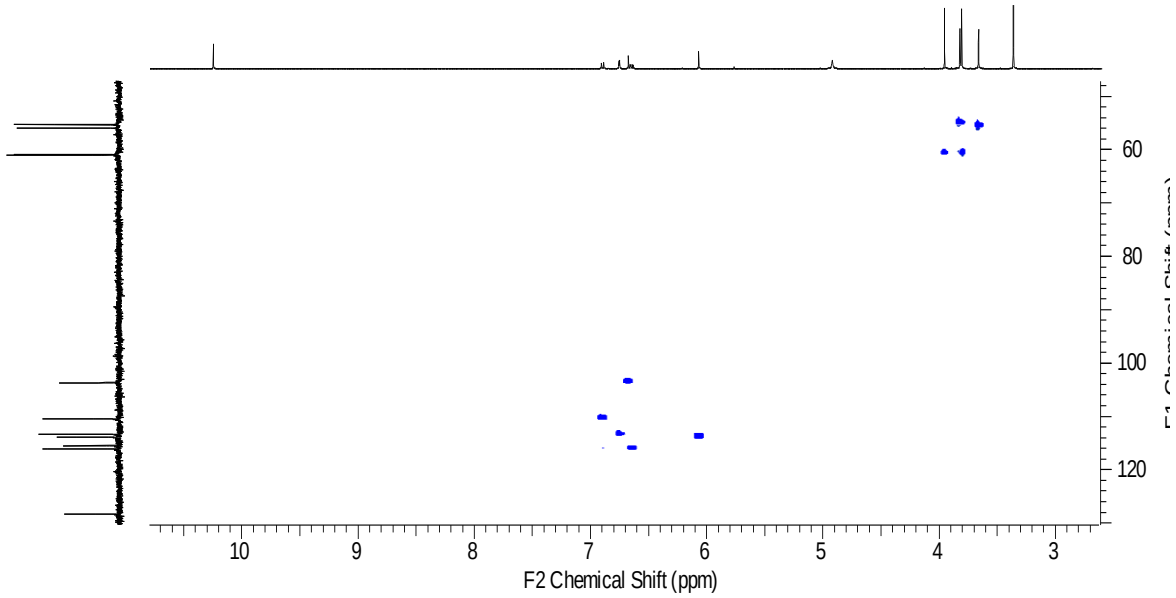

Figure 2.22. HSQC spectrum of oxime (2.20)

2.5 Phenolic C-ring analogue-triflate coupling

After the synthesis of our aniline based compounds we turned our attention to the synthesis of compounds based on our phenolic C-ring (**2.10).** For this purpose the boronic acid **(2.10)** was coupled to triflate **(2.05)** using the same conditions as were utilised before for the coupling of the aniline C-ring analogue, to give silyl ether **(2.21)** (Scheme 2.18). The success of the coupling reaction was confirmed by ^{1}H NMR spectrum (figure 2.23) of **(2.21)** where the dimethyl (0.21 ppm) and *tert*-butyl (1.02 ppm) substituents were present. Moreover an additional methoxy group was confirmed by the presence of the extra sharp singlet resonating in the region between 3.70-4.10 ppm and finally the aromatic region also had the expected three additional protons for the aromatic ring.

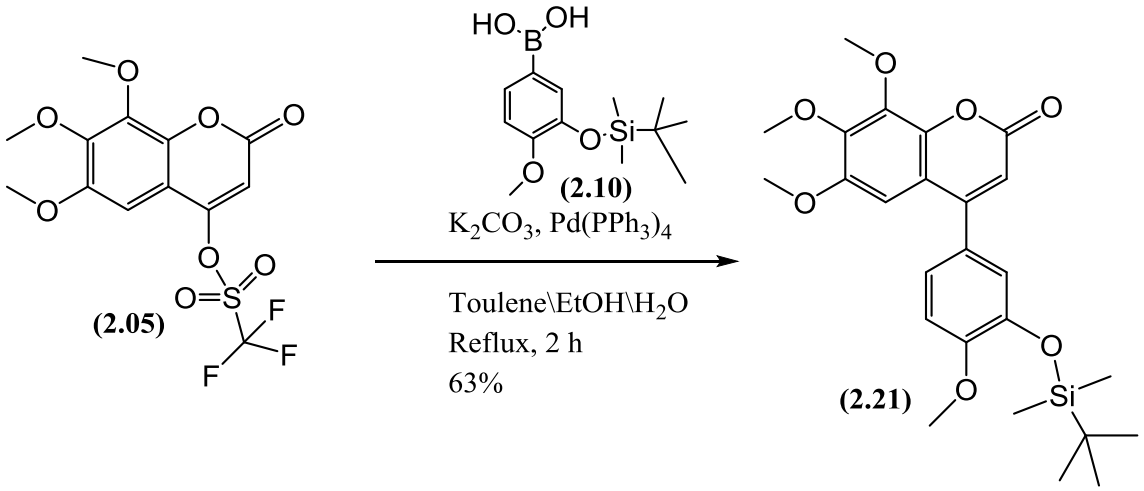

Scheme 2.18. Suzuki coupling of triflate **(2.05)** with boronic acid **(2.10)** to give 4-arylcoumarin intermediate **(2.21)**

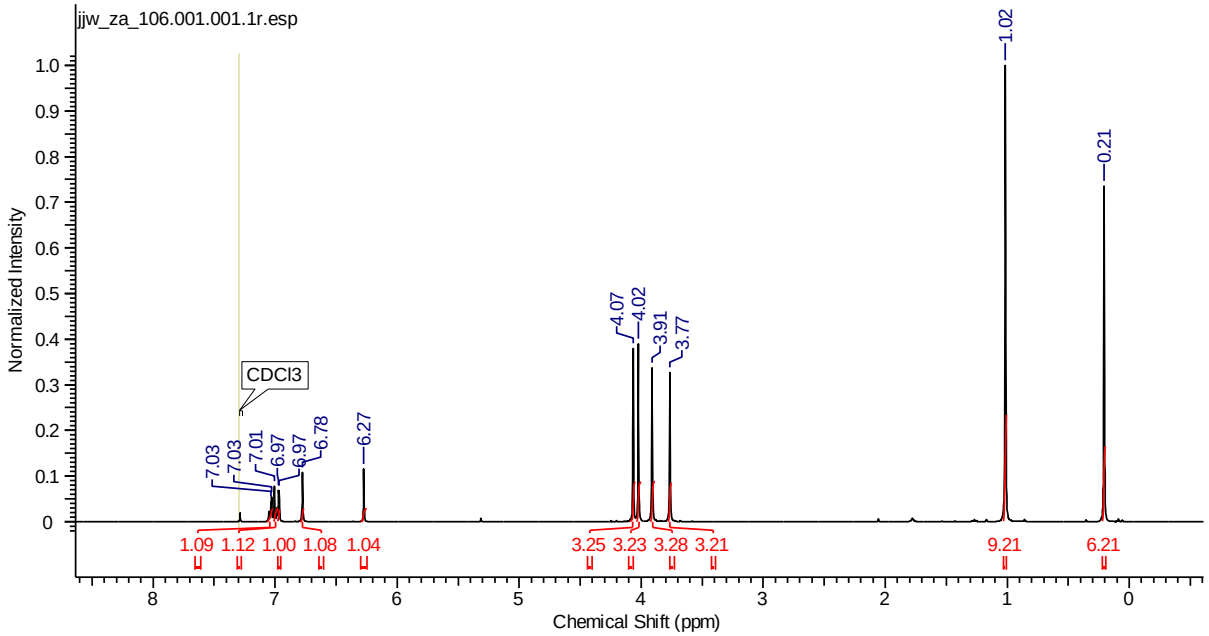

Figure 2.23. ^{1}H NMR spectrum of (2.21)

The resultant silyl ether **(2.21)** was deprotected with TBAF (scheme 2.19) to give phenol **(2.22)**. The structural confirmation was achieved through the disappearance of *tert*-butyl and dimethyl peaks of the silyl protecting group as well as by the appearance of the phenolic OH at 9.43 ppm in the ^{1}H NMR spectrum (figure 2.24). The HRMS further confirmed the identity of **(2.22)** by finding the molecular ion of mass 381.0944 as sodium adduct ($M+Na^{+}$).

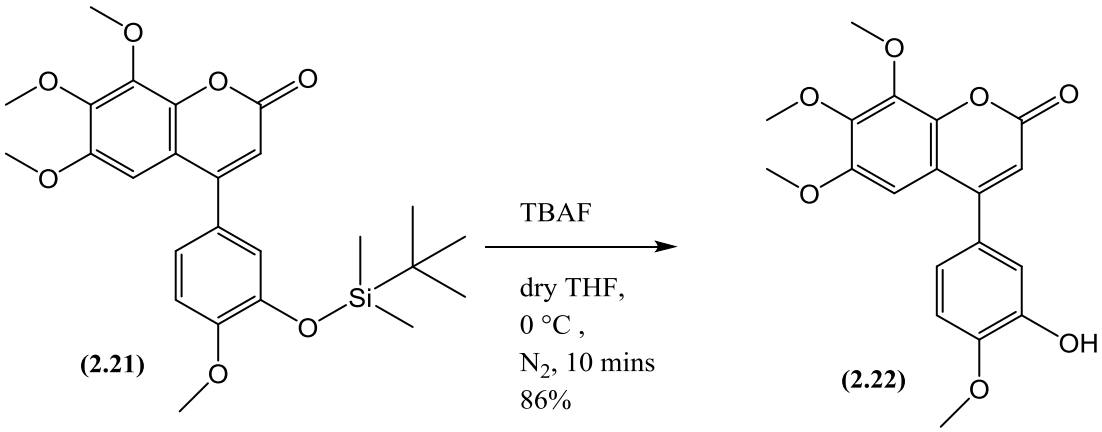

Scheme 2.19. Deprotection of silyl ether **(2.21)** to give phenol **(2.22)**

.

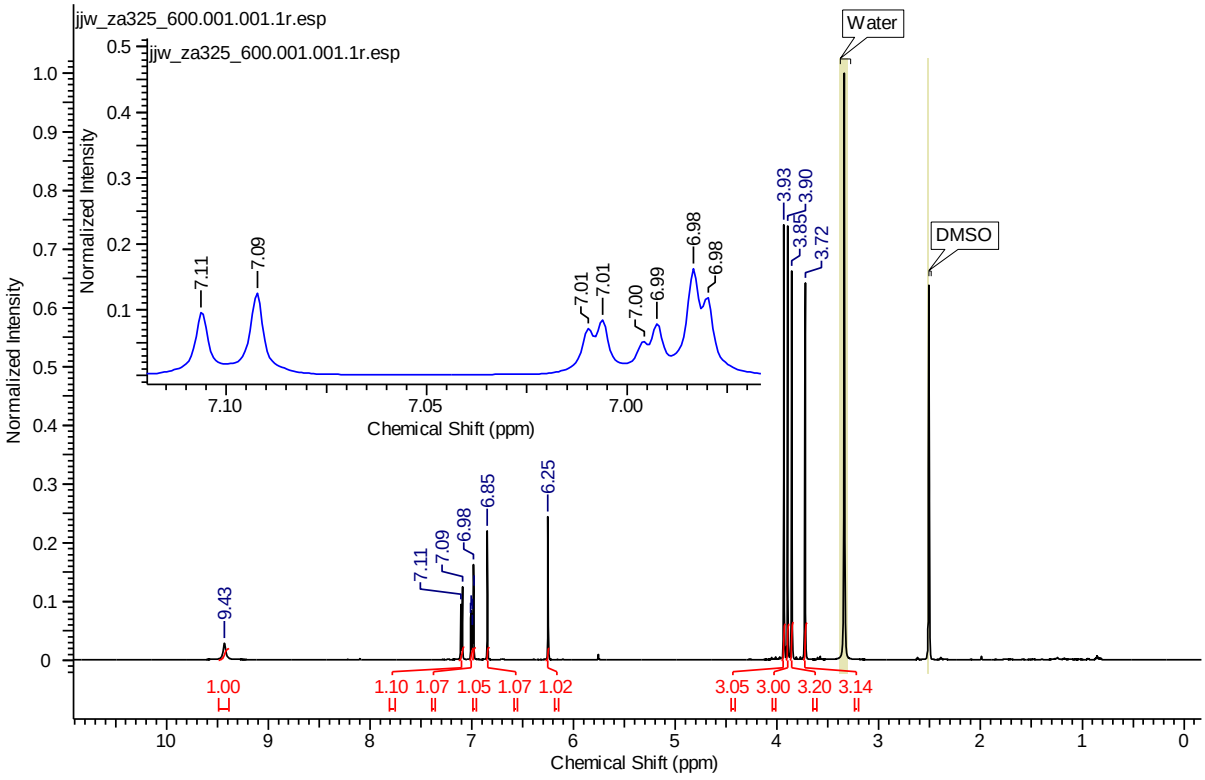

Figure 2.24. ^{1}H NMR spectrum of phenol (2.22)

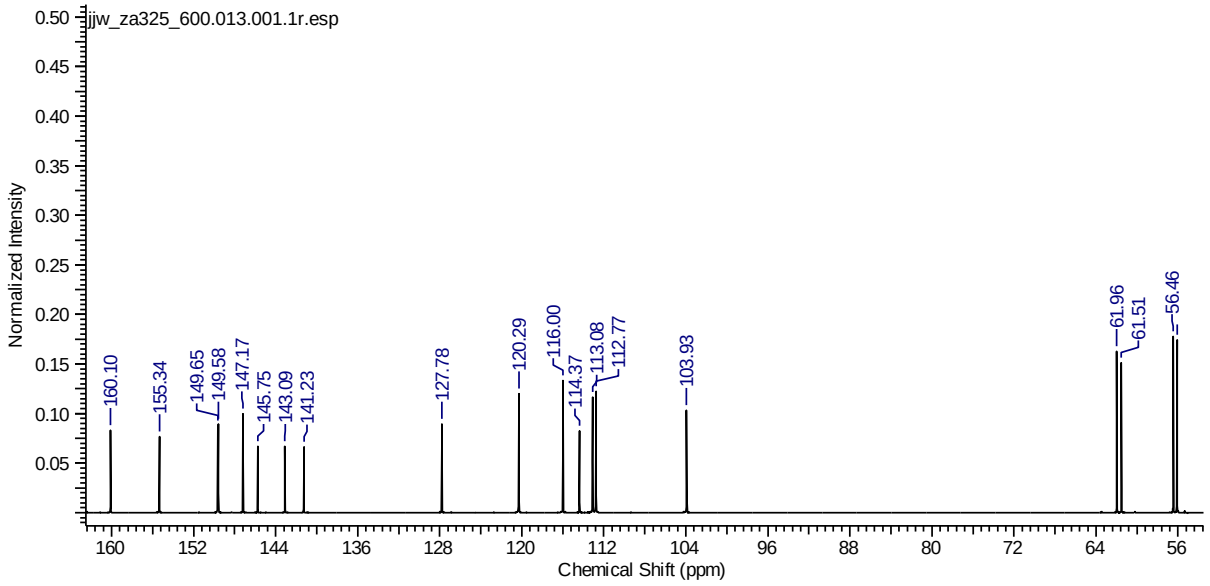

Figure 2.25. ^{13}C NMR spectrum of phenol (2.22)

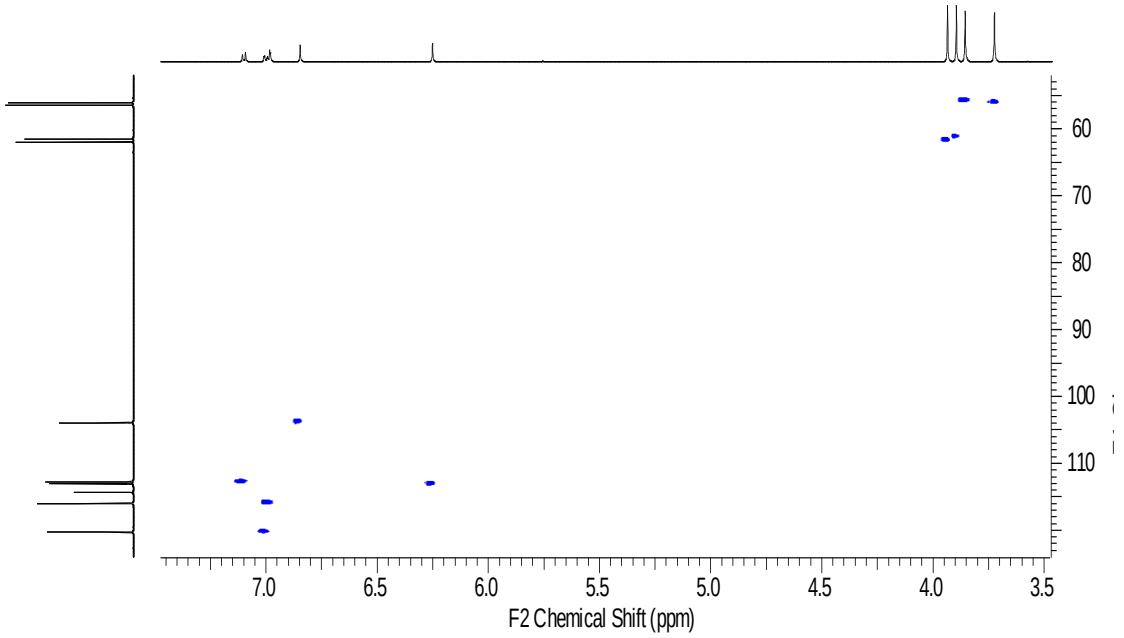

Figure 2.26. HSQC spectrum of phenol (2.22)

2.5.1 Thione derivative of coumarin compound (2.22)

Next we had to convert the carbonyl functionality of **(2.21)** into the thione by refluxing 4-arylcoumarin **(2.21)** with Lawesson's reagent in toluene, which was followed by TBAF removal of the silyl protecting group to afford the final thione **(2.24)** (Scheme 2.20). The identity of phenol **(2.24)** was confirmed through a range of spectroscopic techniques. The ^{1}H NMR spectrum (figure 2.27) shows a total count of 17 protons while the signal for OH was difficult to detect. The ^{13}C-NMR spectrum (figure 2.28) represents all the peaks for 19

carbons. HRMS analysis of **(2.24)** found the relative molecular ion of mass 397.0728 (M + Na^+).

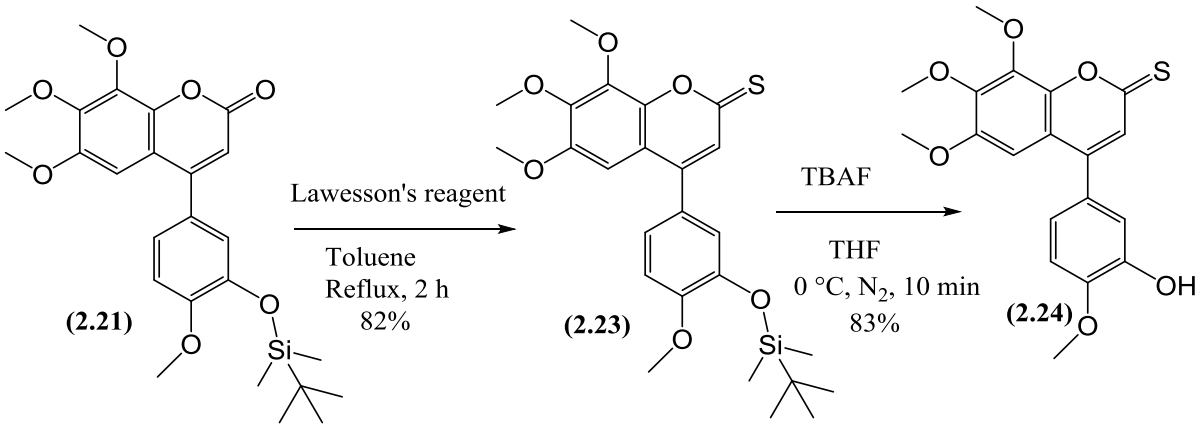

Scheme 2.20. Thionation of ketone **(2.21)**, followed by subsequent deprotection to give phenol **(2.24)**

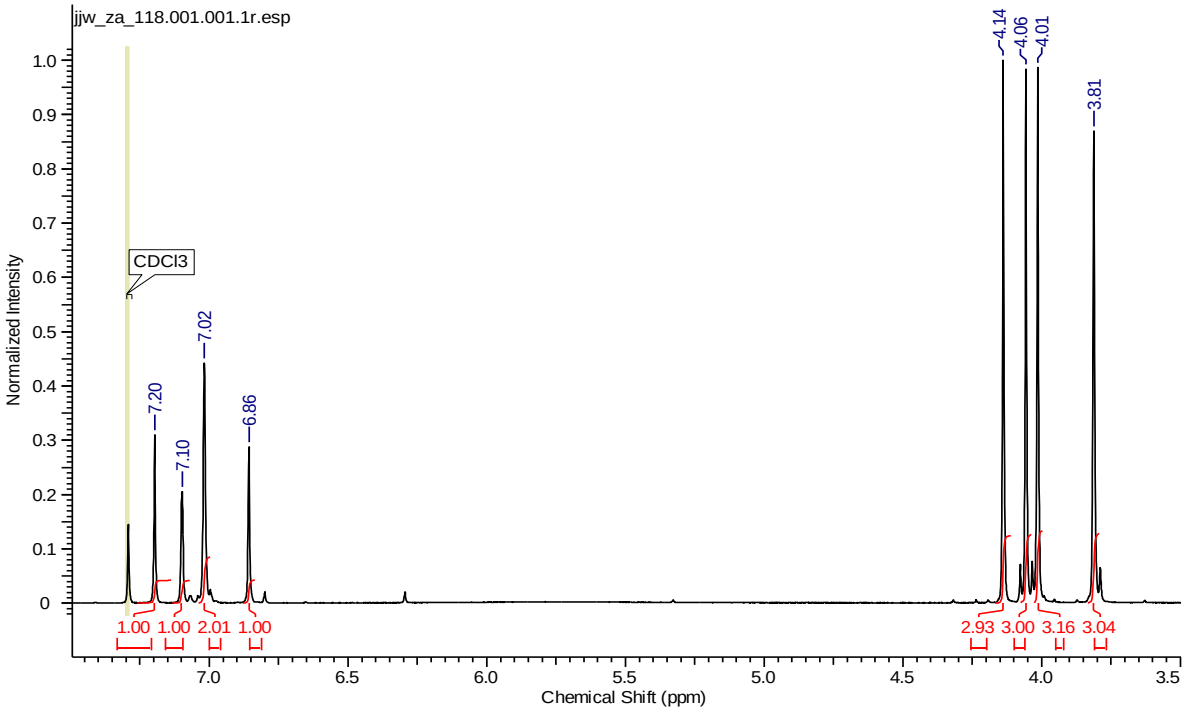

Figure 2.27. ^{1}H NMR spectrum of phenol (2.24)

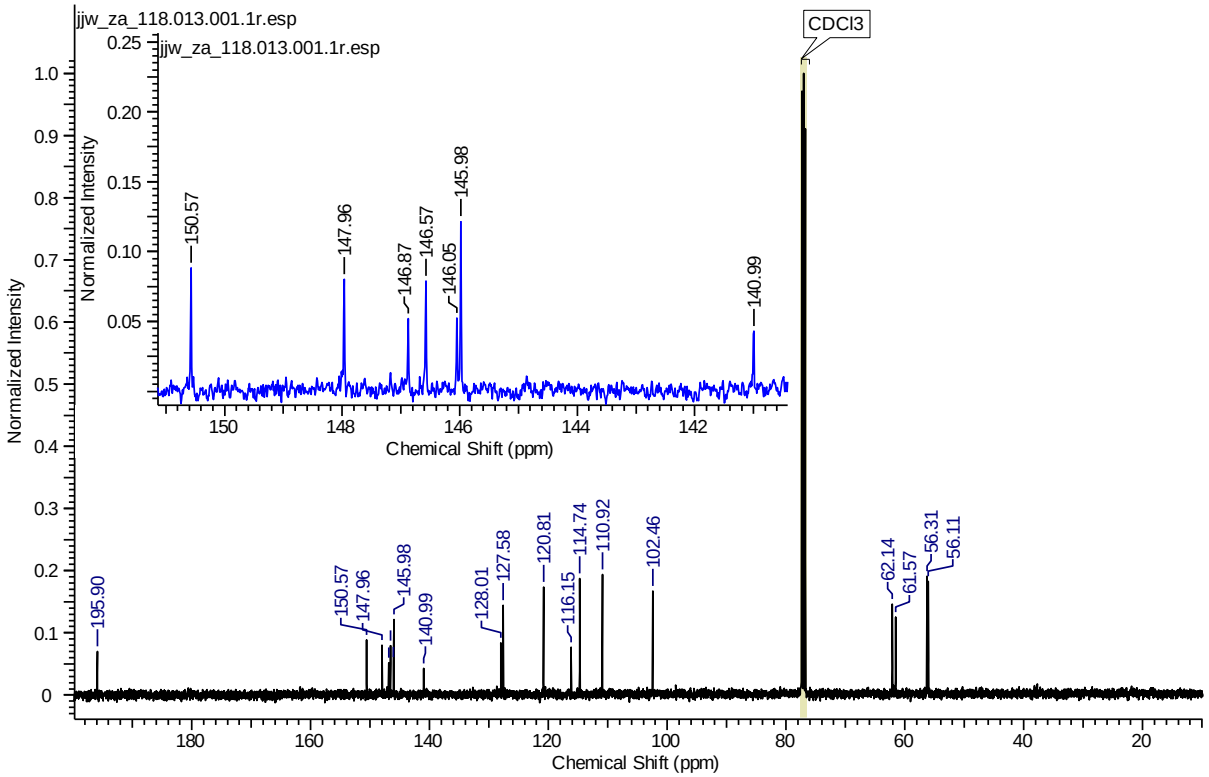

Figure 2.28. ^{13}C NMR spectrum of phenol (2.24)

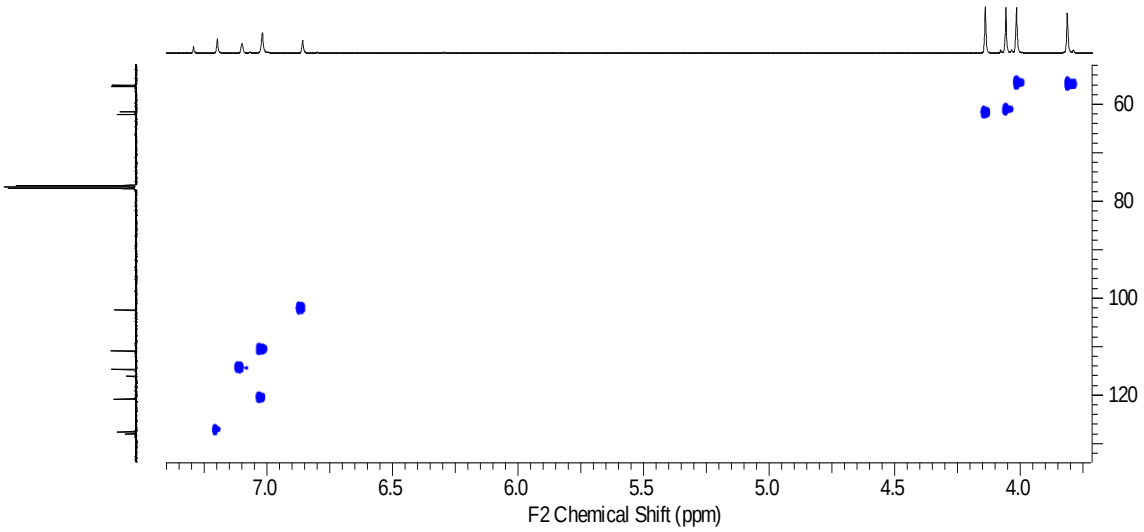

Figure 2.29. HSQC spectrum of phenol (2.24)

2.5.2 Oxime derivative of coumarin compound (2.24)

Next the simple oxime derivatives of phenol **(2.24)** was synthesised, using hydroxylamine hydrochloride with diisopropylethylamine as base and DMF as solvent (Scheme 2.21). After the aqueous work-up and purification by flash column chromatography, the oxime

derivative **(2.25)** was afforded in a yield of 80%. The structural confirmation was achieved by the disappearance of thiocarbony signal at 195.90 ppm in the ^{13}C NMR spectrum (figure 2.31) and the appearance of OH of the oxime functionality at 10.26 ppm in the ^{1}H NMR spectrum (figure 2.30). Along with NMR spectroscopy, the HRMS also found the relative molecular ion of mass 396.1068 as sodium adduct ($M+Na^{+}$).

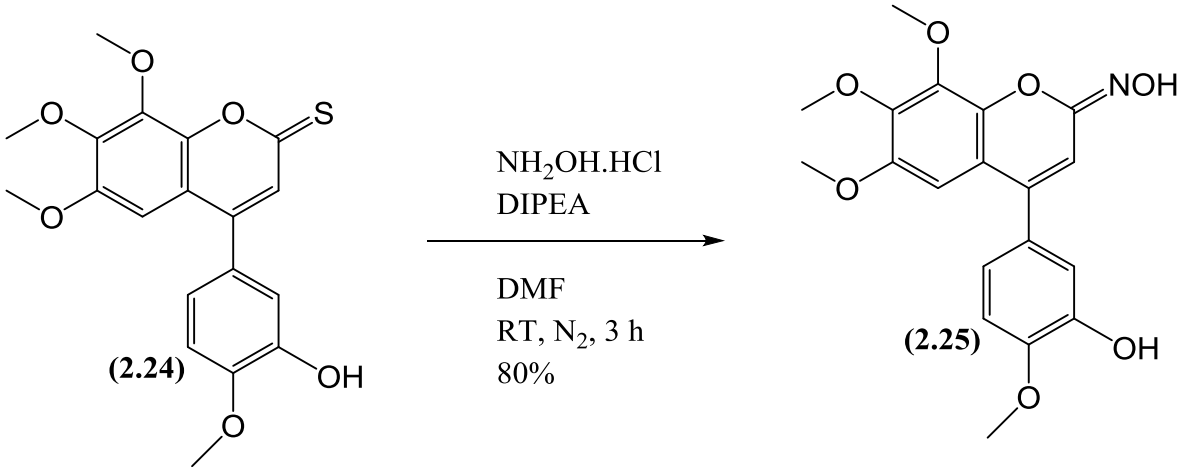

Scheme 2.21. Synthesis of oxime **(2.25)**

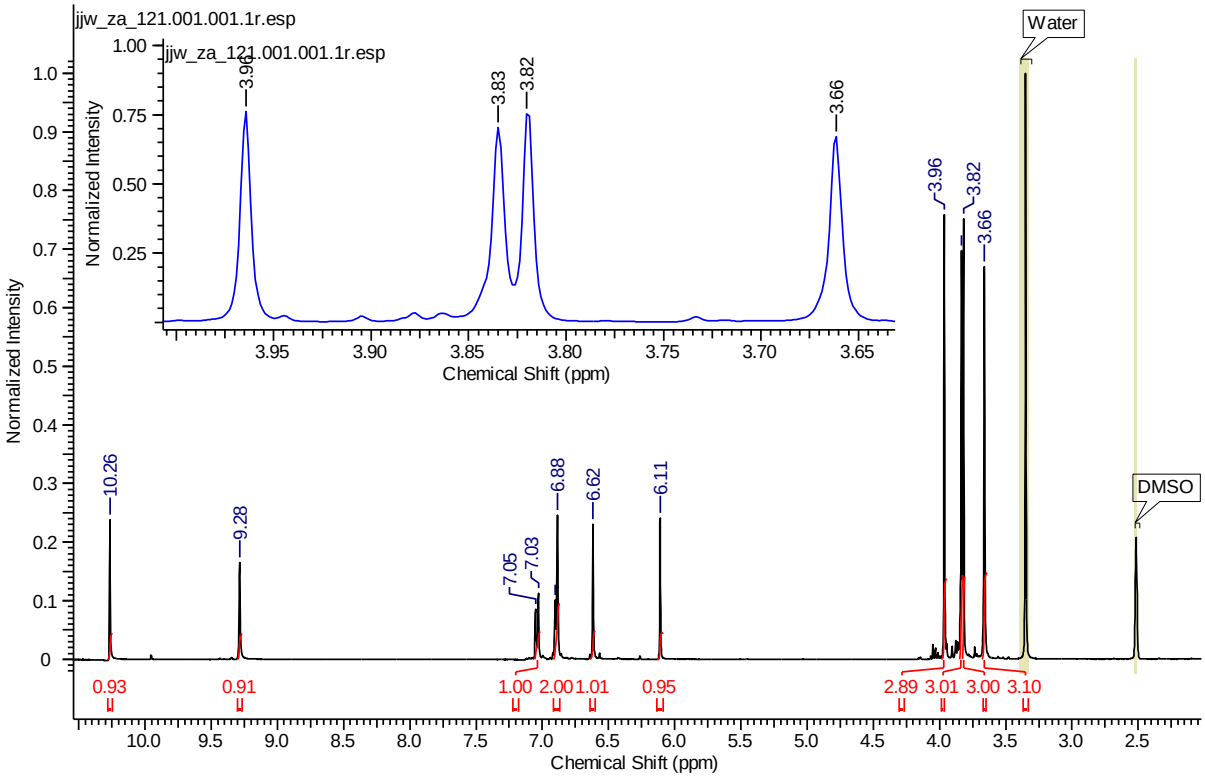

Figure 2.30. ^{1}H NMR spectrum of oxime (2.25)

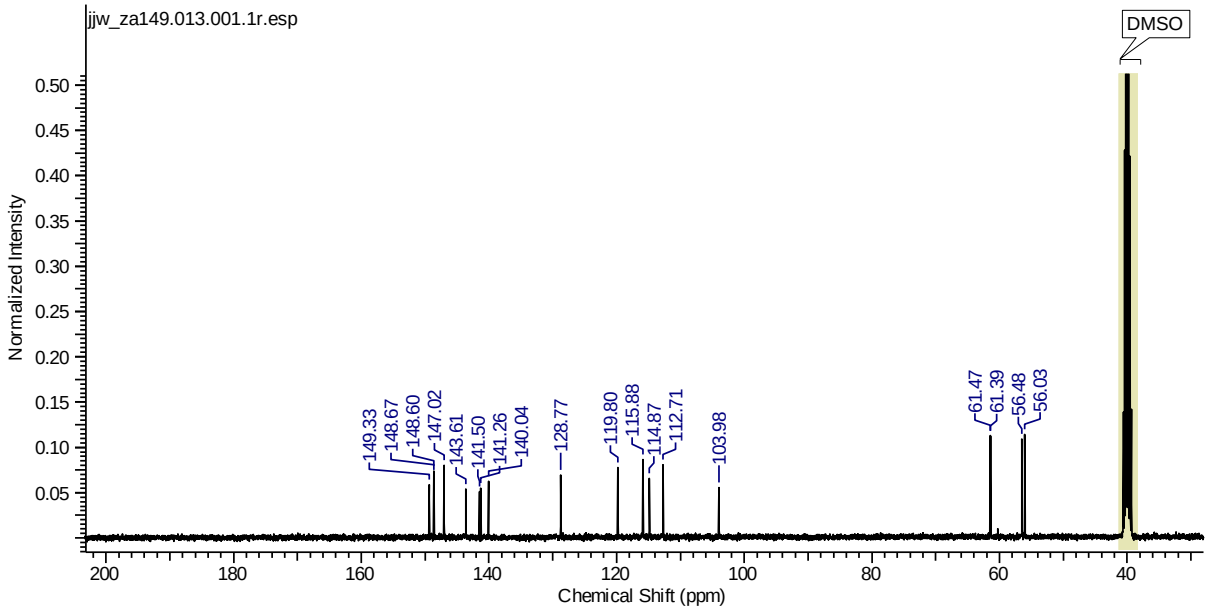

Figure 2.31. ^{13}C NMR spectrum of oxime (2.25)

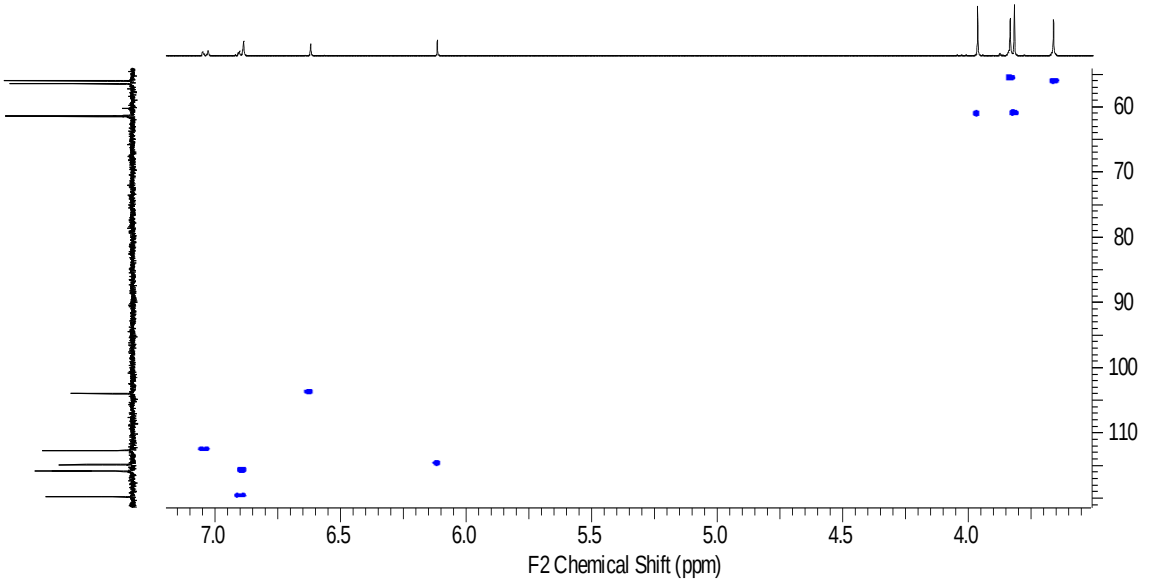

Figure 2.32. HSQC spectrum of oxime (2.25)

2.5.3 Methyl oxime derivative of coumarin compound (2.24)

Having synthesised the simple oxime derivative, we decided to obtain the methyl oxime derivative in order to compare the effect of different substituents at that specific position. For this purpose phenol **(2.24)** was refluxed with methoxyamine hydrochloride and sodium acetate in ethanol and water (Scheme 2.22) to afford the product **(2.26)** with a yield of 72%.

The proton ^{1}H NMR spectrum (figure 2.33) confirmed the presence of all 21 protons. The additional feature of the ^{1}H NMR spectrum of **(2.26)** as compared **(2.24)** includes the presence of an extra CH_3 at 3.93 ppm representing the methyl protons of methoxy amine.

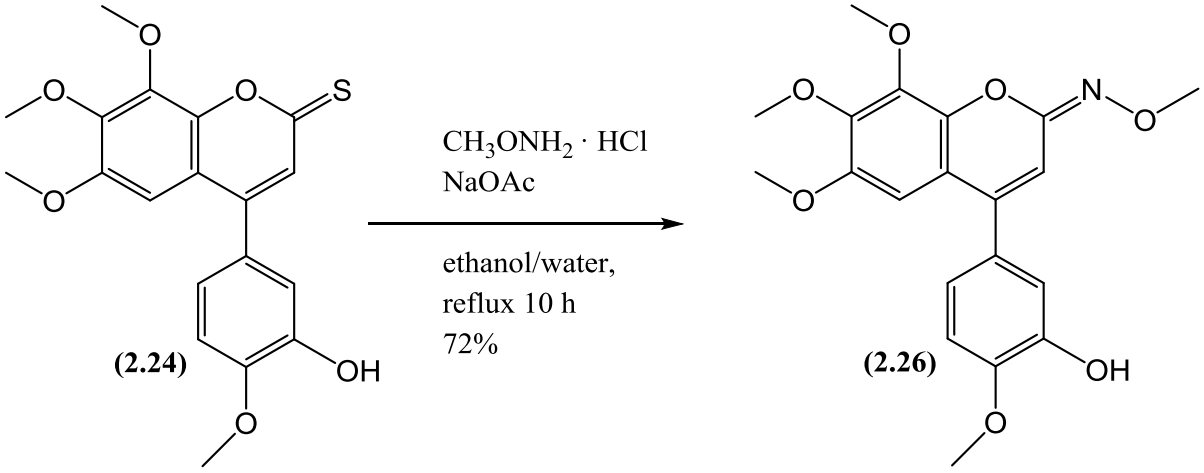

Scheme 2.22. Synthesis of methyl oxime **(2.26)**

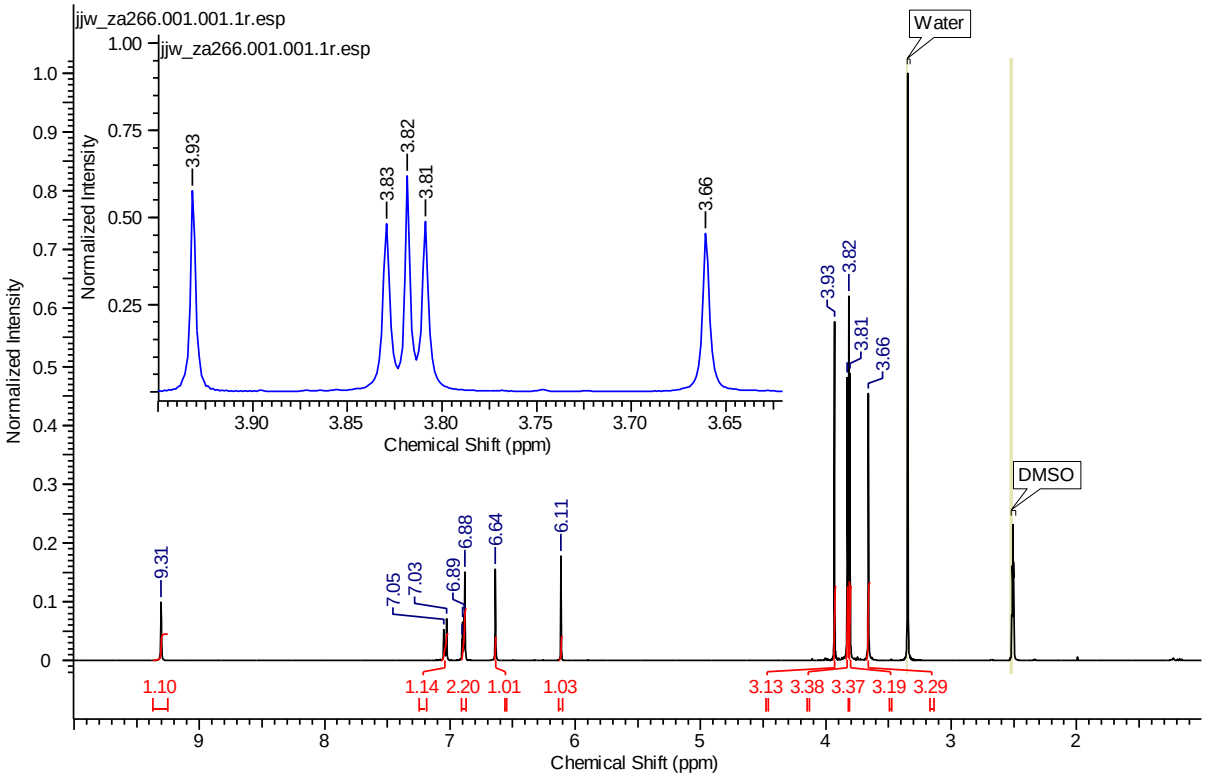

Figure 2.33. ^{1}H NMR spectrum of methyl oxime (2.26)

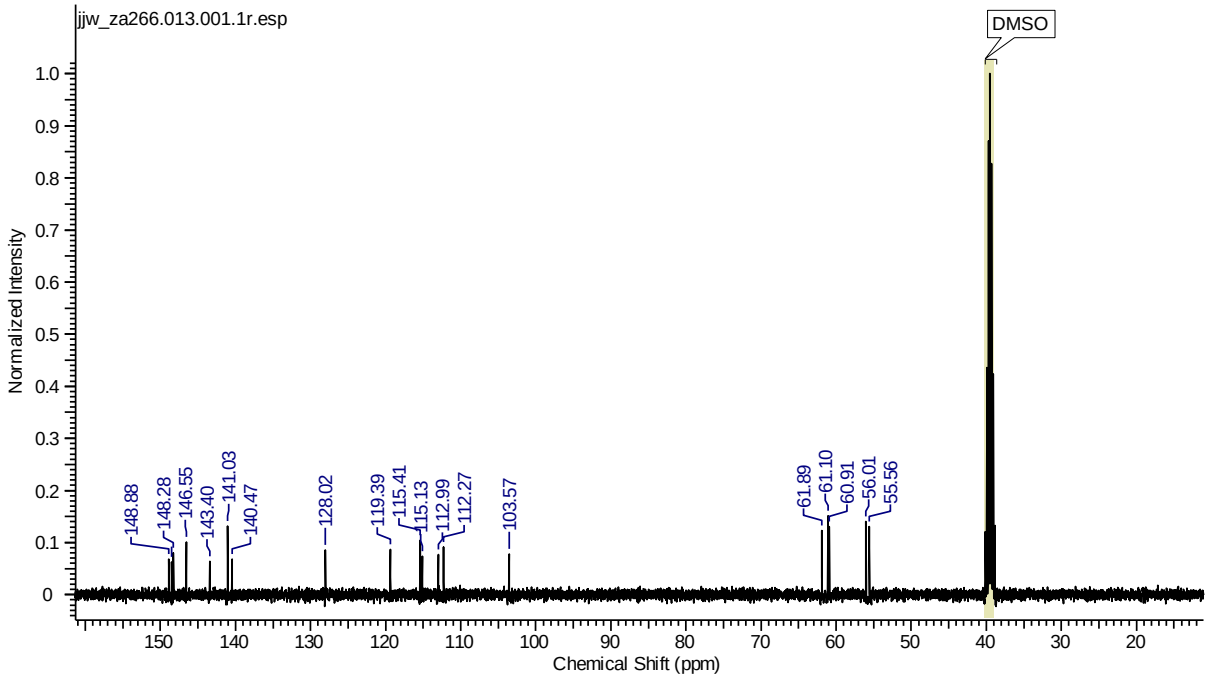

Figure 2.34. ^{13}C NMR spectrum of methyl oxime (2.26)

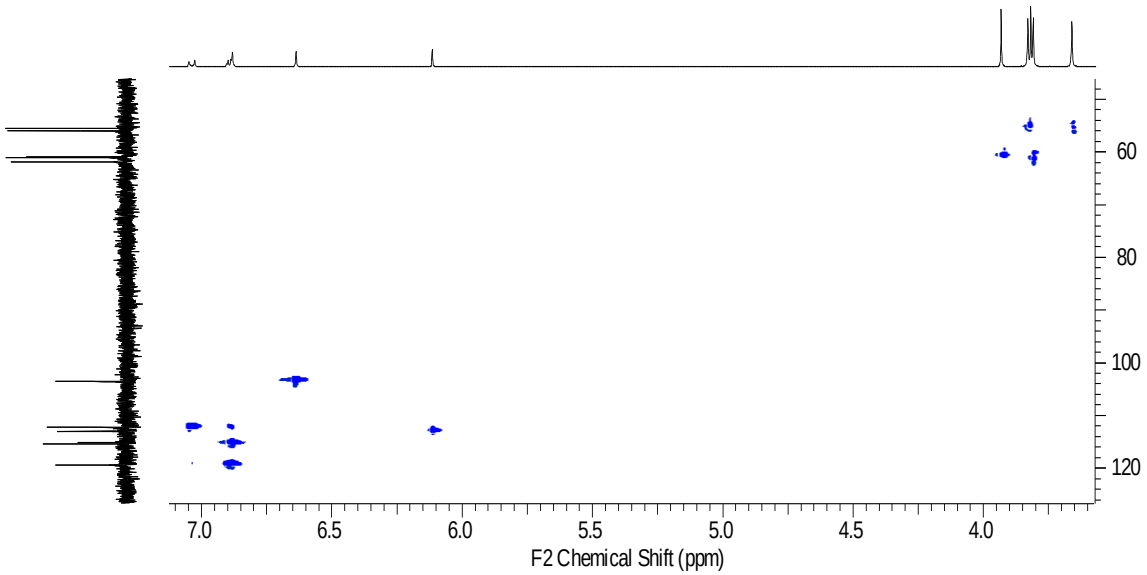

Figure 2.35. HSQC spectrum of methyl oxime (2.26)

2.6 Synthesis of Coumarin derivatives with reference to carbon (3)

One of the initial objectives of our research project was to introduce different substituents at carbon 3 of the 4-aryl coumarin derivatives (figure 2.36).

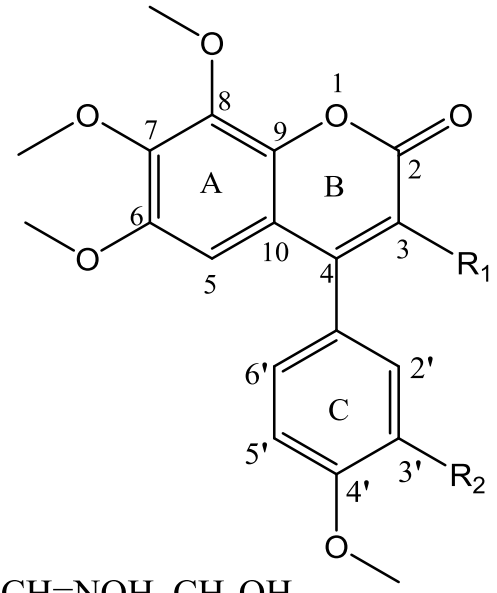

R_1=COOH, CHO,CH=NOH, CH_2OH

R_2= OH or NH_2

Figure 2.36. Proposed synthesis of 3-substituted derivatives of 4-arylcoumarins

The aim of our synthesis was to introduce carboxylate functionality at carbon 3 (C3) of 4-arylcoumarins as we were interested to assess the effects of different substituents at C3 on tubulin polymerization. It was proposed that introducing a polar functional group at C3 would improve the overall aqueous solubility of the compounds. Moreover introducing different substituents at C3 would also enable us to synthesise hybrids by attaching peptidal APN inhibitors that in turn will facilitate their targeted delivery to the tumor tissue. Along with that, the carboxylic acid functionality will enable us to introduce a hydroxamic acid functionality on to C3 to create designed multiple ligands that will have both the APN and tubulin polymerization inhibition activities.

Starting from phenol **(2.01)** the following synthetic route was suggested (Scheme 2.23).

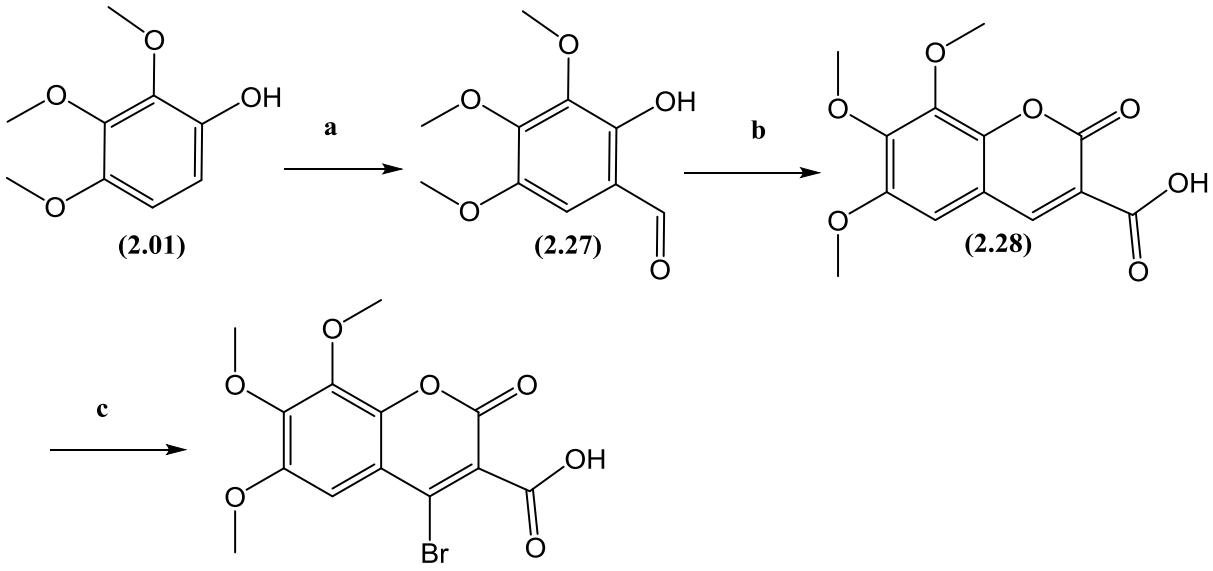

a- Orthoformylation; b-reaction with Meldrum's acid; c- attempted bromination

Scheme 2.23. Initial synthetic strategy for synthesis of 3-carboxycoumarin

The first step involved in our synthetic strategy was the orthoformylation of phenol **(2.01)**. This was successfully achieved by refluxing the phenol (**2.01)** with paraformaldehyde, anhydrous magnesium chloride beads and triethylamine in anhydrous THF (Scheme 2.24). The success of orthoformylation was confirmed by ^{1}H NMR spectrum (figure 2.37) due to the disappearance of one aryl proton as well as the appearance of proton of aldehyde at11.01 ppm. Moreover ^{13}C spectrum also has an additional carbonyl peak of the aldehyde at 194.43 ppm.

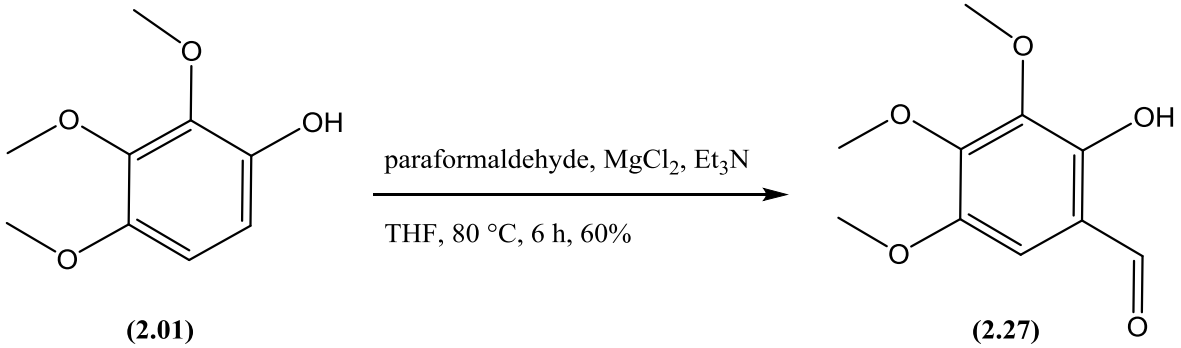

Scheme 2.24. Orthoformylation of phenol **(2.01)**

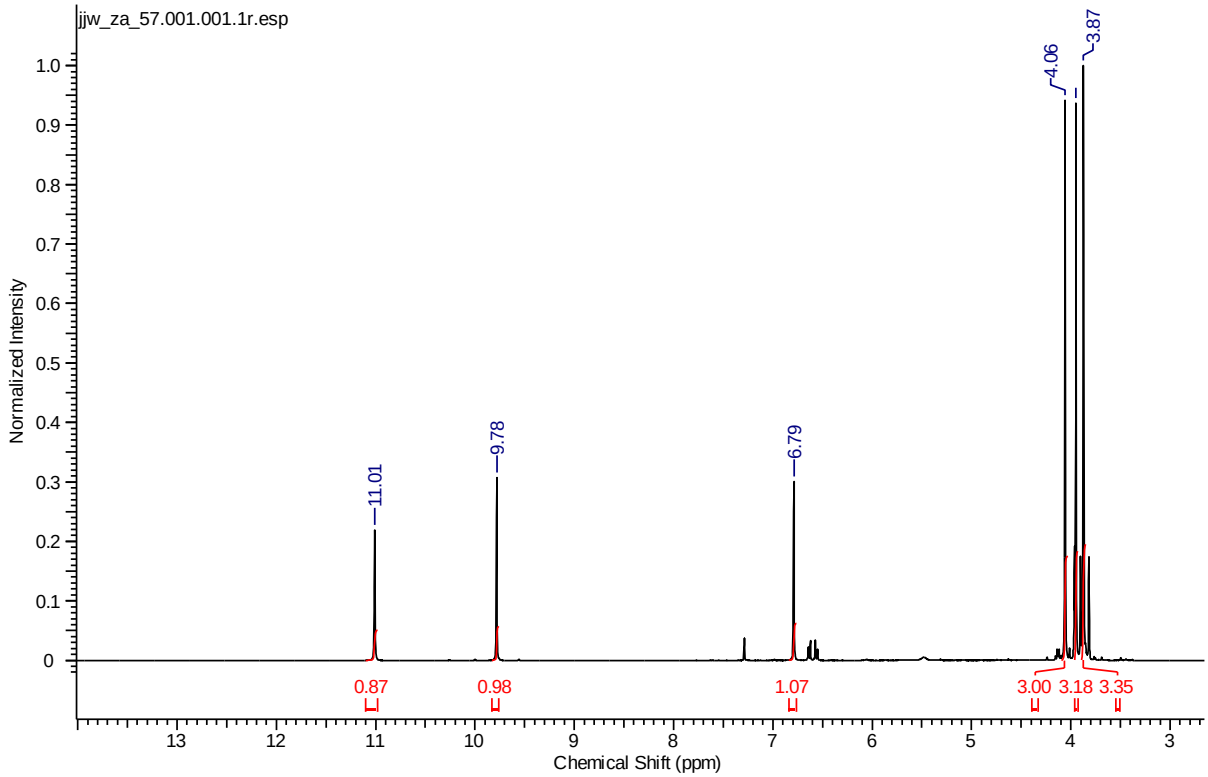

Figure 2.37. ^{1}H NMR spectrum of ortho hydroxybenzaldehyde (2.27)

Having secured the hydroxybenzaldehyde **(2.27)**, our next step was the reaction with Meldrum's acid. This was achieved by refluxing hydroxybenzaldehyde with Meldrum's acid in pyridine (Scheme 2.25). After the completion the reaction mixture was quenched with 2 M HCl and extracted with DCM. Upon evaporating the organic solvent, the crude solid obtained was washed with methanol to afford the carboxycoumarin **(2.28)** in 63% yield. The presence of alkene and carboxylic protons at 6.89 and 12.34 ppm respectively in the ^{1}H NMR spectrum (figure 2.38) confirmed the generation of carboxycoumarin **(2.28)** .

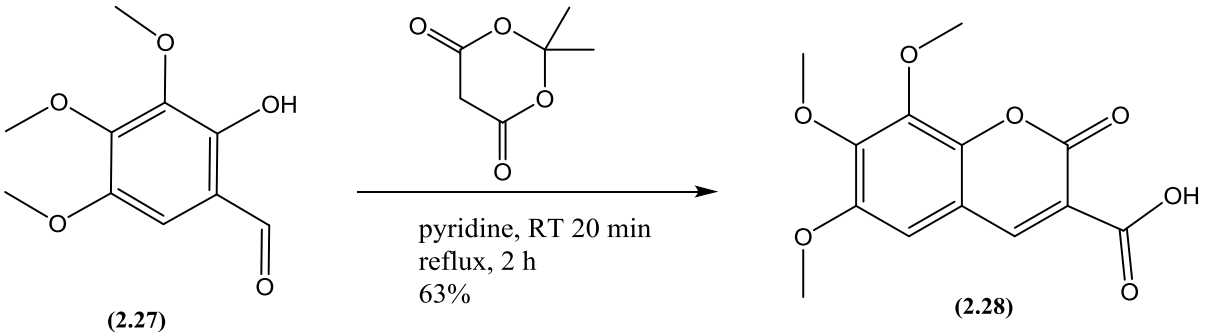

Scheme 2.25. Coupling of 2-hydroxy-3,4,5-trimethoxybenzaldehyde **(2.27)** to Meldrum's acid

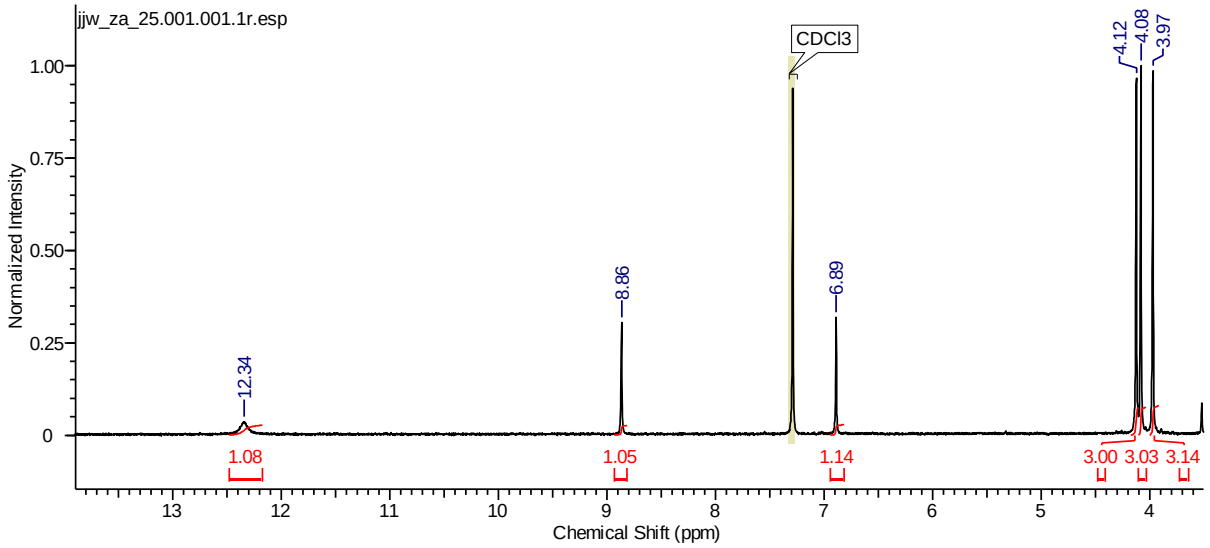

Figure 2.38. ^{1}**H NMR spectrum of 3-carboxycoumarin (2.28)**

Once we synthesised 3-carboxycoumarin, we decided to brominate compound **(2.28)** in order to convert it into a suitable substrate for Suzuki coupling that would allow us to couple the C-ring on to it. For this purpose the coumarin-3-carboxylic acid **(2.28)** was treated with pyridinium tribromide in DCM at room temperature. After the acidic work-up and purification the product obtained was analysed by NMR spectroscopy, which confirmed the bromination of aryl Carbon 5 instead of desired carbon 4 (Scheme 2.26).

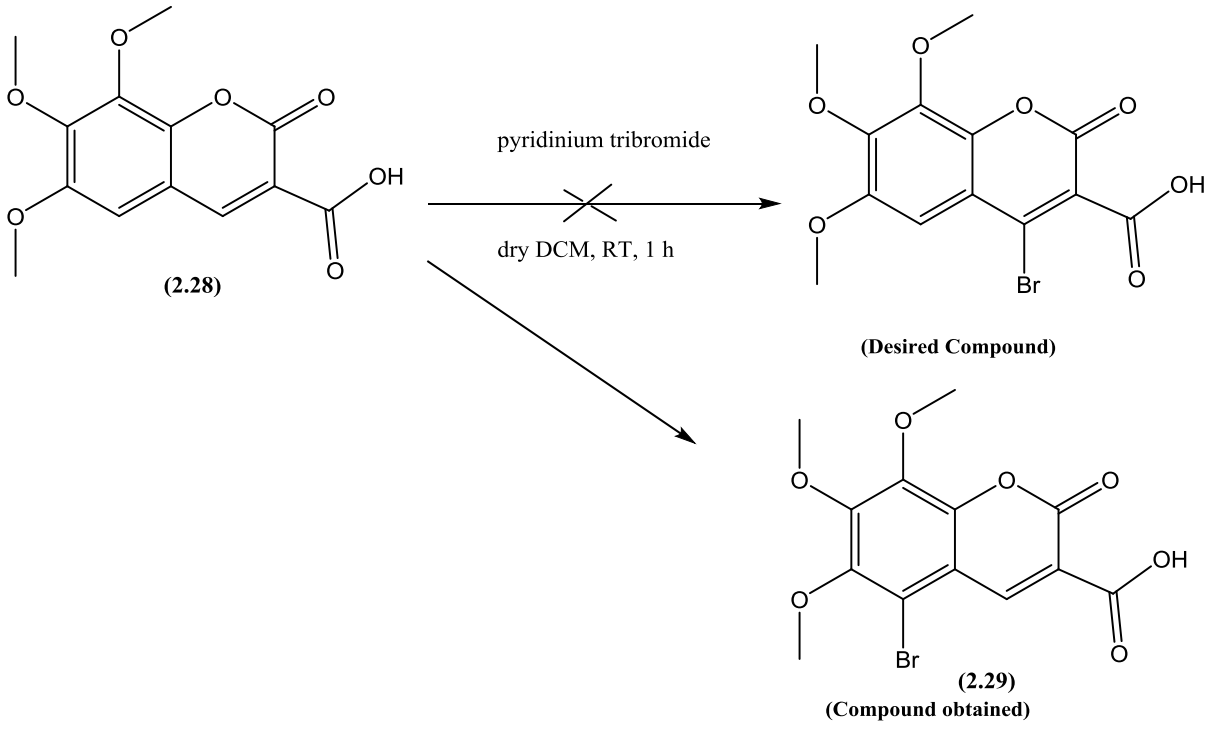

Scheme 2.26. Attempted bromination of 3-carboxycoumarin **(2.28)**

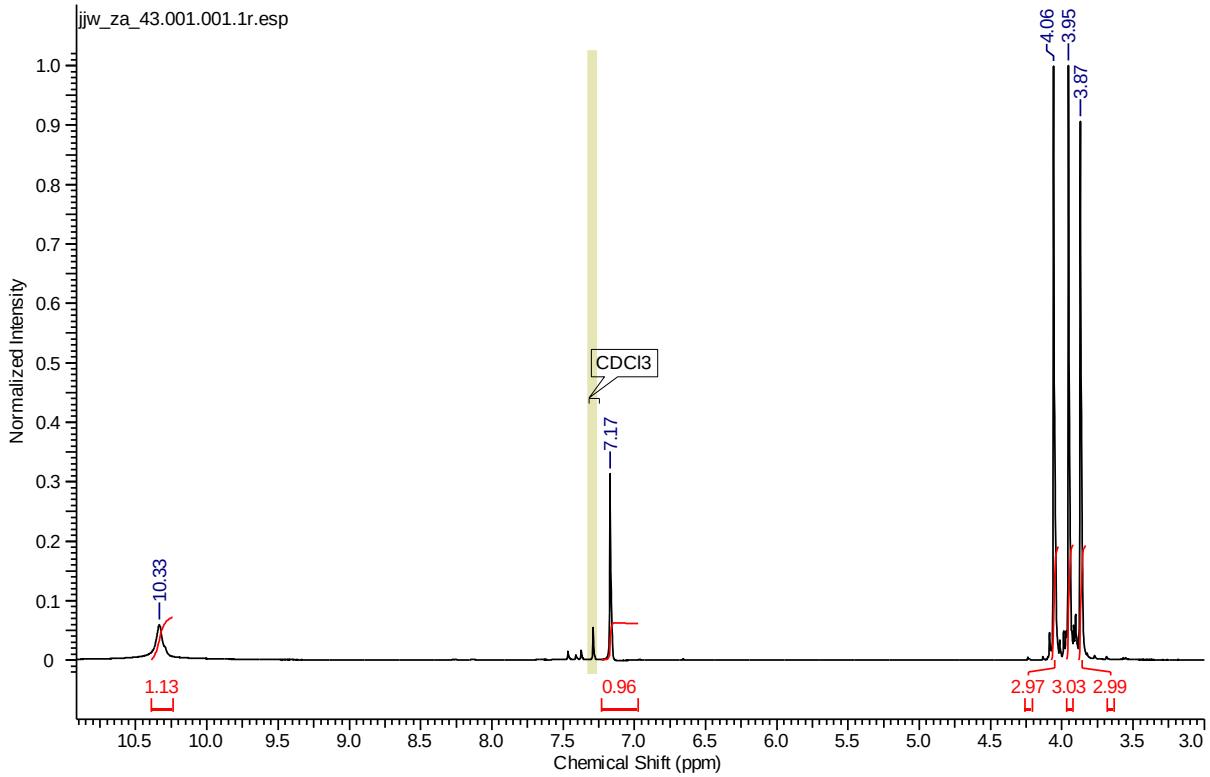

Figure 2.39. ^{1}**H NMR spectrum of compound (2.29)**

2.6.1 Different strategy for synthesis of 3-carboxycoumarin

Since our previous attempt to synthesis 4-bromo-3-carboxycoumarin ended with failure because of the unwanted bromination at aryl C5. As it was desired to have a bromo or triflate group at C4 because both of them would serve as excellent substrates for Suzuki coupling of our Aryl C-ring which is crucial for tubulin binding activity. We decided to adopt another alternate stepwise approach to synthesise 4-hydroxy-3-carboxycoumarin where in the final step, the hydroxy functionality could be converted to a triflate group which would be useful for coupling of our C-aryl ring. The following alternate stepwise approach was suggested (Scheme 2.27).

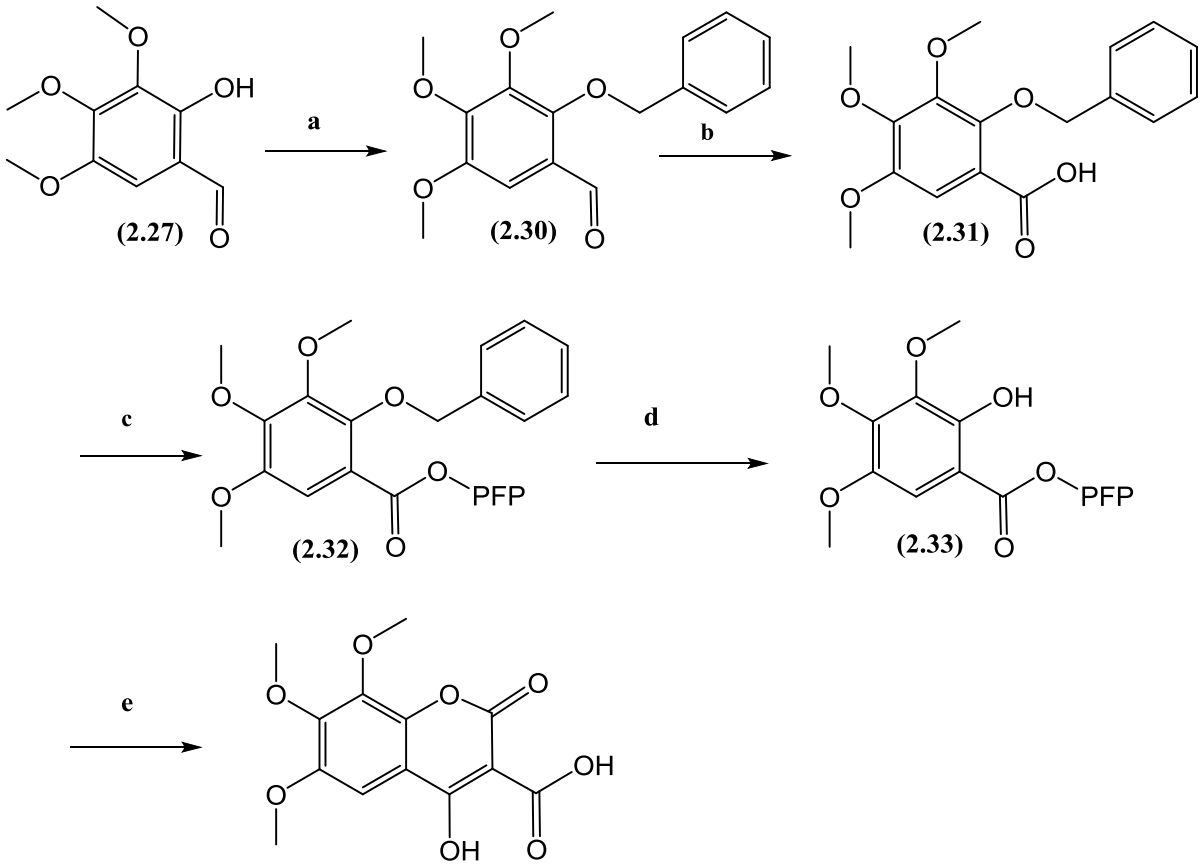

a- Benzyl protection ; b- Oxidation of benzaldehyde ; c- Activation of acid as pentafluorophenyl ester d- Deprotection of benzyl group e- Reaction with Meldrum's acid

Scheme 2.27. Different Synthetic approach for synthesis of 3-carboxycoumarin

According to our new approach to synthesise 3-carboxy coumarin, the phenolic functional group of *ortho* hydroxy benzaldehyde **(2.27)** was protected with a benzyl protecting group. This was achieved by stirring *ortho* hydroxy benzaldehyde with benzyl bromide and caesium carbonate in anhydrous DMF under an atmosphere of nitrogen (Scheme 2.28). After the aqueous work-up and purification by flash column chromatography the benzyl protected compound **(2.30)** was afforded with the yield of 57%. The protection of the phenol was confirmed by the presence of the CH_2 of the benzyl group resonating as singlet at 5.14 ppm, with an integral value of 2 H, and the additional five aromatic protons spanning 6.5-7.5 ppm in the ^{1}H NMR spectrum (figure 2.40).

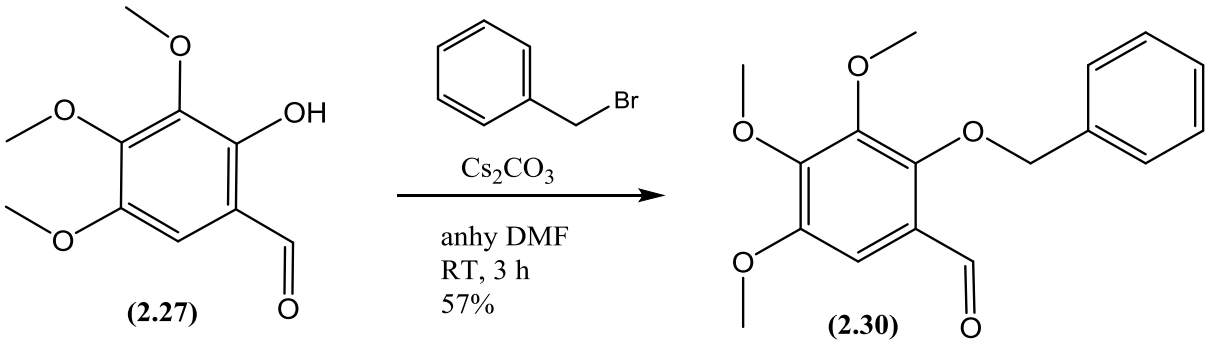

Scheme 2.28. Benzyl protection of hydroxy benzaldehyde **(2.27)**

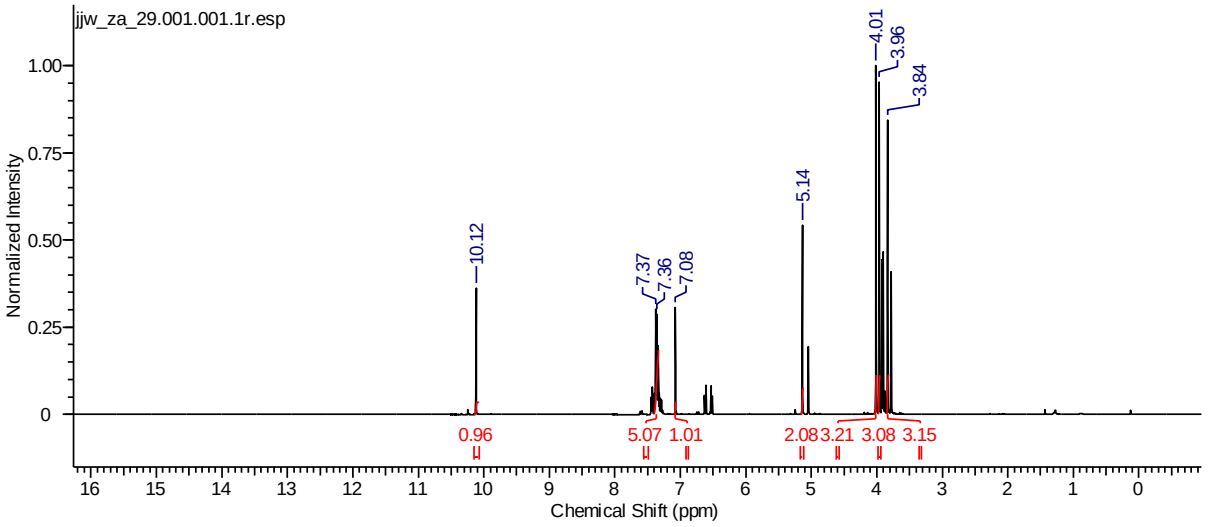

Figure 2.40. ^{1}H NMR spectrum of Compound (2.30)

The resultant benzyl protected benzaldehyde **(2.30)** was oxidized to benzoic acid using $KMnO_4$ as an oxidizing agent in an acetone (8.5 mL), water (1.9 mL) and acetic acid (0.4 mL) solution (Scheme 2.29). After aqueous work-up and purification by column chromatography the desired product **(2.31)** was obtained in 71% yield. The structural identity was confirmed by the presence of carbonyl carbon of the acid at 164.5 ppm in the ^{13}C spectrum (figure 2.42). Moreover the ^{1}H NMR spectrum (figure 2.41) also contains the desired number of aryl, methylene and methoxy protons.

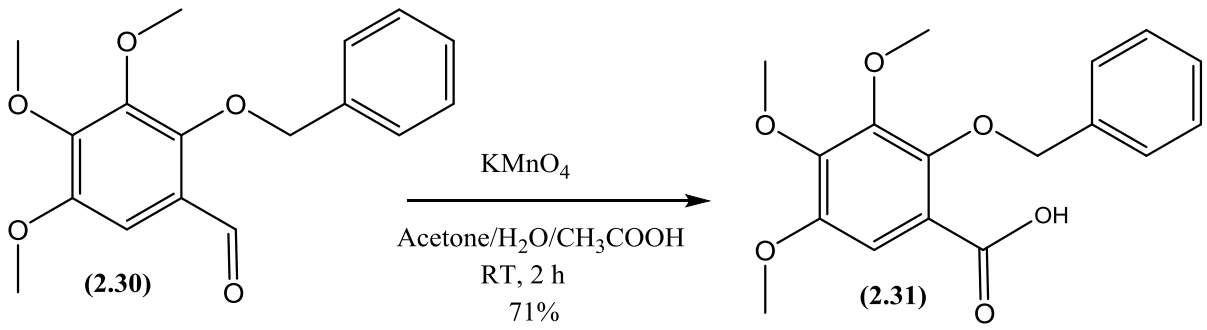

Scheme 2.29. Oxidation of benzaldehyde **(2.30)**

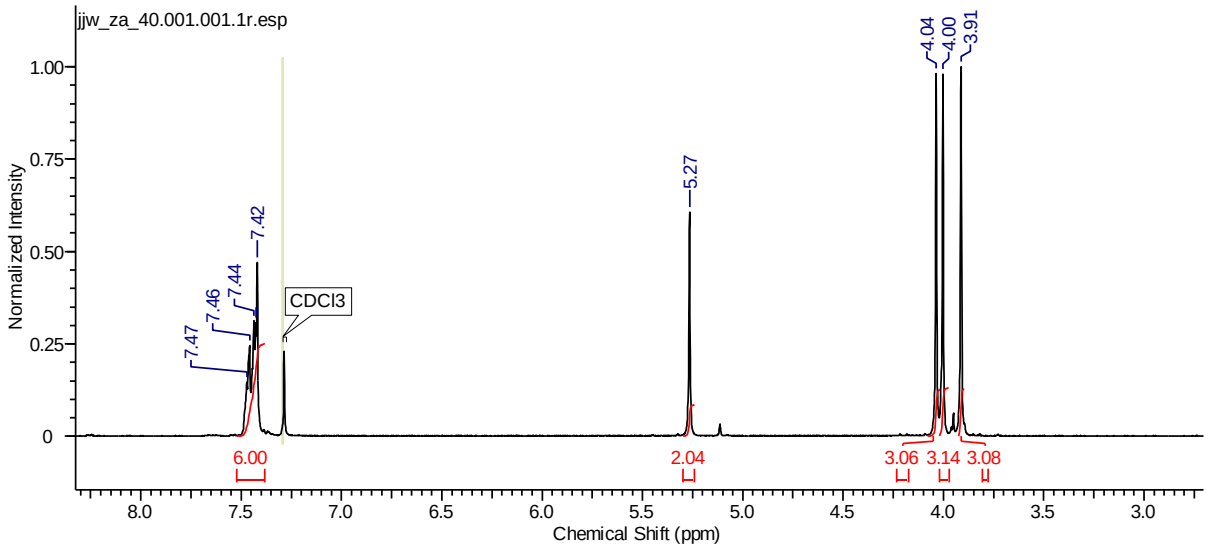

Figure 2.41. ^{1}H NMR spectrum of benzoic acid (2.31)

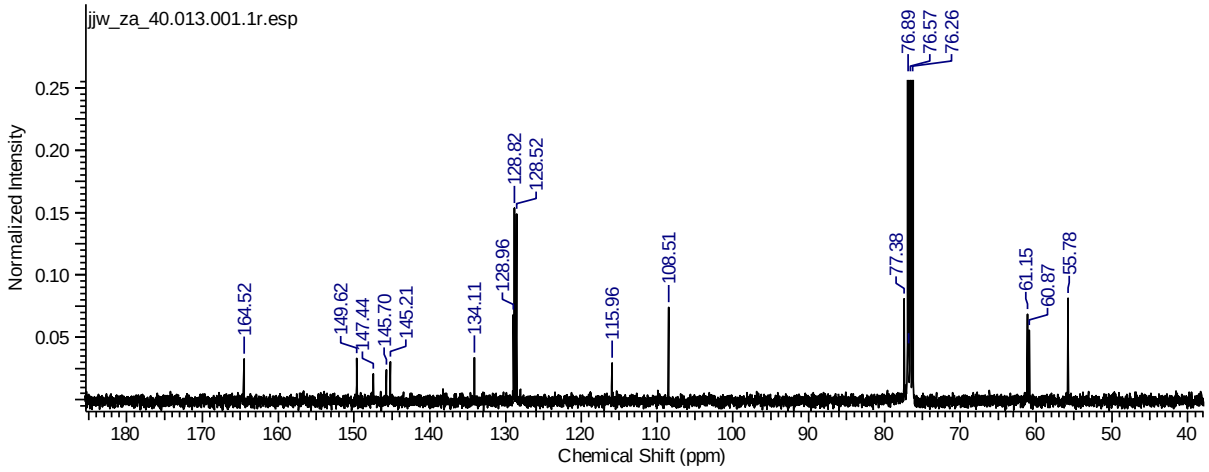

Figure 2.42. ^{13}C NMR spectrum of benzoic acid (2.31)

Having secured the protected benzoic acid **(2.31)**, our next step was to convert the acid in to the pentafluorophenyl ester in order to have a better leaving group. For that purpose, the

benzoic acid was stirred with pentafluorophenol in dry DCM using EDC.HCl as coupling reagent (Scheme 2.30).

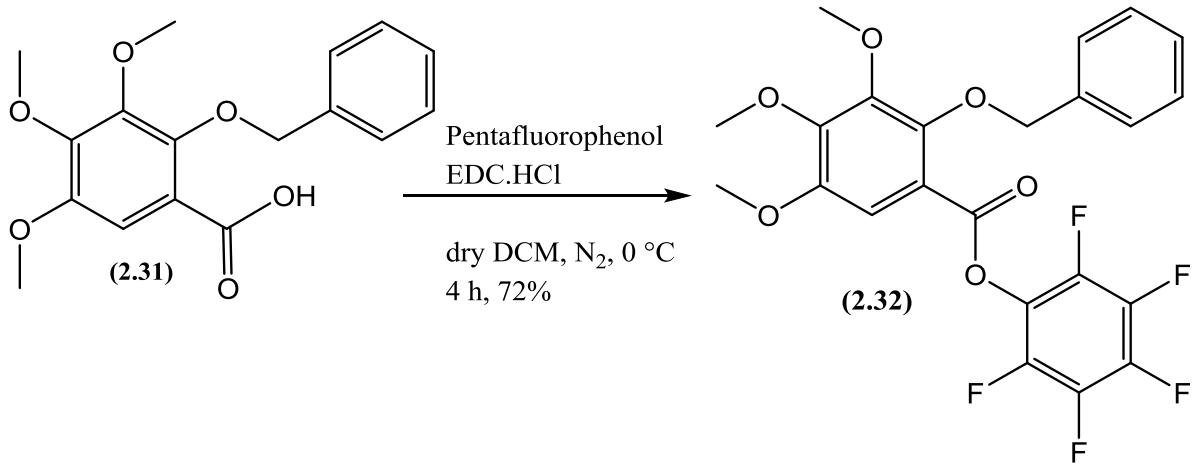

Scheme 2.30. Activation of benzoic acid (2.31)

The next step involved in the synthesis was the removal of benzyl protecting group. This was achieved by treating compound **(2.32)** with Pd/C (10% by weight) under the atmosphere of hydrogen (Scheme 2.31). Once isolated and purified, the structural identity was confirmed by the disappearance of benzyl protecting group as well as the appearance of phenolic OH (9.80 ppm) in the ^{1}H NMR spectrum (figure 2.43) of compound **(2.33)**.

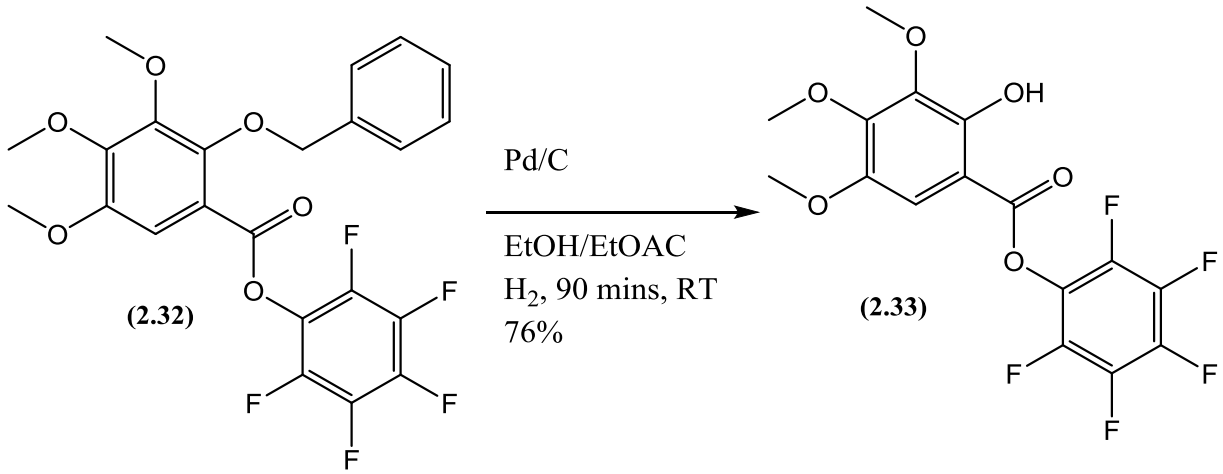

Scheme 2.31. Removal of benzyl protecting group

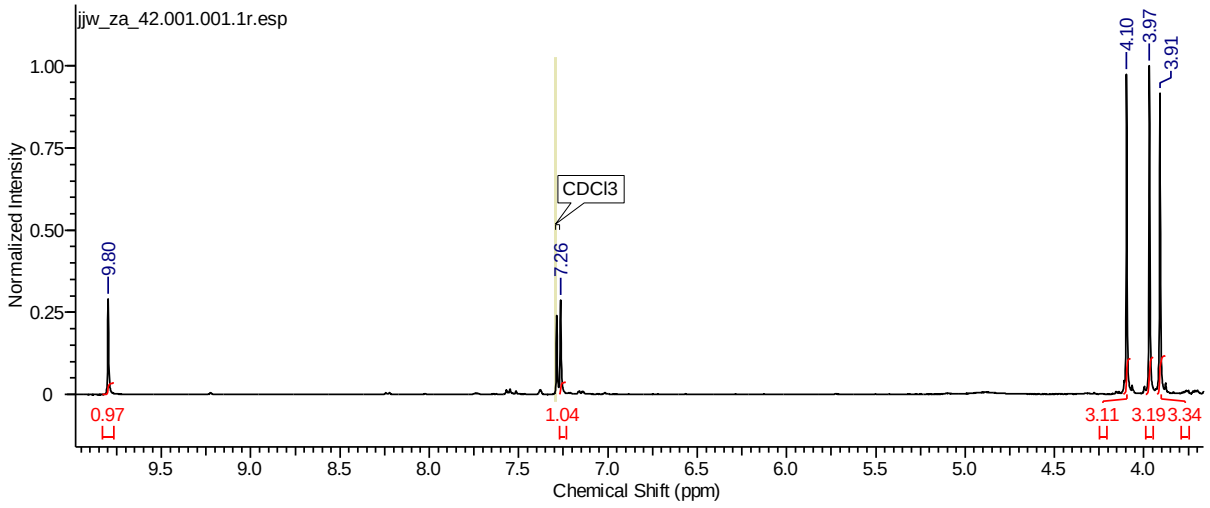

Figure 2.43. ^{1}H NMR spectrum of (2.33)

Once the activated ester **(2.33)** was obtained, the final step in our synthetic sequence was coupling with Meldrum's acid and intramolecular cyclization. For this purpose the activated ester was stirred and refluxed with Meldrum's acid in pyridine. After acidic work-up and purification by column chromatography, the unfortunate hydrolysis of the pentafluorophenyl ester and the generation of hydroxybenzoic acid was confirmed by the ^{1}H NMR spectrum (figure 2.44) and ^{13}C NMR spectrum (figure 2.45), instead of the desired carboxycoumarin compound (Scheme 2.32).

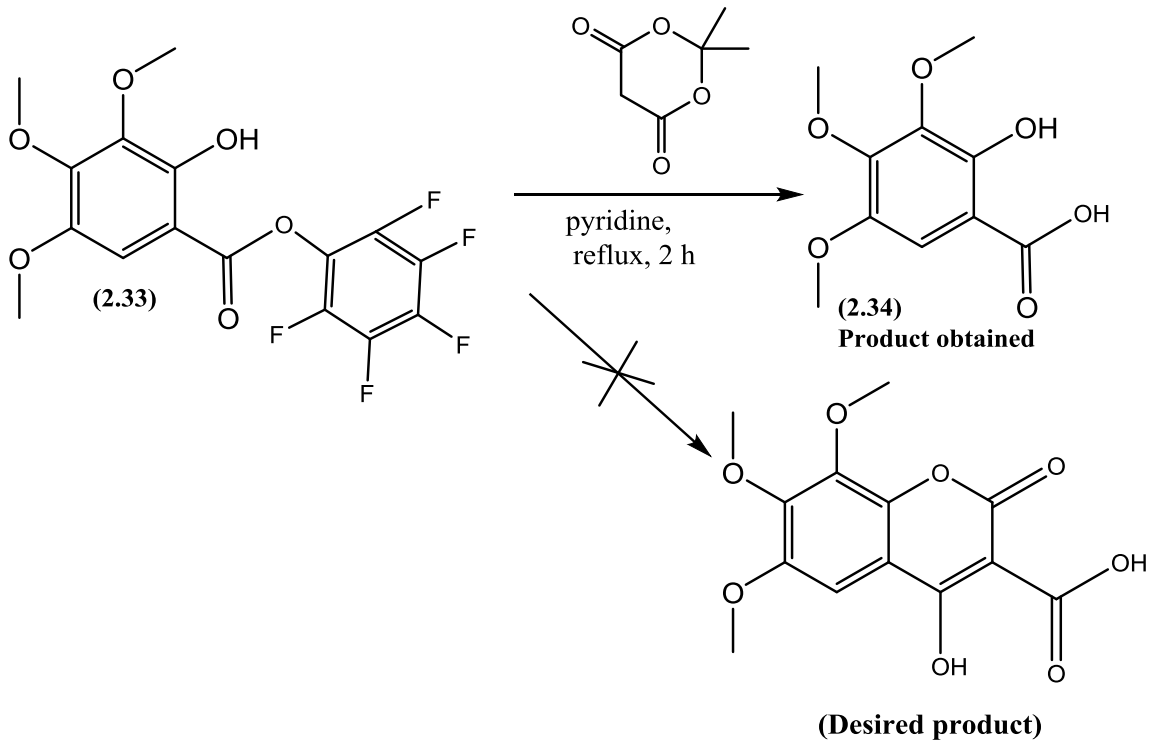

Scheme 2.32. Hydrolysis of pentafluorophenyl ester **(2.33)**

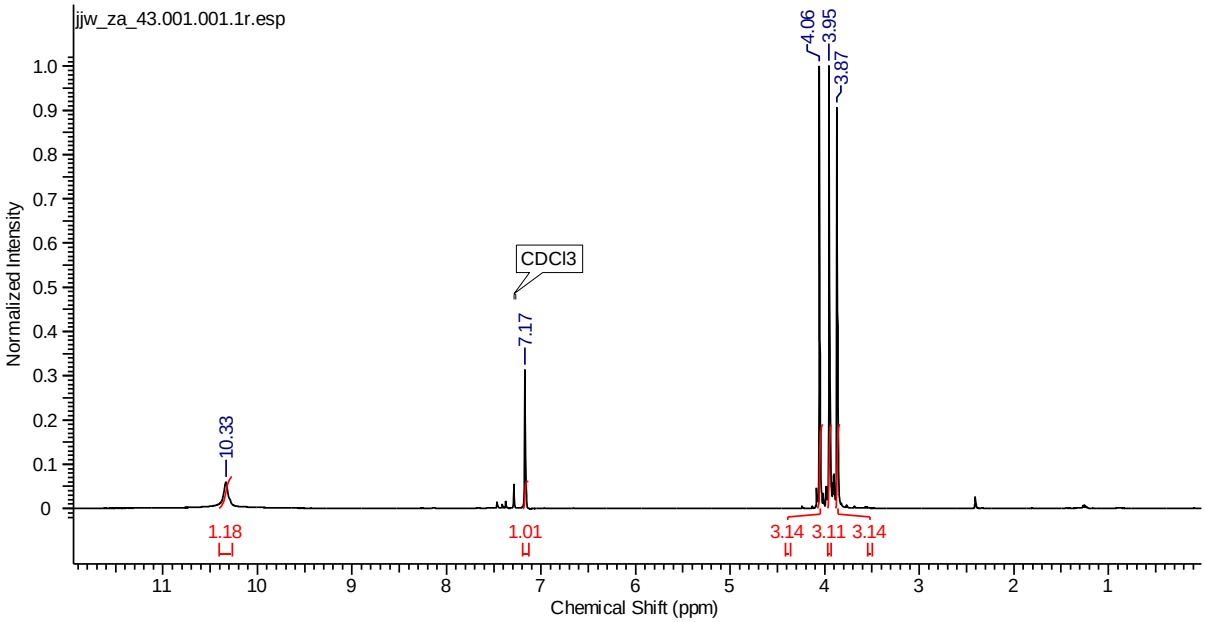

Figure 2.44. ^{1}H NMR spectrum of hydroxybenzoic acid (2.34)

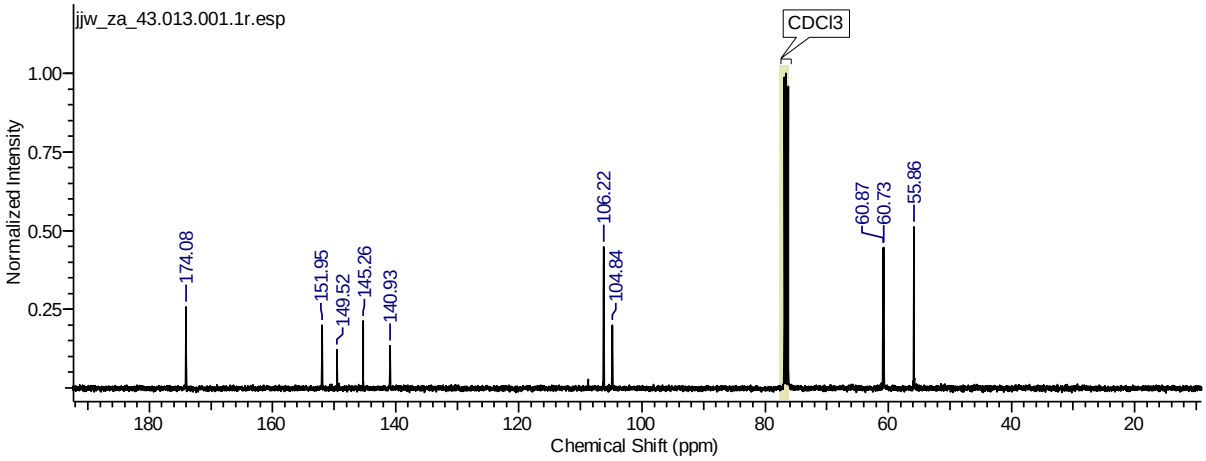

Figure 2.45. ^{13}C NMR spectrum of (2.34)

2.6.2 Attempted synthesis of 3-carboxy-4-phenyl coumarin through Grignard reaction

Having been unsuccessful up to this point with the introduction of the carboxylic functionality at position 3, an alternative approach was adopted centring on first synthesising a phenstatin intermediate employing Grignard coupling as the key step in its synthesis (Scheme 2.33).

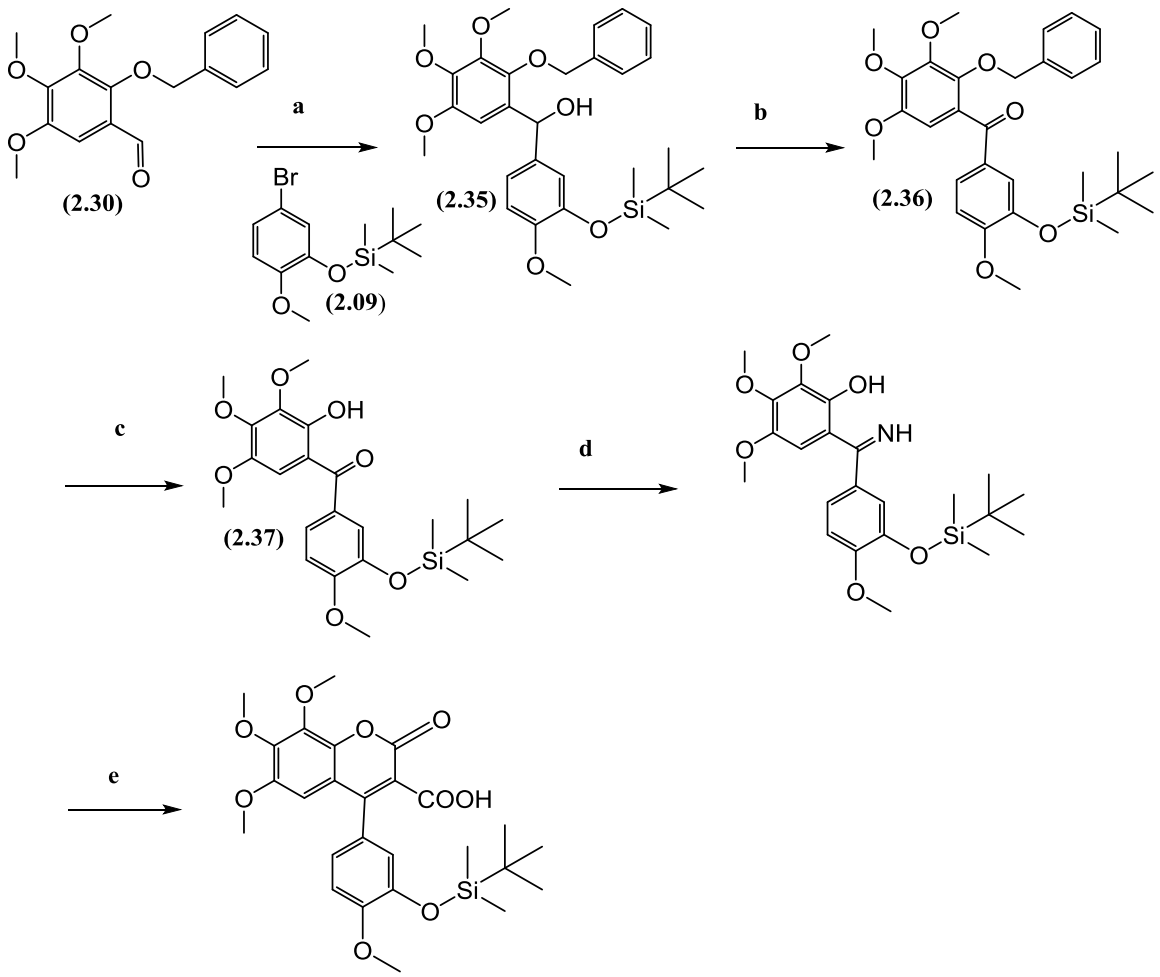

a- Grignard reaction ; b- Oxidation ; c- Removal of benzyl group d- conversion of ketone to the corresponding ketimines e- reaction with meldrum's acid

Scheme 2.33. Attempted route for synthesis of 3-carboxy-4-phenylcoumarin

The first step involves the Grignard reaction of the protected hydroxy benzaldehyde **(2.30)** with the C-ring **(2.09)** (Scheme 2.34). The reaction was carried out under strict anhydrous conditions under nitrogen atmosphere. After acidic work-up and purification by column chromatography, the structural identity of the compound **(2.35)** was confirmed by inspection of its ^{1}H NMR spectrum (figure 2.46) which showed the desired number of aryl protons, methoxy groups as well as both the silyl and benzyl protecting groups.

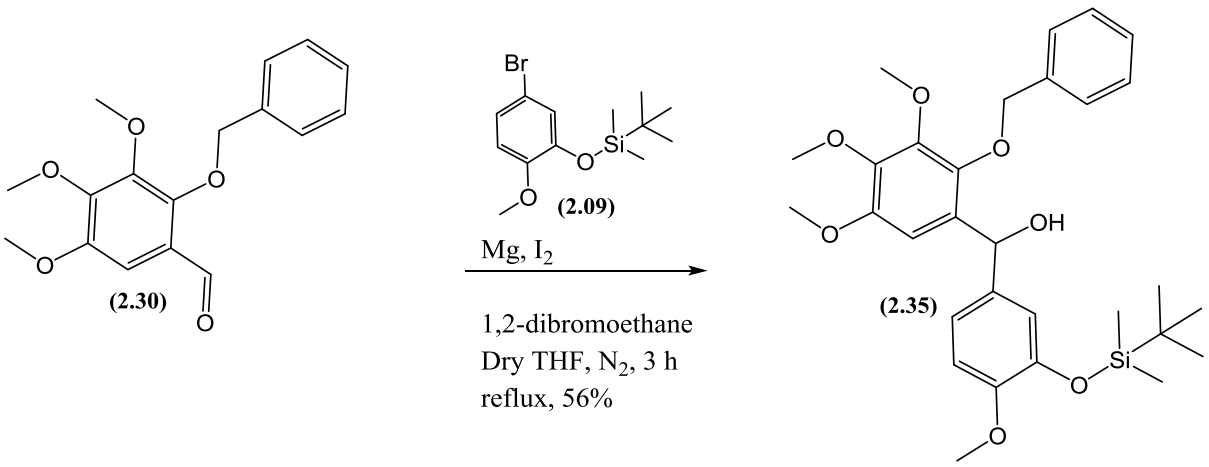

Scheme 2.34. Grignard coupling

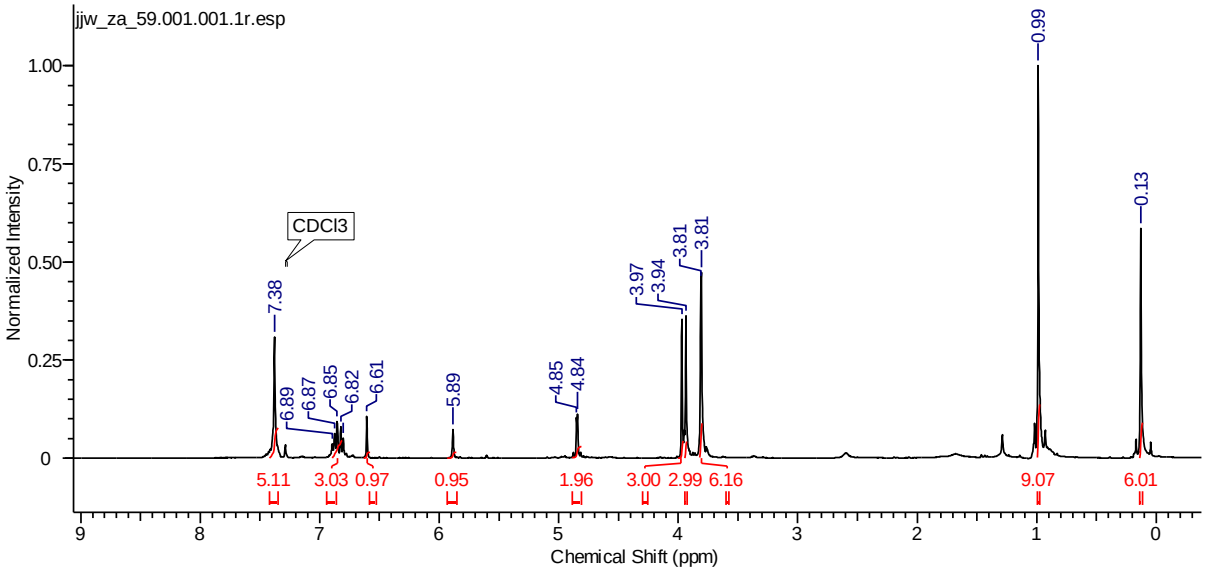

Figure 2.46. ^{1}H NMR spectrum of (2.35)

The alcohol functionality of the compound **(2.35)** was oxidized to its corresponding ketone derivative using Dess-Martin periodinane in DCM at 0 °C (Scheme 2.35). Work-up and purification by flash column chromatography afforded the desired benzophenone intermediate **(2.36)** in 83% yield. The oxidation product was confirmed by following analysis of its NMR spectra. In the ^{1}H NMR spectrum (figure 2.47) the expected absence of the proton signals for CHOH as well as the presence of carbonyl functionality (193.74 ppm) in the ^{13}C spectrum (figure 2.48) of compound **(2.36)** confirmed the oxidation reaction had occurred.

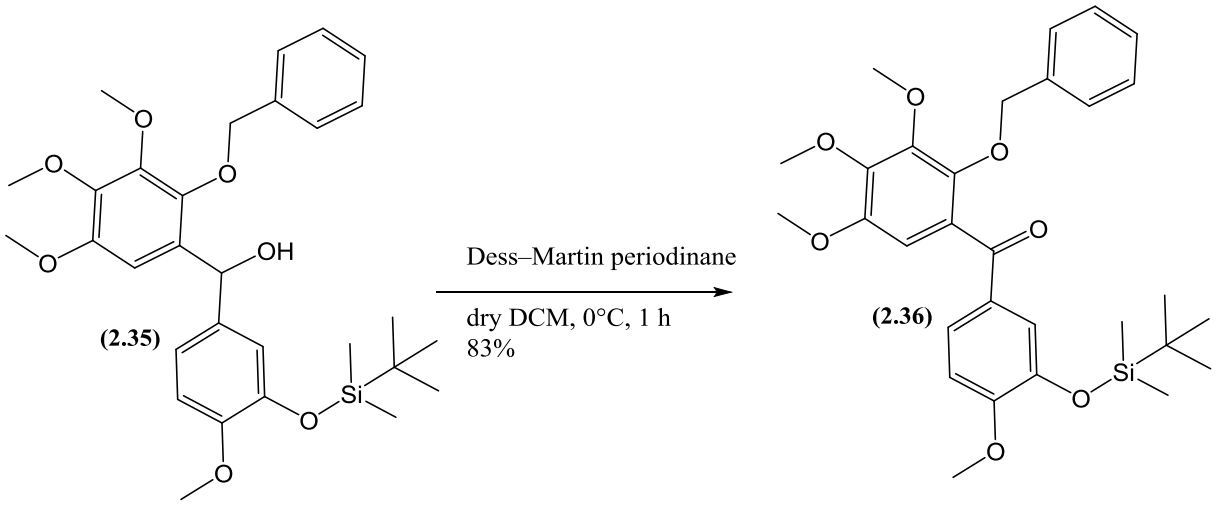

Scheme 2.35. Oxidation of alcohol to ketone

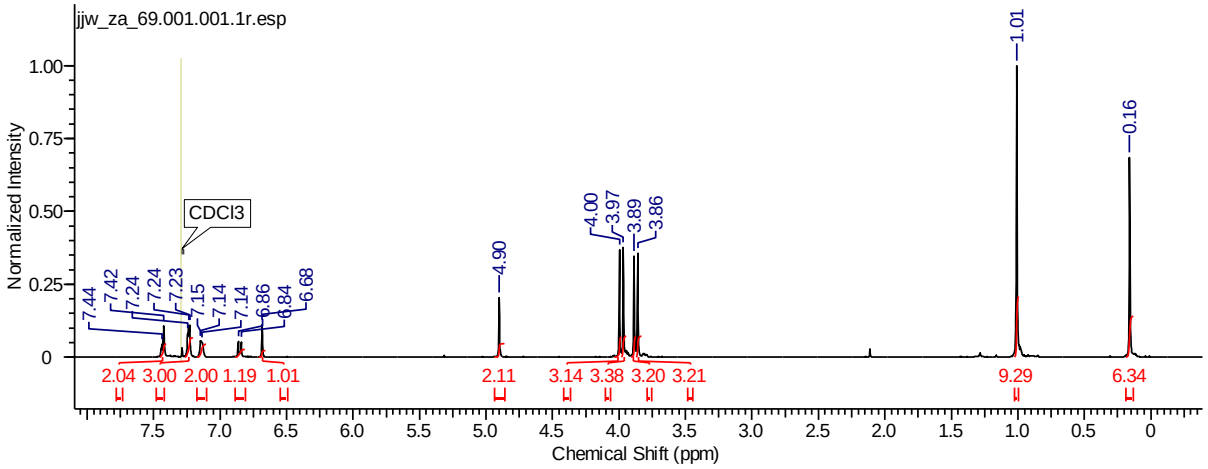

Figure 2.47. ^{1}H NMR spectrum of (2.36)

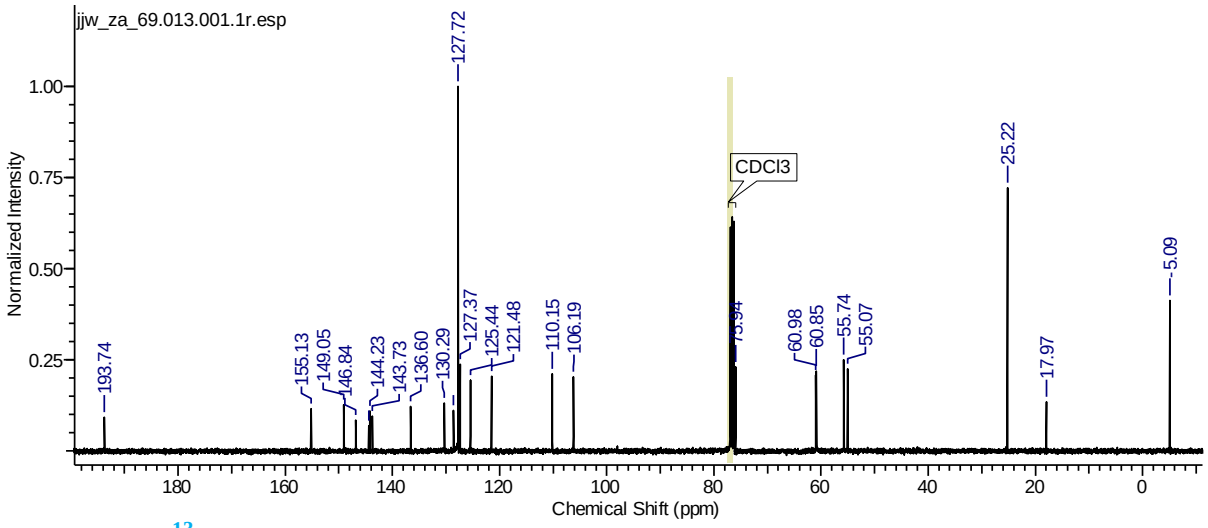

Figure 2.48. ^{13}C NMR spectrum of compound (2.36)

The next step in the synthetic sequence was the removal of benzyl protecting group. This was achieved by treating the compound **(2.36)** with 10% Pd/C in a 1:1 solvent mixture of ethanol and ethyl acetate under the atmosphere of hydrogen (Scheme 2.36). The identity of the debenzylated product; namely (3-((*tert*-butyldimethylsilyl)oxy)-4-methoxyphenyl)(2-hydroxy-3,4,5-trimethoxyphenyl)methanone **(2.37)** was confirmed by ^{1}H NMR spectrum (figure 2.49) due to the expected loss of the benzyl methylene protons at 4.90 ppm as well as the five aromatic protons and the appearance of the broad phenolic OH signal observed at 12.20 ppm.

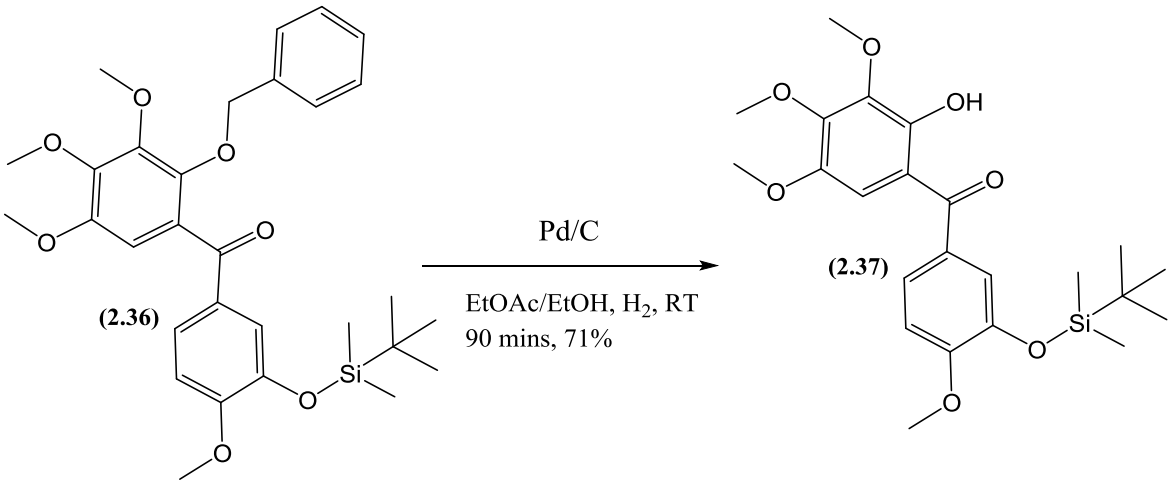

Scheme 2.36. Removal of benzyl protecting group

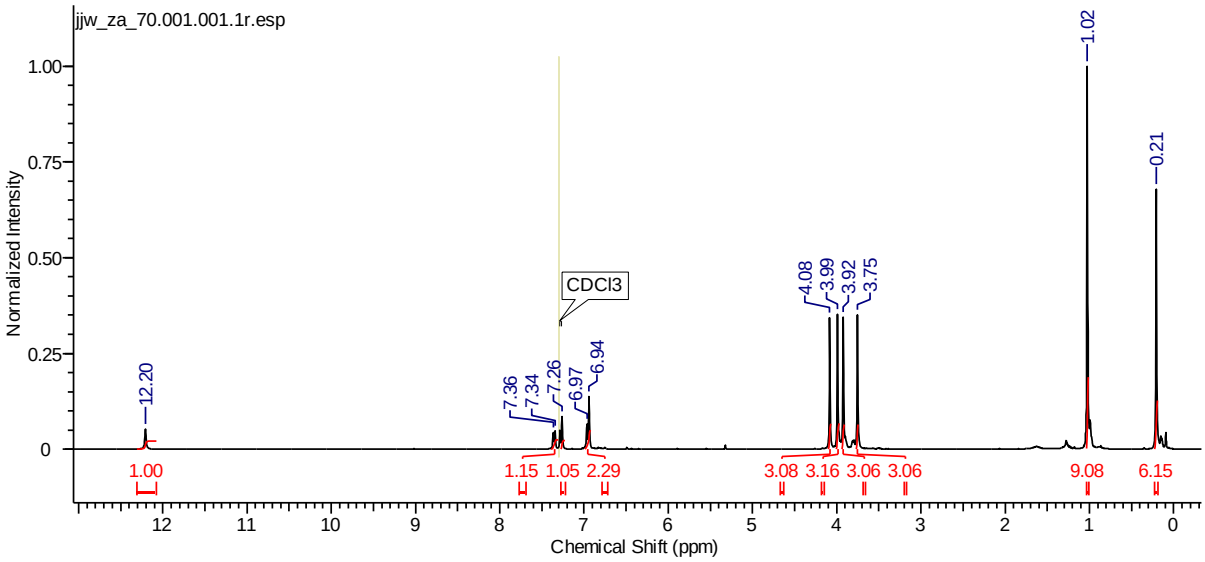

Figure 2.49. ^{1}H NMR spectrum of (2.37)

Once the phenol is deprotected, the next step was the activation of ketone functionality towards nucleophilic attacks by converting it to an imine. As our previous attempts to treat ketone **(2.37)** with Meldrum's acid to get 4-arylcoumarin failed, most probably due to the lack of the ketone reactivity to nucleophilic attack. For this purpose the compound **(2.37)** was treated with ammonia solution in methanol (7 M) overnight at room temperature [156], that resulted in the undesirable deprotection of silyl protecting group (Scheme 2.37) that was evident in the ^{1}H NMR spectrum (figure 2.50).

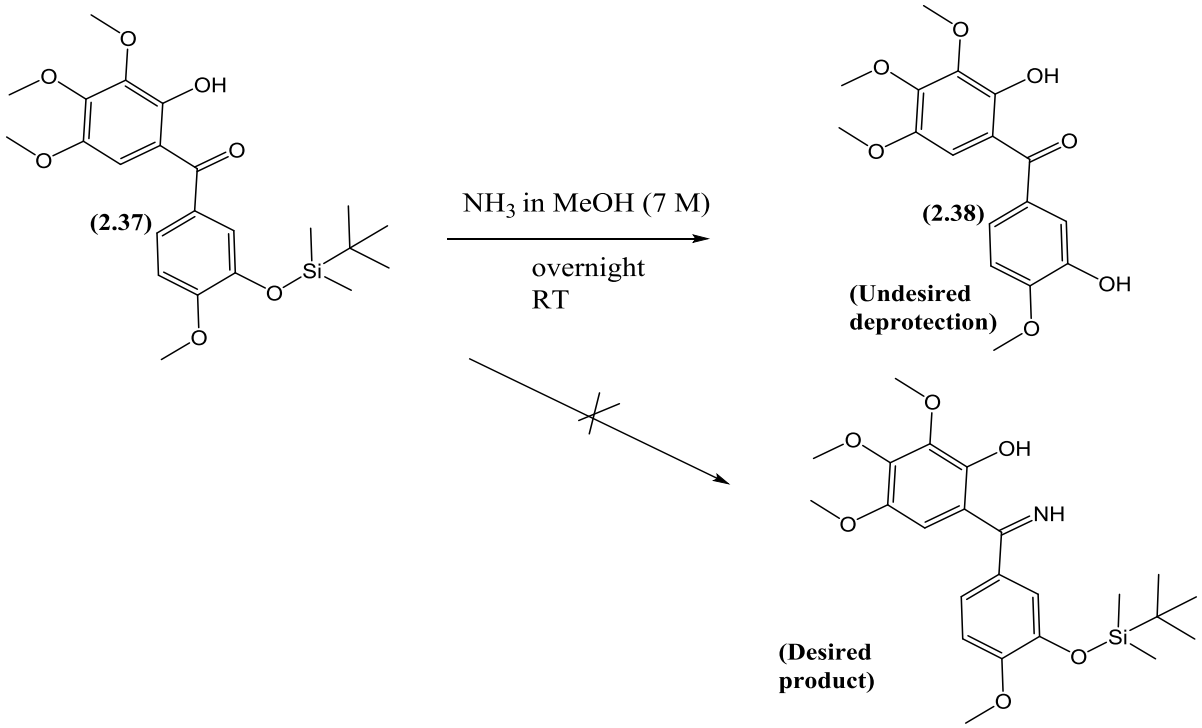

Scheme 2.37. Deprotection of silyl protecting group

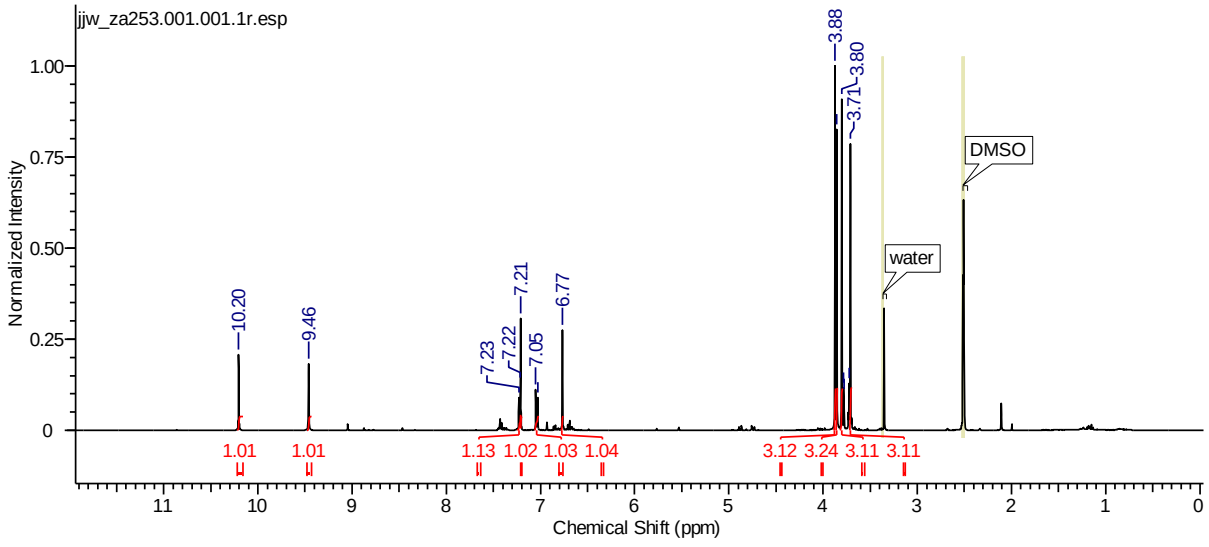

Figure 2.50. ^{1}H NMR spectrum of (2.38)

2.6.3 Synthesis of 3-carboxy-4-phenylcoumarin through Vilsmeier-Haack formylation

After several failed attempts to incorporate the carboxylic acid functionality on to our 4-phenylcoumarin, we decided to employ Vilsmeier-Haack formylation on our 4-hydroxy coumarin **(2.04)** since it has been successfully employed in *ortho*formylation of many heterocyclic compounds. Incorporating aldehyde functionality would enable us to introduce a range of different substituents at carbon-3. For this purpose compound **(2.04)** was brominated at position-4 while simultaneously introducing the aldehyde functionality into position-3 by reaction with phosphorus oxybromide and DMF in dry DCM at 80 °C (Scheme 2.38). Upon completion, the more volatile solvent was evaporated while the remainder was poured onto ice and quenched with cooled 5% sodium bicarbonate due to the exothermic nature of the reaction mixture. Following extraction with diethyl ether and purification by column chromatography the generation of the product **(2.39)** was confirmed by the disappearance of alkene proton and the appearance of aldehyde proton at 10.32 ppm in the ^{1}H NMR spectrum (figure 2.51).

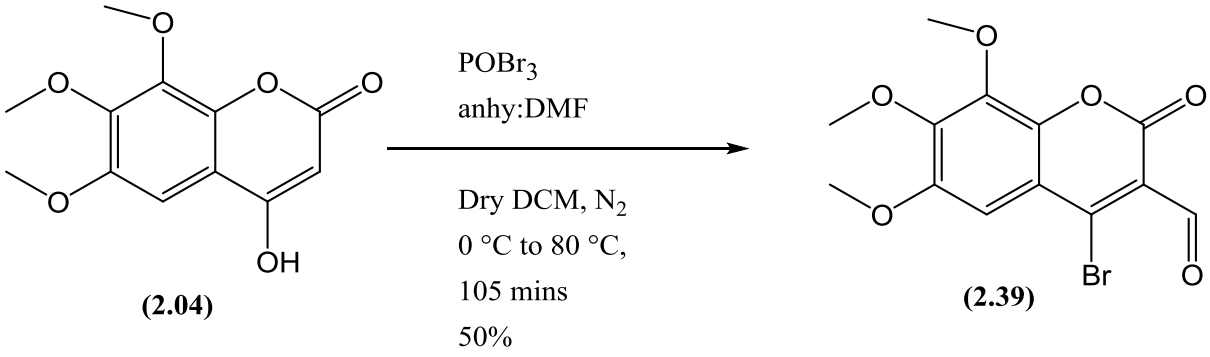

Scheme 2.38. Formylation of 4-hydroxycoumarin **(2.04)**

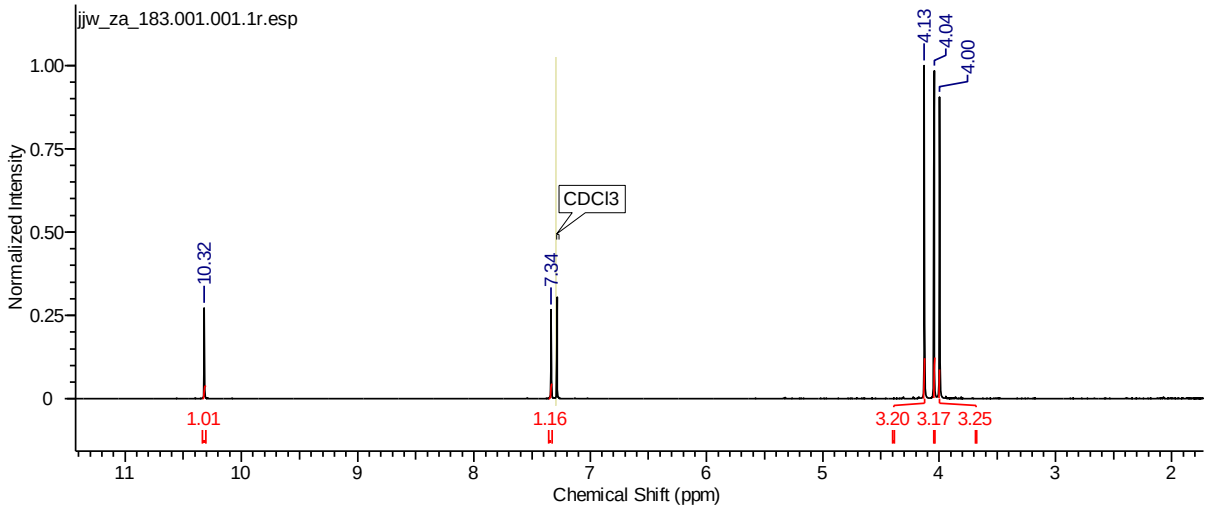

Figure 2.51. ^{1}H NMR spectrum of (2.39)

After formylation our next step was to Suzuki couple the C-ring onto **(2.39)**. For this purpose we tried using different palladium based catalysts, including $Pd(dppf)Cl_2$, $Pd(OAc)_2$ with 2-Dicyclohexylphosphino-2′,6′-dimethoxybiphenyl (Sphos) and $Pd(PPh_3)_4$. The maximum yield obtained was 5% with $Pd(PPh_3)_4$ which was very low to proceed with further. The main product getting formed was probably some kind of dimer with the aldehyde functionality. We tried to employ many different conditions including changing temperature and solvents in order to improve the yield but with no positive results. We decided to protect the aldehyde functionality as an acetal with the hope that it would be useful in preventing the formation of dimer. For this purpose the bromoaldehyde **(2.39)** was stirred with ethylene glycol, triethyl orthoformate and a crystal of *p*-toluenesulfonic acid monohydrate at room temperature under nitrogen atmosphere (Scheme 2.39). After work-up and purification by flash column chromatography, protection of the aldehyde was confirmed by ^{1}H NMR spectrum (figure 2.52) that shows the presence of two methylene groups and one CH of the acetal resonating at 4.06, 4.36 and 6.41 ppm respectively.

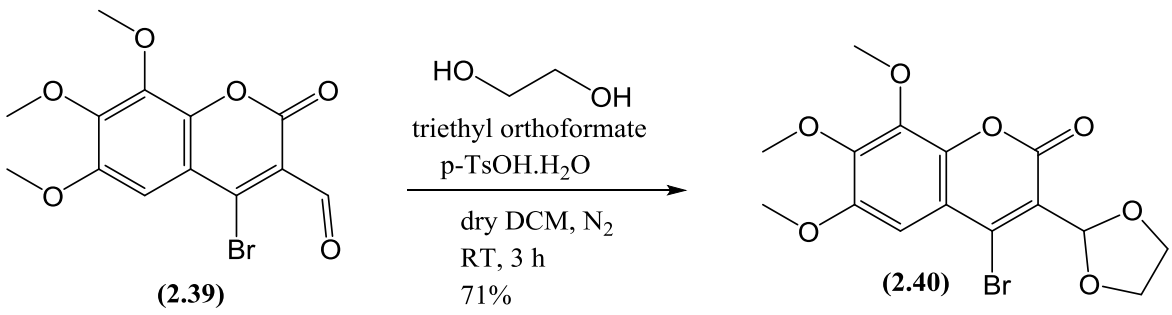

Scheme 2.39. Protection of aldehyde **(2.39)**

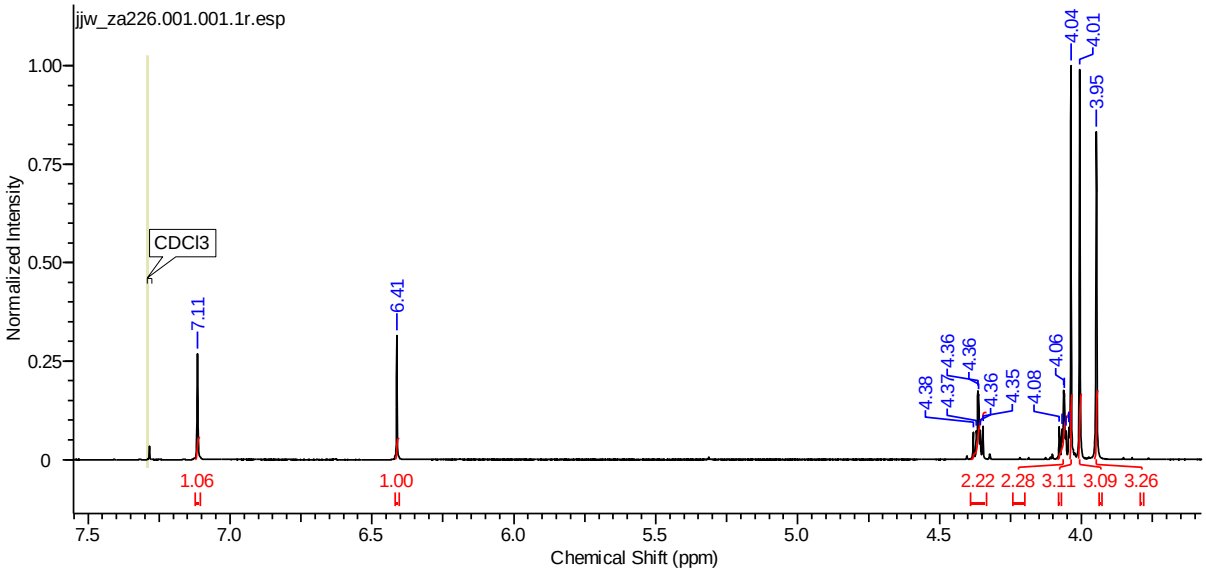

Figure 2.52. ^{1}H NMR spectrum of (2.40)

2.6.3.1 Suzuki coupling bromo acetal (2.40) with boronic ester (2.14)

After securing the protected aldehyde **(2.40)**, we were in a position to go for the Suzuki coupling reaction again. Aryl boronic ester **(2.14)** was coupled with protected aldehyde **(2.40)** using tetrakis (triphenylphosphine) palladium (0) as catalyst and potassium carbonate as a base (Scheme 2.40). The coupling of boronic ester **(2.14)** was confirmed by the ^{1}H NMR spectrum (figure 2.53). The additional feature in the ^{1}H NMR spectrum as compared to bromo acetal **(2.40)** included the presence of characteristic *t*-butyl signal for the Boc group at 1.50 ppm. An additional methoxy group was confirmed in the region 3.5-4.5 ppm and finally the aromatic region signals also had the expected 3 additional protons for the aromatic ring.

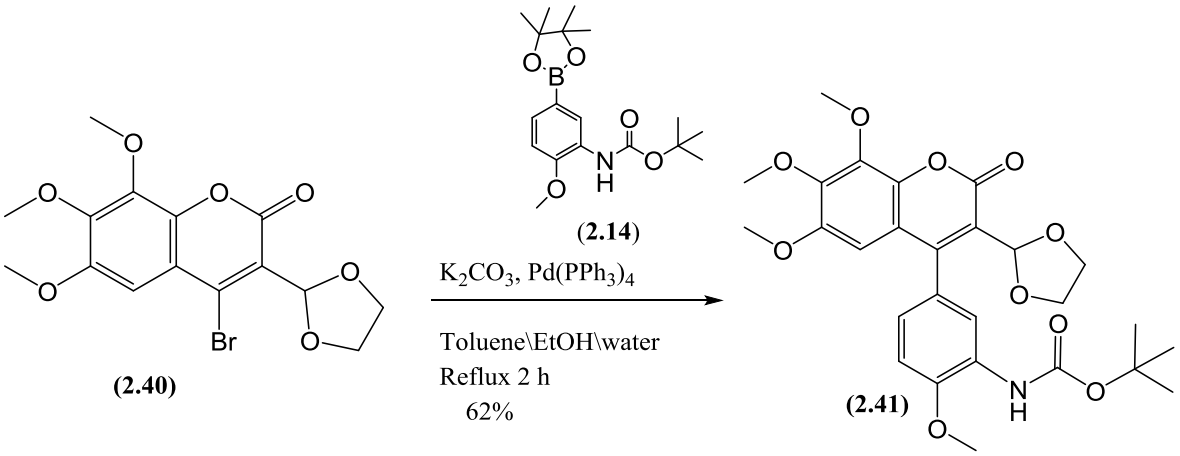

Scheme 2.40. Suzuki coupling of bromo acetal **(2.40)**

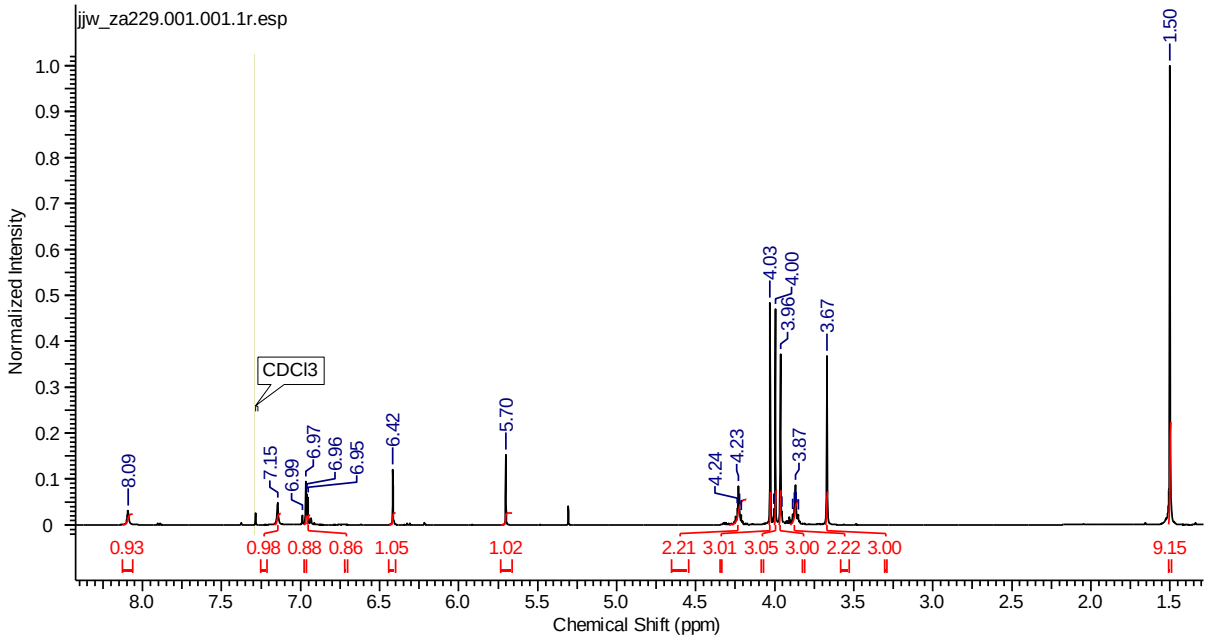

Figure 2.53. ^{1}H NMR spectrum of (2.41)

The next step in the synthetic sequence was the deprotection of the aldehyde functional group. This was achieved by heating *N*-Boc protected aniline **(2.41)** with iodine in DCM:acetone (1:1) at 50 °C for 1 hour [157] (Scheme 2.41). Upon completion and purification by column chromatography the structural identity of compound **(2.42)** was confirmed by the disappearance of the methylene protons of the acetal protecting group and the appearance of an aldehyde signal at 9.89 ppm, in the ^{1}H NMR spectrum (figure 2.54) of aldehyde **(2.42)**.

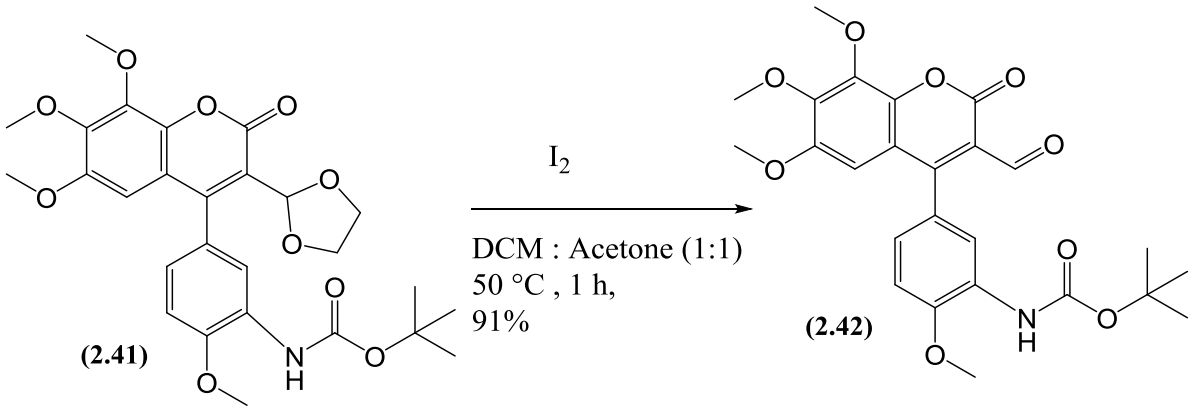

Scheme 2.41. Deprotection of aldehyde **(2.41)**

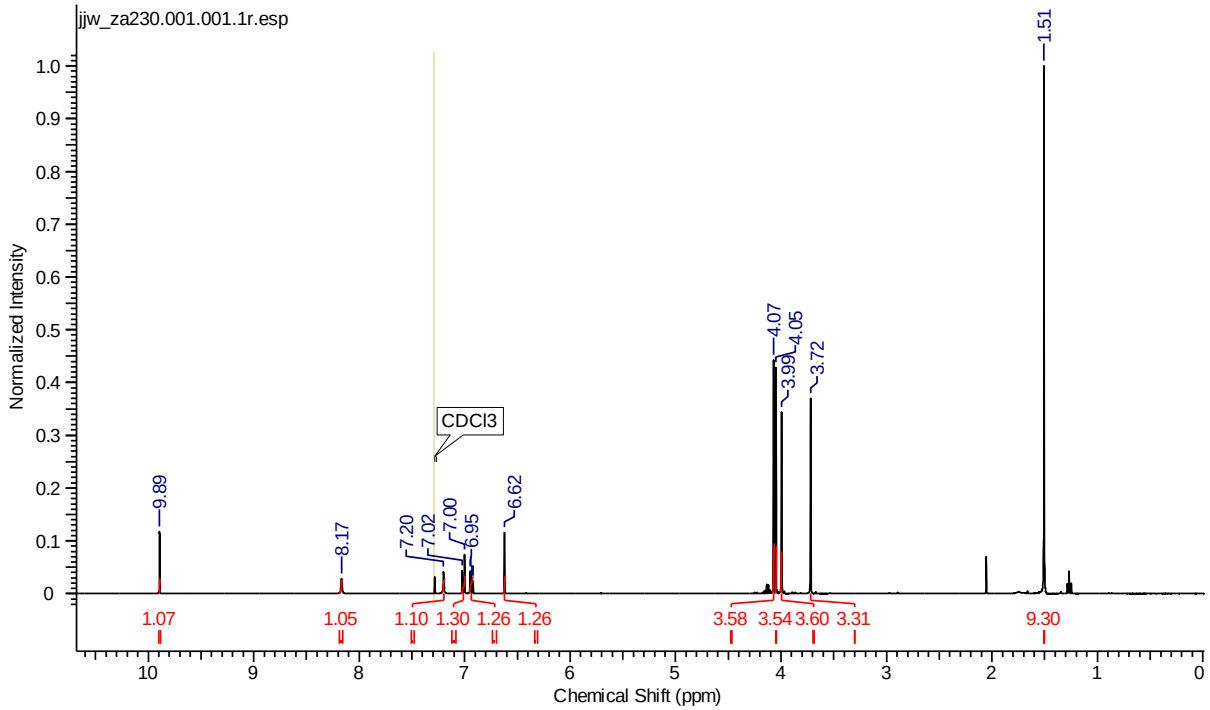

Figure 2.54. ^{1}H NMR spectrum of aldehyde (2.42)

Once we incorporated the aldehyde functional group on to carbon-3 of our 4-arylcoumarin we were in position to introduce different substituents at carbon-3 in order to assess their effect on the tubulin binding activity. So it was decided to oxidize the aldehyde functional group in order to synthesise the 3-carboxy derivative of our 4-phenylcoumarin compounds. For this purpose sodium chlorite (aq. solution) was used as an oxidizing agent along with sodium phosphate monobasic monohydrate (aq. solution) and hydrogen peroxide as a scavenger (Scheme 2.42).

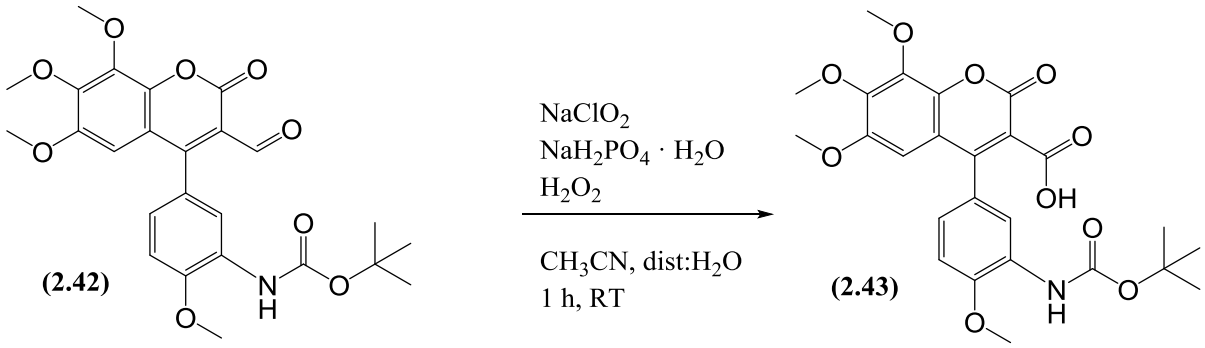

Scheme 2.42. Oxidation of aldehyde **(2.42)**

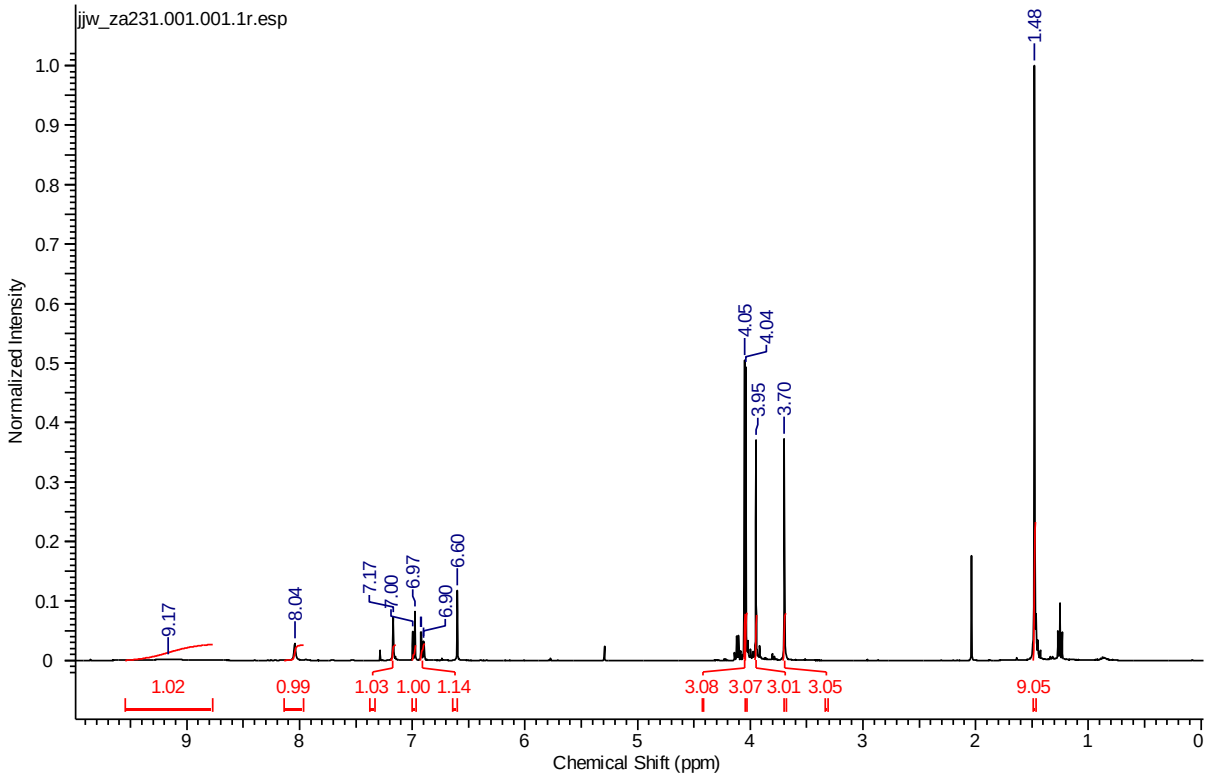

Figure 2.55. ^{1}H NMR spectrum of carboxylic acid (2.43)

The resultant carboxycoumarin **(2.43)** was *N*-Boc deprotected with 25% TFA in DCM (Scheme 2.43) to give aniline **(2.44).** The structural confirmation was done by NMR spectra where the ^{1}H NMR spectrum (figure 2.56) showed the expected loss of the BOC protecting group and also indicated presence of NH_2 signal resonating at 4.80 ppm with an integral value of 2. Moreover the ^{13}C spectrum (figure 2.57) also showed the presence of carbonyl carbon (C=O) of the acid resonating at 167.36 ppm.

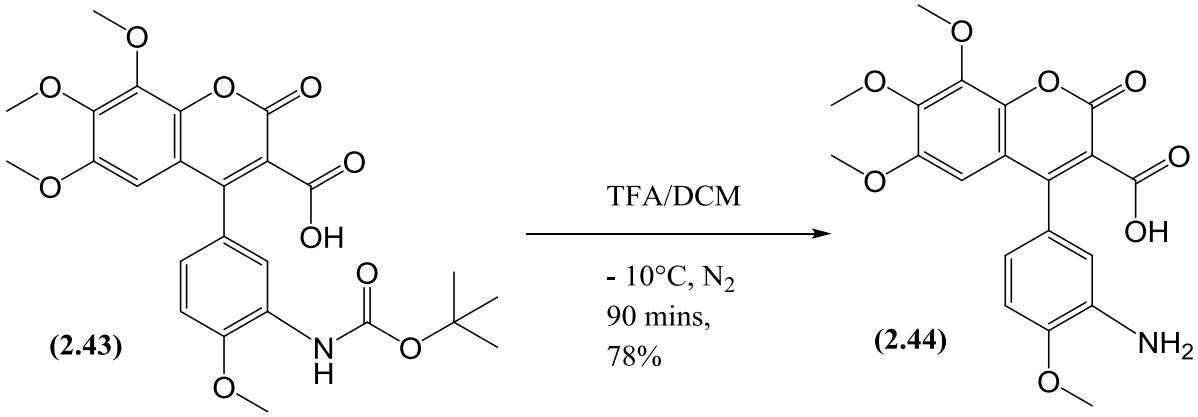

Scheme 2.43. Removal of Boc group

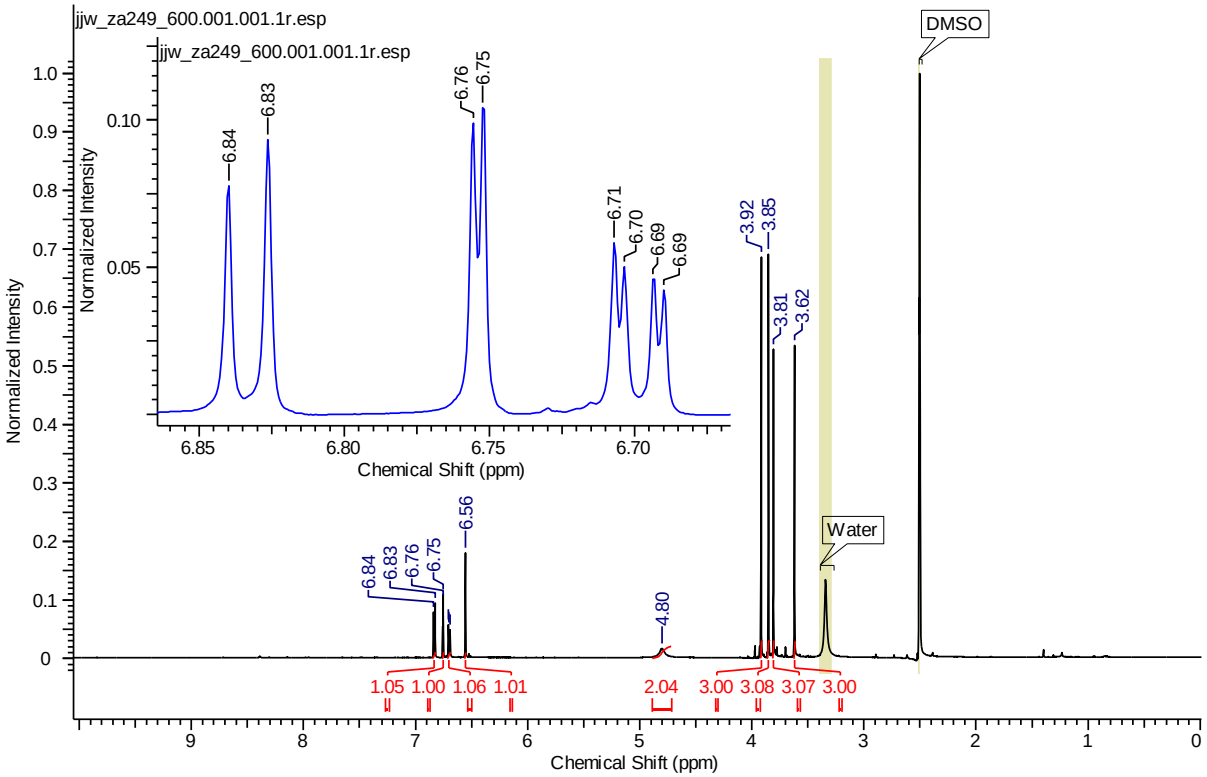

Figure 2.56. ^{1}H NMR spectrum of aniline carboxylate (2.44)

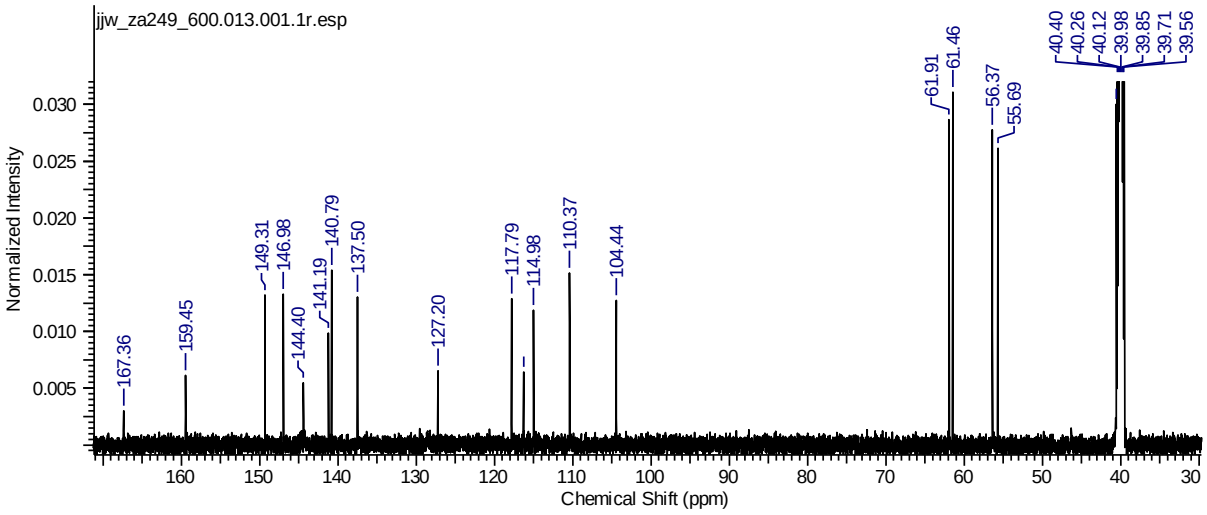

Figure 2.57. ^{13}C NMR spectrum of aniline carboxylate (2.44)

After formation of the carboxylic acid derivative **(2.44)**, we decided to introduce the oxime functionality at carbon 3 by condensation of hydroxylamine hydrochloride with the aldehyde **(2.42)** using diisopropylethylamine as base, in anhydrous DMF under nitrogen atmosphere. After the aqueous work-up and purification by flash column chromatography, *N*-Boc protected aldoxime was afforded with an excellent yield of 81%. The resultant Boc protected aldoxime **(2.45)** was than deprotected with TFA:DCM (1:3) to afford the

aldoxime **(2.46)** (Scheme 2.44). For the Structural identification of Aldoxime **(2.46)** spectroscopic techniques including NMR and mass spectrometry was used. The ^{1}H NMR spectrum of aldoxime (figure 2.58) shows a total proton count of 20 while the ^{13}C-spectrum (figure 2.59) shows the presence of all expected 20 carbons. The striking feature present in the ^{1}H NMR spectrum includes the presence of signal at 5.01 ppm with an integral value of 2 representing NH_2 and a singlet at 11.43 ppm indicating OH of the aldoxime. Moreover the presence of 1 CH proton, 4 aryl protons and 4 methoxy groups was also evident in the ^{1}H NMR spectrum.

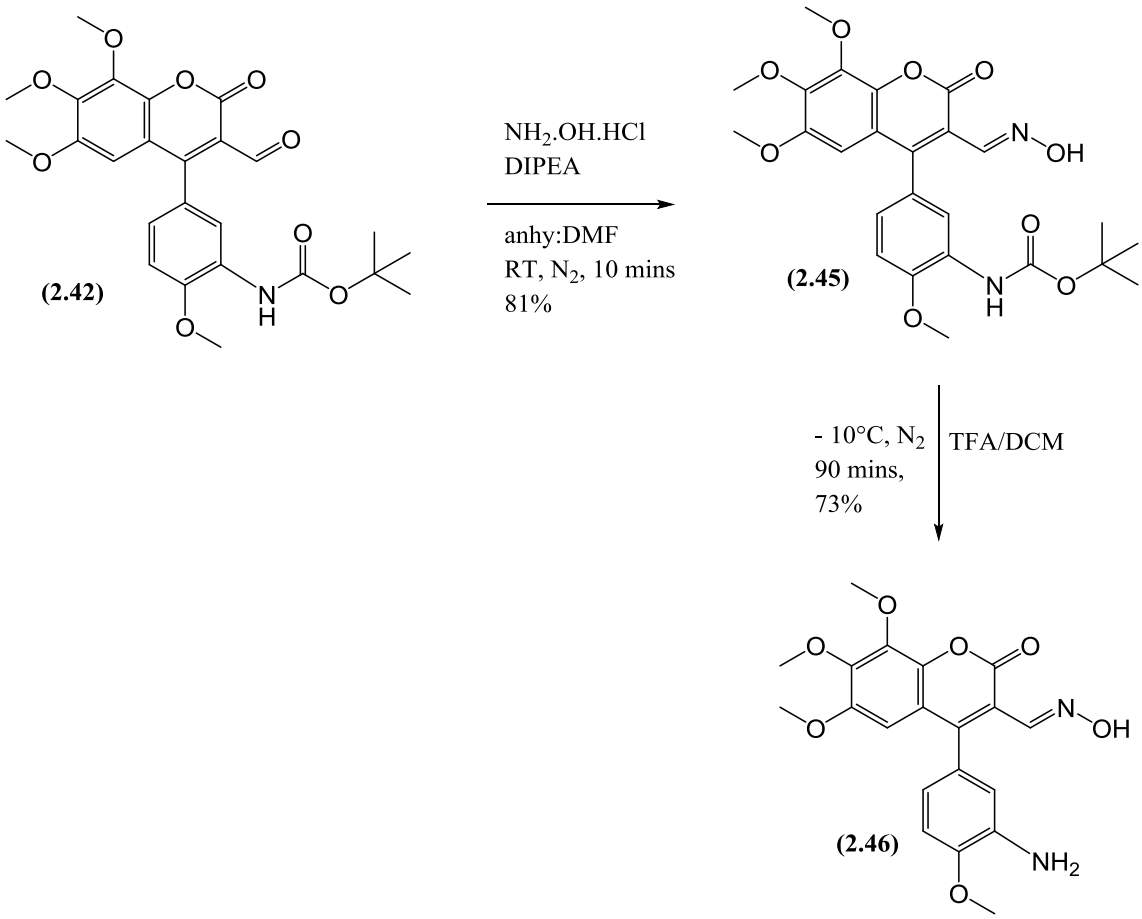

Scheme 2.44. Aldoxime formation and subsequent deprotection

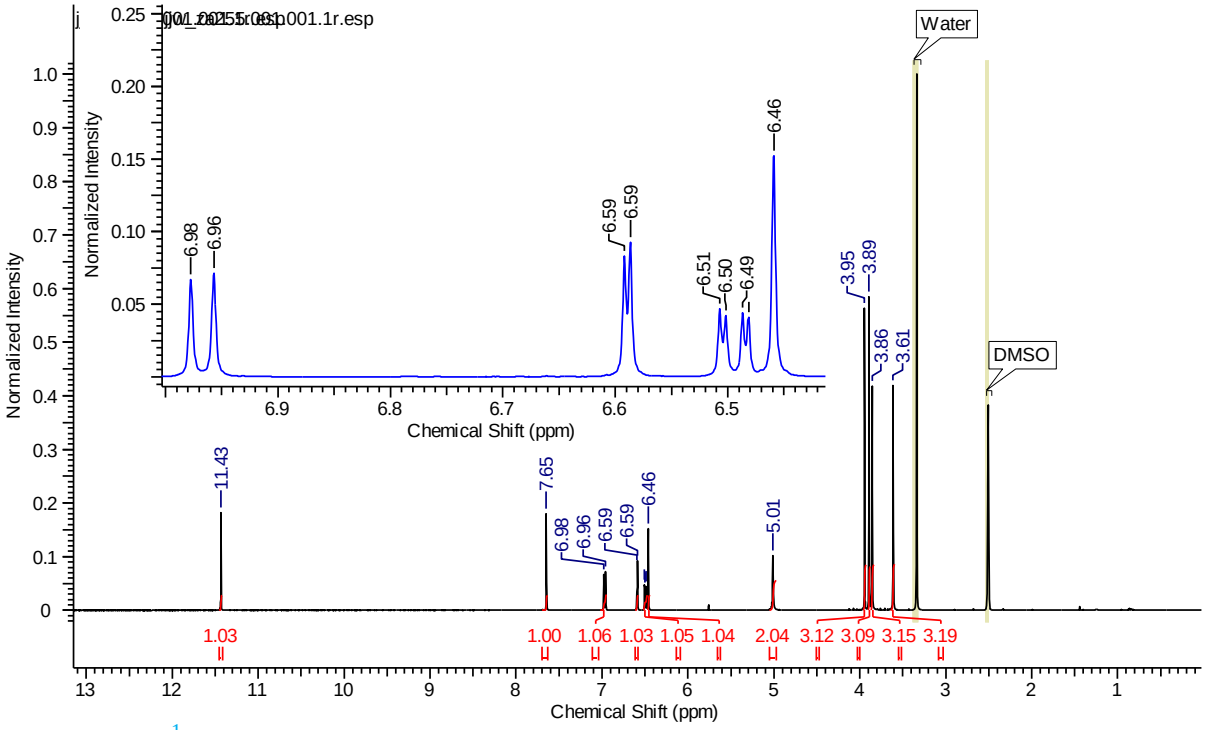

Figure 2.58. ^{1}H NMR spectrum of aldoxime (2.46)

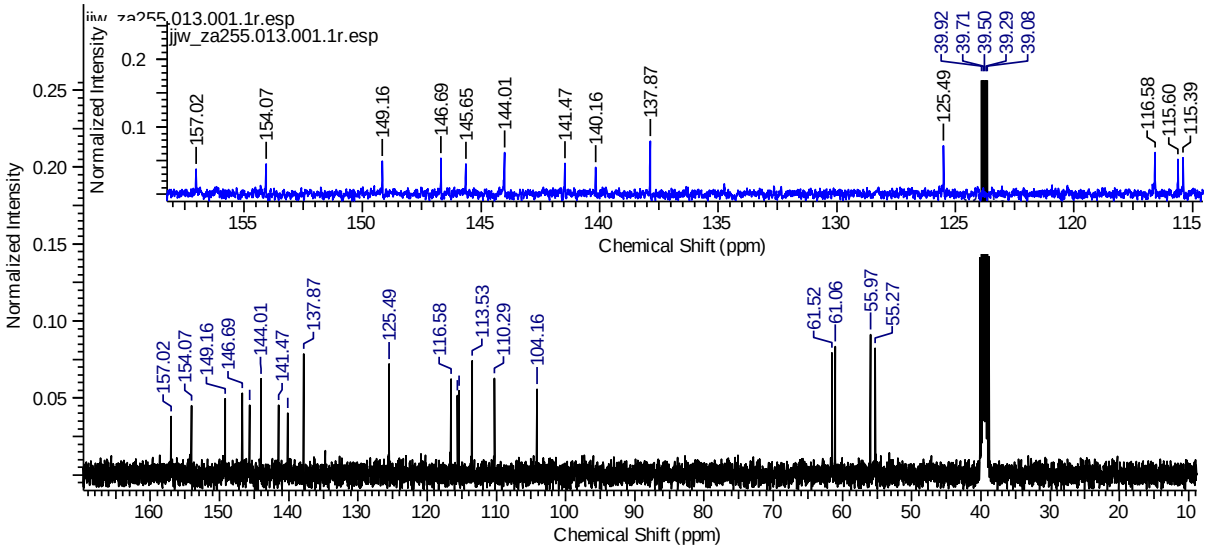

Figure 2.59. ^{13}C NMR spectrum of aldoxime (2.46)

Alcohol functionality was introduced by treating the compound **(2.42)** with sodium borohydride in methanol:DCM (4:1). After completion the reaction was quenched with saturated aqueous NaCl solution and extracted with diethyl ether. After evaporation of the organic solvent the remainder was purified by flash column chromatography to afford the *N*-Boc protected alcohol **(2.47)** with the yield of 78%. The *N*-Boc group of the alcohol **(2.47)** was then removed with TFA:DCM (1:3) to afford the compound **(2.48)** (Scheme 2.45). The structural confirmation was done by NMR spectroscopy. The ^{1}H NMR spectrum

(figure 2.60) indicates the presence of 20 protons while the ^{13}C spectrum (figure 2.61) shows the presence of all expected 20 carbons. The OH proton didn't show up in the ^{1}H NMR spectrum most probably due to deuterium exchange. The main characteristic features in ^{1}H NMR spectrum include the presence of singlet at 3.26 ppm with an integral value of 2 representing NH_2 and a quartet at 4.01 ppm (showing geminal coupling) with an integral value of 2 representing the CH_2. Moreover the ^{1}H NMR spectrum also indicated the presence of 4 methoxy groups and expected 4 aryl protons.

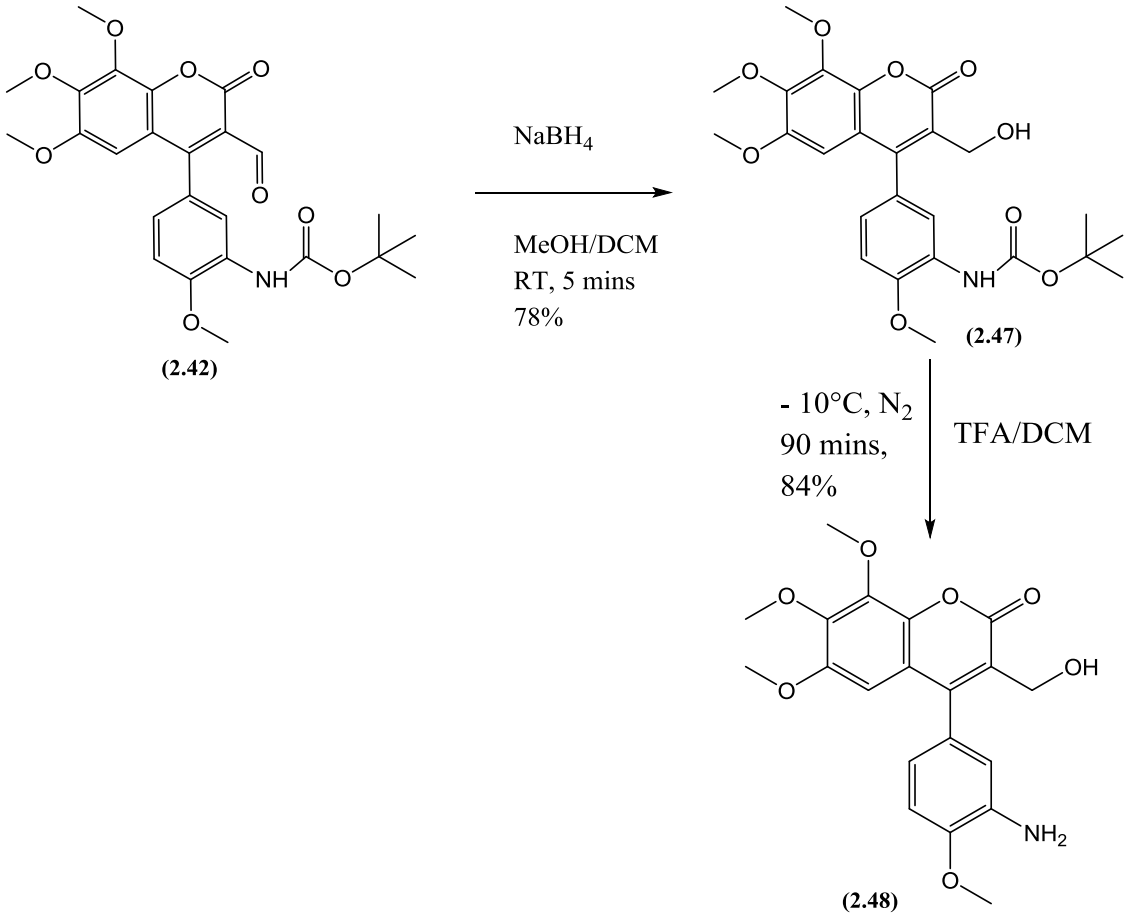

Scheme 2.45. Aldehyde reduction and subsequent deprotection

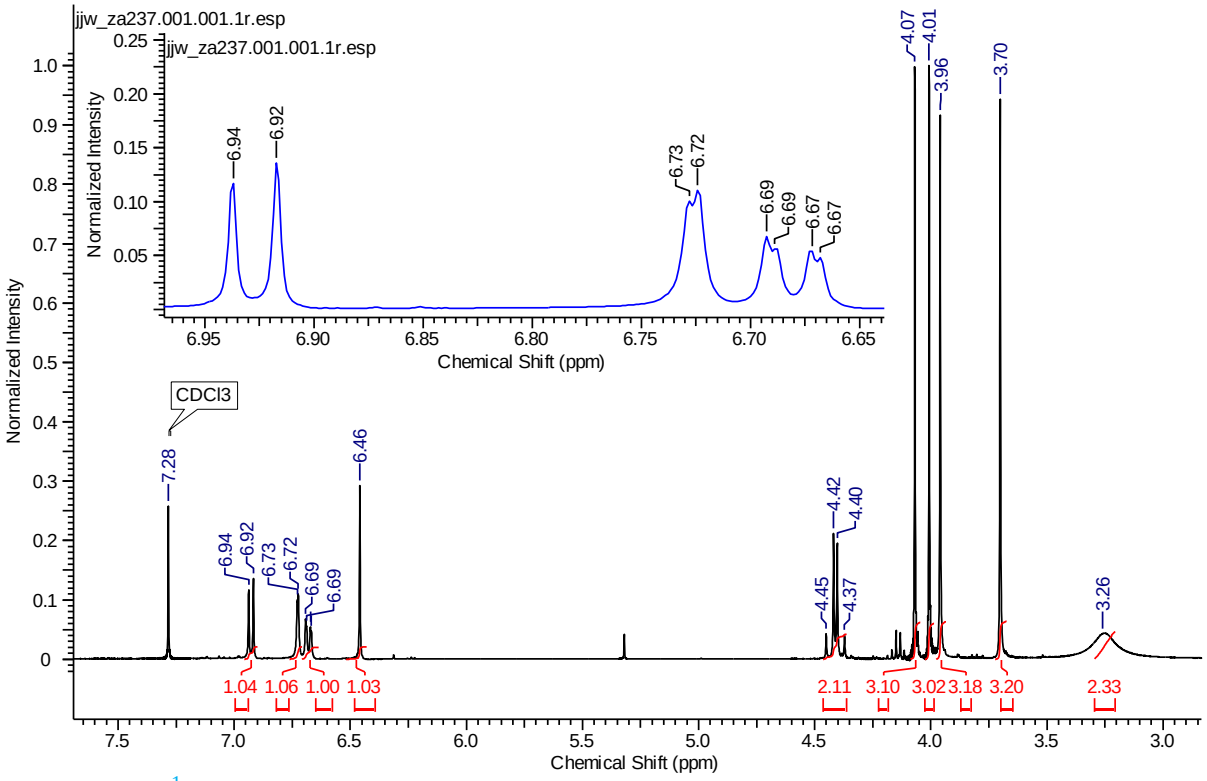

Figure 2.60. ^{1}H NMR spectrum of alcohol (2.48)

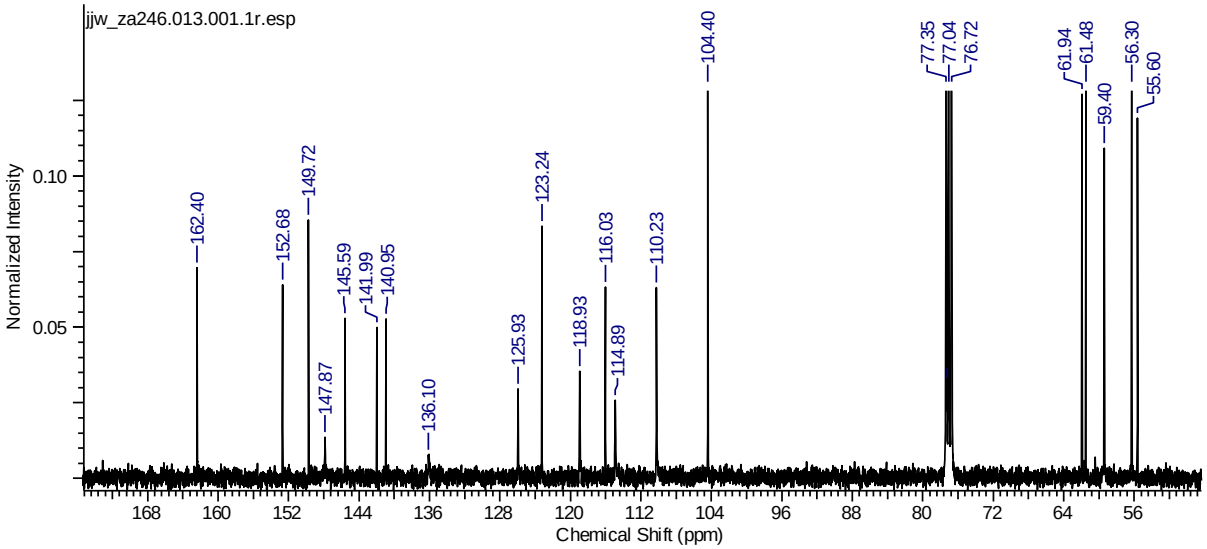

Figure 2.61. ^{13}C NMR spectrum of alcohol (2.48)

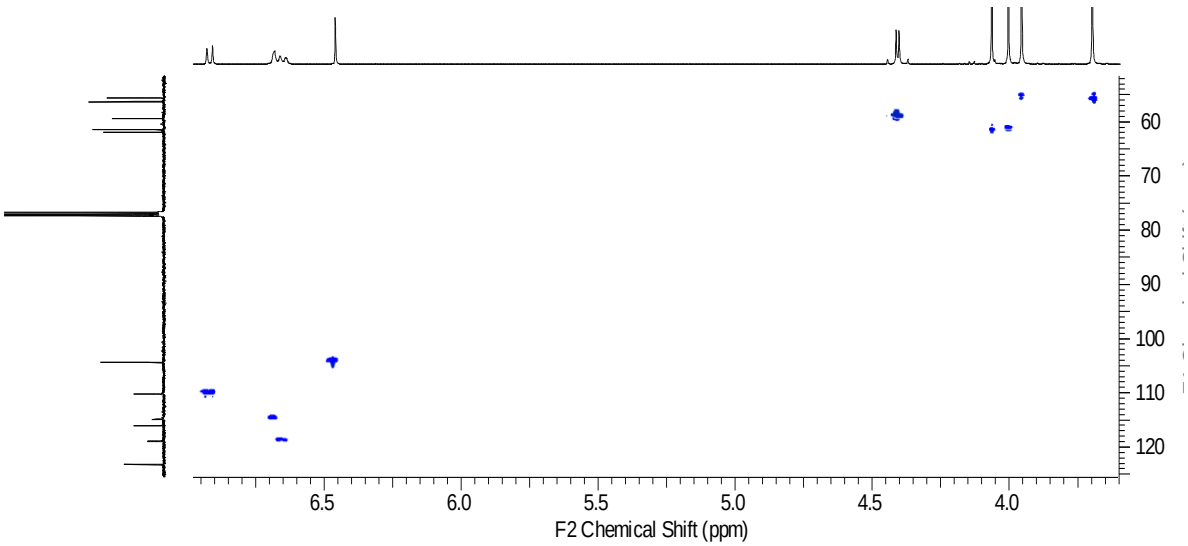

Figure 2.62. HSQC of alcohol (2.48)

2.6.3.2 Suzuki coupling bromo acetal (2.40) with boronic acid (2.10)

Aryl boronic acid **(2.10)** was coupled with bromo acetal **(2.40)** using the same conditions employed before for the Suzuki coupling reactions, to give the tricyclic compound **(2.49)**. TBAF deprotection of the *tert*-butyldimethylsilyl ether protecting group resulted in the formation of the acetal protected phenol **(2.50)** (Scheme 2.46). After purification by column chromatography, the structural identity of the phenol **(2.50)** was confirmed by NMR spectroscopy where the presence of all expected 22 protons was evident in the ^{1}H NMR spectrum (figure 2.63) while the ^{13}C spectrum (figure 2.64) also represents a total carbon count of 22.

The distinctive characteristics of the compound in the ^{1}H NMR spectrum include the presence of the two CH_2 groups of the acetal protecting group resonating as multiplets at 3.89 and 4.24 ppm, each with an integral value of 2. Along with that the presence 4 methoxy groups, 4 aryl protons, 1 CH and 1 OH was also indicated by the proton NMR spectrum.

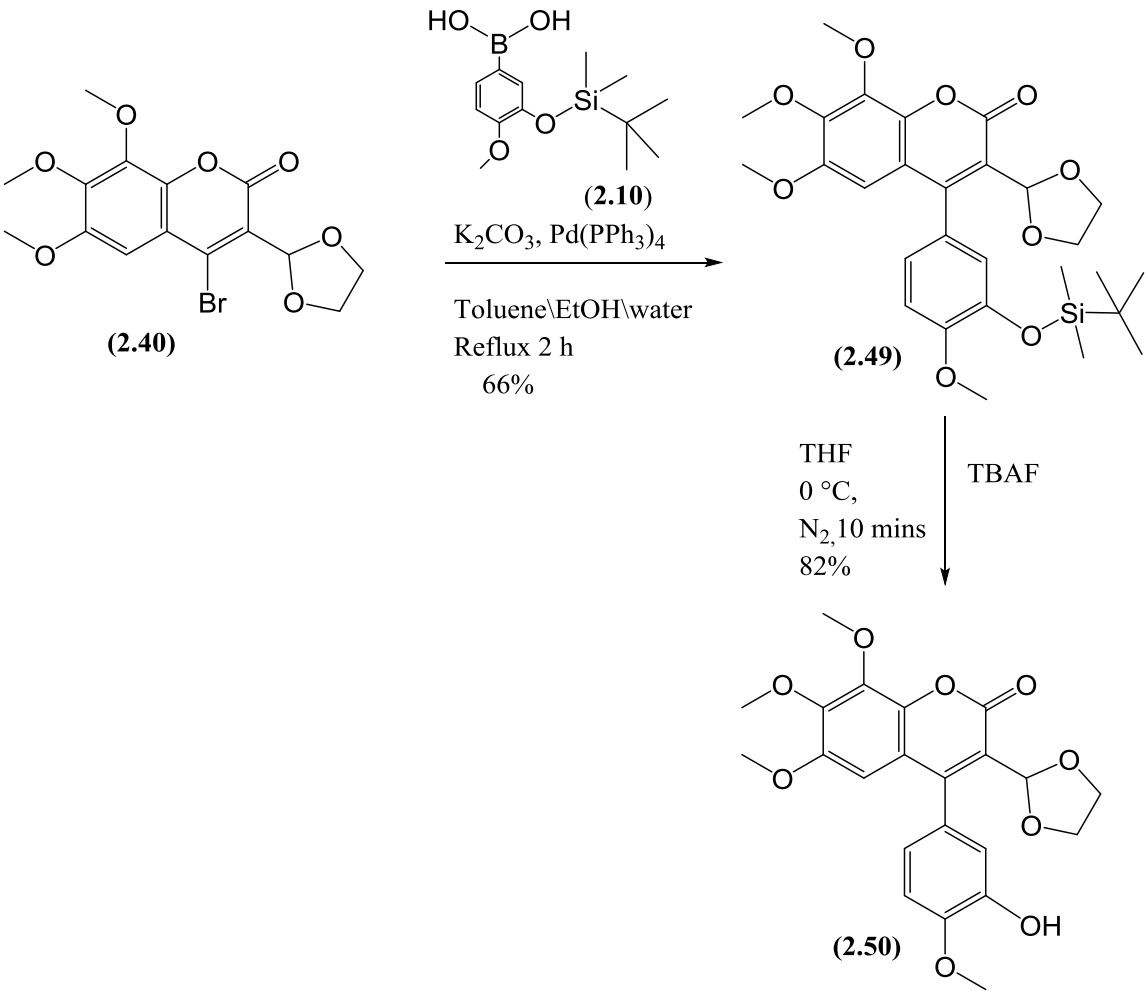

Scheme 2.46. Suzuki coupling and subsequent deprotection

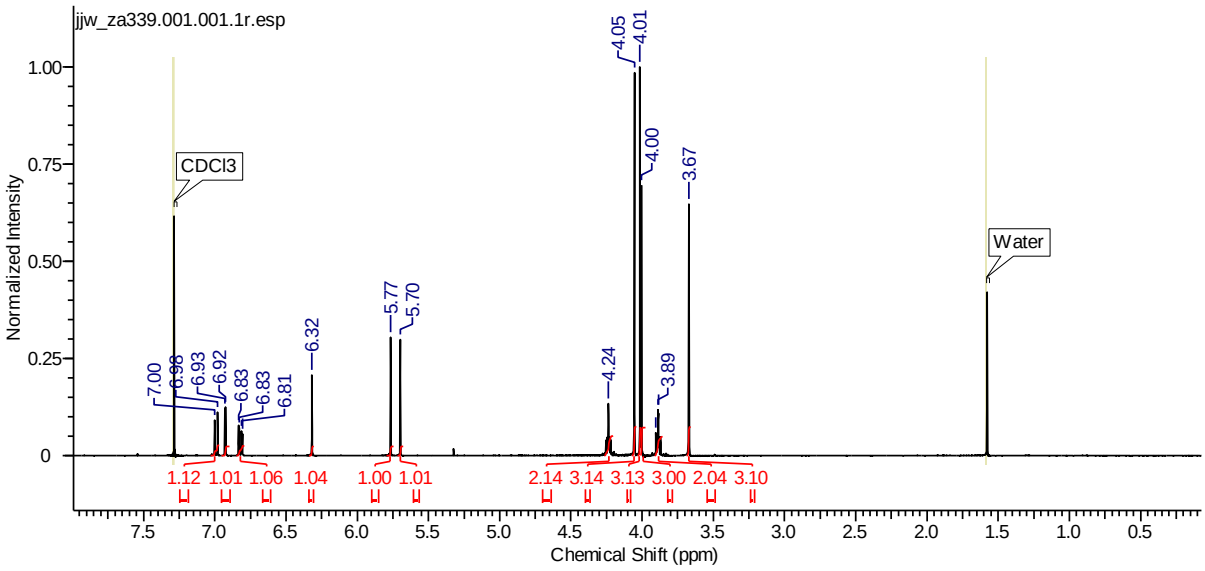

Figure 2.63. ^{1}H NMR spectrum of phenol (2.50)

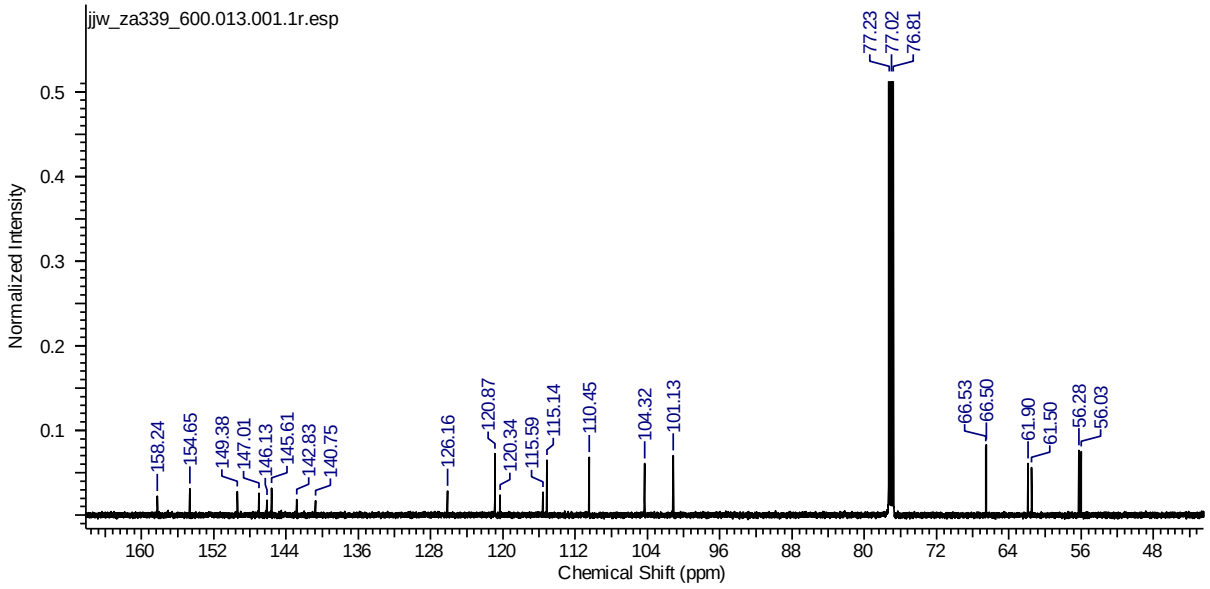

Figure 2.64. ^{13}C-NMR spectrum of phenol (2.50)

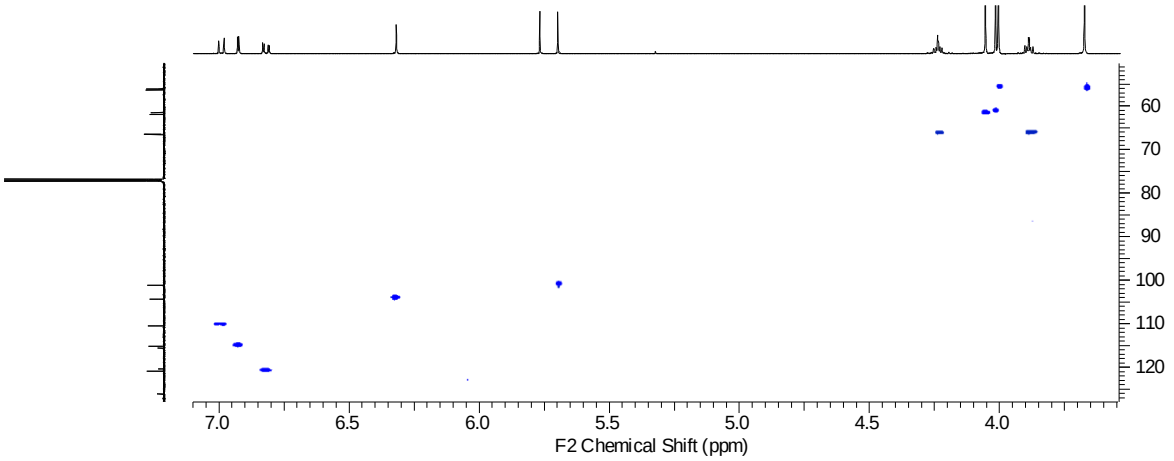

Figure 2.65. HSQC spectrum of phenol (2.50)

Next we had to remove the acetal protecting group in order to get the aldehyde derivative of 4-arycoumarin. For this purpose the phenol **(2.50)** was stirred with iodine in DCM:acetone (1:1) at 50 °C for 1 hour (Scheme 2.47), affording the aldehyde **(2.51)** in a 75% yield, after work-up and purification by flash column chromatography. The structural confirmation was done by NMR spectroscopy where the signals for all the expected 18 protons are present in ^{1}H NMR spectrum (figure 2.66) while the ^{13}C spectrum (figure 2.67) also shows the presence of 20 carbons. The singlet at 9.91 ppm in the ^{1}H NMR spectrum with an integral value of 1 represents the aldehyde proton while the phenolic OH is found to be resonating at 5.84 ppm as broad singlet with an integral value of 1. The remaining

structural features of the compound **(2.51)**, including the 4 methoxy groups and 4 aryl protons are also evident in the ^{1}H NMR spectrum.

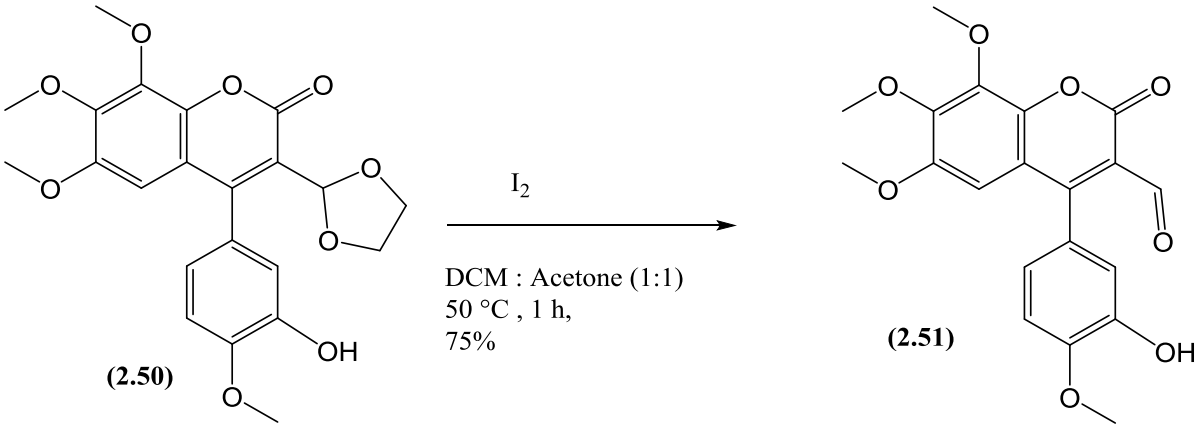

Scheme 2.47. Deprotection of acetal protecting group

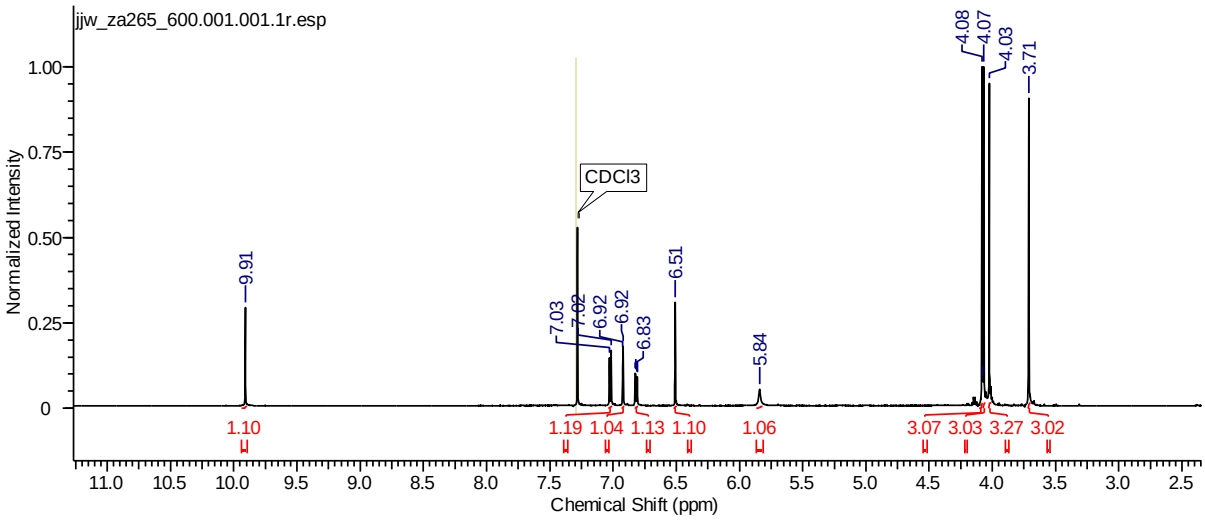

Figure 2.66. ^{1}H NMR spectrum of aldehyde (2.51)

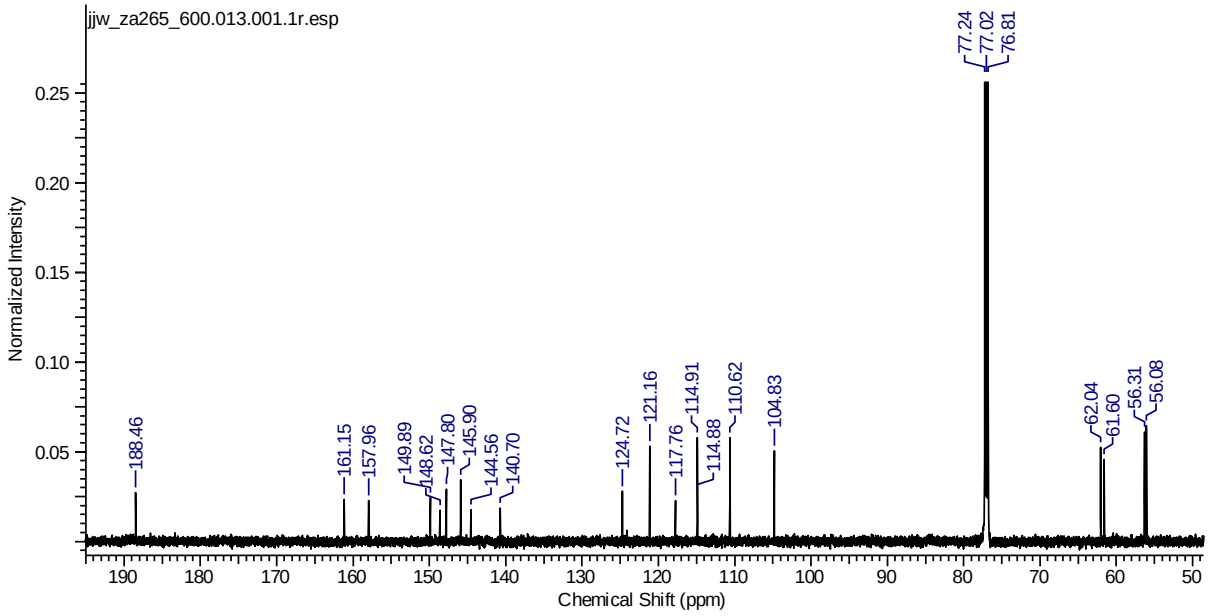

Figure 2.67. ^{13}C-NMR spectrum of aldehyde (2.51)

2.7 Synthesis of dimethoxy A-ring coumarin compounds

A library of novel coumarin compounds with dimethoxy A-ring were synthesised by our former colleague, D. Ropero that demonstrated potent inhibition of tubulin polymerisation. The most active among them was compound (**4.37)**. These coumarin based compounds hold the same structural arrangement as our previous compounds that include methoxy substituted aryl ring (A ring), a six membered aliphatic ring (B-ring) and a monomethoxy substituted aryl ring (C ring). The only difference was the presence of 6,8-dimethoxy arrangement at A-ring instead of 6,7,8-trimethoxy (figure 2.68). The methoxy of the A-ring at position 7 was replaced by an OH substituent. Moreover it was also found in the tubulin binding assays of the compounds that were synthesised that position 7 also accommodated bulky substituents, including benzyloxy **(4.36)** and dimethylallyl oxy **(4.44)** substituents without having a significant negative effect on tubulin binding activity. With this in mind we decided to further increase the library of these compounds. Our initial focus was to scale up the quantity of various intermediates that would allow us to introduce different substituents at carbon 7. With this in mind a particular focus was to optimise yields of reactions where possible during the course of the synthesis.

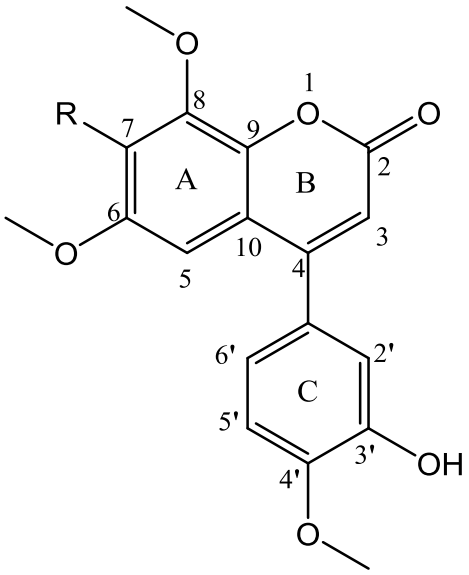

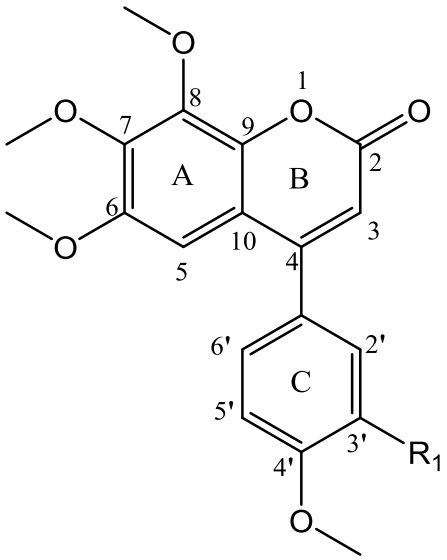

D.Ropero compounds

R= $C_6H_5CH_2O$ **(4.36)**, OH **(4.37)**, O-prenyl **(4.44)**

Compounds with trimethoxy substituted A ring

R_1= OH, NH_2

Figure 2.68. General structures of 4-arylcoumarins

2.7.1 Synthesis of 4-hydroxycoumarin backbone

For the synthesis of dimethoxycoumarins, we followed the synthetic route established by a former colleague D. Ropero. Starting with 2,6-dimethoxyphenol **(2.52)**, our first step was the protection of phenol functional group. This was achieved by stirring the phenol **(2.52)** with benzyl bromide and caesium carbonate in anhydrous DMF at room temperature. In the next step the benzyl protected phenol **(2.53)** underwent formylation with phosphorous oxychloride ($POCl_3$) using dry DMF as solvent at 80 °C (Scheme 2.48). After 7 hours the reaction flask was cooled to -10 °C and very slowly poured on to ice and then quenched with ice cooled solution of sodium acetate (10%). Ice cooled aqueous sodium acetate was used for quenching because our previous attempt to quench the reaction directly at room temperature resulted in the deprotection of **(2.54)** due to the exothermic nature of the reaction mixture thereby reducing the yield to 7%. After quenching, the aqueous layer was extracted with diethyl ether, dried with $MgSO_4$ and evaporated using rotary evaporator. The crude product obtained was purified by flash column chromatography to afford the benzaldehyde **(2.54)** with a yield of 65%. The success of the formylation reaction was confirmed by the ^{1}H NMR spectrum (figure 2.69) of the benzaldehyde **(2.54)** that shows the presence of aldehyde proton signal at 10.27 ppm. Moreover in the aromatic region of

the spectrum the presence of two *ortho* coupling protons resonating at 6.78 and 7.65 ppm evidenced the accurate regio-positioning of the aldehyde functional group.

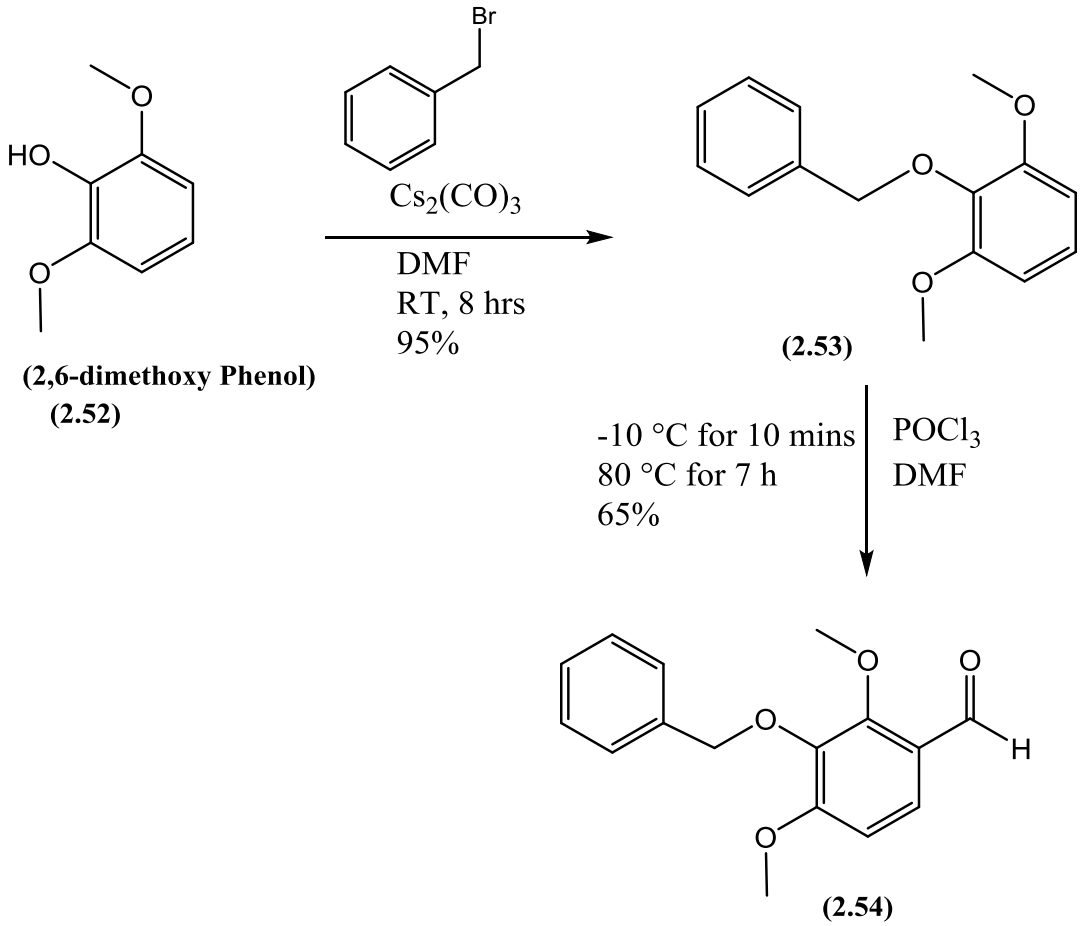

Scheme 2.48. Protection of phenol followed by subsequent formylation

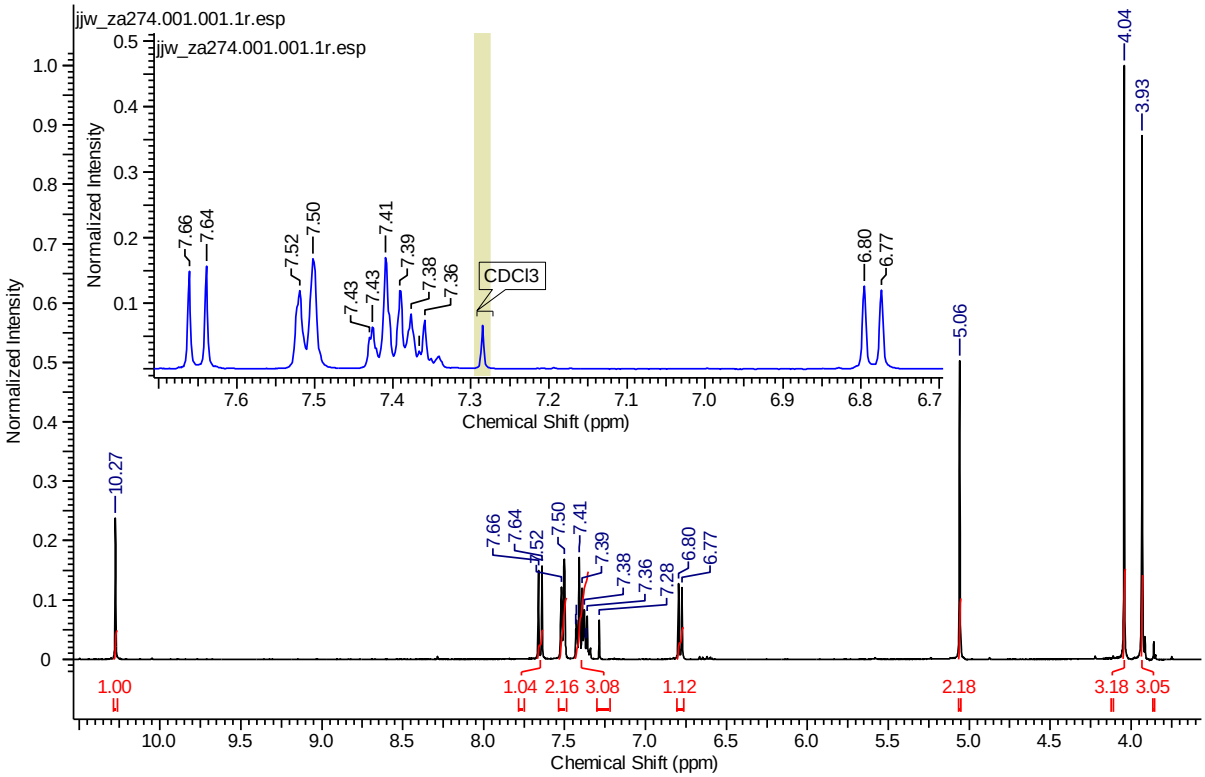

Figure 2.69. ^{1}H NMR spectrum of benzaldehyde (2.54)

The next step in the synthetic sequence was the Baeyer-Villiger oxidation of 3-(benzyloxy)-2,4-dimethoxybenzaldehyde **(2.54)** with *meta*-chloroperoxybenzoic acid (*m*CPBA) to give the formate ester **(2.55)**. The transformation of benzaldehyde to formate ester was straight forward however the complete removal of *m*CPBA was quite difficult. The formate ester was next hydrolysed using 2 M aqueous NaOH to afford the phenol **(2.56)** (Scheme 2.49). After the acidic work-up, the product was further purified by flash column chromatography. The structural identity of the phenol was confirmed due to the absence of the peak for the formate ester proton and the appearance of broad phenolic signal at 5.48 ppm in the ^{1}H NMR spectrum (figure 2.70).

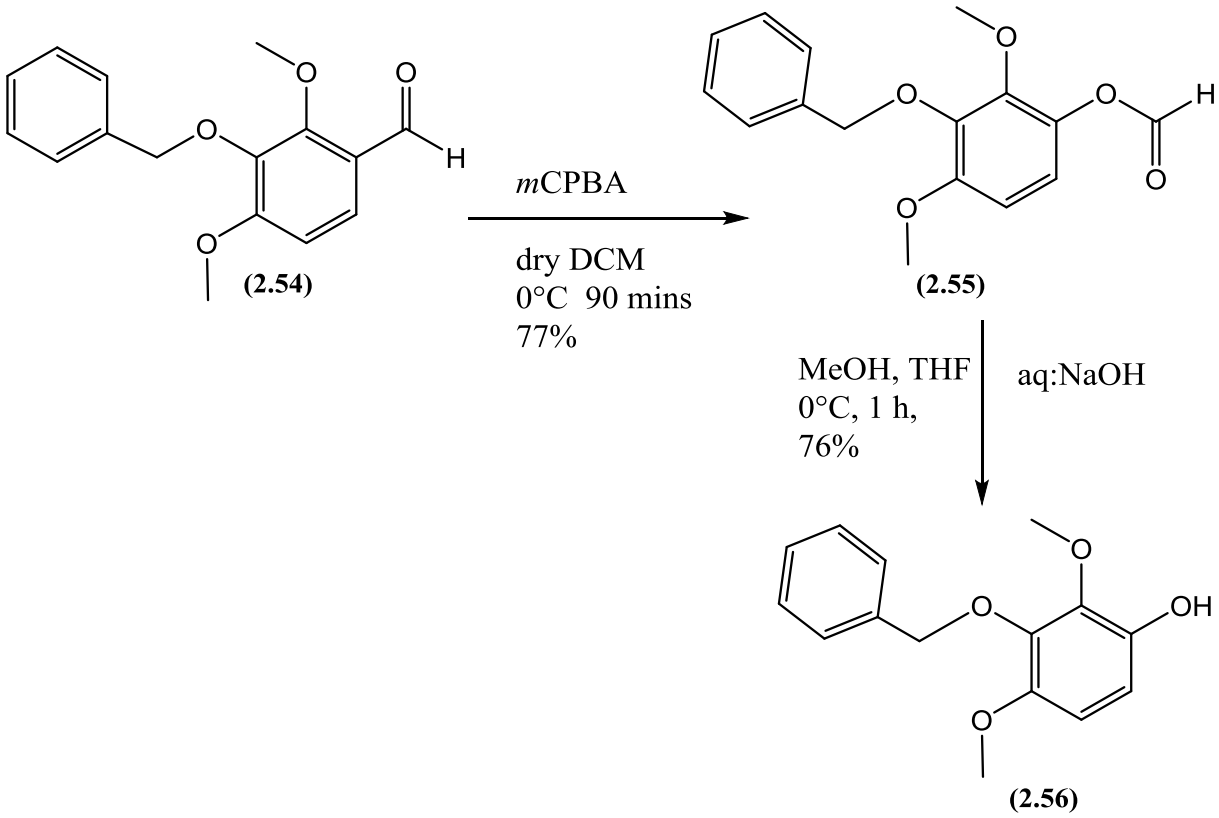

Scheme 2.49. Baeyer-Villiger oxidation and subsequent hydrolysis

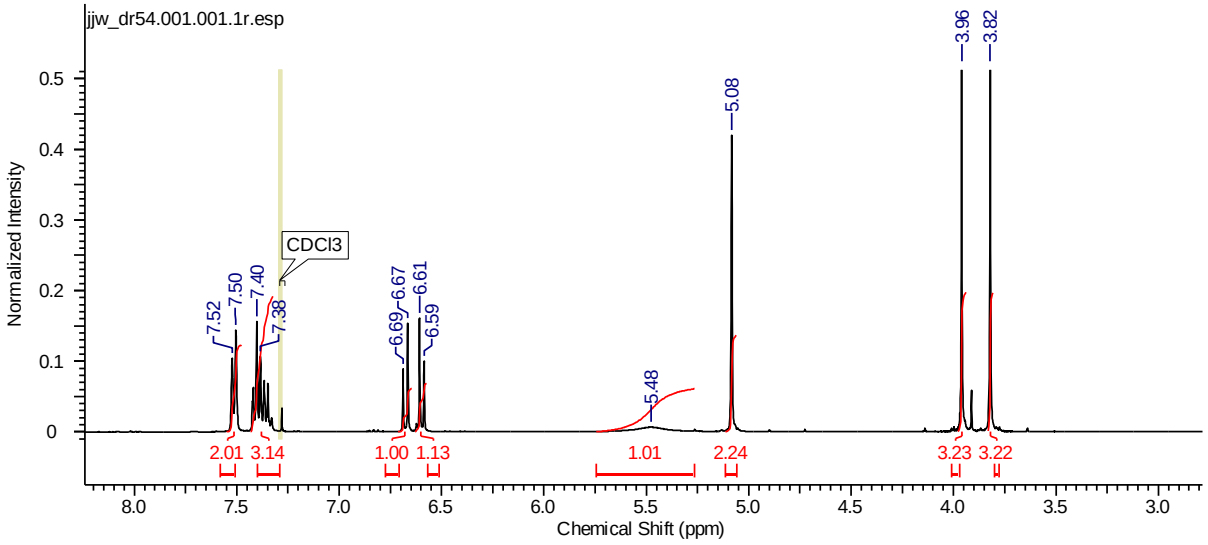

Figure 2.70. ^{1}H NMR spectrum of phenol (2.56)

The resultant phenol **(2.56)** was ortho-formylated using freshly dried and distilled triethylamine, paraformaldehyde and anhydrous magnesium chloride in dry THF at 75 °C, under anhydrous conditions [158] (Scheme 2.50). After the work-up and purification by flash column chromatography, the structural identity of the product, obtained in a satisfactory yield of 59%, was confirmed by the ^{1}H NMR spectrum (figure 2.71) of the

ortho-hydroxy benzaldehyde **(2.57)** that shows the presence of both aldehyde and hydroxyl protons resonating at 9.80 and 10.96 ppm respectively. Moreover the disappearance of one aryl proton was also evident in the spectrum.

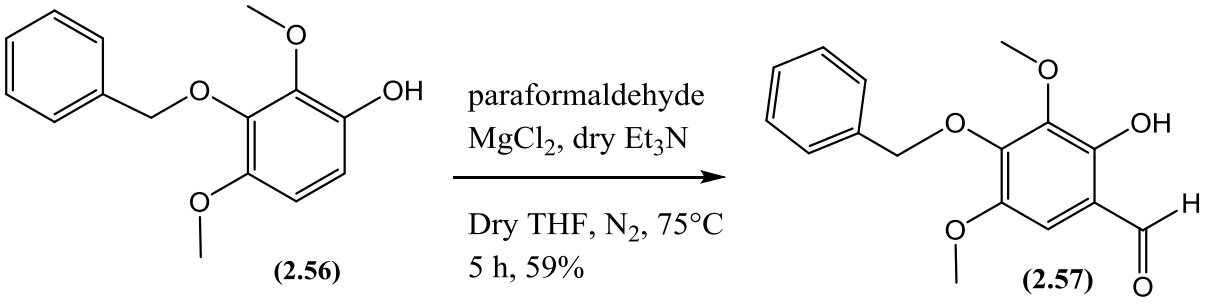

Scheme 2.50. Ortho-formylation of Phenol **(2.56)**

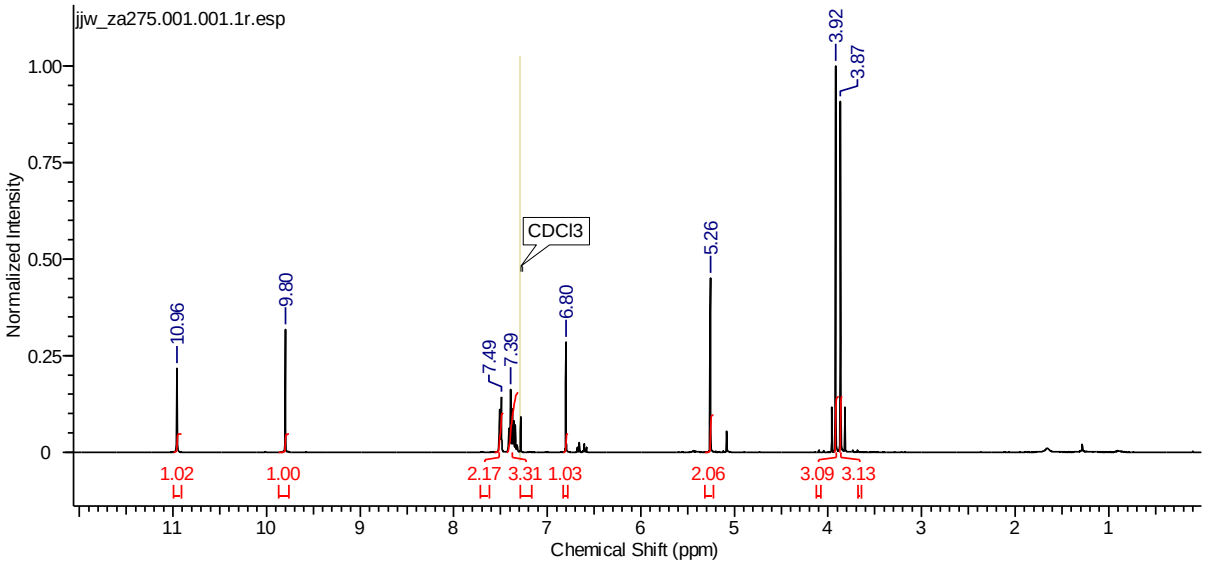

Figure 2.71. ^{1}H NMR spectrum of *ortho*-hydroxybenzaldehyde (2.57)

The phenol functional group of hydroxybenzaldehyde **(2.57)** was protected with a silyl protecting group using *tert*-butyl dimethylsilyl chloride and imidazole in anhydrous DMF under the atmosphere of nitrogen. The resultant silyl protected benzaldehyde **(2.58)** was then treated with the Grignard reagent methylmagnesium bromide in dry THF for one hour to afford 1-(4-(benzyloxy)-2-((*tert*-butyldimethylsilyl)oxy)-3,5-dimethoxyphenyl)ethan-1-ol **(2.59)** with a yield of 78% (Scheme 2.51). After purification by column chromatography its structural identity was confirmed by the analysis of its ^{1}H NMR spectrum (figure 2.72) which showed the presence of a doublet at 1.47 ppm for the methyl group and a quartet at 5.28 ppm corresponding to the CHOH proton.

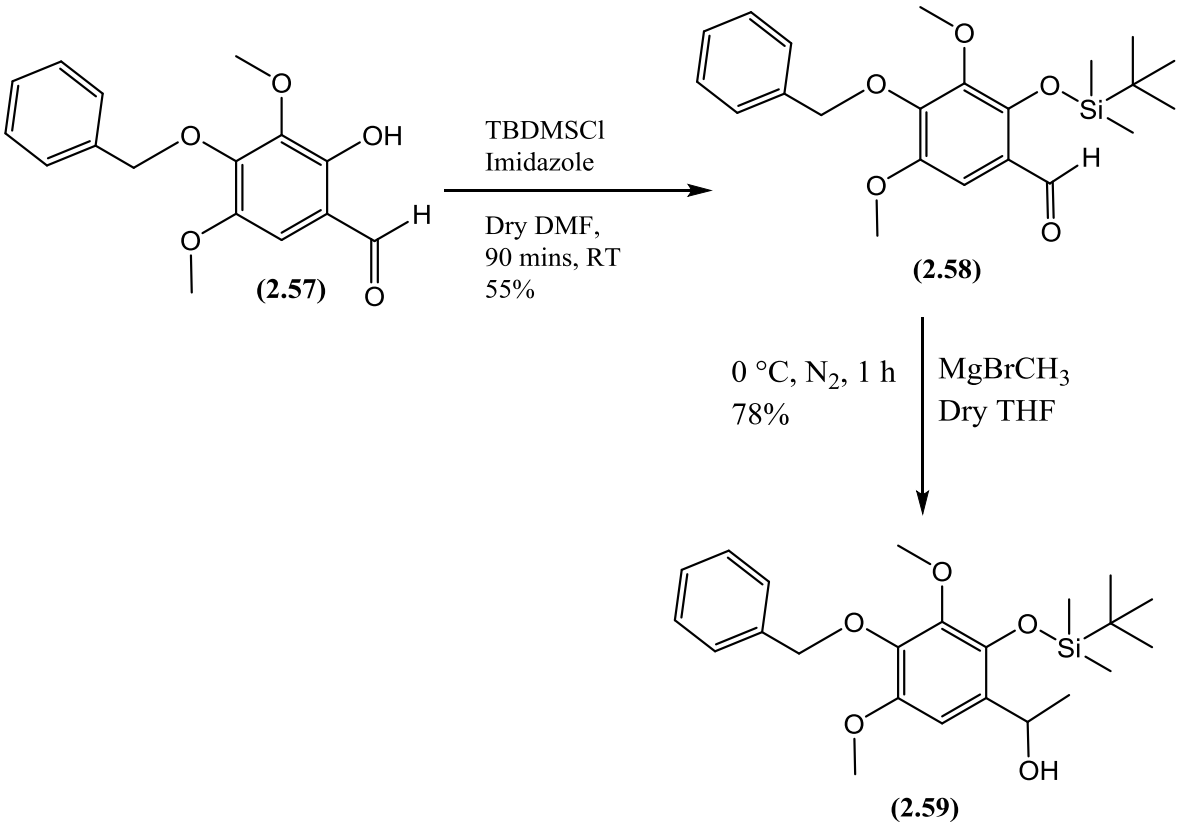

Scheme 2.51. Protection of phenol followed by Grignard reaction

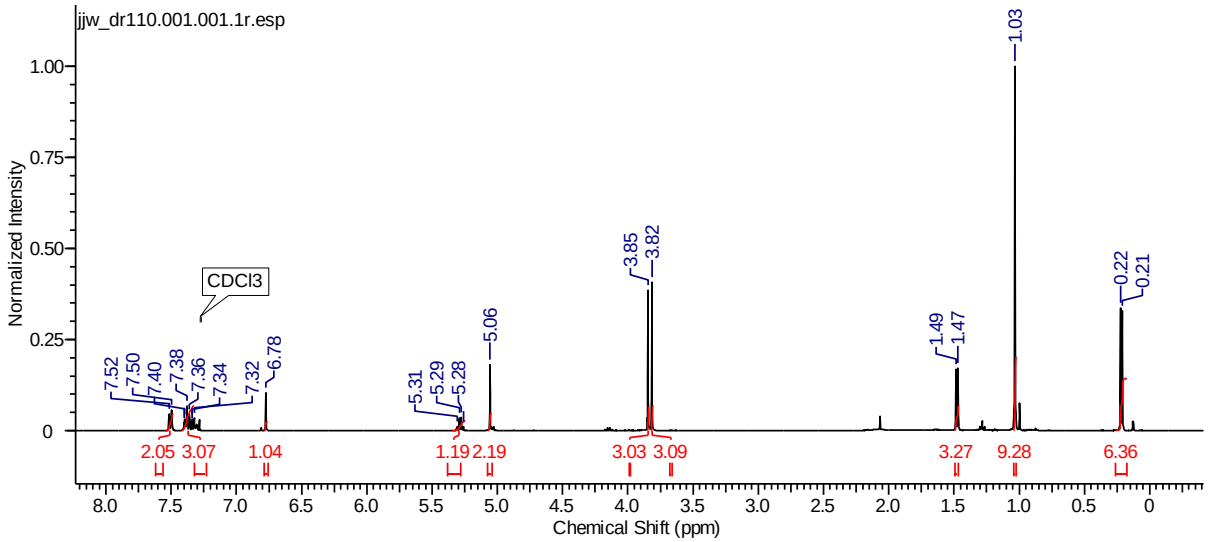

Figure 2.72. ^{1}H NMR spectrum of (2.59)

The next step in the synthetic sequence involved the oxidation of the alcohol **(2.59)** with Dess-Martin periodinane in dry DCM at 0 °C (Scheme 2.52). Upon completion the reaction was quenched with 5% $NaHCO_3$ and extracted with diethyl ether before being evaporated

and purified by flash column chromatography to afford the product namely 1-(4-(benzyloxy)-2-((*tert*-butyldimethylsilyl)oxy)-3,5-dimethoxyphenyl)ethan-1-one **(2.60)** with a yield of 74%. Its identity was confirmed due to the absence of the CHOH proton signals and the appearance of methyl-keto protons as a singlet at 2.62 ppm, in the ^{1}H NMR spectrum (figure 2.73).

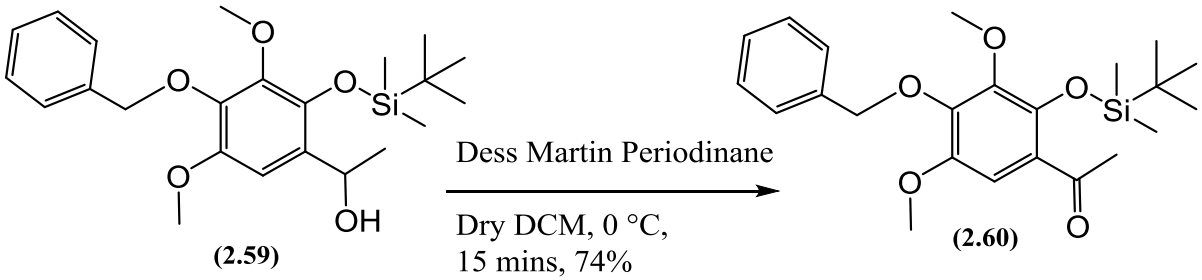

Scheme 2.52. Oxidation of alcohol to ketone

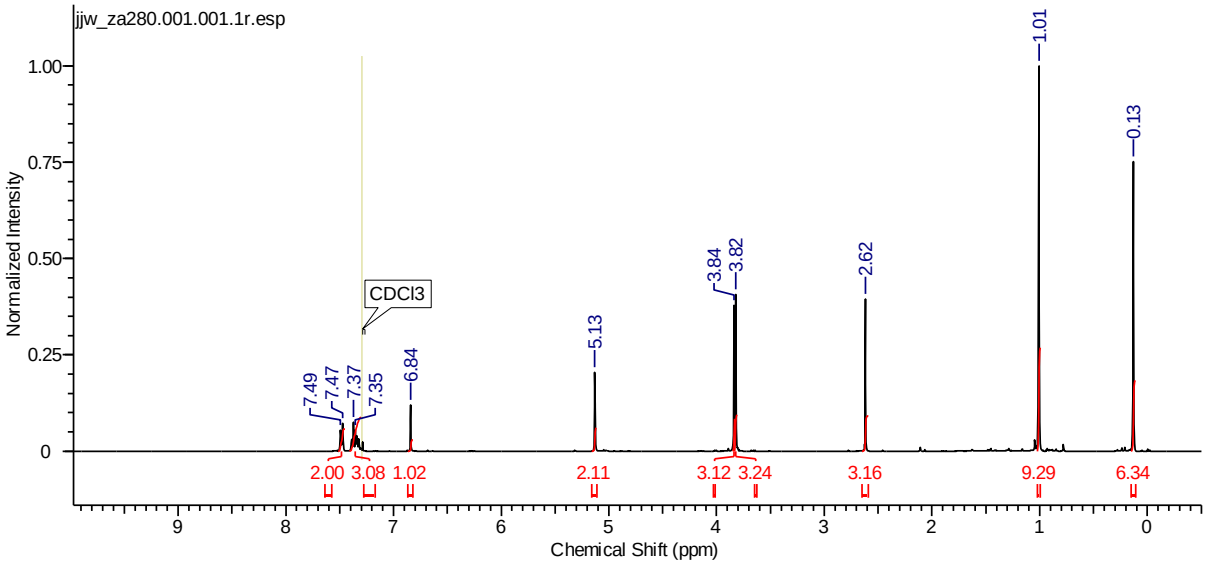

Figure 2.73. ^{1}H NMR spectrum of Ketone (2.60)

Removal of the *tert*-butyldimethyl silyl group of **(2.60)** was carried out in the presence of TBAF and THF at 0 °C to afford the keto-phenol **(2.61)**. The resultant keto-phenol underwent condensation with diethyl carbonate to give ethyl 3-(4-(benzyloxy)-2-hydroxy-3,5-dimethoxyphenyl)-3-oxopropanoate **(2.62)** in a yield of 90% (Scheme 2.53). Its structural identity was confirmed through inspection of its ^{1}H NMR spectrum (figure 2.74) which shows the characteristic triplet, at 1.30 ppm, integrating for 3 protons and a quartet, at 4.24 ppm, integrating for 2 protons for the ethyl side chain. The dicarbonyl methylene protons were also seen to resonate as a singlet at 3.96 ppm.

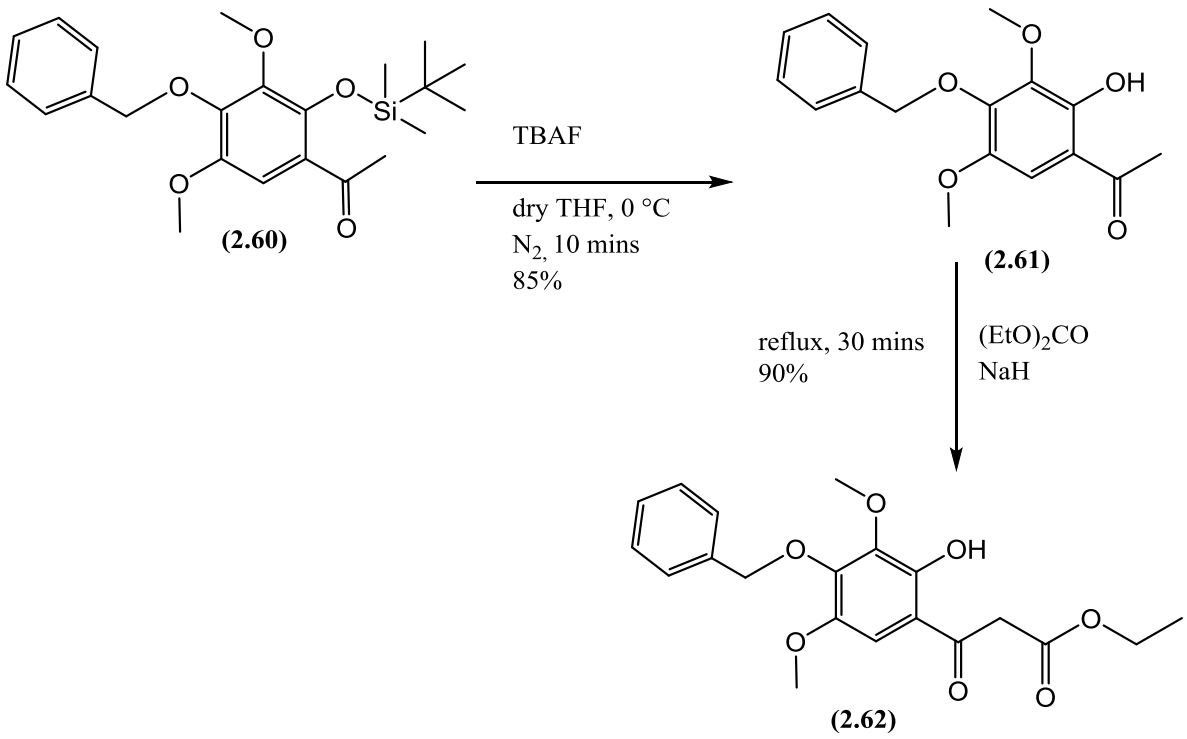

Scheme 2.53. Deprotection followed by condensation with diethyl carbonate

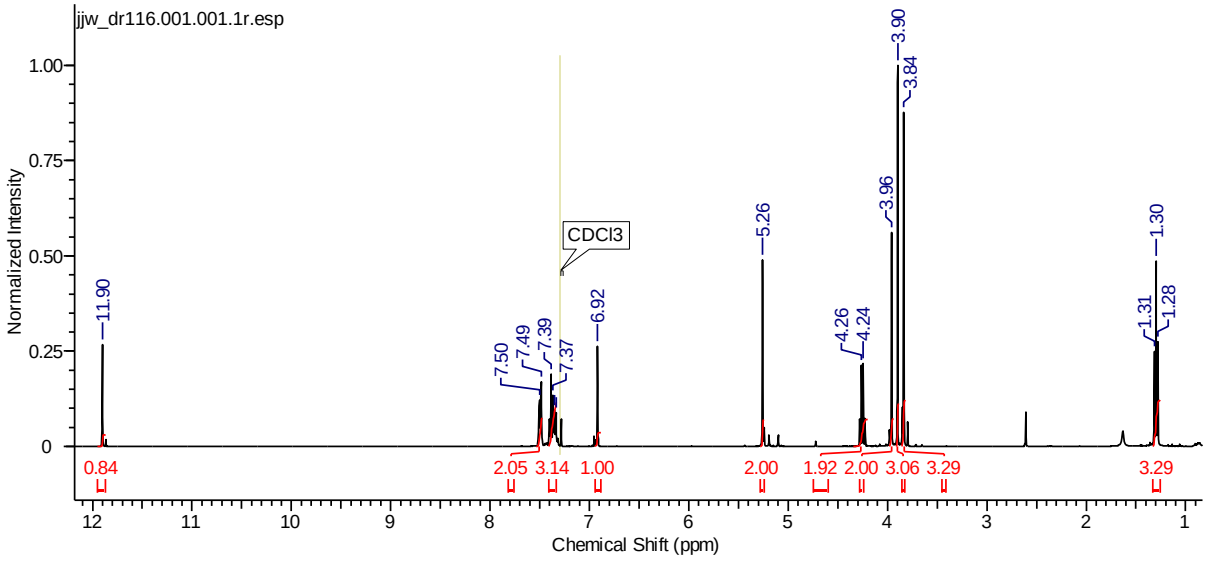

Figure 2.74. ^{1}H NMR spectrum of (2.62)

In order to get our desired 4-hydroxycoumarin, compound, **(2.62)** was cyclised by heating it in toluene at 120 °C for 16 hours. Upon evaporation of the organic solvent, the crude solid obtained was washed a few times with diethyl ether to afford the desired 7-(benzyloxy)-4-hydroxy-6,8-dimethoxy-2*H*-chromen-2-one **(2.63)** in an excellent yield of 82% (Scheme 2.54). Confirmation of its structure was achieved by analysis of its ^{1}H NMR

spectrum (figure 2.75) which showed the presence of the characteristic alkene proton resonating at 5.92 ppm and the complete absence of the ethyl side chain protons on **(2.62)** as expected.

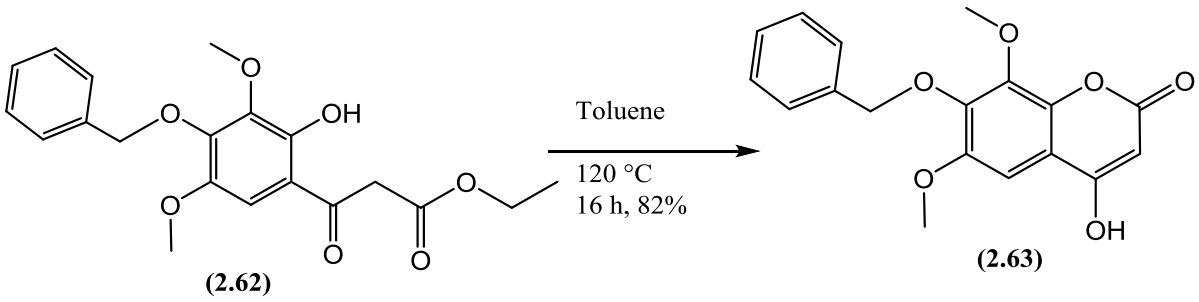

Scheme 2.54. Cyclization of compound (**2.62)**

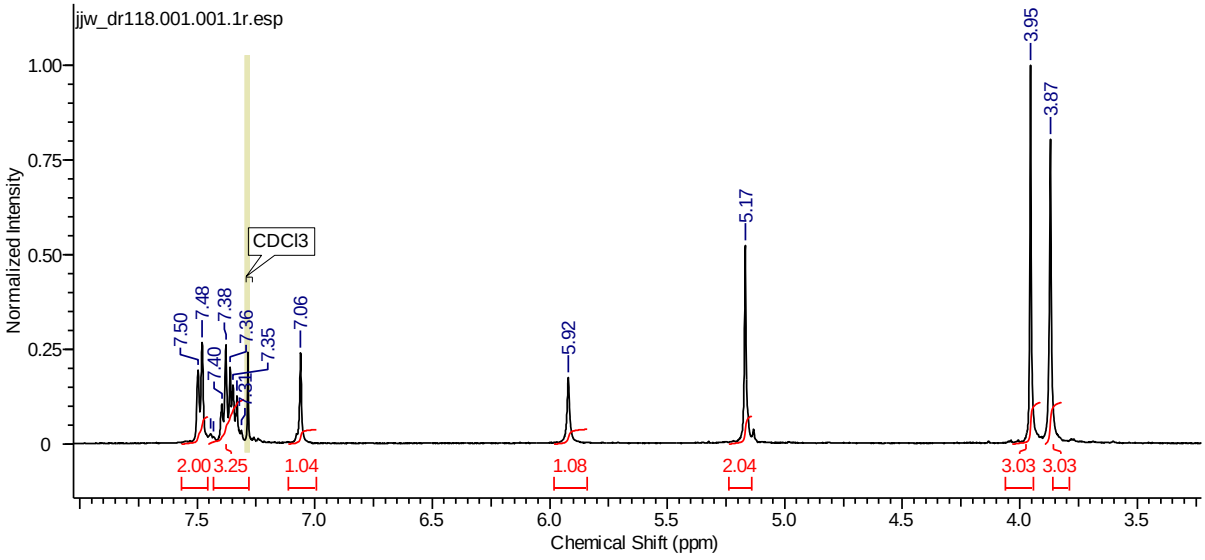

Figure 2.75. ^{1}H NMR spectrum hydroxycoumarin (2.63)

As we know a triflate derivative of 4-hydroxycoumarins serves as a useful leaving group when trying to form carbon-carbon bonds at this position under Suzuki coupling conditions. Thus 4-hydroxycoumarin **(2.63)** was converted into its triflate derivative by treating it with trifluoromethanesulfonic anhydride, using triethylamine as base in dry DCM under anhydrous conditions (Scheme 2.55). Due to the unstable nature of the triflate **(2.64)** structural characterization was not carried out and it was immediately subjected to the Suzuki coupling conditions to directly couple the boronic ester **(2.14)** to it.

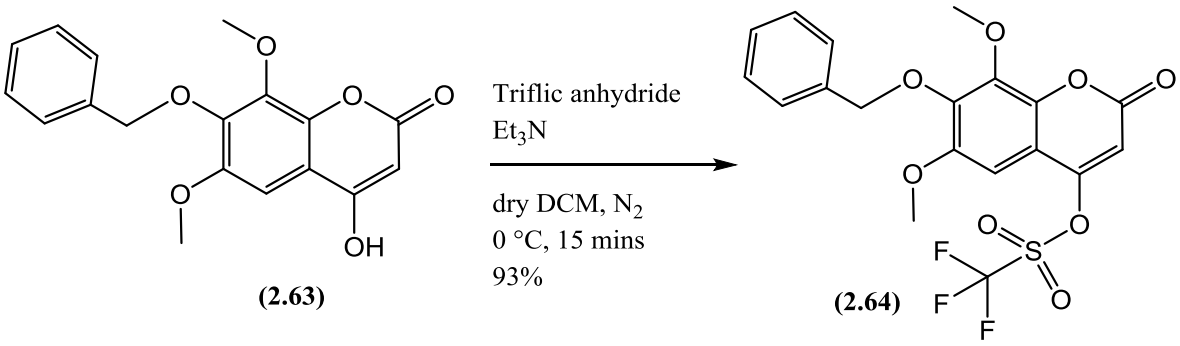

Scheme 2.55. Triflation of 4-hydroxycoumarin **(2.63)** with triflic anhydride

2.7.2 Coupling of chromenone precursor (2.64) to boronic ester (2.14)

Suzuki coupling was achieved by refluxing a biphasic mixture of toluene, ethanol and water containing $Pd(PPh_3)_4$ as catalyst, K_2CO_3 as a base, and both the triflate **(2.64)** and boronic ester **(2.14)** (Scheme 2.56). Following work-up and purification by column chromatography the coupled product **(2.65)** was obtained in 73% yield. The typical features of its ^{1}H NMR spectrum included the presence of the characteristic *t*-butyl signal of the Boc group at 1.53 ppm. Moreover the presence of an additional methoxy group and 3 additional aryl protons were also evident in the ^{1}H NMR spectrum (figure 2.76) of compound **(2.65)**.

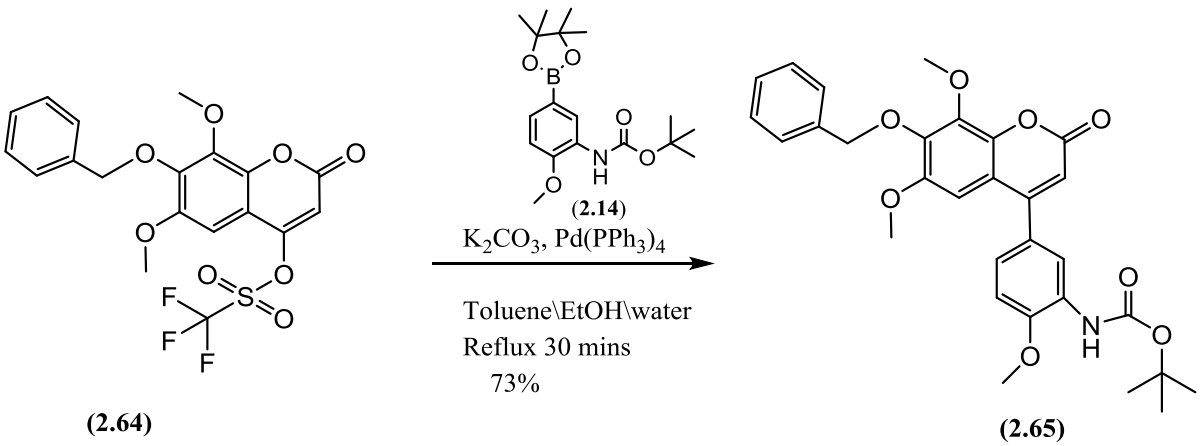

Scheme 2.56. Suzuki coupling of triflate **(2.64)** with boronic ester **(2.14)**

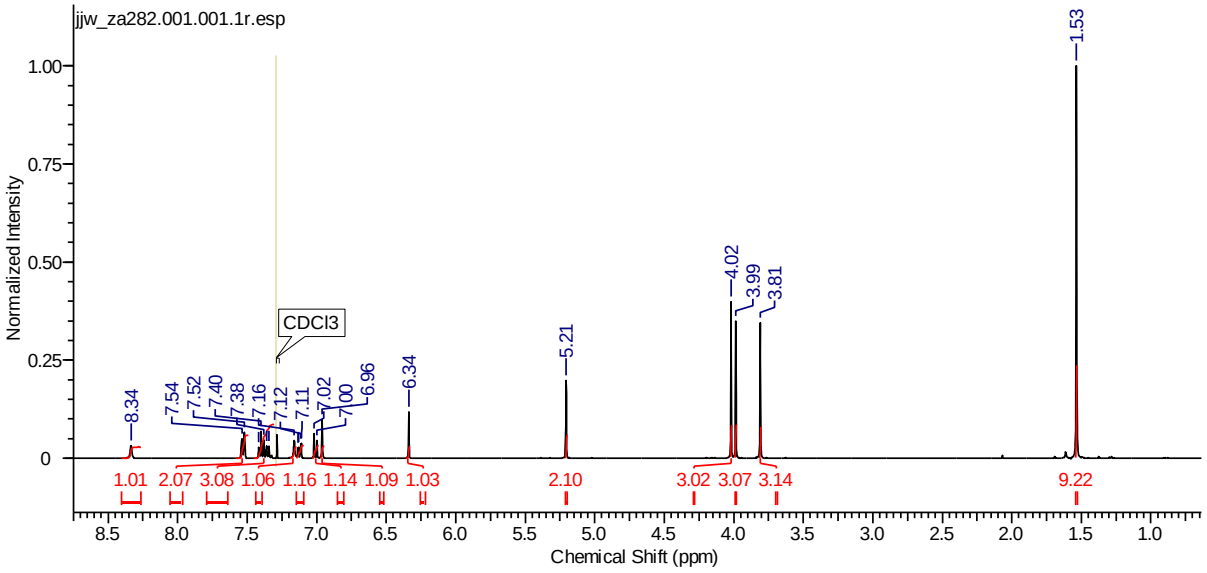

Figure 2.76. ^{1}H NMR spectrum of 2.65

Before the compound could be evaluated for its potential activity as tubulin polymerization inhibitor it was necessary to remove the Boc protecting group. This was achieved by stirring the compound **(2.65)** at -10 °C with cooled TFA:DCM (1:3) for 90 minutes (Scheme 2.57). Upon completion the reaction mixture was diluted with cold water and then quenched with 5% aq.$NaHCO_3$. Following extraction with diethyl ether and purification by flash column chromatography the structural identity of aniline **(2.66)** was confirmed due to the disappearance of *t*-Boc group signals in the ^{1}H (figure 2.77) and ^{13}C (figure 2.78) NMR spectra. ^{1}H NMR spectrum represents a total proton count of 23 while the ^{13}C-spectrum shows the presence of all 25 carbons. Moreover ^{1}H NMR spectrum also showed the presence of other expected signals including 3 methoxy groups (3.76, 3.96 and 4.02 ppm), benzyl protecting group and the aryl and alkene signals. The NH_2 also appeared to be resonating as broad overlapping signal at 3.71 ppm.

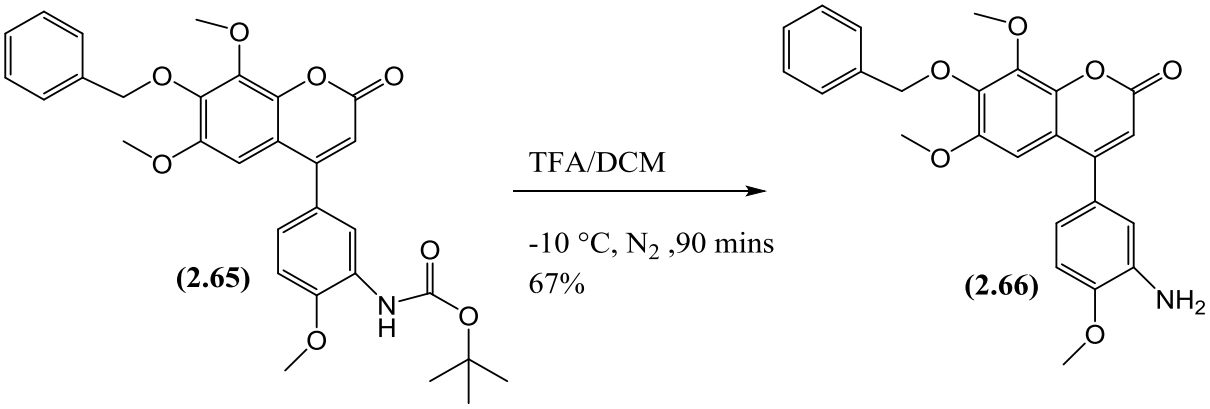

Scheme 2.57. Deprotection of Boc protecting group

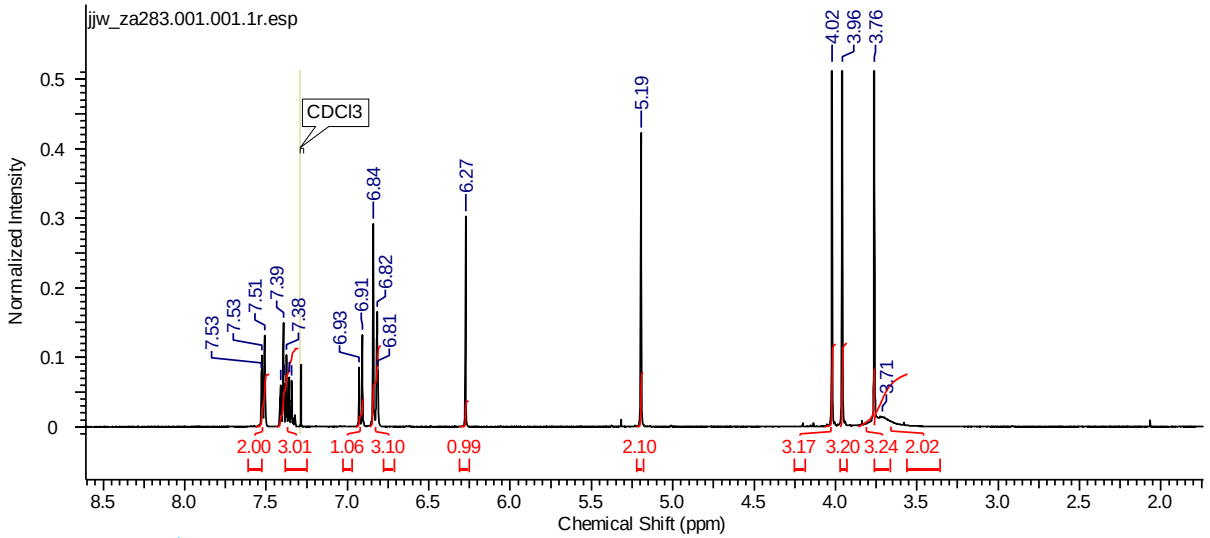

Figure 2.77. ^{1}H NMR spectrum of aniline (2.66)

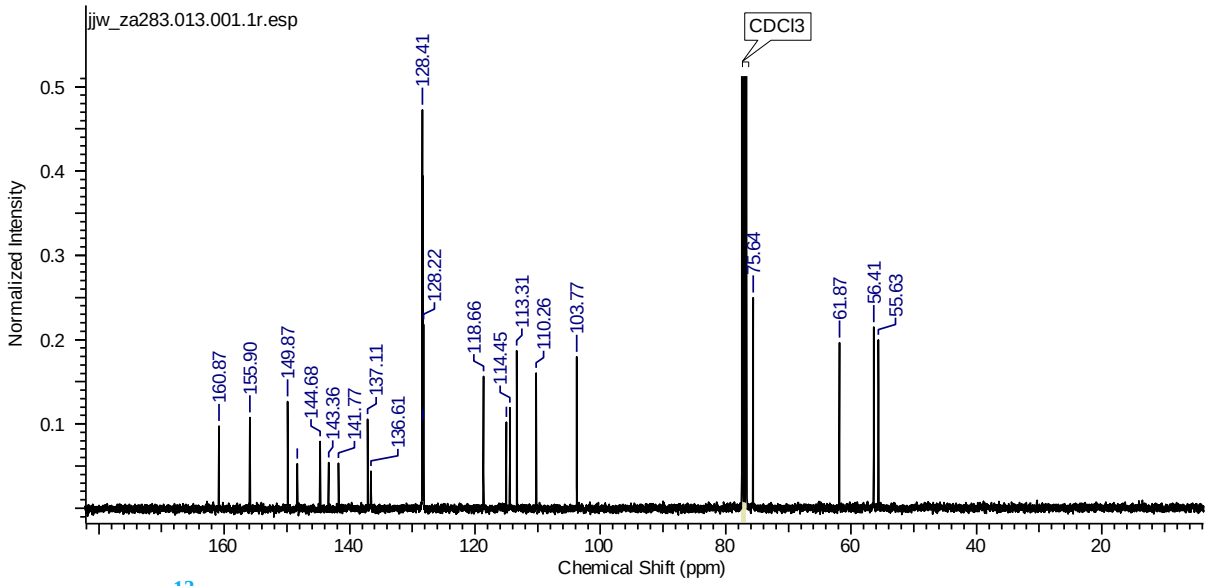

Figure 2.78. ^{13}C NMR spectrum of aniline (2.66)

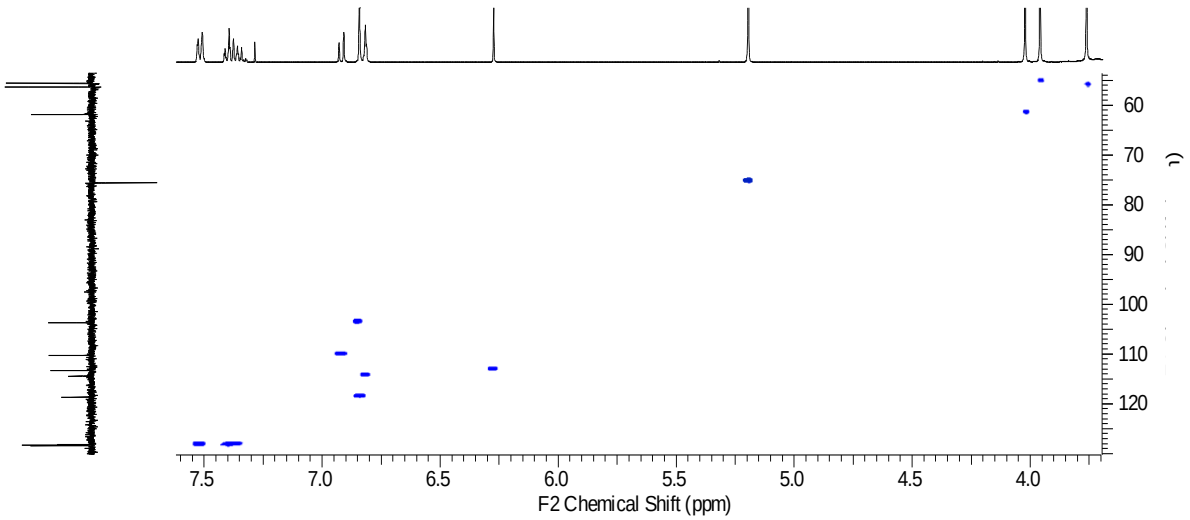

Figure 2.79. HSQC spectrum of aniline (2.66)

2.7.3 Synthesis of 4-(3-amino-4-methoxyphenyl)-7-hydroxy-6,8-dimethoxy-2H-chromen-2-one (2.68)

For the synthesis of 4-(3-amino-4-methoxyphenyl)-7-hydroxy-6,8-dimethoxy-2H-chromen-2-one **(2.68)**, the compound **(2.65)** was first debenzylated under hydrogenolysis, using Pd/C in methanol and dichloromethane to afford the phenol **(2.67)** with a yield of 84% (scheme 2.58). The removal of benzyl protecting group was confirmed by the ^{1}H NMR spectrum (figure 2.80) of the phenol due to the absence signals for CH_2 and 5 aryl protons of the benzyl protecting group. Moreover the presence of phenolic OH was also found resonating as broad singlet at 8.32 ppm.

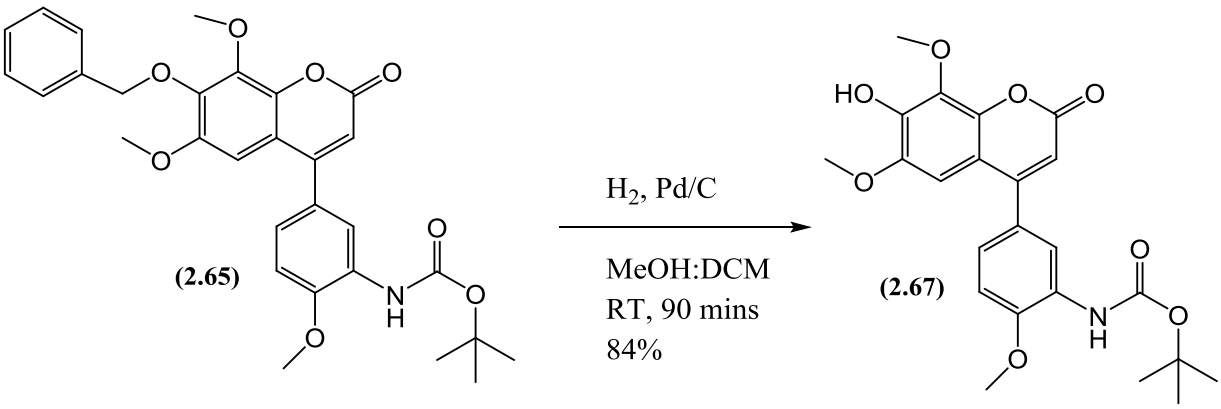

Scheme 2.58. Removal of benzyl protecting group

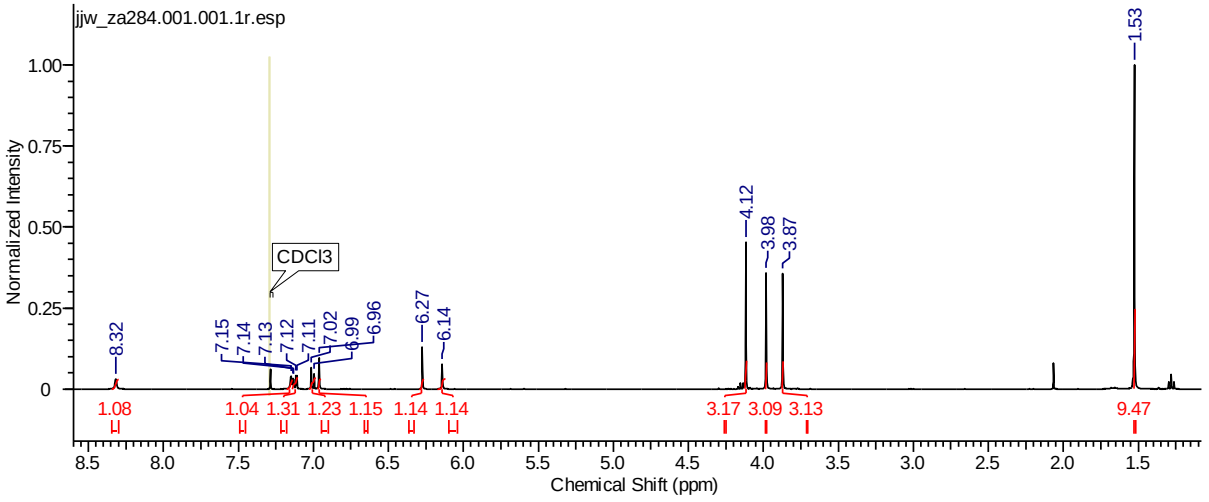

Figure 2.80. ^{1}H NMR spectrum of phenol (2.67)

In the final step the Boc protecting group was removed using cooled TFA in dry DCM (1:3) to get our desired final compound **(2.68)** in an excellent yield of 93% (Scheme 2.59). Structural confirmation was carried out using NMR spectroscopy. The ^{1}H NMR spectrum (figure 2.81) represents a total proton count of 17 while the ^{13}C-spectrum (figure 2.82) shows the presence of all 18 carbons. The striking feature of the ^{1}H NMR spectrum includes the presence of NH_2 signal at 5.00 ppm and phenolic OH signal at 10.00 ppm. Moreover the ^{1}H NMR spectrum also shows the presence of 3 methoxy groups, 4 aryl protons and 1 alkene proton that was also confirmed by the HSQC spectrum of the compound **(2.68)** (figure2.83).

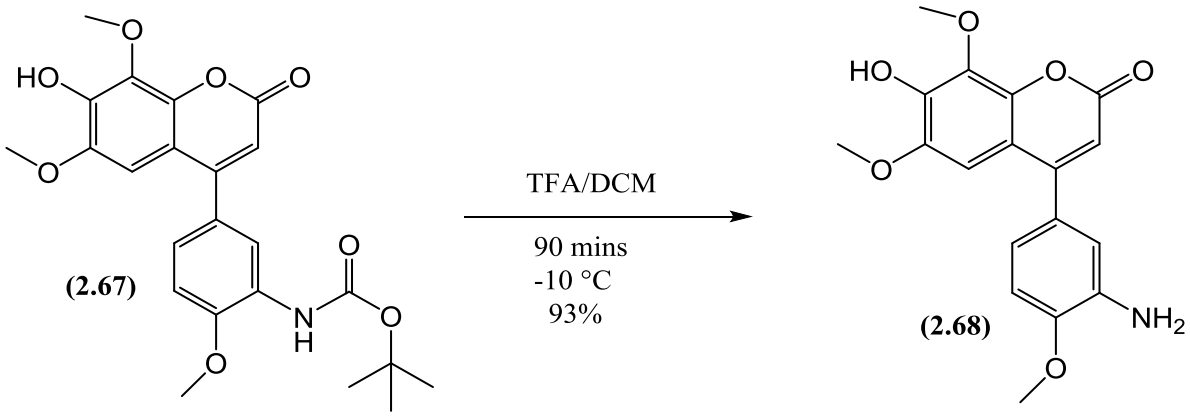

Scheme 2.59. Removal of Boc protecting group

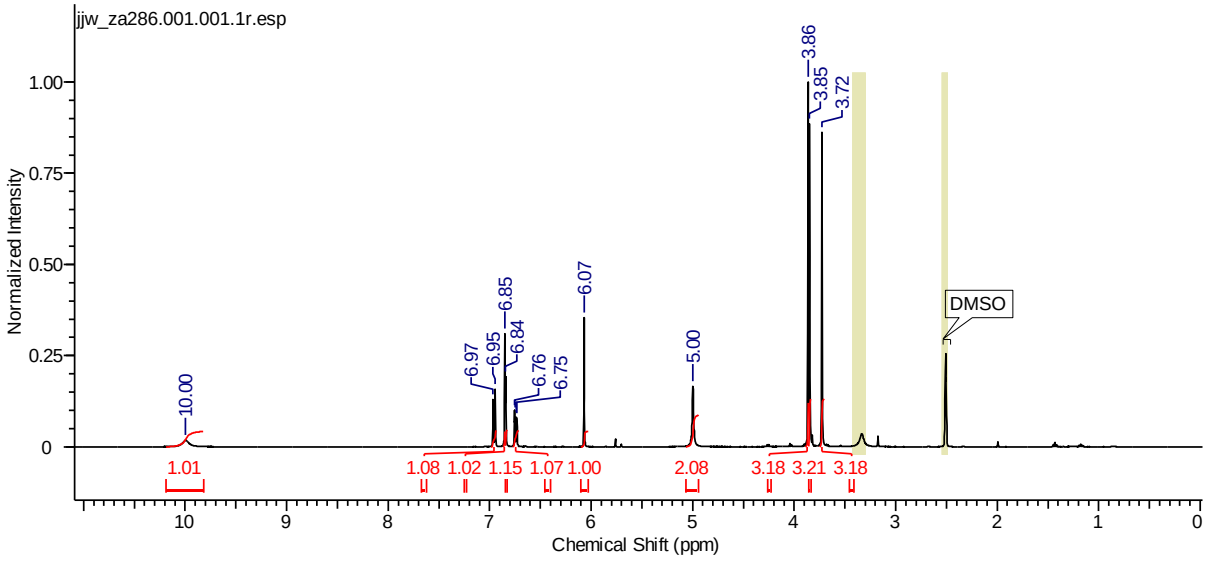

Figure 2.81. ^{1}H NMR spectrum of aniline (2.68)

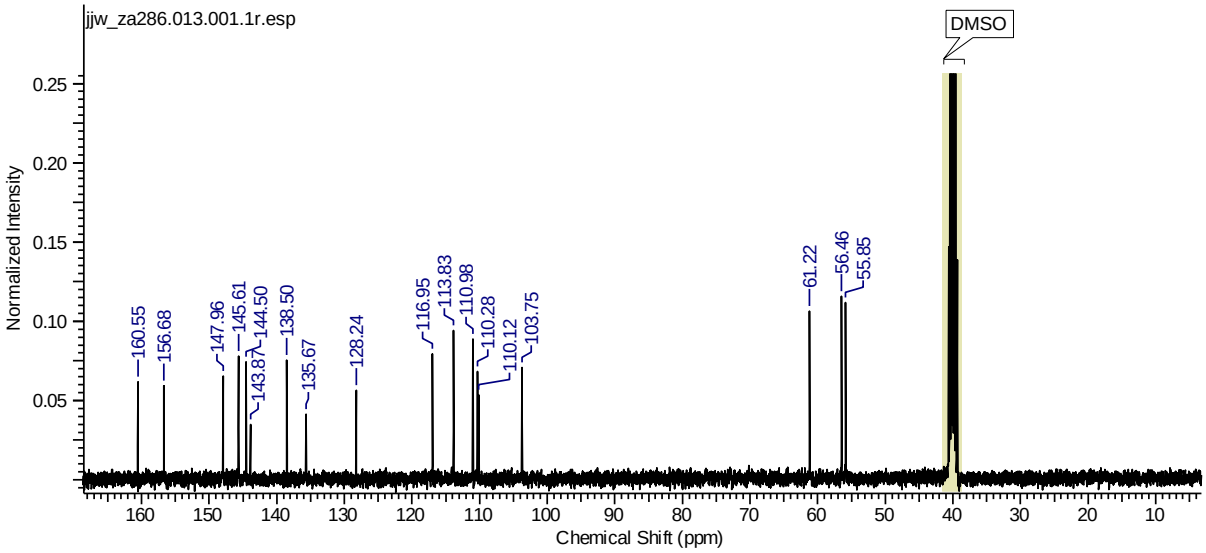

Figure 2.82. ^{13}C NMR spectrum of aniline (2.68)

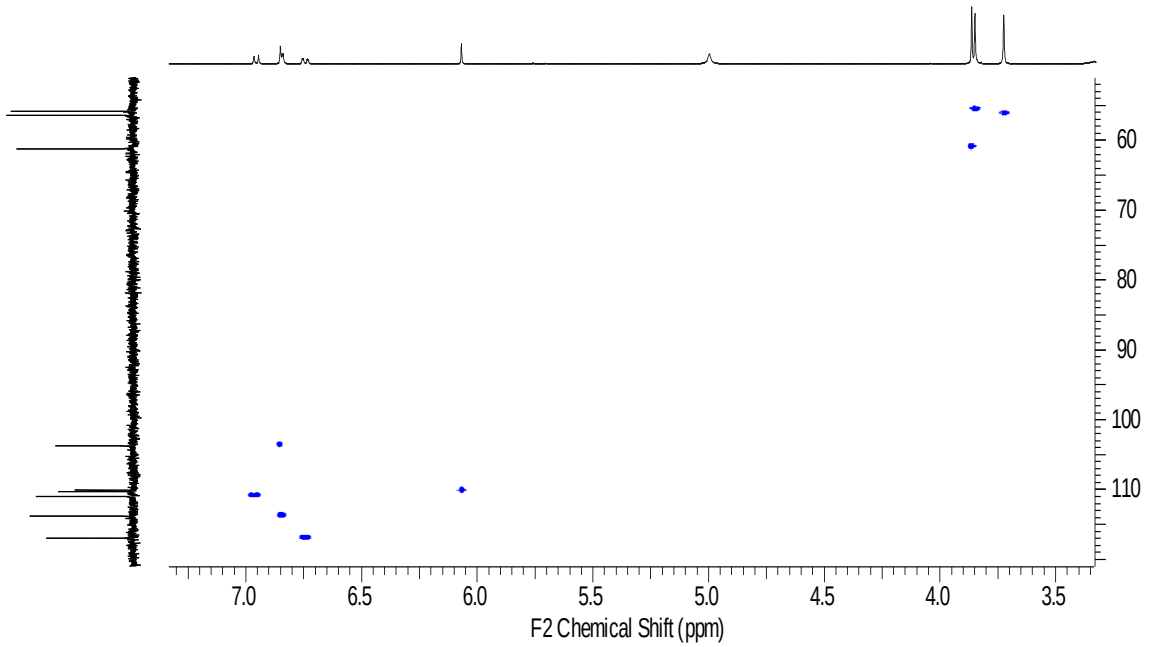

Figure 2.83. HSQC spectrum of aniline (2.68)

2.7.4 Synthesis of 2-((4-(3-amino-4-methoxyphenyl)-6,8-dimethoxy-2-oxo-2H-chromen-7-yl)oxy)acetic acid (2.71)

For the synthesis of 2-((4-(3-amino-4-methoxyphenyl)-6,8-dimethoxy-2-oxo-2H-chromen-7-yl)oxy)acetic acid **(2.71)**, the phenol **(2.67)** was refluxed with benzyl bromoacetate in the first step using potassium carbonate as base and acetone as solvent (scheme 2.60). Upon completion the organic solvent was evaporated and the remainder was purified by flash column chromatography to afford the product **(2.69)** in 90% yield. The presence of additional features in the ^{1}H NMR spectrum (figure 2.84) including 2 methylene groups

(4.89, 5.26 ppm) and 5 aryl protons of the benzyl protecting group confirmed the synthesis of desired product.

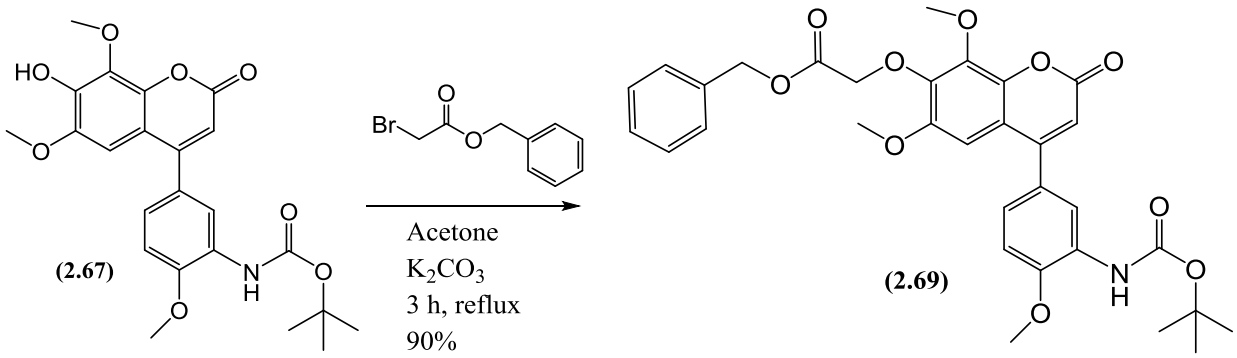

Scheme 2.60. Alkylation of phenol **(2.67)**

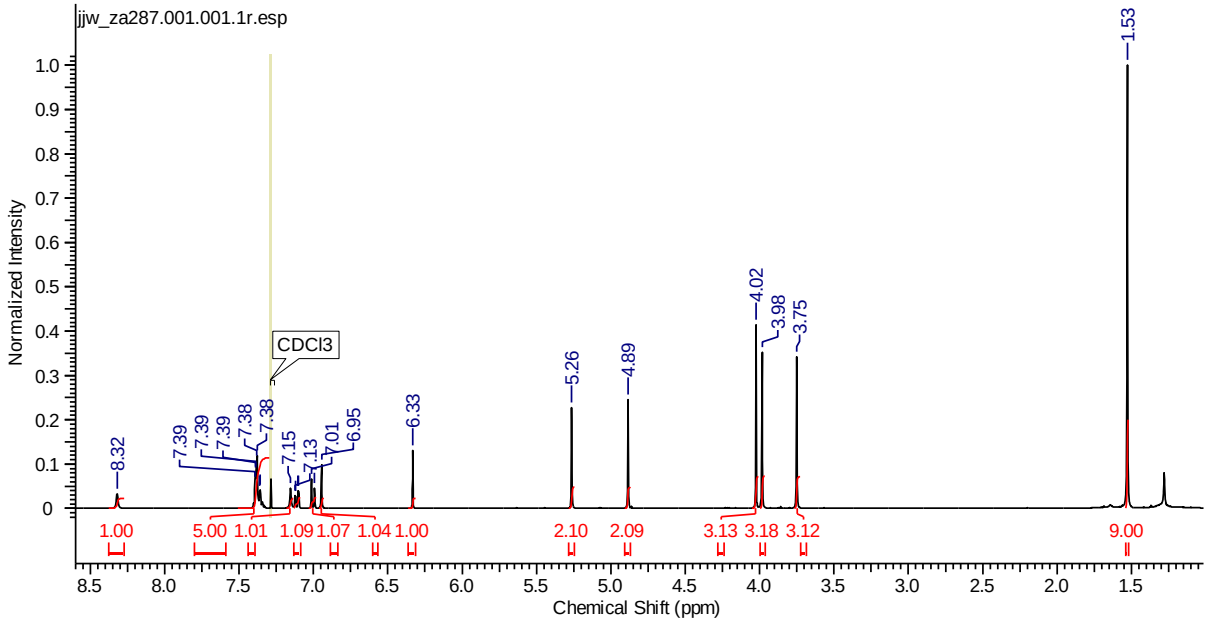

Figure 2.84. ^{1}H NMR spectrum of (2.69)

In the next step the benzyl protecting group was removed under exactly the same conditions as that required for **(2.67)** thereby affording the product with a yield of 96% (scheme 2.61). The structural identity of the intermediate **(2.70)** was confirmed by ^{1}H NMR spectrum (figure 2.85) where the expected loss of the benzyl group was evident.

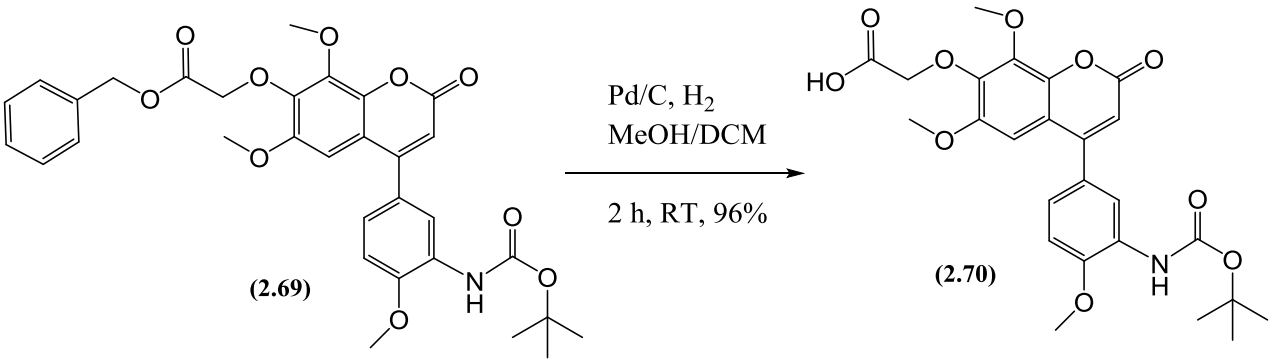

Scheme 2.61. Removal of benzyl protecting group

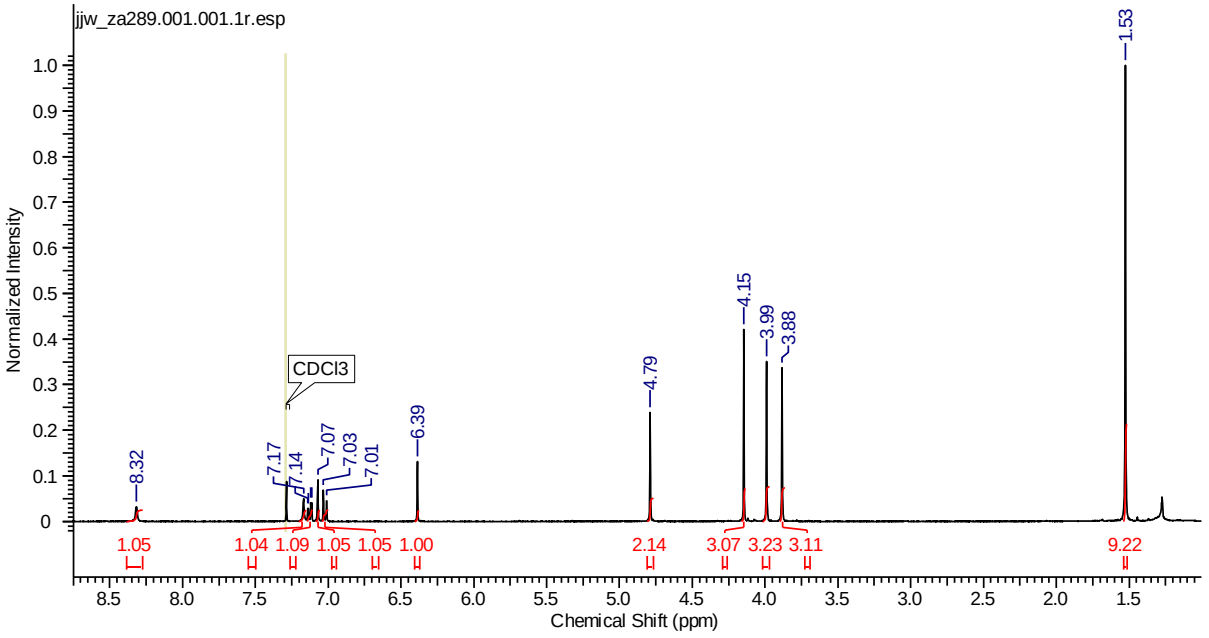

Figure 2.85. ^{1}H NMR spectrum of Acid (2.70)

The final step towards the synthesis of our desired aniline compound **(2.71)** was the removal of Boc protecting group. That was achieved by stirring the compound with cooled TFA:DCM (1:3) at -10 $^{\circ}$C for two hours (scheme 2.62). Upon work-up and purification the structural identity of the product was confirmed mainly by NMR spectroscopy. The ^{1}H NMR spectrum (figure 2.86) of compound **(2.71)** represents a total proton count of 18 while the ^{13}C-spectrum (figure 2.87) gives a total count of 20 carbons. The signal for the OH proton was absent most probably due to deuterium exchange. The confirmation of the deprotection was achieved due the absence of signal for *t*-Boc group and the appearance of NH_2 signal at 5.02 ppm in the ^{1}H NMR spectrum. Moreover the HSQC spectrum (figure

2.71) was used to identify the corresponding carbons of four aryl protons, one alkene proton, one CH_2 group and 3 methoxy groups.

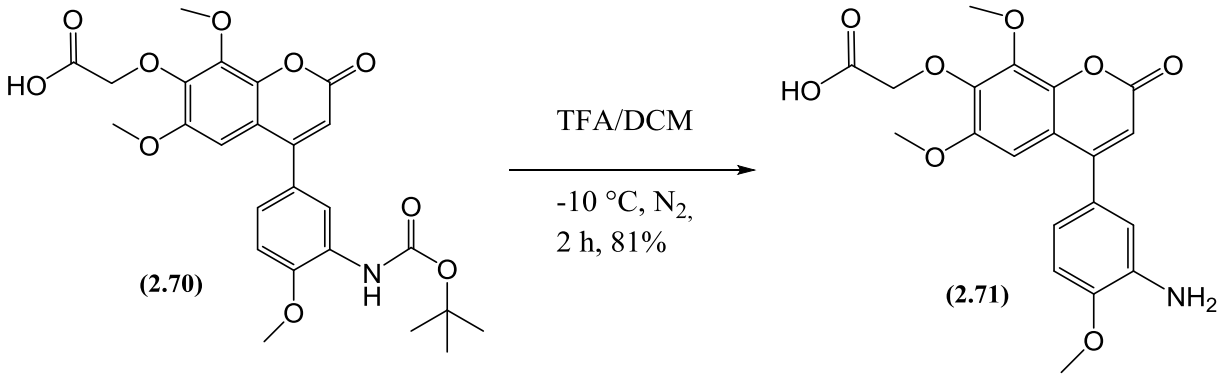

Scheme 2.62. Removal of Boc protecting group

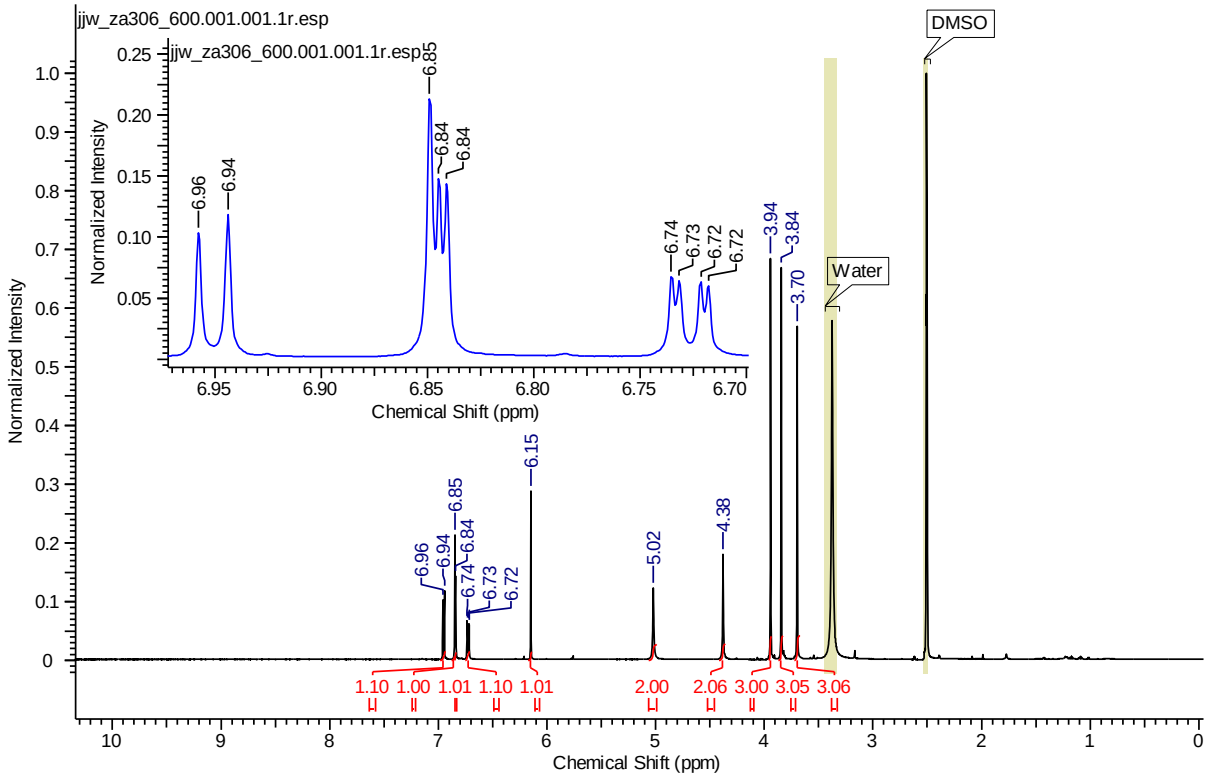

Figure 2.86. ^{1}H NMR spectrum of aniline (2.71)

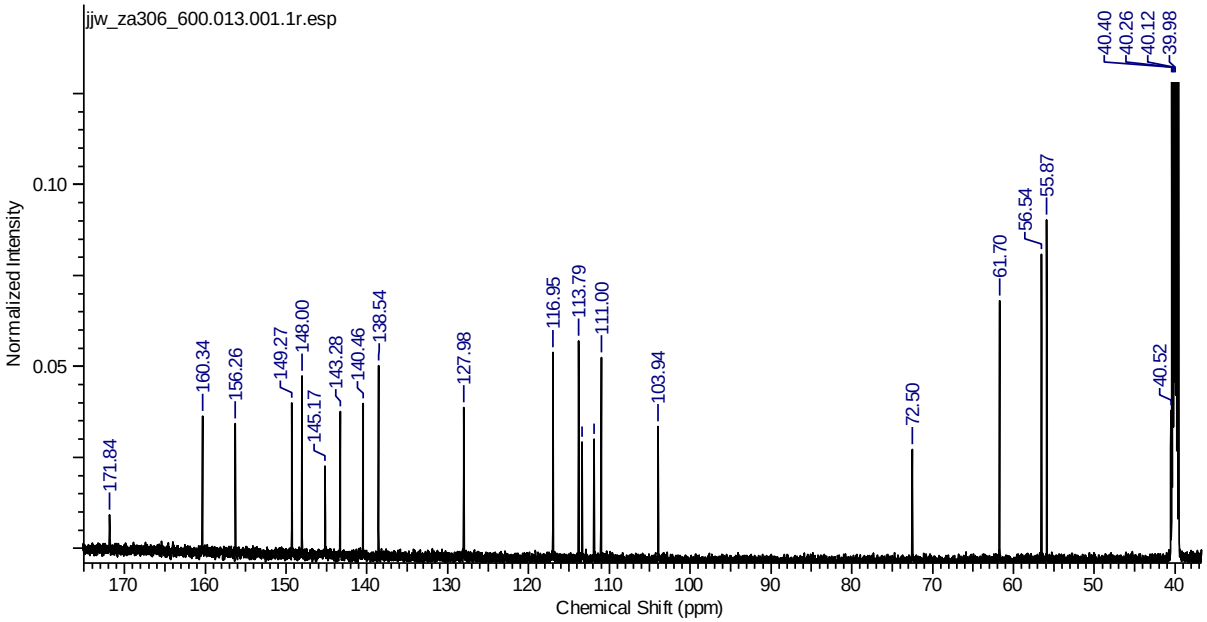

Figure 2.87. ^{13}C NMR spectrum of aniline (2.71)

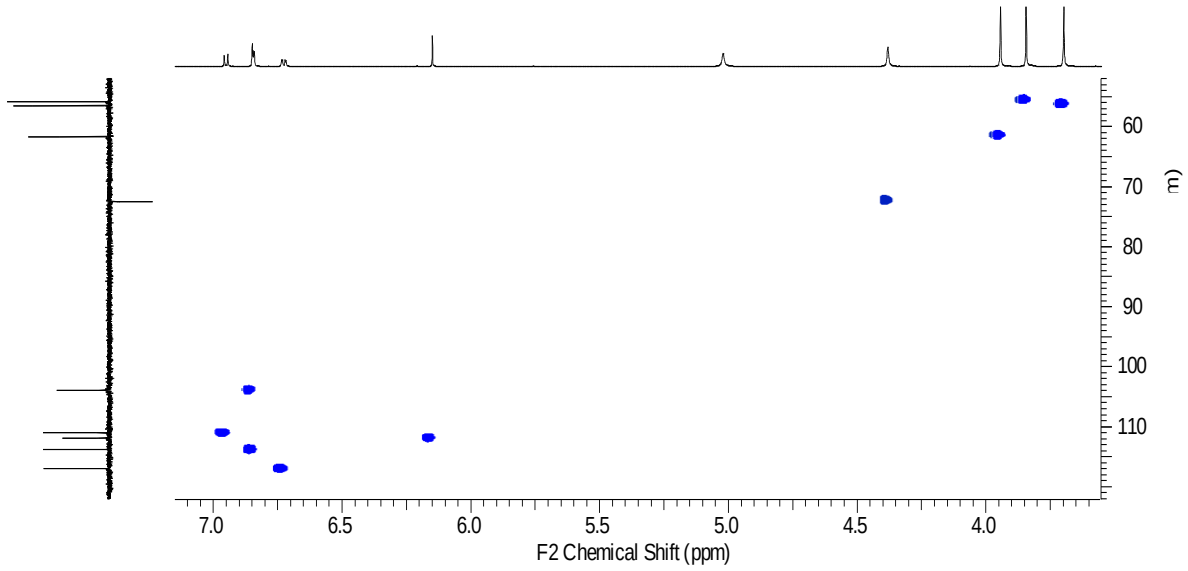

Figure 2.88. HSQC spectrum of aniline (2.71)

2.8 Tubulin polymerisation inhibition data and conclusions

All the compounds synthesised in chapter 2 were evaluated for their activity as tubulin polymerisation inhibitors. The assay procedure employed is given at the end of experimental chapter. The general structure of the compounds tested is shown in the figure 2.89 while the results are summarised in the table (figure 2.90). Of all the compounds

synthesised in this chapter, only six demonstrated inhibition of tubulin polymerisation. From the assay results it is concluded that replacing the carbonyl functionality (C2) of the 4-arylcoumarin with thione or oxime resulted in the reduced activity. This was observed when the carbonyl functionality of compound **(2.16)** (IC_{50}= 1.413 µM) was replaced with thiocarbonyl **(2.18)** (IC_{50} = 7.116 µM) and with oximes **(2.20** and **2.26)** (Inactive). From these observations it was concluded that the presence of carbonyl functionality at position 2 (C2) of 4-arylcoumarins is essential for activity. Furthermore introducing different functionalities at carbon 3 (C3) of 4-arylcoumarins rendered these compounds **(2.50, 2.44, 2.46, 2.48, 2.51)** inactive as tubulin polymerisation inhibitors. It was demonstrated that replacing the trimethoxy arrangement at the aromatic A-ring of 4-arylcoumarin **(2.16)** (IC_{50}= 1.413 µM) with a dimethoxy substitution **(2.68)** (IC_{50}= 3.094 µM) has a negligible effect on the tubulin polymerisation inhibition activity. Moreover, bulky groups can be introduced at the A-ring phenolic functionality of the 4-arylcoumarin **(2.68)** without having any major reduction in the tubulin binding activity of the compound and this was observed in the case of compound **(2.66) (**IC_{50}= 3.299 µM).

(2.16), R= OCH_3, R_1= O, R_2= H, R_3= NH_2

(2.18), R= OCH_3, R_1= S, R_2= H, R_3= NH_2

(2.20), R= OCH_3, R_1= NOH, R_2= H, R_3= NH_2

(2.22), R= OCH_3, R_1= O, R_2= H, R_3= OH

(2.24), R= OCH_3, R_1= S, R_2= H, R_3= OH

(2.25), R= OCH_3, R_1= NOH, R_2= H, R_3= OH

(2.26), R= OCH_3, R_1= $NOCH_3$, R_2= H, R_3= OH

(2.44), R= OCH_3, R_1= O, R_2= COOH, R_3= NH_2

(2.46), R= OCH_3, R_1= O, R_2= HCNOH, R_3= NH_2

(2.48), R= OCH_3, R_1= O, R_2= CH_2OH, R_3= NH_2

(2.50), R= OCH_3, R_1= O, R_2= acetal, R_3= OH

(2.51), R= OCH_3, R_1= O, R_2= CHO, R_3= OH

(2.66), R= OBn, R_1= O, R_2= H, R_3= NH_2

(2.68), R= OH, R_1= O, R_2= H, R_3= NH_2

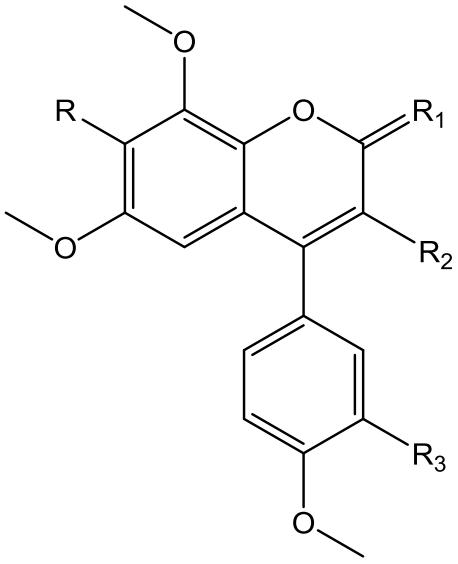

Figure 2.89. General structure of 4-phenylcoumarin derivatives

Compound	IC_{50} (μM)	(R^2)
(2.16)	**1.413**	**0.9191**
(2.18)	**7.116**	**0.8983**
2-oxime derivative (2.20)	**Inactive**	
(2.22)	**2.745**	**0.9289**
(2.24)	**6.905**	**0.9205**
2-oxime derivative (2.25)	**Inactive**	
2-methyloxime derivative (2.26)	**Inactive**	
3-carboxycoumarin (2.44)	**Inactive**	
3-aldoxime derivative (2.46)	**Inactive**	
3-alcohol derivative (2.48)	**Inactive**	
3-acetalcoumarin (2.50)	**Inactive**	
3-aldehyde derivative (2.51)	**Inactive**	
(2.66)	**3.299**	**0.9332**
(2.68)	**3.094**	**0.9412**
CA-4	**2.736**	**0.9775**

Figure 2.90. IC_{50} values obtained from tubulin polymerisation assay

Figures 2.91, 2.92, 2.93, 2.94, 2.95 and 2.96 present the results obtained for the synthesized compounds, together with combretastatin A-4 (CA-4) as positive control and DMSO as negative control.

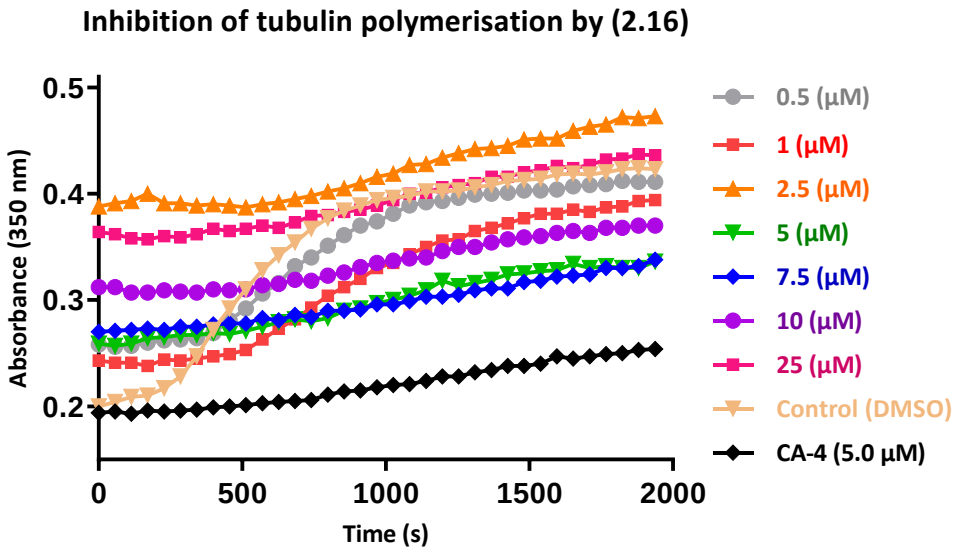

Figure 2.91. Results obtained for the *in vitro* tubulin polymerization assay of (2.16) in different concentrations

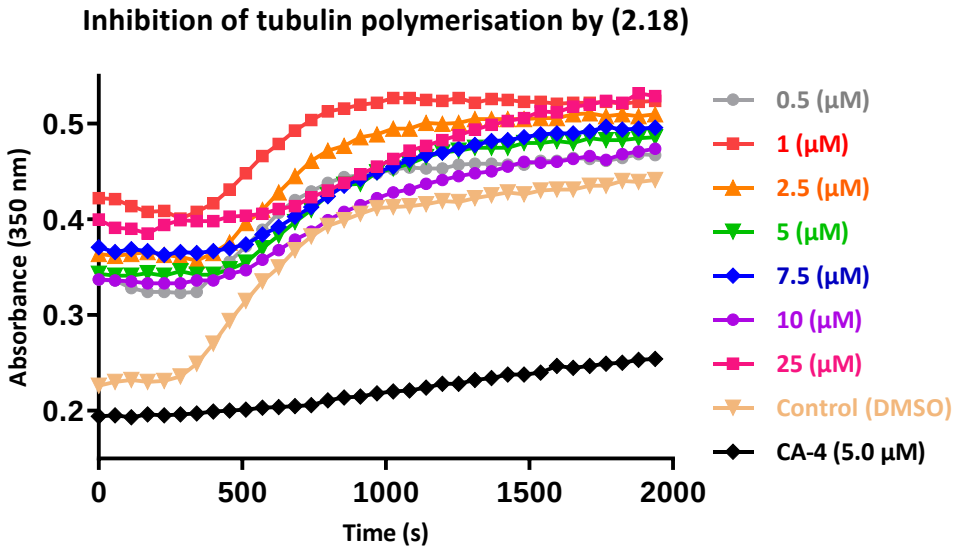

Figure 2.92. Results obtained for the *in vitro* tubulin polymerization assay of (2.18) in different concentrations

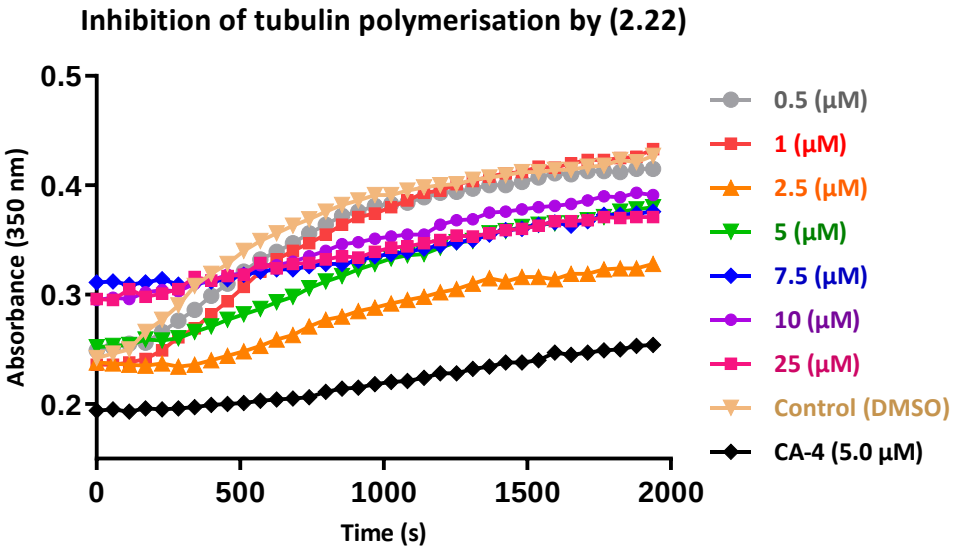

Figure 2.93. Results obtained for the *in vitro* tubulin polymerization assay of (2.22) in different concentrations

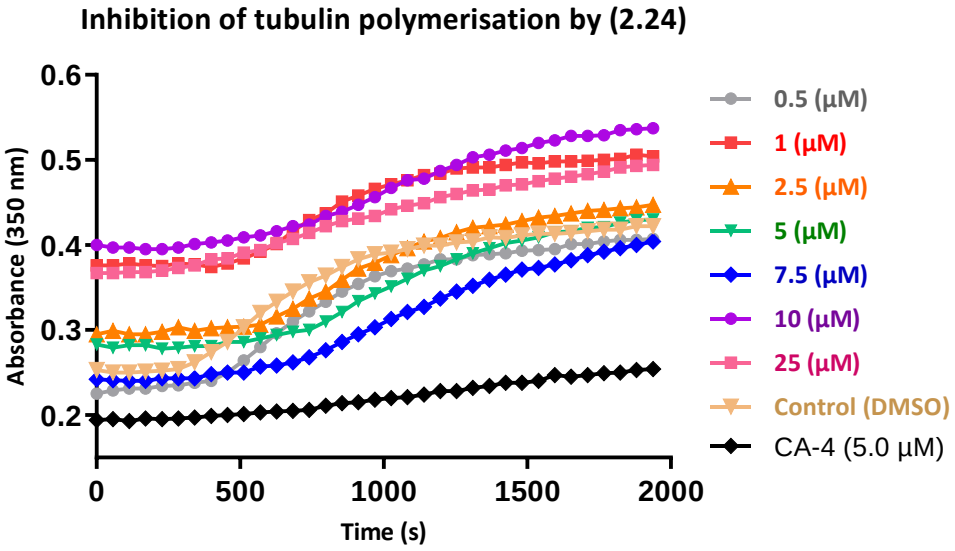

Figure 2.94. Results obtained for the *in vitro* tubulin polymerization assay of (2.24) in different concentrations

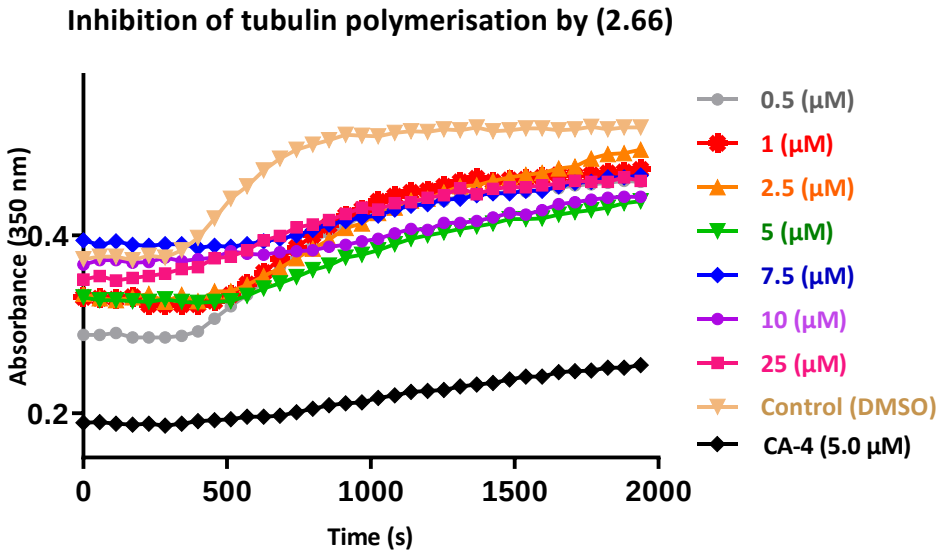

Figure 2.95. Results obtained for the *in vitro* tubulin polymerization assay of (2.66) in different concentrations

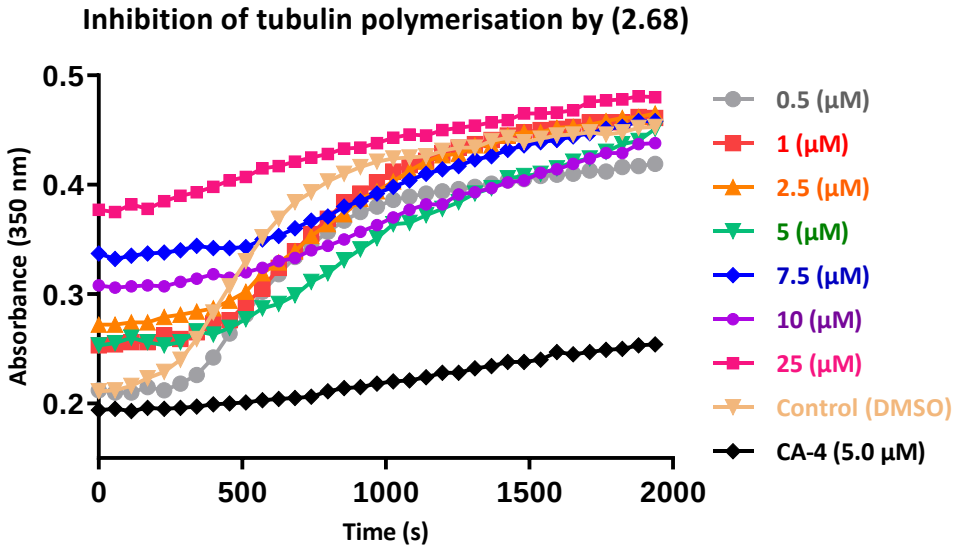

Figure 2.96. Results obtained for the *in vitro* tubulin polymerization assay of (2.68) in different concentrations

The percent tubulin polymerisation inhibition of five compounds at 5 µM was compared to CA-4 (figure 2.97). The compound **(2.16)** presented 69.74 ± 6.44% inhibition, followed by **(2.66)** 58.11 ± 3.44%, **(2.22)** 48.64 ± 10.99% and **(2.68)** 47.61 ± 3.31%. The two thiocarbonyl compounds **(2.18)** and **(2.24)** demonstrated 20.73 ± 5.12 and 25.85 ± 7.06% inhibition activities respectively. The control CA-4 gave 63.01 ± 1.90% inhibition.

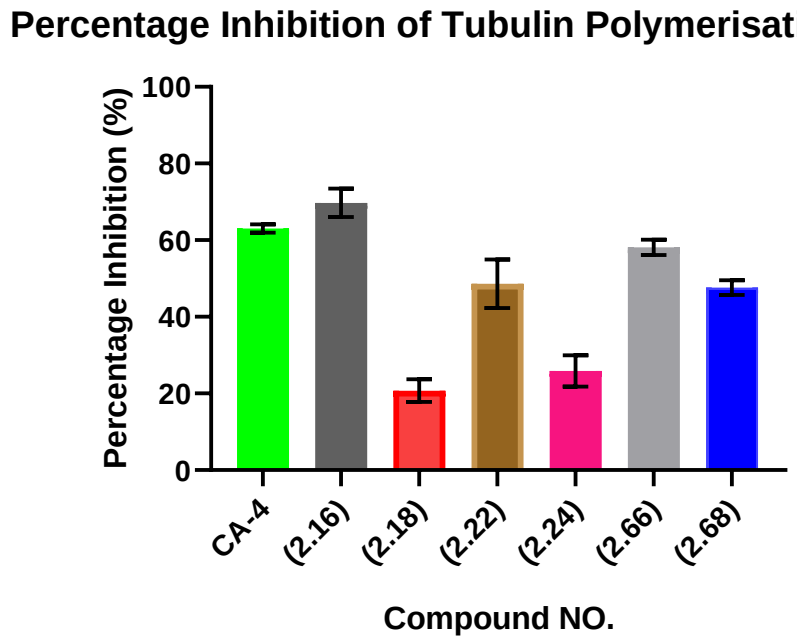

Figure 2.97. Percentage inhibition of tubulin polymerisation for coumarin derivatives at 2.5 µM concentration

The percentage inhibition of tubulin polymerisation was plotted against log concentration (M) to obtain dose responsive curve for compounds **(2.16)**, **(2.18)**, **(2.22)**, **(2.24)**, **(2.66)**, **(2.68)** and **CA-4** (figure 2.98)**.**

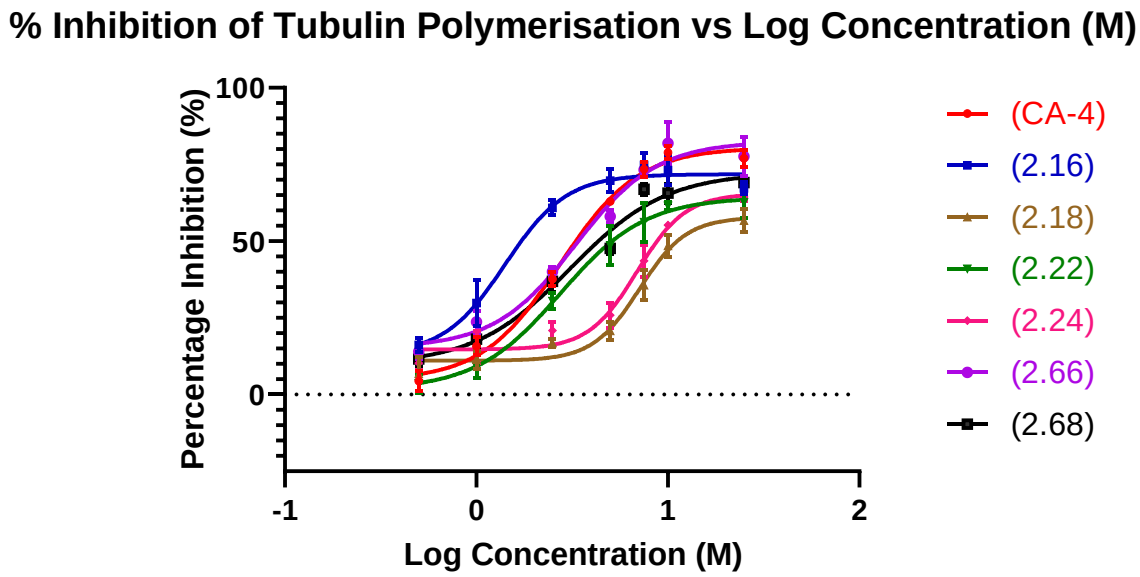

Figure 2.98. Percent inhibition vs log concentration for tubulin polymerisation inhibitors (2.16), (2.18), (2.22), (2.24), (2.66), (2.68) and (CA-4). (error bars represent SEM of n = 3, in triplicate)

Chapter 3

Synthesis of phenstatin based compounds

3.0 Introduction

The purpose of the work described in this chapter was to generate a further set of potent tubulin inhibitors with additional linker units for loading of the peptide-based APN inhibitors. In particular a catechol-like structure on the A-ring was deemed desirable with the option of a phenolic or aniline structure on the B-ring akin to phenstatin **(1.11)** or aminophenstatin **(1.13)** (figure 3.1) by utilising phenstatin and its derivatives have proven to be potent inhibitors of tubulin polymerisation that act by binding at the colchicine binding site of tubulin. For example phenstatin showed comparable antiproliferative activity to combretastatin A-4 when evaluated in the NCI (National Cancer Institute USA) 60 cell line human tumour screen and proved to be a potent inhibitor of tubulin polymerization [85, 87].

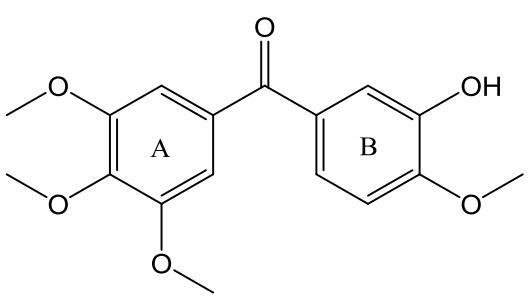

Phenstatin **(1.11)**

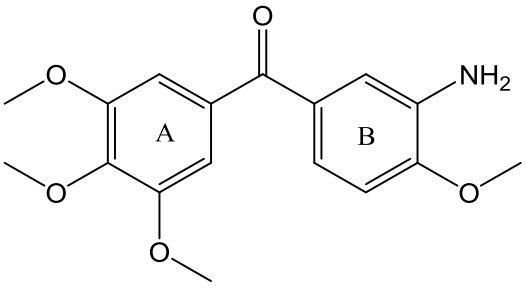

Aminophenstatin **(1.13)**

Figure 3.1 Structures of phenstatin compounds

By keeping in mind the highly active nature of phenstatins as cytotoxic agents it was decided to synthesise derivatives that would allow us to attach tumor specific peptides with the aim of optimising their targeted delivery to tumour vasculature. As we know APN is zinc dependent, membrane-bound ectopeptidase that is highly expressed on endothelial cells of neoangiogenic but not on normal vasculature so we will be utilizing APN targeting peptides as the homing device for the selective delivery of our phenstatin based compounds to the tumor tissue.

3.1 Synthesis of phenstatin compounds based on phenolic B-ring (2.09)

During our research, while we were working on 3-carboxycoumarin derivatives, a phenstatin based compound **(2.38)** with the trimethoxy arrangement on the A-ring was synthesised that demonstrated potent inhibition of tubulin polymerisation. This compound was already synthesised by Pettit *et al.* However as the essential target of our work in this

chapter was to create additional phenstatin-like compounds with a greater number of linker sites on them we set about the synthesis of **(3.04)**, **(3.09)** and **(3.20)** (figure 3.2).

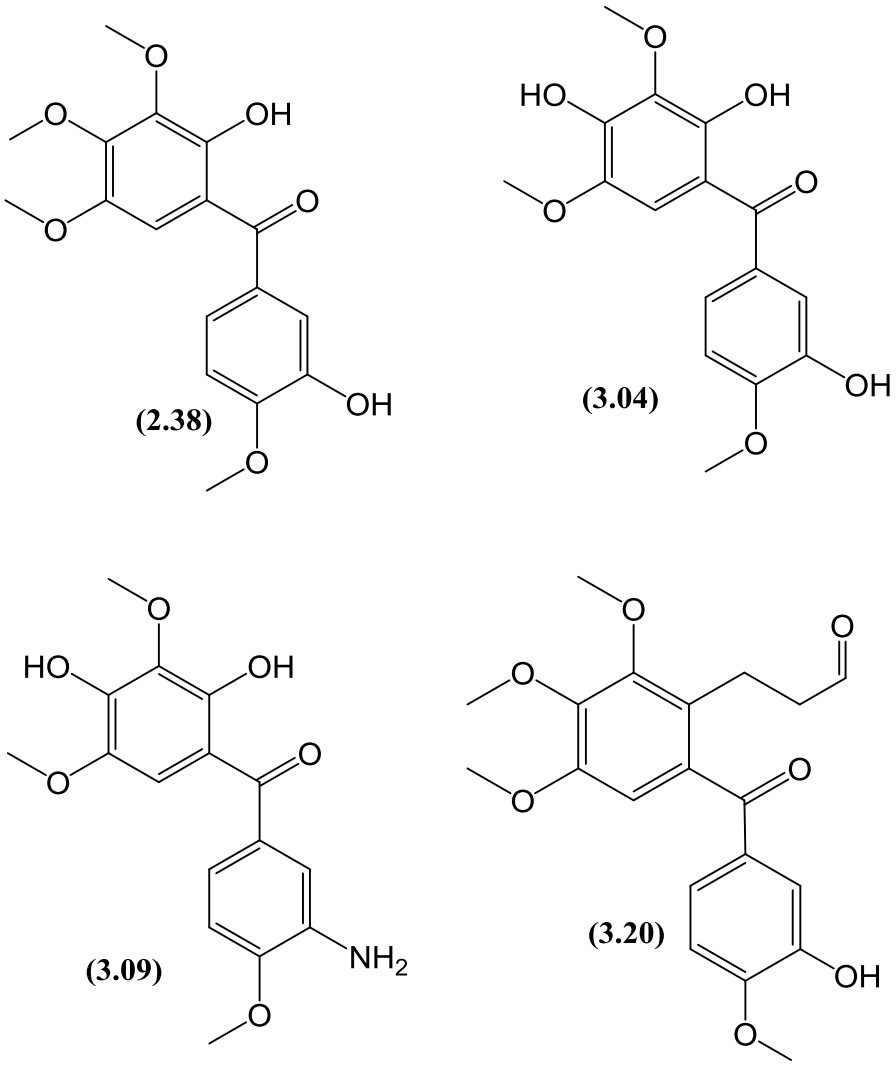

Figure 3.2 Structures of phenstatin derivatives

The starting point for the synthesis of **(3.04)** and **(3.09)** was **(2.57)**, a building block that we used in the synthesis of the compounds outlined in Chapter 2. The silyl protected bromophenol **(2.09)** was directly coupled to it through a Grignard reaction but unfortunately the yield of the reaction was very low. In order to solve this problem we decided to use an alternate method of organolithium coupling. The reaction was carried out using *n*-butyl lithium (2.5 M in hexane) in dry THF at -80 for one hour and then at -50 °C for one hour (scheme 3.1). After the work-up and purification by column chromatography, the structural identity of **(3.01)** was confirmed by analysis of its ^{1}HNMR spectrum (figure 3.3) which shows the expected presence of the 3 methoxy groups (3.71, 3.82 and 3.82 ppm) and 2 *tert*-butyldimethyl silyl protecting groups (0-1.5 ppm).

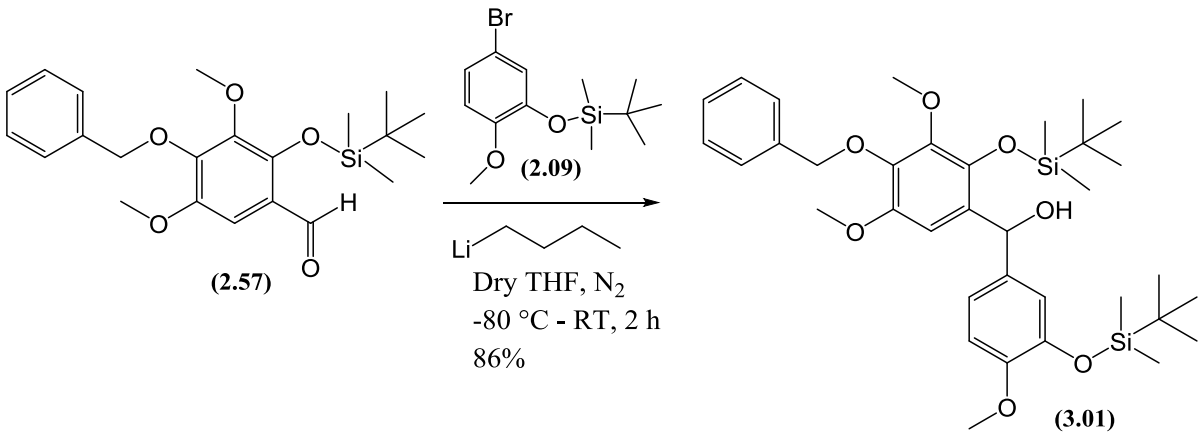

Scheme 3.1. Organolithium coupling of benzaldehyde **(3.01)**

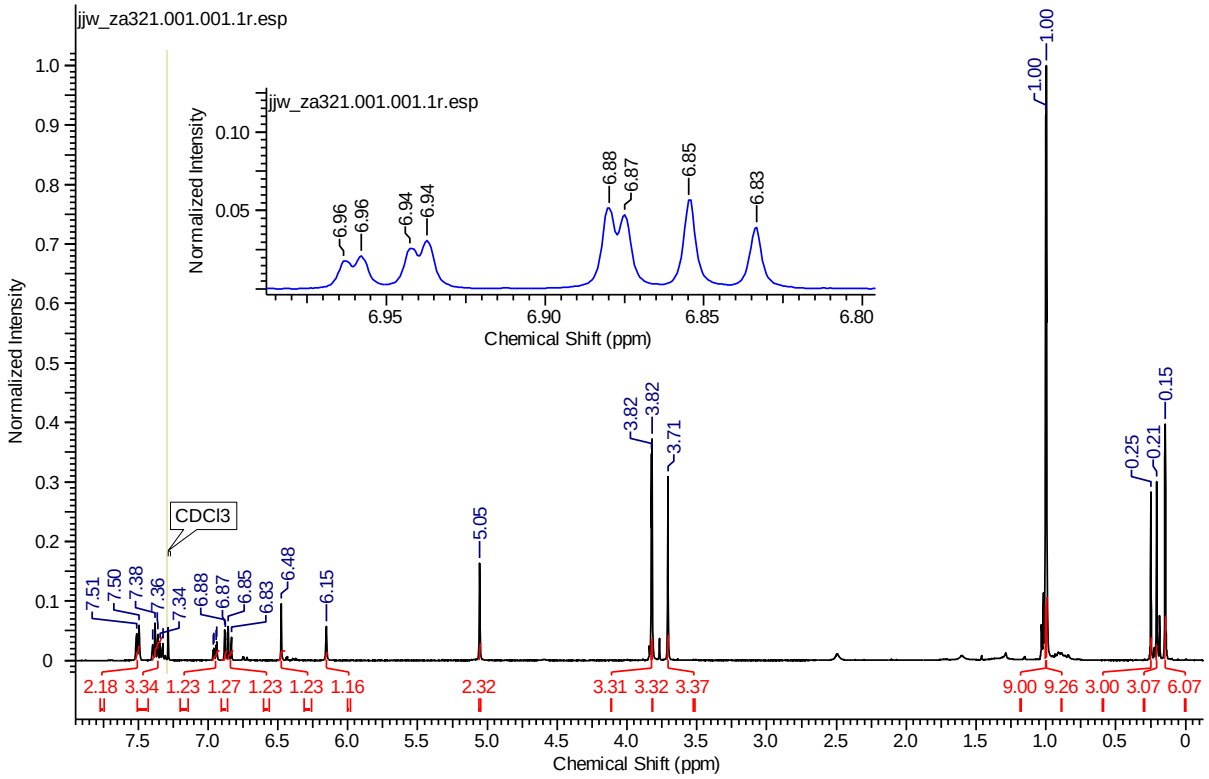

Figure 3.3. ^{1}H-NMR spectrum of diphenylmethanol (3.01)

In order to have the desired ketone functionality, the alcohol functional group of **(3.01)** was oxidized with Dess Martin Periodinane using dry DCM as solvent at 0 °C (scheme 3.2). Upon completion, the reaction mixture was quenched with 5% aq. $NaHCO_3$ and extracted with DCM. After evaporating the organic solvent and purification by flash column chromatography, the product **(3.02)** was obtained in 84% yield. The structural identity of the product was confirmed by NMR spectroscopy where the ^{1}H NMR spectrum (figure 3.4)

shows the absence of the -CH- proton (6.15 ppm) while the ^{13}C spectrum (figure 3.5) confirmed the presence of the carbonyl functional group resonating at 195.00 ppm.

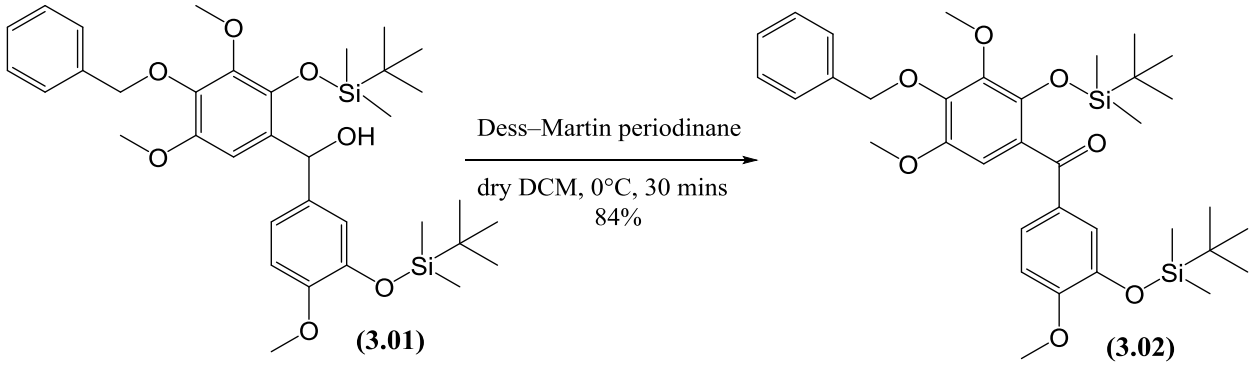

Scheme 3.2. Oxidation of alcohol **(2.71)**

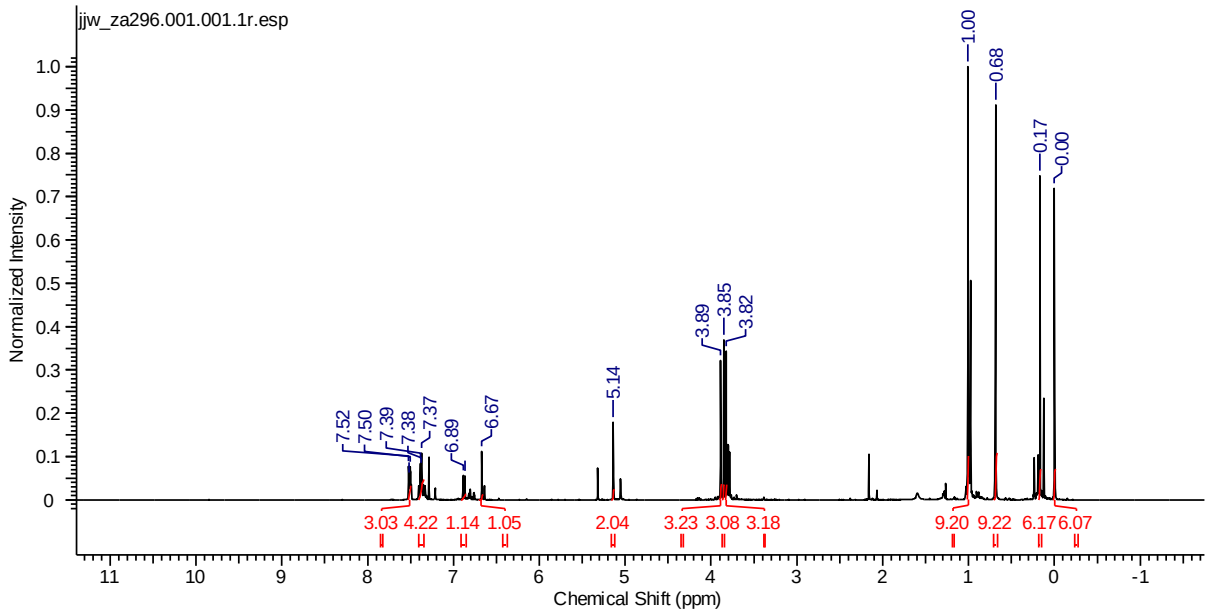

Figure 3.4. ^{1}H-NMR spectrum of benzophenone (3.02)

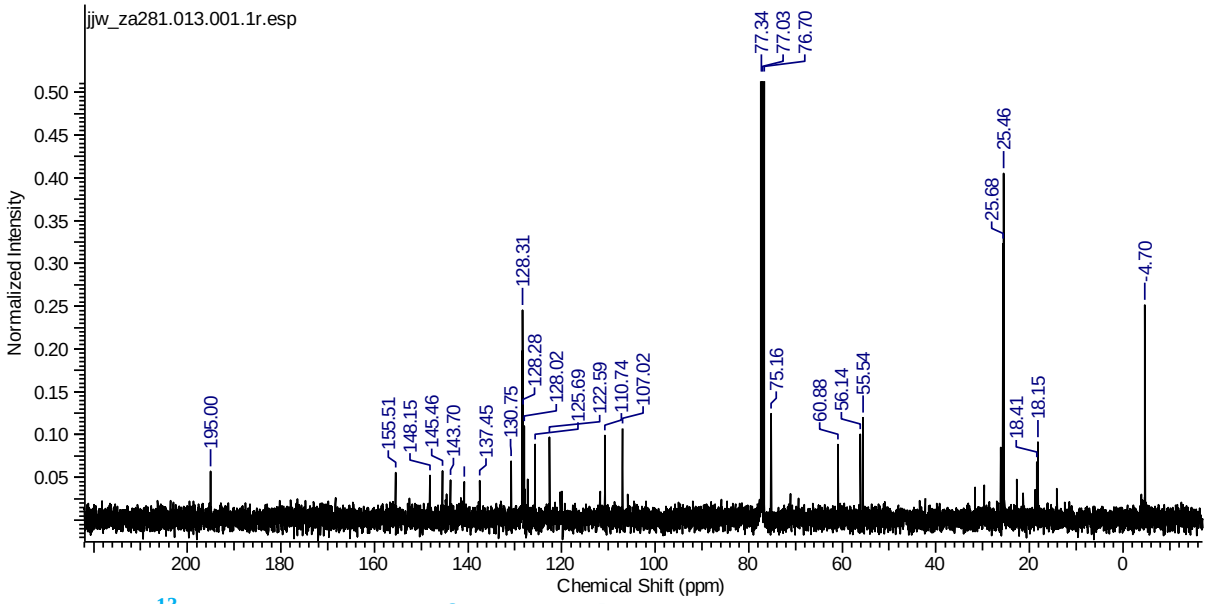

Figure 3.5. ^{13}C NMR spectrum of compound (3.02)

In the next step both silyl protecting groups were removed using TBAF in dry THF at 0 °C to afford the di-phenolic benzophenone compound **(3.03)** (scheme 3.3). The structural characterization of the di-phenolic benzophenone was carried out using NMR spectroscopy. The disappearance of the two *tert*-butyldimethylsilyl protecting groups was clearly evident in the ^{1}H NMR spectrum (figure 3.6). Moreover the two phenolic OH protons were also present in the spectrum resonating at 5.77 and 12.10 ppm.

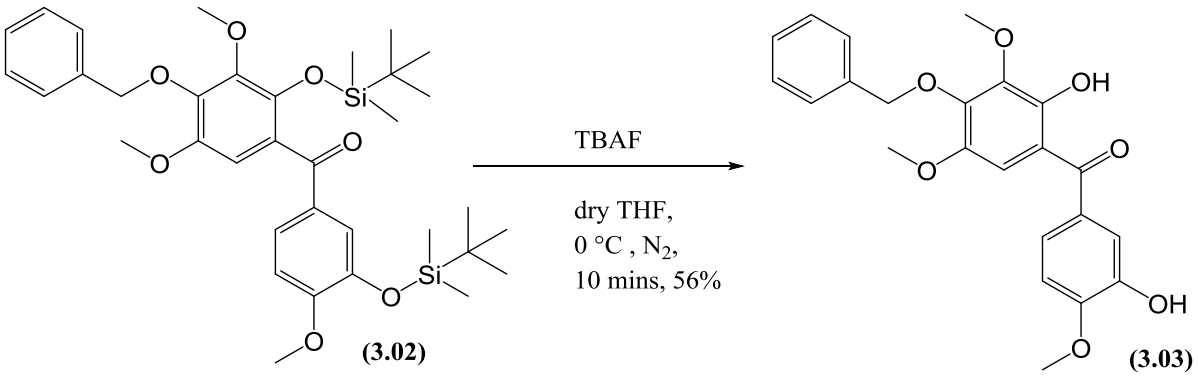

Scheme 3.3. Removal of silyl protecting groups

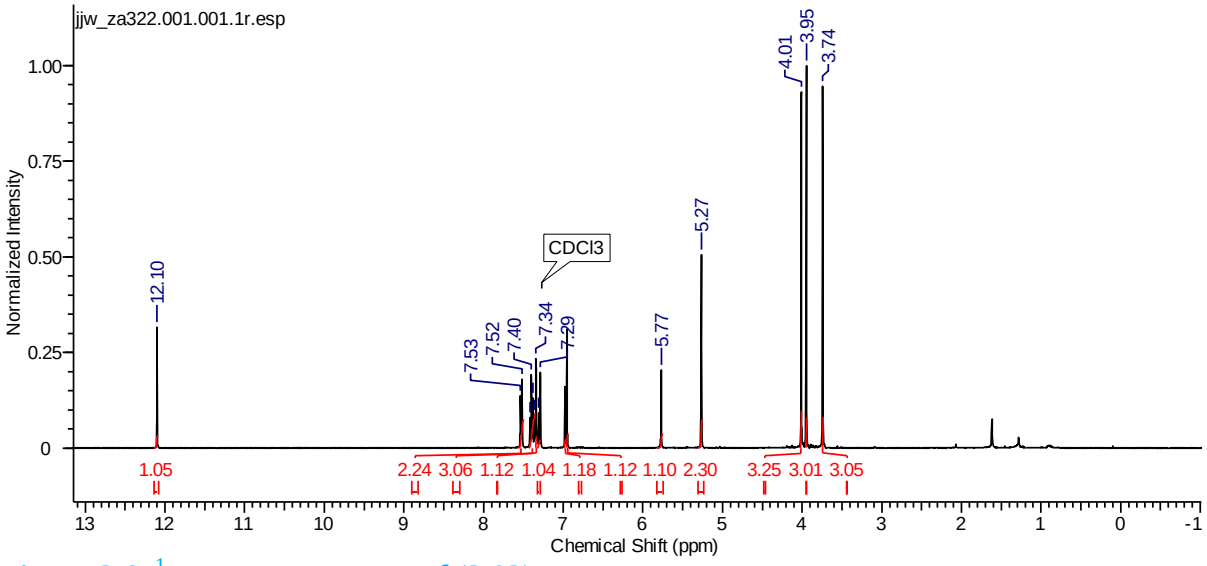

Figure 3.6. ^{1}H-NMR spectrum of (3.03)

The final step towards the synthesis of the triphenolic phenstatin compound was the removal of the benzyl protecting group. This was achieved by stirring the compound **(3.03)** with Pd/C (10% by weight) in methanol:DCM (2:1) under an atmosphere of hydrogen (scheme 3.4). After 90 minutes the palladium species were filtered through a cotton plug and upon evaporating the solvent the remainder was purified by flash column chromatography to afford the benzophenone **(3.04)** with a yield of 85%. The initial confirmation of the product was achieved by HRMS that detected the protonated molecular ion of mass 321.0963. In addition to mass spectroscopy, the ^{1}H NMR spectrum (figure 3.7) also confirmed the removal of benzyl protecting group due to the disappearance of methylene (CH_2) protons as well as the absence of 5 aryl protons of the benzyl protecting group. Moreover the ^{1}H NMR spectrum also confirmed the presence of all expected 16 protons while the ^{13}C spectrum (figure 3.8) shows the presence of all 16 carbons.

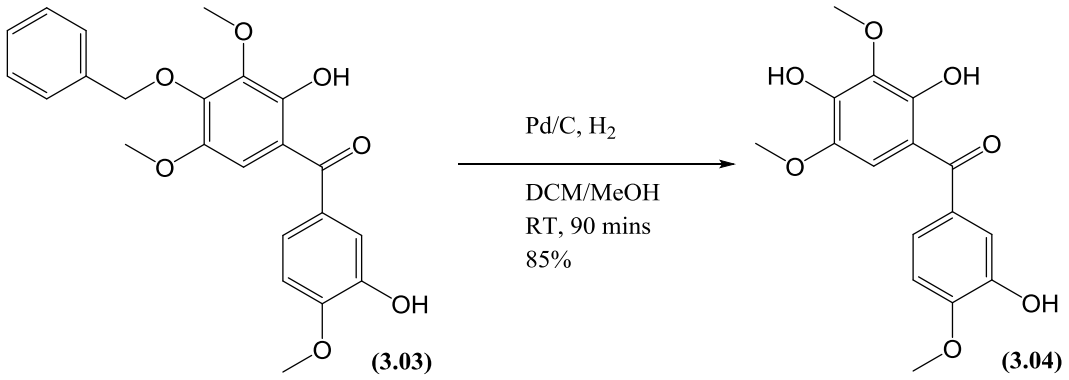

Scheme 3.4. Removal of benzyl protecting group

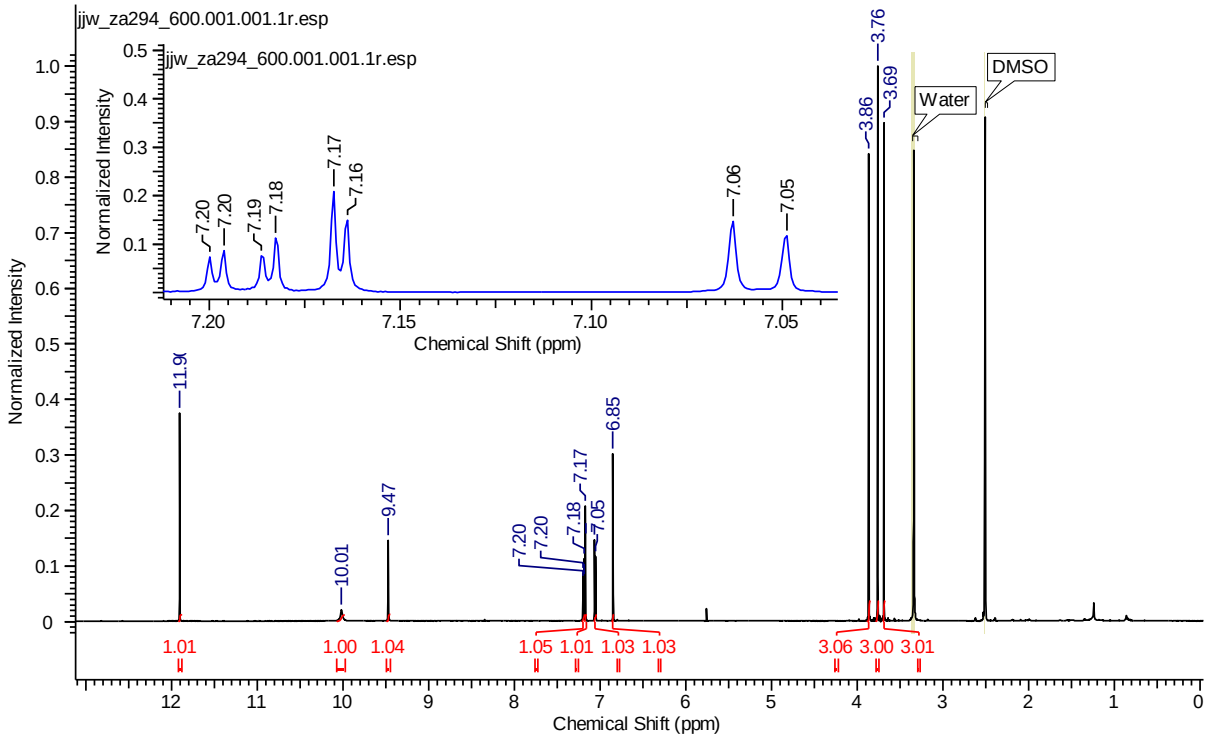

Figure 3.7. ^{1}H-NMR spectrum of compound (3.04)

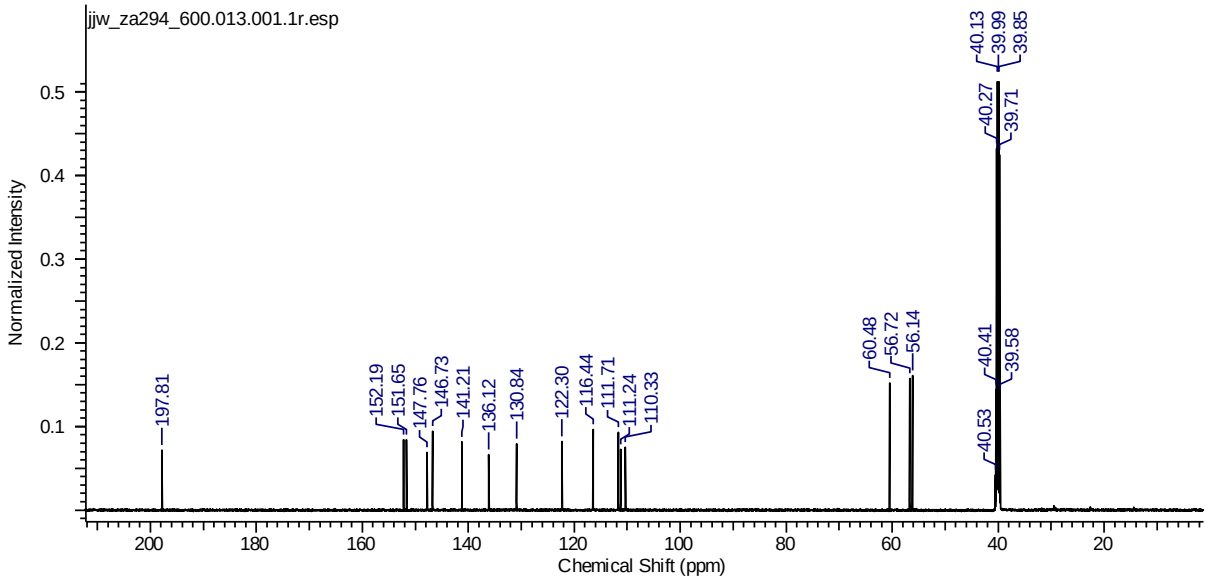

Figure 3.8. ^{13}C spectrum of compound (3.04)

3.2 Synthesis of (3.09), the aniline analogue of (3.04)

The principal reason for trying to furnish this compound **(3.09)** was to utilise the aniline moiety for the attachment of a substrate for APN, usually based on neutral amino acids like leucine or alanine as examples. Since the *N*-Boc protecting group that we utilised previously for aniline protection during Suzuki coupling proved to be unstable during organolithium coupling conditions, an alternative protecting group was required. For that purpose we decided to utilise the *N*-*N*-dibenzyl protecting group. So initially the dibenzyl protection of the aniline **(2.12)** was carried out using benzyl bromide and caesium carbonate in dry DMF at room temperature but unfortunately that resulted in the generation of both mono and dibenzyl protected products which were difficult to separate using flash column chromatography. We decided to change the reaction conditions by using benzyl bromide in a mixture of ethanol and water as solvent and potassium carbonate as base (scheme 3.5). Initially the reaction was carried out at room temperature but the reaction proceeded at a very slow rate. By rising the temperature to 70 °C the reaction was gone to completion within 7 hours, with the generation of only the dibenzylated product **(3.05)**. The structural identity of the *N*-*N*-dibenzyl aniline **(3.05)** was confirmed by ^{1}H NMR spectrum (figure 3.9) that shows the presence of expected 2×CH_2 of the benzyl protecting groups resonating as a singlet at 4.27 ppm with an integral value of 4. Moreover the 10 aryl protons of the two benzyl groups were also found to be resonating as multiplet at 7.31 ppm.

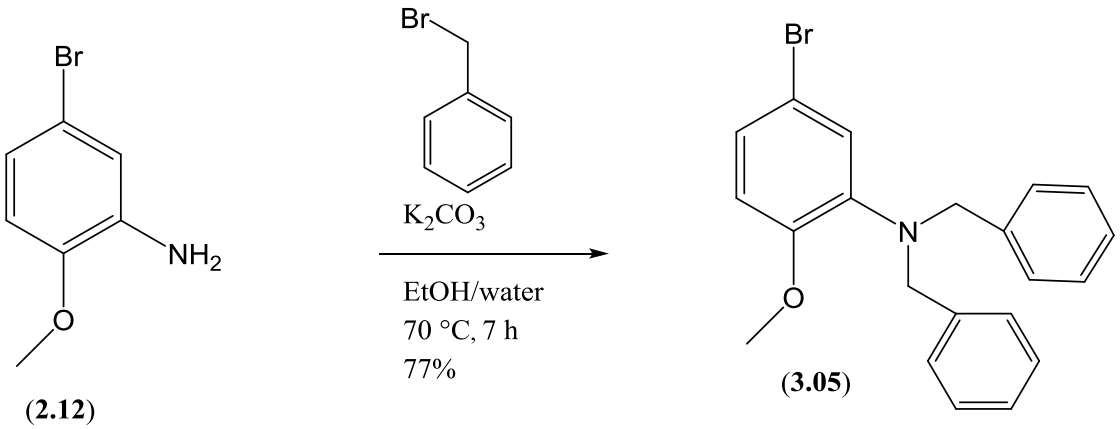

Scheme 3.5. *N*-*N*-dibenzylation of aniline **(2.12)**

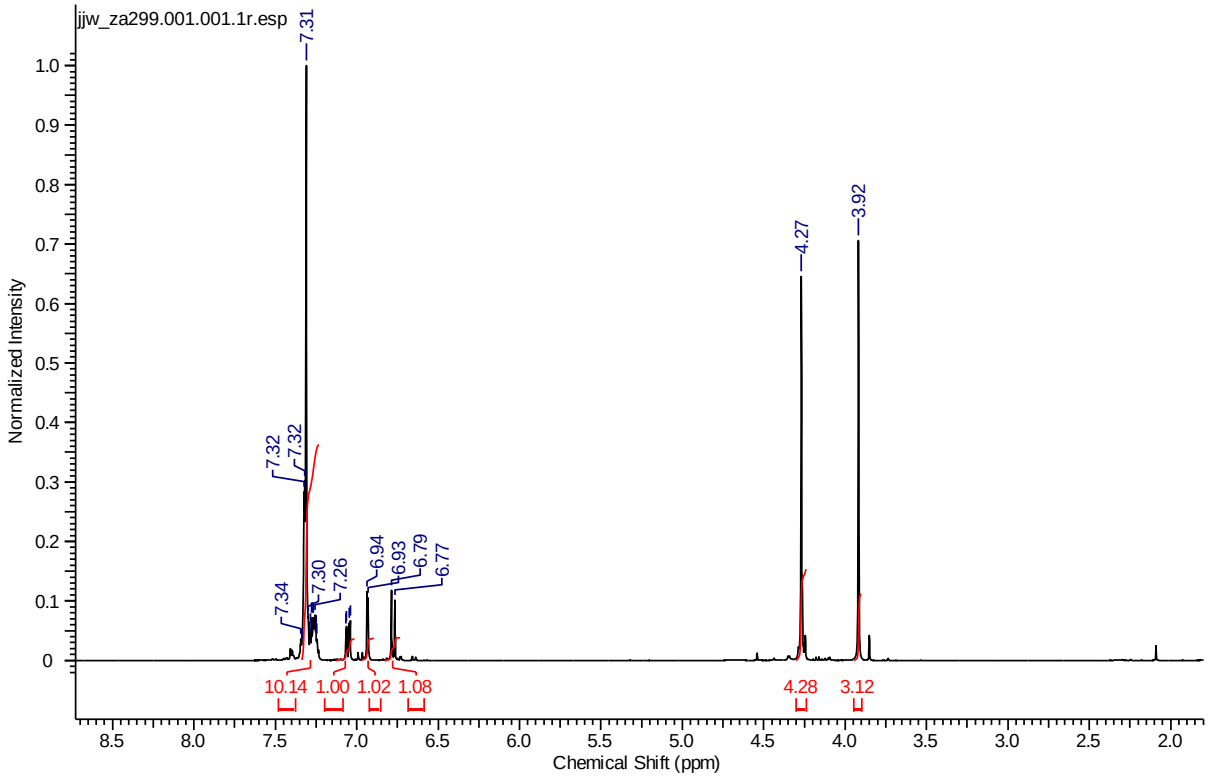

Figure 3.9. ^{1}H-NMR spectrum of compound (3.05)

Once the dibenzyl protected product was obtained we were in a position to couple it directly to the benzaldehyde **(2.57)** utilizing the organolithium coupling conditions. The reaction was carried out by dissolving the *N*-*N*-dibenzyl aniline **(3.05)** in dry THF under nitrogen atmosphere and cooling it to -80 °C over 30 minutes before the dropwise addition of *n*-butyl lithium (2.5 M in hexane). Following this, the benzaldehyde **(2.57)** was added and reaction was maintained at the same temperature for one hour, then at -50 °C for one hour (scheme 3.6). After the aqueous work-up and purification by column chromatography structural confirmation **(3.06)** was done by ^{1}H NMR analysis (figure 3.10) which shows the presence of *tert*-butyl dimethylsilyl protecting group (0-1.0 ppm) as well as the CH of the methanol functional group (appearing as a doublet at 6.10 ppm). Moreover the presence of 3 benzyl protecting groups was also evident in the spectrum at 7.20-7.54 ppm.

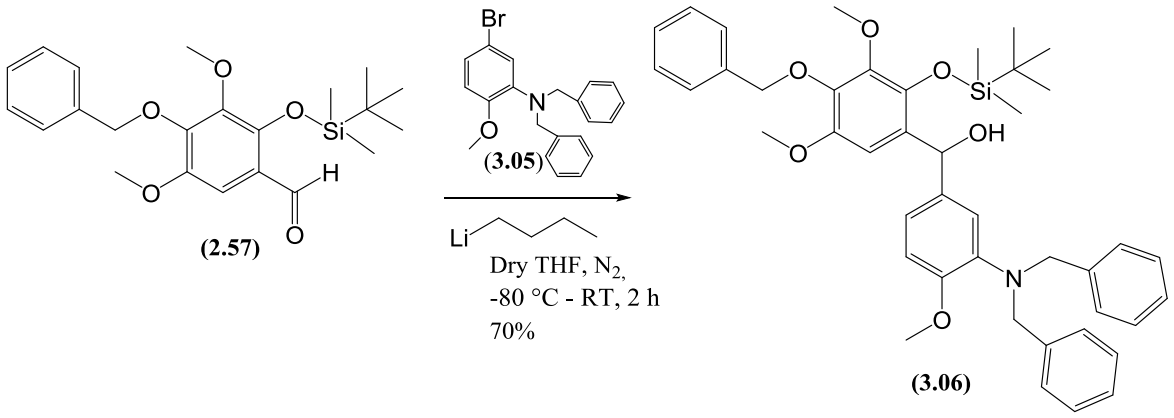

Scheme 3.6. Organolithium coupling to give **(3.06)**

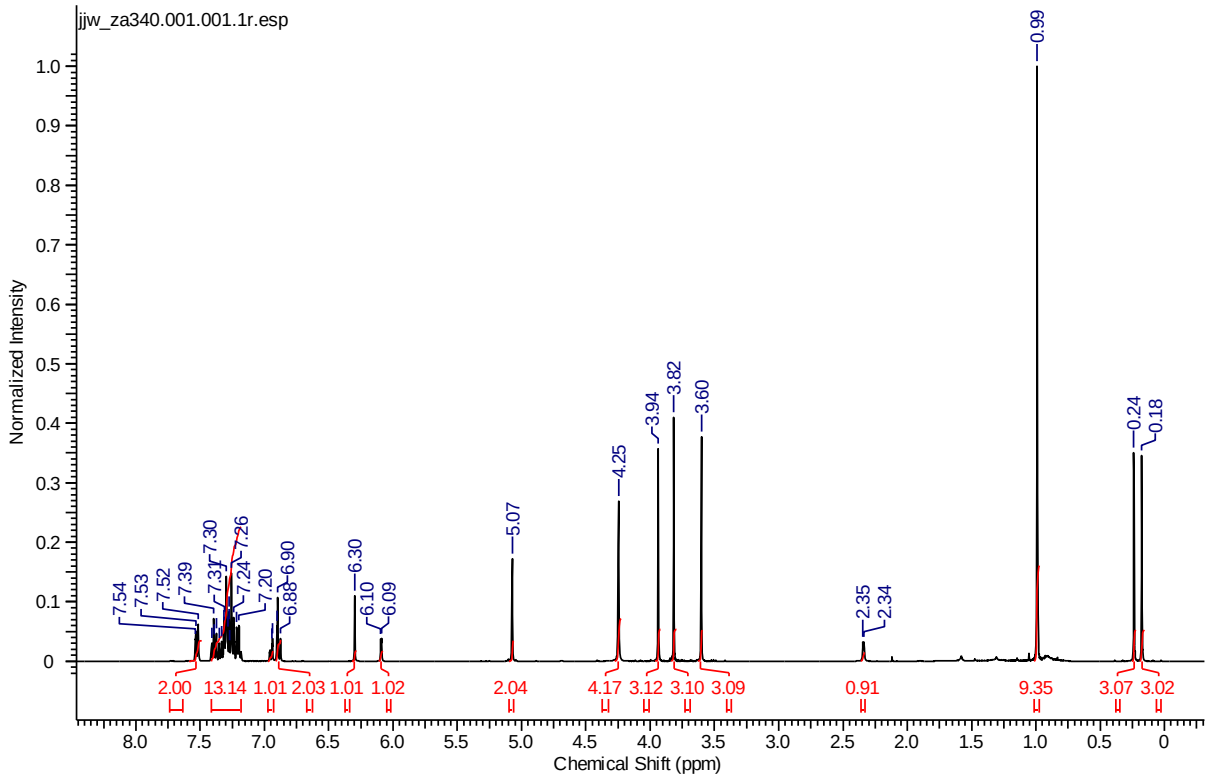

Figure 3.10. ^{1}H-NMR spectrum of (3.06)

Diphenylmethanol **(3.06)** was oxidized to diphenylketone **(3.07)** using Dess Martin periodinane in dry DCM at 0 °C (scheme 3.7). Upon completion the reaction was quenched with 5% $NaHCO_3$ and extracted with DCM. After purification by flash column chromatography, the success of the oxidation reaction was confirmed by the ^{1}H NMR spectrum (figure 3.11) due to the disappearance of CH proton of the methanol functional group as well as the appearance of the ketone signal in the ^{13}C spectrum (figure 3.12) resonating at 194.90 ppm.

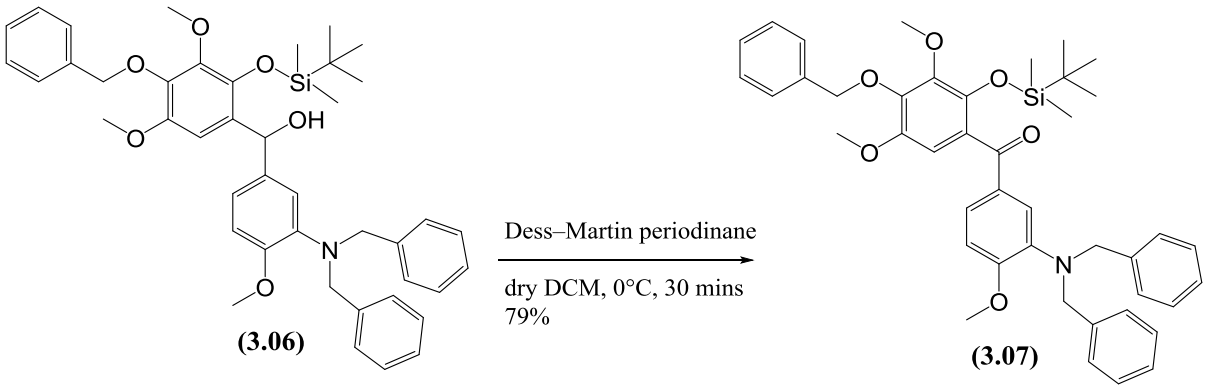

Scheme 3.7. Oxidation of alcohol functionality to ketone

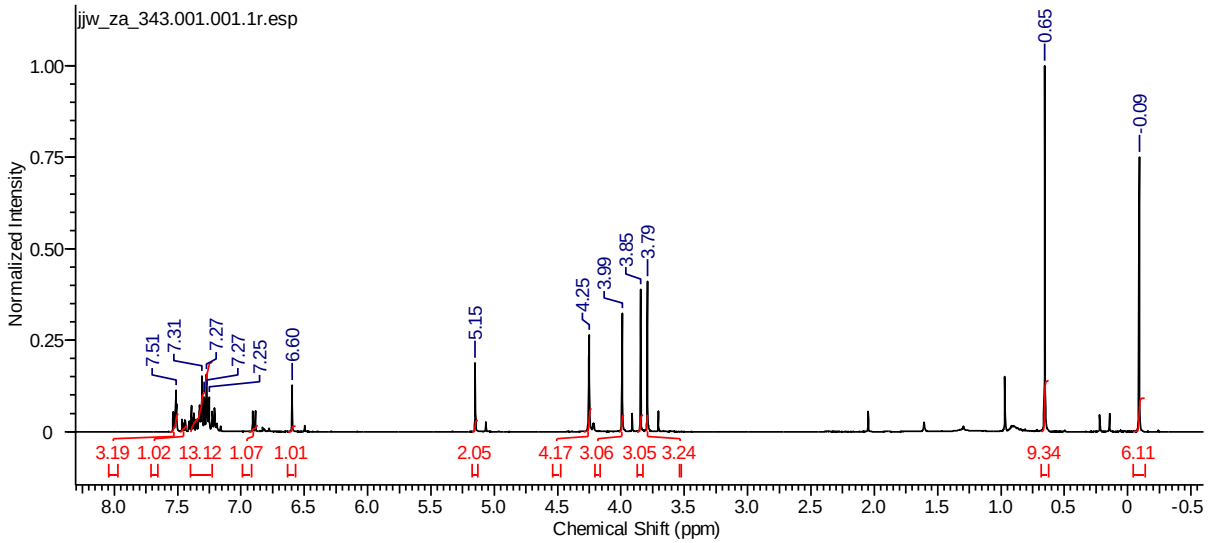

Figure 3.11. ^{1}H-NMR spectrum of (3.07)

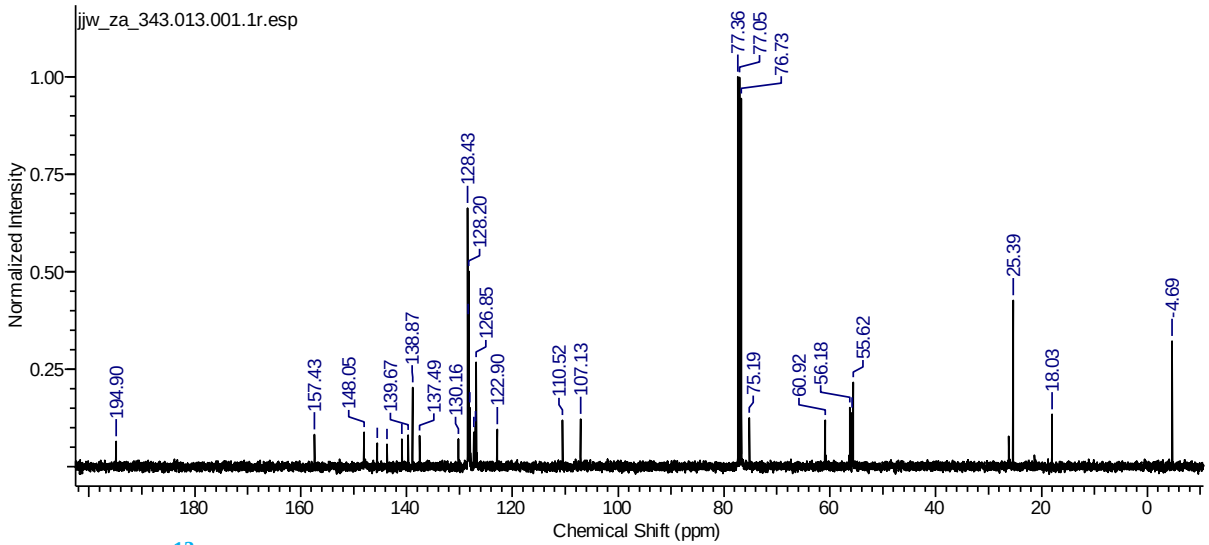

Figure 3.12. ^{13}C NMR spectrum of compound (3.07)

The silyl protecting group of **(3.07)** was removed using with TBAF in dry THF at °C to give the phenol **(3.08)** (scheme 3.8). The silyl deprotection was confirmed by the disappearance of *tert*-butyl and dimethyl protons in the ^{1}H NMR spectrum (figure 3.13) and also by the appearance of the phenolic OH at 12.08 ppm.

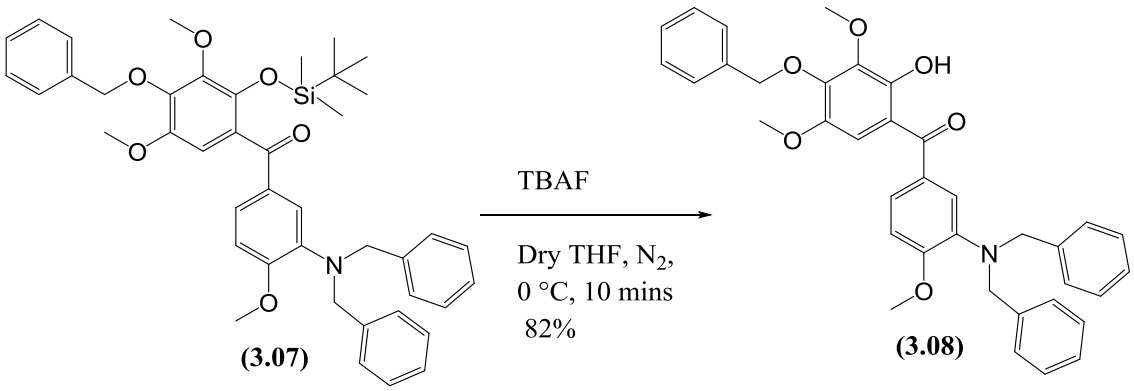

Scheme 3.8. Removal of silyl protecting group

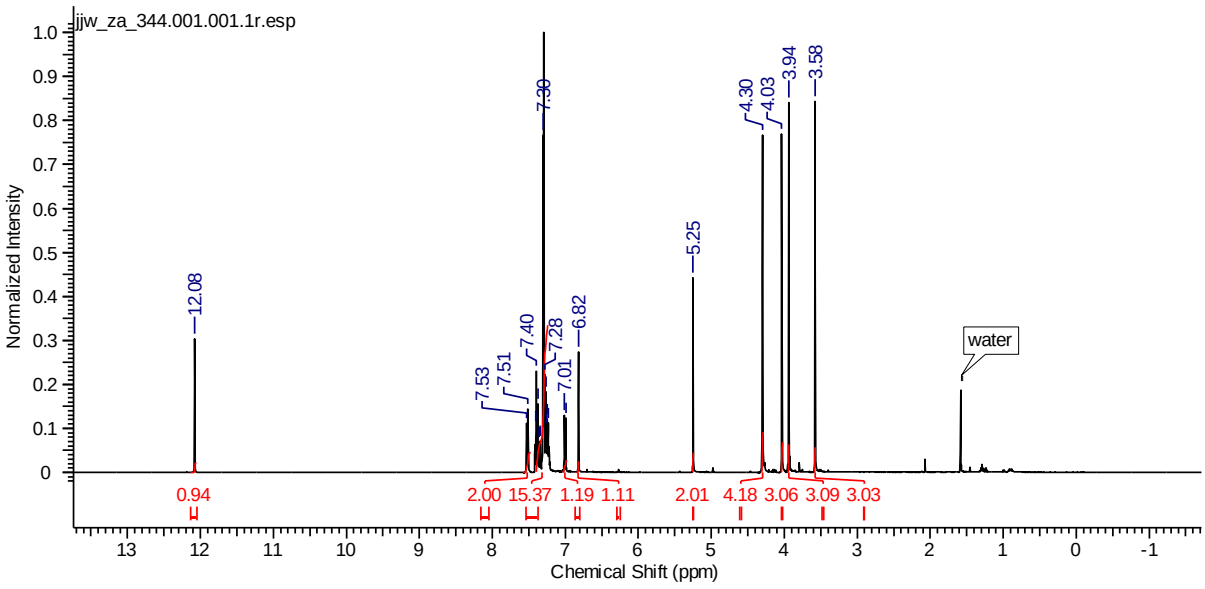

Figure 3.13. ^{1}H-NMR spectrum of (3.08)

The final step towards the synthesis of the di-hydroxy aniline phenstatin **(3.09)** was the removal of both benzyl and dibenzyl protecting groups. This was achieved by stirring compound **(3.08)** with $Pd(OH)_2/C$ (20% by weight) in DCM:MeOH (1:2) under an atmosphere of hydrogen (scheme 3.9). After 90 minutes the Pd species was filtered by passing the reaction mixture through a cotton wool plug. Upon evaporating the organic solvent, the remainder was purified by flash column chromatography to afford the product in 63% yield. The HRMS analysis confirmed the identity of the compound **(3.09)** with the molecular ion of mass 320.1130 corresponding to the ($M+H^+$) ion. Further confirmation

was done by using the ^{1}H NMR spectrum (figure 3.14) where the loss of 3 benzyl protecting groups, and the presence of two phenolic OHs (10.01 and 12.12 ppm) and amino NH_2 (5.02 ppm) was evident. Moreover the ^{13}C spectrum (figure 3.15) also showed the presence of all 16 carbons.

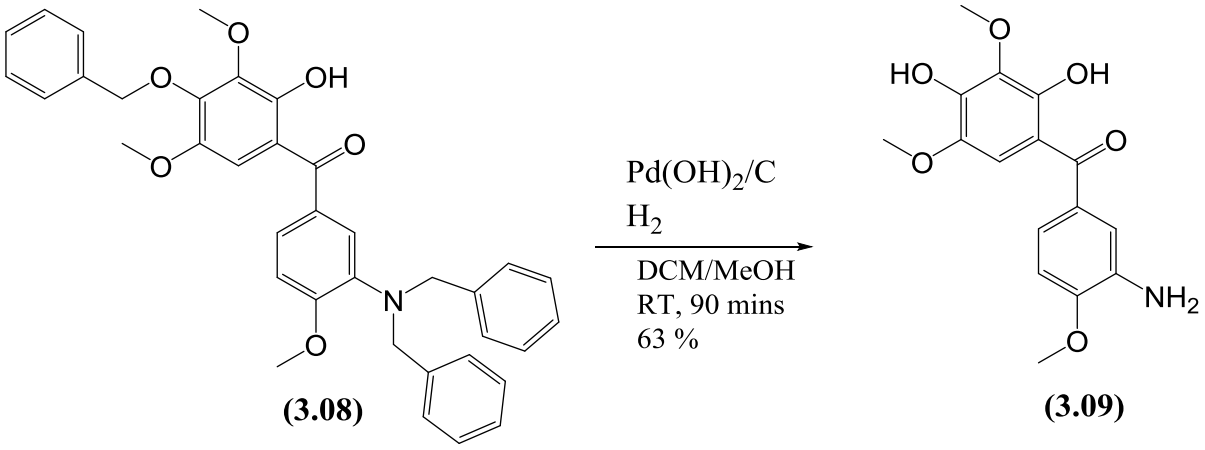

Scheme 3.9. Deprotection of benzyl protecting groups

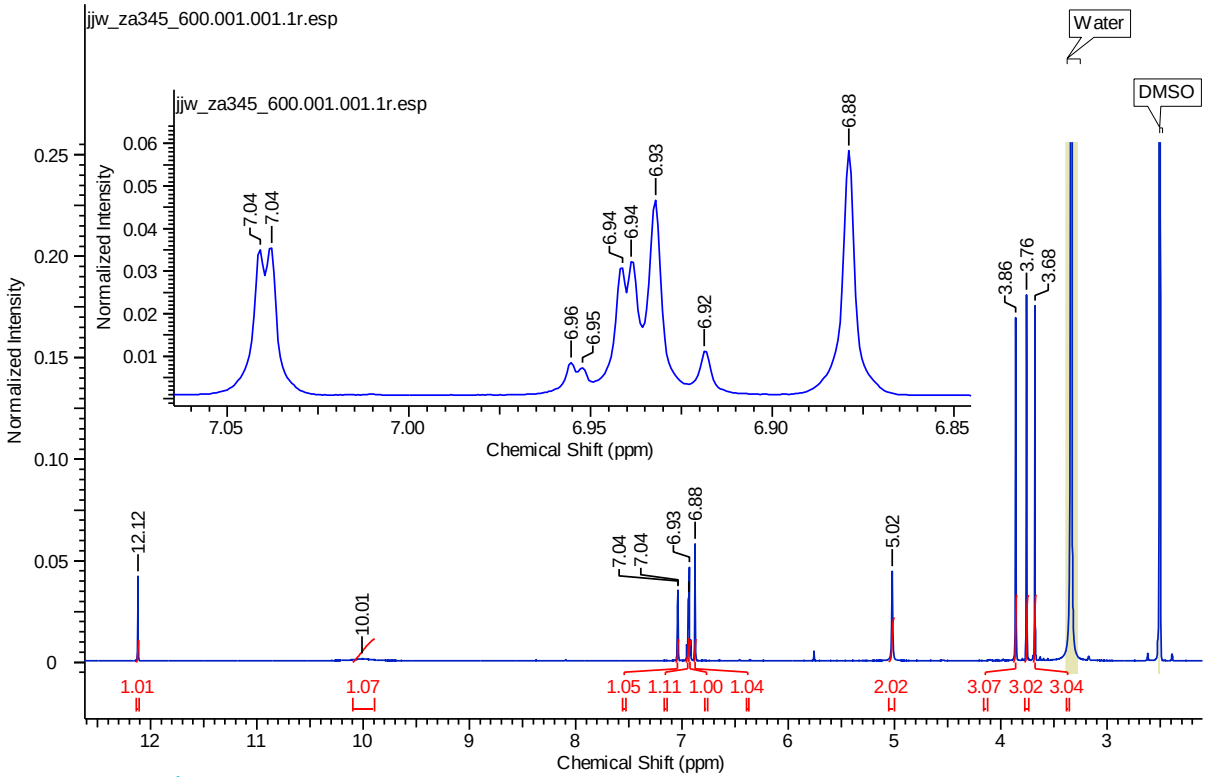

Figure 3.14. ^{1}H NMR spectrum of compound (3.09)

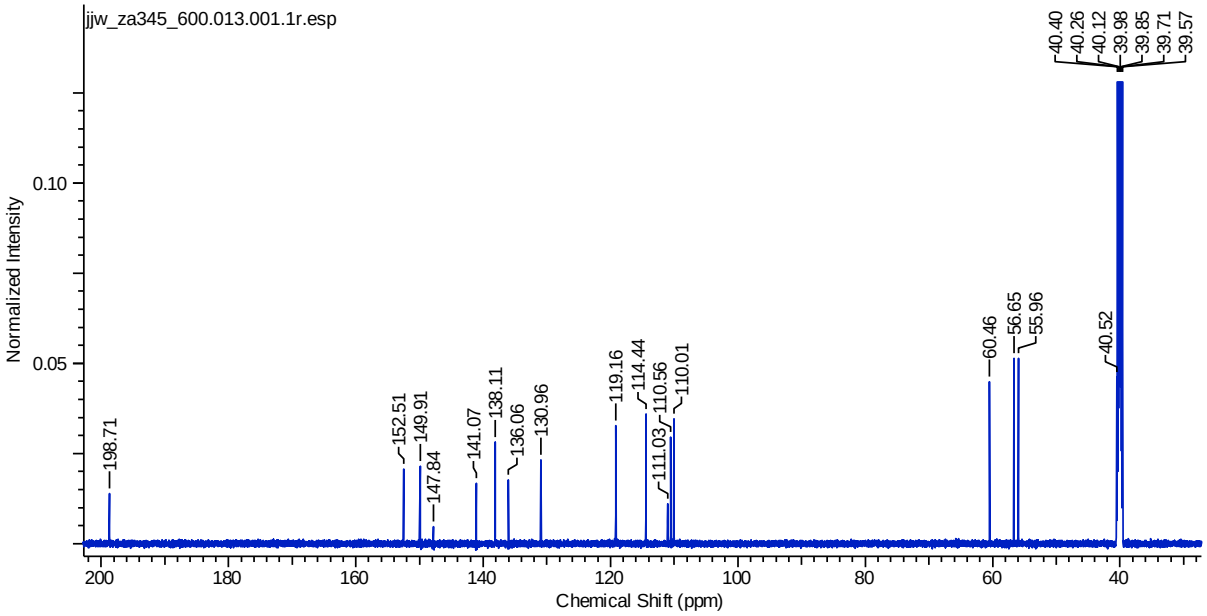

Figure 3.15. ^{13}C NMR spectrum of compound (3.09)

3.3 Synthesis of phenstatin (3.20) with a C3 aldehyde side chain

A series of phenstatin like compounds has been synthesised previously by the former PhD students of our lab, namely R.Shah and M.White by the oxidative cleavage of 7-membered ring compound **(3.10)** using potassium dichromate ($K_2Cr_2O_7$) as oxidizing agent. The compounds share structural similarities with the known phenstatin compound **(1.11)** by having a trimethoxy substituted A-ring and a monomethoxy substituted phenolic B-ring connected through a carbonyl bridge. The only difference as compared to phenstatin was the presence of butanal side chain (figure 3.16). In the tubulin polymerisation assay the most active compound was the keto-aldehyde **(3.11)** that exhibited an IC_{50} value of 9.85 µM [159].

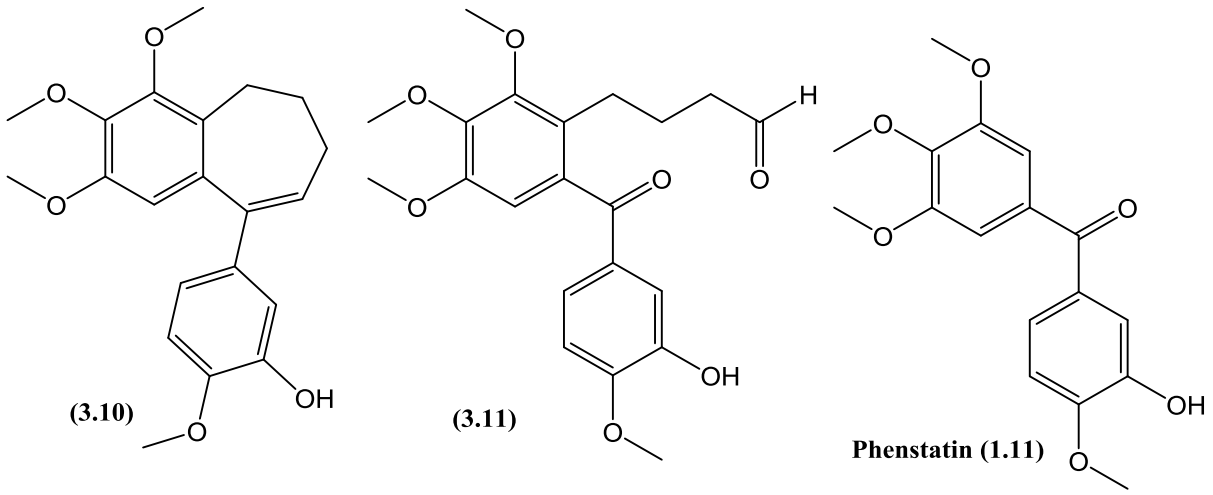

Figure 3.16. Structures of compound (3.10), its ring open derivative (3.11) and phenstatin (1.11).

By keeping in mind the tubulin binding activity of the keto-aldehyde **(3.11)**, it was decided to further expand the library shortening the length of the butanal side chain by one carbon to generate a propanal side chain. The idea being that the aldehyde could serve as a useful linker for the attachment of the APN inhibitory peptides. Starting with the commercially available trimethoxybenzene the following synthetic route was proposed to give the 6-membered protected analogue of **(3.10)**. Ring opening of this intermediate should then furnish the propanal side chain.

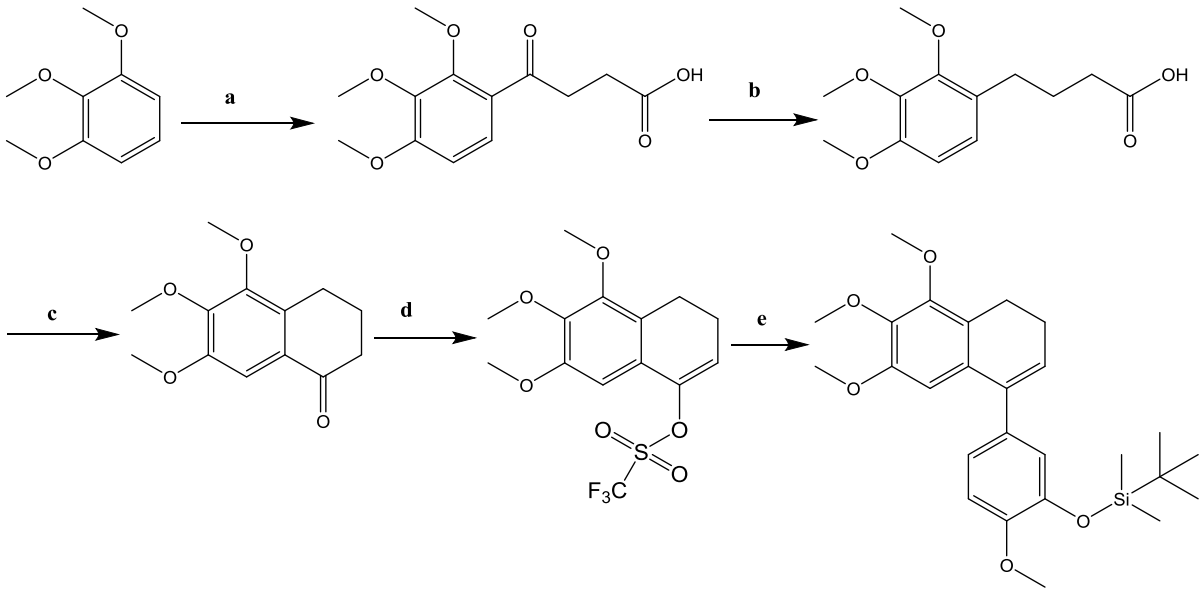

Scheme 3.10. (a) Reaction with succinic anhydride; (b) Carbonyl reduction; (c) Cyclization; (d) Triflation; (e) . Suzuki coupling

Based on the synthetic sequence trimethoxybenzene **(3.12)** was treated with succinic anhydride in the first step using aluminium trichloride ($AlCl_3$) as a catalyst and dry DCM as a solvent at -10 °C (scheme 3.11). After 6 hours, and following an aqueous acidic work-up (2 M HCl) and extraction with DCM, the organic layer was dried, reduced in volume to afford and oil which was purified by flash column chromatography to yield the desired carboxylic acid **(3.13)**. The ^{1}H NMR spectrum (figure 3.17) clearly showed the success of the reaction due to the presence two *ortho*-coupling protons in the aromatic region as well as by the presence of two triplets at 2.78 and 3.33 ppm representing two CH_2 groups of the side chain.

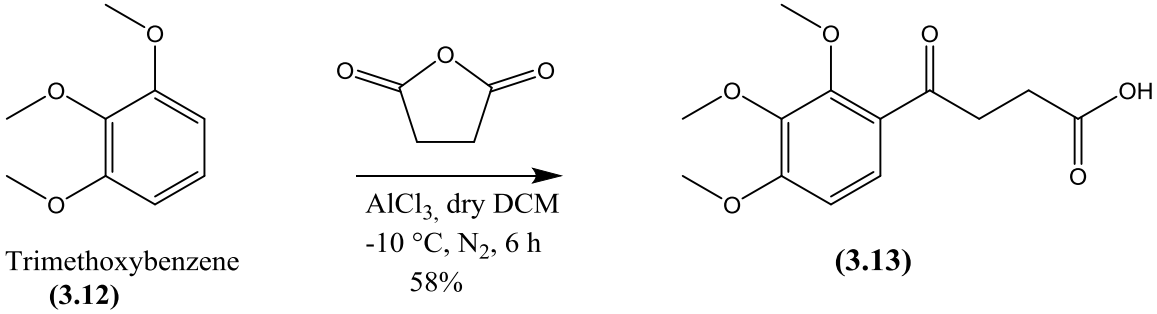

Trimethoxybenzene **(3.12)**

(3.13)

Scheme 3.11. Synthesis of compound **(3.13)**

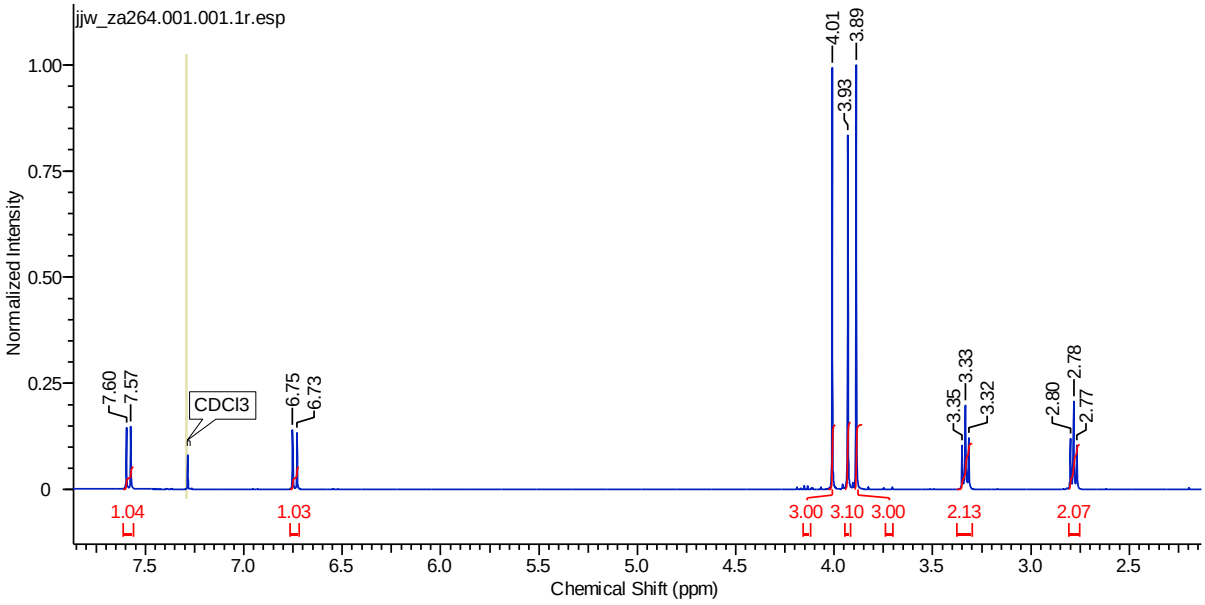

Figure 3.17. ^{1}H NMR spectrum of compound (3.13)

The carbonyl group of the resulting keto acid **(3.13)** underwent reduction with 10% Pd/C in EtOH:acetic acid (1:3) under an atmosphere of hydrogen (scheme 3.12). The reaction was kept on for 12 hours and upon completion was concentrated under reduced pressure using a

rotary evaporator. Following purification, structural confirmation was achieved by the appearance of an extra CH_2 signal in the aliphatic region of the ^1H NMR spectrum (figure 3.18) of compound **(3.14)**.

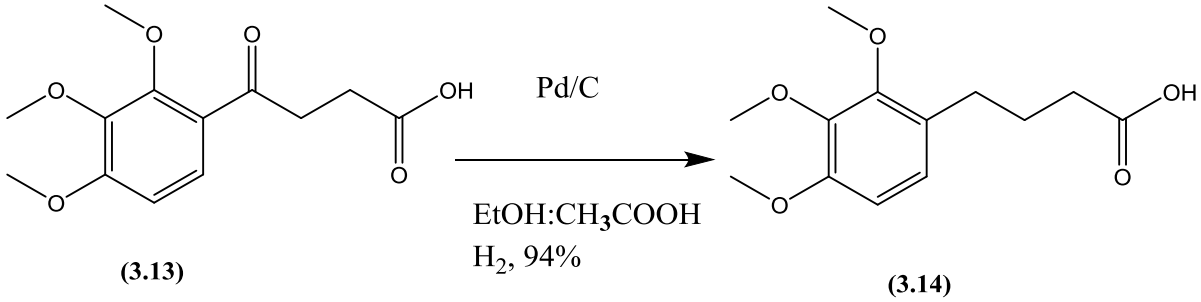

(3.13) **(3.14)**

Scheme 3.12. Reduction of compound **(3.13)**

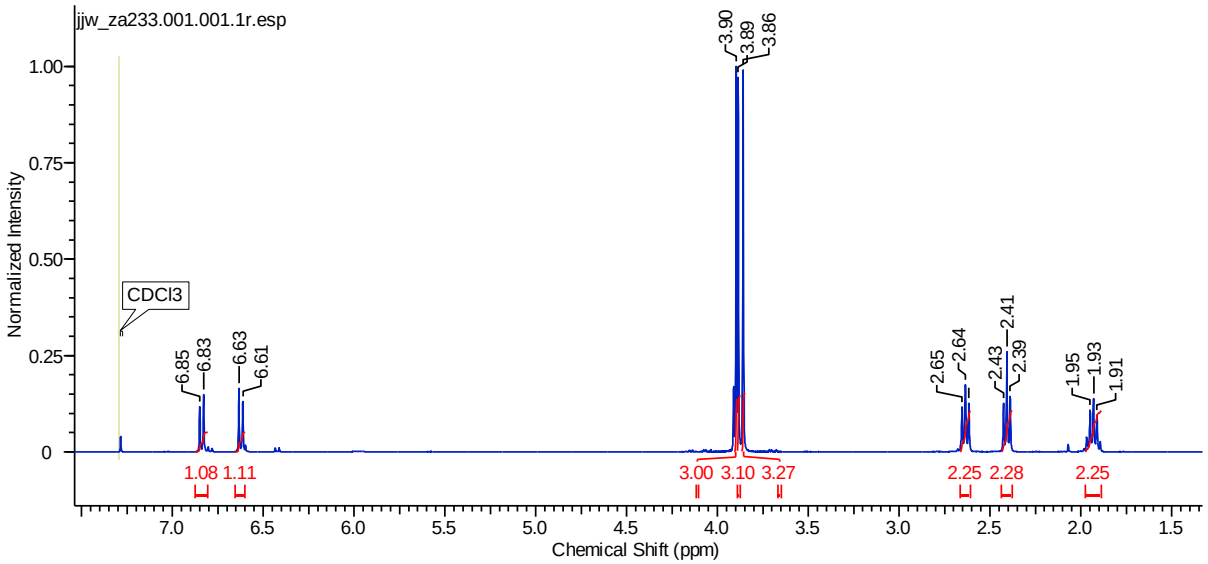

Figure 3.18. ^1H NMR spectrum of compound (3.14)

In the next step, intramolecular cyclization of the acid **(3.14)** was carried out by stirring it with polyphosphoric acid at 75 °C (scheme 3.13). After one hour the reaction mixture was quenched with water and extracted with DCM. The identity of the tetralone compound **(3.15)** was confirmed by the expected loss of one aryl proton in its ^1H NMR spectrum (figure 3.19) and the remaining one aryl proton now appeared as singlet at 7.40 ppm.

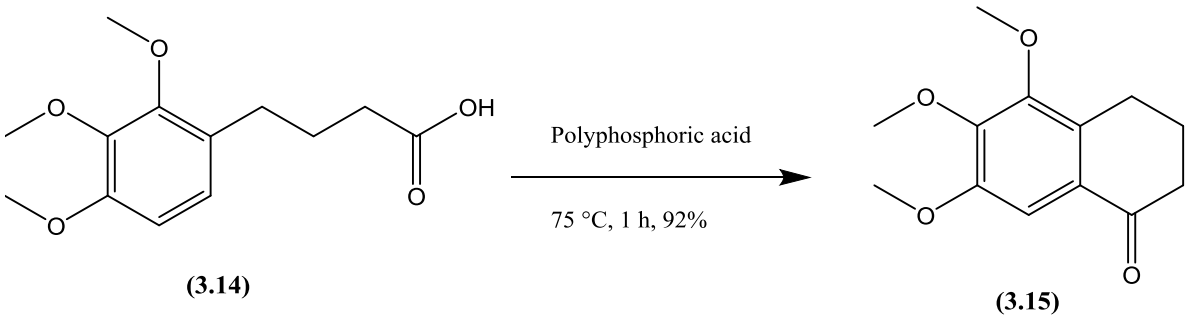

Scheme. 3.13. Cyclization of **(3.14)** to give tetralone compound **(3.15)**

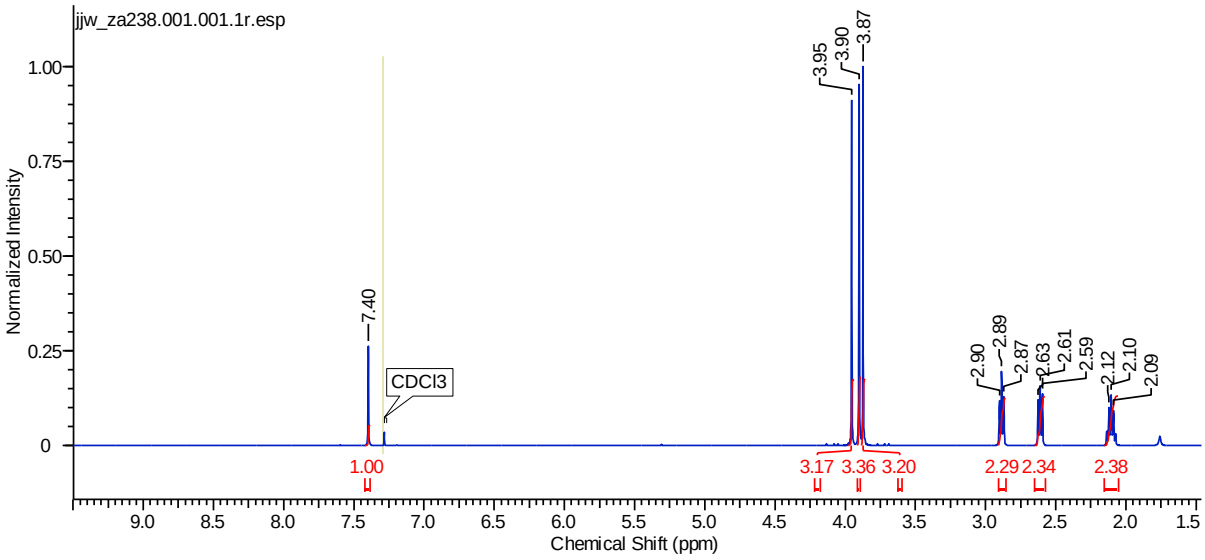

Figure 3.19. ^{1}H NMR spectrum of compound (3.15)

Due to our success with the triflate as a substrate for Suzuki coupling, compound **(3.15)** was converted into its triflate derivative using triflic anhydride and *N*,*N*-diisopropylethylamine (DIPEA) in anhydrous DCM (scheme 3.14). The inspection of the ^{1}H NMR spectrum (figure 3.20) of triflate **(3.16)** showed the loss of one CH_2 group in the aliphatic region as well as the appearance of the alkene proton as a triplet at 5.98 ppm. Further confirmation was achieved by the presence of a fluorine signal at -78.38 ppm in the ^{19}F NMR spectrum (figure 3.21).

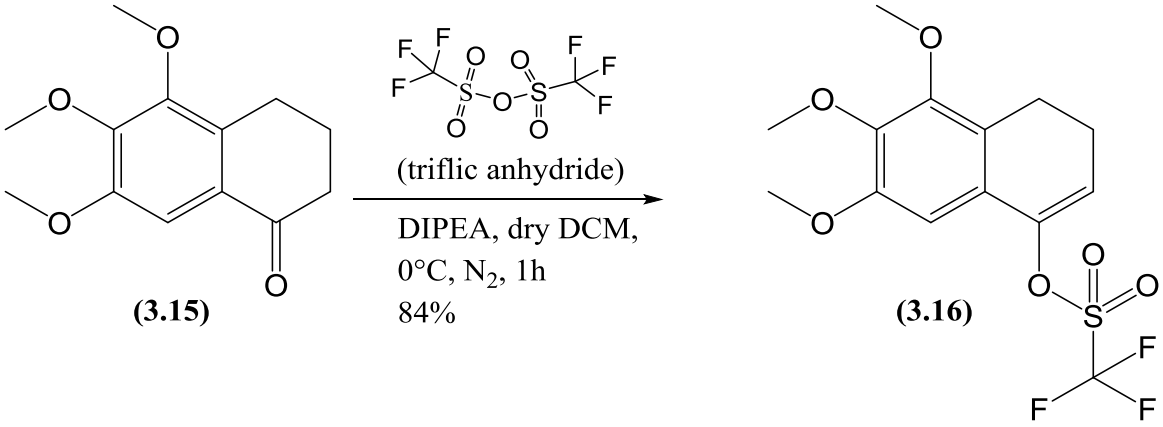

Scheme 3.14. Triflation of compound **(3.15)**

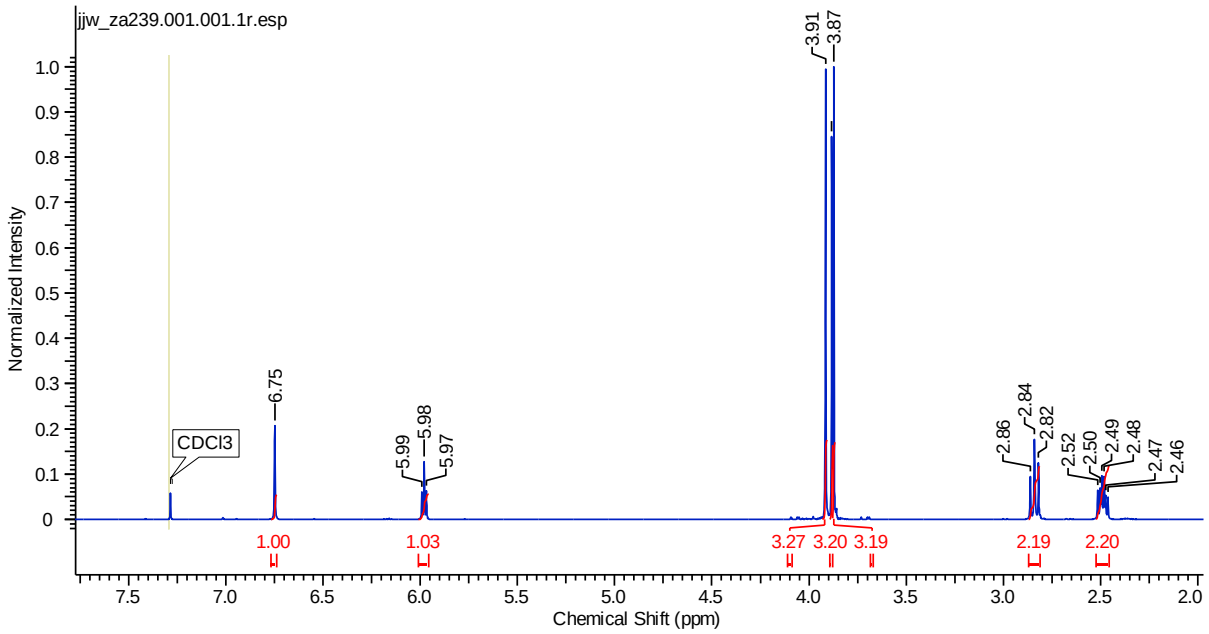

Figure 3.20. ^{1}H NMR spectrum of triflate (3.16)

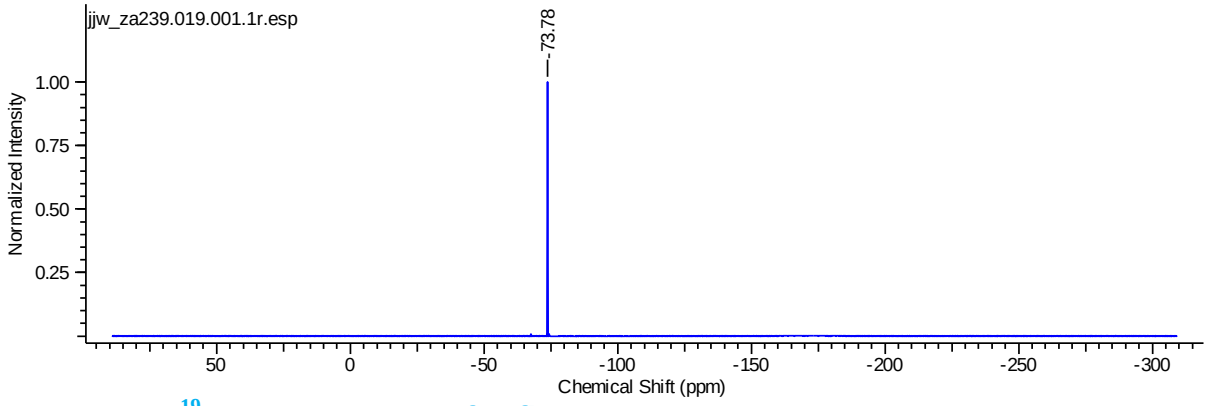

Figure 3.21. ^{19}F NMR spectrum of triflate (3.16)

Once we hand the triflate **(3.16)**, the next step was coupling of the aryl boronic acid **(2.10)** onto it. This was achieved using the same conditions employed for the Suzuki coupling

reactions discussed in chapter 2 (scheme 3.15). The tricyclic compound **(3.17)** afforded was structurally confirmed by investigation of its ^{1}H NMR spectrum (Figure 3.22) that shows additional features as compared to compound **(3.16)** including the presence of silyl protecting group, three extra aryl protons and one extra methoxy group.

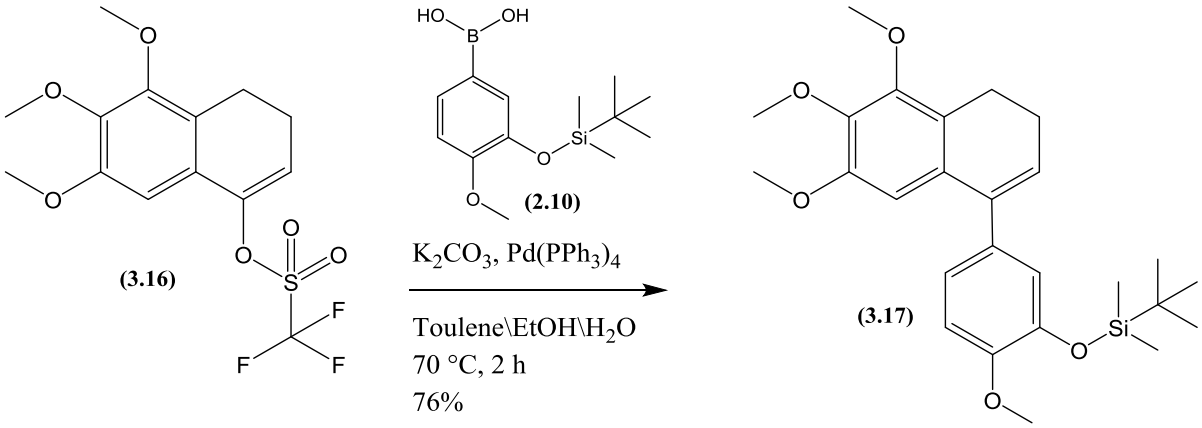

Scheme 3.15. Suzuki coupling triflate **(3.16)** and aryl boronic acid **(2.10)**

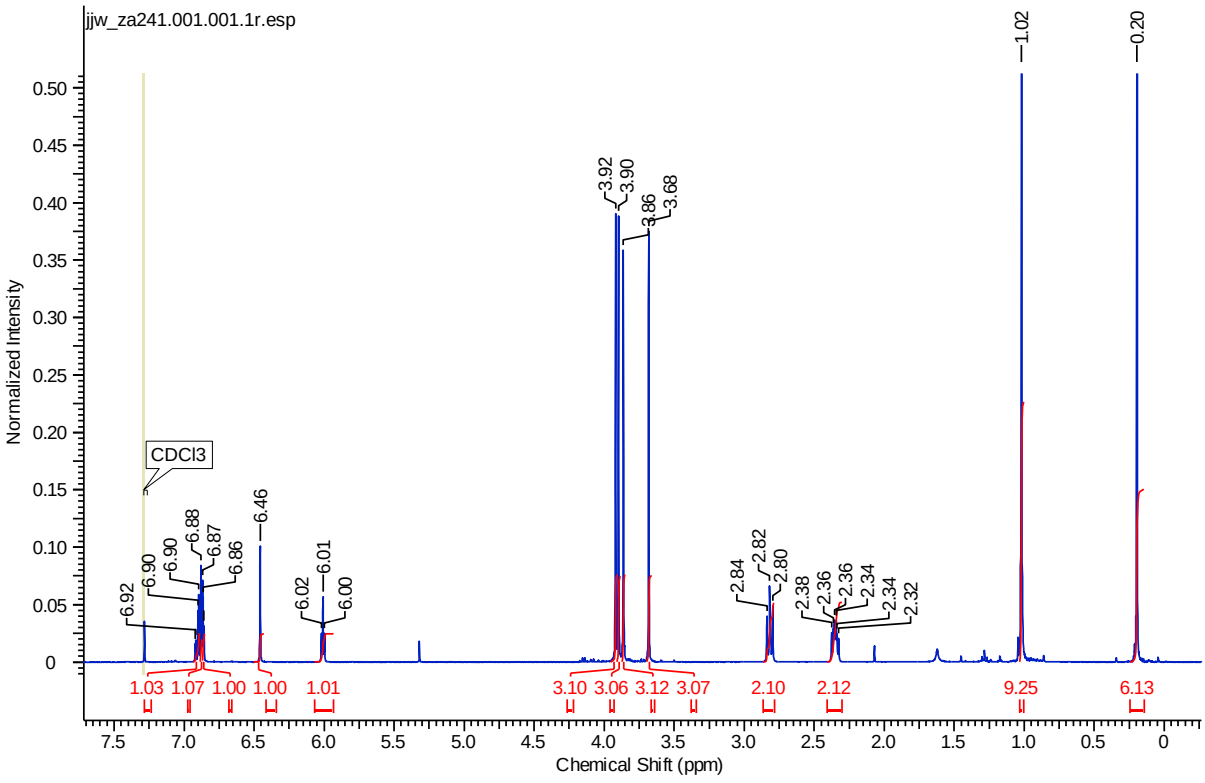

Figure 3.22. ^{1}H NMR spectrum of compound (3.17)

In order to evaluate the compound as tubulin polymerization inhibitor, it was necessary to de-protect the phenolic functionality and that was achieved by treating the compound **(3.17)**

with a solution of TBAF in THF at 0 °C (scheme 3.16). The loss of silyl protecting group was confirmed by the ^{1}H NMR spectrum (figure 3.23) of phenol **(3.18)**.

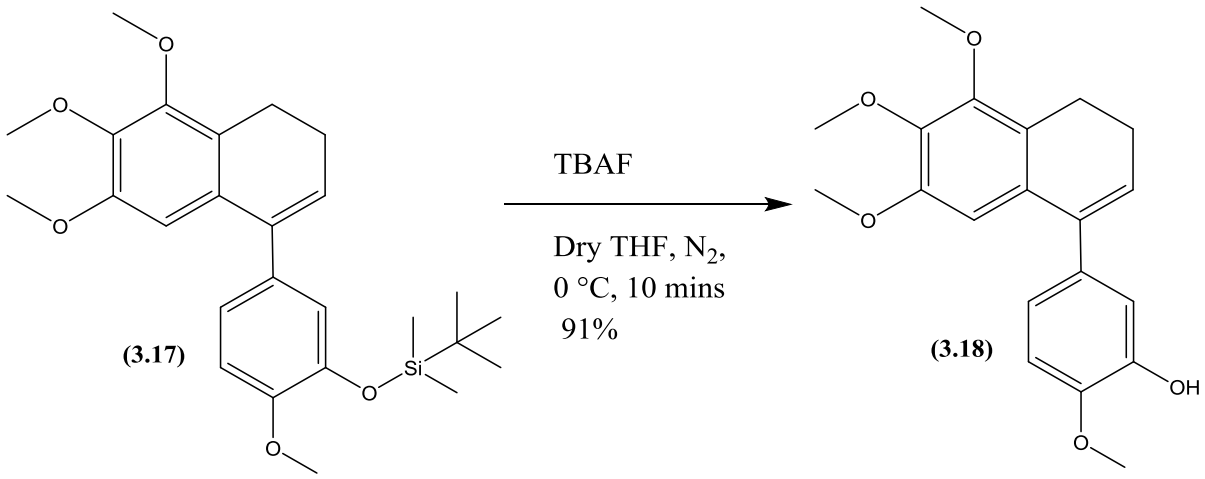

Scheme 3.16. Removal of silyl protecting group

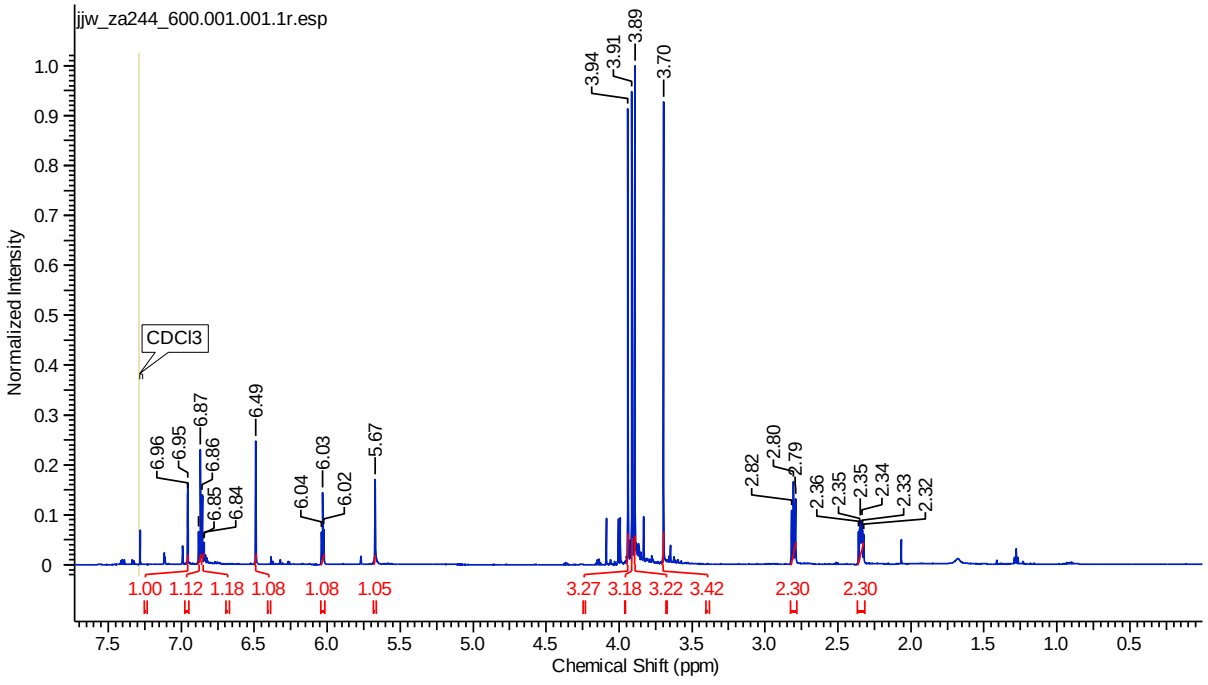

Figure 3.23. ^{1}H NMR spectrum of phenol (3.18)

After securing the phenol **(3.18)**, our next step was to synthesise the ring opened compound **(3.19)**. To a stirred solution of the silyl protected phenol **(3.17)** in acetic acid:acetic anhydride (2:1) at 40 °C was added $K_2Cr_2O_7$ portion wise (scheme 3.17). Upon completion the reaction was quenched with cooled 5% $NaHCO_3$ and extracted with diethyl ether. Upon

evaporation of the organic solvent the residue was purified by flash column chromatography to give the desired benzophenone compound **(3.19)**. Its structure was confirmed by ^{1}H and ^{13}C NMR analysis. The ^{1}H NMR spectrum (figure 3.24) shows the presence of the characteristic aldehyde peak (9.73 ppm) along with the loss of the alkene proton while in the ^{13}C NMR spectrum (figure 3.25) the presence of both ketone (196.20 ppm) and aldehyde (202.07 ppm) signals confirmed the identity of the structure.

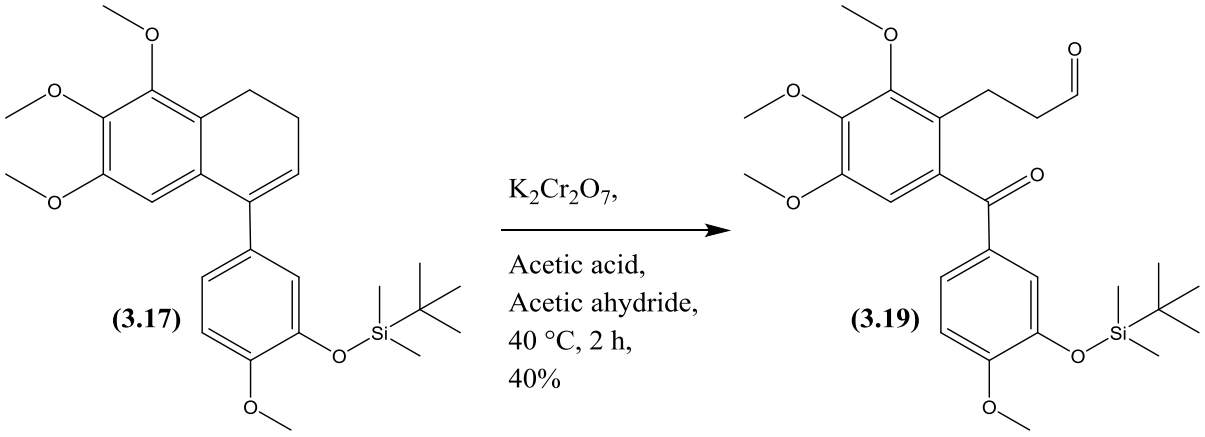

Scheme 3.17. Oxidative ring opening of compound **(3.17)**

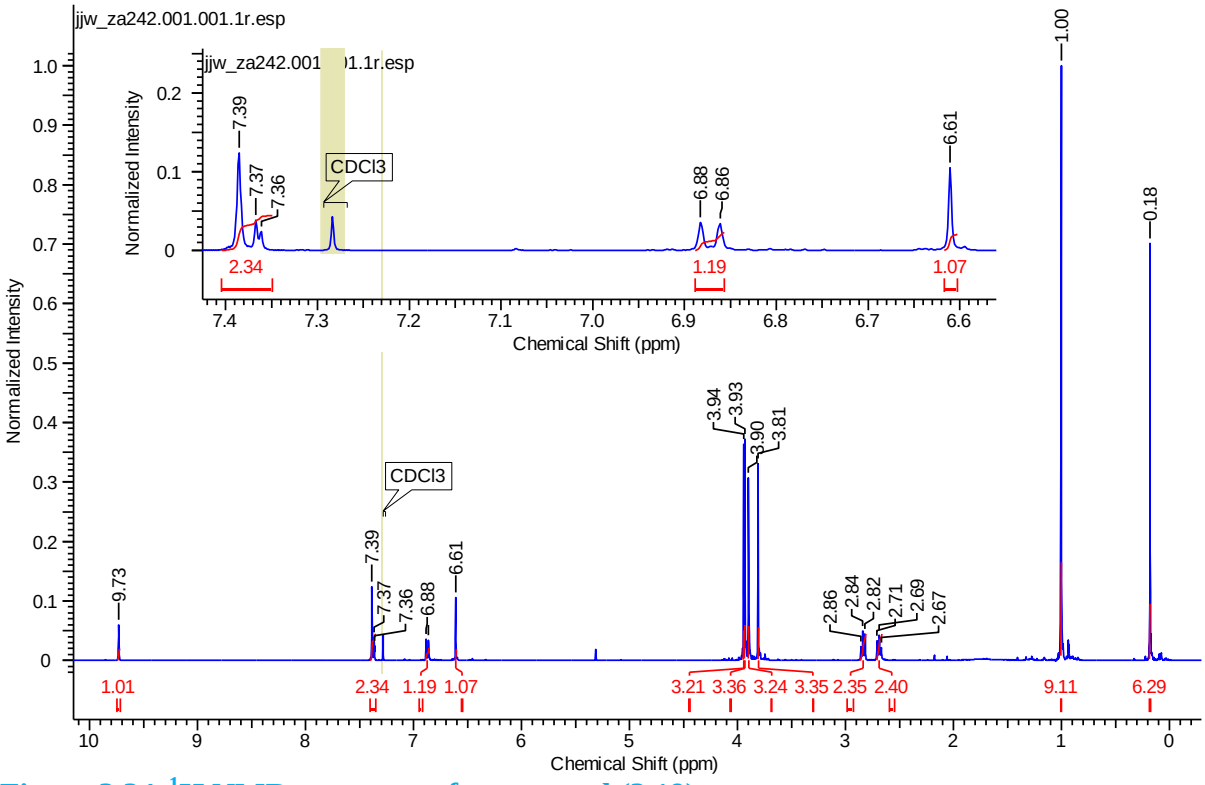

Figure 3.24. ^{1}H NMR spectrum of compound (3.19)

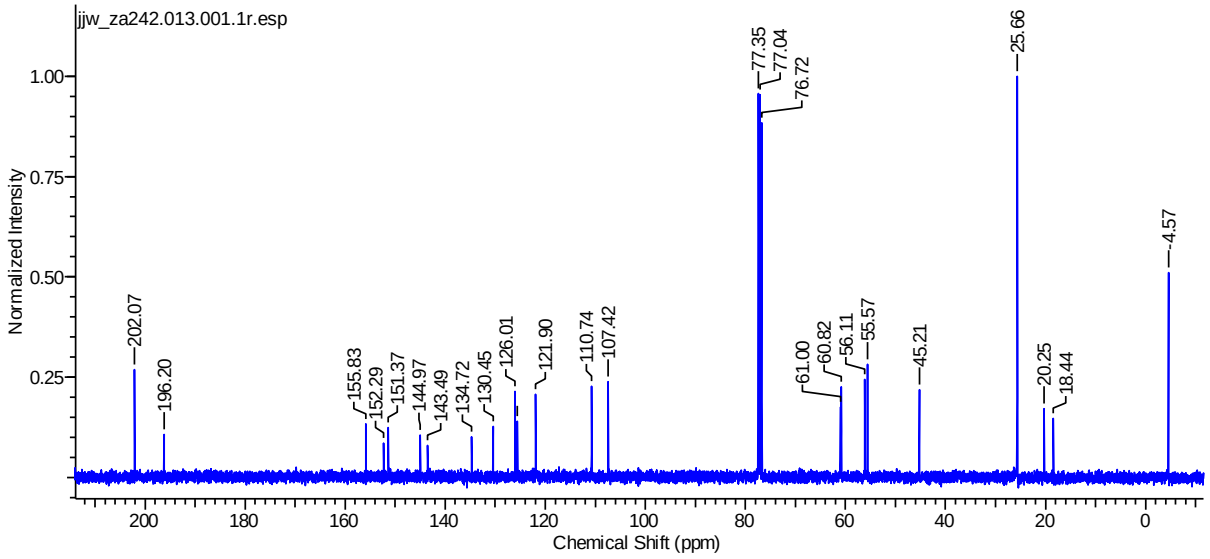

Figure 3.25. ^{13}C NMR spectrum of compound (3.19)

In the final step, silyl deprotection was carried out using TBAF in THF at 0 °C (scheme 3.18). The loss of the silyl protecting group was confirmed by analysis of its ^{1}H NMR spectrum (figure 3.26).

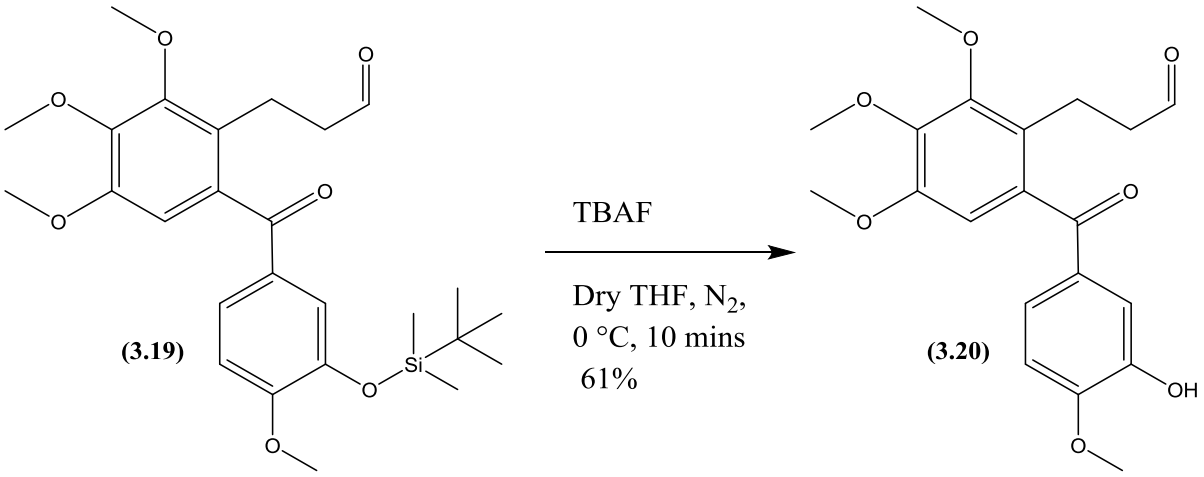

Scheme 3.18. Removal of silyl protecting group

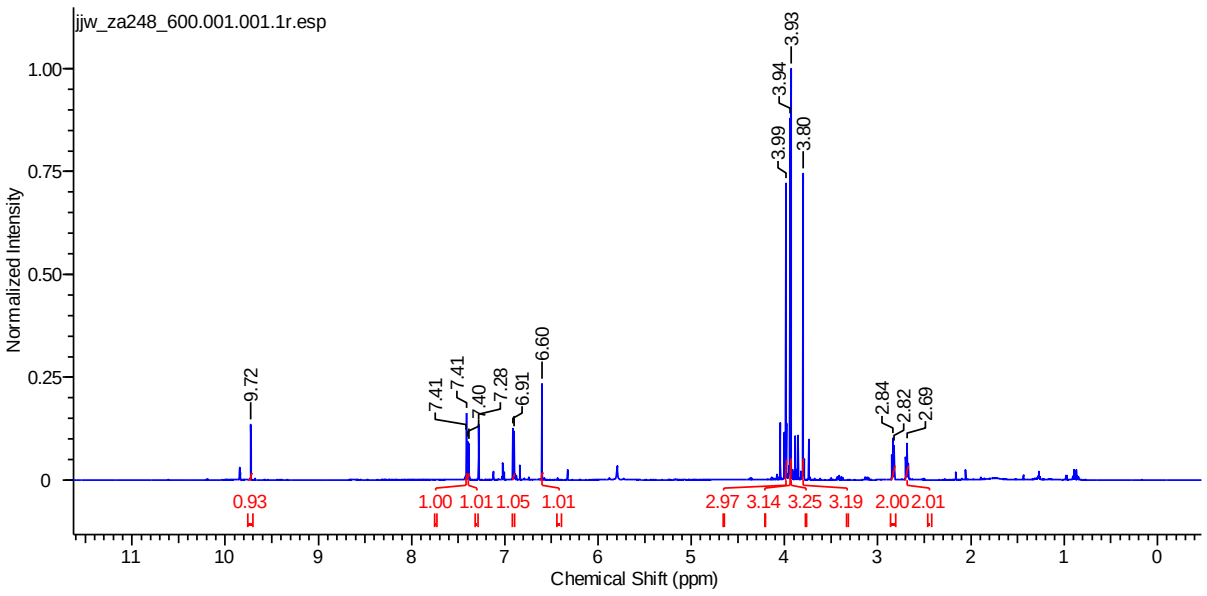

Figure 3.26. ^{1}H NMR spectrum of compound (3.20)

3.4. Tubulin polymerisation inhibition data and conclusions

Among the compounds synthesised in this chapter, four of them were evaluated as tubulin polymerisation inhibitors. The general structure of the compounds is presented in figure 3.27 while their IC_{50} values are shown in the table (figure 3.28).

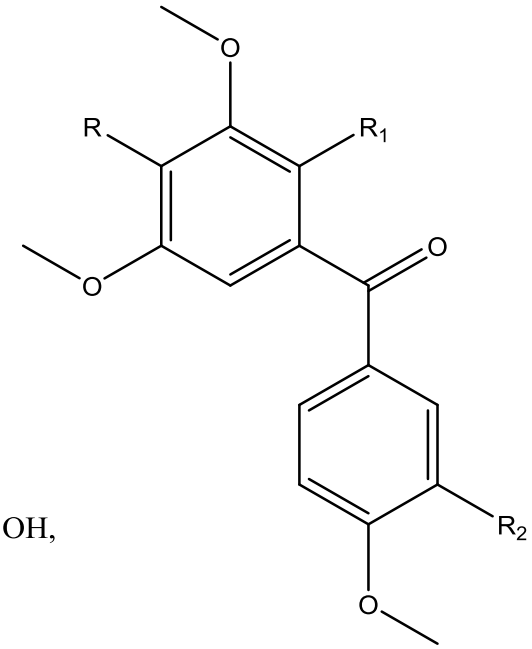

(3.03), R = OBn, R_1 = OH, R_2 = OH,

(3.04), R = OH, R_1 = OH, R_2 = OH,

(3.09), R OH= , R_1 = OH, R_2 = NH_2,

(3.20), R = OCH_3, R_1 = $(CH_2)_2$-CHO, R_2 = OH,

Figure 3.27. General structure of phenstatin derivatives

Compound	IC_{50} (μM)	(R^2)
(3.03)	**15.99**	**0.9568**
(3.04)	**7.816**	**0.9499**
(3.09)	**8.627**	**0.9248**
(3.20)	**inactive**	
CA-4	**1.838**	**0.8225**

Figure 3.28. IC_{50} values of phenstatin derivatives

Figures 3.29, 3.30 and 3.31 present the results obtained for the synthesized compounds, together with combretastatin A-4 (CA-4) as positive control and DMSO as negative control.

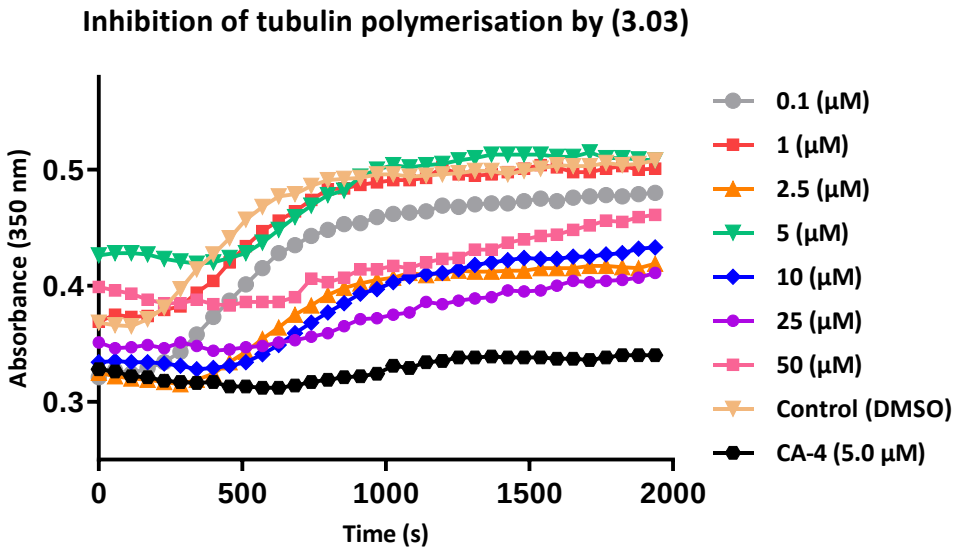

Figure 3.29. Results obtained for the *in vitro* tubulin polymerization assay of (3.03) in different concentrations

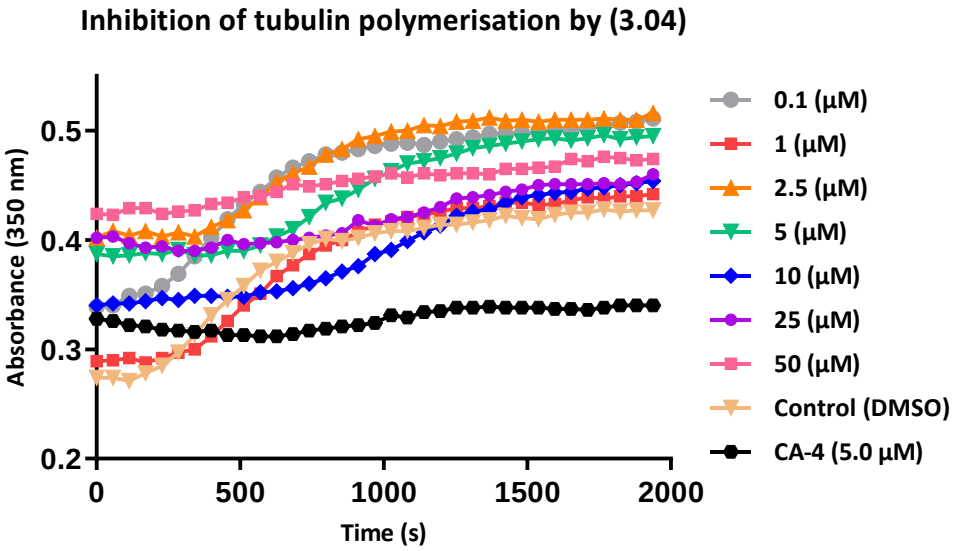

Figure 3.30. Results obtained for the *in vitro* tubulin polymerization assay of (3.04) in different concentrations

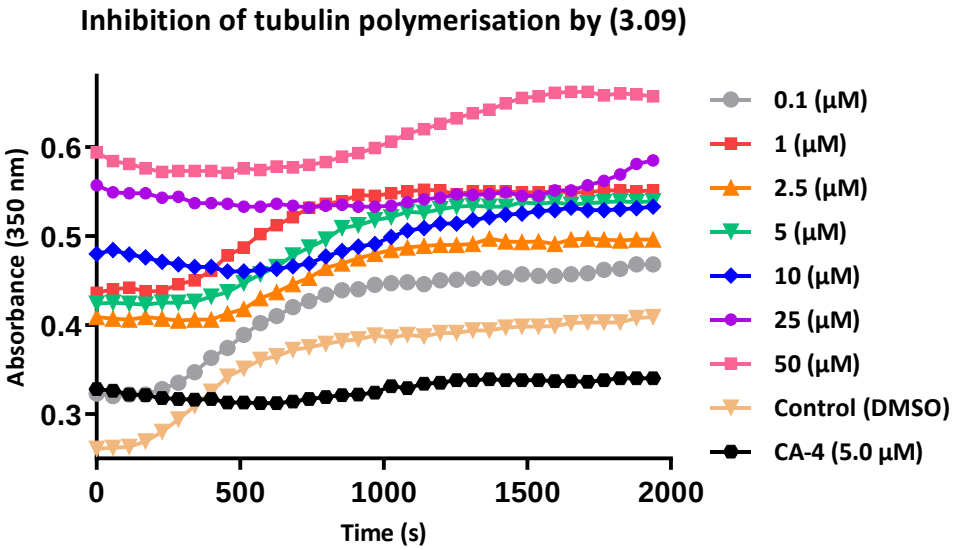

Figure 3.31. Results obtained for the *in vitro* tubulin polymerization assay of (3.09) in different concentrations

The percent inhibition of tubulin polymerisation by the three compounds **(3.03, 3.04, 3.09)** was compared to CA-4 at 10 µM and is shown in figure 3.32. The syntheised compound **(3.03)** presented 28.03 ± 8.92% inhibition, followed by **(3.09)** 43.11 ± 8.08% and **(3.04)** 50.60 ± 4.34% inhibition while CA-4 presented 73.25 ± 5.83% inhibition.

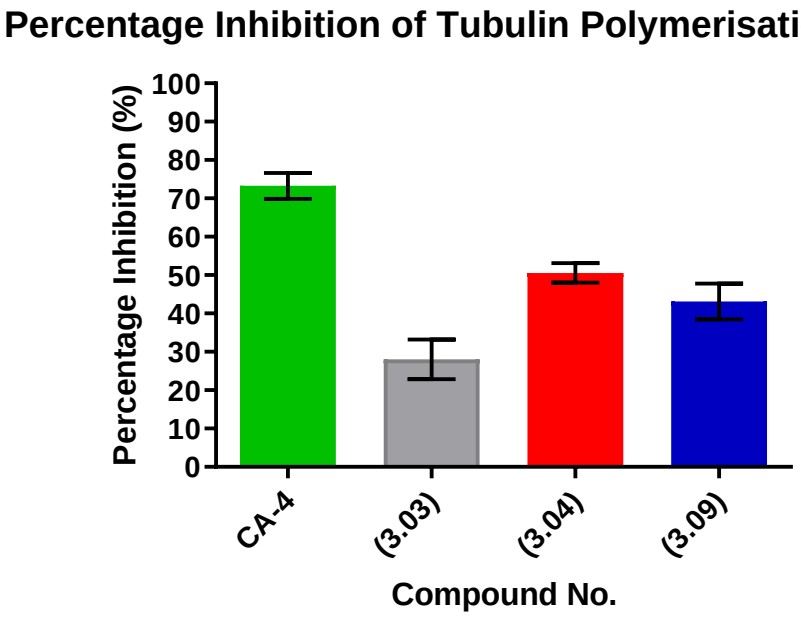

Figure 3.32. Percent inhibition of tubulin polymerisation for the synthesised phenstatin derivatives at 10 µM concentration

The percentage inhibition of tubulin polymerisation was plotted against log concentration (M) to obtain dose responsive curve for compounds **(3.03)**, **(3.04)**, **(3.09)** and **CA-4** (figure 3.33)**.**

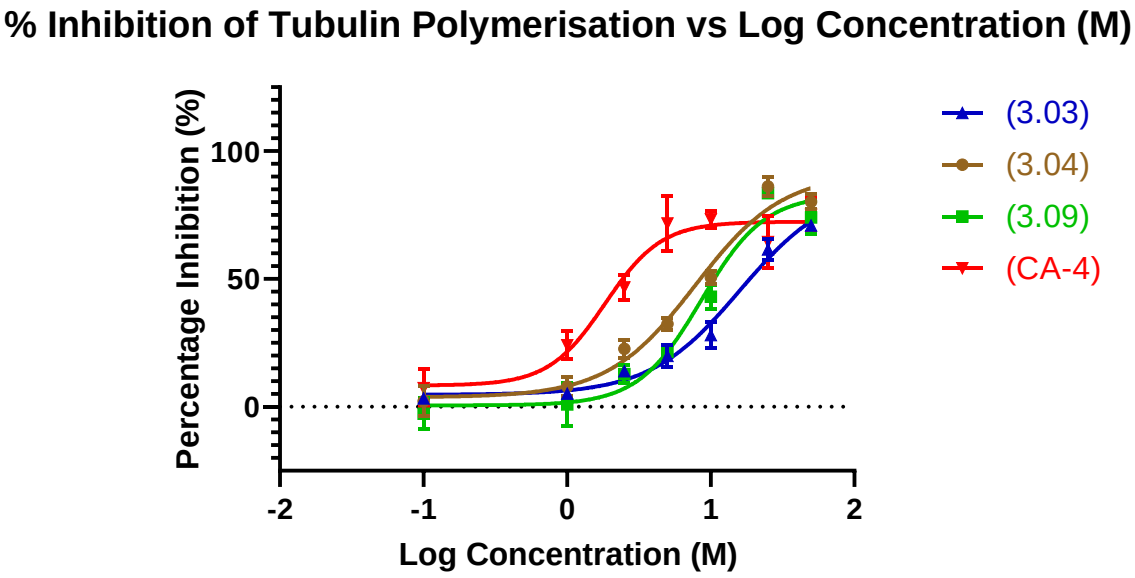

Figure 3.33. Percent inhibition vs log concentration for tubulin polymerisation inhibitors (3.03), (3.04), (3.09) and (CA-4). (error bars represent SEM of n = 3, in triplicate)

The main objective of this chapter was to synthesise a series of potent tubulin inhibitors with additional linker units for loading of the peptide-based APN inhibitors. The compound **(3.03)** (IC_{50} = 15.99 µM) synthesised demonstrated that the presence of bulky group like benzyl slight reduces the tubulin polymerisation inhibition activitity of the compound **(3.04)** (IC_{50} = 7.816 µM). Moreover, the presence of three phenolic functionalities of the compound **(3.04)** will enable us to introduce one to three APN targetting moities that will be useful in determining the optimal ratio of the APN targeting to tubulin binding moiety. Moreover the presence of aniline fuctionality of **(3.09)** could be utilised for the attachment of a substrate for APN, usually a neutral amino acid, that will present the compound **(3.09)** in its pro-drug form. The pro-drug will be converted in to its active form by the high expression of APN at the tumor tissue, as APN is known to catalyse the removal of neutral amino acids from the *N*-terminus of peptides.

Chapter 4

Synthesis of a series of novel APN- targetting hybrid drugs

4.0 Introduction

Hybrid drug therapy is a growing area of interest that involves merging the concept of combination therapy in a single agent. The concept of combination therapy in the field of cytotoxic agents was introduced by Frei E 3rd *et al.* in 1965 for acute leukemia[96]. Combination therapy has shown to produce a synergistic response as compared to monotherapy, however its efficacy is sometimes compromised due to drug-drug interaction [160, 161]. By keeping in mind the synergism associated with combination therapy many different hybrid drug therapies have emerged including the use of hybrid drug approach for the selective delivery of cytotoxic agents [125]. It was thus intuitive to employ this concept to our tubulin binding agents for their selective delivery to the tumor vasculature. In this regard, APN was chosen as a target receptor because of its high expression on endothelial cells of neoangiogenic but not on normal vasculature [134]. Moreover APN has also been found to have high expression levels in various different cancers including human uterine cervical cancer, pancreatic carcinoma and human colon cancer [136-138]. Martinez *et al*. demonstrated the enhanced aminopeptidase activity in breast tumor tissue as compared to normal tissues [162]. Several different classes of APN inhibitors have been investigated including those based around bestatin and hydroxamic acids. Bestatin, in particular, was shown to inhibit the growth of leukemic cell lines as well as to lead to an increase in survival time of patients with resected stage I squamous-cell lung carcinoma [149, 150]. Shapiro *et al.* showed in an *in vitro* assay of angiogenesis that at high concentration, bestatin significantly abolishes capillary tube formation using human umbilical vein endothelial cells (HUVECs) [135]. While later studies by Mishima showed the same effect at a much lower concentration of bestatin following continuous treatment of the newly formed tubes with this agent [163]. Taking these observations into consideration the design concepts presented in this chapter is to build hybrids with the facility to slowly release the more potent tubulin component from the hybrid while at the same time allowing for the bestatin component to be presented at levels found *in vivo* to allow it to be therapeutically effective. In effect the tubulin binding component is presented in pro-drug form while APN targeting moiety is in an active presentation. Two approaches will be used, those based on bestatin-like tripeptides and those based on hydroxamic acids to serve as the APN inhibitors.

The aim of the work presented in this chapter was to;

- Synthesize hybrids based on the most active tubulin binding agents whose synthesis is outlined in Chapters 2 & 3, namely **(2.16)**, **(2.22)**, **(2.68)**, **(3.04)** and **(3.09)**, utilizing bestatin-like tripeptides as the APN inhibitor for their targeted delivery to the tumor vasculature.
- Synthesize hydroxamic acid based hybrids of **(2.16)**, **(2.22)**, **(2.68)**.
- Present the hybrids in pro-drug form by linking an APN cleavable peptide on to C-ring of our tubulin binding agents.
- Investigate the release profile of both the APN substrate and inhibitor from **(2.22)**, **(2.68) and (3.04)** by LCMS.

4.1 Peptide based hybrid drugs

In chapter 2 and 3 we have discussed different tubulin binding agents (TBAs) that demonstrated promising activity as tubulin polymerization inhibitors. The most active among them were phenolic 4-arylcoumarin **(2.22)**, aniline based 4-arylcoumarin **(2.16)**, chromenone **(2.68)** and triphenolic phenstatins **(3.04)** and **(3.09)** (figure 4.1).

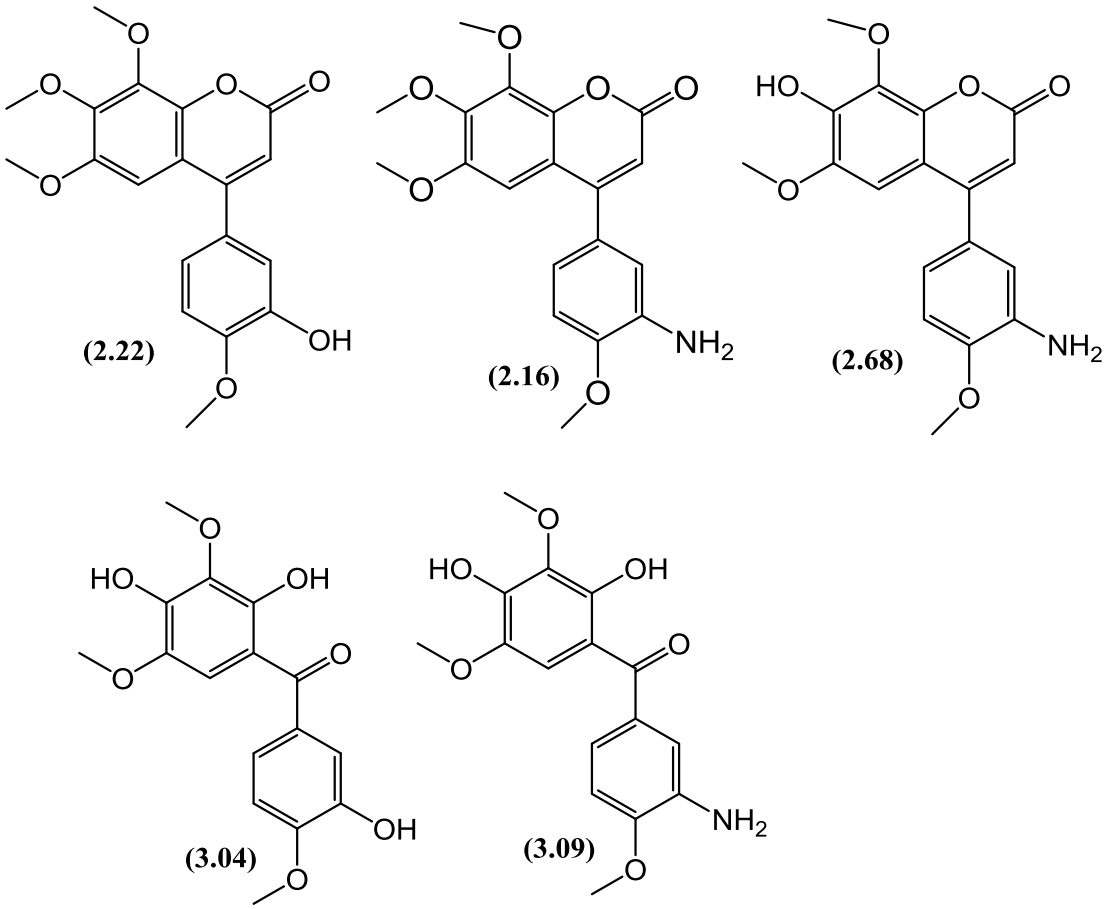

Figure 4.1. Chemical structures of different tubulin binding agents

The two main functional groups that are utilized for the attachment of APN inhibitory peptides on to these tubulin binding agents include (i) phenolic functionality that will form an ester linkage to the APN inhibitor and would most likely be cleaved quickly by hydrolysis at physiological pH or via esterase enzymes found in the blood (ii) aniline functional group that will form an amide linkage to the APN inhibitor and would be relatively resistant to hydrolysis so will be therefore dependent on peptidases including APN for its cleavage.

4.1.1 Tripeptide-based hybrids of 4-arylcoumarin (2.22) with ester linkage

Bestatin is a potent inhibitor of Aminopeptidase N (APN) [147] and exerts its inhibitory effect by interacting with zinc ion at the active site of APN through carbonyl and hydroxyl group. The positively charged free amine group is also found to interact with the 2-3 glutamate residues on the APN active site. The phenylalanine side chain interacts with the $\mathbf{S_1}$ hydrophobic pocket while the leucine group is found to be closely bound in another hydrophobic pocket $\mathbf{S_1'}$. Apart from these binding pockets some other unoccupied hydrophobic clefts have also been identified on APN such as $\mathbf{S_2'}$ that are not occupied by bestatin and longer chain peptides are able to bind to these pockets (figure 4.2).

With this in mind we decided to introduce a peptide chain onto the phenolic functionality of 4-arylcoumarin (**2.22)**, containing an amino acid like leucine or valine that would be able to occupy the $\mathbf{S_2'}$ binding pocket and then to couple bestatin to create a tripeptide based hybrid. We propose that it would potentiate the APN binding and APN inhibitory effect.

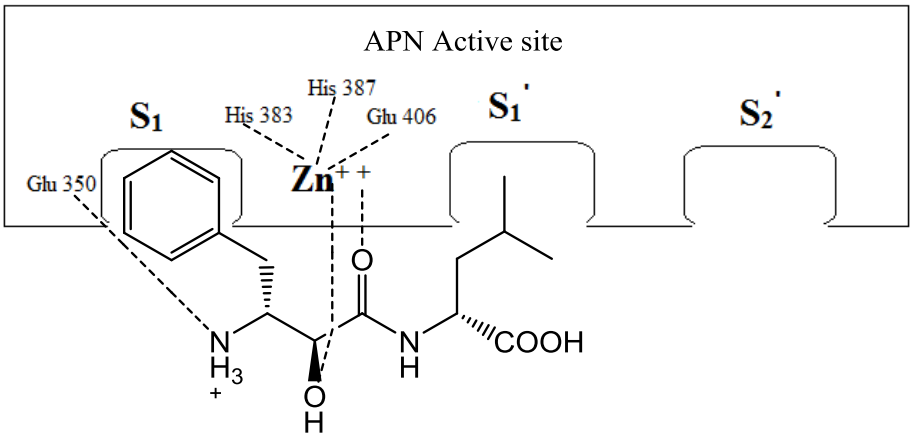

Figure 4.2 Simple schematic representation of APN binding site and interactions of bestatin with the hydrophobic pockets S_1, S_1' and S_2' [164].

During our synthetic approach for hybrids we preferred to couple bestatin directly on to our compounds by converting it to an activated pentafluorophenyl ester. In order to avoid the intermolecular cyclization, bestatin was first protected as an *N*-Boc carbamate using di-*tert*-butyl dicarbonate and potassium carbonate in a mixture of THF:water (1:1) at room temperature (scheme 4.1). After the reaction time of 7 hours, the less volatile organic solvent was evaporated under reduced pressure while the remainder was quenched with aqueous NaOH (2 M) and extracted with diethyl ether. The aqueous fraction was then acidified with aqueous HCl (2 M) and extracted with DCM. Upon drying and evaporating the organic layer, the Boc-protected bestatin **(4.01)** was afforded with a yield of 84%.

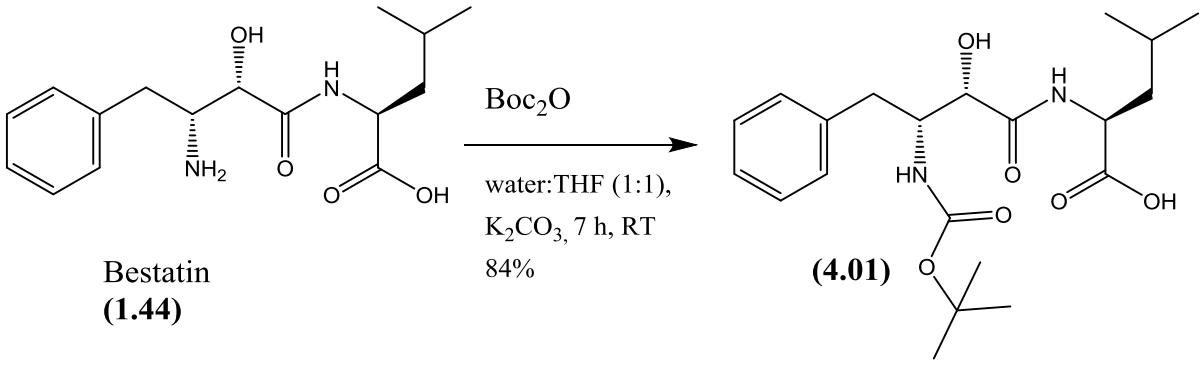

Bestatin
(1.44)

(4.01)

Scheme 4.1. Boc protection of bestatin

For the coupling of Boc bestatin **(4.01)** on to our compounds it was converted it into activated pentafluorophenyl (PFP) ester in order to avoid the use of a coupling reagent in the next step. For this purpose Boc bestatin **(4.01)** was treated with pentafluorophenol using EDC.HCl as coupling reagent in DCM at 0 °C (scheme 4.2). EDC.HCl was preferred as a coupling reagent because the reagent itself as well as its by-products are soluble in water and can easily be removed from the reaction mixture by washing with water. Following completion of the reaction the product was partitioned between diethyl ether and water, the organic layer was dried with Na_2SO_4 in order to avoid the hydrolysis of the pentafluorophenyl ester **(4.02)**.

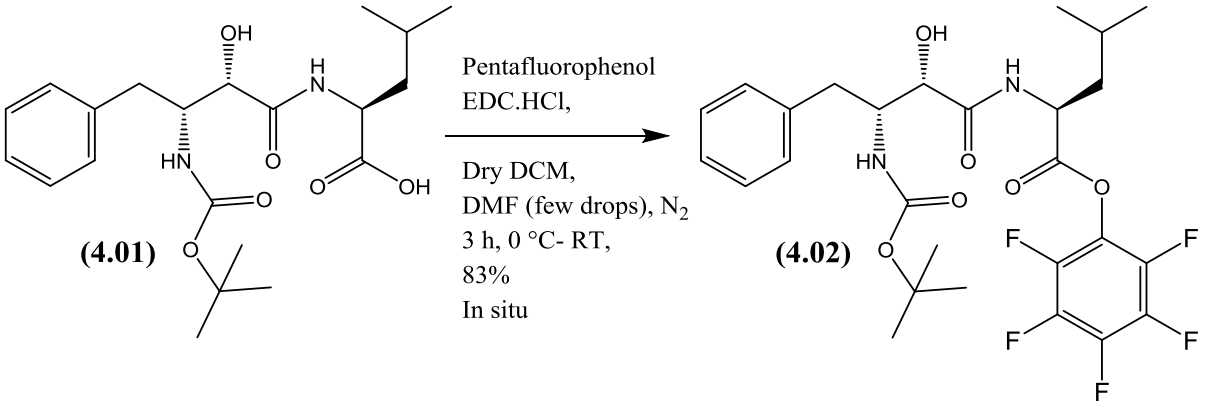

Scheme 4.2. Formation of PFP ester of Boc bestatin **(4.01)**

4.1.1.1 Leucine based tripeptide hybrid of 4-arylcoumarin (2.22)

The first step towards the synthesis of this hybrid was coupling of *N*-Cbz-leucine to phenol **(2.22)**. This was achieved by stirring the phenol **(2.22)** with *N*-Cbz-leucine in dry DCM at 0 °C using EDC.HCl as coupling reagent (scheme 4.3). After 3 hours the reaction was diluted with DCM, washed once with water and quickly dried. Upon evaporation of the organic solvent, the residue was purified by flash column chromatography to afford the leucine coupled product **(4.03)** in 89% yield. The coupling of Cbz leucine was confirmed by ^{1}H NMR analysis (figure 4.3) due to the presence of the characteristic 6 protons of leucine side chain at 1.05 ppm as well as by the additional CH_2 (5.15 ppm)and 5 aryl protons, at 7.36 ppm, for the Cbz protecting group.

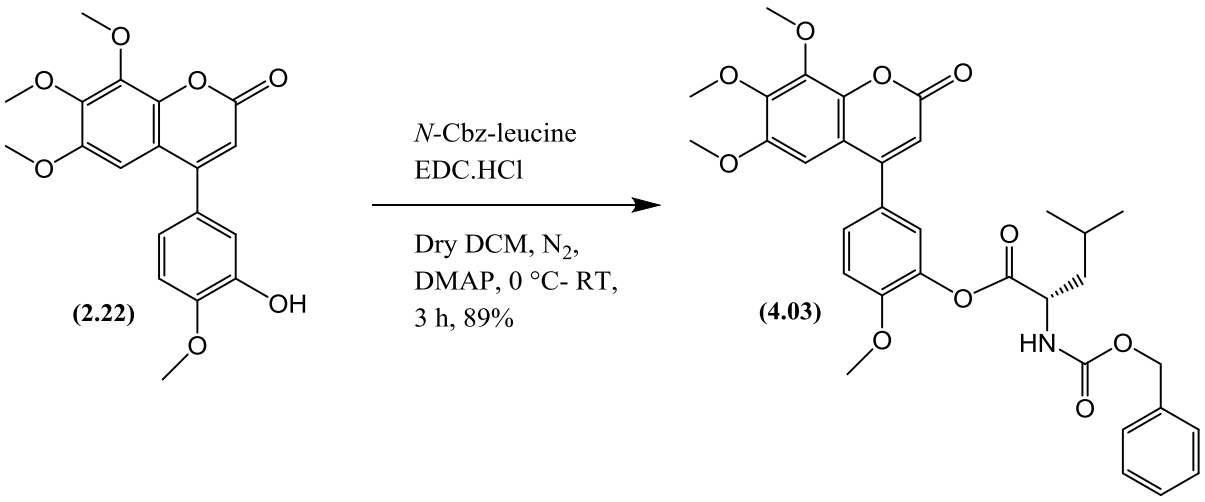

Scheme 4.3. EDC coupling of *N*-Cbz-leucine on to phenol **(2.22)**

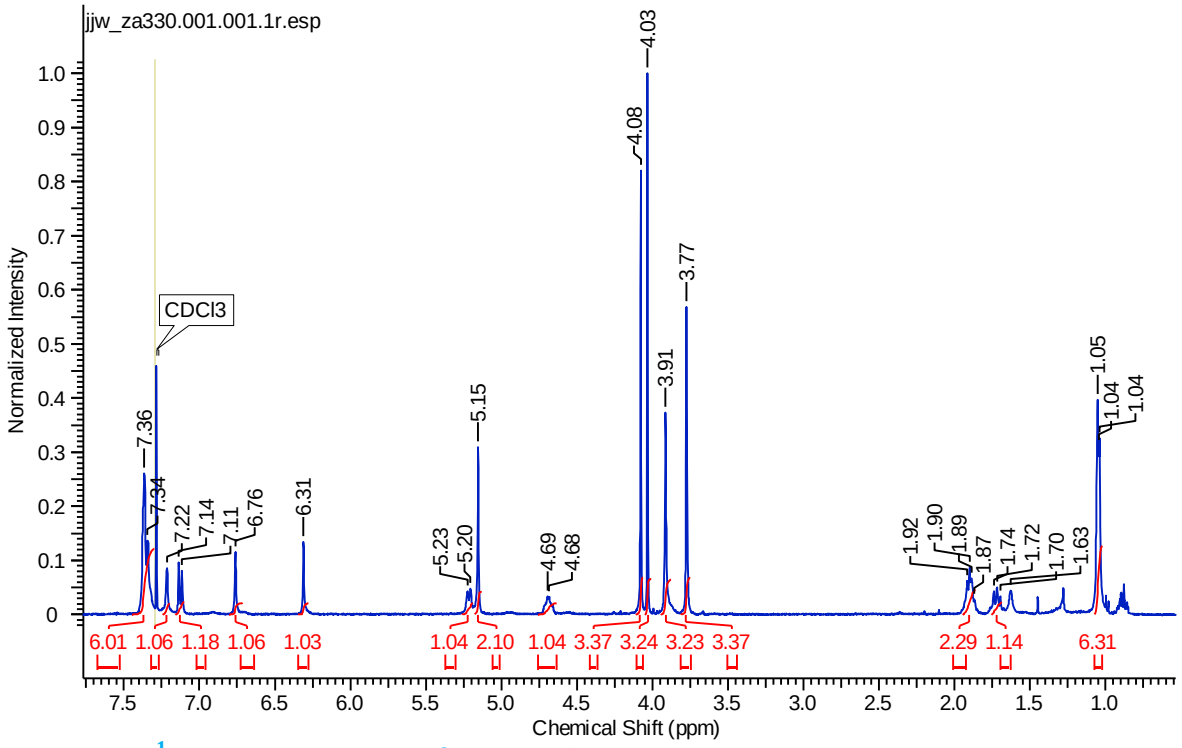

Figure 4.3. ^{1}H NMR spectrum of intermediate (4.03)

Next steps in the synthetic sequence involved the deprotection of Cbz protecting group and coupling of the PFP ester of bestatin **(4.02)**. Due to the nucleophilic nature of free amine of the leucine and the presence of activated ester linkage at the C-ring we decided to carry out both the deprotection and coupling of PFP ester **(4.02)** in one single step. For this purpose compound **(4.03)** was deprotected in the presence of PFP ester of bestatin **(4.02)** using 10% Pd/C in EtOAc:EtOH (1:1) under an atmosphere of hydrogen (scheme 4.4). After 90 minutes, the palladium/carbon was filtered through a cotton plug and the organic solvent was evaporated at 35 °C under reduced pressure, following which the product was purified by flash column chromatography to afford compound **(4.04)** in 56% yield. The coupling of Boc bestatin was confirmed due to the presence of additional features, including the characteristic Boc group at 1.41 ppm, 5 extra aryl protons and 6 extra CH_3 protons of the second leucine residue, in the ^{1}H NMR spectrum (figure 4.4). Along with the NMR, HRMS analysis by APCI found the relative protonated molecular ion of mass 862.4115 ($M+H^{+}$).

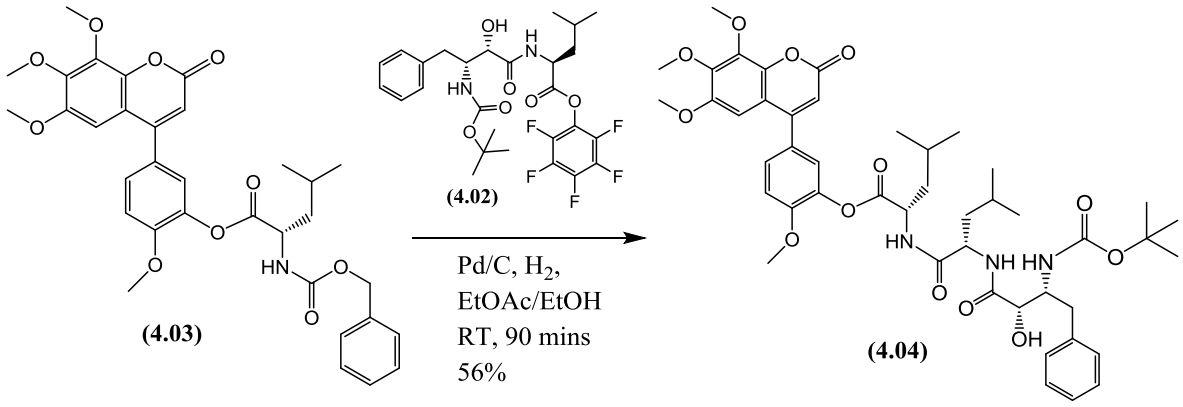

Scheme 4.4. Cbz-deprotection and coupling of PFP ester

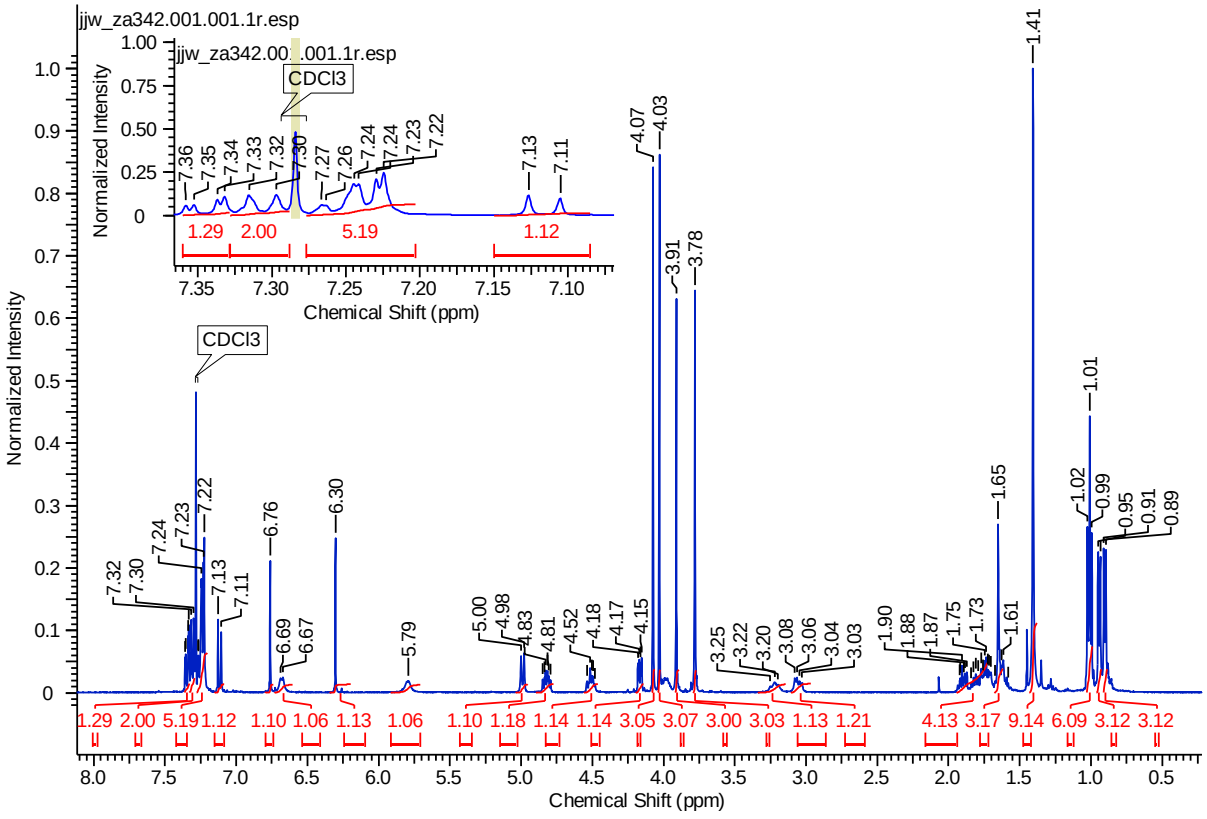

Figure 4.4. ^{1}H NMR spectrum of compound (4.04)

The final step towards the synthesis of our first hybrid drug was the deprotection of the Boc group and this was achieved under strict anhydrous conditions. *N*-Boc protected compound **(4.04)** was dissolved in dry DCM under an atmosphere of nitrogen and cooled to -10 °C with salted ice. To this was added TFA (already cooled in salted ice) and the reaction allowed to proceed for 90 minutes before being diluted with DCM. The solvent was then evaporated at 35 °C under reduced pressure to afford the product **(4.05)** in 98% yield as the TFA salt (scheme 4.5).

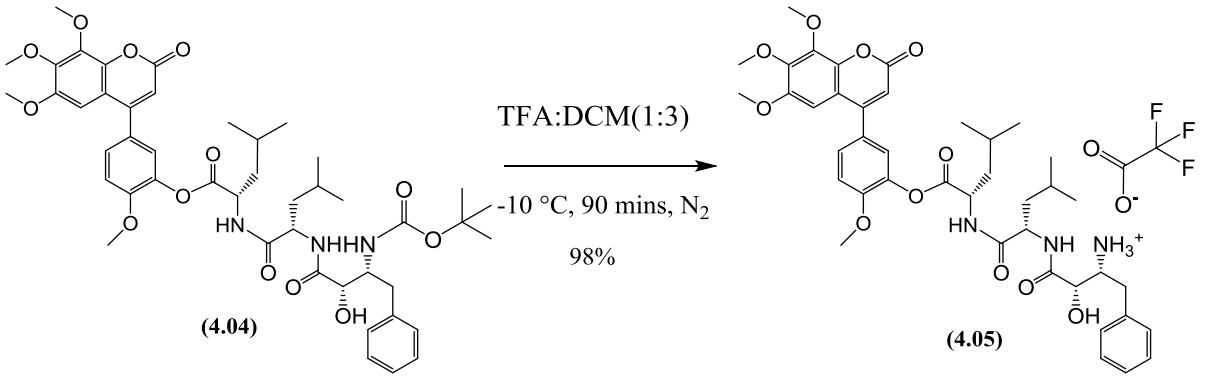

Scheme 4.5. Removal of Boc group

4.1.1.2 Structure elucidation of compound (4.05)

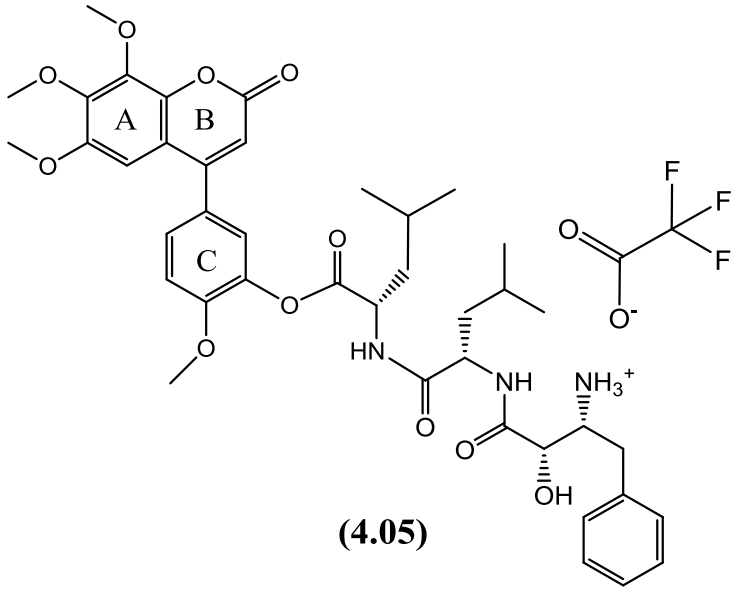

Linking a tripeptide chain onto phenol **(2.22)** resulted in the overall increase in the molecular weight of compound along with the sharp increase in the level of complexity associated with its structural elucidation. For the structural confirmation of tripeptide **(4.05)** mainly HRMS and NMR spectroscopic techniques were used. The ^{1}H NMR spectrum (figure 4.5) shows the presence of all 52 protons while the ^{13}C spectrum (figure 4.6) gives a total carbon count of 43.

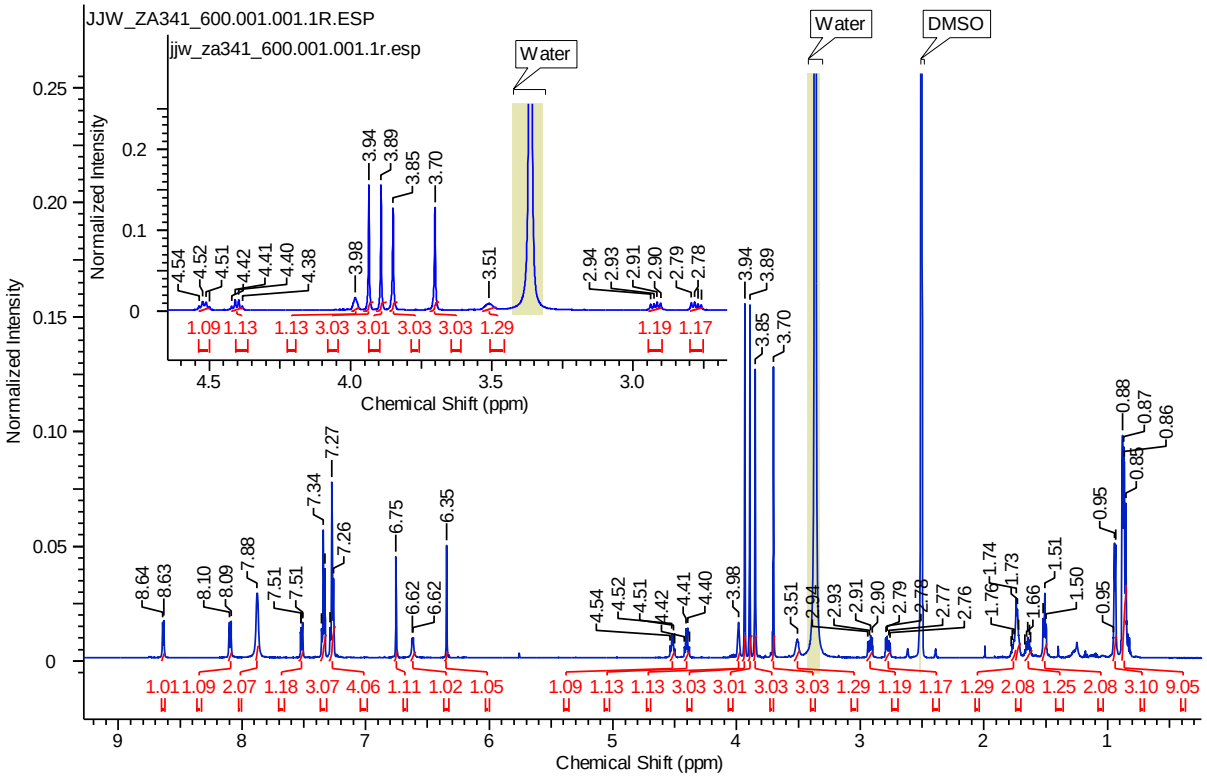

Figure 4.5. ^{1}H NMR spectrum of (4.05)

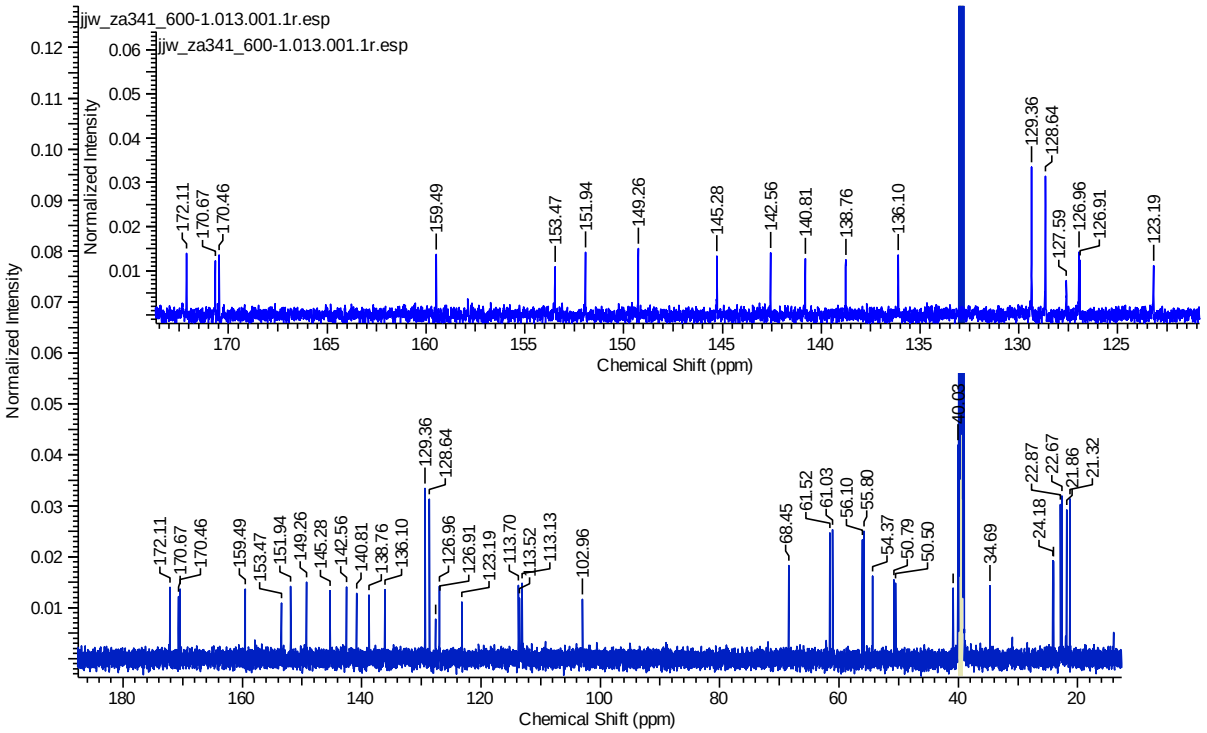

Figure 4.6. ^{13}C NMR spectrum of (4.05)

Starting with the expanded ^{1}H NMR spectrum the most upfield signals in the region 0.5-1.0 ppm appearing as two overlapping doublets (integral value 9 protons) and one doublet

(integral value 3 protons) represent the four methyl groups of the two leucine residues. The next signal appearing as triplet at 1.51 ppm with an integral value of 2 corresponds to the CH_2 of the leucine side chain and is distinguished from the remaining two CH_2 groups by the fact that in HMBC it shows coupling to CH_3 carbons of the leucine (figure 4.8) and do not show any coupling to aryl carbons while CH_2 of the AHPA (2.78, 2.91 ppm) show coupling to aryl carbons (figure 4.9). The two singlets at 3.51 and 3.98 ppm corresponds to two CH groups of the AHPA and the methoxy groups are found to be resonating as four singlets at 3.70, 3.85, 3.89 and 3.94 ppm each with an integral value of 3. Towards the aromatic region the next two quartets at 4.40 and 4.50 ppm each with an integral value of 1 represent the CH protons on each leucine attached to NH.

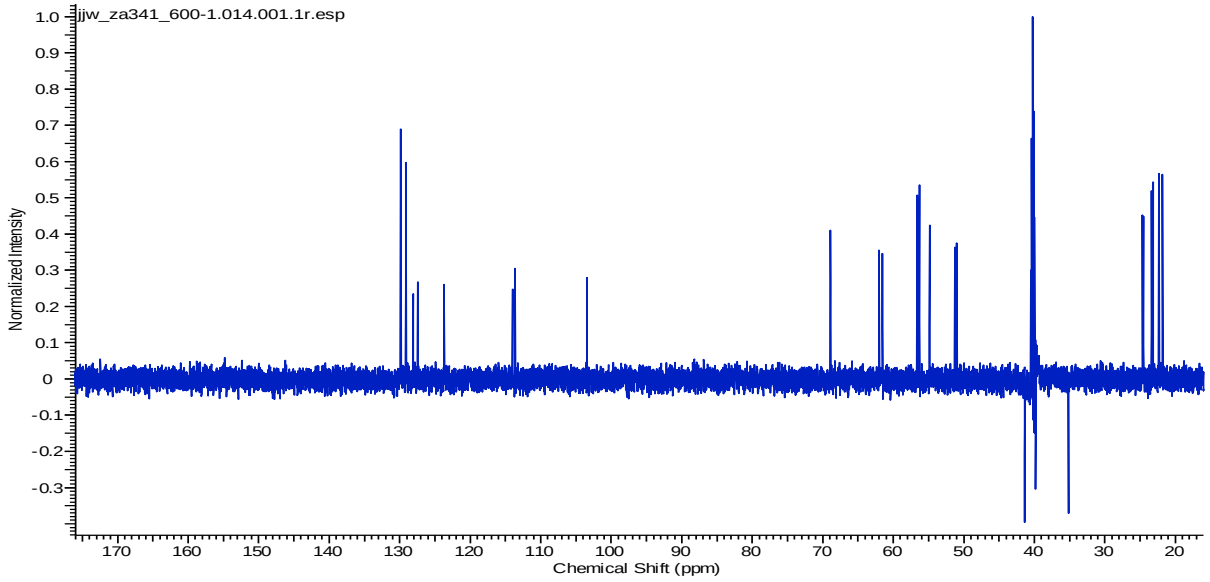

Figure 4.7. Dept 135 spectrum of compound (4.05)

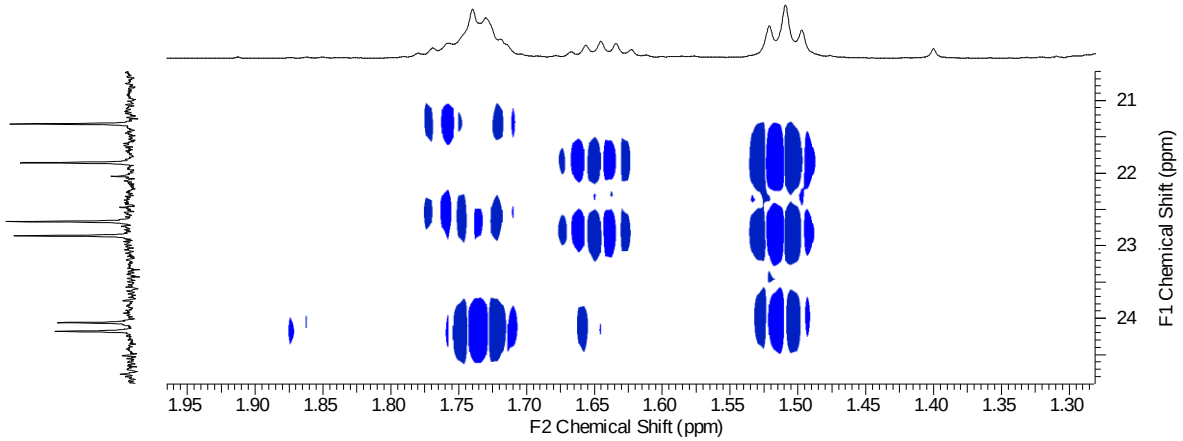

Figure 4.8. Expansion of HMBC spectrum of (4.05)

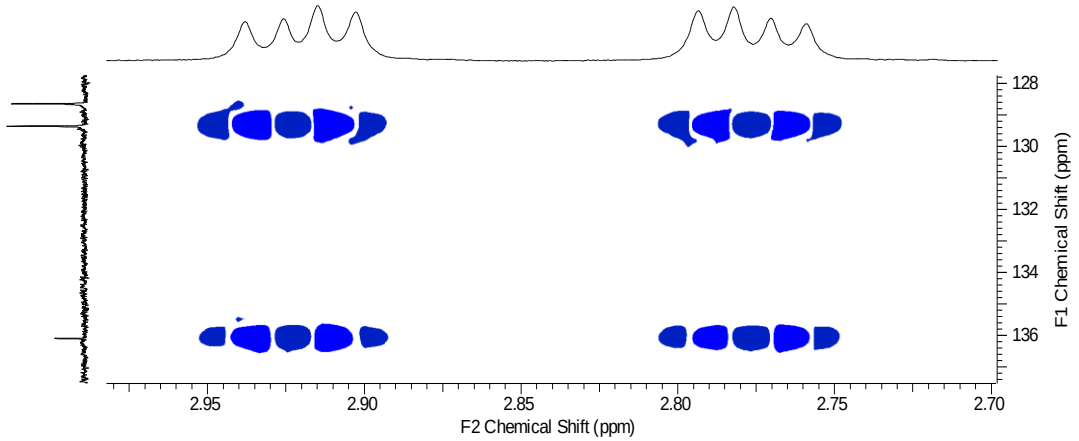

Figure 4.9. Expansion of HMBC spectrum of (4.05)

The next singlet at 6.35 ppm corresponds to the alkene proton while the signal at 6.75 ppm represents the A-ring aryl proton. The overlapping signals in the region spanning 7.25-7.40 ppm represent the 5 aryl protons of AHPA and 2 aryl protons of C-ring. The final proton of C-ring appears as double-doublet (showing *ortho-meta* coupling) at 7.51 ppm. Among the last remaining signals two NH groups were found using NH COSY, resonating as doublets at 8.10 and 8.62 ppm because each having one proton attached to their adjacent carbons while the NH_2 was found resonating as a broad singlet at 7.88 ppm.

All the carbons related to these protons are easily identified using the HSQC spectrum (figure 4.10) and ^{13}C NMR spectrum (figure 4.6) where the four CH_3 groups of two leucine residues resonates at 21.32, 21.86 , 22.67 and 22.87 ppm and the two CH groups attached to them appear at 24.06 and 24.18 ppm. Four methoxy groups resonates at 55.80, 56.10, 61.03 and 61.52 ppm while the carbon peak for the CH_2 group of AHPA is found resonating at 34.69 ppm while the two CH_2 carbons of leucine resonate at 39.33 and 40.87 ppm. Four CH signals at 50.50, 50.79, 54.37 and 68.45 ppm correspond to the CHNH of leucine, CHNH of second leucine residue, $CHNH_2$ of AHPA and CHOH of AHPA. In the aromatic region of the ^{13}C spectrum the signals for the four aromatic CH's of A and C rings are identified at 102.96, 113.52, 123.19 and 127.59 ppm while the C=CH signal is at 113.13ppm. Five aryl CH's of the AHPA are also present in the aryl region and appear as one CH at 126.96, two at 128.64 and two at 129.36 ppm. Out of ten quaternary carbons identified in the region between 113-154 ppm, nine represent aromatic quaternary carbons while one represent the carbon of the alkene. Of the remaining signals, the carbonyl of the B-ring was found resonating at 159.49 ppm while the three carbonyls of the tripeptide were found at 170.46, 170.67 and 172.11 ppm.

The HRMS analysis of **(4.05)** revealed a protonated molecular ion of mass 762.3601 ($M+H^+$) as free base form of the TFA salt.

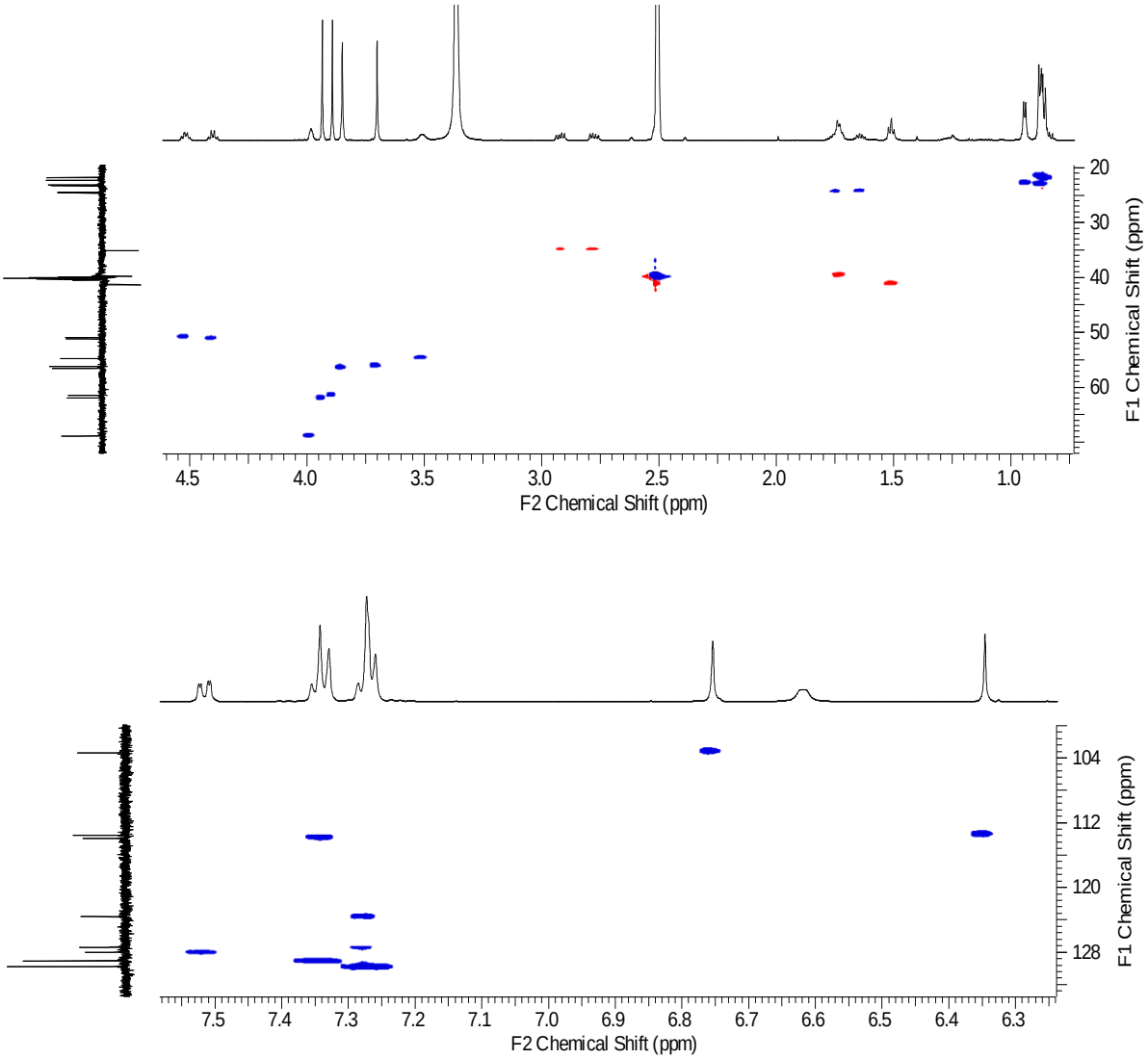

Figure 4.10. Partial HSQC spectra of (4.05), CH_2 protons (red contours)

4.1.1.3 Valine based tripeptide hybrid of 4-arylcoumarin (2.22)

Next it was decided to synthesize valine based tripeptide hybrid in order to investigate a suitable substrate for $\mathbf{S_2'}$ binding pocket. We followed exactly the same synthetic route that we employed for the synthesis of hybrid drug **(4.05)** except in the first step, as required, the Cbz leucine amino acid was replaced by Cbz valine. Again starting with phenol **(2.22)**, in the first step EDC coupling of Cbz valine was performed to synthesize the valine coupled product **(4.06)** that was followed by single step Cbz deprotection and coupling of the

bestatin ester **(4.02)** to give the *N*-Boc protected tripeptide **(4.07)** (scheme 4.6). The success of the coupling was first confirmed by HRMS that detected the molecular mass of 848.396875 ($M+H^+$) as a protonated ion. Further confirmation was achieved following inspection of its ^1H NMR spectrum (figure 4.11).The presence of the characteristic peaks including the Boc group (1.41 ppm), 4 CH_3 groups of the side chain of valine and leucine (0.80-1.10 ppm), 4 methoxy groups (3.78, 3.91, 4.03 and 4.08 ppm) and 5 extra aryl protons of AHPA.

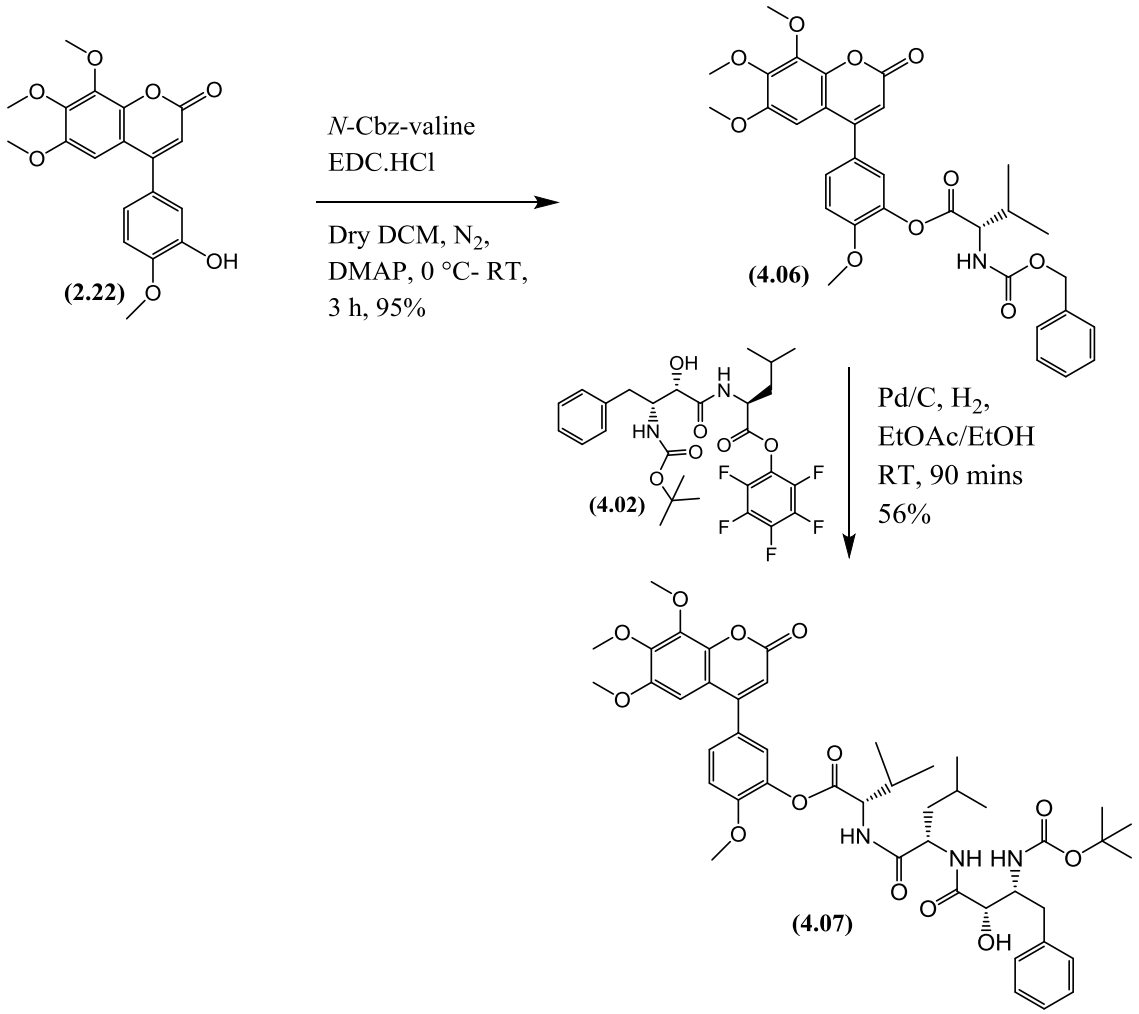

Scheme 4.6. Coupling of tripeptide chain onto phenol **(2.22)**

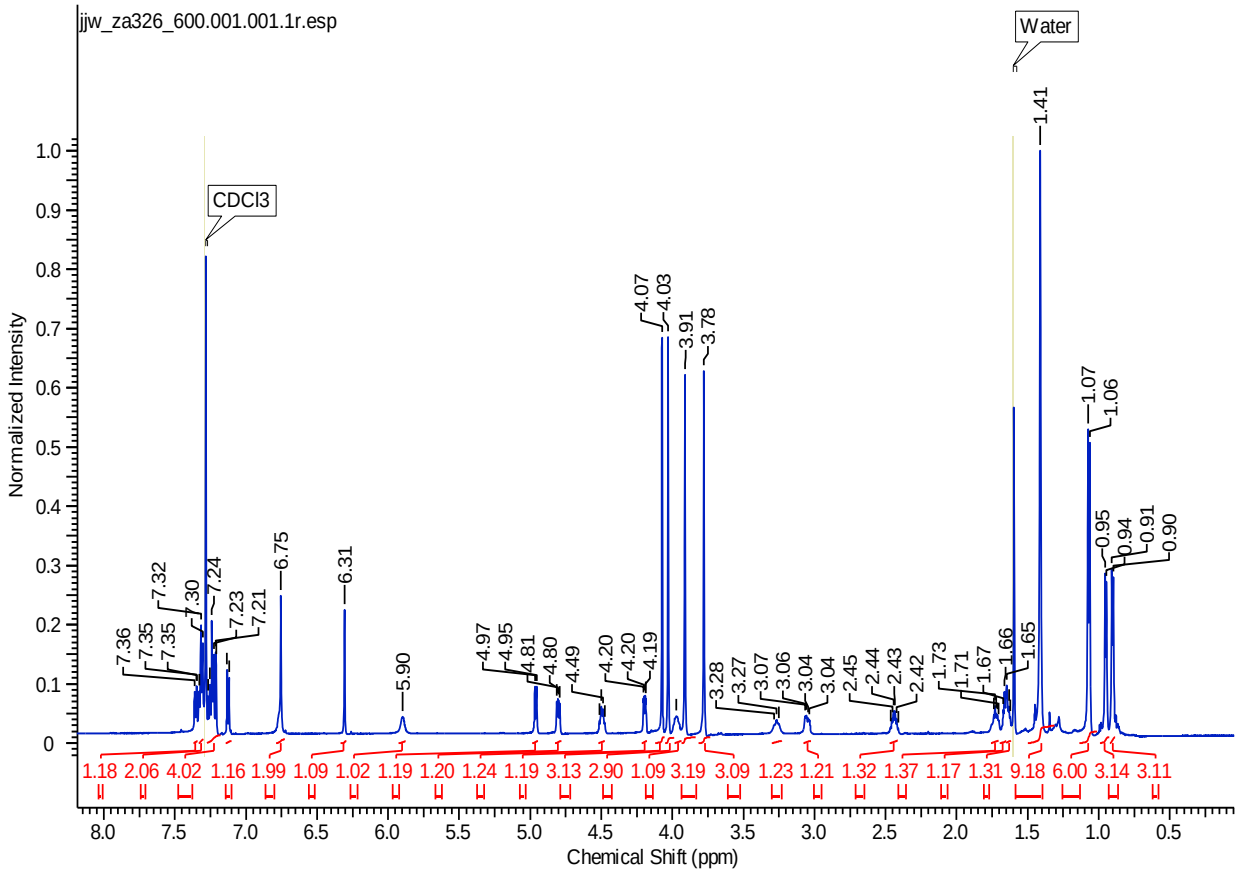

Figure 4.11. ^{1}H NMR spectrum of Boc protected tripeptide (4.07)

In the final step *N*-Boc deprotection was carried out using cooled anhydrous DCM and TFA (3:1) under the atmosphere of nitrogen to afford the valine based tripeptide hybrid drug **(4.08)** in a yield of 98%, in the same manner as conducted for the leucine analogue **(4.05)** discussed above (scheme 4.7).

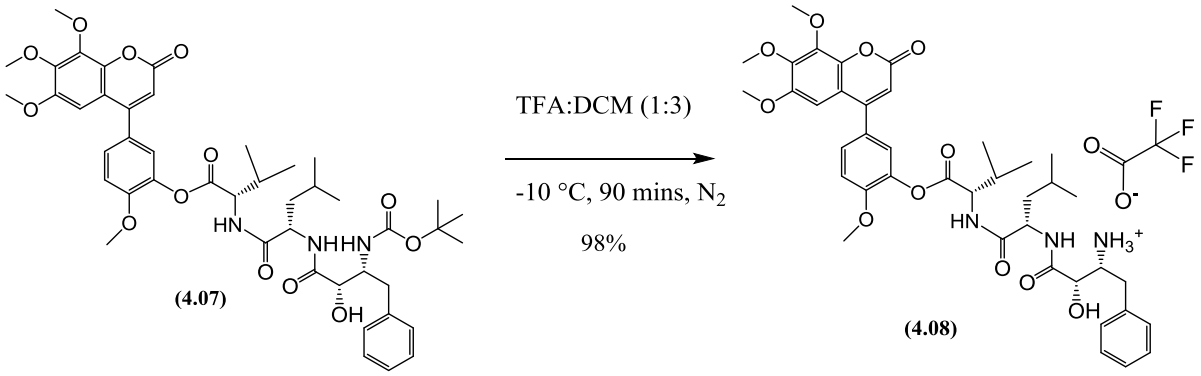

Scheme 4.7. Removal of Boc group

The synthesis of the hybrid compound **(4.08)** was confirmed by the disappearance of the signal for *N*-Boc protecting group at 1.41 ppm in the ^{1}H NMR spectrum (figure 4.12).

Moreover, the ^{1}H NMR spectrum also shows distinctive signals for **(4.08)** including the four methoxy groups (3.71, 3.86, 3.90 and 3.94 ppm), four CH_3 groups of valine and leucine (0.80-1.10 ppm) and the five extra aryl protons of AHPA. The ^{13}C NMR spectrum (figure 4.13) shows the presence of all expected 40 carbons. As the compound **(4.08)** shares most of the structural features with the hybrid compound **(4.05**), its complete elucidation will not be discussed here (see experimental for the complete assignments). The only difference was the presence of two CH_2 groups (figure 4.14) as compared to three for **(4.05)**.

HRMS analysis of **(4.08)** also confirmed the synthesis of compound **(4.08)** with the presence of the molecular ion peak of mass 748.3423 corresponding to the ($M+H^+$) ion.

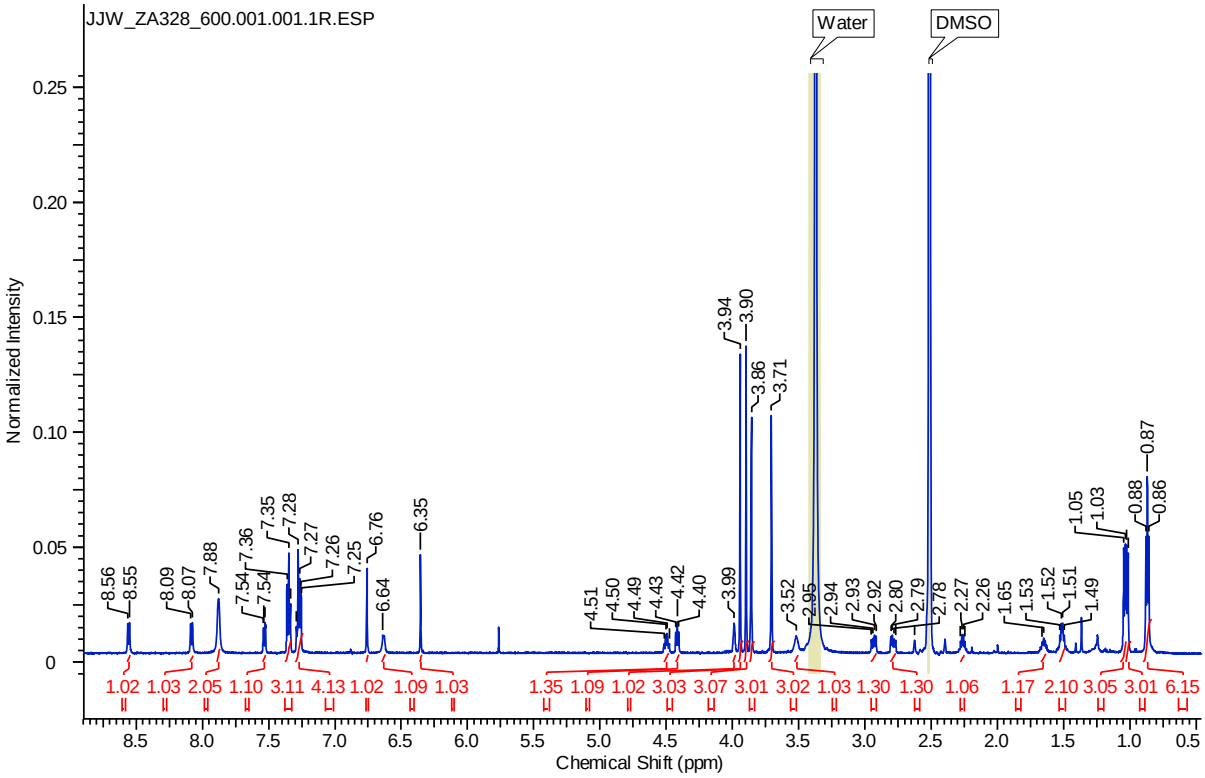

Figure 4.12. ^{1}H NMR spectrum of compound (4.08)

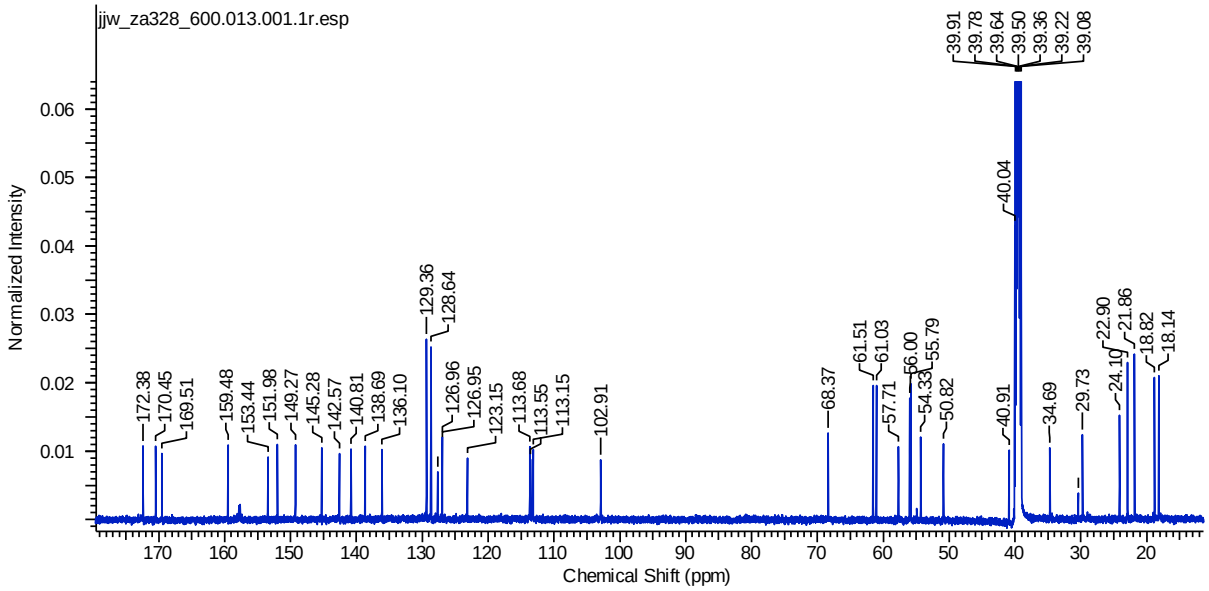

Figure 4.13. ^{13}C NMR spectrum of (4.08)

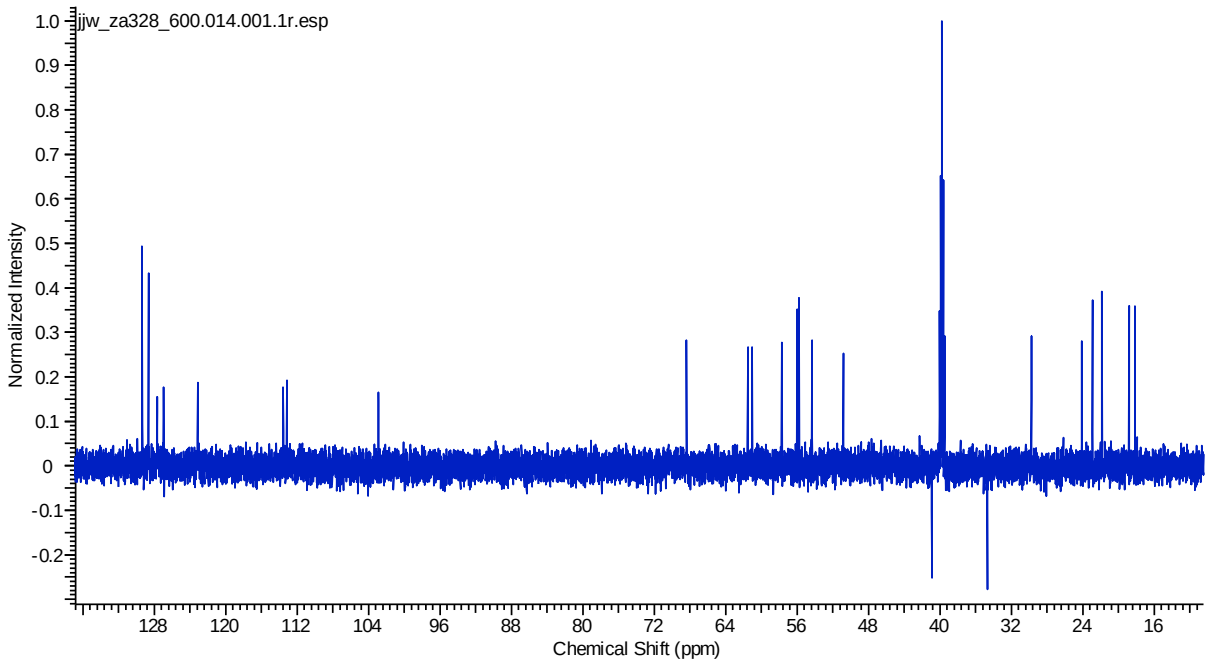

Figure 4.14. DEPT 135 spectrum of (4.08)

4.1.2 Tripeptide based hybrids of 4-arylcoumarin (2.68) with ester linkage

Having completed the synthesis of the 4-arylcoumarin **(2.68)** and shown it to be a significant inhibitor of tubulin polymerization, our next strategy was to use the phenolic position on the A-ring for the attachment of the APN binding peptide (figure 4.15). Our

rationale for doing so was based on the premise that positioning the APN binding peptide between two relatively bulky methoxy groups with their associated positive inductive effect on substituents *ortho* to them should offer greater resistance to hydrolysis over the less crowded analogues on the C-ring namely **(4.05)** and **(4.08)** thus allowing for slower release of the tubulin binding component.

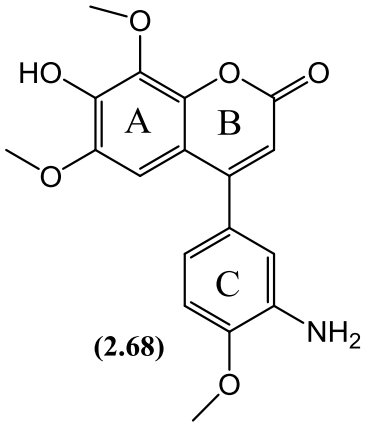

(2.68)

Figure 4.15. 4-arylcoumarin with dimethoxy substituted aryl (A-ring)

Starting with the intermediate **(2.67)**, the first step required coupling of Cbz valine to it using EDC.HCl as coupling reagent in dry DCM at 0 °C to give compound **(4.09)**. The next step involved the deprotection of Cbz protecting group and coupling of the bestatin ester **(4.02)** employing the same conditions as we used before during the synthesis of tripeptide hybrids (scheme 4.8). The structural confirmation of **(4.10)** was achieved by the HRMS analysis that showed the protonated molecular ion of mass 933.445807 ($M+H^+$). Moreover the ^1H NMR spectrum (figure 4.16) of compound **(4.10)** also confirmed the structural identity by having the expected characteristic peaks including 2 Boc groups (1.41 and 1.52 ppm), 4 methyl groups of the leucine and valine side chains (0.85-1.10 ppm), 3 methoxy groups (3.76, 3.98 and 4.04 ppm) and 5 additional aryl protons of the phenyl ring of AHPA.

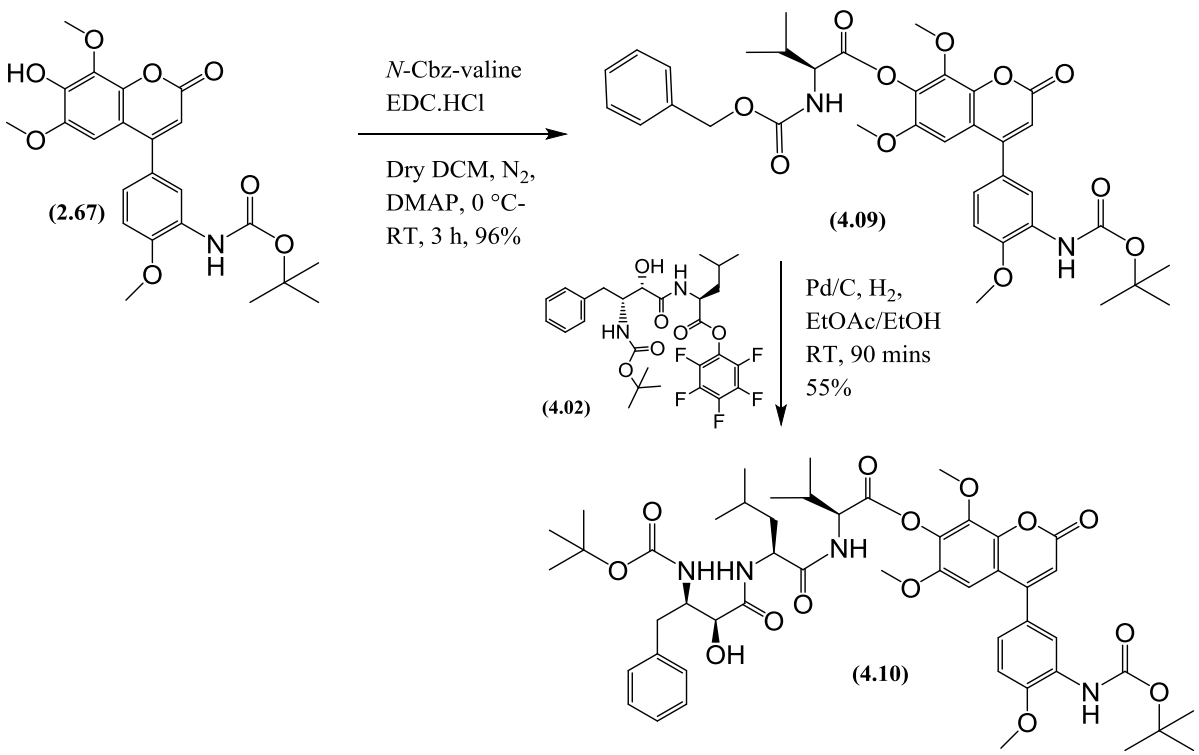

Scheme 4.8. Coupling of tripeptide onto phenol **(2.67)**

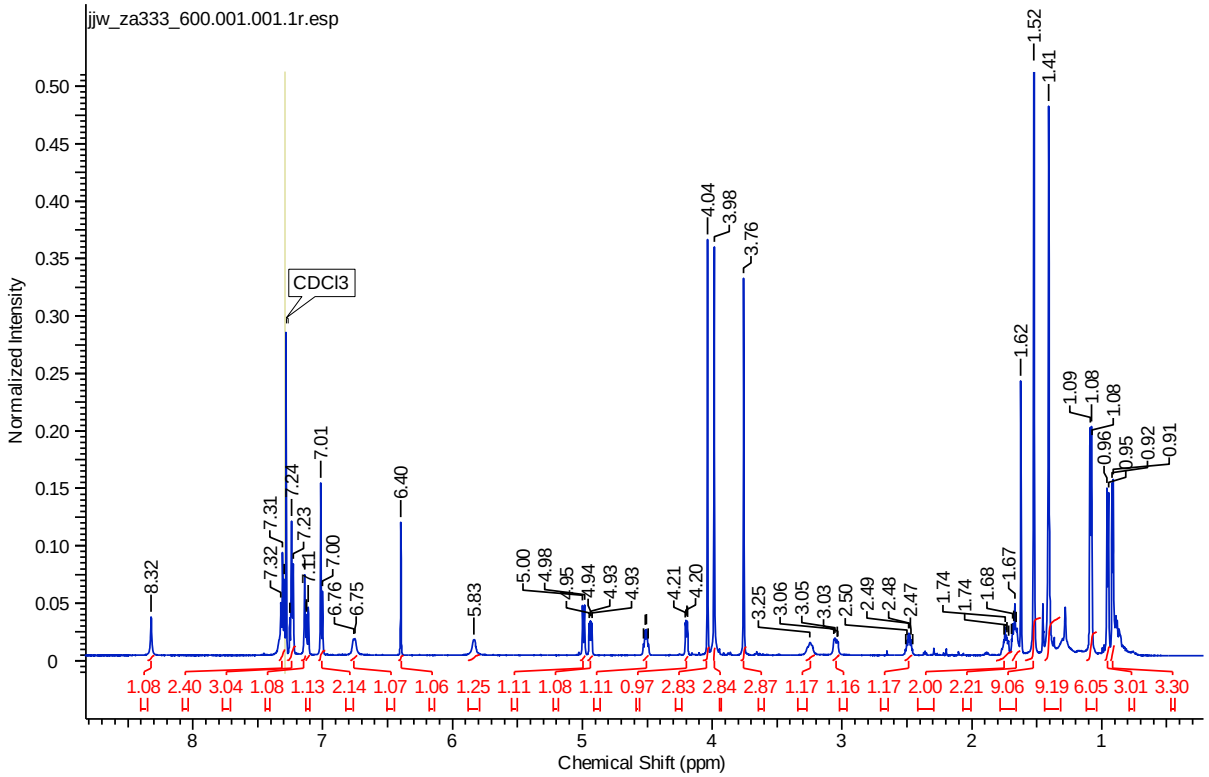

Figure 4.16. ^{1}H NMR spectrum of compound (4.10)

Removal of the two *N*-Boc protecting groups was achieved under anhydrous conditions using dry DCM:TFA (3:1) at -10 °C to afford the desired hybrid compound **(4.11)** in 97% yield (scheme 4.9).

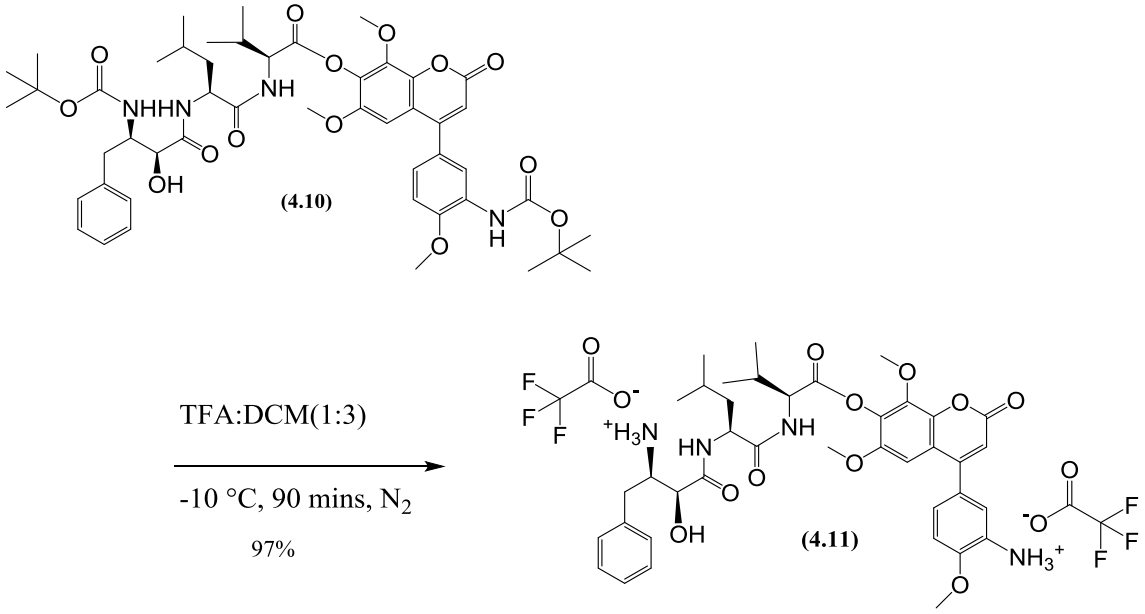

Scheme 4.9. Removal of Boc groups

4.1.2.1 Structure elucidation of (4.11)

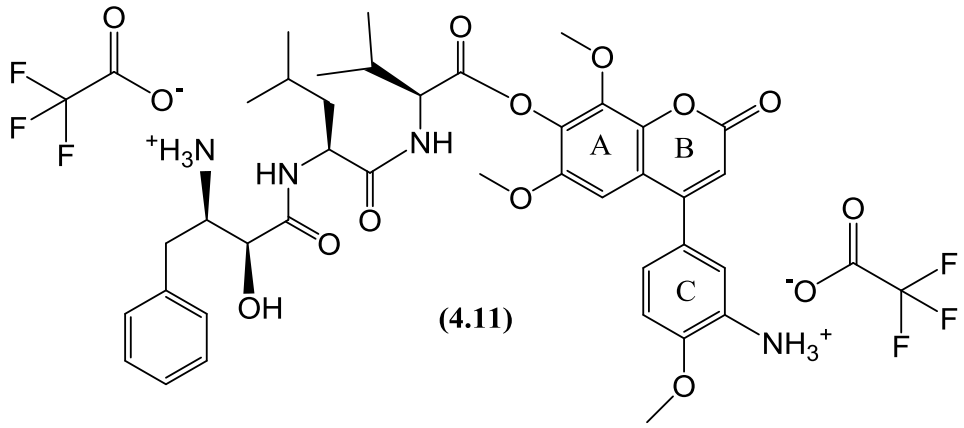

A cursory inspection of the ^{1}H NMR spectrum (figure 4.17) of compound **(4.11)** clearly showed the successful generation of the desired compound due to the disappearance of the two sharp singlets for the *N*-Boc protecting groups at 1.41 and 1.52 ppm. A more comprehensive analysis of the ^{1}H NMR spectrum showed the presence of a total of 46 protons while the ^{13}C NMR spectrum (figure 4.18) showed signals for the presence of all 39 carbons.

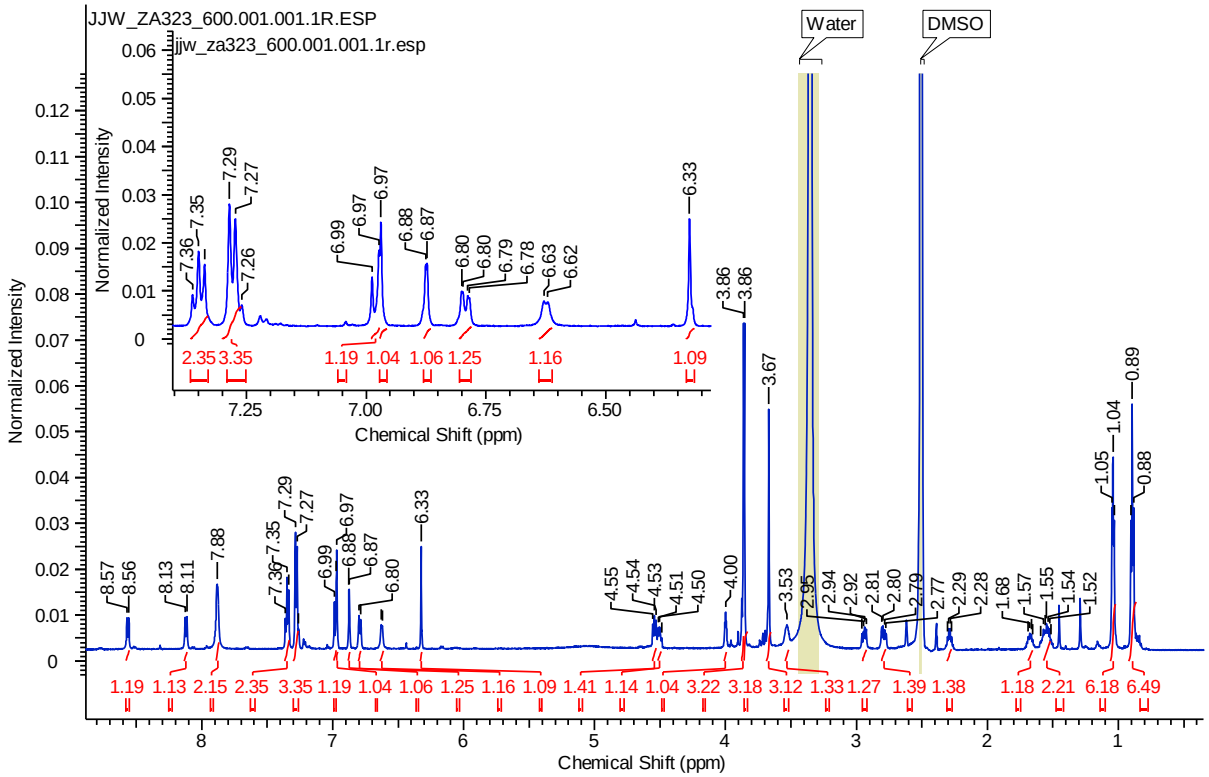

Figure 4.17. ^{1}H NMR spectrum of (4.11)

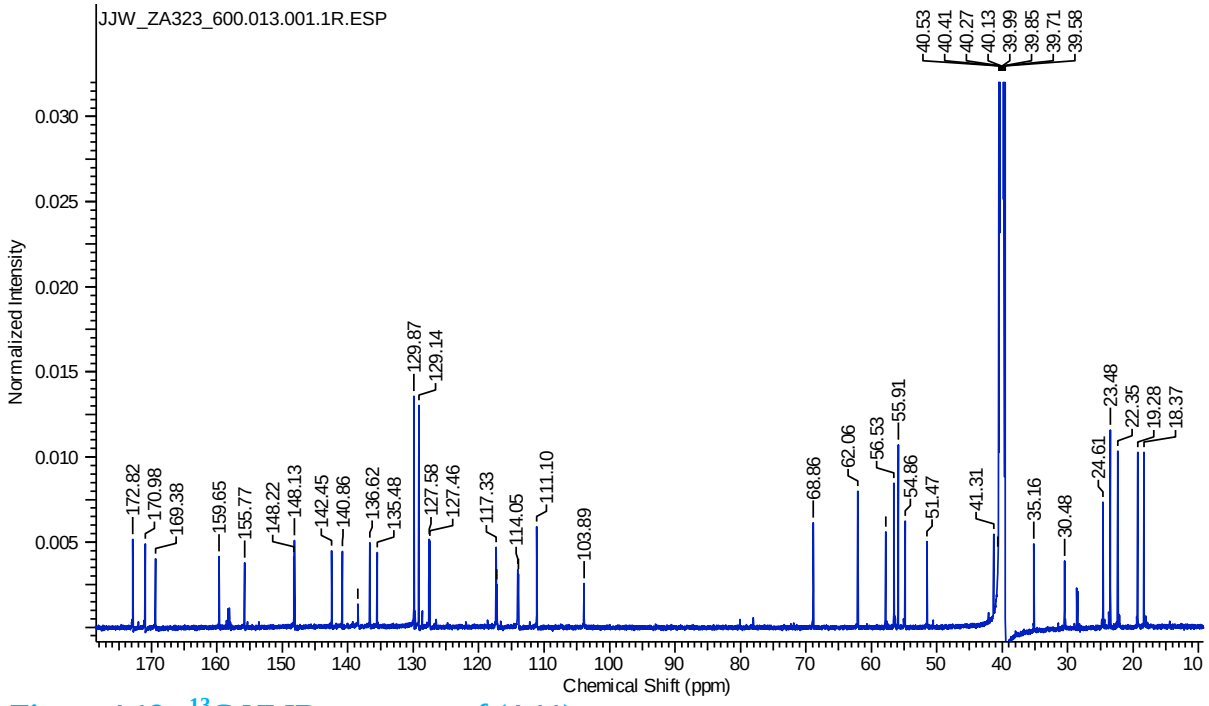

Figure 4.18. ^{13}C NMR spectrum of (4.11)

The main characteristic features of the ^{1}H NMR spectrum includes the two triplets in the most upfield region (0.5-1.1 ppm) of the spectrum, each with an integral value of 6 representing the 4 methyl groups of leucine and valine. The CH_2 of the leucine residue resonates as a multiplet at 1.54 ppm and can be seen as a red contour in the HSQC

spectrum (figure 4.19) while the signal for CH_2 of the AHPA splits into two peaks (red contours) and appear as two double doublets at 2.79 and 2.94 ppm. The ^1H NMR spectrum also has 3 distinct peaks for the methoxy groups at 3.67, 3.86 and 3.86 ppm.

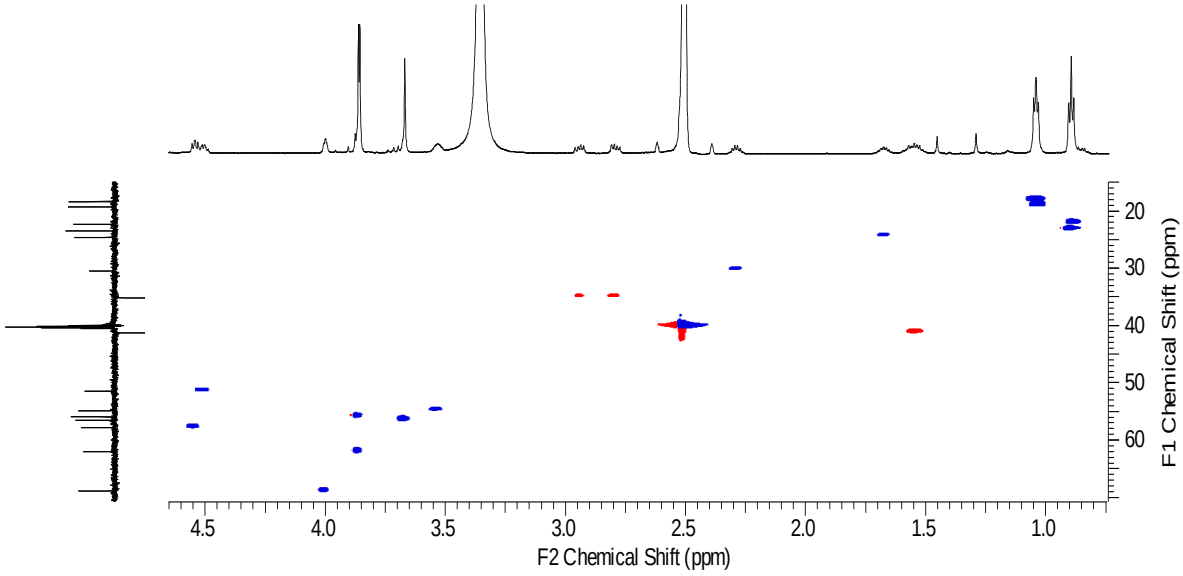

Figure 4.19. Expansion of HSQC spectrum having DEPT 135 on Y-axis

Towards the aromatic region the signal for the alkene proton of the B-ring appears at 6.33 ppm and the remaining four aryl protons of the A and C-rings are seen resonating at 6.79, 6.87, 6.97 and 6.98 ppm while the remaining five aryl protons of the AHPA residue appear as two multiplets in the region between 7.2-7.4 ppm. The most downfield signals in the ^1H NMR spectrum represent the two NHs and one NH_2 that was confirmed by the NH-COSY spectrum (figure 4.21).

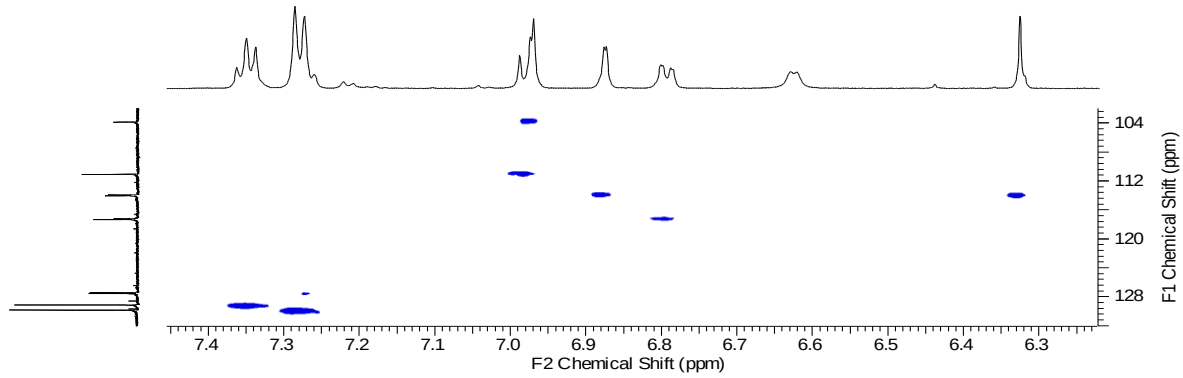

Figure 4.20. Expansion of aromatic region of HSQC spectrum of (4.11)

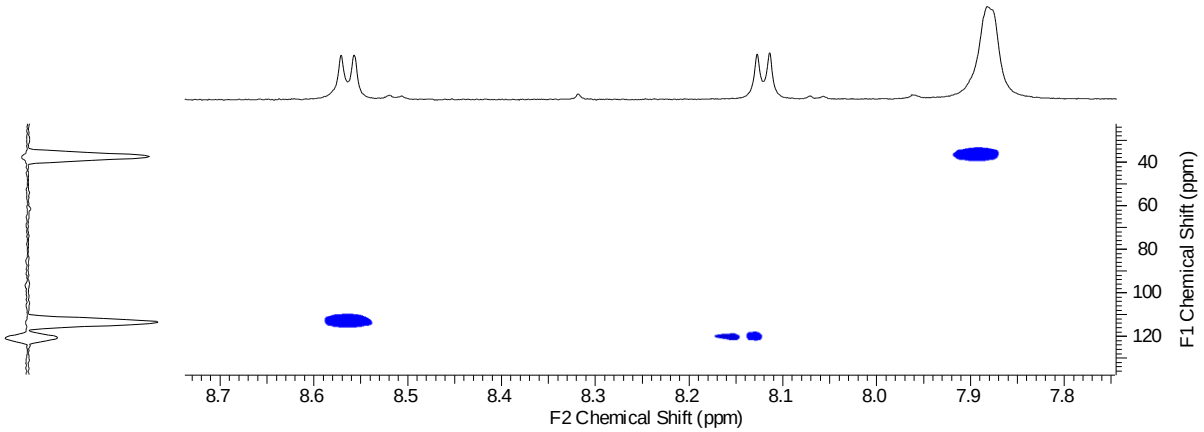

Figure 4.21. NH-COSY spectrum of (4.11)

The ^{13}C NMR spectrum along with HSQC, HMBC and DEPT 135 aided further to the structural elucidation of compound **(4.11)** and the most striking distinctive features present in the ^{13}C NMR spectrum includes the CH_3 groups of the valine (18.37 and 19.28 ppm) and leucine (22.35 and 23.48 ppm) along with the presence of three methoxy peaks (55.91, 56.53 and 62.06 ppm). The CH_2 of the leucine residue resonates at 41.31 ppm while the CH_2 of the AHPA appears at 35.16 ppm. Furthermore in the aromatic region four aryl CHs of the A and C ring and one alkene CH of the B-ring are seen resonating between (100-118 ppm) while the five aryl CH's of AHPA are found in the region between 127-130 ppm. Of the remaining signals nine quaternary aryl carbons appear in the region 117-150 ppm while the carbon of the alkene appears at 155.77 ppm. Finally in the most downfield region, the carbonyl of the B-ring resonates at 159.65 ppm while the three peaks at 169.38 (Ar-O-C=O), 170.98 (Leu-HN-C=O), 172.82 (Val-HN-C=O) represent the three carbonyls of the tripeptide.

HRMS analysis of compound **(4.11)** gave the molecular ion of mass 733.3422 ($M+H^+$).

4.1.2.2 Synthesis of control release hybrid of compound (4.11)

While we know in principle that certain "bulky" groups like benzyl and dimethylally derivatives can be tolerated on the A-ring **(2.68)** without having any major effect on tubulin polymerization inhibition activity, it is nevertheless predicted that a tripeptide at this position is likely to be too bulky to allow this hybrid presentation to bind to tubulin and inhibit tubulin polymerization in its intact form. Nevertheless, we suspect that it will be possible to cleave this phenolic ester tripeptide overtime under standard physiological conditions thus allowing for the liberation of **(2.68)**. It is envisaged that the tripeptide can

act as the molecular magnet to sequester the hybrid at the APN rich site undergoing tumor angiogenesis while sequentially allowing for hydrolysis of the intact hybrid to occur at this site. Attachment of a substrate for APN onto the C-ring to present **(2.68)** in pro-drug form while also having the APN inhibitor attached to the A-ring should in theory prevent premature hydrolysis of the substrate by APN in circulation or other aminopeptidases, thus keeping **(2.68)** in true pro-drug form while in circulation. APN and other aminopeptidases are present in lower concentrations in blood. Neutral amino acids like leucine and alanine are preferred substrates for APN. APN catalyzes the removal of neutral amino acids from the *N*-terminus of peptides. The cleavage of the leucine residue from the aniline functionality of **(2.16)** by APN has previously been demonstrated by Breen [165] in her studies on prodrugs.

We began the synthesis of controlled release hybrid with the coupling of *N*-Boc-leucine on to aniline **(2.66)** using bromotripyrrolidinophosphonium hexafluorophosphate **(**PyBroP) as coupling reagent, *N*,*N*-diisopropylethylamine (DIPEA) as base and dry DCM as solvent at 0 °C (Scheme 4.10). Upon completion the reaction was quenched with 1 M aq. HCl and extracted with DCM. After drying the organic layer with Na_2SO_4, it was evaporated under reduced pressure and the resulting residue was purified by flash column chromatography to afford **(4.12)**. The confirmation of the coupling reaction was achieved due to the presence of a peak for *N*-Boc group at 1.50 ppm as well as two CH_3 groups at1.00 ppm for the leucine side chain in the ^1H NMR spectrum (figure 4.22). Moreover the HRMS data also confirmed the structure by detecting the protonated molecular ion of mass 647.2943 (M + H^+).

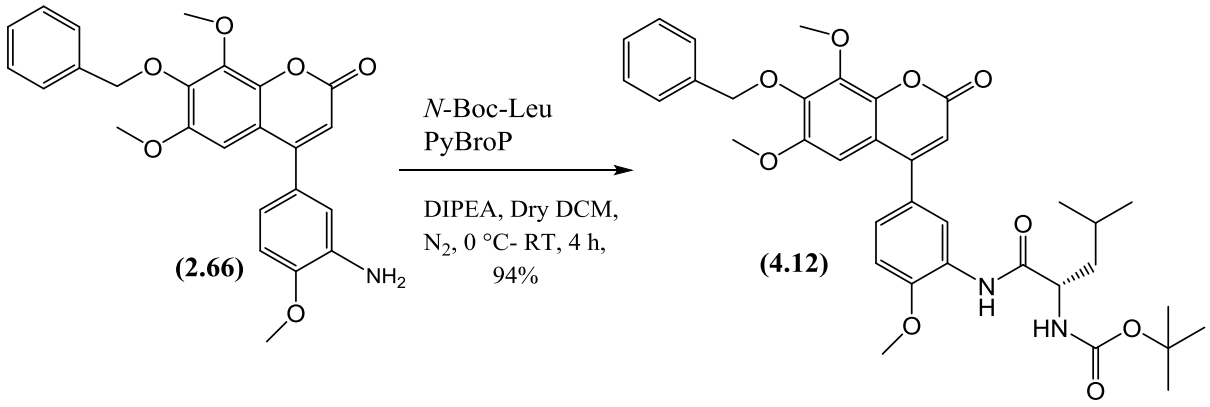

Scheme 4.10. Coupling of Boc leucine on to aniline **(2.66)**

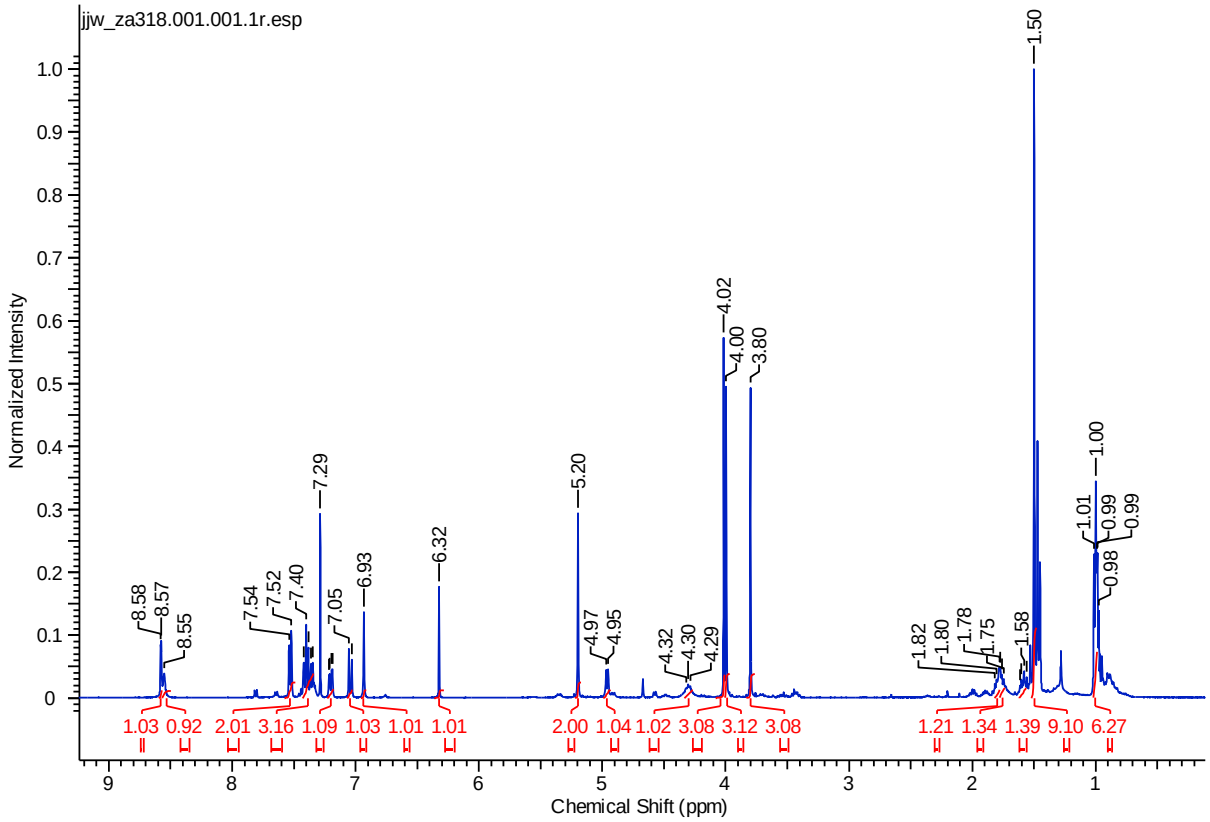

Figure 4.22. ^{1}H NMR spectrum of compound (4.12)

In order to introduce the ester linked tripeptide onto **(4.12)**, the benzyl protecting group was removed by hydrogenolysis using 10% Pd/C (10% by weight) in DCM and methanol (scheme 4.11). The deprotection was confirmed by the ^{1}H NMR analysis of the phenol **(4.13)** (figure 4.23) due to the disappearance of CH_2 and 5 aryl protons of the benzyl protecting group and by the appearance of the broad phenolic signal at 6.12 ppm.

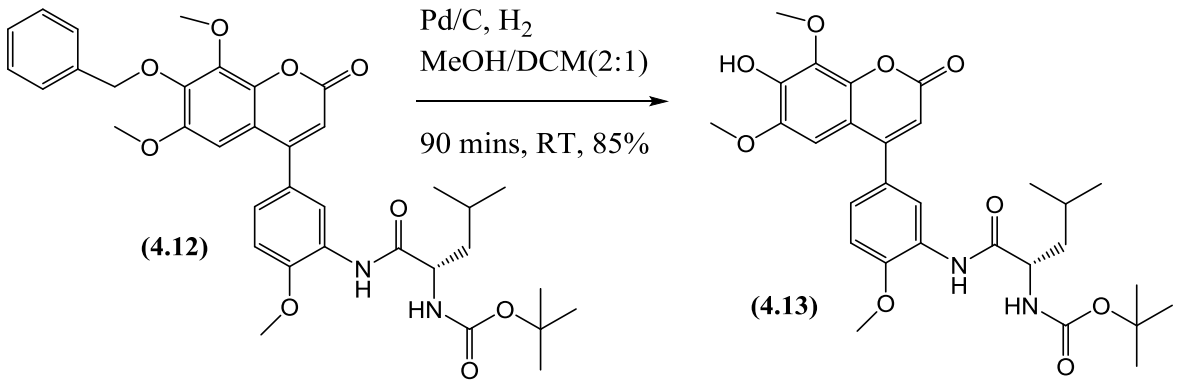

Scheme 4.11. Hydrogenolysis of compound **(4.12)**

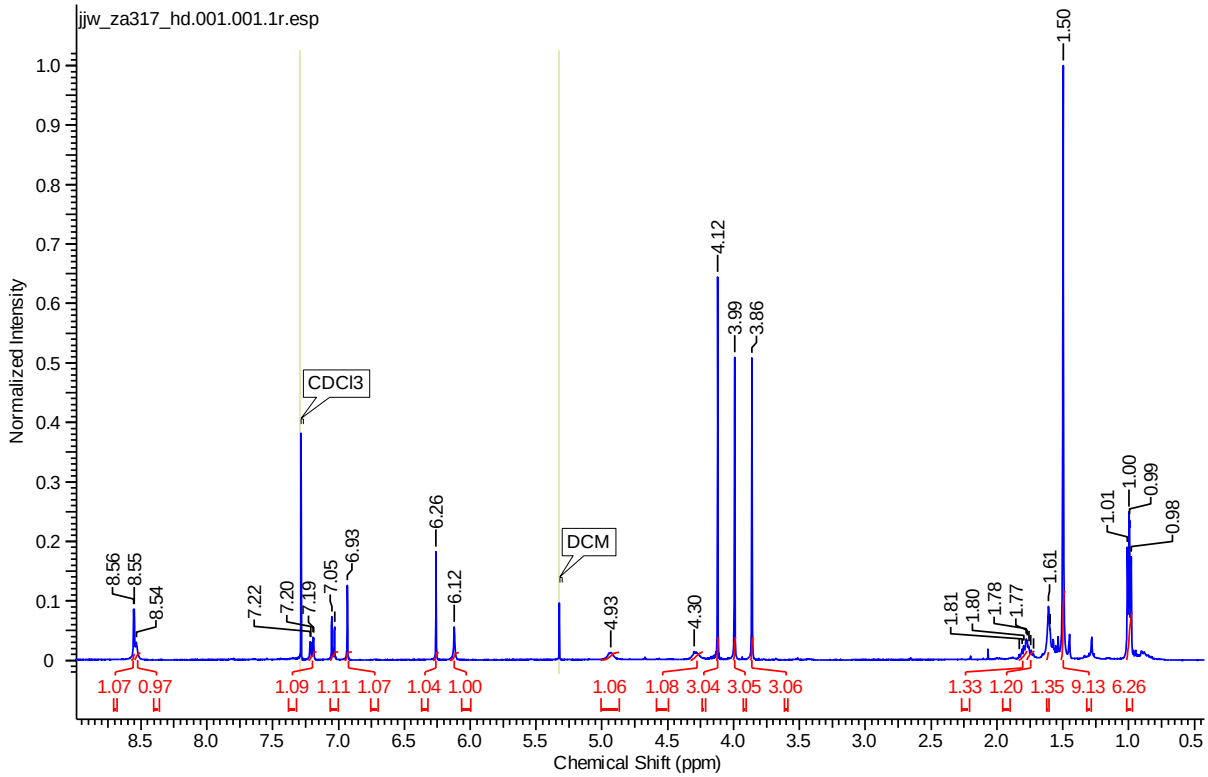

Figure 4.23. ^{1}H NMR spectrum of phenol (4.13)

The deprotection of the benzyl protecting group was followed by EDC coupling of *N*-Cbz valine in dry DCM under anhydrous conditions (scheme 4.12). After aqueous work-up and extraction with DCM, the organic layer was dried, reduced in volume and purified by flash column chromatography to give **(4.14)**. Its structural identity was confirmed through NMR spectroscopy. The additional characteristic features in the ^{1}H NMR spectrum of compound **(4.14)** (figure 4.24) as compared to phenol **(4.13)** includes the presence of two extra CH_3 groups of valine in the aliphatic region, CH_2 (5.18 ppm) and five extra aryl protons (7.40 ppm) of the Cbz protecting group.

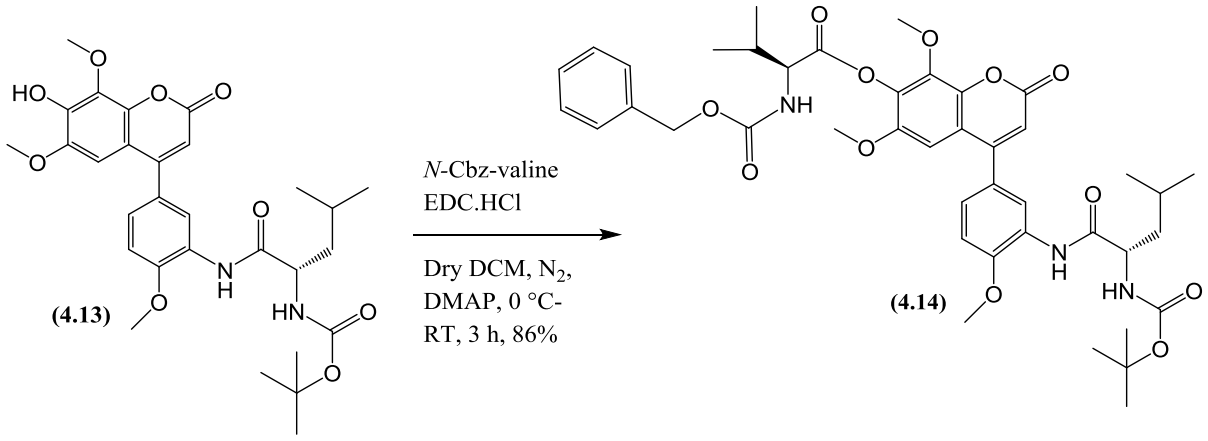

Scheme 4.12. EDC coupling of Cbz valine

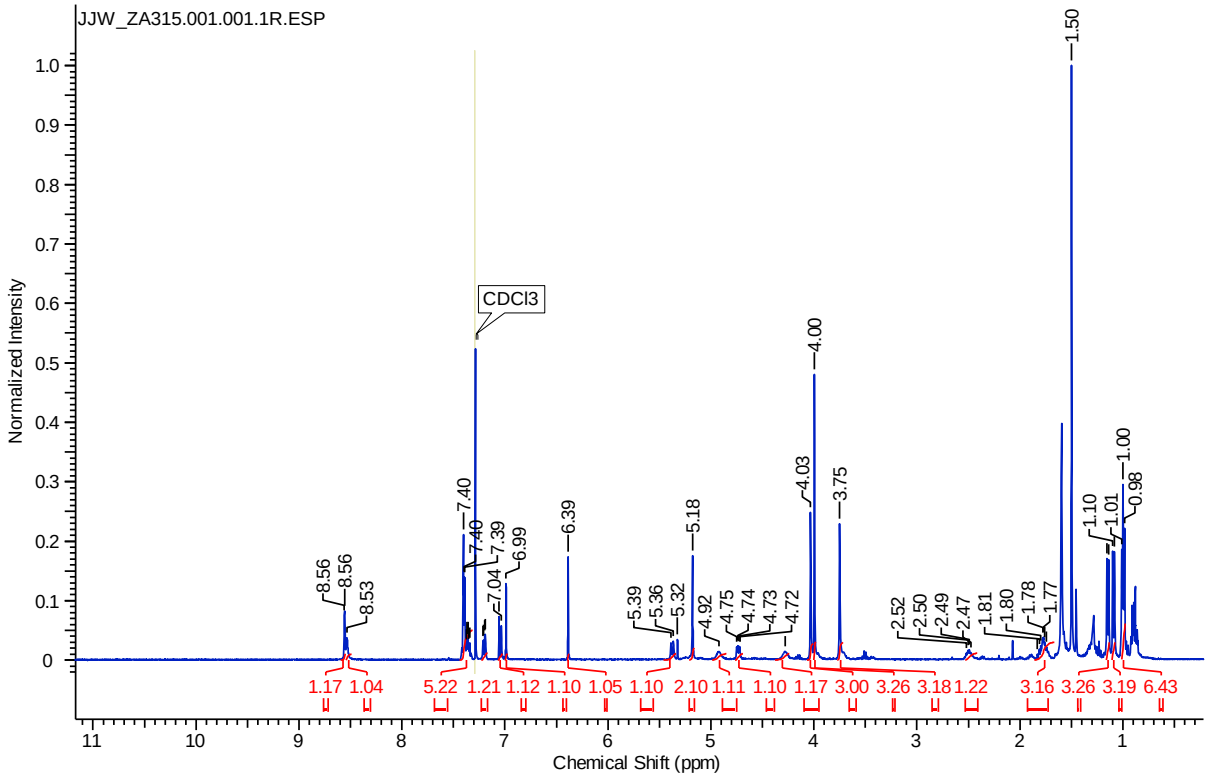

Figure 4.24. ^{1}H NMR spectrum of compound (4.14)

Deprotection of the Cbz group and coupling of PFP ester of bestatin was carried out in a single step by stirring the carbamate compound **(4.14)** with pentafluorophenyl ester of bestatin **(4.02)** in the presence of 10% Pd/C using ethanol and ethyl acetate (1:1) under the atmosphere of hydrogen (scheme 4.13). Synthesis of the desired compound **(4.15)** was confirmed by the analysis of its ^{1}H NMR spectrum (figure 4.25) where the presence of distinctive signals including the two Boc groups at 1.41 and 1.49 ppm, 3 methoxy groups and six CH_3 groups (four leucine and two valine) are clearly evident.

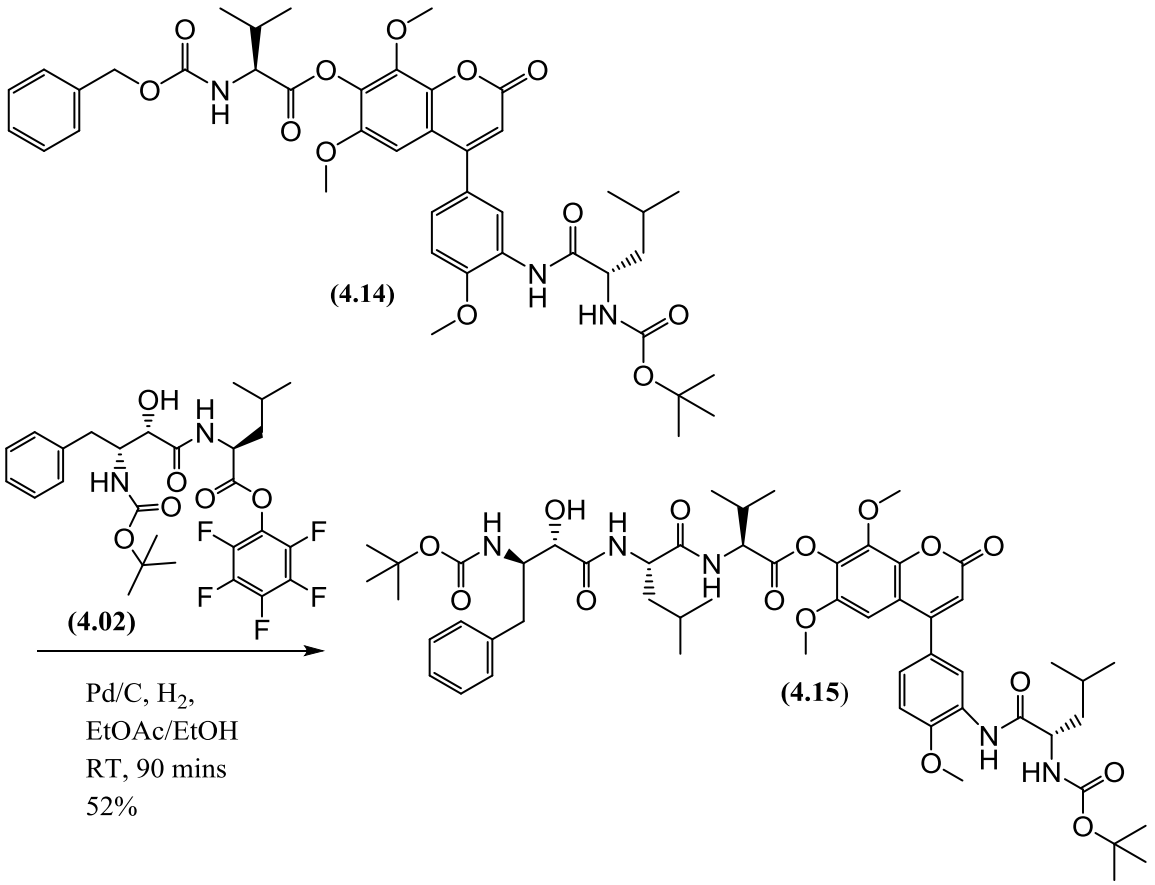

Scheme 4.13. One pot deprotection and coupling of bestatin.

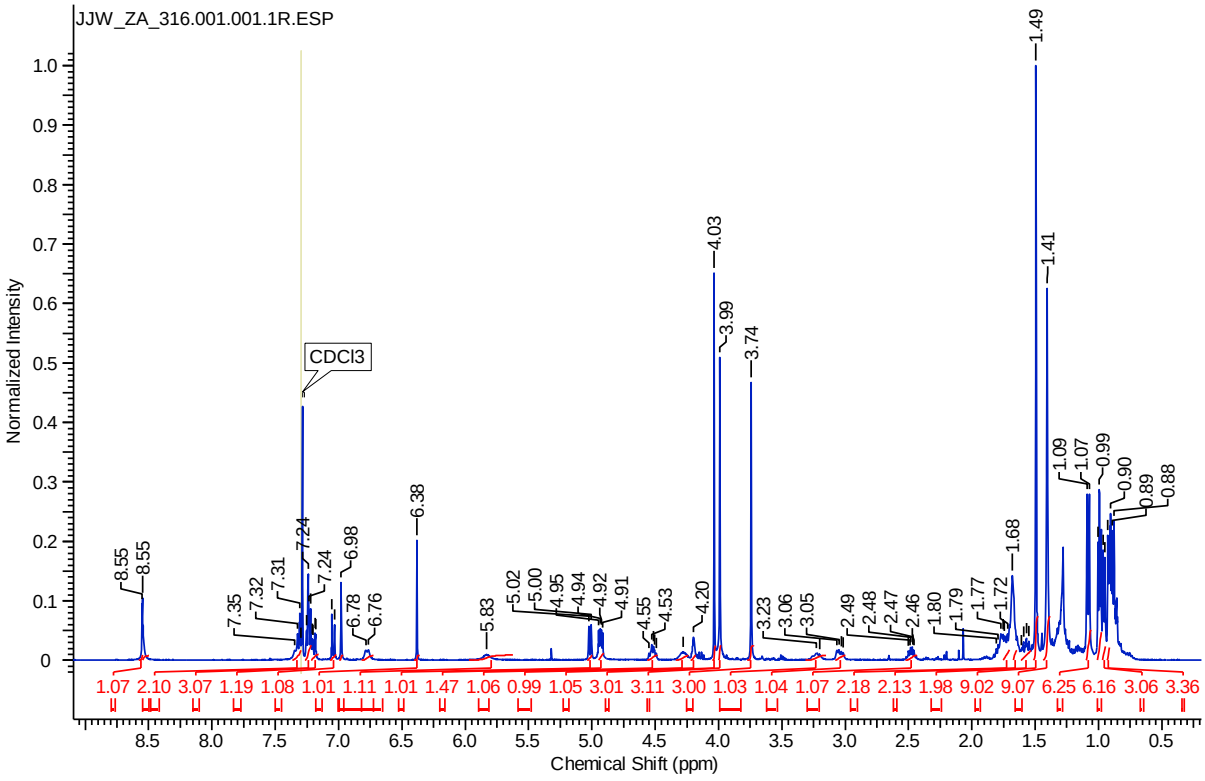

Figure 4.25. ^{1}H NMR spectrum of compound (4.15)

Again in the final step deprotection of the two Boc groups was carried out using cooled 25% TFA in DCM at -10 °C (scheme 4.14). After 90 minutes the reaction mixture was diluted with DCM and solvent was evaporated at 35 °C under reduced pressure to afford the final control release hybrid **(4.16)** as TFA salt with a yield of 98%.

.

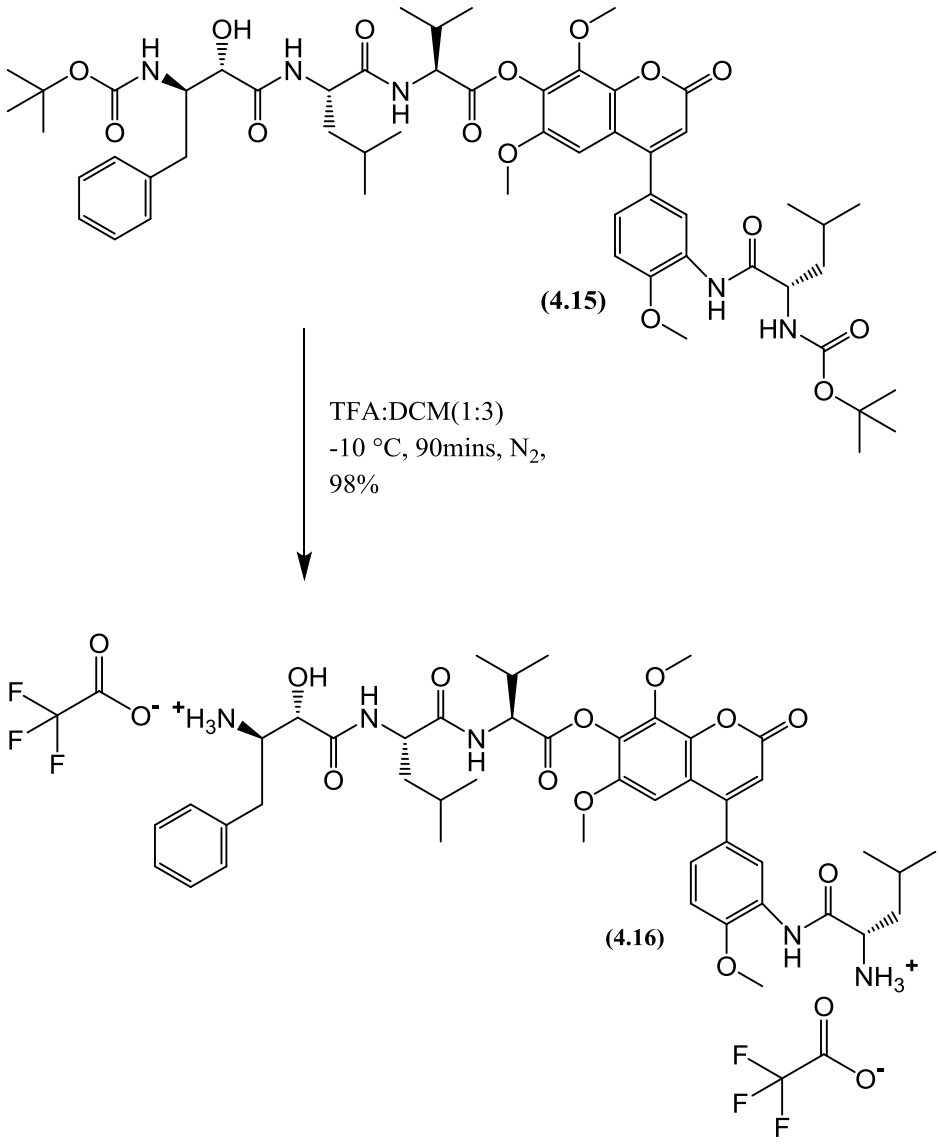

Scheme 4.14. Removal of Boc groups

4.1.2.3 Structure elucidation of compound (4.16)

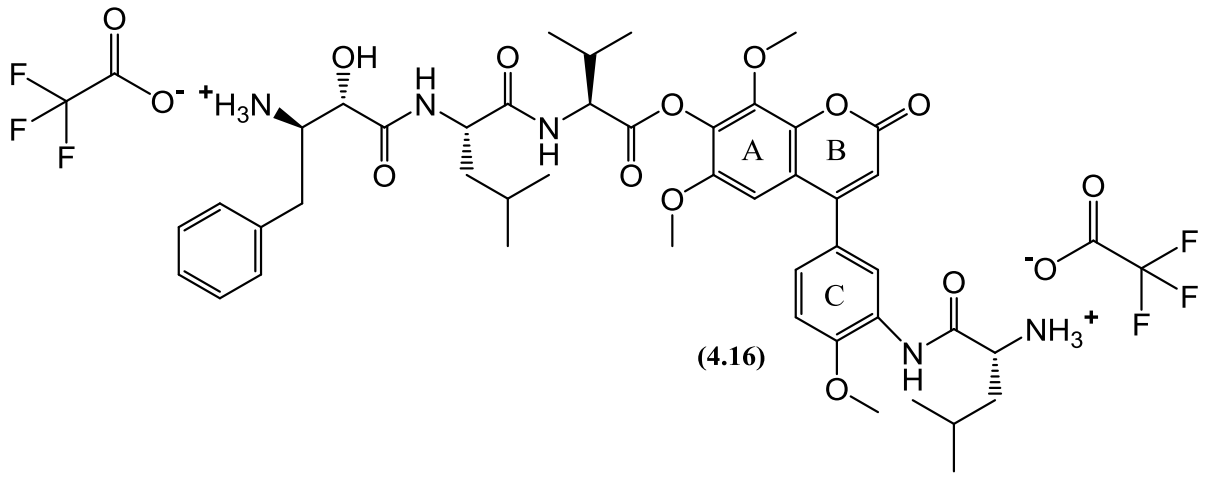

Confirmation of the structure of (**4.16)** was mainly by NMR and mass spectroscopy. The ^{1}H NMR spectrum (figure 4.26) shows the presence of all 59 protons while the ^{13}C spectrum (figure 4.30) represents a total carbon count of 45.

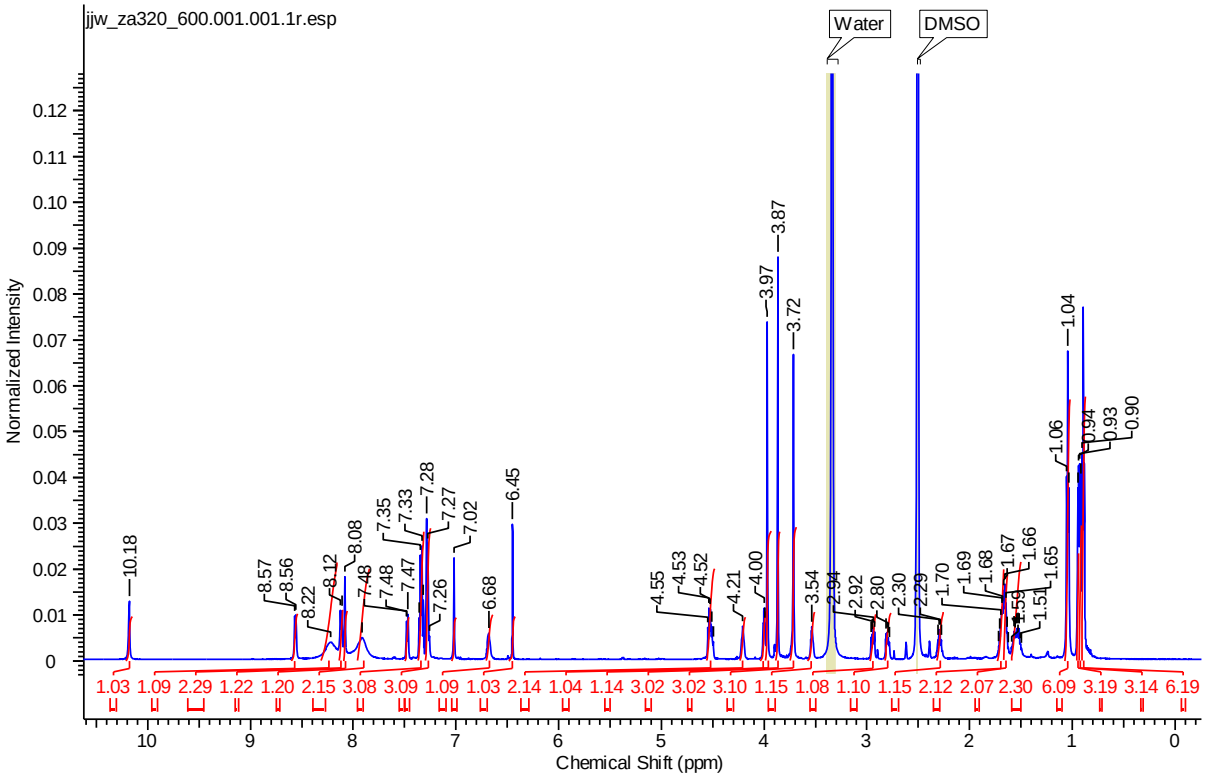

Figure 4.26. ^{1}H NMR spectrum of compound (4.16)

The most upfield signals in the expanded ^{1}H NMR spectrum (figure 4.27) from 0.5-1.2 ppm represent the four CH_3 groups of leucine and two CH_3 groups of valine. The DEPT 135 spectrum (figure 4.28) confirm the presence of three CH_2 groups and among them two

methylene groups of two leucine residues are found resonating as multiplets at 1.54 and 1.66 ppm while the signal for the CH_2 of AHPA splits into two and appear as two double doublets at 2.80 and 2.94 ppm. The ^{1}H NMR spectrum also confirmed the presence of three methoxy peaks (3.72, 3.87 and 3.97 ppm), two CHs attached to NH (4.51 and 4.53 ppm) and two CHs attached to NH_2 (4.21 and 3.54 ppm).

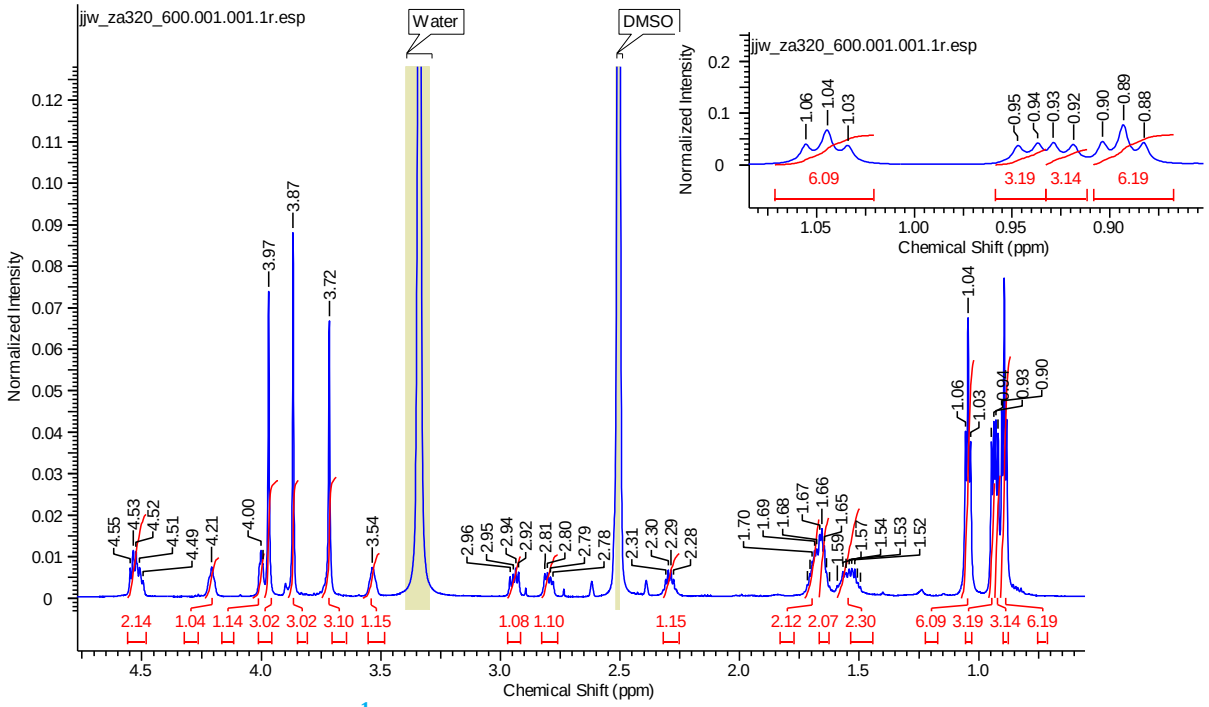

Figure 4.27. Expansion of ^{1}H NMR spectrum of compound (4.16)

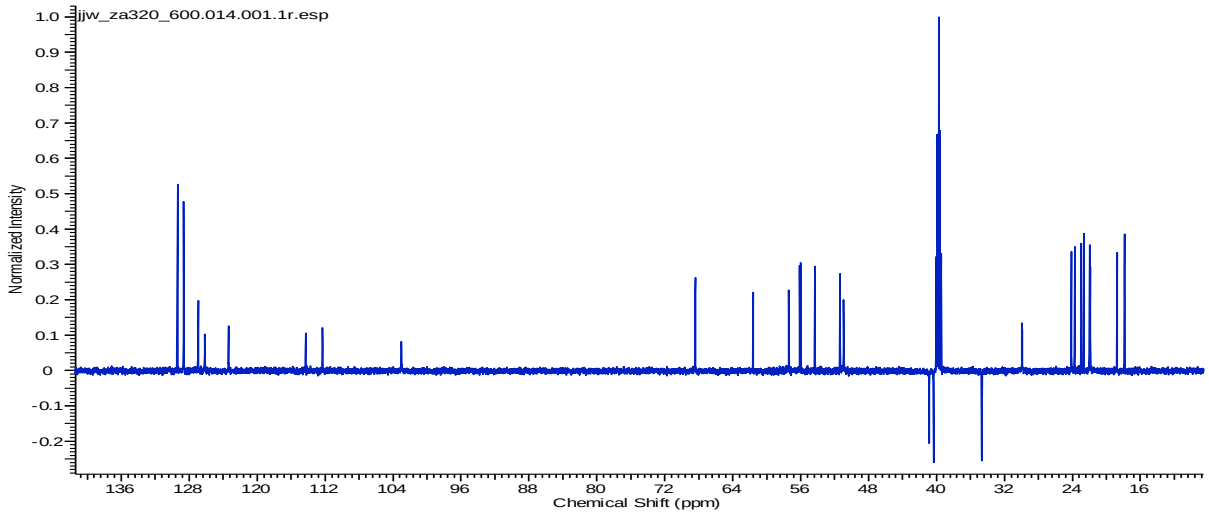

Figure 4.28. DEPT 135 spectrum of compound (4.16)

In the aromatic region of the expanded ^{1}H NMR spectrum (figure 4.29) the alkene CH of the B-ring appears at 6.45 ppm and the four aryl CHs of the A and B ring resonates at 7.02, 7.32, 7.47 and 8.08 ppm while the five aryl protons of AHPA residue appear as two

multiplets at 7.28 and 7.35 ppm. Among the other remaining signals the two NH_2 protons resonate at 7.91 and 8.22 ppm while the three NH proton signals are present at 8.12, 8.56 and 10.18 ppm

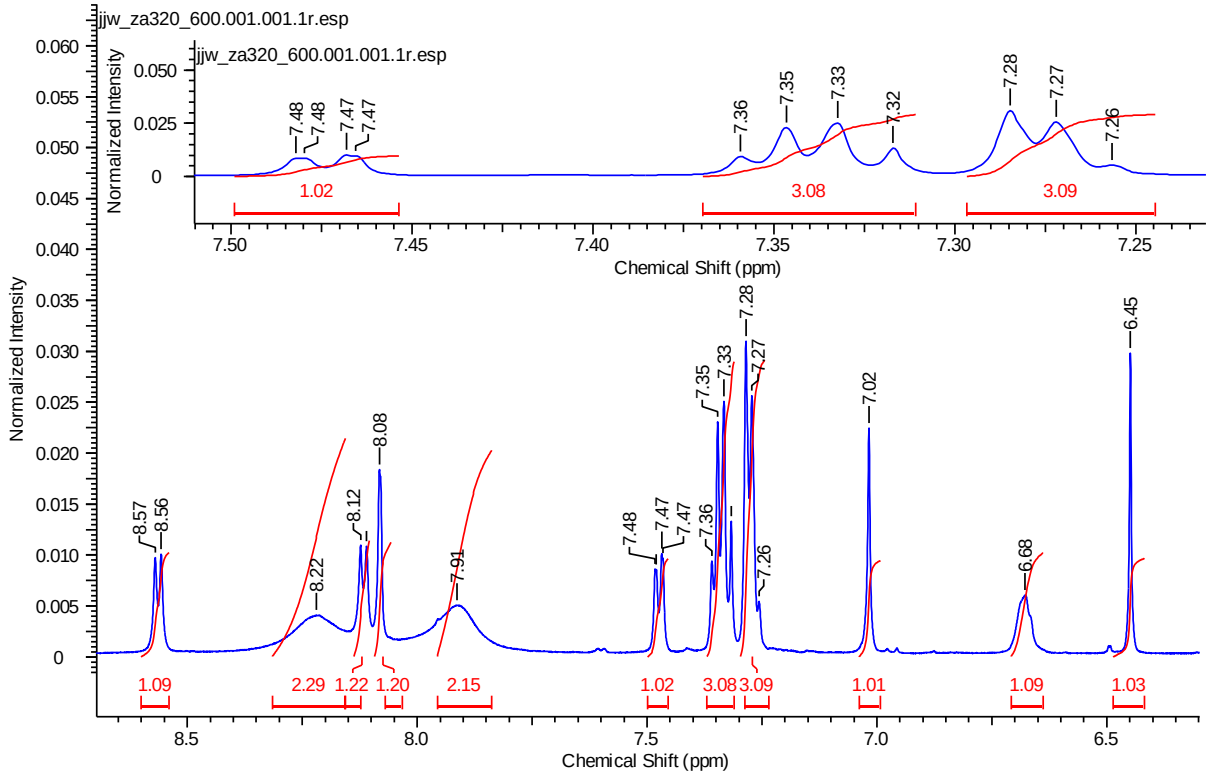

Figure 4.29. Expansion of ^{1}H NMR spectrum of compound (4.16)

The ^{13}C spectrum (figure 4.30), along with HSQC and HMBC spectra aided in elucidating the structure of the controlled release hybrid **(4.16)**. The three methoxy peaks are found resonating at 55.99, 56.12 and 61.61 ppm, while the DEPT 135 shows three CH_2 protons at 34.67, 40.35 and 40.86 ppm. The signals for the CH_3 groups of two leucine residues appears at 21.89, 21.99, 22.66 and 22.97 ppm while the CH_3 protons of the valine resonates at 17.86 and 18.76 ppm.

In the aromatic region of the ^{13}C spectrum the signals for four aromatic CHs of A and C rings are identified at 103.01, 112.29, 123.36 and 126.17 ppm while the C=CH signal is at 114.30 ppm. Five aryl CHs of the AHPA are also present in the aryl region and appear as one CH at 126.95, two at 128.64 and two at 129.37 ppm. Out of ten quaternary carbons identified in the region between 113-154 ppm, nine represent aromatic quaternary carbons while one represent the carbon attached to alkene. Of the remaining signals the carbonyl of the B-ring was found resonating at 159.04 ppm while the remaining four carbonyls were found at 168.77, 168.95, 170.49 and 172.36 ppm.

Final confirmation of the compound was received by HRMS analysis that detected the protonated molecular ion of mass 846.4283 ($M+H^+$).

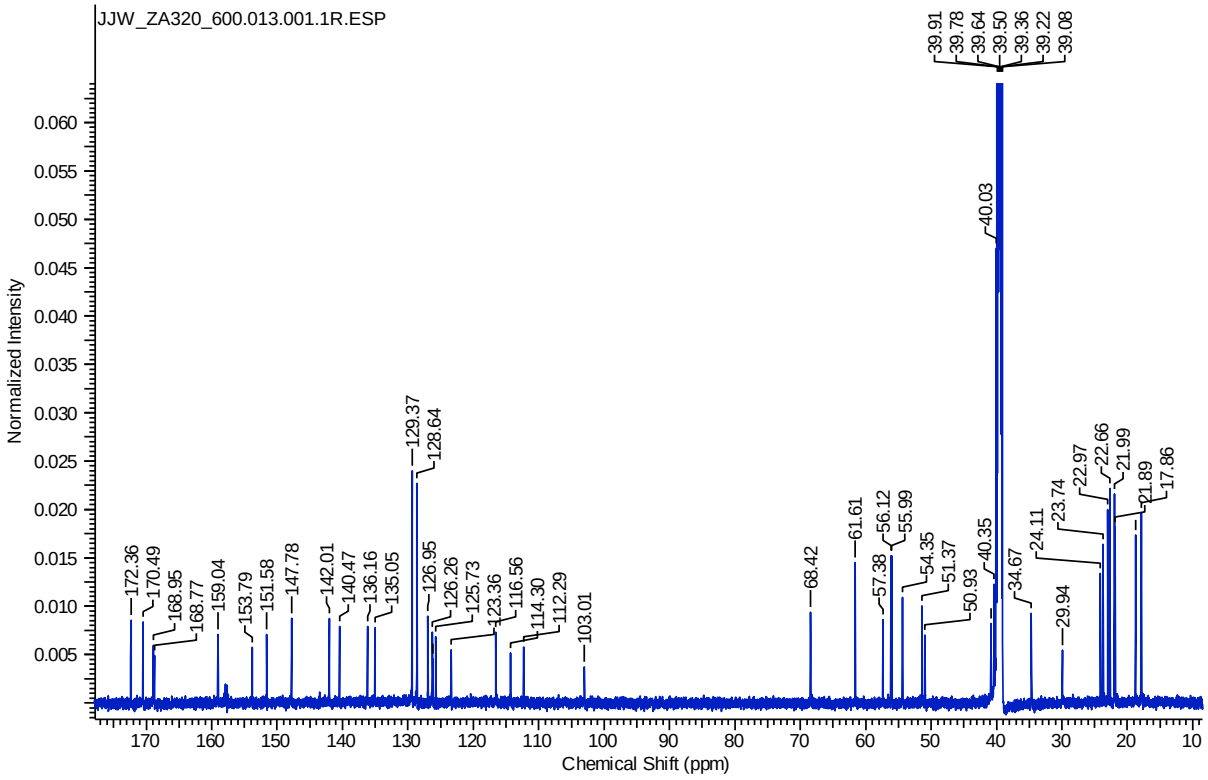

Figure 4.30. ^{13}C NMR spectrum of compound (4.16)

4.1.3 Synthesis of peptide based hybrid of phenstatin compound (3.04)

This section deals with the synthesis of a hybrid based on the phenstatin derivative **(3.04)**. The essential difference here is the loading of two tripeptide moieties onto the tubulin inhibitor **(3.04)**. The design of the phenstatin compounds that are the subject of this work was solely focused on optimizing the number of possible linker units onto their structure. In this way the optimal peptide ratio to tubulin moiety could be discerned. Also it is envisaged as before that this design will also allow for the peptide moieties to remain active while attached onto the tubulin binding unit. Moreover, it is predicted that the release of the tubulin unit from these peptides can be controlled when the pH of the formulation is carefully controlled.

The synthetic sequence involved EDC coupling of Cbz valine onto the "di-phenolic" benzophenone **(3.04)** in dry DCM under anhydrous conditions at 0 °C (scheme 4.15). Due to the presence of two reactive phenolic groups, three equivalents of Cbz valine were used

and upon completion, the reaction mixture was diluted with DCM and washed with water. After drying and evaporating the organic layer, the residue was purified by flash column chromatography to afford **(4.17)** in 94% yield. The structural confirmation of the purified product was achieved through the inspection of its ^{1}H NMR spectrum (figure 4.31) that clearly shows the presence of four CH_3 groups of the two valine residues at 0.5-1.2 ppm. Moreover the presence of three methoxy groups (3.5-4.0 ppm), three CH_2 (5.15 ppm) and fifteen aryl protons of the three benzyl groups confirms the identity of **(4.17)**.

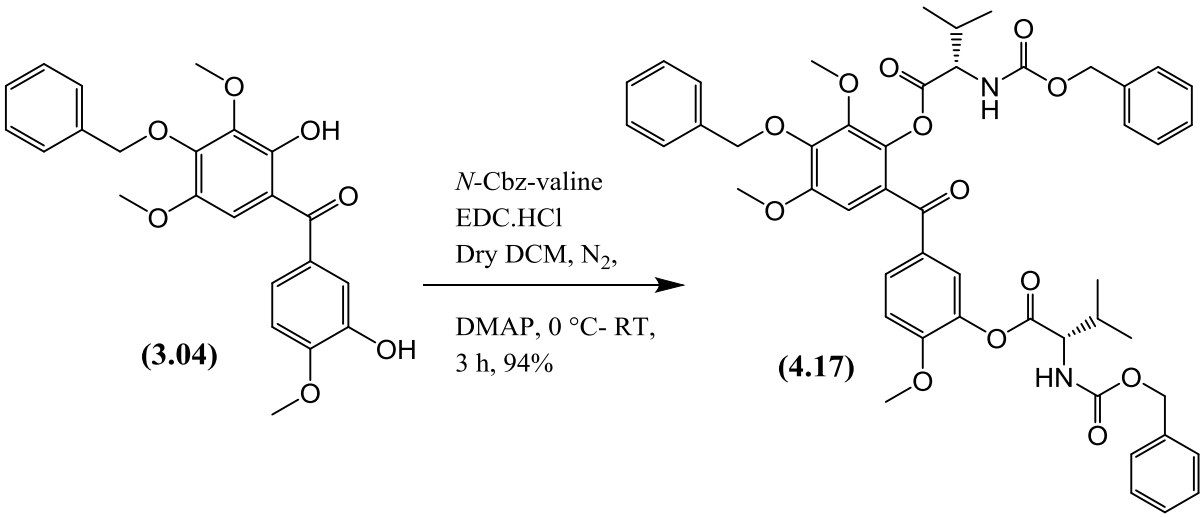

Scheme 4.15. EDC coupling of Cbz valine on to compound **(3.04)**

\

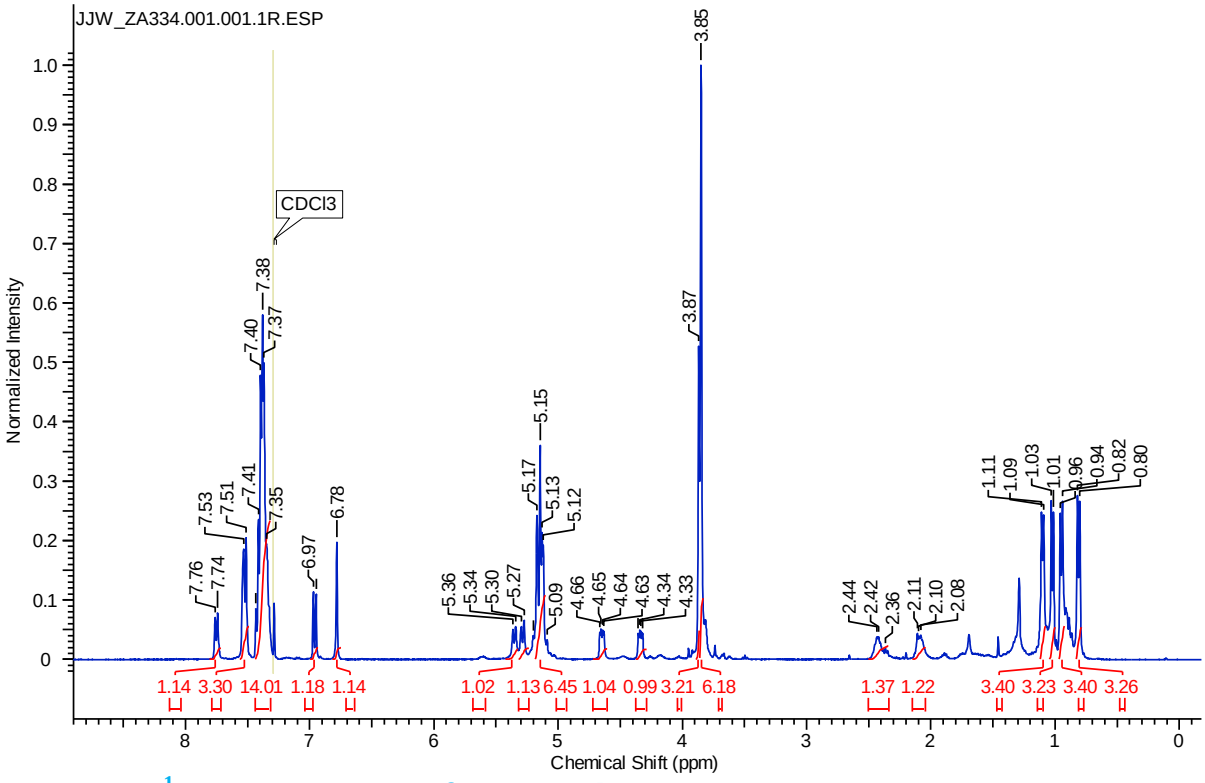

Figure 4.31.^{1}H NMR spectrum of compound (4.17)

Removal of benzyl groups and coupling of the PFP ester of *N*-BOC bestatin **(4.02)** was performed utilizing the same reaction conditions employed in the synthesis of compound **(4.15)**, however, as required, the quantity of the PFP ester **(4.02)** was doubled due to the present of two reactive amine functionalities of two valine amino acid residues (scheme 4.16). After the reaction duration of 90 minutes, the product was passed through a cotton wool plug to remove palladium and carbon, the resulting filtrate was concentrated under reduced pressure to afford a residue which was purified by flash column chromatography to give **(4.18)**. The structural confirmation was achieved through HRMS and NMR spectroscopy. HRMS analysis found the protonated molecular ion of mass 1299.6625 ($M+H^+$), while the ^1H NMR spectrum (figure 4.32) shows the presence of characteristic peaks including the presence of the two Boc groups at 1.28 and 1.29 ppm and eight CH_3 groups (0.5-1.02 ppm) corresponding to two leucine and two valine residues. Furthermore the presence of three methoxy groups (3.70, 3.77 and 3.85 ppm) and 10 extra aryl protons of the two phenyl rings of AHPA are also evident in the spectrum.

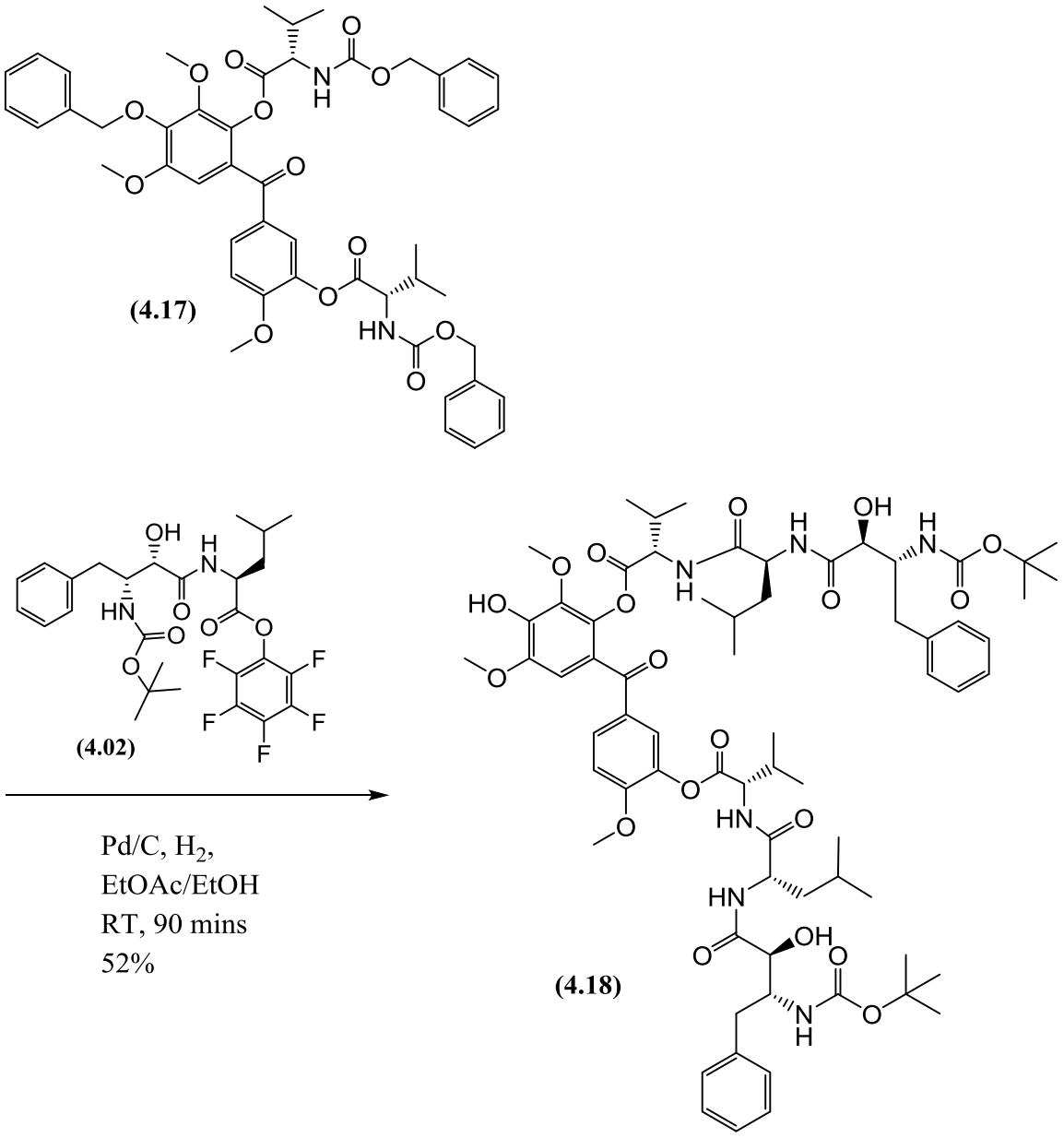

Scheme 4.16. Debenzylation and coupling of PFP ester **(4.02)**

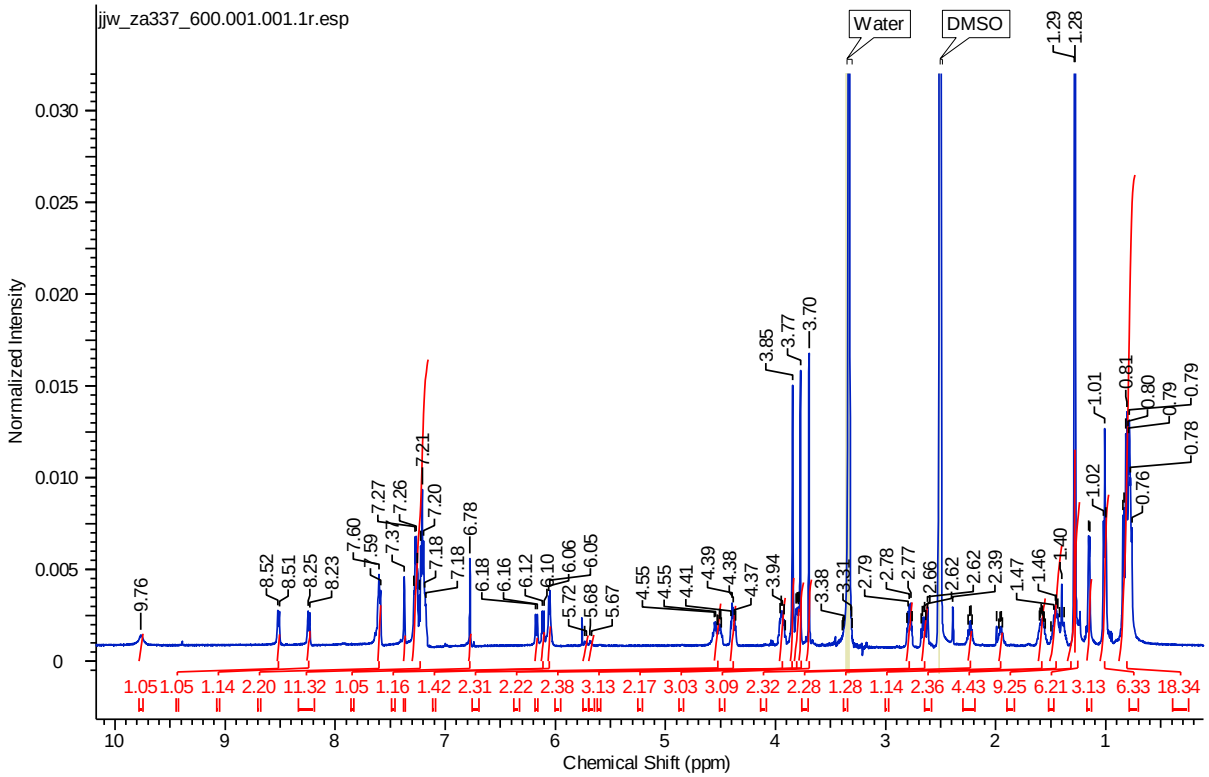

Figure 4.32. ^{1}H NMR spectrum of compound (4.18)

In the final step, the two Boc groups were removed with TFA:DCM (1:3) to obtain the hybrid compound **(4.19)** with two tri-peptides chains (scheme 4.17). The generation of the product was confirmed by HRMS, which detected the protonated molecular ion of mass 1099.5616 ($M+H^{+}$) while the ^{1}H NMR spectrum (figure 4.33) also aided to the confirmation of the structure by the disappearance of signals for two Boc protecting groups at 1.28 and 1.29 ppm.

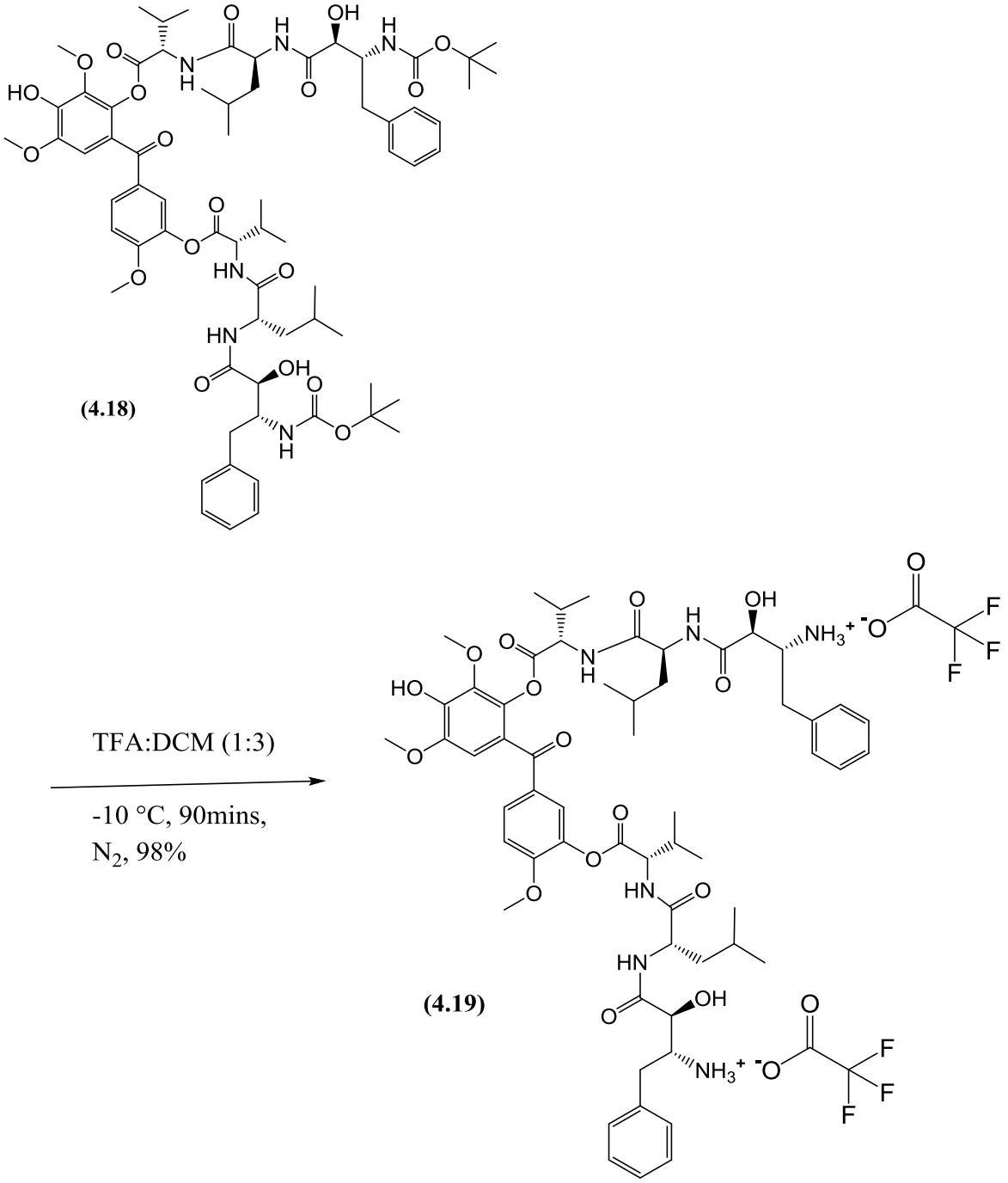

Scheme 4.17. Removal of Boc protecting groups to give final compound **(4.19)**

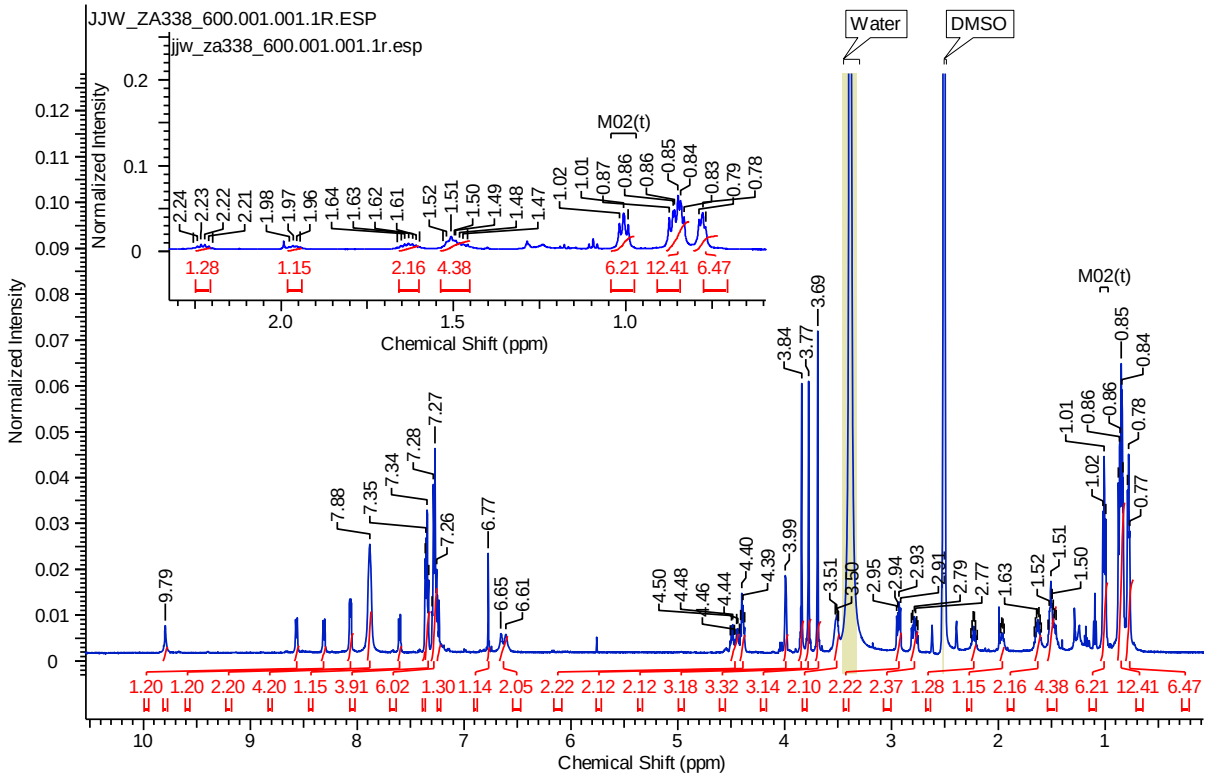

Figure 4.33. ^{1}H NMR spectrum of compound (4.19)

4.1.4 Synthesis of peptide based hybrid with amide linkage

After the successful synthesis of different phenolic ester-linked hybrids we decided to utilize the aniline functionality on the C-ring of compound **(2.16)** to synthesize hybrids with a more robust linkage. The more robust linker unit would require sequential removal of the amino acids from the tripeptide to allow the tubulin component to become active. As previous attempts within the group to couple bestatin directly to the aniline functional group ended with failure it was decided to employ a stepwise approach. In the first step, aniline **(2.16)** was coupled to Boc-leucine using PyBroP as coupling reagent and DIPEA as base in dry DCM at 0 °C. Upon completion, an aqueous/organic work-up and purification by flash column chromatography afforded the *N*-Boc-leucine coupled product **(4.20)** with a yield of 66%. The *N*-Boc protecting group of (**4.20)** was then removed using 25% TFA in dry DCM under an atmosphere of nitrogen to afford **(4.21)** (scheme 4.18).

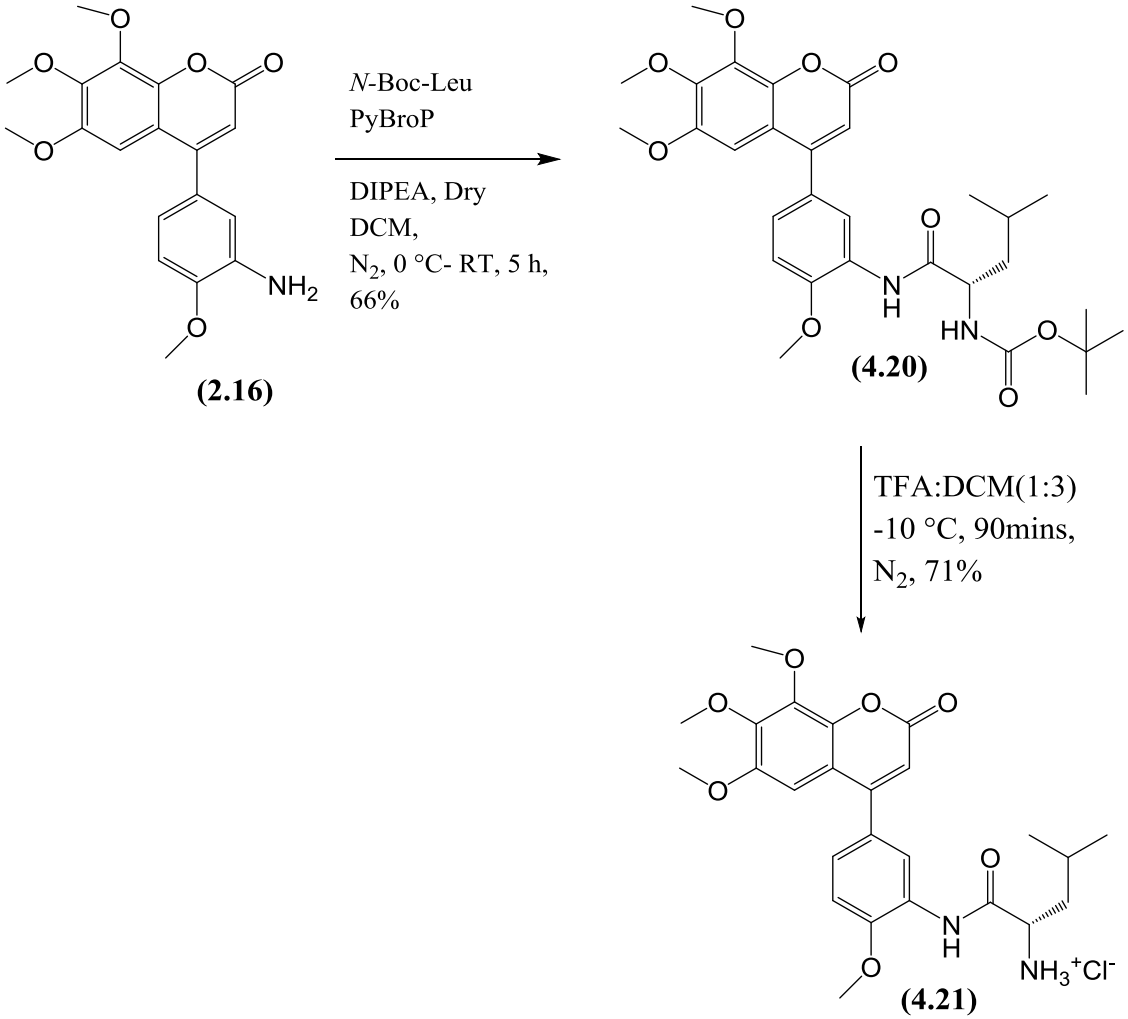

Scheme 4.18. Boc leucine coupling followed by subsequent deprotection of Boc group

Before **(4.21)** could be coupled to (2S,3R)-3-Amino-2-hydroxy-4-phenylbutyric acid (AHPA) it was necessary to protect the free amine of AHPA using di-*tert*-butyldicarbonate and potassium carbonate, as base, in a solution consisting of methanol, THF and water. Next the carboxylic acid group of the compound **(4.23)** was activated by converting it into its corresponding pentafluorophenyl ester **(4.24)**, using EDC coupling with pentafluorophenol (scheme 4.19).

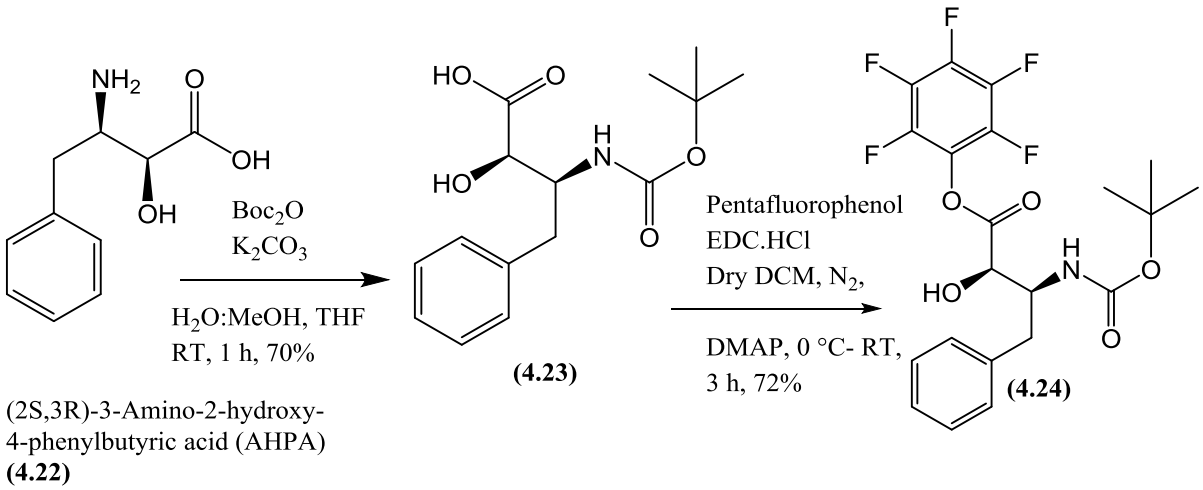

Scheme 4.19. *N*-Boc protection of AHPA and subsequent activation of carboxylic group

The PFP ester **(4.24)** was directly reacted with the free amine **(4.21)**, using diisopropylethyl amine as base under anhydrous conditions at 0 °C (scheme 4.20). Upon completion the reaction was concentrated under reduced pressure at 35 °C and the remainder was purified by flash column chromatography to afford the compound **(4.25)**.

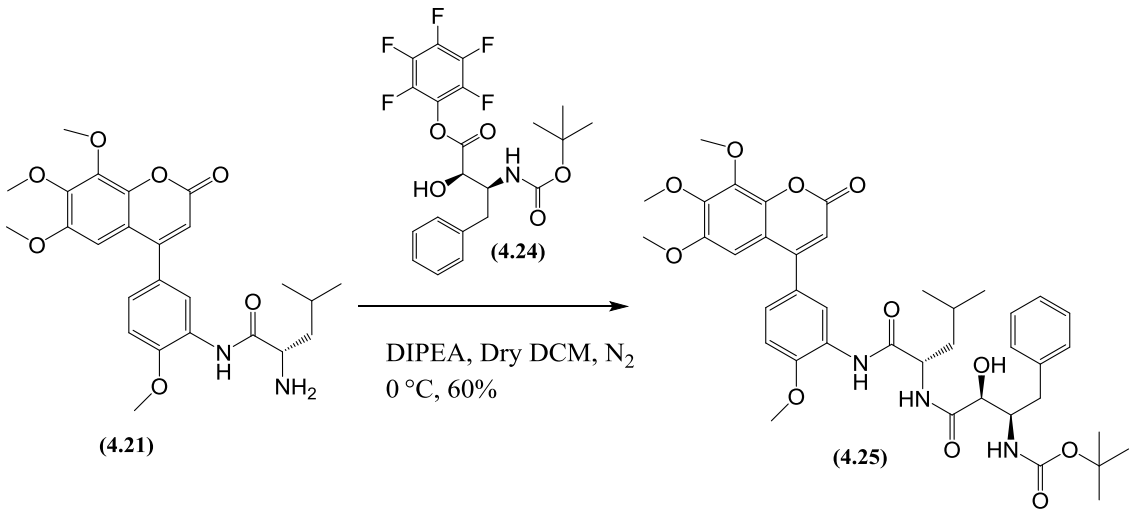

Scheme 4.20. Coupling of PFP ester **(4.24)** onto compound **(4.21)**

Once again the removal of the *N*-Boc group from compound **(4.25)** was carried out using with 25% TFA in dry DCM (scheme 4.21). Upon completion, the reaction mixture was diluted with DCM and solvent evaporated using the rotary evaporator at 35 °C. The resultant TFA salt was re-dissolved in DCM and stirred with 5% aqueous $NaHCO_3$ to give free amine **(4.26)**. HRMS analysis confirmed the synthesis of the **(4.26)** with the molecular ion of mass 648.2904 corresponding to the ($M+H^+$). Further confirmation was received by

the inspection of its ^{1}H NMR spectrum (figure 4.34) where the presence of distinct features including two CH_3 groups of leucine (0.96-1.00 ppm), four methoxy groups (3.77, 3.94, 4.01 and 4.05 ppm) and five extra aryl protons of AHPA (7.22 and 7.29 ppm) is evident.

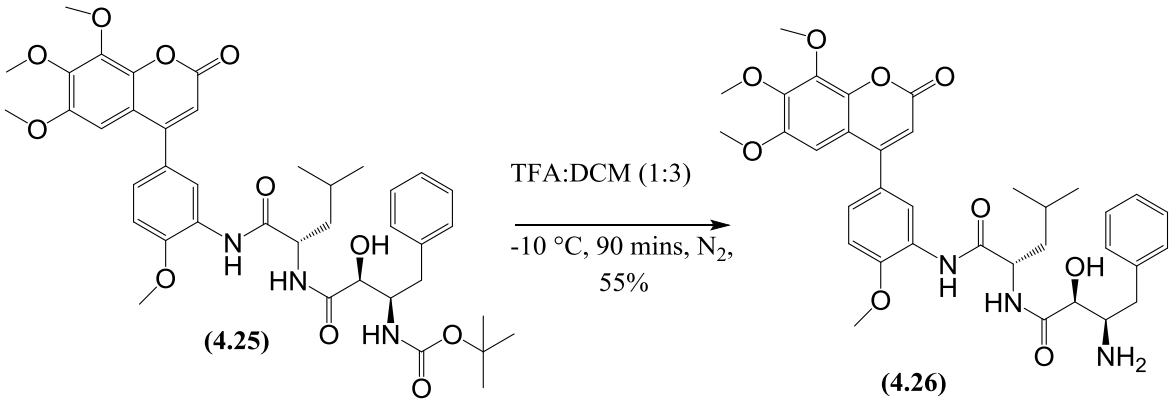

Scheme 4.21. Removal of Boc protecting group

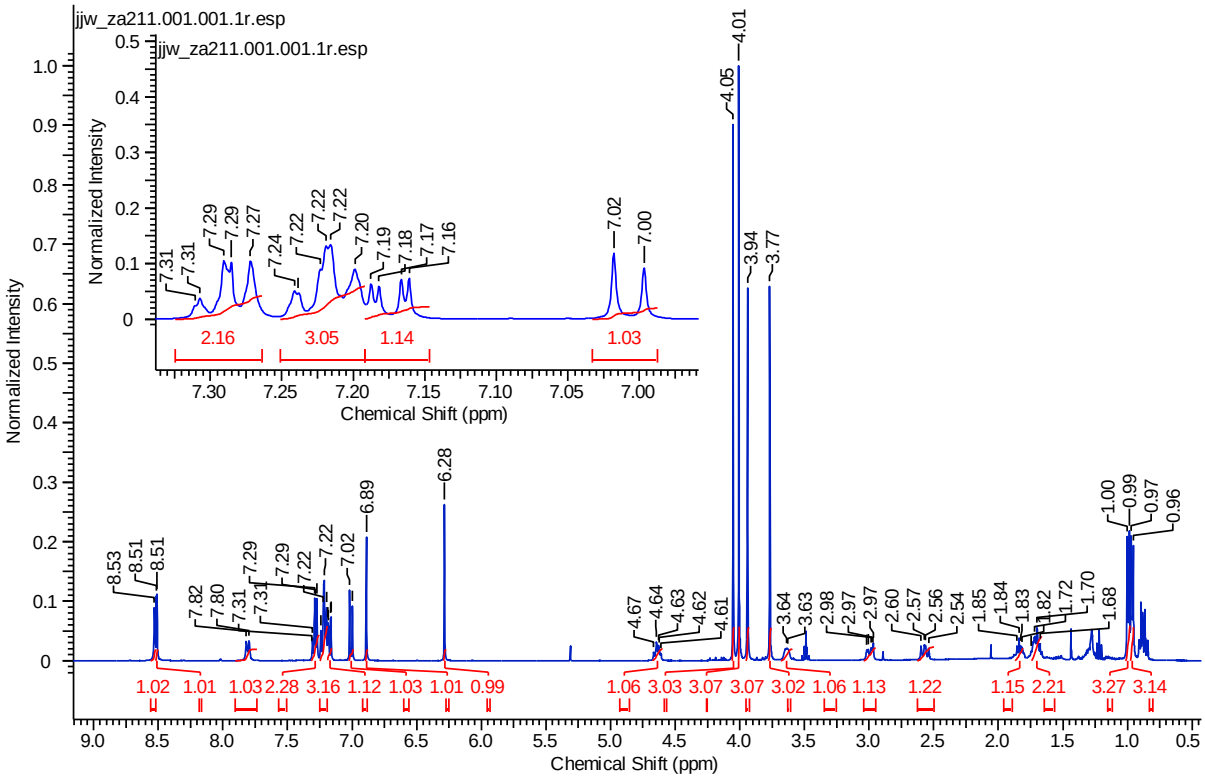

Figure 4.34. ^{1}H NMR spectrum of compound (4.26)

4.2. Synthesis of hydroxamic acid based hybrids

4.2.1 Synthesis of aniline hydroxamic acid-based hybrid

Previous studies conducted by our lab group have shown that hydroxamic acid-based derivatives of our tubulin-binding agents exhibit inhibition of APN as well as tubulin binding activity. As the thione derivative **(2.17)** is susceptible to attack by amine based nucleophiles the purpose of this study was to utilize this fact to prepare an analogous series of hybrids of our 4-phenylcoumarin series of tubulin binding agents. As we were able to introduce the simple oxime functionality onto the B-ring of **(2.17)** we decided to introduce a modified oxime functionality onto the B-ring thione **(2.17)** using the reagent o-carboxymethyl hydroxylamine *hemi*-hydrochloride as a nucleophile, with sodium acetate as a base in water/ethanol (Scheme 4.22). The reaction proceeded efficiently to give **(4.27)**.

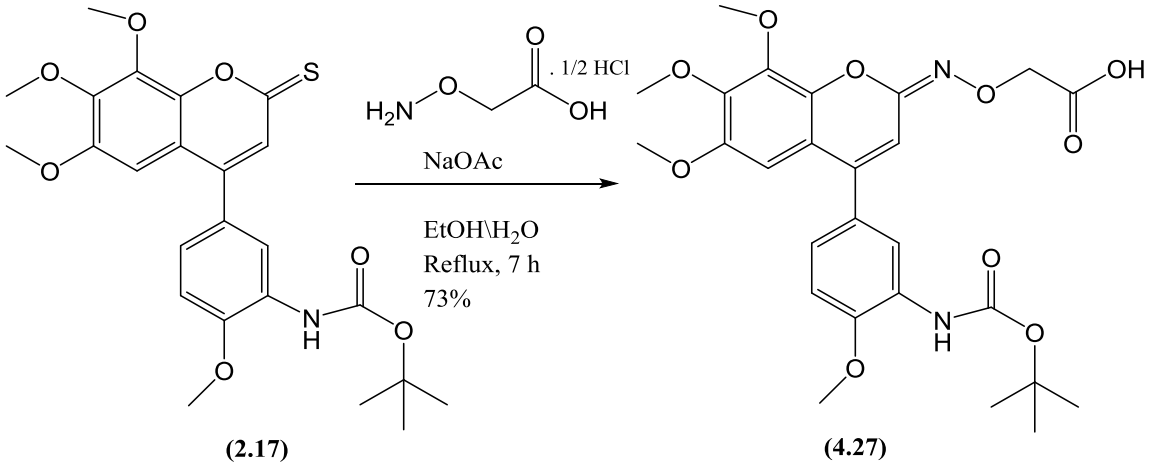

Scheme 4.22. Synthesis of oxime carboxylic acid **(4.27)**

In order to introduce hydroxamic acid functionality onto the carboxylic group of **(4.27)**, it was required to have a better leaving group instead of OH of carboxylic acid. So we decided to form *in situ* the pentafluorophenyl ester of carboxylate compound **(4.27)**, using pentaflourophenol**,** EDC as coupling reagent, and anhydrous DCM as solvent. With pentafluorophenyl ester **(4.28)** in place, we were able to introduce the hydroxamic acid functionality by simply coupling hydroxylamine hydrochloride to **(4.28)** using DIPEA as a base in dry DMF. The reaction was quick and went to completion within 10 minutes at room temperature to generate the hydroxamic acid **(4.29)** (Scheme 4.23).

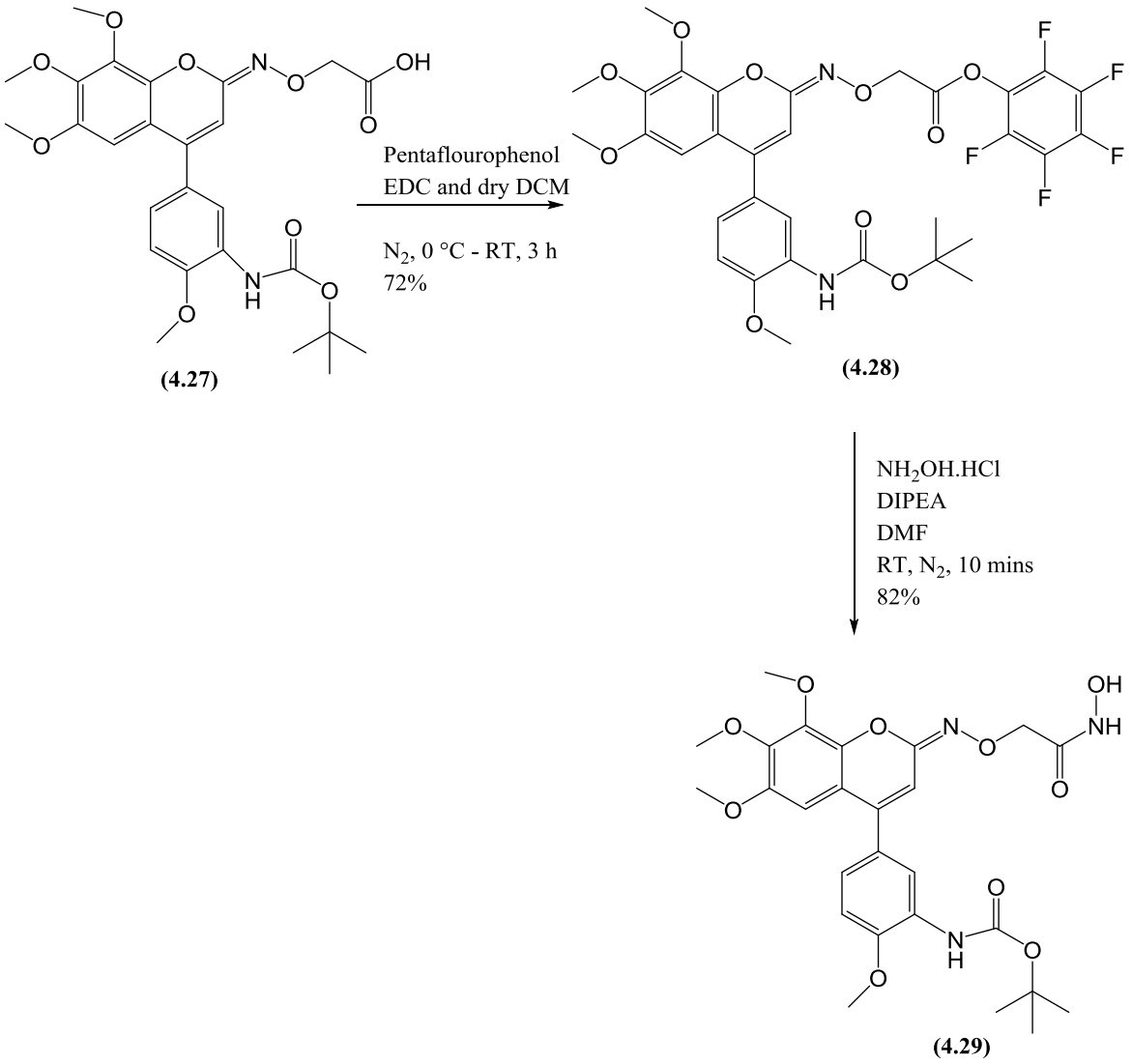

Scheme 4.23. *In situ* pentafluorophenyl ester **(4.28)** synthesis, followed by conversion to hydroxamic acid **(4.29)**

Finally the Boc-group on hydroxamic acid **(4.29)** was removed with 50% TFA in DCM to afford our desired final hydroxamic acid DML **(4.30) (**Scheme 4.24).

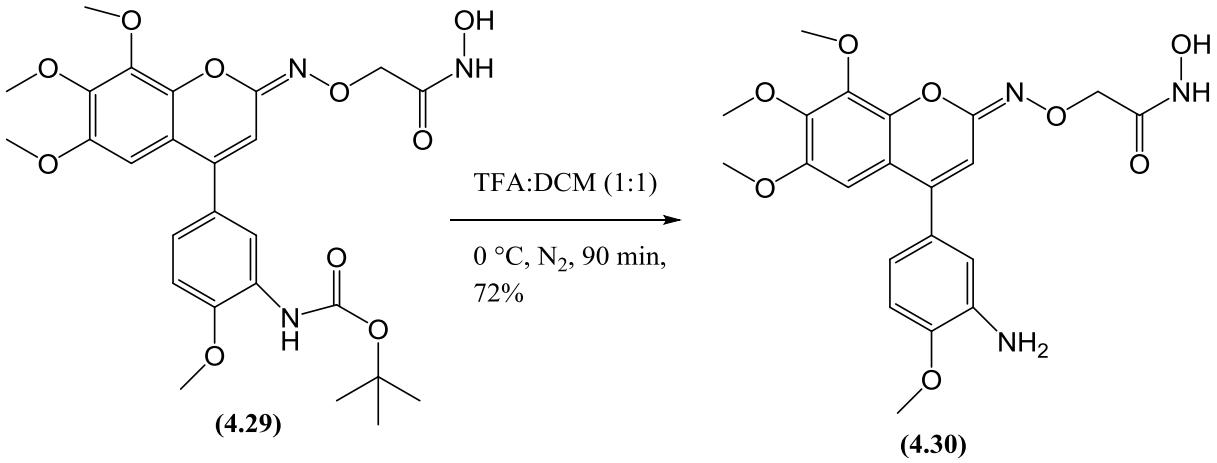

Scheme 4.24. Removal of Boc-group to give final hydroxamic acid DML **(4.30)**

4.2.1.1. Structural elucidation of hydroxamic acid (4.30)

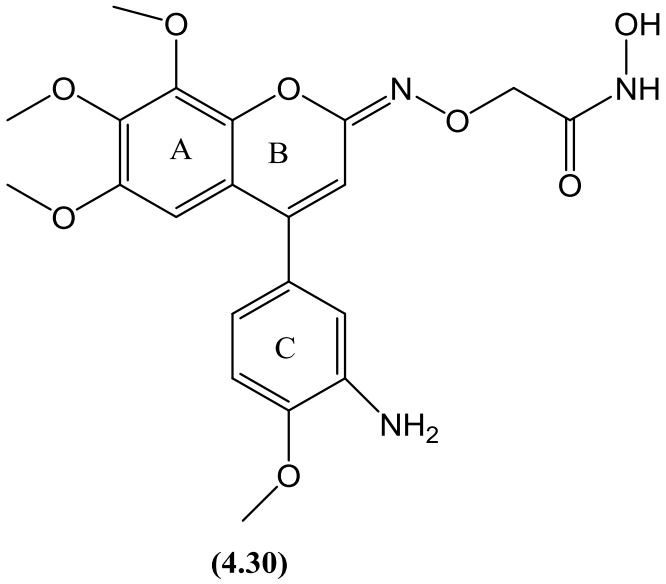

The structural identification of the hydroxamic acid **(4.30)** was confirmed using mainly NMR and mass spectroscopy. The ^{1}H-NMR spectrum (figure 4.35) shows a total count of 23 protons while the ^{13}C-NMR spectrum (figure 4.38) gives a total count of 21 carbons. The most upfield signals between 3.5-4.0 ppm are those of the methoxy protons representing a total of 12 protons in this region. Two methoxy signals in this region are overlapping at 3.83 ppm with an integral value of 6. The corresponding carbons can be easily identified with the help of HSQC (figure 4.39) where the methoxy protons show coupling to four carbons at 55.31, 55.96, 60.93 and 61.22 ppm.

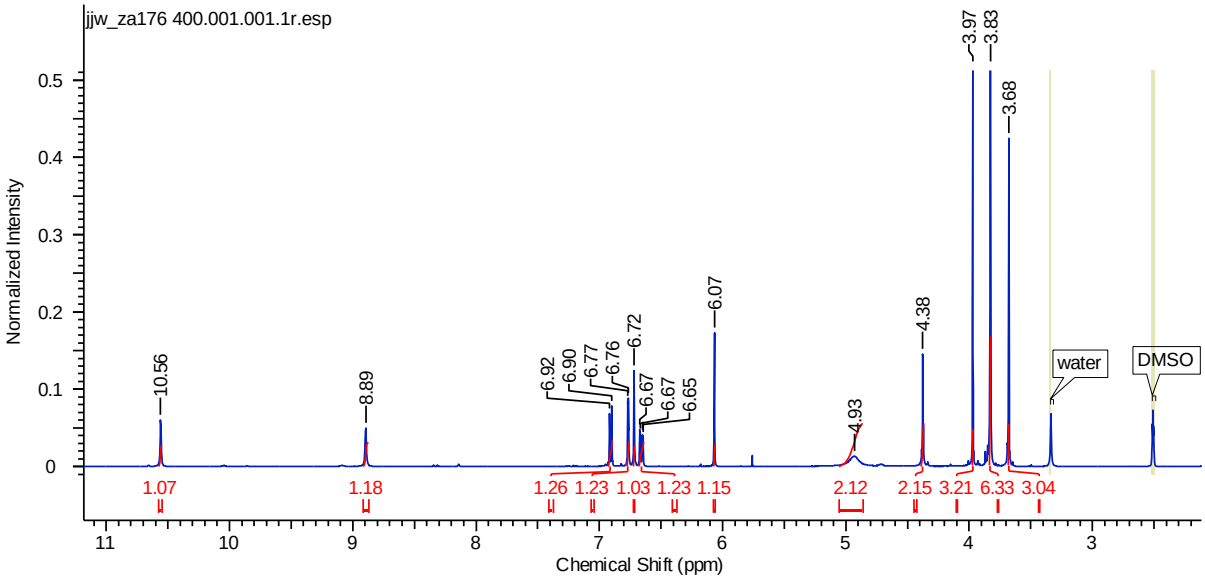

Figure 4.35. ^{1}H-NMR spectrum of hydroxamic acid (4.30)

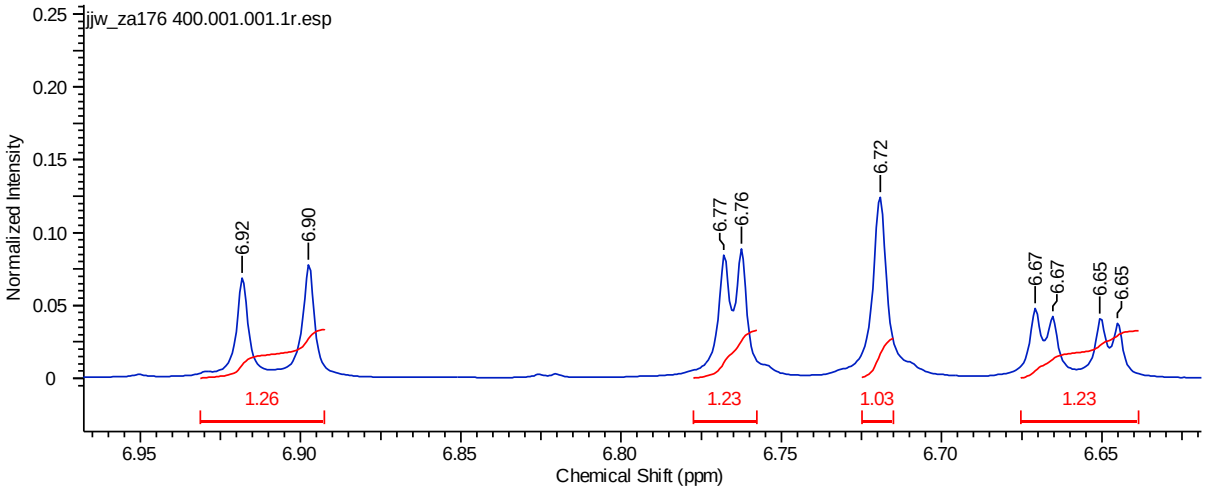

Figure 4.36 Expansion of selected region of ^{1}H-NMR spectrum of hydroxamic acid (4.30)

The next downfield signal in the ^{1}H-NMR spectrum is at 4.38 ppm that represents the methylene protons (CH_2) while their corresponding carbon can be identified using DEPT 135° (figure 4.37), pointing downward at 71.98 ppm. Further downfield to methylene proton is a broad peak for NH_2 at 4.93 ppm.

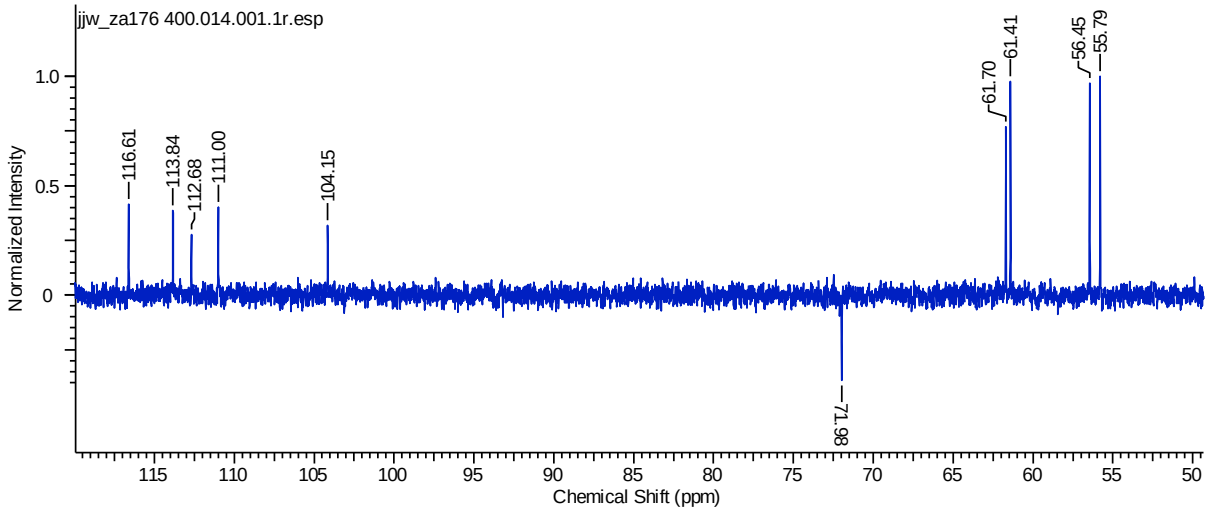

Figure 4.37. DEPT 135° of hydroxamic acid (4.30)

Moving further downfield towards the aromatic region, the next peak at 6.07 ppm represents the alkene proton of the B-ring while the other singlet in the aromatic region at 6.72 ppm represents the aryl proton of the A-ring. The remaining three protons in the aromatic region are the C-ring aryl protons and appear as a double-doublet at 6.67 ppm (showing *ortho*-*meta*-coupling), a doublet at 6.77 ppm (showing *meta*-coupling) and a doublet at 6.92 ppm (showing *ortho* coupling). The last and most downfield remaining two singlets at 8.90 and 10.56 ppm are for NH and OH of the hydroxamic acid functionality. All the carbons related to these aromatic protons are easily identified using HSQC. Of the remaining signals the C=N was found resonating at 150.40 ppm, the carbonyl carbon was found at 165.83 ppm and while the dept 90° spectrum distinguished the aromatic and double bond CHs from remaining aromatic quaternary carbons that were identified using HMBC.

HRMS found the relevant protonated molecular ion of mass 446.1543 corresponding to the ($M+H^+$) ion.

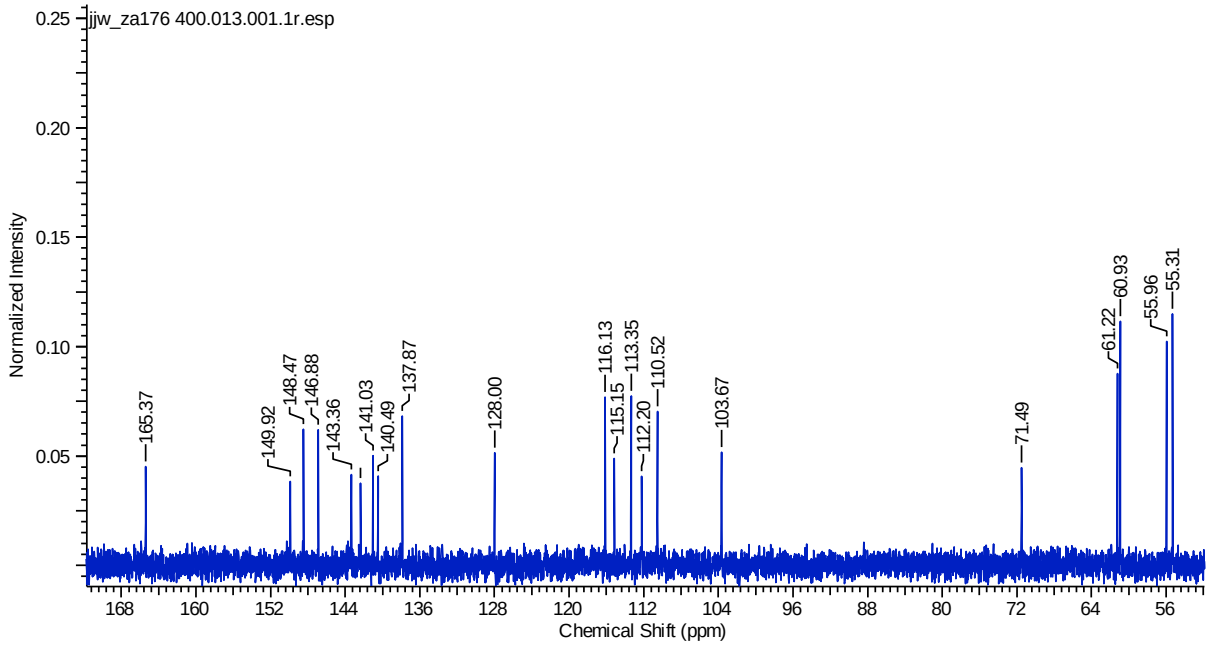

Figure 4.38. ^{13}C NMR spectrum of hydroxamic acid (4.30)

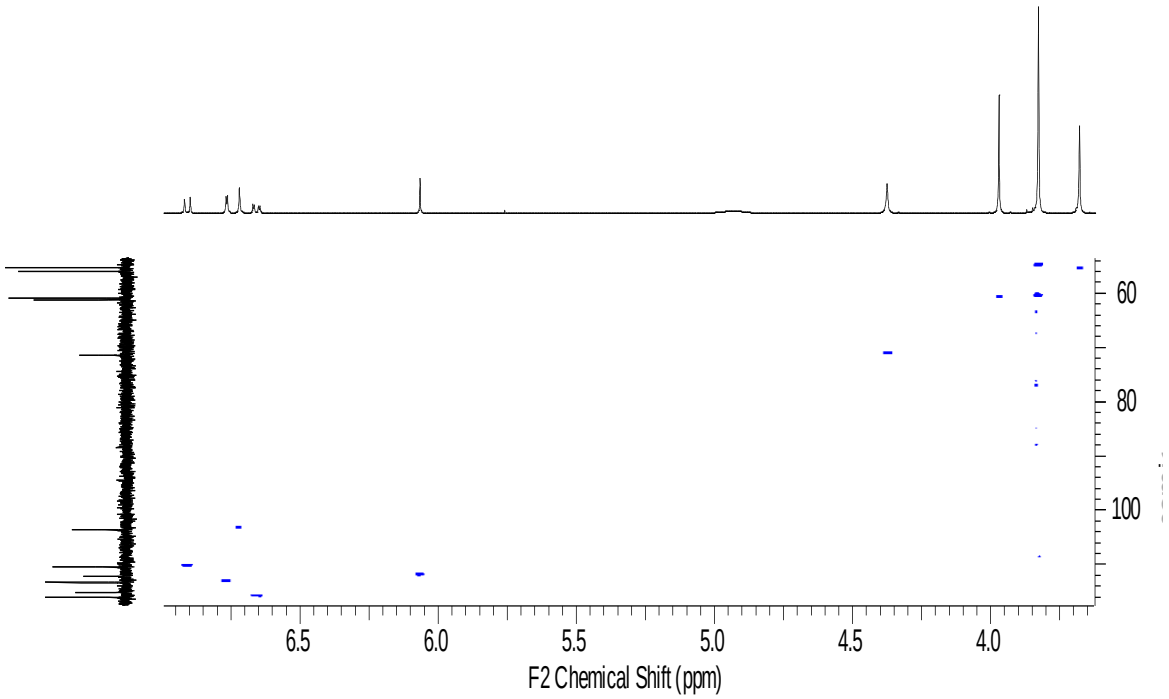

Figure 4.39. HSQC spectrum of hydroxamic acid (4.30)

4.2.2 Synthesis of phenol hydroxamic acid DML (4.33)

Our next target was to procure the phenol hydroxamic acid derivative **(4.33).** We started the synthesis with phenol **(2.24)** by refluxing it with *O*-carboxymethyl hydroxylamine hemihydrochloride and sodium acetate in ethanol\water mixture. The carboxylic acid **(4.31)** obtained was converted to its pentafluorophenyl ester **(4.32)** derivative using similar conditions as we used before for making the pentafluorophenyl ester **(4.28)** of aniline. The PFP ester was quickly converted to the hydroxamic acid **(4.33)** using hydroxylamine hydrochloride and DIPEA, as tertiary base, along with DMF as a solvent (Scheme 4.25). The only problem was the poor solubility of the compound **(4.33)**, so after quenching the reaction with water, the product precipitated which necessitated several extractions with diethyl ether and each time the aqueous layer was carefully removed without losing any of the compound that had precipitated. The diethyl ether containing the precipitated product was directly evaporated without being dried with $MgSO_4$. After evaporation, the solid residue was washed several times with diethyl ether to remove any residual moisture and dried under high vacuum. This was an effective approach despite the fact that water exhibits very poor solubility in ether. All the spectra were obtained in deutrated DMSO.

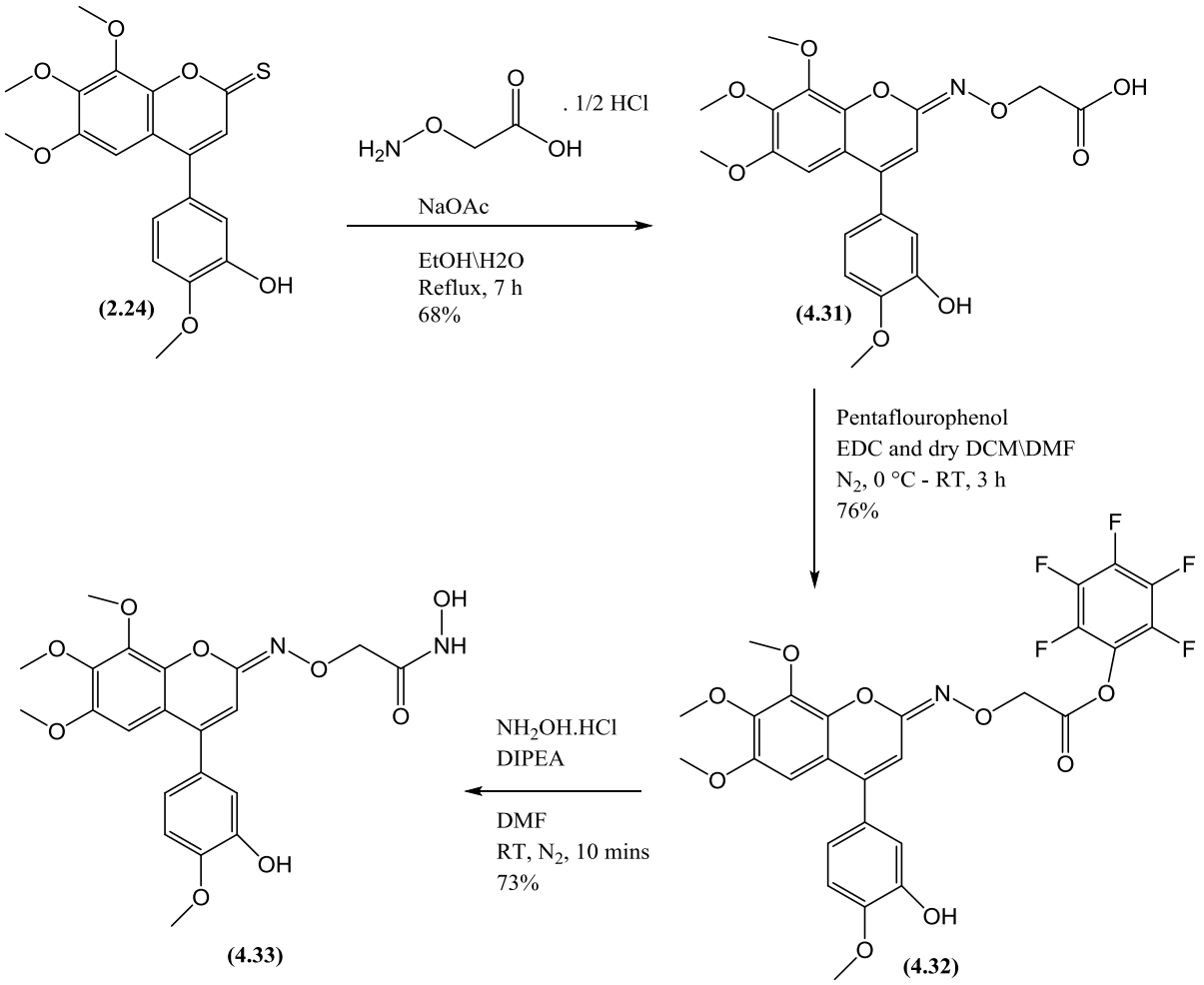

Scheme 4.25. Steps involved in the synthesis of hydroxamic acid **(4.33)**

4.2.2.1. Structural elucidation of (4.33)

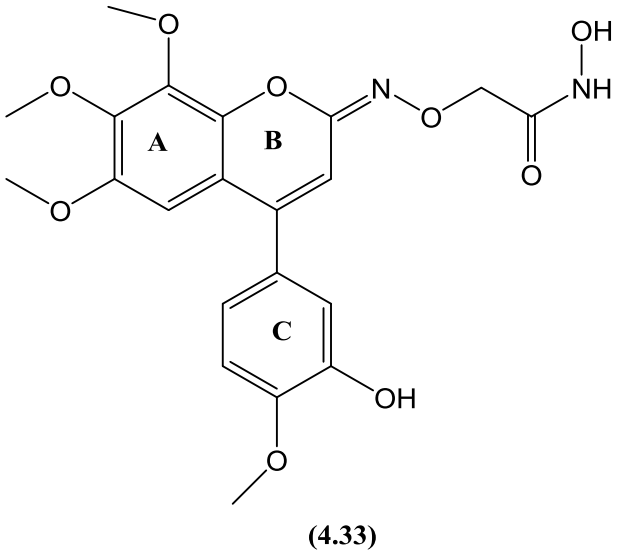

The identity of hydroxamic acid **(4.33)** was confirmed by NMR and mass spectroscopy. In the ^{1}H NMR spectrum (figure 4.40) 22 protons are present while the ^{13}C spectrum (figure 4.41) represents a total carbon count of 21.

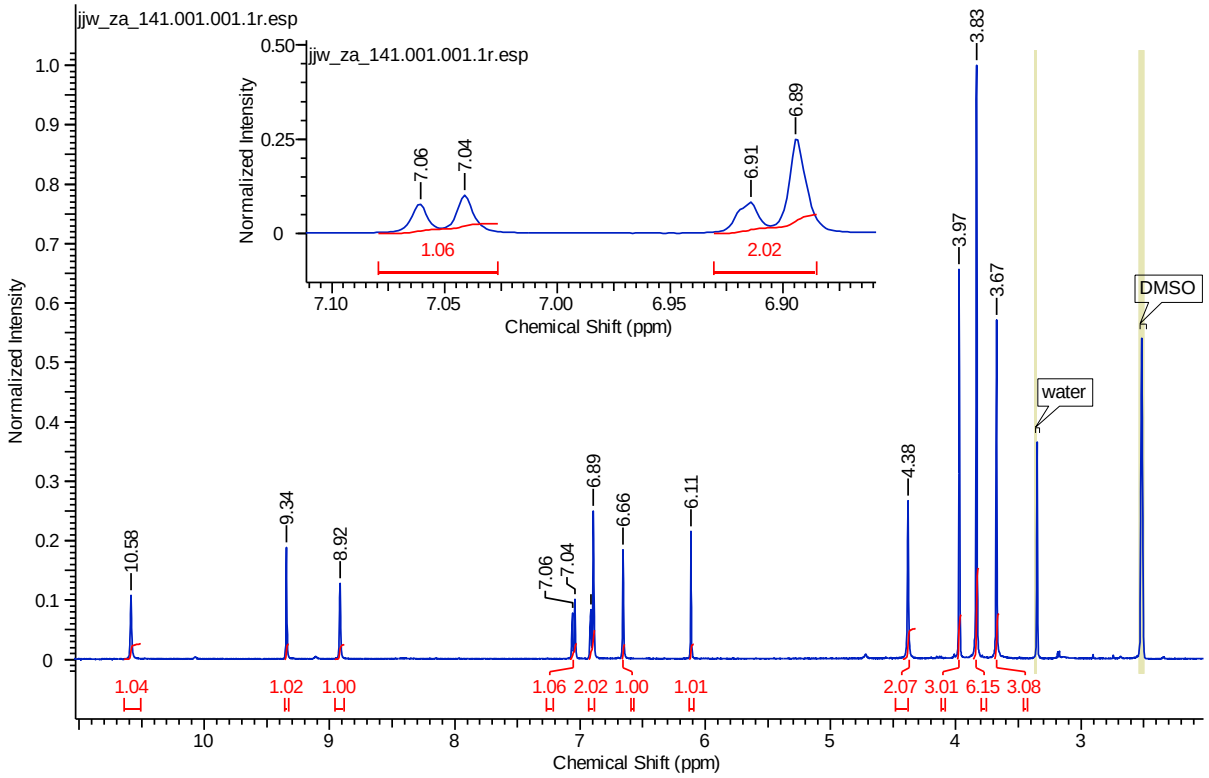

Figure 4.40. ^{1}H-NMR spectrum of hydroxamic acid (4.33)

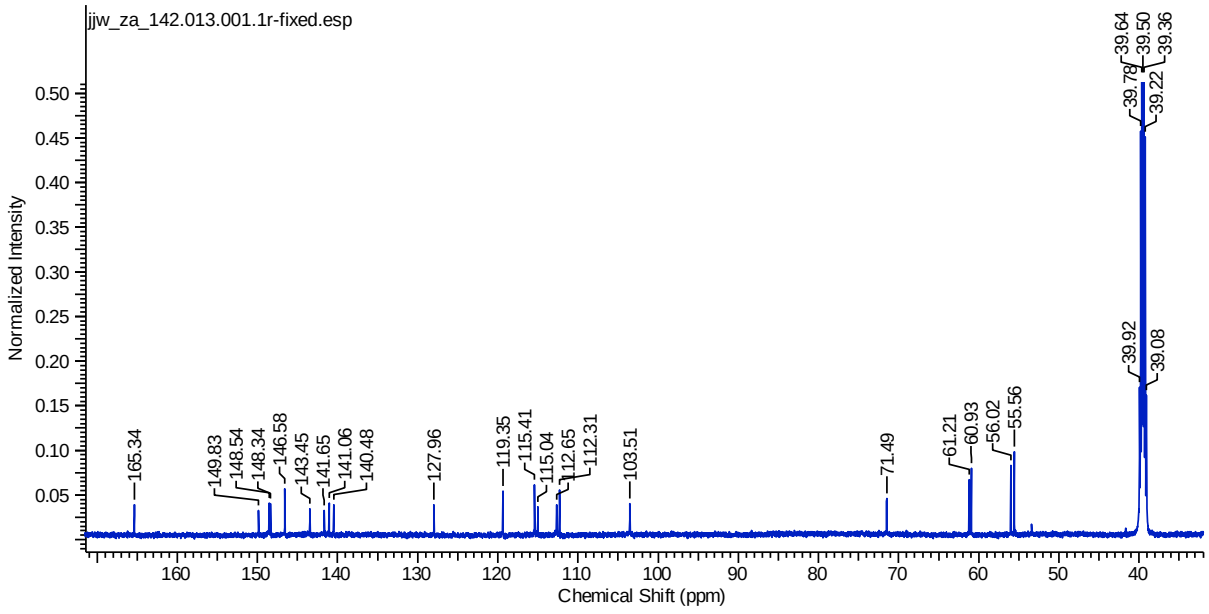

Figure 4.41. ^{13}C NMR spectrum of hydroxamic acid (4.33)

The most upfield signals in the ^{1}H NMR spectrum between 3.5-4.0 ppm are those for the methoxy protons, representing a total 12 protons in this region. Two methoxy signals in this region are overlapping at 3.83 ppm with an integral value of 6. Their corresponding carbons can be easily identified with the help of the HSQC spectrum (figure 4.42) where the methoxy protons show coupling to 4 carbons at 55.56, 56.02, 60.93 and 61.21 ppm.

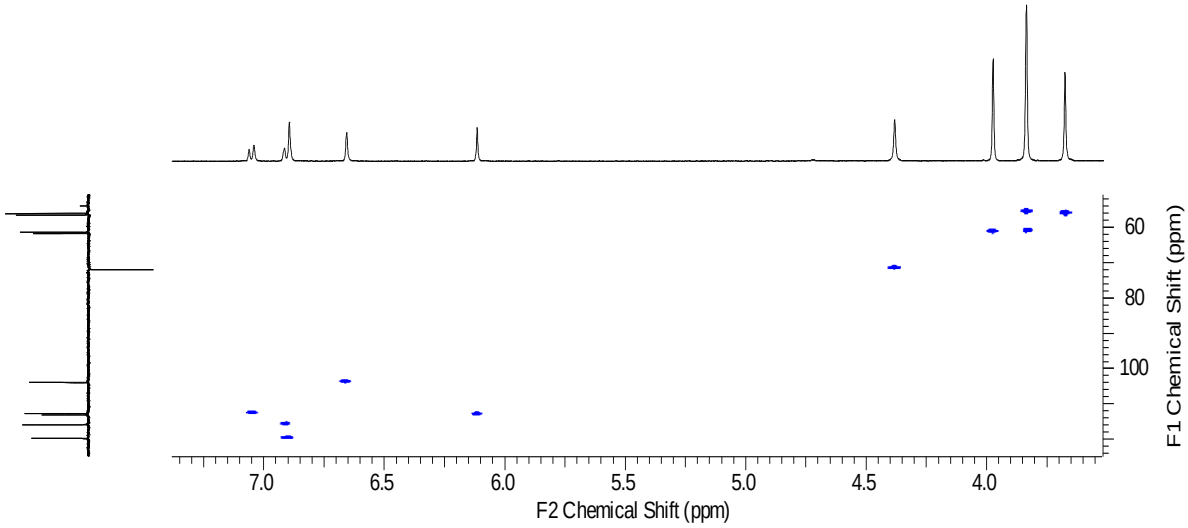

Figure 4.42. HSQC spectrum of hydroxamic acid (4.33)

The next downfield signal in the ^{1}H NMR spectrum is at 4.38 ppm that represents the methylene protons (CH_2) while their corresponding carbon can be identified using DEPT 135° spectrum (figure 4.43), pointing downwards at 71.99 ppm.

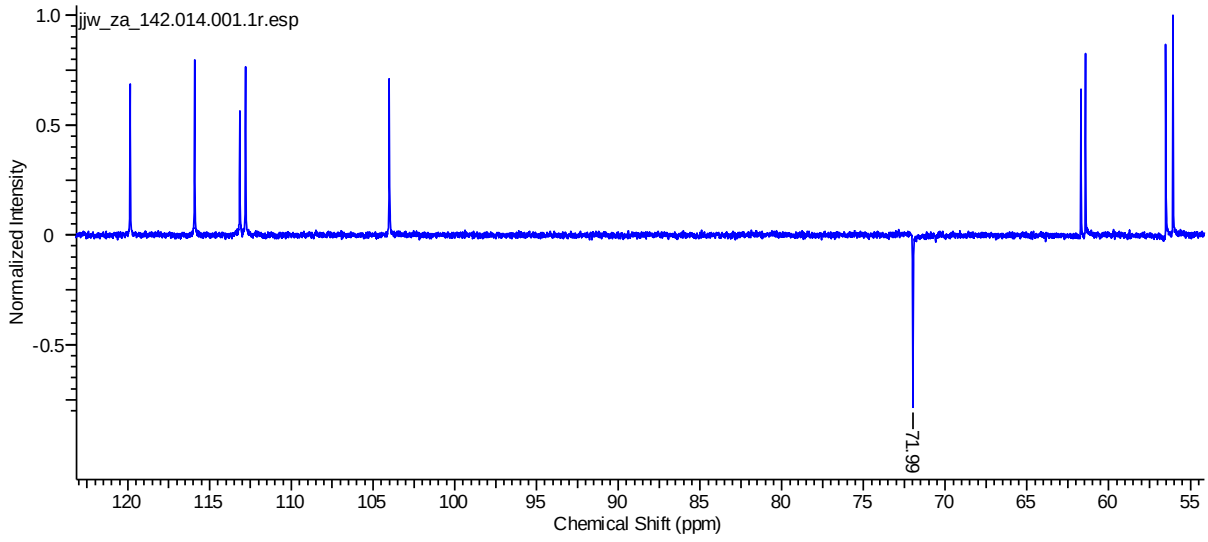

Figure 4.43. DEPT 135° spectrum of hydroxamic acid (4.33)

Moving further downfield towards the aromatic region, the next singlet at 6.11 ppm represents the alkene proton of the B-ring while the two remaining singlets in the aromatic region are represented by the proton of the A-ring (6.66 ppm) while the other represents the proton of the C-ring (6.89 ppm). Next we have a broad doublet at 6.90 ppm that shows overlapping with a singlet and the other doublet at 7.05 ppm. Both of these doublets correspond to C-ring aryl protons.

The furthest downfield singlet at 10.58 ppm corresponds to NH, confirmed by the NH-COSY spectrum (figure 4.44). Out of the remaining last 2 singlets in the downfield region, the singlet at 9.34 represents the OH attached to C-ring while the singlet at 8.92 corresponds to the OH of the hydroxamic acid functionality. The CH carbons related to the four aryl and one alkene proton are easily identified following examination of the HSQC spectrum (figure 4.42) while for the remaining quaternary aryl carbons a combination of the DEPT 135 and HMBC spectra were used. The last signal at 165.34 ppm in the ^{13}C NMR spectrum represents the carbonyl carbon. HRMS found the relevant protonated molecular ion of mass 447.1427 ($M+H^+$).

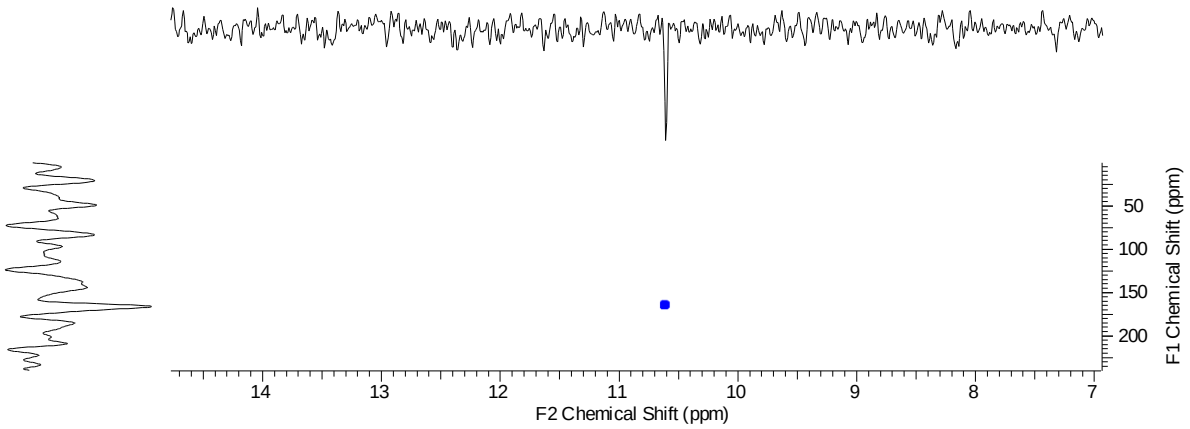

Figure 4.44. NH-COSY of hydroxamic acid (4.33)

4.2.3 Synthesis of controlled release designed multiple ligand (DML) (4.38)

The design strategy under investigation here is to determine if it is possible to create a DML version of **(4.16)** with equivalent levels of efficacy. According to the Lipinski rule of 5, it is most desirable for a potential candidate drug molecule to have a molecular weight of

less than 500. However this rule is not always adhered to as a significant number of the clinically approved drugs do not necessarily obey this rule. None more so than in the cancer field with examples including vincristine, vinblastine, doxorubicin and paclitaxel. For the synthesis of controlled release DML **(4.38)**, we began by coupling *N*-Boc alanine onto aniline compound **(2.18)** using PyBrop as coupling reagent to give compound **(4.34)** (Scheme 4.26). The ^{1}H NMR spectrum (figure 4.45) confirmed the coupling reaction due to the presence of CH_3 group of alanine at 1.46 ppm and Boc group at 1.49 ppm.

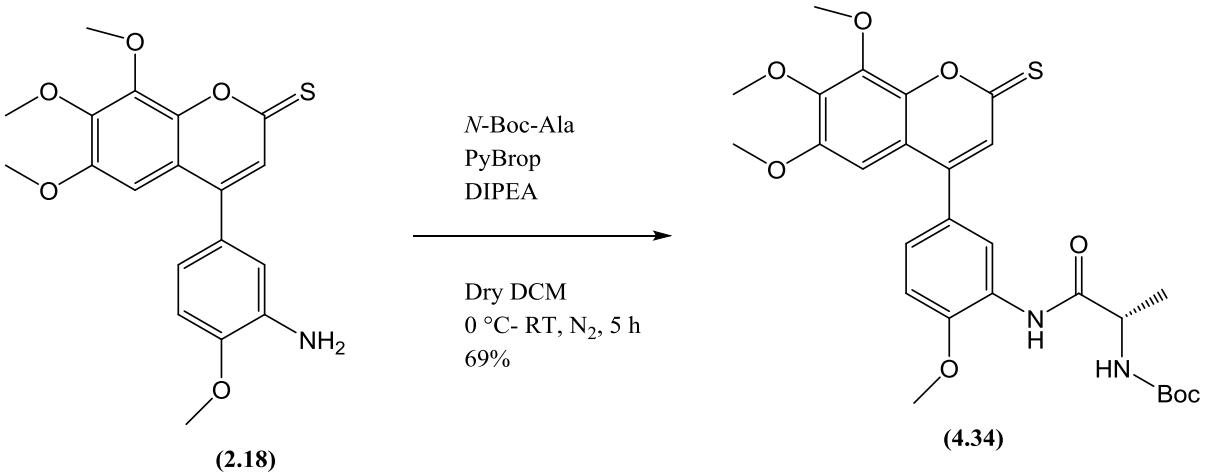

Scheme 4.26. Coupling of *N*-Boc alanine on to aniline **(2.18)**

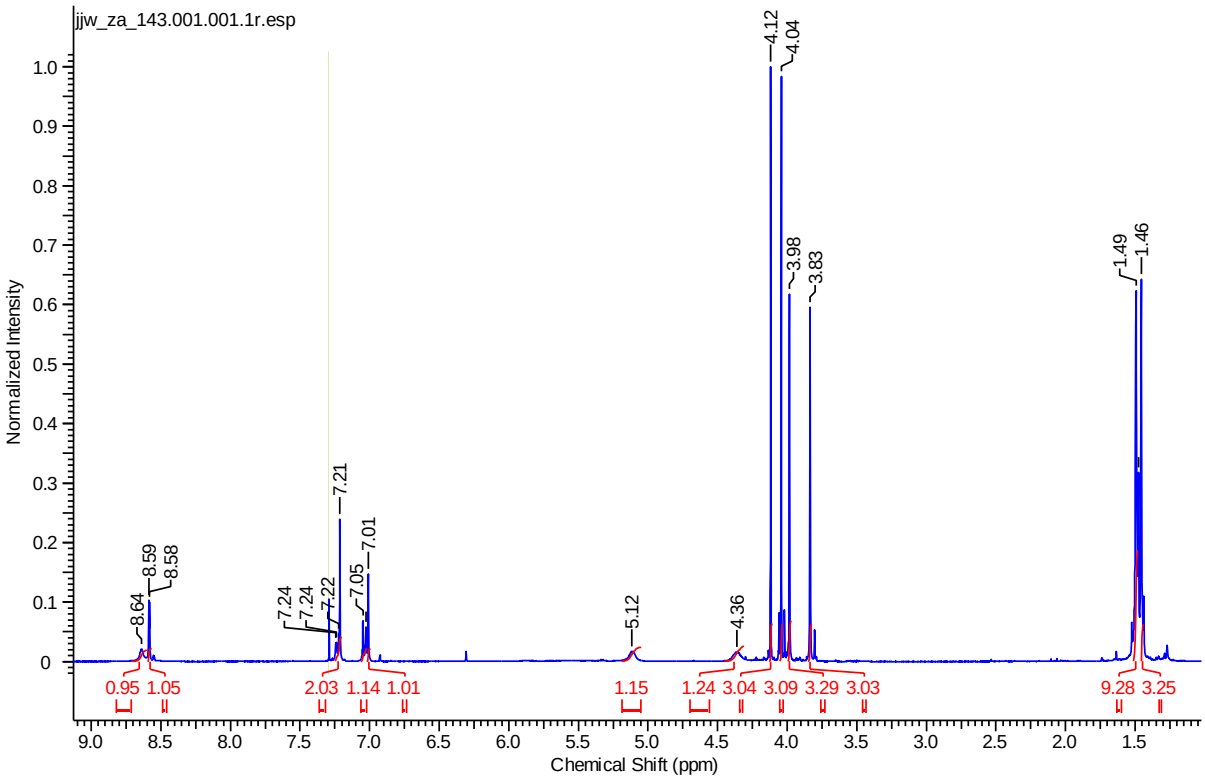

Figure 4.45.^{1}H-NMR spectrum of compound (4.34)

After coupling *N*-Boc-alanine onto the C-ring, we introduced the oxime carboxylic acid moiety by using the reagent *O*-carboxymethyl hydroxylamine hemihydrochloride and sodium acetate in ethanol\water. In the subsequent steps we essentially followed the same steps as we used for the synthesis of **(4.27)** and converted the carboxylic group of **(4.35)** into its pentafluorophenyl ester derivative using pentaflourophenol and EDC. After the final work-up with DCM and water to remove the EDC by-product, the product **(4.36)** was dried quickly to reduce the risk of hydrolysis of the pentafluorophenyl ester. Next, the pentafluorophenyl ester was treated with hydroxylamine hydrochloride to afford the hydroxamic acid **(4.37)** (Scheme 4.27) and its synthesis was confirmed by HRMS analysis that found the molecular ion of mass 639.2258 as sodium adduct ($M+Na^+$). Moreover, further confirmation was achieved by the presence of the CH_2 group of the hydroxamic acid side chain at 4.69 ppm in the ^1H NMR spectrum (figure 4.46) of compound **(4.37)**.

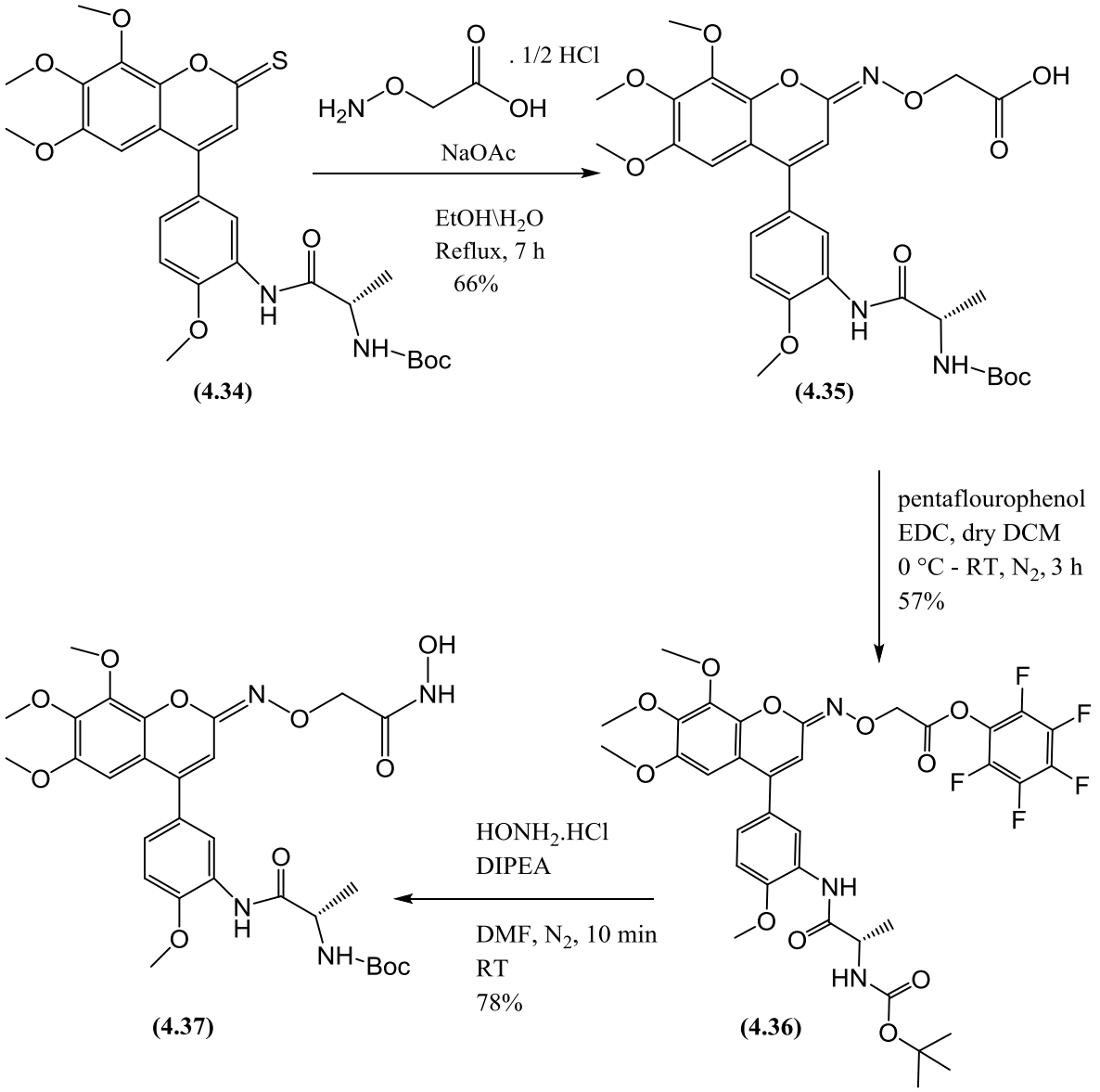

Scheme 4.27. Steps involved in synthesis of **(4.37)** from compound **(4.34)**

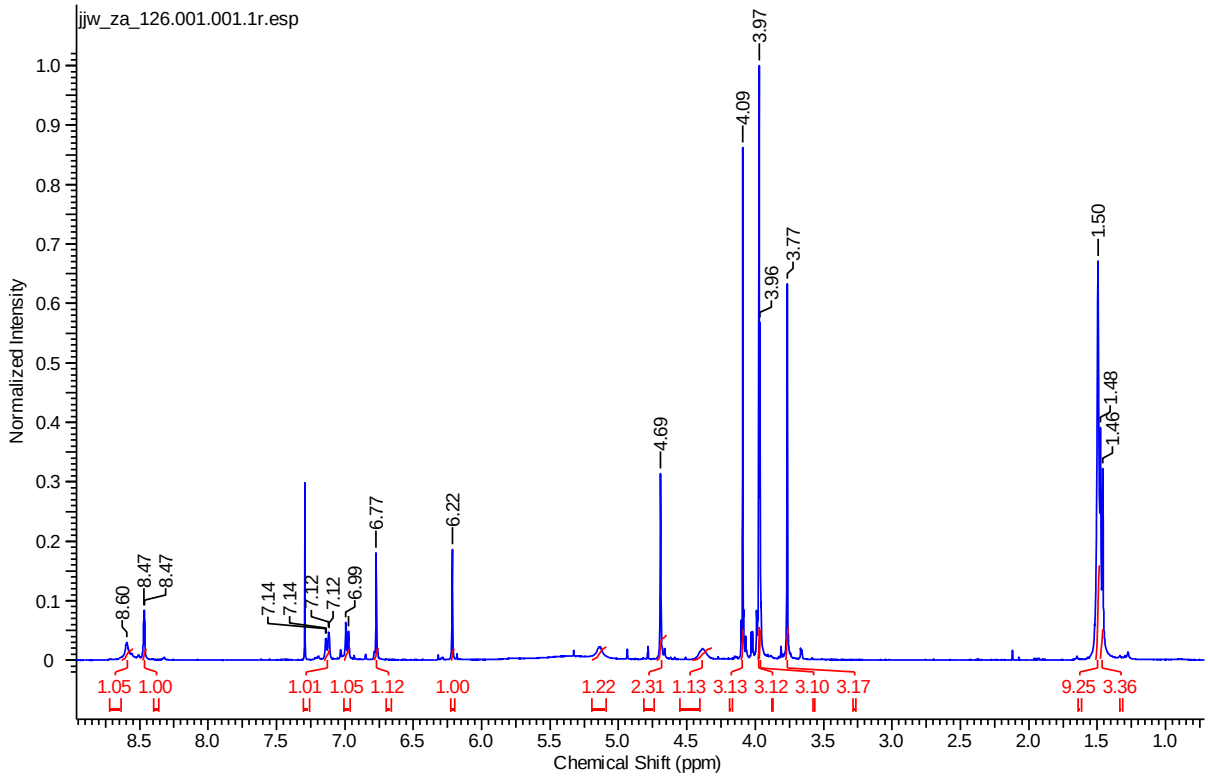

Figure 4.46. ^{1}H-NMR spectrum of compound (4.37)

Finally removal of the *N*-Boc protecting group was achieved with 50% TFA in DCM to afford the desired controlled release compound **(4.38)** (Scheme 4.28). *N*-Boc deprotection was confirmed by the disappearance of the signal for the Boc group at 1.50 ppm in the ^{1}H NMR spectrum (figure 4.47).

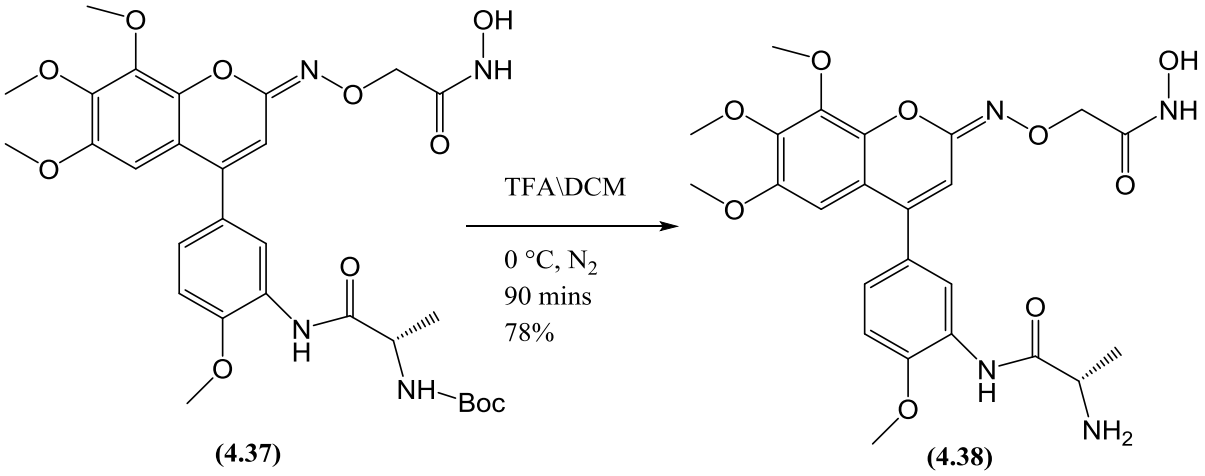

Scheme 4.28. Deprotection to give final control release compound **(4.38)**

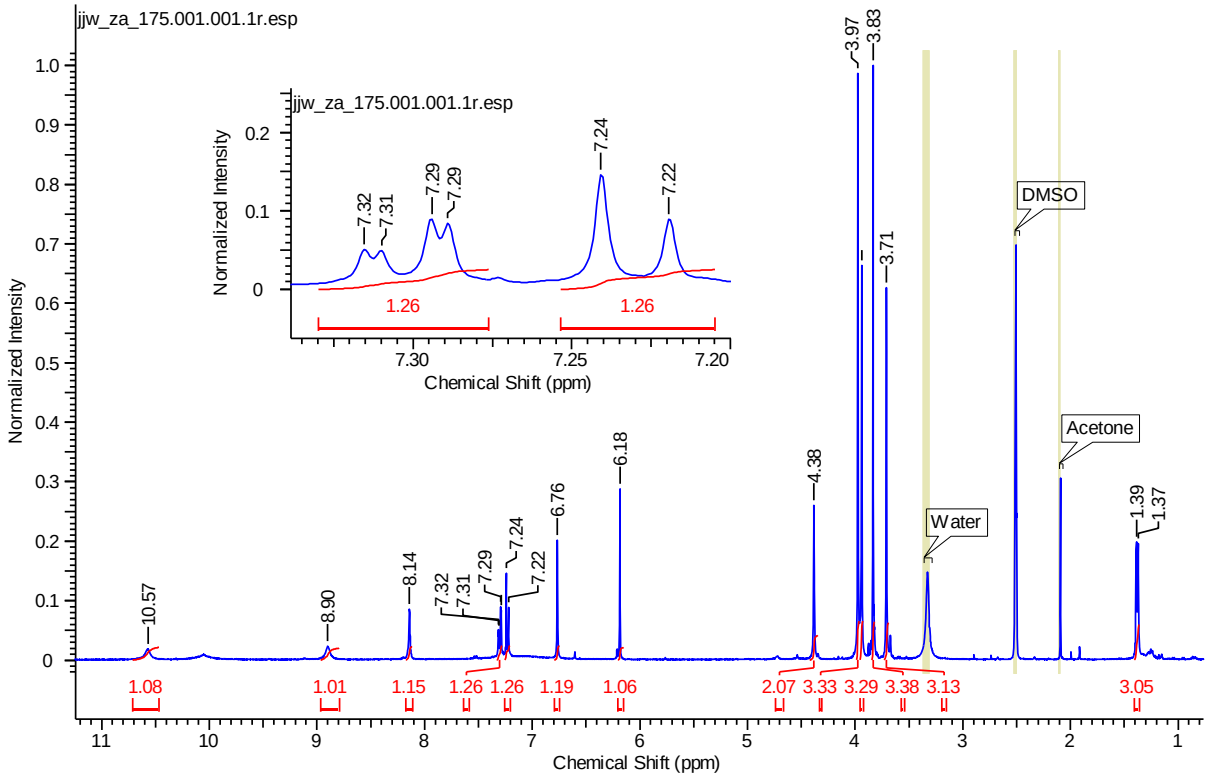

Figure 4.47. ^{1}H-NMR spectrum of compound (4.38)

4.2.4. Synthesis of hydroxamate compound (4.41)

Another aim of the work in this chapter was to introduce the hydroxamic acid functionality onto the A-ring of our compounds. For this purpose, the intermediate **(2.70)** was first converted into PFP ester using the same EDC coupling conditions employed for synthesis of compound **(4.36)**. The PFP ester **(4.39)** was directly treated with hydroxylamine hydrochloride and diisopropylethylamine in DMF to afford the hydroxamic acid **(4.40)** (Scheme 4.29). The HRMS analysis of the compound **(4.40)** found the molecular ion of mass 539.1615 ($M+Na^{+}$). Further confirmation of the product was received through the inspection of its ^{1}H NMR spectrum (figure 4.48) that shows signals for the presence of NH and OH at 7.16 and 10.38 ppm.

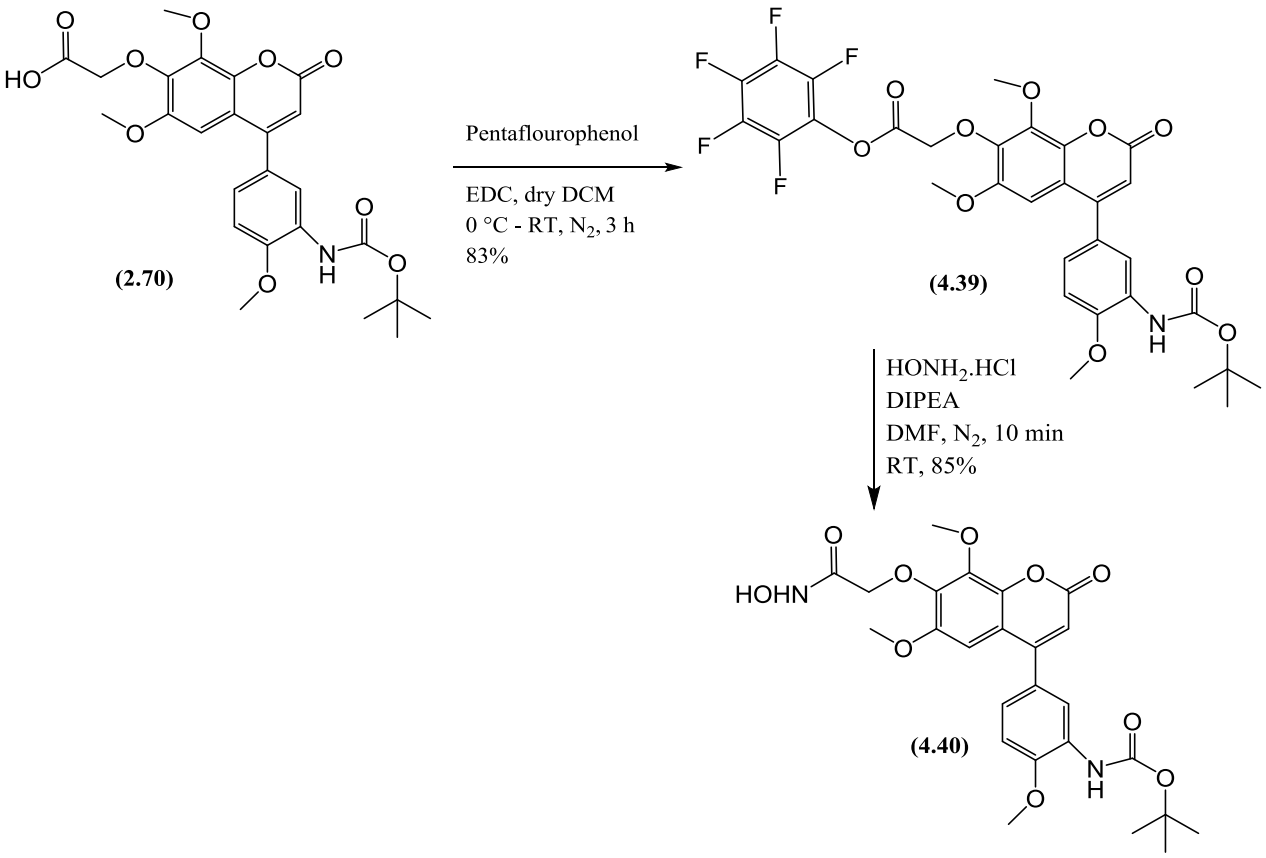

Scheme 4.29. Synthesis of compound **(4.40)**

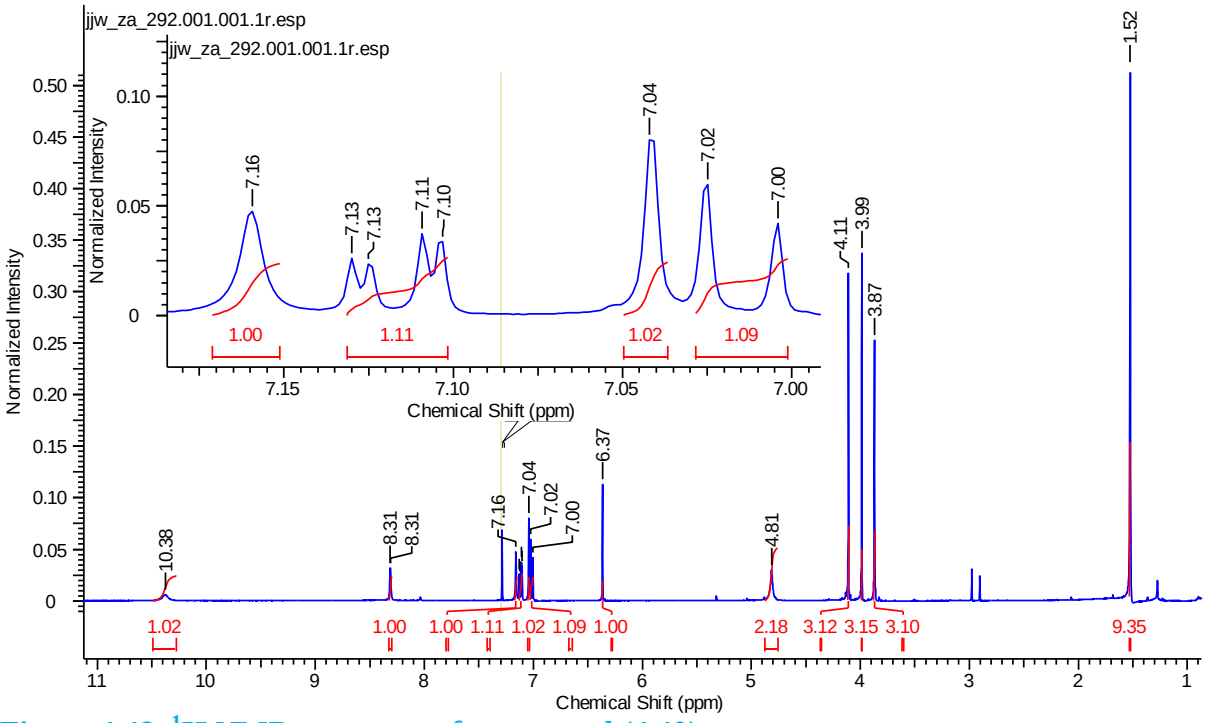

Figure 4.48. ^{1}H NMR spectrum of compound (4.40)

Finally *N*-Boc deprotection with 25% TFA in dry DCM afforded the aniline hydroxamic acid **(4.41)** (Scheme 4.30). The success of deprotection step was confirmed by the

disappearance of signal for Boc protecting group at 1.52 ppm as well as by the appearance of a peak for the NH_2 group at 5.02 ppm in the ^1H NMR spectrum (figure 4.49) of the compound **(4.41)**. Moreover ^{13}C NMR spectrum (figure 4.50) also shows the presence of all expected 20 carbons. The HRMS analysis also found the relative protonated molecular ion of mass 417.1306 ($M+H^+$).

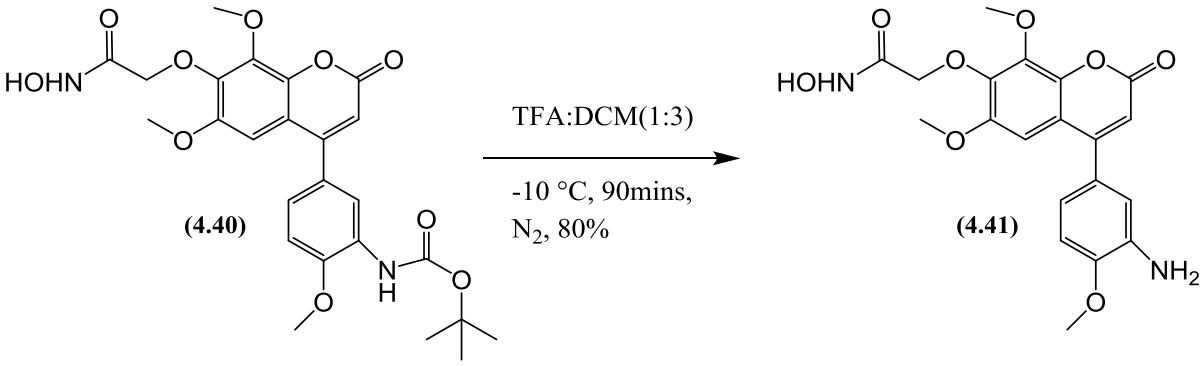

Scheme 4.30. Deprotection to give aniline hydroxamic acid **(4.41)**

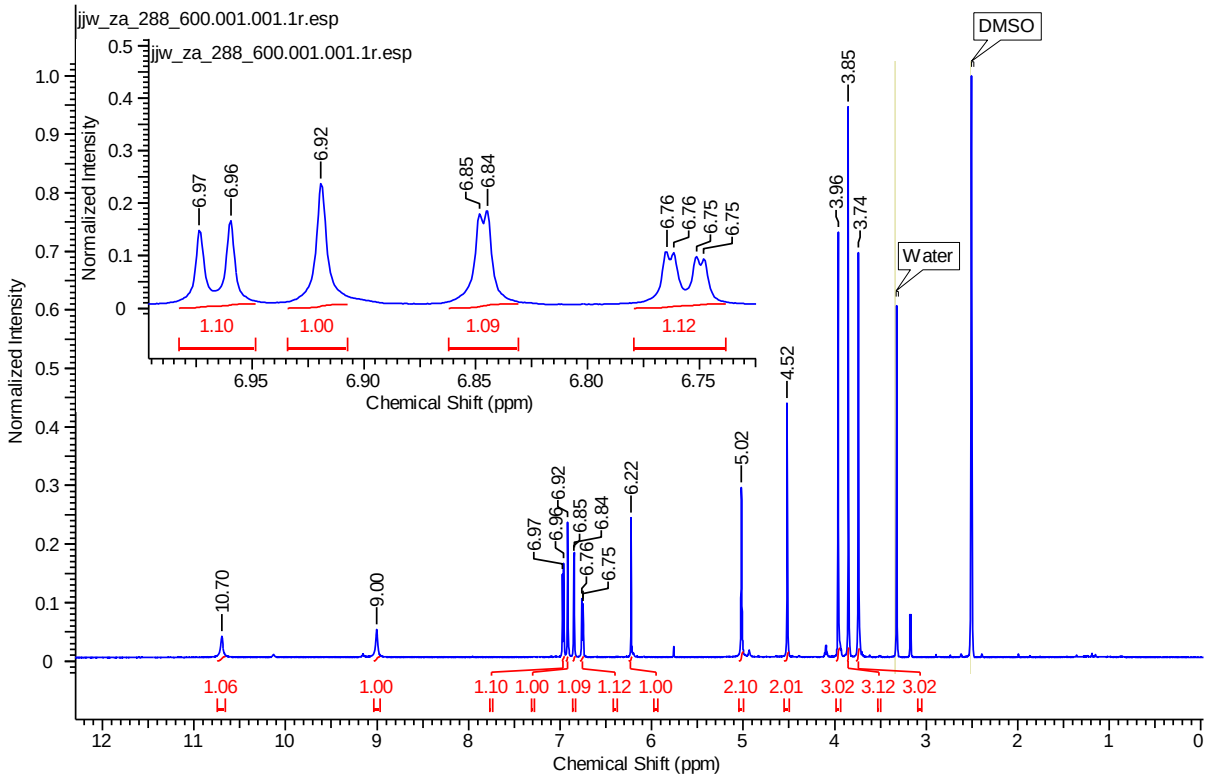

Figure 4.49. ^1H NMR spectrum of compound (4.41)

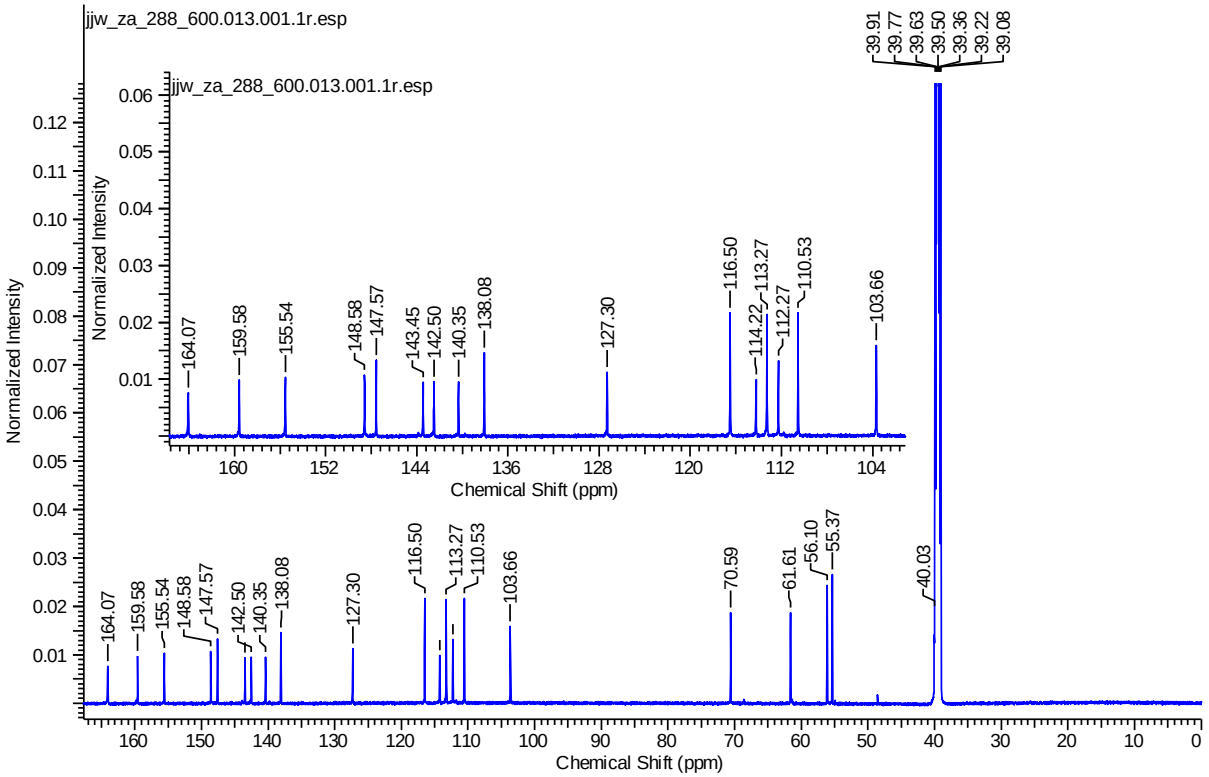

Figure 4.50. ^{13}C NMR spectrum of compound (4.41)

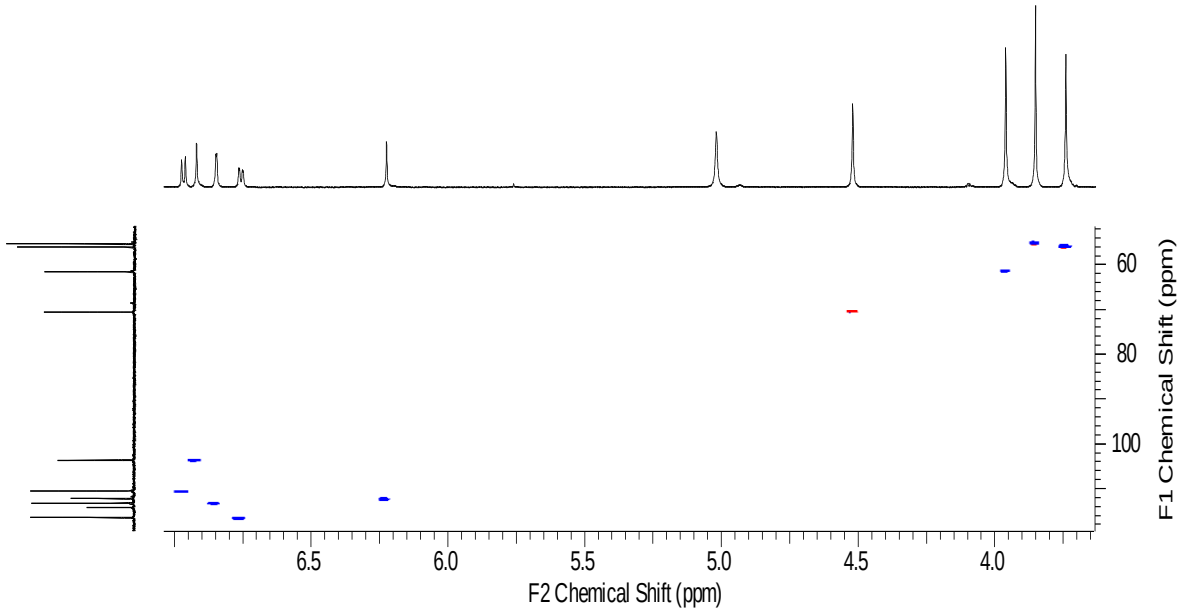

Figure 4.51. HSQC spectrum of compound (4.41), CH_2 as red contour

4.3 APN inhibition assay

For the determination of APN inhibitory activity of the compounds synthesized in this chapter, an APN inhibition assay was carried out. The assay measures the ability of the compounds to inhibit the cleavage of L-leucine-*p*-nitroanilide by the APN enzyme [166]. The main purpose of attaching an APN targeting moieties onto anti-vascular agents was their targeted delivery to the tumor site. APN converts the L-leucine-*p*-nitroanilide (colourless in solution) into its metabolite *p*-nitroaniline (yellow colour in solution) (Scheme 4.31). This colorimetric assay basically compares the extent to which the L-leucine-*p*-nitroanilide is converted into *p*-nitroaniline by the APN enzyme in the presence of an APN inhibitor, relative to the absence of inhibitor. All compounds were screened on three separate occasions (N=3) for their APN inhibition activity at different concentrations (1, 2.5, 5, 10, 20, 30, 40, 50, and 75 µM) and bestatin was used alongside as a control. The percent APN inhibition was determined using the formula:

% APN inhibition = [100 - mX / mB] x 100

mX = mean absorbance of test compound

Mb = mean absorbance of negative control (Enzyme + substrate without drug)

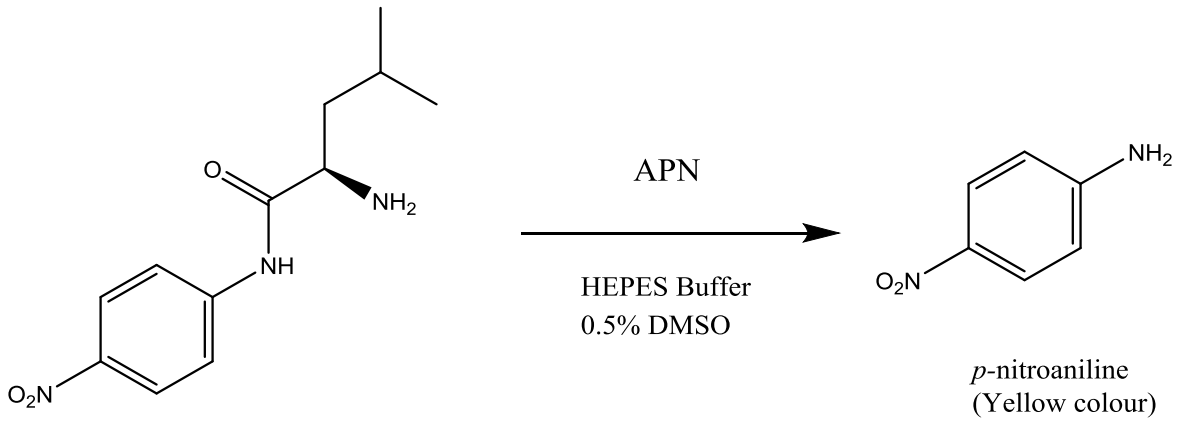

Scheme 4.31 APN-catalyzed cleavage of L-leucine-*p*-nitroanilide to form coloured *p*-nitroaniline

Compound	IC_{50} (μM) ±SD
Phenolic tripeptide hybrid (4.05)	**16.67 ± 1.05**
Phenolic tripeptide hybrid (4.08)	**22.62 ± 1.39**
Phenolic tripeptide hybrid (4.11)	**20.91 ± 1.34**
Control release tripeptide hybrid (4.16)	**28.21 ± 2.13**
Phenstatin based tripeptide hybrid (4.19)	**1.94 ± 1.96**
Anilide dipeptide hybrid (4.26)	**8.31 ± 1.47**
Aniline hydroxamic acid (4.30)	**22.50 ± 3.67**
Control release hydroxamic acid (4.38)	**35.63 ± 2.33**
Hydroxamic acid (4.41)	**28.01 ± 2.24**
Hydroxamic acid (4.33)	**Not soluble**
Bestatin	**22.94 ± 1.44**

Figure 4.52. IC_{50} values of APN inhibition assay

4.4 Conclusions

In this chapter a range of bestatin based tripeptide hybrid compounds were synthesised containing the most promising tubulin binding agents from chapters 2 and 3; namely **(2.16)**, **(2.22)**, **(2.68)** and **(3.04)**. The valine based tripeptide hybrids **(4.08)** (IC_{50} 22.62 ± 1.39 μM) and **(4.11)** (22.62 ± 1.39 μM) displayed comparative APN inhibition to bestatin (22.94 ± 1.44 μM) while the leucine based tripeptide hybrid (**4.05)** proved to have slightly better activity than bestatin with an IC_{50} value of 16.67 ± 1.05 μM. Another bestatin based hybrid **(4.16)** was synthesised by coupling a leucine residue on to the aniline functionality of **(4.11)**, with the aim of presenting the hybrid **(4.11)** in its prodrug form and upon reaching the tumor vasculature will be converted in to its active form by the peptidase enzyme such as APN. The hybrid displayed the APN inhibition with an IC_{50} value of 28.21 ± 2.13 μM.

Among the compounds synthesised, the most active APN inhibitor was the phenstatin based hybrid **(4.19)** consisting of two tripeptide moieties onto the tubulin inhibitor **(3.04)** and it is predicted that the release of the tubulin unit from these peptides will be dependent

on the pH. The compound **(4.19)** proved to be very active as an APN inhibitor with an IC_{50} value of 1.94 ± 1.96 µM.

Moreover a series of hydroxamic acid based designed multiple ligands was also synthesized by merging both an APN targeting and tubulin inhibiting pharmacophores together on to a single structure. Among them the hydroxamic acid **(4.30)** (IC_{50} value 22.50 ± 3.67 µM) has shown comparable activity to bestatin while the hydroxamic acid **(4.41)** demonstrated an IC_{50} value of 28.01 ± 2.24 µM. The control release hydroxamic acid **(4.38)** has shown APN inhibition activity with an IC_{50} value of 35.63 ± 2.33 µM.

4.5 Preliminary studies on the peptide release profile of hybrids

Having completed the synthesis of the bestatin-related hybrids and their evaluation as APN inhibitors, the next step was to evaluate the release of these peptides over time from the conjugates. In essence, these hybrids were designed to exhibit potent inhibition of APN in their hybrid form but the tubulin binding component is essentially in pro-drug form for its effective delivery to the tumour vasculature. Thus it is pertinent to investigate their release profile before establishing their activity in *in vitro*, *ex vivo* and *in vivo* test systems. The controlled release system having both a substrate and inhibitor for APN, as in **(4.16)** (figure 4.74), is envisaged to only be in active form where the presentation of the enzyme is in high concentration, as in tumour vasculature, but less so in the circulating system where the concentration of this enzyme is lower. In the other examples what will determine the rate of activation will be a combination of pH and the presence of amine or thiol-based nucelophiles in tumour vasculature to release of the peptide from the conjugate. It is envisaged that thiol based nucleophiles in particular in the form of glutathione (present in mM concentrations inside cells) could also effect the release of the tubulin binding component by a *trans*thiolation reaction.

In the preliminary studies conducted to date, the main focus was on establishing a time course experiment to establish how readily the active tubulin inhibitor would be generated from the cell culture medium that would be used in subsequent *in vitro* studies, when incubated in the presence of 25 mU/mL of APN. This necessitated establishing a suitable LCMS method. We ultimately decided to use a gradient elution method consisting of 0.1% formic acid in water and 0.1% formic acid in acetonitrile and a liquid-liquid extraction protocol, using *tert*butyl methyl ether as extraction solvent, prior to analysis of the samples by LCMS. While the liquid-liquid extraction step is time-consuming, it nevertheless overcomes the significant issue of ion suppression caused by cationic substances that are

present in the cell medium after the reaction is quenched with acetonitrile and used directly in the analysis. A double extraction step with *tert*-butyl methyl ether was conducted, the combined organic layers were reduced to dryness and the residue reconstituted in methanol (200 μL) prior to analysis by LCMS. It was decided to settle on a concentration of 5 μM of each test compound. The first two hybrids studied were the *O*-leucine-bestatin **(4.05)** (figure 4.53) and *O*-valine-bestatin **(4.08)** (figure 4.58). With both hybrids the phenolic ester linkage was slowly cleaved to generate the active 4-phenyl coumarin **(2.22)** (figure 4.53 and figure 4.58), this happened slowly over time and in both examples was seen to go to completion within 24 hours. With regard to the *O*-valine bestatin hybrid **(4.11)** (figure 4.63), where the peptide fragment was switched onto the A-ring, most of the active form was generated within the first hour but the hydrolysis ceased after this time-point. Cleavage of the phenolic esters in dibestatin **(4.19)** proceeded slowly to first generate the intermediate monobestatin conjugate(s) either **(4.52)** or **(4.53)** before proceeding to the active phenstatin analogue **(3.04)** (figure 4.68). The majority of this hybrid was still intact after 4 days. While the release of the peptide from the slow release hybrid **(4.16)** proceeded efficiently over 37 hours, it did so with some evidence showing by LCMS that a tetrapeptide derivative formed, where the leucine residue on the C-ring coupled to the tri-peptide on the A-ring to give **(4.55)** (figure 4.74). Increasing the pH of the reaction medium to 8.0 and conducting the experiment in Hepes buffer resulted in faster hydrolysis of the A-ring phenolic ester to give the pro-drug **(4.54)** with very limited formation of the tetrapeptide on the C-ring, (see Figure 4.76) while the leucine substrate was slowly hydrolysed to generate the active tubulin inhibitor **(2.68)** (figure 4.74). While these studies can only be considered preliminary, at this point, they nevertheless indicate that design concepts under investigation are worthy of further studies.

4.5.1 Generalised Method

For each time-point measurement a solution of the test compounds in DMSO were added to a solution containing 148 μL of cell culture medium and 50 μL of 100 mU/mL of APN enzyme in Hepes Buffer. The final concentration of DMSO was 1% and the final concentrations of test compounds were 5 μM. After each time-point 200 μL x 2 of *tert*butyl methyl ether was added, mixed thoroughly using a Velp Scientifica Rx3® vortex mixer, organic layer was removed and the aqueous phase re-extracted. The combined organic layers were reduced to a residue by use of a Pierce manifold to blow the solvent off. The residue was reconstituted in methanol (200 μL) for LCMS analysis.

4.5.2 LCMS conditions

Chromatographic analysis was carried out on a Thermo Accela® liquid chromatograph. The detector was a Thermo LTQ-XL-Orbitrap Discovery® mass spectrometer. The column used for chromatographic separation was an Acquity UPLC® HSS T3, 2.1x 150 mm 1.8 µm at 30 ºC. Mobile Phase A: 0.1% formic acid in water. Mobile Phase B: 0.1% formic acid in acetonitrile. Flow rate: 250 µL/min, Injection volume: 6µL, run time: 10 min. Gradient, 20% B to 95% B over 5.10 min, hold until 7.00 min. 20% B at 7.10 min and equilibrate for 3 min. The needle was washed with 0.1% formic acid in acetonitrile between runs.

The LTQ-XL ion trap mass spectrometer was coupled to the Accela LC system via an electrospray ionisation (ESI) probe. The capillary temperature was maintained at 400 ºC, sheath gas flow rate 50 arbitrary units, auxiliary gas flow rate 5 arbitrary units, sweep gas flow rate 0 arbitrary units, source voltage 3.20 kV, source current 100 µA, capillary voltage 43.00 V and tube lens 100 V. All compounds were detected in positive ion mode using selected ion monitoring (SIM). The optimum detector conditions were found by tuning the instrument to the highest sensitivity for each compound.

4.5.3 Release of peptide from hybrid (4.05)

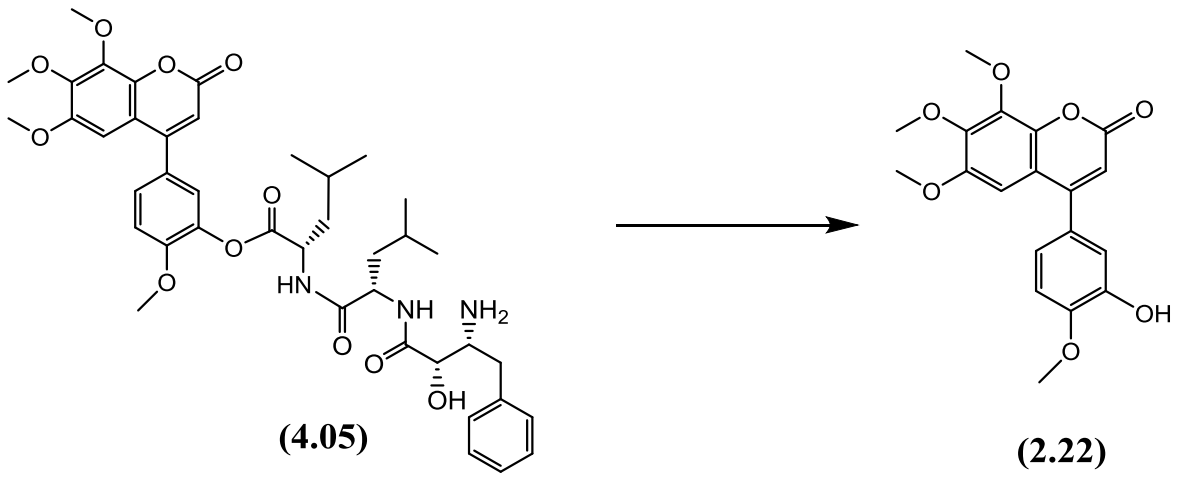

Figure 4.53. Conversion of hybrid drug (4.05) to phenol (2.22)

Chromatogram	Duration (h)	Compound present	Retention time (minutes)
(A)	0	**(4.05)**	6.70
(B)	1.5	**(4.05)** + **(2.22)**	6.70 + 7.06
(C)	2.5	**(4.05)** + **(2.22)**	6.71 + 7.07
(D)	5	**(4.05)** + **(2.22)**	6.71 + 7.07
(E)	7	**(4.05)** + **(2.22)**	6.71 + 7.07
(F)	9	**(4.05)** + **(2.22)**	6.71 + 7.07
(G)	24	**(2.22)**	7.07

Figure 4.54 Timepoint measurements for (4.05) together with respective Rts for both (4.05) and (2.22)

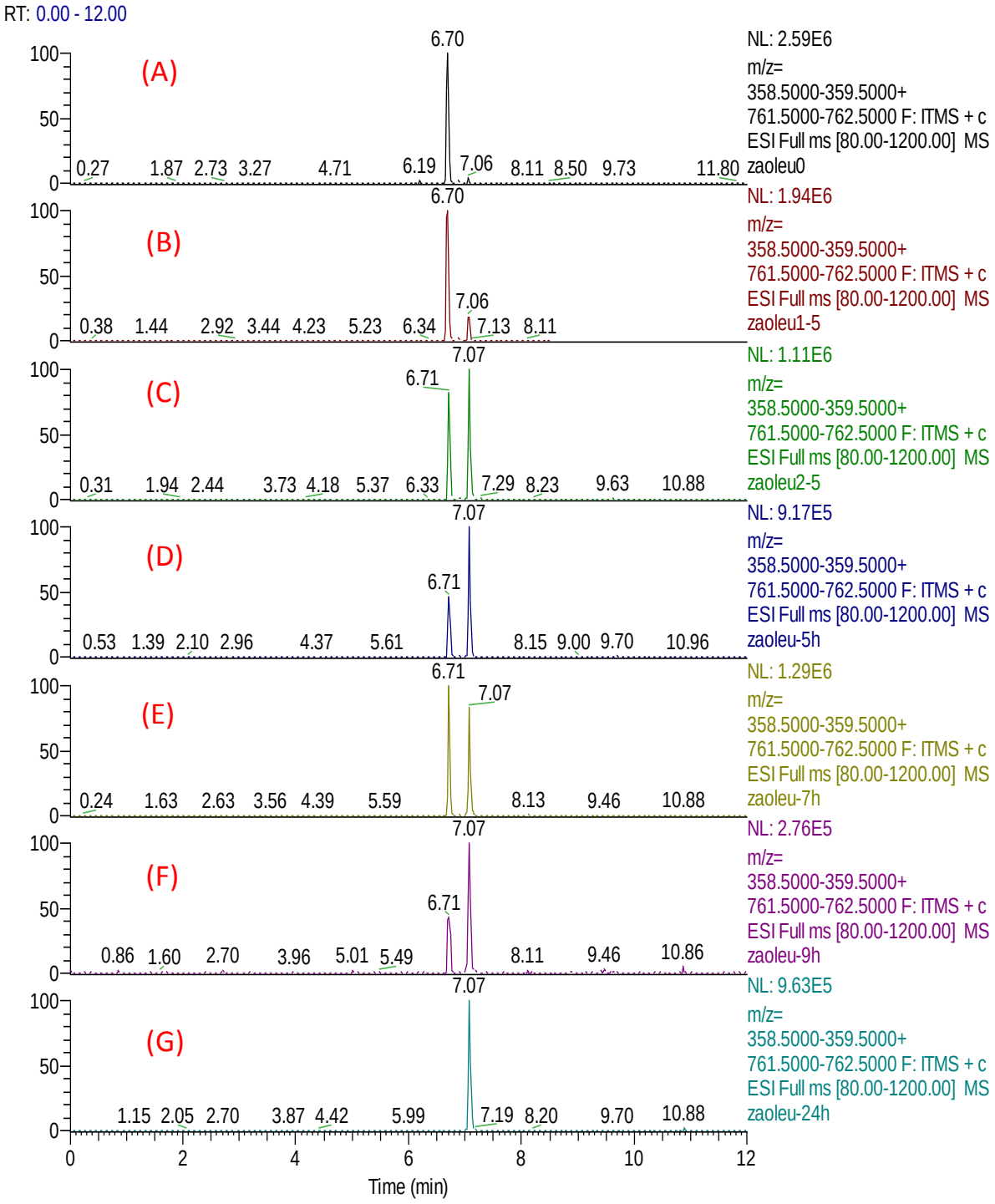

Figure 4.55. Chromatograms of the *O*-leucinebestatin conjugate (4.05) (Rt ~ 6.71 minutes) over the time course of the experiment showing generation of the active 4-phenylcoumarin (2.22) (Rt ~ 7.06 minutes)

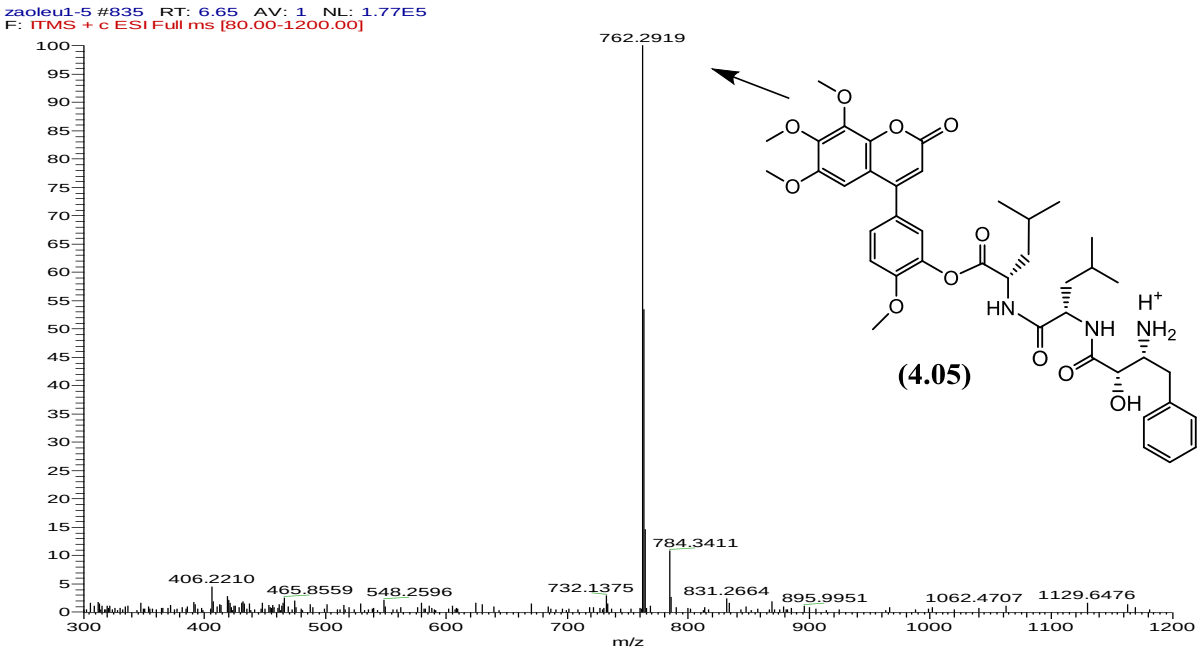

Figure 4.56. (M+H$^+$) Low resolution mass spectrum for (4.05)

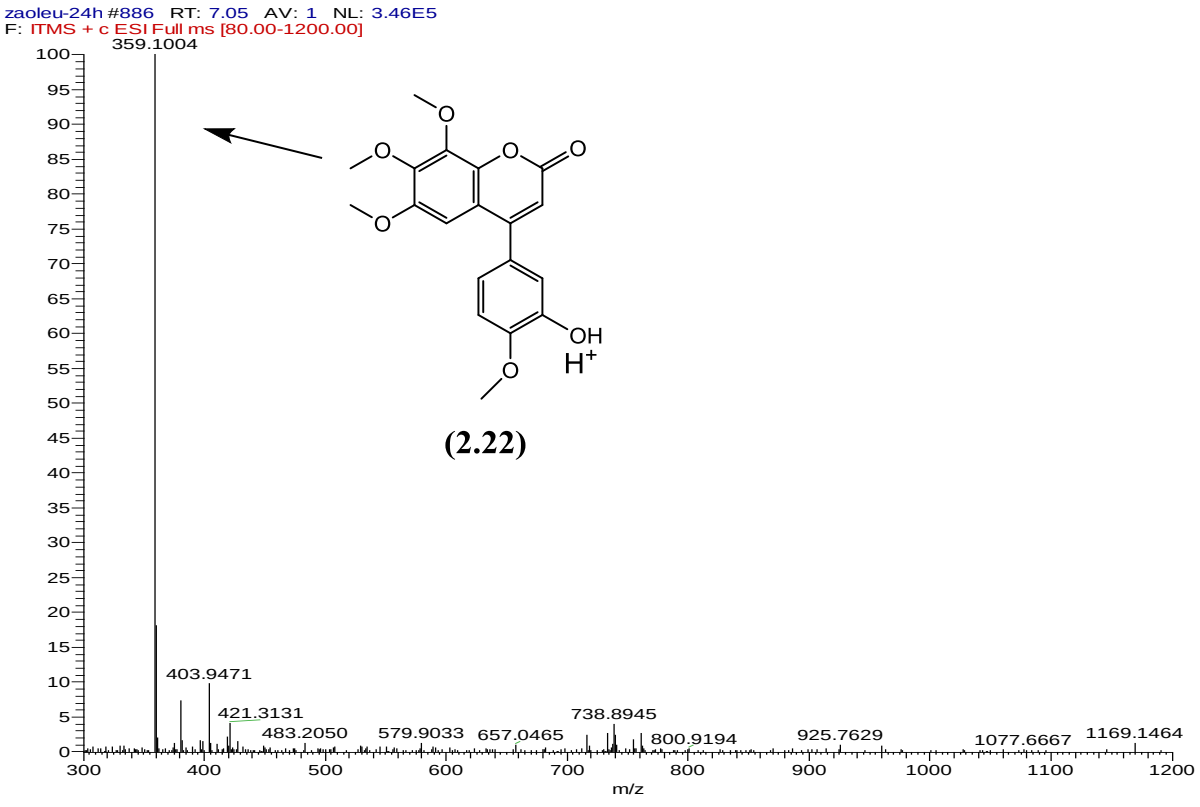

Figure 4.57. (M+H$^+$) Low resolution mass spectrum for the 4-phenylcoumarin (2.22)

4.5.4 Release of peptide from hybrid (4.08)

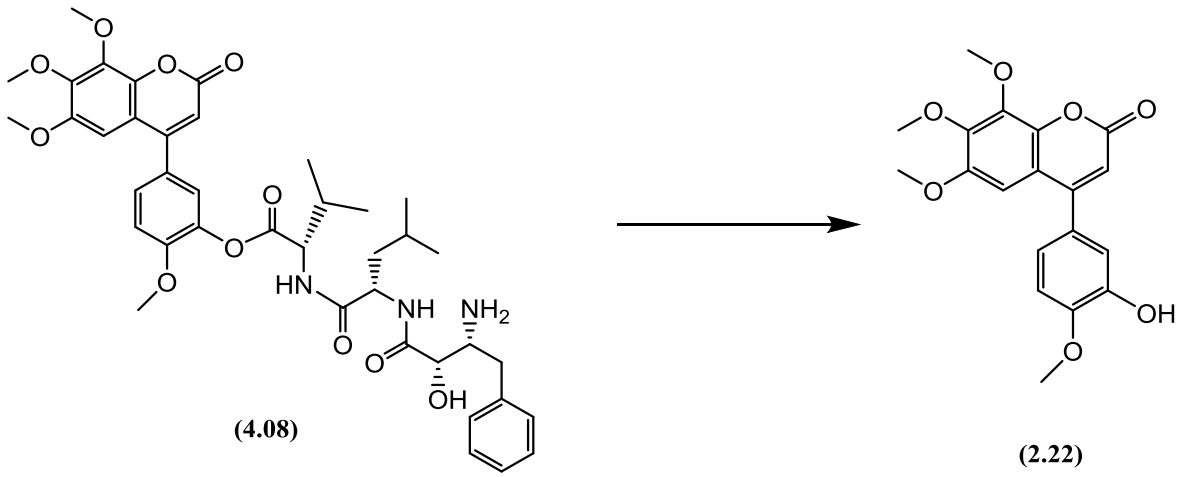

Figure 4.58. Generation of phenol (2.22) from hybrid drug (4.08)

Chromatogram	Duration (h)	Compound present	Retention time (minutes)
(A)	0	**(4.08)**	6.51
(B)	1.5	**(4.08)** + **(2.22)**	6.50 + 7.06
(C)	2.5	**(4.08)** + **(2.22)**	6.50 + 7.06
(D)	5	**(4.08)** + **(2.22)**	6.52 + 7.07
(E)	7	**(4.08)** + **(2.22)**	6.52 + 7.07
(F)	9	**(4.08)** + **(2.22)**	6.55 + 7.07
(G)	24	**(2.22)**	7.07

Figure 4.59. Timepoint measurements for (4.08) together with respective Rts for both (4.08) and (2.22)

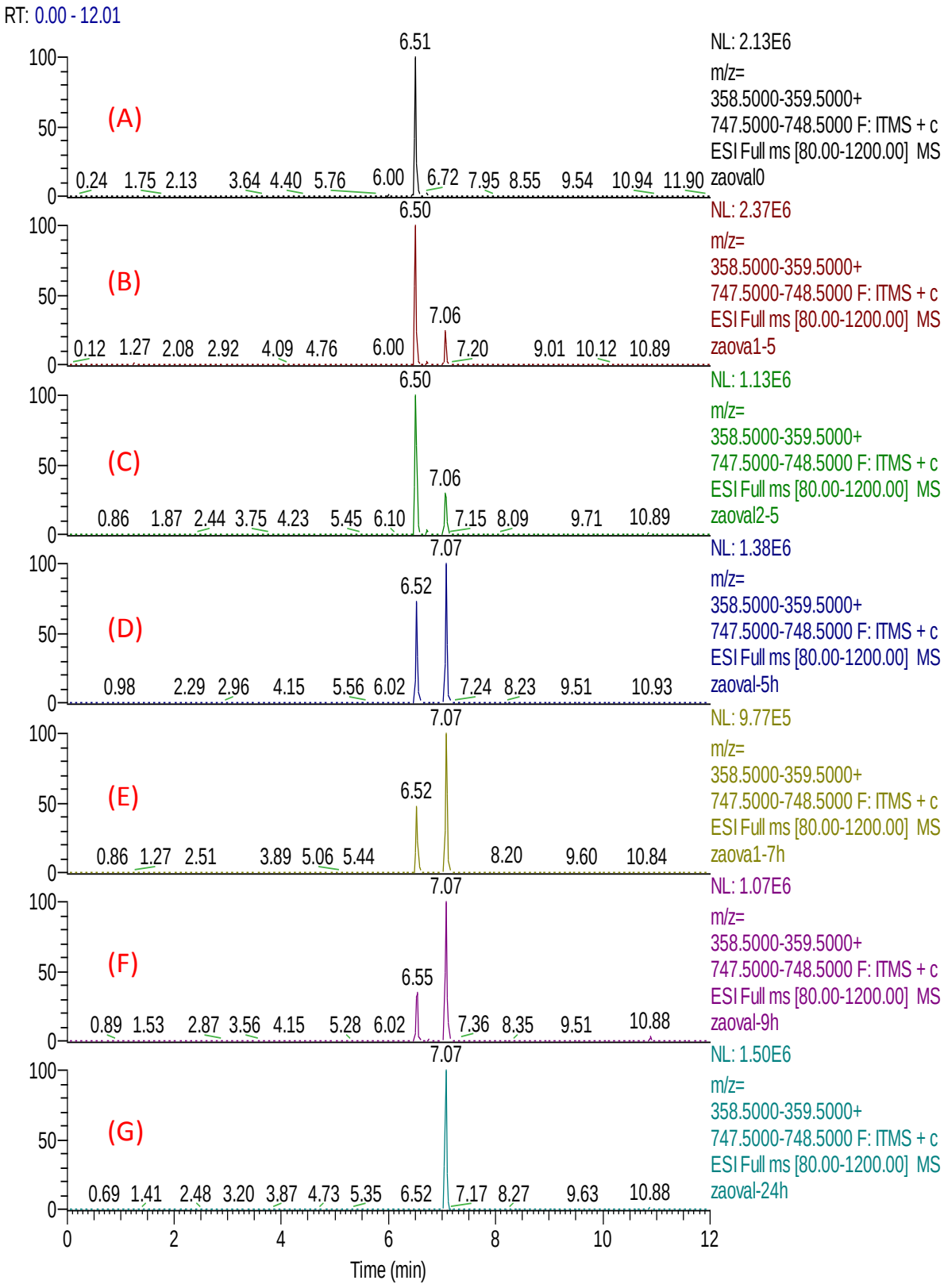

Figure 4.60. Chromatograms of the *O*-valinebestatin conjugate (4.08) (Rt ~ 6.51 minutes) over the time course of the experiment showing the generation of the active 4-phenylcoumarin (2.22) (Rt ~ 7.06 minutes)

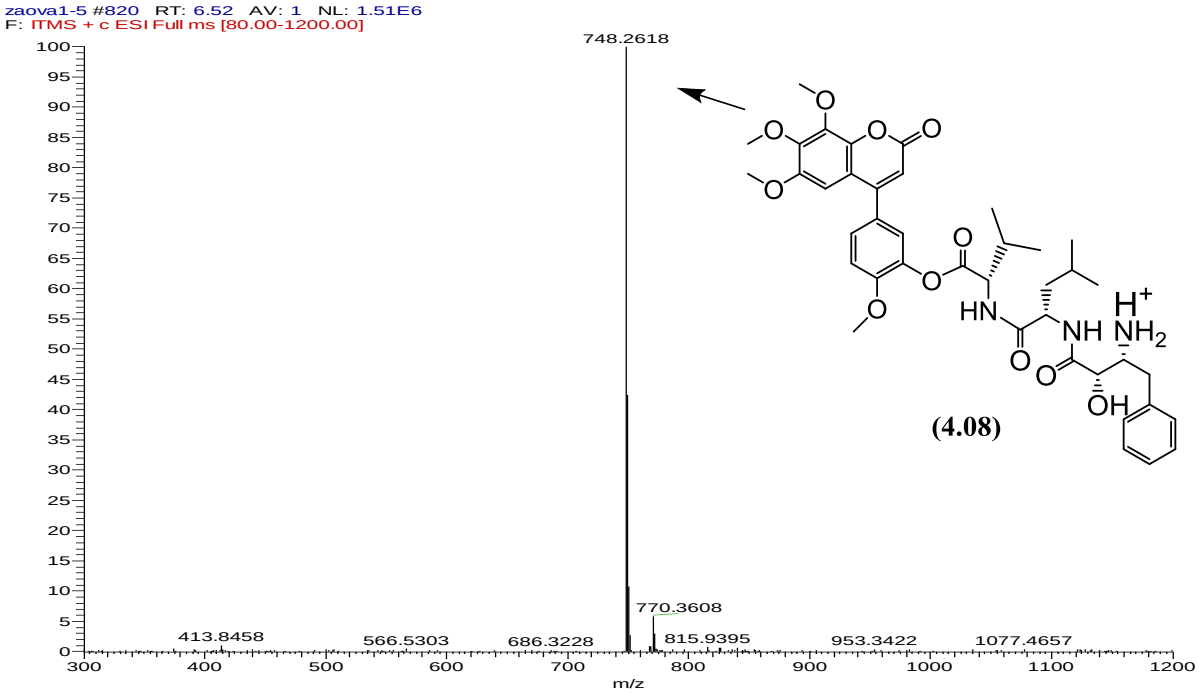

Figure 4.61. ($M+H^+$) Low resolution mass spectrum for (4.08)

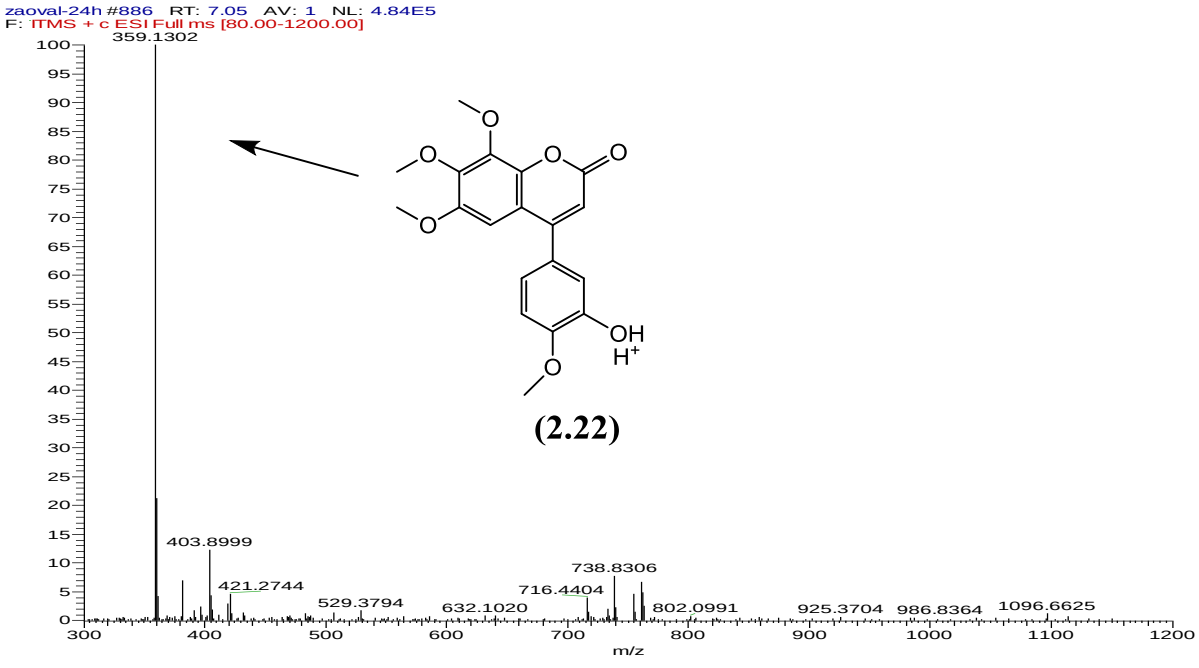

Figure 4.62. ($M+H^+$) Low resolution mass spectrum for (2.22)

4.5.5 Release of peptide from hybrid (4.11)

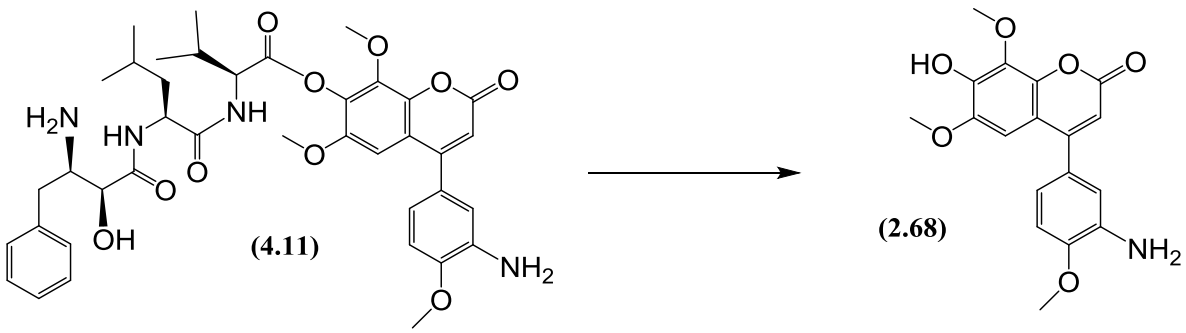

Figure 4.63. Generation of aniline (2.68) from hybrid drug (4.11)

Chromatogram	Duration (h)	Compound present	Retention time (minutes)
(A)	0	**(4.11)**	6.25
(B)	2	**(2.68)** + **(4.11)**	5.97 + 6.28
(C)	3	**(2.68)** + **(4.11)**	5.97 + 6.28
(D)	5	**(2.68)** + **(4.11)**	5.97 + 6.28
(E)	6	**(2.68)** + **(4.11)**	5.94 + 6.25
(F)	8	**(2.68)** + **(4.11)**	5.95 + 6.26
(G)	9	**(2.68)** + **(4.11)**	5.95 + 6.26
(H)	22	**(2.68)** + **(4.11)**	5.95+ 6.26

Figure 4.64. Timepoint measurements for (4.11) together with respective Rts for both (4.11) and (2.68)

Figure 4.65. Chromatograms of the *O*-valinebestatin conjugate (4.11) (Rt ~ 6.25) over the time course of the experiment showing generation of the active 4-phenylcoumarin (2.68) (Rt ~ 5.97 minutes)

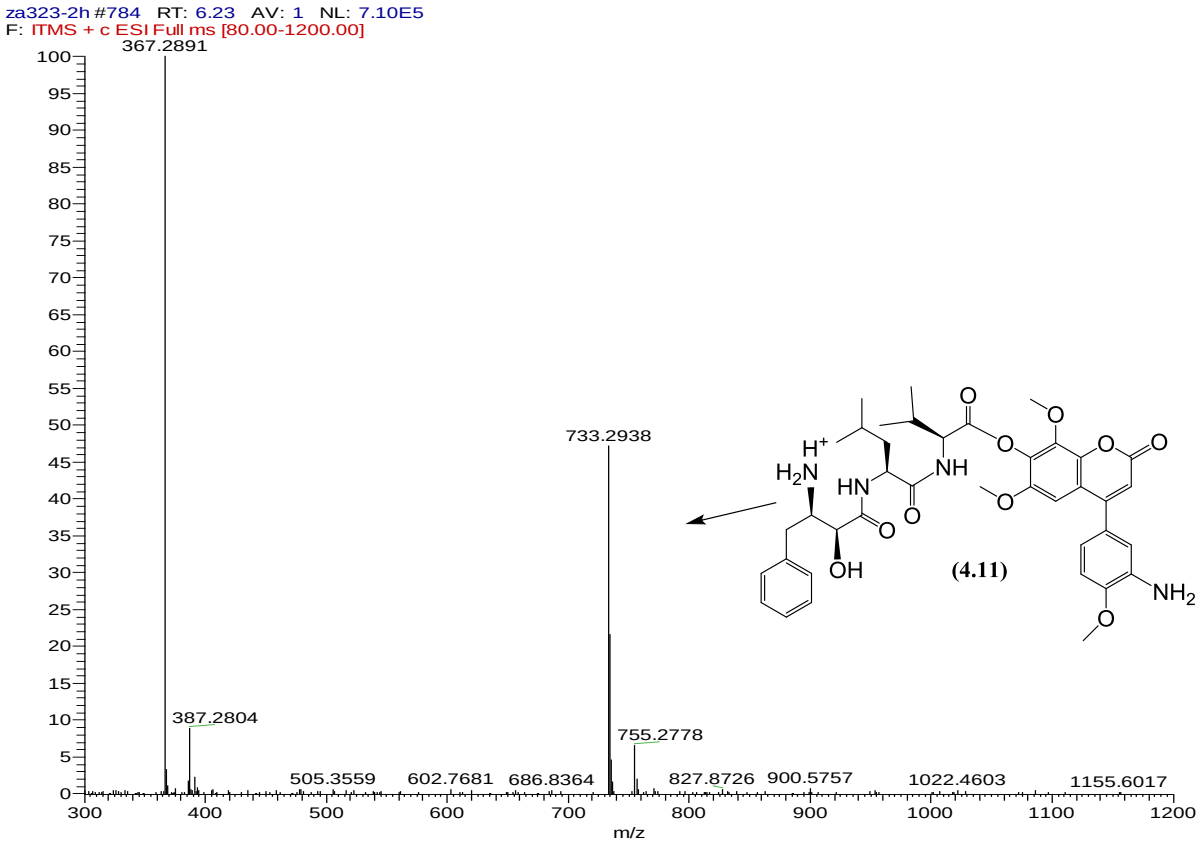

Figure 4.66. (M+H$^+$) Low resolution mass spectrum for (4.11)

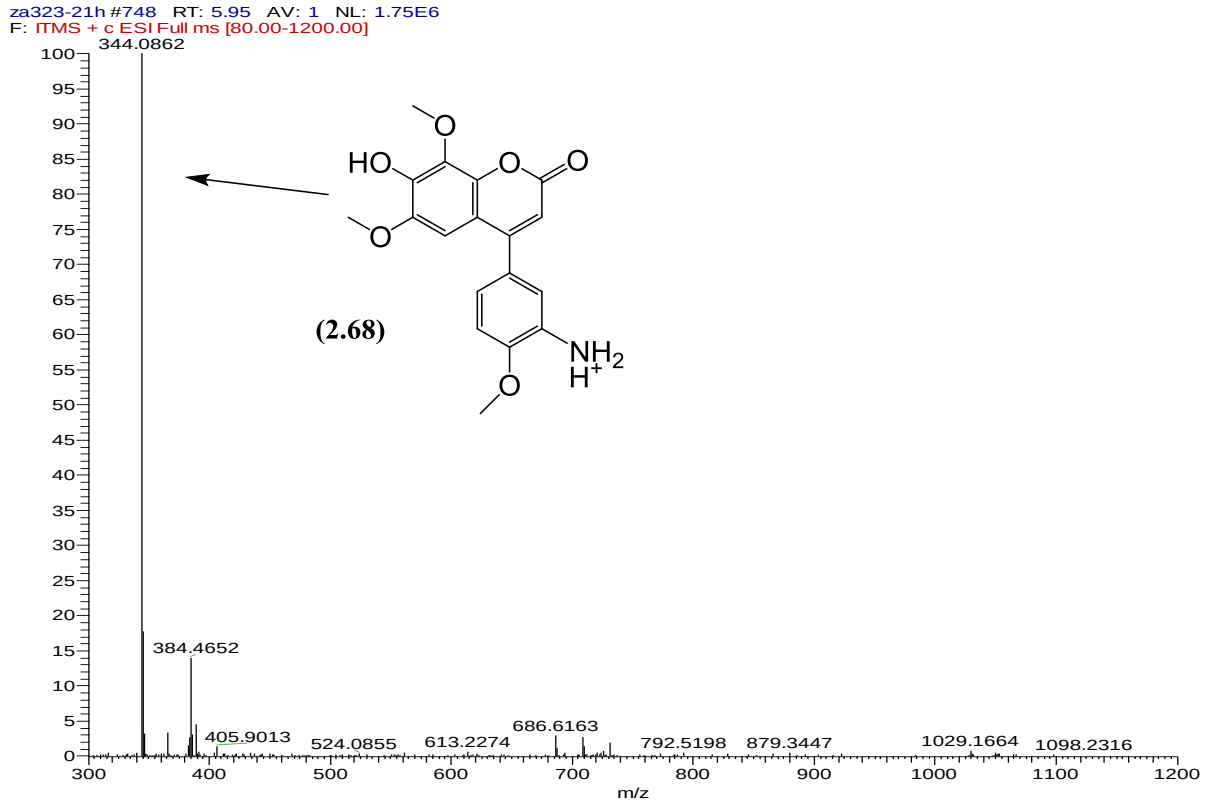

Figure 4.67. (M+H$^+$) Low resolution mass spectrum for (2.68)

4.5.6 Release of peptides from hybrid (4.19)

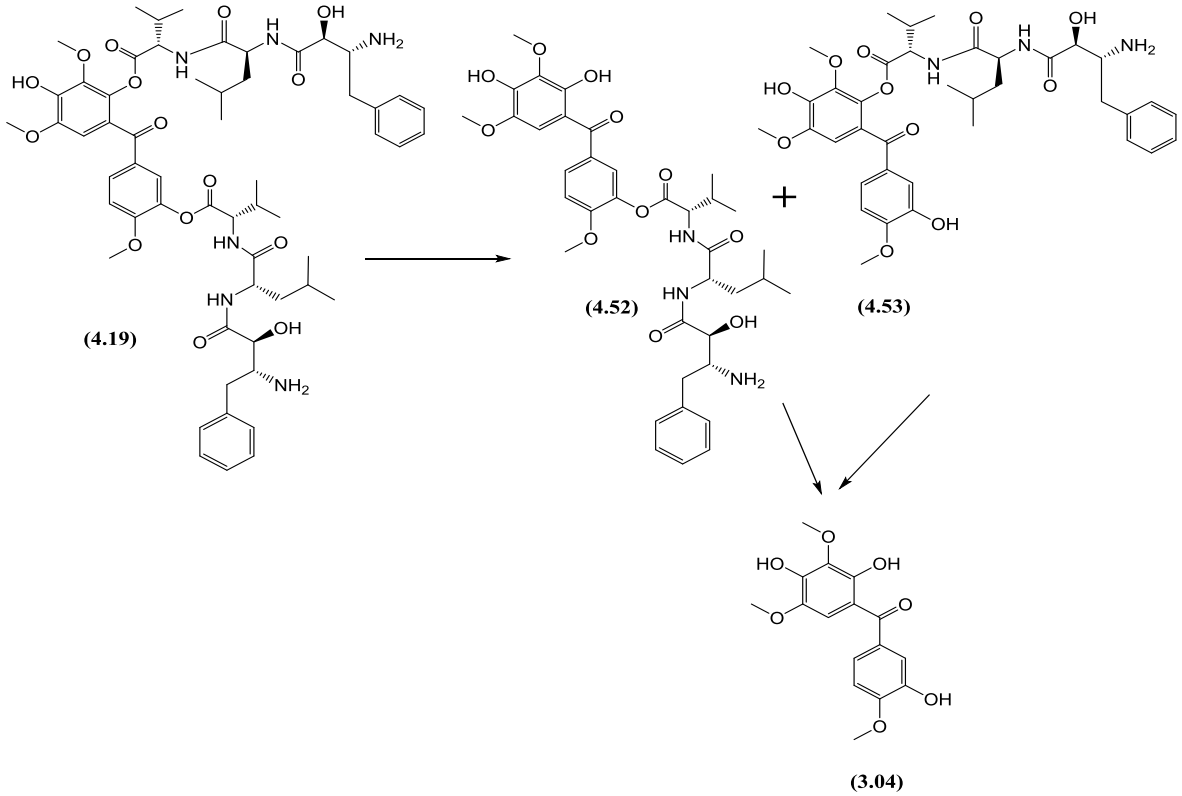

Figure 4.68. Generation of (4.52), (4.53) and (3.04) from hybrid drug (4.19)

Chromatogram	Duration (h)	Compound present	Retention time (minutes)
(A)	0	**(4.19) + (4.52) or (4.53)**	5.52 + 5.68
(B)	1	**(4.19) + (4.52) or (4.53)**	5.52 + 5.68
(C)	2	**(4.19) + (4.52) or (4.53)**	5.52 + 5.68
(D)	4	**(4.19) + (4.52) or (4.53)**	5.52 + 5.68
(E)	28	**(4.19) + (4.52) or (4.53) + (3.04)**	5.52 + 5.68 + 6.23
(F)	46	**(4.19) + (4.52) or (4.53) + (3.04)**	5.52 + 5.68 + 6.23
(G)	After 72	**(4.19) + (4.52) or (4.53) + (3.04)**	5.52 + 5.68 + 6.23

Figure 4.69 Timepoint measurements for (4.19) together with respective Rts for both (4.52), (4.53) and (3.04)

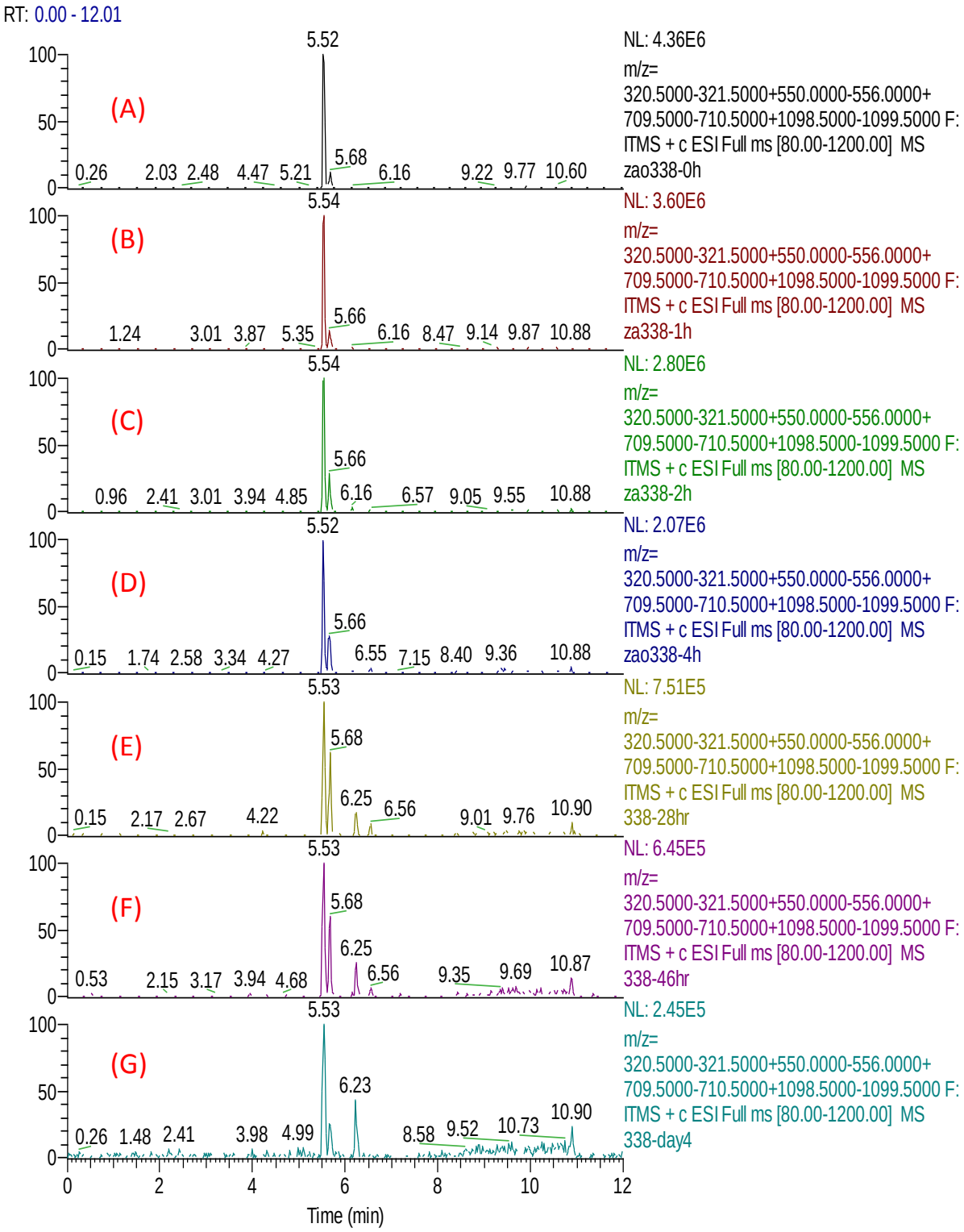

Figure 4.70. Chromatograms of the di bestatin conjugate (4.19) (Rt ~ 5.52) over the time course of the experiment showing generation of the mono-bestatin intermediate hybrid (4.52) or (4.53) (Rt ~ 5.66 minutes) and the active phenstatin derivative (3.04) (Rt ~ 6.23 minutes)

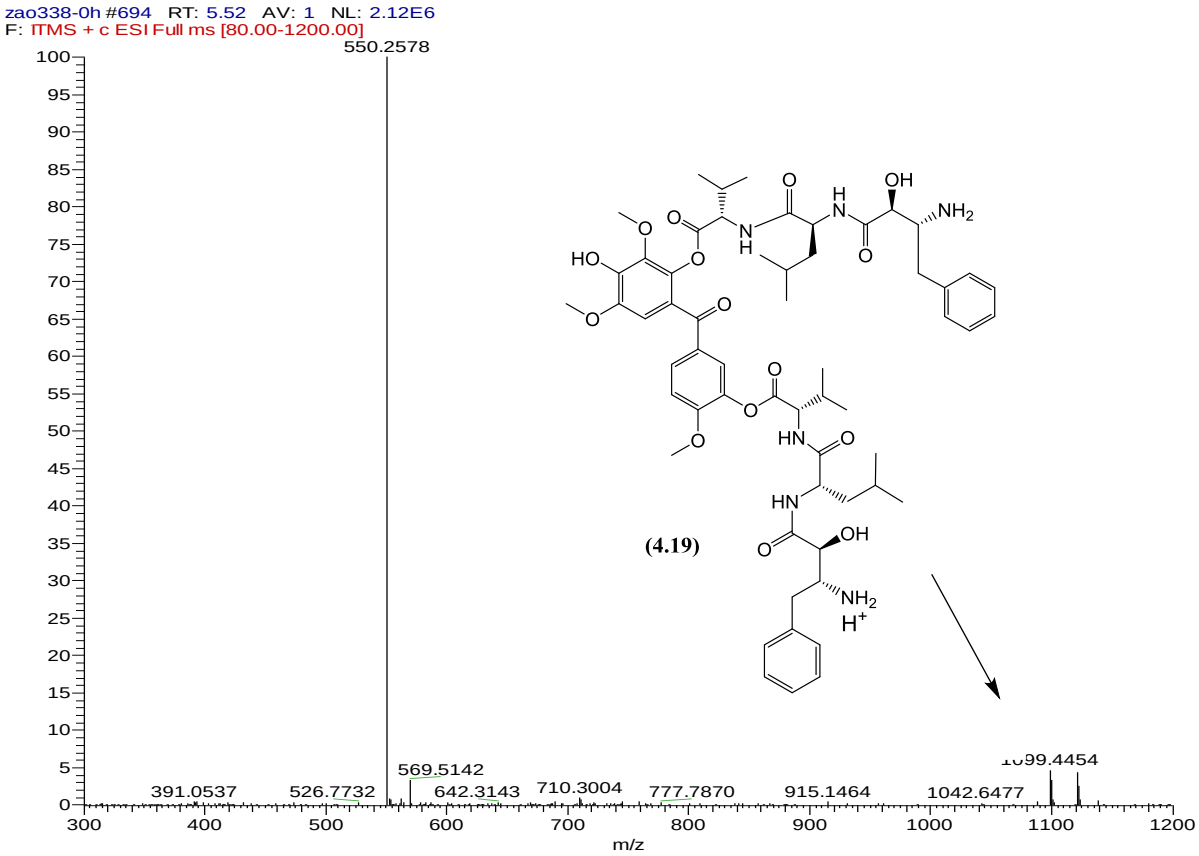

Figure 4.71. Low resolution mass spectrum of (4.19)

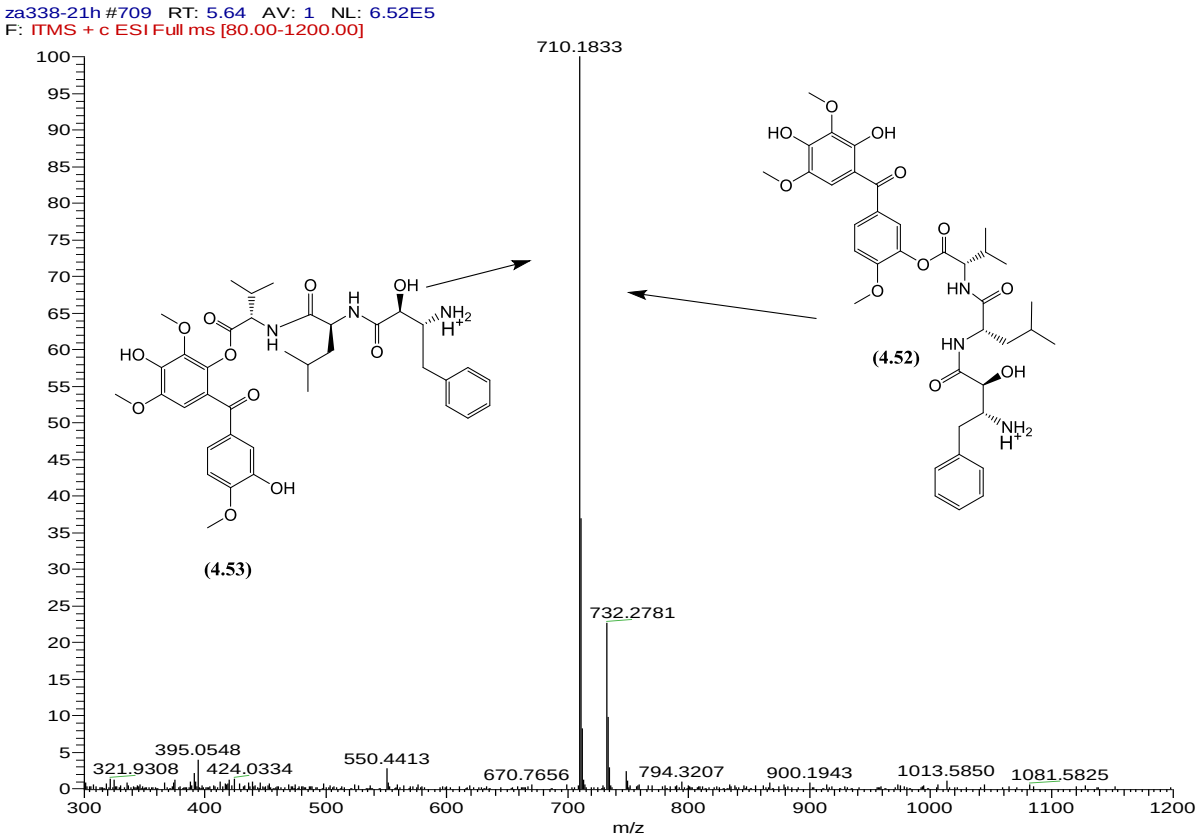

Figure 4.72. Low resolution mass spectrum of (4.52) or (4.53)

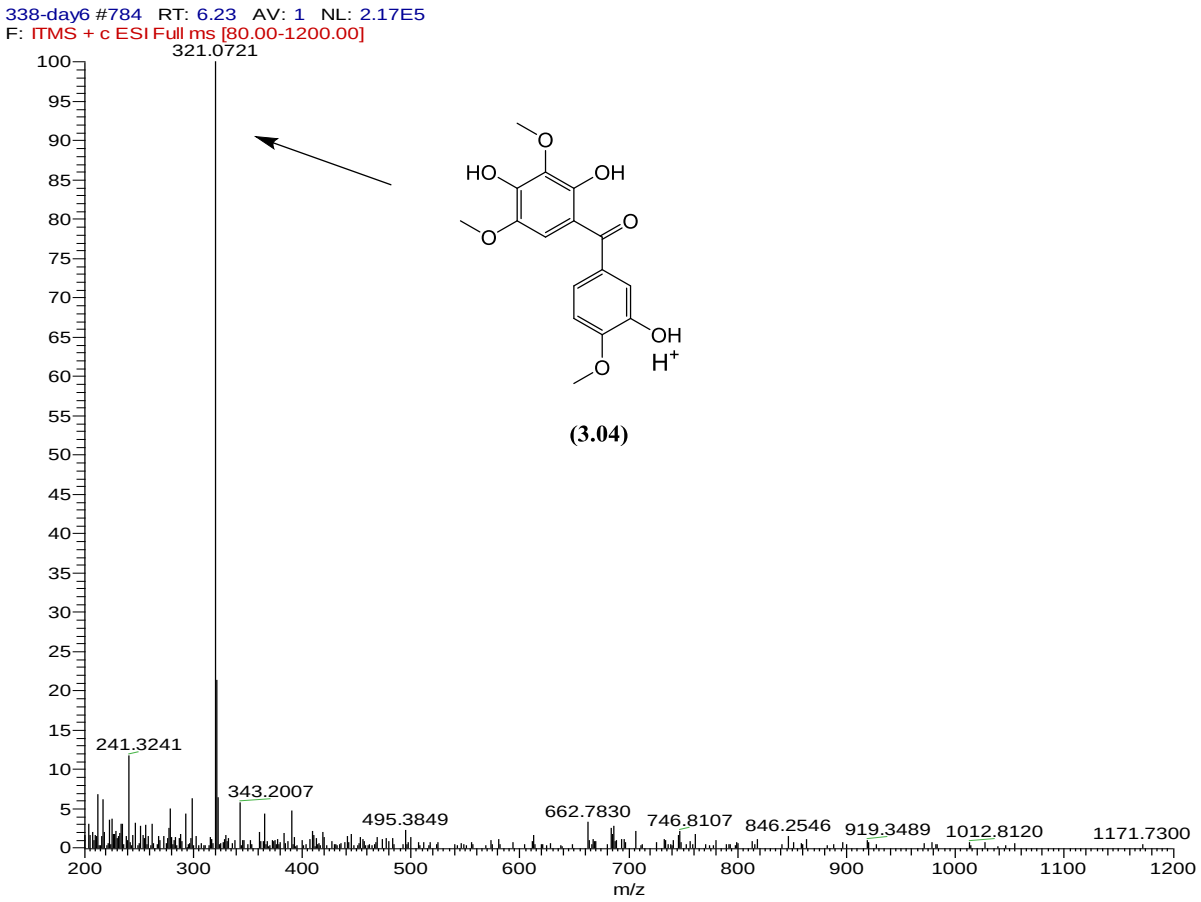

Figure 4.73. Low resolution mass spectrum of (3.04)

4.5.7 Release of peptides from hybrid (4.16)

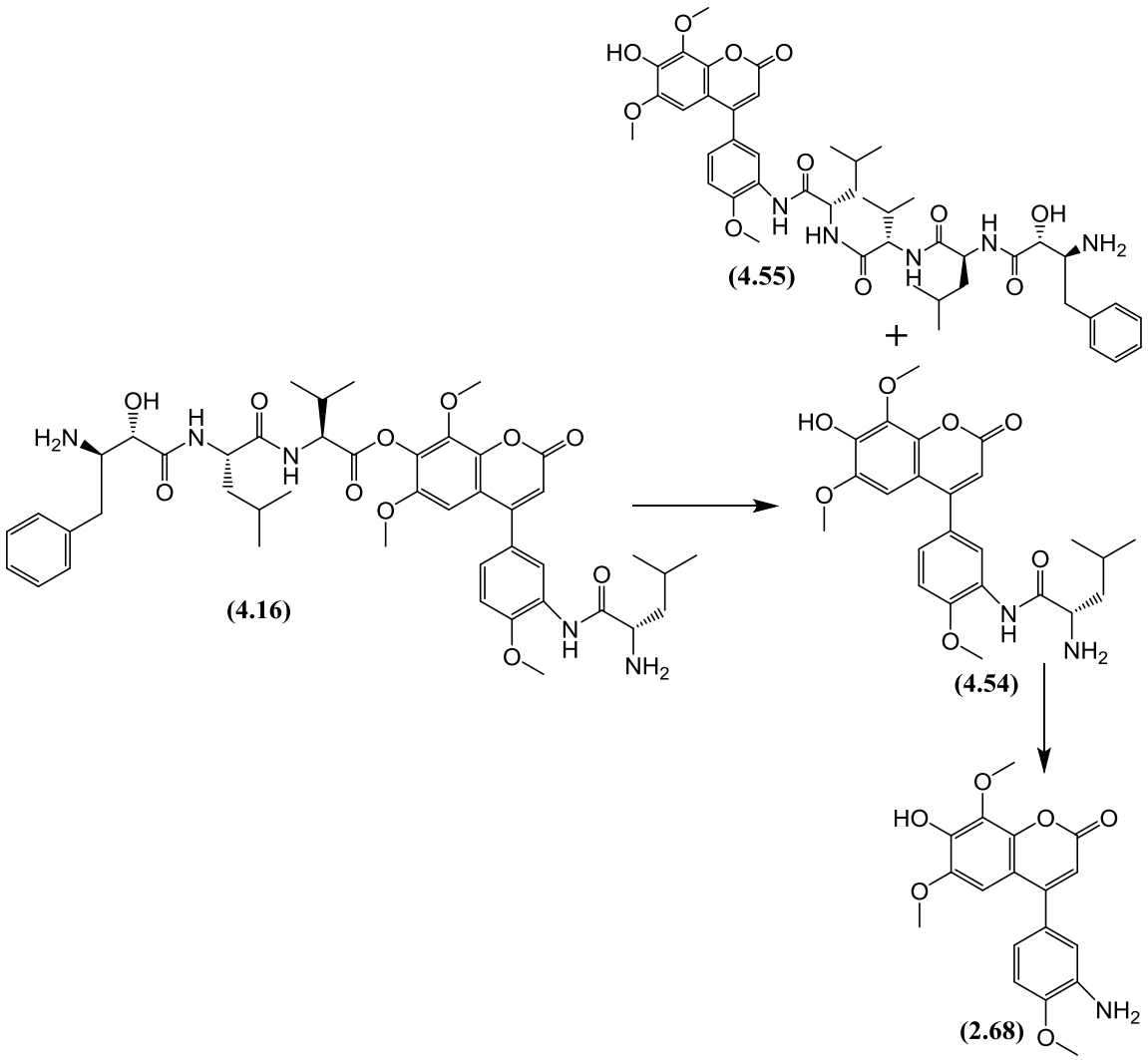

Figure 4.74. Generation of phenol (4.54), tetrapeptide (4.55) and aniline (2.68) from hybrid drug (4.16)

Chromatogram	Duration (h)	Compound present	Retention time (minutes)
(A)	0	**(4.16)**	5.42
(B)	1	**(4.54)** + **(4.16)**	5.27 + 5.42
(C)	2	**(4.54)** + **(4.16)**	5.27 + 5.44
(D)	4	**(4.54)** + **(4.16)** + **(2.68)**	5.27 + 5.44 + 5.94
(E)	10	**(4.54)** + **(2.68)**	5.27 + 5.97
(F)	28	**(4.54)** + **(2.68)** + **(4.55)**	5.30 + 5.94 + 6.18
(G)	37	**(4.54)** + **(2.68)** + **(4.55)**	5.29 + 5.95 + 6.17
(H)	Tb1	**(4.54)** + **(2.68)** + **(4.55)**	5.30+ 5.97 + 6.18

Figure 4.75. Timepoint measurements for (4.16) together with respective Rt for both (4.54) and (2.68)

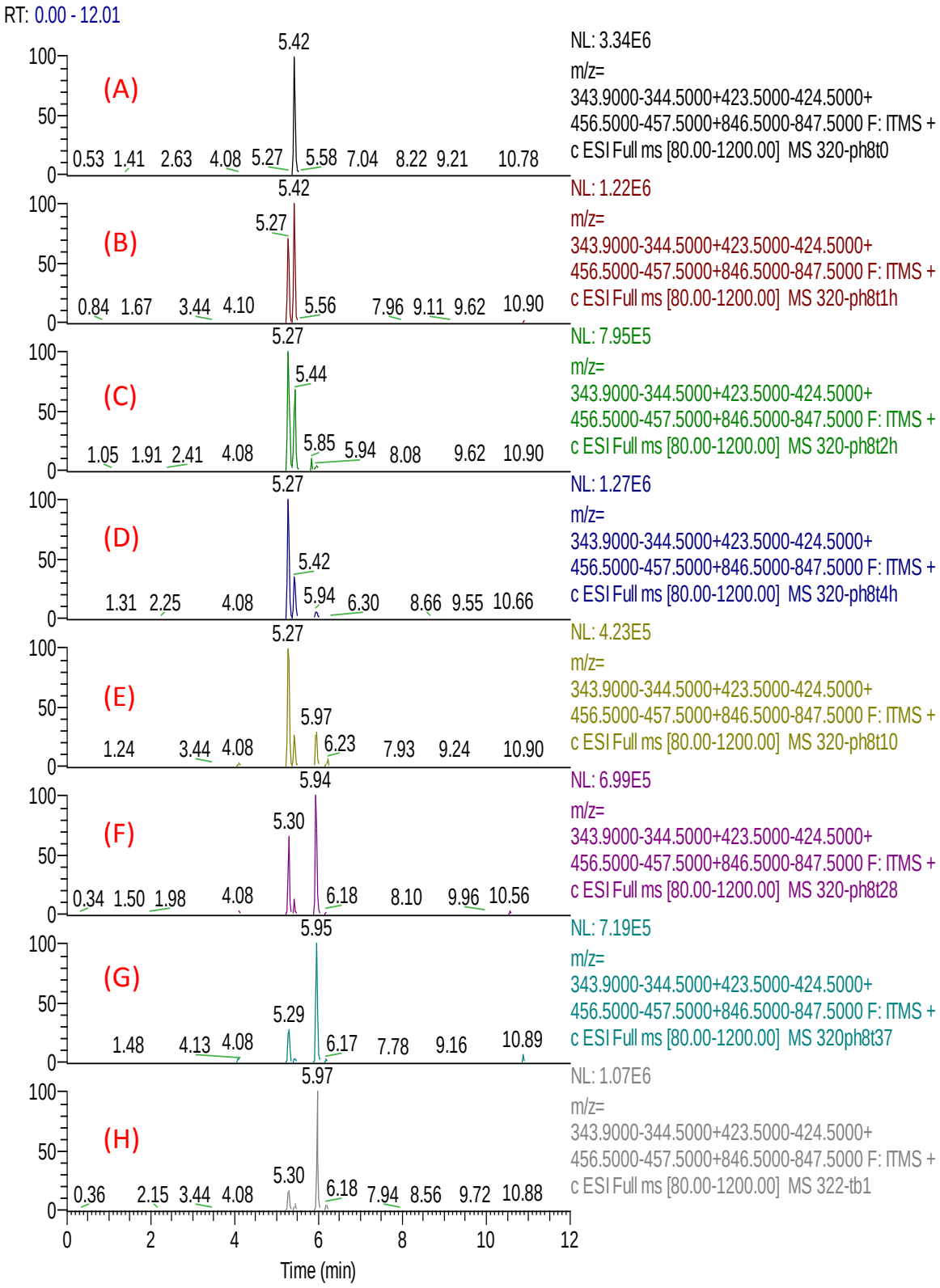

Figure 4.76. Chromatograms of (4.16) (Rt ~ 5.42) over the time course of the experiment showing generation of the pro-drug intermediate (4.54) (Rt ~ 5.27) minutes and the active 4-phenylcoumarin derivative (2.68) (Rt ~ 5.97 minutes)

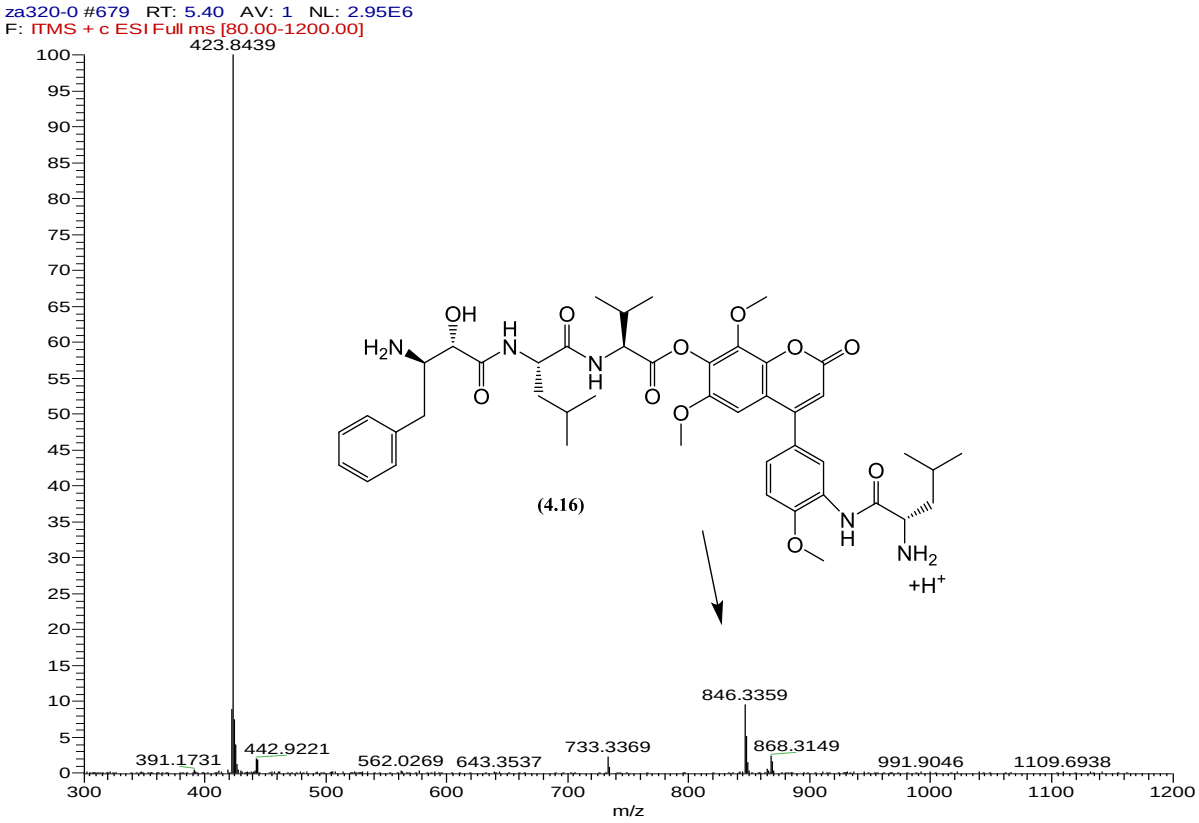

Figure 4.77. Low resolution mass spectrum of (4.16)

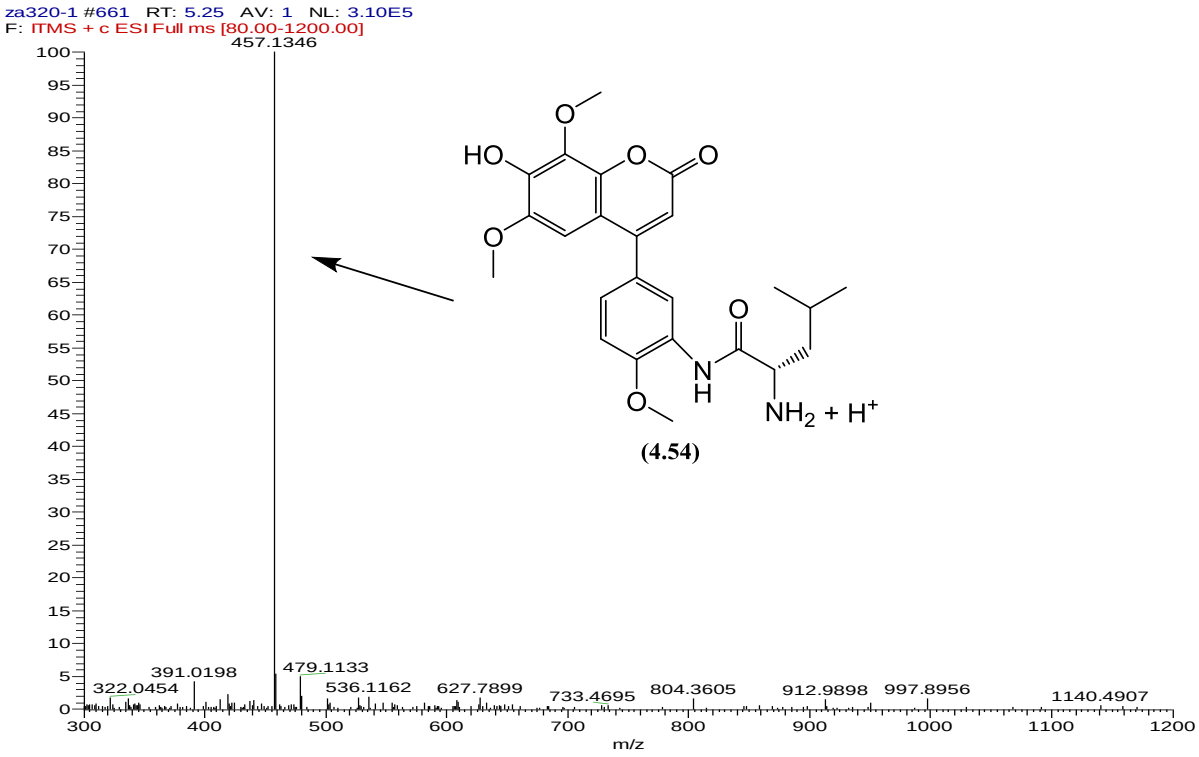

Figure 4.78: Low resolution mass spectrum of (4.54)

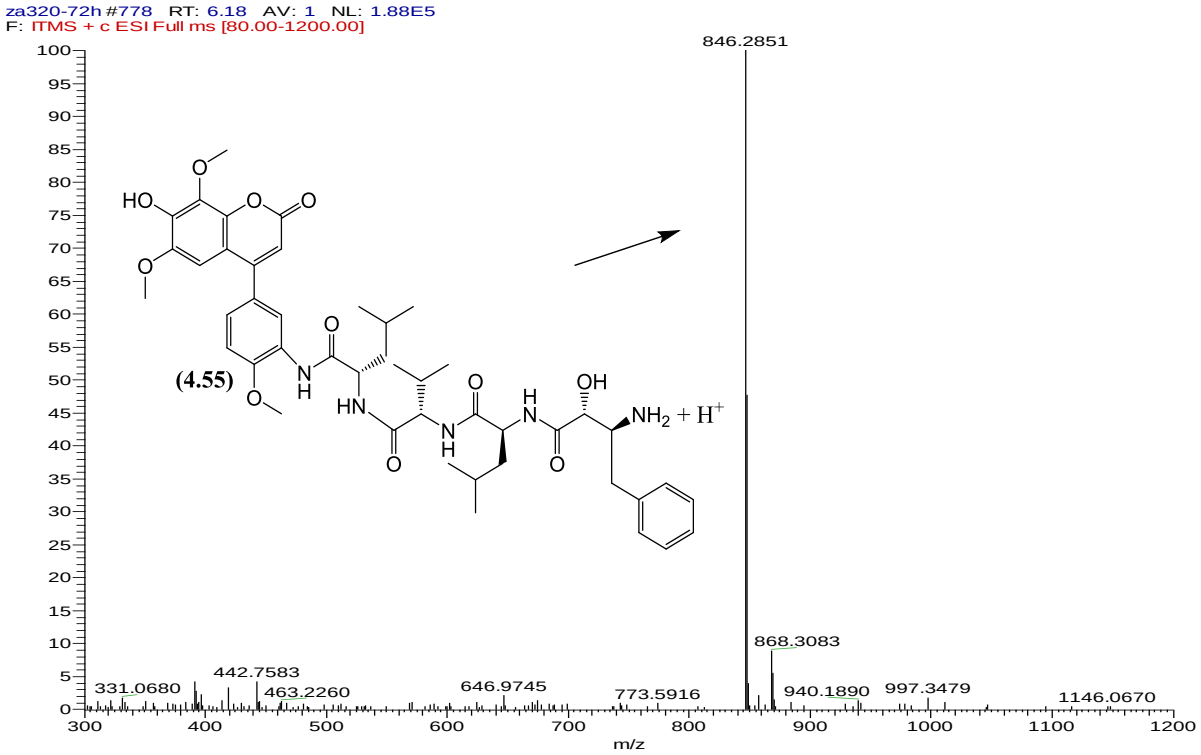

Figure 4.79. Low resolution mass spectrum of tetra-peptide (4.55)

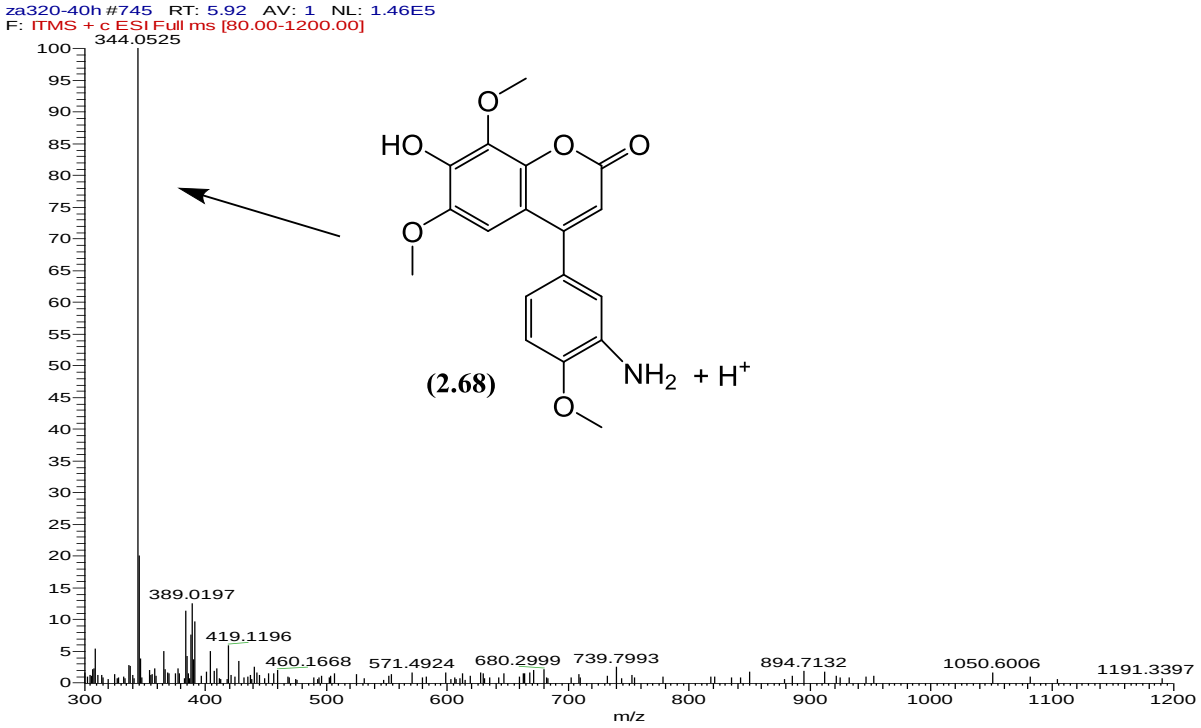

Figure 4.80. Low resolution mass spectrum of (2.68)

Chapter 5

Experimental

5.0 General methods and instruments

Most of the chemical were obtained from Sigma Aldrich and were not characterised.

High resolution mass spectroscopy (HRMS) data was obtained from a Thermo Scientific® LTQ-Orbitrap and analysis of mass spectra was carried out using the Xcalibur program.

Nuclear Magnetic Resonance (NMR) spectra were obtained primarily using a Bruker Avance III 400 and Bruker Avance II 600 NMR spectrophotometer at 25 °C. NMR spectra were analysed using ACD/NMR Processor Academic Edition software version12.01. The following abbreviations were used during NMR assignments; s=singlet, d=doublet, t=triplet, q=quartet, m=multiplet, br=broad, dd=double doublet, ArH=aromatic hydrogen, ArC=aromatic quaternary carbon, ArCH=aromatic carbon having hydrogen attached.

Infrared (IR) spectra were obtained using Perkin Elmer® FT-IR spectrophotometer spectrum 100.

Melting points were determined using Electrotherm® melting point apparatus.

Compound were named using ChemDraw Professional version 15.0.

Column chromatography was performed using silica gel 60 (230-400 mesh) while thin layer chromatography was carried out using Merck silica gel F254 pre-coated aluminium sheets. For visualisation of compounds, UV light at 254 and 365 nm wavelength along with the variety of spray reagents was used.

Anhydrous DCM was obtained by distillation over powdered calcium hydride. Anhydrous THF was prepared by refluxing over lithium aluminium hydride as well as obtained from fisher scientific Ireland.

5.1 Experimental Chapter 2

Synthesis of 2,3,4-trimethoxyphenol (2.01)

2,3,4–trimethoxybenzaldehyde (50 g, 0.255 moles) and hydrogen peroxide (37.6 mL, 30% solution) were stirred together at 0 °C, followed by addition of concentrated sulphuric acid (5 mL) drop wise very slowly during one hour with proper stirring. The reaction mixture was further stirred for 30 minutes at 0 °C. Methanol (250 mL) was carefully added portion wise and kept the reaction at 0 °C for one hour. After which the reaction was quenched with aq.NaOH (200 mL, 2 M) and methanol removed using rotary evaporator. The remaining aqueous layer was washed with dichloromethane (3×250 mL).The aqueous layer was then acidified with aq.HCl (250 mL, 2M) and extracted with dichloromethane (3×250 mL). The solvent was evaporated to afford the crude product which was further purified by column chromatography (1:4, ethyl acetate:hexane) to afford the phenol **(2.01)** (38.5 g, 0.190 moles, 82%) as brown oil.

^{1}H NMR (400 MHz, CHLOROFORM-*d*) δ_H ppm: 3.83 (3 H, s, OCH_3), 3.92 (3 H, s, OCH_3), 3.98 (3H, s, OCH_3), 5.43 (1H, br.s, OH), 6.58 (1H, d, ArH, J = 8.6 Hz), 6.64 (1 H, d, ArH, J= =8.6 Hz);

^{13}C NMR (101 MHz, CHLOROFORM-*d*) δ_C ppm: 56.6 (OCH_3), 60.9 (OCH_3), 61.3 (OCH_3), 107.6 (ArCH), 108.5 (ArCH), 140.7 (ArC), 142.3 (ArC), 143.3 (ArC), 146.9 (ArC);

V_{max} cm^{-1}: 3423, 2940, 2835, 1601, 1491, 1480, 1091;

HRMS: Calculated 184.0736, found 183.0675 ($M - H^+$).

Synthesis of intermediate 2, 3, 4-trimethoxyphenyl acetate (2.02)

Phenol **(2.01)** (4.28 g, 0.023 moles) and sodium acetate (4.19 g, 0.0511 moles) were stirred together in acetic anhydride (22 mL). The resultant solution was refluxed for 4 hours. Afterwards the reaction mixture was concentrated using rotary evaporator under strong vacuum and the remainder was dissolved in water (50 mL) and extracted with DCM (3×50 mL). After evaporation of the organic solvent, the reaction was re-dissolved in diethyl ether (50 mL) and washed successively with water (3×50 mL). The organic layer was dried

with magnesium sulphate and concentrated under reduced pressure to afford the product **(2.02)** (4.08 g, 0.018 moles, 78%) as light brown oil.

^{1}H NMR (400 MHz, CHLOROFORM-*d*) δ_H ppm: 2.33 (3 H, s, CH_3), 3.87 (3 H, s, OCH_3), 3.91 (3 H, s, OCH_3), 3.91 (3 H, s, OCH_3), 6.64 (1 H, d, ArH, J = 9 Hz), 6.76 (1 H, d, ArH, J = 9 Hz);

^{13}C NMR (101 MHz, CHLOROFORM-*d*) δ_C ppm: 20.8 (CH_3), 55.7 (OCH_3), 60.5 (OCH_3), 60.6 (OCH_3), 105.9 (ArCH), 116.2 (ArCH), 137.3 (ArC), 142.6 (ArC), 145.3 (ArC), 151.3 (ArC), 169.1 (C=O);

V_{max} cm^{-1}: 3509, 2995, 2942, 2837, 1768, 1635, 1600, 1490, 1241, 1207, 1095, 1051;

HRMS: Calculated 226.0841 found 249.0729 ($M + Na^+$), 227.2266 (M + H).

Synthesis of 1-(2-hydroxy-3, 4, 5-trimethoxyphenyl) ethan-1-one (2.03)

Ester **(2.02)** (4.08 g, 0.018 moles) was dissolved in glacial acetic acid (5 mL), followed by the dropwise addition of boron trifluoride diethyl etherate (7.76 mL, 0.063 moles). The reaction was refluxed for 2 hours. Afterward reaction mixture was cooled to room temperature, poured into aq.NaOH (100 mL, 2.5 M) and extracted with DCM (3×100 mL). The reaction was then dried using magnesium sulphate and concentrated *in vacuo*. Finally the brown solid was purified by flash column chromatography (1:2, ethyl acetate:hexane) to afford the product **(2.03)** (3.11 g, 0.014 moles, 76%) as yellow solid.

^{1}H NMR (400 MHz, CHLOROFORM-*d* δ_H ppm: 2.52 (3 H, s, CH_3), 3.79 (3 H, s, OCH_3), 3.85 (3 H, s, OCH_3), 3.97 (3 H, s, OCH_3), 6.87 (1 H, s, ArH), 12.39 (1 H, s, OH);

^{13}C NMR (101 MHz, CHLOROFORM-*d*) δ_C ppm: 26.3 (CH_3), 56.3 (OCH_3), 60.6 (OCH_3), 60.9 (OCH_3), 106.9 (ArCH), 113.7 (ArC), 140.9 (ArC), 144.6 (ArC), 149.4 (ArC), 152.7 (ArC), 202.7 (C=O);

V_{max} cm^{-1}: 3007, 2976, 2938, 2834, 1625, 1489, 1269, 1070, 961, 812, 726;

HRMS: Calculated 226.0841, found 227.0905 ($M + H^+$);

MP: 75 – 78 °C.

Synthesis of intermediate 4-hydroxy-6, 7, 8-trimethoxychromen-2-one (2.04)

Keto-phenol **(2.03)** (3.11 g, 0.014 moles) was dissolved in diethyl carbonate (40 mL) and stirred while sodium hydride (5.5 g, 0.229 moles, 60% dispersion in oil) was very slowly added. The resultant green mixture was refluxed for 5 hours and then left stirring overnight at room temp. After completion the reaction was quenched with minimum amount of methanol. The reaction was then poured into diethyl ether (100 mL) and extracted with water (5×50 mL). The combined aqueous layers were then acidified with dilute aq.HCl (50 mL) and extracted with DCM (5×50 mL). The organic layers were dried with magnesium sulphate, filtered and solvent evaporated using rotary evaporator. The solid residue obtained was washed with diethyl ether and dried under high vacuum to afford the product **(2.04**) (2.50 g, 0.010 moles, 72%) as white solid.

^{1}H NMR (400 MHz, DMSO-d_6) δ ppm: 3.86 (3 H, s, OCH_3), 3.87 (3 H, s, OCH_3), 3.90 (3 H, s, OCH_3), 5.55 (1 H, s, C=CH), 7.07 (1 H, s, ArH), 12.56 (1 H, br.s, OH);

^{13}C NMR (101 MHz, DMSO-d_6) δ ppm: 56.0 (OCH_3), 61.0 (OCH_3), 61.4 (OCH_3), 90.0 (C=CH), 99.2 (ArCH), 111.1 (ArC), 140.5 (ArC), 142.4 (ArC), 145.6 (ArC), 149.3 (ArC), 161.8 (C=CH), 165.7 (C=O);

V_{max} cm^{-1}: 3332, 2931, 1742, 1554, 1433, 1381;

HRMS: Calculated 252.0634, found 251.0571 ($M - H^+$).

Synthesis of intermediate 6, 7, 8-trimethoxy-2-oxochromen-4-yl trifluoromethanesulfonate (2.05)

4-hydroxycoumarin intermediate **(2.04)** (3 g, 0.012 moles) was stirred with triethylamine (2.2 mL, 0.015 moles) in anhydrous DCM (30 mL) at 0 °C under the atmosphere of nitrogen. To this solution was added trifluoromethanesulfonic anhydride (4.4 g, 2.6 mL, 0.0156 moles) dropwise at 0 °C through a syringe. Reaction was allowed to stir for 1 hour. After 1 hour the reaction mixture was directly poured on to silica column and purified by column chromatography (1:9, ethyl acetate:hexane) to afford the triflate **(2.05)** (3.6 g, 0.009 moles, 79%) as light yellow oil that solidified on further vacuum drying.

^{1}H NMR (400 MHz, CHLOROFORM-*d*) δ_H ppm: 3.95 (3 H, s, OCH_3), 4.06 (6 H, s, 2×OCH_3), 6.44 (1 H, s, C=CH), 6.85 (1 H, s, ArH);

^{13}C NMR (101 MHz, CHLOROFORM-*d*) δ_C ppm: 55.9 (OCH_3), 61.2 (OCH_3), 61.6 (OCH_3), 97.3 (C=<u>C</u>H), 104.1 (ArCH), 108.1 (ArC), 116.4 (CF_3), 140.9 (ArC), 142.6 (ArC), 147.4 (ArC), 150.3 (ArC), 156.7 (<u>C</u>=CH), 159.1 (C=O);

^{19}F NMR (376 MHz, CHLOROFORM-*d*) δ_F ppm: 73.3 (CF_3);

V_{max} cm^{-1}: 2947, 1737, 1571, 1422, 1396, 1282, 1262, 1174, 1037;

HRMS: Calculated 384.0127, found 385.0198 ($M + H^+$);

MP: 151-153 °C.

Synthesis of 3-oxo-3-(2,3,4-trimethoxyphenoxy)propanoic acid (2.06)

Phenol **(2.01)** (1 g, 0.0054 moles) was dissolved in toluene (20 mL). To this was added Meldrum's acid (0.865 g, 0.006 moles) and the resultant mixture was refluxed for 6 hours. Afterwards the solvent was evaporated using rotary evaporator, while the remainder was purified by column chromatography (1:3:0.03, ethyl acetate:hexane:formic acid) to afford the product **(2.06)** (0.933 g, 0.0034 moles, 63%) as brown viscous oil.

^{1}H NMR (400 MHz, DMSO-d_6) δ ppm: 3.66 (2 H, s, CH_2), 3.74 (3 H, s, OCH_3), 3.76 (3 H, s, OCH_3), 3.79 (3 H, s, OCH_3), 6.81 (2 H, q, ArH);

^{13}C NMR (101 MHz, DMSO-d_6) δ ppm: 41.7 (CH_2), 56.5 (OCH_3), 61.0 (OCH_3), 61.4 (OCH_3), 107.4 (ArCH), 117.3 (ArCH), 137.4 (ArC), 142.9 (ArC), 145.7 (ArC), 152.0 (ArC), 166.1 (<u>C</u>=O), 168.1 (<u>C</u>=O);

V_{max} cm^{-1}: 3353, 2930, 1433, 1269, 1155;

HRMS: Calculated 270.0740, found 293.3559 ($M + Na^+$).

Synthesis of 4-hydroxy-6,7,8-trimethoxy-2H-chromen-2-one (2.04) using Eaton's reagent

Acid **(2.06)** (7.5 g, 0.028 moles) was stirred in Eaton's reagent (30 mL) at 70 °C for 2 hours. After 2 hours the reaction mixture was cooled to room temperature, quenched with 150 mL of ice cooled water and extracted with DCM and methanol (8:2, 5×100 mL). The crude residue obtained was finally washed several time with diethyl ether to afford the 4-Hydroxy coumarin **(2.04)** (5 g, 0.020 moles, 71%) as off-white solid.

^{1}H NMR (400 MHz, DMSO-d_6) δ ppm: 3.86 (3 H, s, OCH_3), 3.87 (3 H, s, OCH_3), 3.90 (3 H, s, OCH_3), 5.55 (1 H, s, C=CH), 7.07 (1 H, s, ArH), 12.56 (1 H, br.s, OH);

^{13}C NMR (101 MHz, DMSO-d_6) δ ppm: 56.0 (OCH_3), 61.0 (OCH_3), 61.4 (OCH_3), 90.0 (C=CH), 99.2 (ArCH), 111.1 (ArC), 140.5 (ArC), 142.4 (ArC), 145.6 (ArC), 149.3 (ArC), 161.8 (C=CH), 165.7 (C=O);

V_{max} cm^{-1}: 3332, 2931, 1742, 1554, 1432, 1381;

HRMS: Calculated 252.0634, found 251.0571 ($M - H^+$).

Synthesis of Phenolic C-ring:

Synthesis of intermediate 5-bromo-2-methoxyphenyl formate (2.07)

To a solution of 5-bromo-2-methoxybenzaldehyde (20 g, 0.093 moles) in DCM (80 ml) was added *m*CPBA (25 g, 0.112 moles, 77% purity) in DCM (160 mL) at 0 °C. The reaction mixture was allowed to stir for 16 hours at the same temperature. Afterwards the reaction mixture was passed through a cotton plug with DCM to remove *m*CPBA precipitate before being concentrated using rotary evaporation. The resultant fraction was then washed with aq.$NaHCO_3$ solution (3×300 mL, 5%), water (500 mL) and saturated NaCl solution (500 mL) sequentially. Finally the organic layer was dried with magnesium sulphate and concentrated to afford the product **(2.07)** (19 g, 0.082 moles, 88%) as brown oil.

1H NMR (400 MHz, CHLOROFORM-*d*) δ_H ppm: 3.95 (3 H, s, OCH_3), 6.92 (1 H, d, ArH, J=8.78 Hz), 7.65 (1H, dd, ArH, J=8.91, 2.64 Hz), 7.93 (1H, d, ArH, J=2.51 Hz), 10.40 (1H, s, CHO);

^{13}C NMR (101 MHz, CHLOROFORM-*d*) δ_C ppm: 56.0 (OCH_3), 113.5 (ArCBr), 113.8 (ArCH), 126.1 (ArC), 131.0 (ArCH), 138.3 (ArCH), 160.8 (ArC), 188.4 (C=O);

V_{max} cm^{-1}: 2971, 2833, 2549, 1677, 1416, 1277, 899;

HRMS: Calculated 229.9579, found 253.2398 ($M + Na^+$).

Synthesis of intermediate 5-bromo-2-methoxyphenol (2.08)

Formate ester **(2.07)** (19 g, 0.082 moles) was dissolved in Methanol (100 mL) and THF (60 mL) at 0 °C. To this was added a solution of NaOH (100 mL, 2.5 M) and allowed to stir at 0 °C for 16 hours. Afterwards the organic solvents were evaporated using rotary and the

remainder was acidified with aq.HCl solution (100 mL, 2 M). The acidic aqueous layer was then extracted with DCM (3×200 mL), dried with magnesium sulphate and concentrated *in vacuo* to afford the phenol **(2.08)** (13 g, 0.064 moles, 78%) as light brown solid.

^{1}H NMR (400 MHz, CHLOROFORM-*d*) δ_H ppm: 3.78 (3H, s, OCH_3), 6.61 (1H, d, ArH, J= 8 Hz), 6.91(1H, d, ArH, J=8 Hz), 7.03 (1H, s, ArH);

^{13}C NMR (101 MHz, CHLOROFORM-*d*) δ_C ppm: 55.8 (OCH_3), 111.3 (ArCH), 112.8 (ArCH), 117.1 (ArCH), 112.1 (ArCH), 145.5 (ArC), 146.3 (ArC);

V_{max} cm^{-1}: 3285, 1629, 1249, 686;

HRMS: Calculated 201.9768, found 224.9666 ($M + Na^+$);

MP: 60-62 °C.

Synthesis of intermediate 5-bromo-2-methoxyphenoxy(*tert*-butyl)dimethylsilane (2.09)

Phenol **(2.08)** (13 g, 0.064 moles) was dissolved in dry DMF (100 mL). To this solution was added imidazole (6.96 g, 0.102 moles) and *tert*-butyldimethylsilyl chloride (14.46 g, 0.096 moles) under an atmosphere of nitrogen and allowed to stir at room temperature for 16 hours. The reaction was then quenched with concentrated aqueous NaCl solution (100 mL), extracted with diethyl ether (3×150 mL) and dried with magnesium sulphate. Finally the mixture was purified by column chromatography using just hexane to afford the product **(2.09)** (16.5 g, 0.052 moles, 81%) as colourless oil.

^{1}H NMR (400 MHz, CHLOROFORM-*d*) δ_H ppm: 0.18 (6 H, s, 2 × Si-$\underline{CH_3}$), 1.02 (9 H, s, $C(CH_3)_3$), 3.81 (3 H, s, OCH_3), 6.74 (1 H, d, ArH, 9 Hz), 7.01 (1 H, d, ArH, J=2.5 Hz), 7.04 (1H, dd, ArH, J=9, 2.5 Hz);

^{13}C NMR (101 MHz, CHLOROFORM-*d*) δ_C ppm: -5.1 (2 × $Si(CH_3)$), 18.0 ($\underline{C}(CH_3)_3$), 25.2 ($C(\underline{C}H_3)_3$, 55.1 (OCH_3), 111.9 (ArCBr), 112.7 (ArCH), 123.6 (ArCH), 123.9 (ArCH), 145.5 (ArC), 150.0 (ArC);

V_{max} cm^{-1}: 3032, 1626, 1261, 690;

HRMS: Calculated 316.0494, found 339.0422 ($M + Na^+$).

Synthesis of (3-((*tert*-butyldimethylsilyl) oxy)-4-methoxyphenyl) boronic acid (2.10)

Aryl bromide **(2.09)** (1.00 g, 0.003 moles) was dissolved in dry THF (5 mL) and cooled to -78 °C under an atmosphere of nitrogen. To this was added *n*-butyl lithium (2 mL, 0.005 moles, 2.5 M solution in hexane) dropwise over 30 mins and allowed further to stir for 30 mins at -78 °C. After this, triisopropyl borate (3.8 mL, 0.0164 moles) was added dropwise over 30 minutes and allowed the reaction to stir at this temperature for 2 hours before a further 2 hours stirring at -20 °C and 2 hours at room temperature. The reaction was quenched with 1 M HCl (20 mL) and extracted with diethyl ether (3×20 mL). Finally the product was dried with $MgSO_4$ and purified by column chromatography (1:4, ethyl acetate:hexane) to afford the product **(2.10)** (0.55 g, 0.002 moles, 62%) as white solid.

^{1}H NMR (400 MHz, CHLOROFORM-*d*) δ_H ppm: 0.26 (6 H, s, 2 × CH_3), 1.10 (9 H, s, (C(C$\underline{H}_3$)$_3$), 3.93 (3 H, s, OCH_3), 7.02 (1 H, d, ArH, J=8.35 Hz), 7.70 (1 H, d, ArH, J=1.5 Hz), 7.83 (1 H, dd, ArH, J=8.35, 1.55 Hz);

^{13}C NMR (101 MHz, CHLOROFORM-*d*) δ_C ppm: -4.9 (2×$SiCH_3$), 18.1 ($\underline{C}(CH_3)_3$), 25.3 (C($\underline{C}H_3$)$_3$), 54.9 (OCH_3), 110.8 (ArCH), 126.9 (ArCH), 129.8 (ArCH), 144.1 (ArC), 154.3 (ArC);

V_{max} cm^{-1}: 3435, 2978, 2935, 1729, 1520, 1368, 1235, 1154;

HRMS: Calculated 282.146, found 281.1370 (M - H^+).

Synthesis of Aniline C-ring Precursor

Synthesis of intermediate 4-bromo-1-methoxy-2-nitrobenzene (2.11)

4-bromo-2-nitrophenol (12.00 g, 0.055 moles) was dissolved in acetone (150 mL). To this was added iodomethane (34 mL, 77.78 g, 0.548 moles), followed by the addition of potassium carbonate (23.00 g, 0.166 moles). The reaction mixture was refluxed while stirring for 3 hours. Solvent was removed *in vacuo* and the remainder was purified by flash column chromatography using (1:9, ethyl acetate:hexane) to isolate the product **(2.11)** (11.60 g, 0.050 moles, 91%) as white solid.

^{1}H NMR (400 MHz, CHLOROFORM-*d*) δ_H ppm: 3.97 (3 H, s, OCH_3), 7.01 (1 H, d, ArH, J= 8.8 Hz), 7.65 (1 H, dd, ArH, J= 8.8, 2.4 Hz), 7.98 (1 H, d, ArH, J= 2.4 Hz);

^{13}C NMR (101 MHz, CHLOROFORM-*d*) δ_C ppm: 56.8 (OCH_3), 111.8 (ArC), 115.2 (ArCH), 128.4 (ArCH), 136.9 (ArC), 140.0 (ArCH), 152.2 (ArC);

V_{max} cm^{-1}: 1604, 1517, 1344, 1148;

HRMS: Calculated 230.9531, found 253.9424 ($M + Na^+$);

MP: 90-91 °C.

Synthesis of intermediate 5-bromo-2-methoxyaniline (2.12)

Nitrobenzene compound **(2.11)** (15 g, 0.065 moles) was dissolved in ethanol (450 mL) (with the aid of small amount of heat just to dissolve completely) at room temperature, followed by the careful addition of concentrated HCl (225 mL). To this solution was added tin powder (15 g, 0.126 moles) and allowed to stir at RT for 5 hours. After this, solvent volume was reduced *in vacuo,* and the resulting oil was stirred and cooled to 0 °C using an ice bath. To the reaction mixture NaOH (cooled with ice) (350 mL, 2.5 M) was slowly introduced. The reaction was then extracted with DCM (3×300 mL), dried with $MgSO_4$, filtered and condensed under reduced pressure. The crude product obtained was then purified by flash column chromatography (1:6, ethyl acetate:hexane) to afford the aniline **(2.12)** (11.26 g, 0.056 moles, 86%) as white solid.

^{1}H NMR (400 MHz, CHLOROFORM-*d*) δ_H ppm: 3.84 (3 H, s, OCH_3), 3.88 (2 H, br.s, NH_2) 6.65 (1 H, d, ArH, J= 9 Hz), 6.83 (1 H, dd, ArH, J=8.5, 1 Hz), 6.84 (1 H, s, ArH);

^{13}C NMR (101 MHz, CHLOROFORM-*d*) δ_C ppm: 55.7 (OCH_3), 111.6 (ArCH), 113.2 (ArC), 117.3 (ArCH), 120.7 (ArCH), 137.7 (ArC), 146.4 (ArC);

V_{max} cm^{-1}: 3472.25, 3380.57, 3004, 2960, 2907, 2837, 1611, 1502, 1221;

HRMS: Calculated 200.9789, found 201.9863 ($M + H^+$);

MP: 88-90 °C.

Synthesis of intermediate *tert*-butyl *N*-(5-bromo-2-methoxyphenyl) carbamate (2.13)

Aniline compound **(2.12)** (11.26 g, 0.056 moles) and di-*ter*t-butyl dicarbonate (24.33 g, 0.111 moles) were dissolved in anhydrous THF (150 mL) and allowed to stir together under an atmosphere of nitrogen. The reaction mixture was refluxed gently over the course of 2 working days. Upon completion, the reaction was quenched with concentrated aqueous

NaCl solution (100 mL) and the organic solvent was evaporated using rotary evaporator. The aqueous layer left behind was then extracted with diethyl ether (3×100 mL) and dried with $MgSO_4$. After filtration and evaporation under reduced pressure, the crude product obtained was further purified by flash column chromatography (1:10, ethyl acetate:hexane) to afford the Boc-protected aniline **(2.13)** (15.98 g, 0.005 moles, 95%) as white solid.

^{1}H NMR (400 MHz, CHLOROFORM-*d*) δ_H ppm: 1.55 (9 H, s, $C(CH_3)_3$), 3.87 (3 H,s, OCH_3), 6.71 (1 H, d, ArH, , J= 8.6 Hz), 7.08 (1 H, overlapping-dd, ArH, J= 2.4, 8.6 Hz), 7.09 (1 H, d, ArH, , J= 2.4 Hz), 8.30 (1 H, br.s, NH);

^{13}C NMR (101 MHz, CHLOROFORM-*d*) δ_C ppm: 28.3 ($C(\underline{C}H_3)_3$), 55.9 (OCH_3), 80.8 ($\underline{C}(CH_3)_3$), 111.2 (ArCH), 113.6 (ArC), 120.7 (ArCH), 124.7 (ArCH), 129.4 (ArC), 146.5 (ArC), 152.4 (C=O);

V_{max} cm^{-1}: 3079, 1632, 1502, 1409;

HRMS: Calculated 301.0314, found 302.0698 (M+H);

MP: 75-78 °C.

Synthesis of *tert*-butyl (2-methoxy-5-(4,4,5,5-tetramethyl-1,3,2-dioxaborolan-2-yl)phenyl)carbamate (2.14)

Potassium acetate (1.55 g, 0.016 moles), [1,1'-Bis(diphenylphosphino)ferrocene] dichloropalladium(II) (0.116 g,0.000159 moles) and bis(pinacolato)diboron (1.47 g, 0.00579 moles) were stirred together in a 2 necked round bottom flask under an atmosphere of nitrogen. To this *tert*-butyl *N*-(5-bromo-2-methoxyphenyl)carbamate **(2.13)** (1.59 g, 0.0053 moles) in DMSO (30 mL) was added and the reaction heated to 80 °C for 6 hours, then left stirring at room temperature overnight. The reaction was quenched with water (100 mL) and then extracted with diethyl ether (100 mL). The palladium species were then filtered through a cotton plug and the remaining organic layer was dried with $MgSO_4$ before being condensed using rotary evaporator. Finally the product was purified by column chromatography (1:12, ethyl acetate:hexane) to afford the boronic ester **(2.14)** (0.45 g, 0.0012 moles, 76%) as white solid.

^{1}H NMR (400 MHz, CHLOROFORM-*d*) δ_H ppm: 1.34 (12 H, s, 4 × CH_3), 1.55 (9 H, s, $C(CH_3)_3$), 3.90 (3 H, s, OCH_3), 6.87 (1 H, d, ArH, J= 8 Hz), 7.06 (1 H, s, ArH), 7.47 (1 H, d, ArH, J= 8 Hz), 8.42 (1 H, br.s, NH);

^{13}C NMR (101 MHz, CHLOROFORM-*d*) δ_C ppm: 24.8 (4 × CH_3), 28.3 (C($\underline{C}H_3)_3$), 55.5 (OCH_3), 74.9 ($\underline{C}(CH_3)_3$, 80.0 (2× $\underline{C}(CH_3)_2$COB), 109.2 (ArCH), 124.0 (ArC), 127.5 (ArC), 129.8 (2 × ArCH), 150.0 (Ar$\underline{C}$-OCH_3), 152.6 (C=O);

V_{max} cm^{-1}: 3052, 1628, 1432, 1178, 1118;

HRMS: Calculated 349.2061, found 348.1989 (M - H^+);

MP: 105 °C.

Synthesis of *tert*-butyl (2-methoxy-5-(6,7,8-trimethoxy-2-oxo-2H-chromen-4-yl)phenyl)carbamate (2.15) via Suzuki coupling

Triflate **(2.05)** (0.115 g, 0.3 mmoles), aryl boronic ester **(2.14)** (0.125 g, 0.36 mmoles) and potassium carbonate (0.125 g, 0.9 mmoles) were dissolved in toluene: ethanol: water mixture (3:1:1, 10 mL). To this tetrakis (triphenylphosphine) palladium (0) (17 mg, 0.015 mmoles) was added and the reaction was refluxed for 2 hours. After 2 hours the reaction mixture was diluted with ethyl acetate (200 mL) and dried with $MgSO_4$. Solvent was evaporated using rotary evaporator and product was purified by column chromatography (1:3, ethyl acetate:hexane) to afford the Boc-protected aniline **(2.15)** (97 mg, 0.21 mmoles, 58%) as light yellowish oil that solidified on further vacuum drying.

^{1}H NMR (400 MHz, CHLOROFORM-*d*) δ_H ppm: 1.51 (9 H, s,$(CH_3)_3$), 3.80 (3 H, s, OCH_3), 3.96 (3 H, s, OCH_3), 4.01 (3 H, s, OCH_3), 4.04 (3 H, s, $0CH_3$), 6.31 (1 H, s, C=CH), 6.94 (1 H, s, ArH), 6.99 (1 H, d, ArH, J= 8.53 Hz),7.10 (1 H, d, ArH, J= 8.03 Hz), 7.17 (1 H, s, ArH), 8.31 (1 H, br.s, NH);

^{13}C NMR (101 MHz, CHLOROFORM-*d*) δ_C ppm: 27.8 (C($\underline{C}H_3)_3$), 55.4 (OCH_3), 55.7 (OCH_3), 61.0 (OCH_3), 61.4 (OCH_3), 80.3 ($\underline{C}(CH_3)_3$), 103.1 (ArCH), 109.8 (ArCH), 112.8 (C=$\underline{C}$H), 114.0 (ArC), 118.1(ArC), 122.1 (ArCH), 127.6 (ArCH), 127.8 (ArC), 140.8 (ArC), 142.9 (ArC), 145.2 (ArC), 148.2 (ArC), 149.1 (ArC), 152.2 ($\underline{C}$=CH), 155.0 (N$\underline{C}$=O), 160.4 (C=O);

V_{max} cm^{-1}: 3453, 2939, 1724, 1531, 1390;

HRMS: Calculated 457.1737, found 480.4556 (M+Na^+).

Synthesis of 4-(3-amino-4-methoxyphenyl)-6,7,8-trimethoxy-2H-chromen-2-one (2.16)

N-Boc protected aniline **(2.15)** (150 mg, 0.328 mmoles) was dissolved in anhydrous DCM (3 mL) under the atmosphere of nitrogen and cooled to -10 °C. To this was added cooled TFA (1.5 mL) and allowed to stir at 0 °C for 90 minutes. After completion the product was diluted with DCM (20 mL) and solvent evaporated at 40 °C using rotary evaporator. The remainder was again dissolved in DCM 10 mL and stirred with sodium bicarbonate (3 mL, 5%) for 5 minutes. The aqueous layer was removed with the help of Pasteur pipette. Organic layer was dried with $MgSO_4$ and solvent evaporated using rotary evaporator. Finally the crude product was further purified by column chromatography (1:2, ethyl acetate:hexane) to afford the aniline **(2.16)** (97 mg, 0.271 mmoles, 83%) as yellow solid.

^{1}H NMR (400 MHz, CHLOROFORM-*d*) δ_H ppm: 3.78 (3 H, s, OCH_3), 3.96 (3 H, s, OCH_3), 4.02 (3 H, s, OCH_3), 4.06 (3 H, s, OCH_3), 6.27 (1 H, s, C=CH), 6.80-6.85 (3 H, m, 3× ArH), 6.91 (1 H, d, ArH, J= 8 Hz);

^{13}C NMR (101 MHz, CHLOROFORM-*d*) : 55.6 (OCH_3), 56.4 (OCH_3), 61.5 (OCH_3), 61.9 (OCH_3), 103.6 (ArCH), 110.2 (ArCH), 113.2 (C=CH), 114.4 (ArCH), 114.7 (ArC), 118.6 (ArCH), 128.3 (ArC), 136.7 (ArC), 141.3 (ArC), 143.4 (ArC), 145.8 (ArC), 148.3 (ArC), 149.5 (ArC), 155.9 (C=CH), 160.9 (C=O);

V_{max} cm^{-1}: 3444, 2956, 2926, 2856, 1730, 1571, 1462, 1384, 1287, 1129;

HRMS: Calculated 357.1717, found 358.2184 ($M + H^+$),

MP: 163-165 °C.

Synthesis of *tert*-butyl (2-methoxy-5-(6,7,8-trimethoxy-2-thioxo-2H-chromene-4-yl)phenyl)carbamate (2.17)

N-Boc protected aniline **(2.15)** (500 mg, 1.094 mmole) was dissolved in toluene (10 mL). To this solution was added Lawesson's reagent (486 mg, 1.202 mmole) and the mixture was refluxed for 2 hours. After completion of the reaction, solvent was evaporated using rotary evaporator and the remainder was purified by column chromatography (1:4, ethyl acetate:hexane) to afford the *N*-Boc protected thione **(2.17)** (395 mg, 0.83 mmoles 76%) as yellow oil that solidified on further vacuum drying.

^{1}H NMR (400 MHz, CHLOROFORM-*d*) δ_H ppm: 1.51 (9 H, s, $(CH_3)_3$), 3.84 (3 H, s, OCH_3), 3.97 (3 H, s, OCH_3), 4.04 (3 H, s, OCH_3), 4.11 (3 H, s, OCH_3), 7.00 (1 H, d, ArH, J= 8.53 Hz), 7.03 (1 H, s, C=CH) , 7.14 (1 H, d, ArH, J= 8 Hz), 7.15 (1 H, s, ArH), 7.22 (1 H, s, ArH), 8.35 (1 H, br.s, NH);

^{13}C NMR (101 MHz, CHLOROFORM-*d*) δ_C ppm: 27.8 ($C(\underline{CH_3})_3$), 55.5 (OCH_3), 55.7 (OCH_3), 61.1 (OCH_3), 61.7 (OCH_3), 80.3 ($\underline{C}(CH_3)_3$), 102.3 (ArCH), 109.9 (ArCH), 115.6 (C=CH), 118.4 (ArC), 122.4 (ArC), 126.7 (ArCH), 126.8 (ArCH), 127.9 (ArC), 140.4 (ArC), 145.4 (ArC), 146.3 (ArC), 146.4 (ArC), 148.5 (ArC),150.2 ($\underline{C}$=CH), 152.2 (N-C=O), 195.4 (C=S);

V_{max} cm^{-1}: 3442, 2932, 1689, 1521, 1393, 1284, 1252, 1121, 1055;

HRMS: Calculated 473.1508, found 496.4327 ($M + Na^+$).

Synthesis of 4-(3-amino-4-methoxyphenyl)-6,7,8-trimethoxy-2H-chromene-2-thione (2.18)

N-Boc protected aniline **(2.17)** (350 mg, 0.74 mmoles) was dissolved in anhydrous DCM (3 mL) under the atmosphere of nitrogen and cooled to -10 °C. To this was added cooled TFA (1.5 mL) and allowed to stir at 0 °C for 90 minutes. After completion the product was diluted with DCM (20 mL) and solvent evaporated at 40 °C using rotary evaporator. The remainder was again dissolved in DCM 10 mL and stirred with sodium bicarbonate (3 mL, 5%) for 5 minutes. The aqueous layer was removed with the help of Pasteur pipette. The organic layer was dried with $MgSO_4$ and solvent evaporated using rotary evaporator. Finally the crude product was further purified by column chromatography (1:2, ethyl acetate:hexane) to afford the aniline **(2.18)** (210 mg, 0.56 mmoles, 76%) as yellow solid.

^{1}H NMR (400 MHz, DMSO-d_6) δ ppm: 3.78 (3 H, s, OCH_3), 3.86 (3 H, s, OCH_3), 3.94 (3 H, s, OCH_3), 4.00 (3 H, s, OCH_3), 5.06 (2 H, br.s, NH_2), 6.84 (1 H, dd, ArH, J= 8.03, 2.01 Hz), 6.91 (1 H, d, ArH, J= 2.01 Hz), 6.98 (1 H, d, ArH, J= 8.03 Hz), 7.01 (1 H, s, ArH) 7.06 (1 H, s, C=CH);

^{13}C NMR (151 MHz, DMSO-d_6) δ ppm: 55.9 (OCH_3), 56.4 (OCH_3), 61.6 (OCH_3), 62.2 (OCH_3), 103.4 (ArCH), 111.1 (ArCH), 113.9 (ArCH), 116.0 (ArC), 117.5 (ArCH), 126.4 (C=CH), 127.0 (ArC), 138.8 (ArC), 140.8 (ArC), 146.1 (ArC), 146.6 (ArC), 148.1 ($\underline{C}$=CH), 148.5 (ArC), 150.7 (ArC), 195.2 (C=S);

V_{max} cm^{-1}: 3357, 2938, 1615, 1539, 1513, 1392, 1281, 1122;

HRMS: Calculated 373.0984, found 374.1073 ($M + H^+$).

Synthesis of *tert*-butyl (Z)-(5-(2-(hydroxyimino)-6,7,8-trimethoxy-2H-chromen-4-yl)-2-methoxyphenyl)carbamate (2.19)

N-Boc aniline **(2.17)** (100 mg, 0.211 mmoles) was dissolved in DMF (3 mL) under the atmosphere of nitrogen at room temperature. To this was added hydroxylamine hydrochloride (18 mg, 0.259 mmoles) and Diisopropylethylamine (45 µL, 0.259 mmoles). The reaction was kept stirring for 3 hours before being quenched with water (40 mL) and extracted with diethyl ether (3×50 mL). After drying with $MgSO_4$ solvent was evaporated and the crude product obtained was further purified by column chromatography (1:3, ethyl acetate:hexane) to afford the *N*-Boc oxime **(2.19)** (85 mg, 0.18 mmoles, 85%) as yellow solid.

^{1}H NMR (400 MHz, CHLOROFORM-*d*) δ ppm: 1.52 (9 H, s, $(CH_3)_3$), 3.77 (3 H, s, OCH_3), 3.94 (3 H, s, OCH_3), 3.97 (3 H, s, OCH_3), 4.11 (3 H, s, OCH_3), 6.26 (1 H, s, C=CH), 6.77 (1 H, s, ArH), 6.95 (1 H, d, ArH, *J*=8.80 Hz), 7.06 (1 H, dd, ArH, *J*=8.31, 1.96 Hz), 7.16 (1 H, s, ArH), 8.24 (1 H, br.s, OH);

^{13}C NMR (101 MHz, CHLOROFORM-*d*) δ ppm : 28.3 ($C(\underline{CH_3})_3$), 55.8 (OCH_3), 56.2 (OCH_3), 61.5 (OCH_3), 61.6 (OCH_3), 103.8 (ArCH), 110.1 (C=<u>C</u>H), 113.8 (ArCH), 115.7 (<u>C</u>=CH), 118.6 (ArCH), 122.4 (ArCH), 128.0 (ArC), 128.9 (ArC), 141.1 (ArC), 141.5 (ArC), 141.8 (ArC), 143.7 (ArC), 148.0 (ArC), 148.8 (ArC), 152.7 (C=N);

V_{max} cm^{-1}: 3435, 2975, 2939, 1724, 1530, 1481, 1381, 1246, 1157, 736;

HRMS: Calculated 472.1846, found 495.1721 ($M + Na^+$).

Synthesis of (Z)-4-(3-amino-4-methoxyphenyl)-6,7,8-trimethoxy-2H-chromen-2-one oxime (2.20)

N-Boc oxime **(2.19)** (50 mg, 0.106 mmoles) was dissolved in anhydrous DCM (2 mL) under the atmosphere of nitrogen and cooled to -10 °C with ice and salt bath. To this was added cooled TFA and allowed to stir at 0 °C for 90 minutes. After which the solvent was evaporated at 40 °C and the remainder was redissolved in DCM (10 mL) and stirred with aqueous sodium bicarbonate (5%, 3 mL) for 5 minutes. After 5 minutes the aqueous layer was removed with the help of pipette while the organic layer was evaporated and the

residue obtained was washed several times with pentane to afford the free amine **(2.20)** (36 mg, 0.097 mmoles, 91%) as a light whitish yellow solid.

^{1}H NMR (400 MHz, DMSO-d_6) δ ppm : 3.66 (3 H, s, OCH_3), 3.81 (3 H, s, OCH_3), 3.82 (3 H, s, OCH_3), 3.95 (3 H, s, OCH_3), 4.92 (2 H, s, NH_2), 6.07(1 H, s, C=CH), 6.65 (1 H, dd, ArH, *J*=8.07, 2.20 Hz), 6.67 (1 H, s, ArH), 6.75 (1 H, d, ArH, *J*= 2.20 Hz), 6.90 (1 H, d, ArH, *J*=8.31 Hz), 10.25 (1 H, s, OH);

^{13}C NMR (101 MHz, DMSO-d_6) δ ppm : 55.3 (OCH_3), 56.0 (OCH_3), 60.9 (OCH_3), 61.0 (OCH_3), 103.7 (ArCH), 110.5 (ArCH), 113.4 (ArCH), 113.9 (C=<u>CH</u>), 115.5 (<u>C</u>=CH), 116.1 (ArCH), 128.3 (ArC), 137.9 (ArC), 140.3 (ArC), 140.8 (ArC), 141.0 (ArC), 143.1 (ArC), 146.7 (ArC), 148.1 (ArC), 149.0 (C=N);

V_{max} cm^{-1}: 3405, 3318, 2941, 2834, 1708, 1637, 1598, 1498, 1380, 1272, 1242, 1129, 1091, 730;

HRMS: Calculated 372.1321, found 373.1383 ($M + H^+$).

Synthesis of 4-(3-((*tert*-butyldimethylsilyl)oxy)-4-methoxyphenyl)-6,7,8-trimethoxy-2H-chromen-2-one (2.21) via Suzuki coupling

Triflate **(2.05)** (0.200 g, 0.00052 moles), boronic acid **(2.10)** (0.180 g, 0.000635 moles) and potassium carbonate (0.216 g, 0.00156 moles) were dissolved and stirred in a biphasic toluene: ethanol: water mixture (3:1:1, 10 mL). To this tetrakis (triphenylphosphine) palladium (0) (0.03 g, 0.000026 moles) was added and the reaction refluxed for 2 h. After 2 hours, the reaction mixture was diluted with ethyl acetate (50 mL), dried with magnesium sulphate and concentrated *in vacuo*. Finally purified by column chromatography (1:4, ethyl acetate:hexane) to afford the biaryl product **(2.21)** (0.150 g, 0.000318 moles, 63%) as a white solid.

[1]H NMR (400 MHz, CHLOROFORM-*d*) δ_H ppm: 0.21 (6 H, s, 2×CH_3), 1.02 (9 H, s, 3×CH_3), 3.77 (3 H, s, OCH_3), 3.91 (3 H, s, OCH_3), 4.02 (3 H, s, OCH_3), 4.07 (3 H, s, OCH_3), 6.27 (1 H, s, C=CH), 6.78 (1 H, s, ArH), 6.97 (1 H, d, ArH, *J*= 2 Hz), 6.99 (1 H, d, ArH, *J*= 8.4 Hz), 7.04 (1 H, dd, ArH, *J*= 2, 8.4 Hz);

^{13}C NMR (101 MHz, CHLOROFORM-*d*) δ_C ppm : -4.9 (2×$SiCH_3$), 17.9 (<u>C</u>(CH_3)$_3$), 25.2 (C(<u>C</u>H_3)$_3$), 55.0 (OCH_3), 55.8 (OCH_3), 61.1 (OCH_3), 61.5 (OCH_3), 102.8 (ArCH), 111.6 (C=<u>C</u>H), 113.0 (ArC), 114.1 (ArCH), 120.5 (ArCH), 121.6 (ArCH), 127.6 (ArC), 140.9

(ArC), 142.9 (ArC), 144.7 (ArC), 145.4 (ArC), 149.1 (ArC), 151.8 (ArC), 154.8 (C=CH), 160.4 (C=O);

V_{max} cm^{-1}: 2916, 1726, 1260, 1092;

HRMS: Calculated 472.1917, found 473.1978 ($M + H^+$).

Synthesis of 4-(3-hydroxy-4-methoxyphenyl)-6,7,8-trimethoxy-2H-chromen-2-one (2.22)

Silyl protected phenol **(2.21)** (100 mg, 0.211 mmole) was dissolved in dry THF (3 mL) under the atmosphere nitrogen and cooled to 0 °C. To this was added tetrabutylamonium fluoride (66 mg, 253 µL, 0.253 mmole) dropwise. The reaction was kept stirring for 10 mins before being quenched with saturated aqueous NaCl solution and extracted with dichloromethane (3×100 mL). After drying with $MgSO_4$ the residue was filtered and concentrated using rotary evaporator. Finally the product was purified (1:1, ethyl acetate:hexane) to afford the phenol **(2.22)** (65 mg, 0.181 mmoles 86%) as light yellow solid.

^{1}H NMR (600 MHz, DMSO-d_6) δ ppm: 3.72 (3 H, s, OCH_3), 3.85 (3 H, s, OCH_3), 3.90 (3 H, s, OCH_3), 3.93 (3 H, s, OCH_3), 6.25 (1 H, s, C=CH), 6.85 (1 H, s, ArH), 6.98 (1 H, d, ArH, *J*= 1.8 Hz), 7.00 (1 H, dd, ArH, *J*= 1.8 , 8.4 Hz), 7.10 (1 H, d, ArH, *J*= 8.4 Hz), 9.43 (1 H, br.s, OH);

^{13}C NMR (151 MHz, DMSO-d_6) δ ppm: 56.1 (OCH_3), 56.5 (OCH_3), 61.5 (OCH_3), 62.0 (OCH_3), 103.9 (ArCH), 112.3 (ArCH), 113.1 (C=CH), 114.4 (ArC), 116.0 (ArCH), 120.3 (ArCH), 127.8 (ArC), 141.2 (ArC), 143.1 (ArC), 145.8 (ArC), 147.2 (ArC), 149.6 (ArC), 149.6 (ArC), 155.3 (C=CH), 160.1 (C=O);

V_{max} cm^{-1}: 3374, 2924, 1722, 1389;

HRMS: Calculated 358.1053, found 381.0944 ($M + Na^+$),

MP: 180-182 °C.

Synthesis of 4-(3-((*tert*-butyldimethylsilyl)oxy)-4-methoxyphenyl)-6,7,8-trimethoxy-2H-chromene-2-thione (2.23)

Silyl ether **(2.21)** (400 mg, 0.847 mmole) was dissolved in toluene (10 mL). To this was added Lawesson's reagent (376 mg, 0.930 mmoles) and the mixture refluxed for 2 hours.

After completion of the reaction solvent was evaporated using rotary evaporator and the remainder was purified by column chromatography (1:5, ethyl acetate:hexane) to afford the silyl protected thione **(2.23)** (340 mg, 0.697 mmoles, 82%) as yellow solid.

^{1}H NMR (400 MHz, CHLOROFORM-*d*) δ_H ppm: 0.21 (6 H, s, 2×CH_3), 1.03 (9 H, s, 3×CH_3), 3.80 (3 H, s, OCH_3), 3.92 (3 H, s, OCH_3), 4.05 (3 H, s, OCH_3), 4.14 (3 H, s, OCH_3), 6.83 (1 H, s, C=CH), 7.00 (1 H, d, ArH, *J*= 1.96 Hz), 7.01 (1 H, d, ArH, *J*= 8 Hz),7.08 (1 H, dd, ArH, *J*= 1.96 Hz, 8 Hz), 7.18 (1 H, s, ArH);

^{13}C NMR (101 MHz, CHLOROFORM-*d*) δ_C ppm : -4.5 (2×$SiCH_3$), 18.4 ($\underline{C}(CH_3)_3$), 25.7 ($C(\underline{C}H_3)_3$), 55.5 (OCH_3), 56.2 (OCH_3), 61.6 (OCH_3), 62.1 (OCH_3), 102.5 (ArCH), 112.1 (C=$\underline{C}$H), 116.3 (ArC), 121.0 (ArCH), 122.3 (ArCH), 127.4 (ArCH), 127.5 (ArC), 141.0 (ArC), 145.3 (ArC), 146.1 (ArC), 146.6 ($\underline{C}$=CH), 146.9 (ArC), 150.6 (ArC), 152.5 (ArC), 195.9 (C=S);

V_{max} cm^{-1}: 3427, 2933, 1643, 1542, 1513, 1281, 1122, 1054;

HRMS: Calculated 488.1689, found 511.1588 (M + Na^+).

Synthesis of 4-(3-hydroxy-4-methoxyphenyl)-6,7,8-trimethoxy-2H-chromene-2-thione (2.24)

Silyl protected thione **(2.23)** (422 mg, 0.864 mmoles) was dissolved in dry THF (10 mL) under the atmosphere nitrogen and cooled to 0 °C. To this was added tetrabutylamonium fluoride (1 mL, 1.036 mmole) dropwise. The reaction was kept stirring for 10 mins before being quenched with brine and extracted with dichloromethane (3×100 mL). After drying with $MgSO_4$ the reaction was filtered and dried using rotary evaporator. Finally the product was purified by flash column chromatography (1:2, ethyl acetate:hexane) to afford the phenol **(2.24)** (270 mg, 0.722 mmoles 83%) as yellow solid.

^{1}H NMR (400 MHz, CHLOROFORM-*d*) δ_H ppm: 3.81 (3 H, s, OCH_3) 4.01 (3 H, s, OCH_3) 4.06 (3 H, s, OCH_3), 4.14 (3 H, s, OCH_3), 6.86 (s, 1 H, ArH), 7.02 (s, 2 H, ArH) 7.10 (s, 1 H, ArH) 7.20 (s, 1 H, C=CH);

^{13}C NMR (101 MHz, CHLOROFORM-*d*) δ_C ppm: 56.1 (OCH_3), 56.3 (OCH_3), 61.6 (OCH_3), 62.1 (OCH_3), 102.5 (ArCH), 110.9 (ArCH), 114.7 (ArCH), 116.2 (ArC), 120.8 (ArCH) , 127.6 (C=$\underline{C}$H), 128.0 (ArC), 141.0 (ArC), 146.0 (ArC), 146.1 (ArC), 146.6 (ArC), 146.9 ($\underline{C}$=CH), 148.0 (ArC), 150.6 (ArC), 195.9 (C=S);

V_{max} cm^{-1}: 3435, 1643, 1542, 1509, 1393, 1280, 1265, 1123;

HRMS: Calculated 374.0824, found 397.0728 ($M + Na^+$).

Synthesis of 4-(3-hydroxy-4-methoxyphenyl)-6,7,8-trimethoxy-2H-chromen-2-one oxime (2.25)

Phenol **(2.24)** (100 mg, 0.267 mmoles) was dissolved in DMF (3 mL) under the atmosphere of nitrogen at room temperature. To this was added hydroxylamine hydrochloride (24 mg, 0.347 mmoles) and DIPEA (60 µL, 0.347 mmoles). The reaction was kept stirring for 3 hours before being quenched with water (40 mL) and extracted with diethyl ether (3×50 mL). After drying with $MgSO_4$ solvent was evaporated and the crude product obtained was further purified by column chromatography (1:1, ethyl acetate:hexane) to afford the oxime **(2.25)** (80 mg, 0.214 mmoles, 80%) as light yellow solid.

^{1}H NMR (400 MHz, DMSO-d_6) δ ppm: 3.66 (3 H, s, OCH_3), 3.82 (3 H, s, OCH_3), 3.83 (3 H, s, OCH_3), 3.96 (3 H, s, OCH_3), 6.11 (1 H, s, C=CH), 6.62 (1 H, s, ArH), 6.88 (1 H, s, ArH), 6.895 (1 H, d, ArH, *J*= 2.3 Hz), 7.04 (1 H, d, ArH, *J*= 9.03 Hz), 9.31 (1 H, s, Ar-OH), 10.29 (1 H, s, N-OH);

^{13}C NMR (101 MHz, DMSO-d_6) δ ppm: 56.0 (OCH_3), 56.5 (OCH_3), 61.4 (OCH_3), 61.5 (OCH_3), 104.0 (ArCH), 112.7 (ArCH), 114.9 (C=CH), 115.8 (ArCH), 115.9 (C=CH), 119.8 (ArCH), 128.8 (ArC), 140.0 (ArC), 141.3 (ArC), 141.5 (ArC), 143.6 (ArC), 147.0 (ArC), 148.6 (ArC), 148.7 (ArC), 149.3 (C=N);

V_{max} cm^{-1}: 3355, 2931, 1644, 1571, 1511, 1465, 1382, 1271, 1221, 1130, 1090, 1049, 968;

HRMS: Calculated 373.1162, found 396.1068 ($M + Na^+$).

Synthesis of (E)-4-(3-hydroxy-4-methoxyphenyl)-6,7,8-trimethoxy-2H-chromen-2-one O-methyl oxime (2.26)

Phenol **(2.24)** (80 mg, 0.214 mmoles) was dissolved in ethanol:water (4:1, 15 mL) at room temperature. To this was added methoxyamine hydrochloride (36 mg, 0.428 mmoles) and sodium acetate (35 mg, 0.428 mmoles). The reaction was refluxed for 10 hours before being quenched with aq.HCl (1 M, 20 mL) and extracted with DCM (3×30 mL). After drying with $MgSO_4$ solvent was evaporated and the crude product obtained was further purified by column chromatography (1:1, ethyl acetate:hexane) to afford the methyl oxime **(2.26)** (60 mg, 0.155 mmole, 72%) as light yellow solid.

^{1}H NMR (400 MHz, DMSO-d_6) δ ppm: 3.66 (3 H, s, OCH_3), 3.81 (3 H, s, OCH_3), 3.82 (3 H, s, OCH_3), 3.83 (3 H, s, OCH_3), 3.93 (3 H, s, N-O$\underline{CH_3}$), 6.11 (1 H, s, C=CH), 6.64 (1 H, s, ArH), 6.88 (1 H, s, ArH), 6.90 (1 H, dd, ArH, *J*= 2.4, 6.8 Hz), 7.04 (1 H, d, ArH, *J*= 8.8 Hz), 9.31 (1 H, br.s, OH);

^{13}C NMR (101 MHz, DMSO-d_6) δ ppm: 55.6 (OCH_3), 56.0 (OCH_3), 60.9 (OCH_3), 61.1 (N-O$\underline{CH_3}$), 61.9 (OCH_3), 103.6 (ArCH), 112.3 (ArCH), 113.0 (C=$\underline{C}$H), 115.1 ($\underline{C}$=CH), 115.4 (ArCH), 119.4 (ArCH), 128.0 (ArC), 140.5 (ArC), 141.0 (ArC), 143.4 (ArC), 146.6 (ArC), 148.3 (ArC), 148.5 (ArC), 148.9 (C=N);

V_{max} cm^{-1}: 3345, 2939, 2887, 1684, 1457, 1257, 1188;

HRMS: Calculated 387.1318, found 388.1393 ($M + H^+$).

Synthesis of 2-hydroxy-3,4,5-trimethoxybenzaldehyde (2.27)

Anhydrous $MgCl_2$ beads (3.4 g, 0.036 moles) and solid paraformaldehyde (1.6 g, 0.053 moles) were added to a well dried 250 mL, two necked round bottom flask already equipped with a stirring bar, rubber septa and reflux condenser attached to a nitrogen source. Dry THF (93 mL) was added by a syringe and the reaction was stirred. Freshly dried and distilled triethylamine (5 mL, 0.036 moles) was added dropwise by a syringe and kept the reaction stirring for 10 minutes. After 10 minutes 2,3,4-trimethoxy phenol **(2.01)** (3.2 g, 0.017 moles) was added dropwise by a syringe and refluxed at 80 °C for 6 hours. The reaction was then allowed to cool to room temperature and 100 mL of ether was added. The resulting organic mixture was then washed successively with 1 N HCl (3×100 mL) and water (2×100 mL), dried over anhydrous $MgSO_4$ and filtered. Finally the solvent was removed using rotary evaporator to obtain the hydroxybenzaldehyde **(2.27)** (2.2 g, 0.010 moles, 60%) as pale yellow oil.

^{1}H NMR (400 MHz, CHLOROFORM-*d*) δ ppm: 3.87 (3 H, s, OCH_3), 3.95 (3 H, s, OCH_3), 4.06 (3 H, s, OCH_3), 6.79 (1 H, s, ArH), 9.78 (CHO), 11.01 (OH);

^{13}C NMR (101 MHz, CHLOROFORM-*d*) δ ppm: 56.0 (OCH_3), 60.7 (OCH_3), 60.9 (OCH_3), 108.8 (ArCH), 114.8 (ArC), 140.5 (ArC), 145.9 (ArC), 149.9 (ArC), 151.3 (ArC), 194.4 (C=O);

V_{max} cm^{-1}: 3295, 1690, 1423, 1287, 1133;

HRMS: Calculated 212.0685, found 235.0594 ($M + Na^+$).

Synthesis of 6,7,8-trimethoxy-2-oxo-2H-chromene-3-carboxylic acid (2.28)

2-Hydroxy-3,4,5-trimethoxybenzaldehyde **(2.27)** (200 mg, 0.942 mmoles) and Meldrum's acid (135 mg, 0.937 mmoles) were stirred together in pyridine (2 mL) at room temperature for 20 minutes. The mixture was then heated at a gentle reflux for further 2 hours. The mixture was then allowed to cool to room temperature and stirred further for 10 minutes. After 10 minutes the mixture was acidified with 2 M HCl (20 mL) and extracted with dichloromethane (3×20 mL). The organic phase was dried with anhydrous $MgSO_4$ and solvent removed by rotary evaporation, leaving behind yellow solid. Finally the solid was washed with methanol to afford the carboxycoumarin **(2.28)** (168 mg, 0.599 mmoles, 63%) as yellow solid.

^{1}H NMR (400 MHz, CHLOROFORM-*d*) δ ppm: 3.97 (3 H, s, OCH_3), 4.08 (3 H, s, OCH_3), 4.12 (3 H, s, OCH_3), 6.89 (1 H, s, C=CH), 8.86 (1 H, s, ArH), 12.34 (1 H, br.s, COOH);

^{13}C NMR (101 MHz, CHLOROFORM-*d*) δ ppm: 56.0 (OCH_3), 61.3 (OCH_3), 61.7 (OCH_3), 104.6 (ArCH), 112.2 (C=<u>C</u>H), 113.3 (<u>C</u>=CH), 140.4 (ArC), 144.0 (ArC), 149.2 (ArC), 151.0 (ArC), 150.9 (ArC), 162.4 (C=O), 163.6 (<u>C</u>OOH);

V_{max} cm^{-1}: 3366, 2934, 1766, 1592, 1424, 2287;

HRMS: Calculated 280.0583, found 303.0492 ($M + Na^+$).

Attempted synthesis of 4-bromo-6,7,8-trimethoxy-2-oxo-2H-chromene-3-carboxylic acid

Coumarin-3-carboxylic acid **(2.28)** (80 mg, 0.285 mmoles) and pyridinium tribromide (93 mg, 0.291 mmoles) were stirred together in DCM (3 mL) at room temperature for one hour. After one hour the solvent was evaporated. The remainder was dissolved in ether (40 mL) and washed with aq.HCl (3×20 mL), dried over anhydrous $MgSO_4$ and filtered. Finally solvent was removed using rotary evaporation and the remainder was purified by column chromatography to afford the product **(2.29)** (40 mg, 0.111 mmoles, 39%) as light yellow solid.

^{1}H NMR (400 MHz, CHLOROFORM-*d*) δ ppm: 3.87 (3 H, s, OCH_3), 3.95 (3 H, s, OCH_3), 4.06 (3 H, s, OCH_3), 7.17 (1 H, s, C=CH), 10.33 (COOH);

^{13}C NMR (101 MHz, CHLOROFORM-*d*) δ ppm: 55.9 (OCH_3), 60.7 (OCH_3), 60.9 (OCH_3), 104.8 (ArC), 106.2 (C=CH), 108.8 (C=CH), 140.9 (ArC), 145.3 (ArC), 149.2 (ArC), 149.5 (ArC), 151.9 (C=O), 174.1 (COOH);

Synthesis of 2-(benzyloxy)-3,4,5-trimethoxybenzaldehyde (2.30)

2-Hydroxy-3,4,5-trimethoxybenzaldehyde **(2.27)** (1.5 g, 0.007 moles) and caesium carbonate (2.7 g, 0.008 moles) were stirred together in anhydrous DMF (15 mL) at room temperature. Benzyl bromide (1.4 g, 1 mL, 0.008 moles) was added dropwise by a syringe and the mixture stirred for 3 hours at room temperature. Afterwards the mixture was dissolved in ether (100 mL) and washed successively with water (3×100 mL), dried over $MgSO_4$ and filtered. Finally the solvent was removed using rotary evaporation to obtain the crude product as light brown oil. The oil was further purified by column chromatography first using just hexane and then (1:4, ethyl acetate:hexane) to afford the product **(2.30)** (1.2 g, 0.004 moles, 57%) as light yellow oil.

^{1}H NMR (400 MHz, CHLOROFORM-*d*) δ ppm: 3.84 (3 H, s, OCH_3), 3.96 (3 H, s, OCH_3), 4.01 (3 H, s, OCH_3), 5.14 (2 H, s, CH_2), 7.08 (1 H, s, ArH), 7.37 (5 H, m, ArH), 10.12 (CHO);

V_{max} cm^{-1}: 2935, 1685, 1533, 1479, 1433, 1352;

HRMS: Calculated 302.1154, found 325.1063 ($M + Na^+$).

Synthesis of 2-(benzyloxy)-3,4,5-trimethoxybenzoic acid (2.31)

A solution of acetone (8.5 mL), water (1.9 mL) and acetic acid (0.4 mL) was prepared. 2 mL of this solution was added to 10 mL round bottom flask containing benzaldehyde **(2.30)** (20 mg, 0.066 mmoles). $KMnO_4$ (44 mg, 0.278 mmoles) was added to the solution and the mixture was stirred for two hours at room temperature. After two hours the mixture was dissolved in ether (30 mL) and washed successively with water (3×20 mL), dried over $MgSO_4$ and filtered. Finally the solvent was removed using rotary evaporation to obtain the product as white powder. The product was further purified by column chromatography (1:1:0.02, ethyl acetate:hexane:formic acid) to afford the benzoic acid **(2.31)** (15 mg, 0.047 mmoles, 71%) as white solid.

^{1}H NMR (400 MHz, CHLOROFORM-*d*) δ ppm: 3.91 (3 H, s, OCH_3), 4.00 (3 H, s, OCH_3), 4.04 (3 H, s, OCH_3), 5.27 (2 H, s, CH_2), 7.42 (6 H, m, ArH);

^{13}C NMR (101 MHz, CHLOROFORM-*d*) δ ppm: 55.8 (OCH_3), 60.9 (OCH_3), 61.2 (OCH_3), 77.4 (CH_2), 108.5 (ArCH), 116.0 (ArC), 128.5 (2×ArCH), 128.8 (2×ArCH), 129.0 (ArCH), 134.1 (ArC), 145.2 (ArC), 145.7 (ArC), 147.4 (ArC), 149.6 (ArC), 164.5 (C=O);

HRMS: Calculated 318.1103, found 341.2032 ($M + Na^+$).

Synthesis of pentafluorophenyl 2-(benzyloxy)-3,4,5-trimethoxybenzoate (2.32)

Carboxylic Acid **(2.31)** (100 mg, 0.314 mmoles) was dissolved in anhydrous DCM (5 mL) at 0 °C under the atmosphere of nitrogen. After that pentaflourophenol (64 mg, 0.348 mmoles) was added by dissolving in dry DCM (2 mL), followed by the addition of EDC.HCl (78 mg, 0.408 mmoles). The reaction mixture was allowed to stir at 0 °C for 4 hours. After 4 hours the reaction was diluted with diethyl ether 100 mL and washed once with water (50 mL) and dried over $MgSO_4$. The organic solvent was removed using rotary evaporation and the crude product was further purified by column chromatography (1:4, ethyl acetate:hexane) to afford the ester **(2.32)** (110 mg, 0.227 mmole, 72%) as white solid.

^{1}H NMR (400 MHz, CHLOROFORM-*d*) δ ppm: 3.94 (3 H, s, OCH_3), 3.96 (3 H, s, OCH_3), 4.06 (3 H, s, OCH_3), 5.11 (2 H, s, CH_2), 7.35 (4 H, m, ArH), 7.51 (2 H, d, ArH);

^{13}C NMR (101 MHz, CHLOROFORM-*d*) δ ppm: 55.9 (OCH_3), 60.9 (OCH_3), 61.1 (OCH_3), 76.0 (CH_2), 108.6 (2×ArC), 115.1 (ArCH), 127.7 (ArCH), 127.9 (2×ArCH), 128.0 (2×ArCH), 136.5 (ArC), 147.6 (ArC), 148.4 (ArC), 148.8 (ArC), 149.0 (ArC), 160.3 (C=O).

Synthesis of pentafluorophenyl 2-hydroxy-3,4,5-trimethoxybenzoate (2.33)

Pentafluorophenyl 2-(benzyloxy)-3,4,5-trimethoxybenzoate **(2.32)** (50 mg, 0.103 mmoles) was dissolved in ethanol:ethyl acetate (1:1, 3 mL). Catalytic amount of Pd/C (5 mg, 10% by weight) was added and the reaction was stirred under the atmosphere of hydrogen for 90 minutes at room temperature. After 90 minutes, the reaction mixture was filtered through a cotton plug and solvent evaporated using rotary evaporation. Finally product was

purified by column chromatography (1:4, ethyl acetate:hexane) to afford the product **(2.33)** (31 mg, 0.079 mmoles, 76%) as light brown oil.

^{1}H NMR (400 MHz, CHLOROFORM-*d*) δ ppm: 3.91 (3 H, s, OCH_3), 3.97 (3 H, s, OCH_3), 4.10 (3 H, s, OCH_3), 7.26 (1 H, s, ArH), 9.80 (OH);

^{13}C NMR (101 MHz, CHLOROFORM-*d*) δ ppm: 56.0 (OCH_3), 60.8 (OCH_3), 61.0 (OCH_3), 103.0 (ArCH), 105.7 (ArC), 141.1 (ArC), 145.7 (ArC), 150.4 (ArC), 152.6 (ArC), 165.5 (C=O).

Hydrolysis of pentafluorophenyl ester (2.33) to form 2-hydroxy-3,4,5-trimethoxybenzoic acid (2.34)

Pentafluorophenyl 2-hydroxy-3,4,5-trimethoxybenzoate **(2.33)** (170 mg, 0.431 mmoles) and Meldrum's acid (62 mg, 0.431 mmoles) were stirred together in pyridine (2 mL) at room temperature for 20 minutes. The mixture was then heated at a gentle reflux for further 2 hours. After 2 hours the reaction mixture was allowed to cool to room temperature and stirred further for 10 minutes. After 10 minutes the mixture was acidified with 2 M HCl and extracted with dichloromethane (3×20 mL). The organic phase was dried with anhydrous $MgSO_4$ and solvent removed by rotary evaporation. Product was further purified by column chromatography first using (1:4, ethyl acetate:hexane) and then (1:1:0.02, ethyl acetate:hexane:formic acid). Finally solvent was evaporated to afford the acid **(2.34)** (60 mg, 0.263 mmoles, 61%) as light brown oil.

^{1}H NMR (400 MHz, CHLOROFORM-*d*) δ ppm: 3.87 (3 H, s, OCH_3), 3.95 (3 H, s, OCH_3), 4.06 (3 H, s, OCH_3), 7.17 (1 H, s, ArH), 10.33 (CO<u>OH</u>);

^{13}C NMR (101 MHz, CHLOROFORM-*d*) δ ppm: 55.9 (OCH_3), 60.7 (OCH_3), 60.9 (OCH_3), 104.9 (ArCH), 106.2 (ArC), 140.9 (ArC), 145.3 (ArC), 149.5 (ArC), 152.0 (ArC), 174.1 (C=O);

HRMS: Calculated 228.0634, found 251.1572 ($M + Na^+$).

Synthesis of (2-(benzyloxy)-3,4,5-trimethoxyphenyl)(3-((*tert*-butyldimethylsilyl)oxy)-4-methoxyphenyl)methanol (2.35)

To a well-stirred dry mixture of Mg (60.52 mg, 2.522 mmoles) in dry THF (5 mL) under nitrogen atmosphere was added iodine (1.2 mg, 0.005 mmoles) and 1,2-dibromoethane (5.4

mg, 0.029 mmoles). The reaction mixture was refluxed for 30 minutes. To this reaction mixture was added phenyl bromide **(2.09)** (400 mg, 1.261 mmoles) through a syringe and maintained the reaction at a gentle reflux for one hour. After one hour the reaction was cooled to room temperature and benzaldehyde **(2.30)** (346 mg, 1.147 mmoles) was added through a syringe by dissolving in THF. The reaction mixture was again refluxed at a gentle heat for two hours. The reaction was cooled to room temperature, filtered and aq. HCl (30 mL, 2M) was added, followed by extraction with ether (3×30 mL). The organic layer was dried with magnesium sulphate and solvent evaporated using rotary evaporation. Finally the product was further purified by column chromatography (1:4, ethyl acetate:hexane) to afford the product **(2.35)** (347 mg, 0.642 mmoles, 56%) as light brown oil.

^{1}H NMR (400 MHz, CHLOROFORM-*d*) δ ppm: 0.13 (6 H, s, 2 × CH_3), 0.99 (9 H, s, $C(CH_3)_3$), 3.81 (3 H, s, OCH_3), 3.81 (3 H, s, OCH_3), 3.94 (3 H, s, OCH_3), 3.97 (3 H, s, OCH_3), 4.84 (2 H, d, CH_2), 5.89 (1 H, s, CH), 6.61 (1 H, s, ArH), 6.85 (3 H, m, ArH), 7.38 (5 H, s, ArH);

^{13}C NMR (101 MHz, CHLOROFORM-*d*) δ ppm: -5.1 (2 × $Si(CH_3)$), 18.0 ($\underline{C}(CH_3)_3$), 25.3 ($C(\underline{C}H_3)_3$, 55.1 (OCH_3), 55.7 (OCH_3), 60.8 (OCH_3), 60.8 (OCH_3), 70.7 (CH), 74.8 (CH_2), 105.0 (ArCH), 111.3 (ArCH), 119.0 (ArCH), 119.3 (ArCH), 127.7 (ArCH), 128.0 (2×ArCH), 128.0 (2×ArCH), 131.9 (ArC), 135.7 (ArC), 136.9 (ArC), 141.9 (ArC), 142.9 (ArC), 144.3 (ArC), 146.6 (ArC), 149.1 (ArC), 149.8 (ArC);
V_{max} cm^{-1}: 3345, 2948, 2957, 1586, 1469, 1438, 1417, 1252, 1168, 832;

HRMS: Calculated 540.2543, found 563.3472 ($M + Na^+$).

Synthesis of (2-(benzyloxy)-3,4,5-trimethoxyphenyl)(3-((*tert*-butyldimethylsilyl)oxy)phenyl)methanone (2.36)

Alcohol **(2.35)** (300 mg, 0.555 mmoles) was dissolved in dry DCM (15 mL) under atmosphere of nitrogen and cooled to 0 °C, followed by addition of Dess-martin Periodinane (259 mg, 0.610 mmoles). The reaction mixture was stirred for one hour at 0 °C. After one hour the reaction was quenched with aq. $NaHCO_3$ (20 mL, 5%) and extracted with DCM (2×30 mL). Finally the organic layer was dried using $MgSO_4$ and solvent removed using rotary evaporation to afford the product as brown oil. The product was

further purified by column chromatography (1:8, ethyl acetate:hexane) to afford the product **(2.36)** (249 mg, 0.462 mmole, 83%) as yellow sticky oil.

^{1}H NMR (400 MHz, CHLOROFORM-*d*) δ ppm: 0.16 (6 H, s, 2 × CH_3), 1.01 (9 H, s, $C(CH_3)_3$), 3.86 (3 H, s, OCH_3), 3.89 (3 H, s, OCH_3), 3.97 (3 H, s, OCH_3), 4.00 (3 H, s, OCH_3), 4.90 (2 H, d, CH_2), 6.68 (1 H, s, ArH), 6.85 (1 H, d, ArH, J = 9.03 Hz, 7.14 (2 H, overlapping signals, ArH), 7.24 (3 H, m, ArH), 7.43 (2 H, m, ArH);

^{13}C NMR (101 MHz, CHLOROFORM-*d*) δ ppm: -5.1 (2 × $Si(CH_3)$), 18.0 ($\underline{C}(CH_3)_3$), 25.2 ($C(\underline{C}H_3)_3$, 55.1 (OCH_3), 55.7 (OCH_3), 60.9 (OCH_3), 61.0 (OCH_3), 75.9 (CH_2), 106.2 (ArCH), 110.2 (ArCH), 121.5 (ArCH), 125.4 (ArCH), 127.4 (ArCH), 127.7 (4×ArCH), 128.6 (ArC), 130.3 (ArC), 136.6 (ArC), 143.7 (ArC), 144.2 (ArC), 144.4 (ArC), 146.8 (ArC), 149.1 (ArC), 155.1 (ArC), 193.7 (C=O);
V_{max} cm^{-1}: 2954, 1675, 1493, 1349, 1155;

HRMS: Calculated 508.2281, found 509.2354 ($M + H^+$).

Synthesis of (3-((*tert*-butyldimethylsilyl)oxy)-4-methoxyphenyl)(2-hydroxy-3,4,5-trimethoxyphenyl)methanone (2.37)

Ketone **(2.36)** (200 mg, 0.371 mmoles) was dissolved in ethyl acetate and ethanol solution (5 mL, 1:1). A catalytic amount of Pd/C (20 mg, 10% by weight) was added and the reaction was stirred under the atmosphere of hydrogen for 90 minutes at room temperature. After 90 minutes the reaction mixture was filtered through a cotton plug and solvent evaporated using rotary evaporation. Finally the crude product was purified by flash column chromatography (1:4, ethyl acetate:hexane) to afford the compound **(2.37)** (118 mg, 0.263 mmoles, 71%) as yellow oil.

^{1}H NMR (400 MHz, CHLOROFORM-*d*) δ ppm: 0.21 (6 H, s, 2 × CH_3), 1.02 (9 H, s, $C(CH_3)_3$), 3.75 (3 H, s, OCH_3), 3.92 (3 H, s, OCH_3), 3.99 (3 H, s, OCH_3), 4.08 (3 H, s, OCH_3), 6.94 (1 H, s, ArH), 6.96 (1 H, overlapping-d, ArH, J = 8.8 Hz, 7.26 (1 H, s, ArH), 7.35 (1 H, d, ArH, J = 8.8 Hz), 12.20 (1 H, br.s, OH);

^{13}C NMR (101 MHz, CHLOROFORM-*d*) δ ppm: -5.0 (2 × $Si(CH_3)$), 18.0 ($\underline{C}(CH_3)_3$), 25.2 ($C(\underline{C}H_3)_3$, 55.1 (OCH_3), 56.2 (OCH_3), 60.7 (OCH_3), 60.9 (OCH_3), 110.1 (ArCH), 110.5

(ArCH), 113.4 (ArC), 121.3 (ArCH), 123.6 (ArCH), 130.3 (ArC), 141.1 (ArC), 144.2 (ArC), 144.3 (ArC), 149.0 (ArC), 153.1 (ArC), 154.0 (ArC), 198.5 (C=O);

V_{max} cm^{-1}: 3423, 2955, 2846, 1664, 1446, 1360, 1147, 940;

HRMS: Calculated 448.1917, found 471.2856 ($M + Na^+$).

Undesirable deprotection to give (2-hydroxy-3,4,5-trimethoxyphenyl)(3-hydroxy-4-methoxyphenyl)methanone (2.38)

Hydroxy benzophenone **(2.37)** was stirred with ammonia (7 M in methanol) overnight at room temperature. Upon completion solvent was evaporated and the remainder was purified by flash column chromatography (1:2, ethyl acetate:hexane) to afford the compound **(2.38)** as yellow solid.

Synthesis of 4-bromo-6,7,8-trimethoxy-2-oxo-2H-chromene-3-carbaldehyde (2.39)

Phosphorus (V) oxybromide (1.72 g, 0.006 moles) was dissolved in dry DCM (30 mL) at 0 °C under the atmosphere of nitrogen and stirred for 5 minutes. To this was added anhydrous DMF (3 mL) dropwise and allowed to stir at 0 °C for 1 hour. After 1 hour the reaction mixture was brought to room temperature and 4-hydroxycoumarin intermediate **(2.04)** (1.26 g, 0.005 moles) was added by dissolving in anhydrous DMF (20 mL). The resultant mixture was refluxed at 80 °C for 45 minutes. Following this step the more volatile solvent was removed using rotary evaporator while the remainder was poured on to ice and quenched with cooled 5% aqueous sodium bicarbonate (70 mL). The aqueous solution was then extracted with diethyl ether (3×100 mL), dried with magnesium sulphate, filtered and solvent evaporated using rotary evaporator. The solid residue obtained was finally purified by column chromatography (1:1, ethyl acetate:hexane) to afford the aldehyde **(2.39)** (0.850 g, 0.0025 moles, 50%) as yellow solid.

^{1}H NMR (400 MHz, CHLOROFORM-*d*) δ_H ppm: 4.00 (3 H, s, OCH_3), 4.04 (3 H, s, OCH_3), 4.13 (3 H, s, OCH_3), 7.34 (1 H, s, ArH), 10.32 (C<u>H</u>O);

^{13}C NMR (101 MHz, CHLOROFORM-*d*) δ ppm: 56.4 (OCH_3), 61.7 (OCH_3), 62.1 (OCH_3), 102.5 (ArCH), 113.4 (C=<u>C</u>H), 116.3 (<u>C</u>=CH), 140.4 (ArC), 143.5 (ArC), 149.5 (ArC), 150.6 (ArC), 153.2 (ArC), 158.5 (C=O), 187.0 (CHO);

V_{max} cm^{-1}: 2956, 1636, 1545, 1433, 1221;

HRMS: Calculated 341.9739, found 365.0667 ($M + Na^+$).

Synthesis of 4-bromo-3-(1,3-dioxolan-2-yl)-6,7,8-trimethoxy-2H-chromen-2-one (2.40)

Bromo-aldehyde **(2.39)** (100 mg, 0.291 mmoles) was dissolved in dry DCM (3 mL) under the atmosphere of nitrogen at room temperature. To this was added ethylene glycol (1 mL), anhydrous triethyl orthoformate (534 mg, 3.603 mmoles, 600 µL) and *p*-Toluenesulfonic acid monohydrate (2 mg, 0.010 mmoles). The resultant mixture was stirred for 3 hours at room temperature. After 3 hours the reaction mixture was diluted with 50 mL of DCM, washed once with 5% aqueous sodium bicarbonate (50 mL) and quickly dried with magnesium sulphate. Upon evaporation of the solvent, the crude residue obtained was purified by column chromatography (1:2, ethyl acetate:hexane) to afford the bromo-acetal **(2.40)** (80 mg, 0.206 mmoles, 71%) as light yellow oil that solidified on further vacuum drying.

^{1}H NMR (400 MHz, CHLOROFORM-*d*) δ_H ppm: 3.95 (3 H, s, OCH_3), 4.01 (3 H, s, OCH_3), 4.04 (3 H, s, OCH_3), 4.06 (2 H, m, CH_2), 4.36 (2 H, m, CH_2), 6.41 (1 H, s, CH), 7.11 (1 H, s, ArH);

^{13}C NMR (101 MHz, CHLOROFORM-*d*) δ ppm: 56.4 (OCH_3), 61.6 (OCH_3), 62.0 (OCH_3), 66.6 ($2\times CH_2$), 100.3 (CH), 101.8 (ArCH), 113.5 (ArC), 120.1 (ArC), 140.6 (C=C), 141.9 (C=C), 147.2 (ArC), 148.9 (ArC), 150.1 (ArC), 157.2 (C=O)

V_{max} cm^{-1}: 2943, 1716, 1564, 1487, 1459, 1419, 1366, 1110, 1062, 941;

HRMS: Calculated 386.0001, found 387.0074 ($M + H^+$).

Synthesis of *tert*-butyl (5-(3-(1,3-dioxolan-2-yl)-6,7,8-trimethoxy-2-oxo-2H-chromen-4-yl)-2-methoxyphenyl)carbamate (2.41) via Suzuki coupling

Bromo-acetal **(2.40)** (758 mg, 1.958 mmoles), boronic ester **(2.14)** (820 mg, 2.349 mmoles) and potassium carbonate (676 mg, 4.895 mmoles) were stirred in a biphasic toluene:ethanol:water mixture (3:1:1, 30 mL). To this was added tetrakis (triphenylphosphine) palladium (0) (103 mg, 0.089 mmoles) and the reaction was refluxed for 2 hours. Upon completion, the reaction was then diluted with ethyl acetate (100 mL),

dried with magnesium sulphate and concentrated *in vacuo*. Finally the crude product was purified by column chromatography (1:2, ethyl acetate:hexane) to afford the product **(2.41)** (640 mg, 1.208 mmoles, 62%) as off white solid.

^{1}H NMR (400 MHz, CHLOROFORM-*d*) δ_H ppm: 1.50 (9 H, s, $(CH_3)_3$), 3.67 (3 H, s, OCH_3), 3.87 (2 H, m, CH_2), 3.96 (3 H, s, OCH_3), 4.00 (3 H, s, OCH_3), 4.03 (3 H, s, OCH_3), 4.23 (2 H, m, CH_2), 5.70 (1 H, s, CH), 6.42 (1 H, s, ArH), 6.95 (1 H, d, ArH, J= 2 Hz), 6.98 (1 H, s, ArH), 7.15 (1 H, br.s, NH), 8.09 (1 H, s, ArH);

^{13}C NMR (101 MHz, CHLOROFORM-*d*) δ ppm: 28.3 (C($\underline{C}H_3)_3$), 55.8 (OCH_3), 56.2 (OCH_3), 61.5 (OCH_3), 61.9 (OCH_3), 66.5 (CH_2), 66.5 (CH_2), 80.7 ($\underline{C}(CH_3)_3$), 101.2 (CH), 104.6 (ArCH), 109.7 (ArCH), 115.6 (ArC), 118.6 (ArCH), 120.2 (C=$\underline{C}$), 123.1 (ArCH), 125.6 (ArC), 128.2 (ArC), 140.7 (ArC), 142.7 (ArC), 146.0 (ArC), 147.9 (ArC), 149.4 (ArC), 152.4 (N$\underline{C}$=O), 155.0 ($\underline{C}$=C), 158.4 (C=O);

V_{max} cm^{-1}: 3434, 2976, 2938, 1728, 1590, 1563, 1531, 1481, 1373, 1244, 1156, 1099;

HRMS: Calculated 529.1948, found 552.2886 ($M + Na^+$).

Synthesis of *tert*-butyl (5-(3-formyl-6,7,8-trimethoxy-2-oxo-2H-chromen-4-yl)-2-methoxyphenyl)carbamate (2.42)

N-Boc protected aniline **(2.41)** (60 mg, 0.113 mmoles) was dissolved in DCM:Acetone (1:1, 5 mL). To this was added iodine (6 mg, 0.024 mmoles) and the resultant solution was refluxed at 50 °C for 1 hour. Following this step the solvent was evaporated and the resultant crude product obtained was purified by column chromatography (1:2, ethyl acetate:hexane) to afford the aldehyde **(2.42)** (50 mg, 0.103 mmoles, 91%) as yellow solid.

^{1}H NMR (400 MHz, CHLOROFORM-*d*) δ_H ppm: 1.51 (9 H, s,$(CH_3)_3$), 3.72 (3 H, s, OCH_3), 3.99 (3 H, s, OCH_3), 4.05 (3 H, s, OCH_3), 4.07 (3 H, s, OCH_3), 6.62 (1 H, s, ArH), 6.94 (1 H, dd, ArH, J= 2.4 Hz , 8.4 Hz), 7.01 (1 H, d, ArH, J= 8.4 Hz), 7.20 (1 H, s, NH), 8.17 (1 H,s, ArH), 9.89 (CHO);

^{13}C NMR (101 MHz, CHLOROFORM-*d*) δ ppm: 28.3 (C($\underline{C}H_3)_3$), 55.9 (OCH_3), 56.2 (OCH_3), 61.6 (OCH_3), 62.0 (OCH_3), 80.9 ($\underline{C}(CH_3)_3$), 105.1 (ArCH), 109.8 (ArCH), 114.9 (ArC), 117.6 (C=$\underline{C}$), 118.3 (ArCH), 123.6 (ArCH), 124.2 (ArC), 128.5 (ArC), 140.7 (ArC),

144.5 (ArC), 148.5 (ArC), 148.7 (ArC), 149.9 (ArC), 152.5 (NH-C=O), 158.0 (C=O), 161.6 (C=C), 188.6 (HC=O);

V_{max} cm^{-1}: 3432, 2976, 2941, 1745, 1720, 1526, 1453, 1378, 1244, 1152, 1052;

HRMS: Calculated 485.1686, found 508.2624 ($M + Na^+$).

Synthesis of 4-(3-((*tert*-butoxycarbonyl)amino)-4-methoxyphenyl)-6,7,8-trimethoxy-2-oxo-2H-chromene-3-carboxylic acid (2.43)

Aldehyde (2.42) (170 mg, 0.350 mmoles) was dissolved in acetonitrile (5 mL). To this was added sodium phosphate monobasic monohydrate (14.5 mg, 0.105 mmoles) in distilled water (2 mL) and hydrogen peroxide (160 µL, 30% solution). This step was followed by the dropwise addition of sodium chlorite (63 mg, 0.701 mmoles) in distilled water (2 mL). The reaction mixture was stirred for one hour at room temperature, then quenched with 2 M HCl (20 mL) and extracted with ethyl acetate (3×20 mL). Upon evaporation of the organic solvent the crude residue obtained was finally purified by column chromatography (1:1:0.02, ethyl acetate:hexane:formic acid) affording the carboxylic acid **(2.43)** (160 mg, 0.319 mmoles, 91%) as reddish oil that solidified on further vacuum drying.

^{1}H NMR (400 MHz, CHLOROFORM-*d*) δ_H ppm: 1.48 (9 H, s,$(CH_3)_3$), 3.70 (3 H, s, OCH_3), 3.95 (3 H, s, OCH_3), 4.04 (3 H, s, OCH_3), 4.05 (3 H, s, OCH_3), 6.60 (1 H, s, ArH), 6.91 (1 H, dd, ArH, J= 2 Hz , 8.4 Hz), 6.98 (1 H, d, ArH, J= 8.4 Hz), 7.17 (1 H, s, NH), 8.04 (1 H, s , ArH), 9.17 (1 H, br.s, OH);

^{13}C NMR (101 MHz, CHLOROFORM-*d*) δ ppm: 28.3 ($C(CH_3)_3$), 55.8 (OCH_3), 56.2 (OCH_3), 61.6 (OCH_3), 62.1 (OCH_3), 80.7 ($C(CH_3)_3$), 105.4 (ArCH), 110.0 (ArCH), 113.0 (ArC), 115.6 (C=C), 117.5 (ArCH), 121.8 (ArCH), 126.6 (ArC), 128.1 (ArC), 140.5 (ArC), 142.7 (ArC), 148.2 (ArC), 148.3 (ArC), 150.4 (ArC), 152.6 (NH-C=O), 161.3 (C=O), 162.8 (OH-C=O), 163.7 (C=C);

V_{max} cm^{-1}: 3434, 2976, 2942, 1722, 1531, 1459, 1246, 1105, 754;

HRMS: Calculated 501.1635, found 524.2573 ($M + Na^+$).

Synthesis of 4-(3-amino-4-methoxyphenyl)-6,7,8-trimethoxy-2-oxo-2H-chromene-3-carboxylic acid (2.44)

Carboxylic acid **(2.43)** (90 mg, 0.179 mmoles) was dissolved in dry DCM (3 mL) under atmosphere of nitrogen and cooled to -10 °C. To this was added dry cooled trifluoroacetic acid (1 mL) and stirred for 90 minutes at 0 °C. Following this step the reaction mixture was diluted with DCM (30 mL), solvent evaporated using rotary evaporator and the oil left behind was redissolved in DCM (8 mL) and stirred with 5% sodium bicarbonate (2 mL) for 3 minutes. After that the aqueous layer was carefully removed with the help of Pasteur pipette and the organic layer was dried with magnesium sulphate. Upon evaporation of the organic solvent, the crude residue obtained was further purified by column chromatography (4:1, DCM:methanol) to afford the aniline **(2.44)** (56 mg, 0.139 mmoles, 78%) as yellow solid.

^{1}H NMR (600 MHz, DMSO-d_6) δ ppm: 3.62 (3 H, s, OCH_3), 3.81 (3 H, s, OCH_3), 3.85 (3 H, s, OCH_3), 3.92 (3 H, s, OCH_3), 4.80 (2 H, br.s, NH_2), 6.56 (1 H, s, ArH), 6.69 (1 H, dd, ArH, J= 1.8 Hz , 8.4 Hz), 6.75 (1 H, d, ArH, J= 1.8 Hz), 6.83 (1 H, d, ArH, J= 8.4 Hz);

^{13}C NMR (151 MHz, DMSO-d_6) δ ppm: 55.7 (OCH_3), 56.4 (OCH_3), 61.5 (OCH_3), 61.9 (OCH_3), 104.4 (ArCH), 110.4 (ArCH), 115.0 (ArCH), 116.3 (ArC), 117.8 (ArCH), 127.2 (ArC), 137.5 (ArC), 140.8 (ArC), 141.2 (ArC), 144.40 (ArC), 147.0 (ArC), 149.3 (ArC), 159.5 (C=O), 167.4 (COOH);

V_{max} cm^{-1}: 332.02, 2926, 1723, 1533, 1453, 1247, 1156, 755;

HRMS: Calculated 401.1111, found 402.1184 ($M + H^+$).

Synthesis of *tert*-butyl (5-(3-((hydroxyimino)methyl)-6,7,8-trimethoxy-2-oxo-2H-chromen-4-yl)-2-methoxyphenyl)carbamate (2.45)

Aldehyde **(2.42)** (120 mg, 0.247 mmoles) was dissolved in anhydrous DMF (2 mL) at room temperature under the atmosphere of nitrogen. To this was added hydroxylamine hydrochloride (26 mg, 0.371 mmoles) and diisopropylethylamine (64 µL, 0.371 mmoles). The reaction mixture was stirred for 10 minutes at room temperature. After 10 minutes the reaction was quenched with water (20 mL), extracted with diethyl ether (3 × 30 mL) and dried with magnesium sulphate. Following this step the organic solvent was evaporated and

the crude product obtained was further purified by column chromatography (2:1, ethyl acetate:hexane) to afford the aldoxime **(2.45)** (100 mg, 0.200 mmoles, 81%) as light yellow solid.

^{1}H NMR (400 MHz, CHLOROFORM-*d*) δ_H ppm: 1.52 (9 H, s,$(CH_3)_3$), 3.70 (3 H, s, OCH_3), 4.00 (3 H, s, OCH_3), 4.03 (3 H, s, OCH_3), 4.06 (3 H, s, OCH_3), 6.50 (1 H, s, ArH), 6.90 (1 H, dd, ArH, J= 2 Hz , 8.4 Hz), 7.01 (1 H, d, ArH, J= 8.4 Hz), 7.20 (OH), 7.87 (1 H, s, ArH), 8.10 (1 H, s, CH);

^{13}C NMR (101 MHz, CHLOROFORM-*d*) δ ppm: 28.3 (C($\underline{C}H_3)_3$), 55.9 (OCH_3), 56.2 (OCH_3), 61.5 (OCH_3), 62.0 (OCH_3), 80.9 ($\underline{C}(CH_3)_3$), 104.3 (ArCH), 110.2 (ArCH), 115.4 (ArC), 115.5 ($\underline{C}$=C), 118.4 (CH), 123.3 (ArCH), 125.4 (ArC), 128.7 (ArC), 140.7 (ArC), 142.3 (ArC), 145.3 (ArCH), 146.6 (ArC), 148.2 (ArC), 149.7 (ArC), 152.5 (HN-$\underline{C}$=O), 155.1 (C=$\underline{C}$), 157.6 (C=O);

V_{max} cm^{-1}: 3345, 2949, 1720, 1685, 1439, 1321, 1155;

HRMS: Calculated 500.1795, found 523.2723 ($M + Na^+$).

Synthesis of 4-(3-amino-4-methoxyphenyl)-6,7,8-trimethoxy-2-oxo-2H-chromene-3-carbaldehyde oxime (2.46)

N-Boc protected Aldoxime **(2.45)** (60 mg, 0.120 mmoles) was dissolved in dry DCM (3 mL) under atmosphere of nitrogen and cooled to -10 °C. To this was added dry cooled trifluoroacetic acid (1 mL) and stirred for 90 minutes at 0 °C. Following this step the reaction mixture was diluted with DCM (30 mL), solvent evaporated using rotary evaporator and the oil left behind was redissolved in DCM (10 mL) and stirred with 5% sodium bicarbonate (2 mL) for 3 minutes. After which the aqueous layer was carefully removed with the help of Pasteur pipette and the organic layer was dried with magnesium sulphate. Upon evaporation of the organic solvent, the crude residue obtained was further purified by column chromatography (3:1, ethyl acetate:hexane) to afford the aniline **(2.46)** (35 mg, 0.087 mmoles, 73%) as yellow solid.

^{1}H NMR (400 MHz, DMSO-d_6) δ ppm: 3.61 (3 H, s, OCH_3), 3.86 (3 H, s, OCH_3), 3.89 (3 H, s, OCH_3), 3.95 (3 H, s, OCH_3), 5.01 (2 H, s, NH_2), 6.46 (1 H, s, ArH), 6.49 (1 H, dd,

ArH, J= 2 Hz , 8.4 Hz), 6.59 (1 H, d, ArH, J= 2 Hz), 6.97 (1 H, d, ArH, J= 8.4 Hz), 7.65 (1 H, s, CH), 11.43 (OH);

^{13}C NMR (101 MHz, DMSO-d_6) δ ppm: 55.3 (OCH_3), 56.0 (OCH_3), 61.1 (OCH_3), 61.5 (OCH_3), 104.2 (ArCH), 110.3 (ArCH), 113.5 (ArCH), 115.4 (ArC), 115.6 (C=C), 116.6 (ArCH), 125.5 (ArC), 137.9 (ArC), 140.2 (ArC), 141.5 (ArC), 144.0 (CH), 145.7 (ArC), 146.7 (ArC), 149.2 (ArC), 154.1 (C=C), 157.0 (C=O);

V_{max} cm^{-1}: 3433, 2932, 2847, 1640, 1596, 1382, 1154;

HRMS: Calculated 400.1271, found 401.1340 ($M + H^+$)

Synthesis of *tert*-butyl (5-(3-(hydroxymethyl)-6,7,8-trimethoxy-2-oxo-2H-chromen-4-yl)-2-methoxyphenyl)carbamate (2.47)

Aldehyde **(2.42)** (115 mg, 0.237 mmoles) was dissolved in Methanol:DCM (4:1, 3mL). To this was added sodium borohydride (3 mg, 0.079 mmoles) and allowed to stir at room temperature for 5 minutes. Following this step the reaction mixture was quenched with saturated aqueous sodium chloride solution (20 mL), extracted with diethyl ether (3 × 20 mL) and dried with magnesium sulphate. Afterwards the organic solvent was evaporated and the remainder was further purified by column chromatography (1:1, ethyl acetate:hexane) to afford the alcohol **(2.47)** (90 mg, 0.185 mmoles, 78%) as light yellow solid.

^{1}H NMR (400 MHz, CHLOROFORM-*d*) δ_H ppm: 1.52 (9 H, s,$(CH_3)_3$), 3.71 (3 H, s, OCH_3), 3.99 (3 H, s, OCH_3), 4.01 (3 H, s, OCH_3), 4.07 (3 H, s, OCH_3), 4.34 (1 H, d, CH_2, J= 12.4 Hz), 4.50 (1 H, d, CH_2, J= 12.4 Hz), 6.51 (1 H, s, ArH), 6.97 (1 H, dd, ArH, J= 2 Hz , 8.4 Hz), 7.01 (1 H, d, ArH, J= 8.4 Hz), 7.18 , 8.08 (1 H, s, ArH)

^{13}C NMR (101 MHz, CHLOROFORM-*d*) δ ppm: 28.3 (C(CH_3)$_3$), 55.9 (OCH_3), 56.2 (OCH_3), 59.5 (CH_2), 61.5 (OCH_3), 62.0 (OCH_3), 80.8 (C(CH_3)$_3$), 104.5 (ArCH), 110.0 (ArCH), 115.8 (C=C), 118.5 (ArCH), 122.8 (ArCH), 123.4 (ArC), 125.9 (ArC), 128.4 (ArC), 141.0 (ArC), 142.0 (ArC), 145.6 (ArC),148.0 (ArC), 149.8 (ArC), 152.3 (HN-C=O), 152.5 (C=C), 162.4 (C=O)

V_{max} cm^{-1}: 3332, 2976, 2938, 1698, 1529, 1480, 1459, 1420, 1380, 1246, 1141, 1104, 1043;

HRMS: Calculated 487.1842, found 488.1928 ($M + H^+$)

Synthesis of 4-(3-amino-4-methoxyphenyl)-3-(hydroxymethyl)-6,7,8-trimethoxy-2H-chromen-2-one (2.48)

N-Boc Alcohol **(2.47)** (90 mg, 0.185 mmoles) was dissolved in dry DCM (3 mL) under atmosphere of nitrogen and cooled to -10 °C with salted ice. To this was added dry cooled trifluoroacetic acid (1 mL) and allowed to stir for 90 minutes at 0 °C. Following this step the reaction mixture was diluted with DCM (30 mL), solvent evaporated using rotary evaporator and the oil left behind was redissolved in DCM (10 mL) and stirred with 5% sodium bicarbonate (2 ml) for 3 minutes. After which the aqueous layer was carefully removed with the help of Pasteur pipette and the organic layer was dried with magnesium sulphate. Upon evaporation of the organic solvent, the crude residue obtained was further purified by column chromatography (2:1, ethyl acetate:hexane) to afford the product **(2.48)** (60 mg, 0.155 mmoles, 84%) as light yellow solid.

^{1}H NMR (400 MHz, CHLOROFORM-*d*) δ_H ppm: 3.26 (2 H, br.s, NH_2), 3.70 (3 H, s, OCH_3), 3.96 (3 H, s, OCH_3), 4.01 (3 H, s, OCH_3), 4.07 (3 H, s, OCH_3), 4.41 (2 H, q , CH_2, , J= 12 Hz), 6.46 (1 H, s, ArH), 6.68 (1 H, dd, ArH, J= 1.5, 8.3 Hz), 6.73 (1 H, d, ArH, , J= 1.5 Hz), 6.93 (1 H, d, ArH, J= 8.3 Hz);

^{13}C NMR (101 MHz, CHLOROFORM-*d*) δ ppm: 55.6 (OCH_3), 56.3 (OCH_3), 59.4 (CH_2), 61.5 (OCH_3), 61.9 (OCH_3), 104.4 (ArCH), 110.2 (ArCH), 114.9 (ArCH), 116.0 (ArC), 118.9 (ArCH), 123.2 (C=C), 125.9 (ArC), 136.0 (ArC), 140.9 (ArC), 142.0 (ArC), 145.6 (ArC), 147.9 (ArC), 149.7 (ArC), 152.7 (C=C), 162.4 (C=O);

V_{max} cm^{-1}: 3433, 2975, 2936, 1697, 1518, 1484, 1459, 11456, 1113, 1049;

HRMS: Calculated 387.1318, found 388.1379 ($M + H^+$).

Synthesis of 3-(1,3-dioxolan-2-yl)-4-(3-hydroxy-4-methoxyphenyl)-6,7,8-trimethoxy-2H-chromen-2-one (2.50) through suzuki coupling intermediate (2.49)

Bromo-acetal **(2.40)** (120 mg, 0.311 mmoles), boronic acid **(2.10)** (96 mg, 0.342 mmoles) and potassium carbonate (107 mg, 0.777 mmoles) were stirred in a biphasic

toluene:ethanol:water mixture (3:1:1, 10 mL). To this was added tetrakis (triphenylphosphine) palladium (0) (17 mg, 0.015 mmoles) and the reaction was refluxed for 2 hours. Upon completion the reaction was then diluted with ethyl acetate (50 mL), dried with magnesium sulphate and concentrated *in vacuo*. Finally the crude product was purified by column chromatography (1:3, ethyl acetate:hexane) to afford the product **(2.49)** (112 mg, 0.206 mmoles, 66%) as off-white solid. The solid obtained was redissolved in dry THF (3 mL) at 0 °C under atmosphere of nitrogen. To this was added tetrabutylamonium fluoride (81 mg, 310 µL, 0.310 mmoles) dropwise. The reaction was kept stirring for 10 minutes before being quenched with brine and extracted with dichloromethane (3×20 mL). After drying with $MgSO_4$, the reaction mixture was filtered and evaporated using rotary evaporator. Finally the product was purified by flash column chromatography (2:1, ethyl acetate:hexane) to afford the phenol **(2.50)** (73 mg, 0.170 mmoles 82%) as white solid.

^{1}H NMR (400 MHz, CHLOROFORM-*d*) δ_H ppm: 3.67 (3 H, s, OCH_3), 3.89 (2 H, m, CH_2), 4.00 (3 H, s, OCH_3), 4.01 (3 H, s, OCH_3), 4.05 (3 H, s, OCH_3), 4.24 (2 H, m, CH_2), 5.70 (1 H, s, CH), 5.77 (1 H, s, OH), 6.32 (1 H, s, ArH), 6.82 (1 H, dd, ArH, *J*=8.19, 2.08 Hz), 6.92 (1 H, d, ArH, *J*=1.96 Hz), 6.99 (1 H, d, ArH, *J*=8.31 Hz);

^{13}C NMR (151 MHz, CHLOROFORM-*d*) δ ppm: 56.0 (OCH_3), 56.3 (OCH_3), 61.5 (OCH_3), 61.9 (OCH_3), 66.5 (CH_2), 66.5 (CH_2), 101.1 (CH), 104.3 (ArCH), 110.5 (ArCH), 115.1 (ArCH), 115.6 (ArC), 120.3 (C=C), 120.9 (ArCH), 126.2 (ArC), 140.8 (ArC), 142.8 (ArC), 145.6 (ArC), 146.1 (ArC), 147.0 (ArC), 149.4 (ArC), 154.7 (C=C) 158.2 (C=O);

V_{max} cm^{-1}: 3332, 2931, 2837, 1621, 1521, 1465, 1257;

HRMS: Calculated 430.1264, found 431.1325 ($M + H^+$).

Synthesis of 4-(3-hydroxy-4-methoxyphenyl)-6,7,8-trimethoxy-2-oxo-2H-chromene-3-carbaldehyde (2.51)

Phenol **(2.50)** (45 mg, 0.105 mmoles) was dissolved in DCM:acetone (1:1, 5 mL). To this was added iodine (4 mg, 0.016 mmoles) and the resultant solution was heated at 30 °C for 30 minutes. Following this step the solvent was evaporated at low temperature and the resultant crude product obtained was purified by column chromatography (1:1, ethyl acetate:hexane) to afford the aldehyde (2.51) (30 mg, 0.078 mmoles, 75%) as yellow solid.

^{1}H NMR (600 MHz, CHLOROFORM-*d*) δ ppm: 3.71 (3 H, s, OCH_3), 4.03 (3 H, s, OCH_3), 4.07 (3 H, s, OCH_3), 4.08 (3 H, s, OCH_3), 5.84 (1 H, s, OH), 6.51 (1 H, s, ArH), 6.82 (1 H, dd, ArH, *J*=8.07, 2.20 Hz), 6.92 (1 H, d, ArH, *J*=1.83 Hz), 7.02 (1 H, d, ArH, *J*=8.07 Hz), 9.91 (1 H, s, CHO);

^{13}C NMR (151 MHz, CHLOROFORM-*d*) δ ppm: 56.1 (OCH_3), 56.3 (OCH_3), 61.6 (OCH_3), 62.0 (OCH_3), 104.8 (ArCH), 110.6 (ArCH), 114.9 (ArC), 114.9 (ArCH), 117.8 (C=C), 121.2 (ArCH), 124.7 (ArC), 140.7 (ArC), 144.6 (ArC), 145.9 (ArC), 147.8 (ArC), 148.6 (ArC), 149.9 (ArC), 158.0 (C=O), 161.2 (C=C), 188.5 (CHO);

V_{max} cm^{-1}: 3374, 2930, 1681, 1530, 1343, 1280;

HRMS: Calculated 386.1002, found 409.1004 ($M + Na^+$).

Synthesis of intermediate 2-(benzyloxy)-1,3-dimethoxybenzene (2.53)

2,6-dimethoxyphenol **(2.52)** (15.00 g, 0.097 moles) was dissolved in 100 mL of dry DMF, then caesium carbonate (35 g, 0.107 moles) and benzyl bromide (18 g, 0.107 moles, 12.5 mL) were added to the solution and stirred for 8 hours at room temperature. The reaction was quenched with 120 mL of water and extracted with diethyl ether (3 x 120 mL). The organic layer was dried with $MgSO_4$, concentrated under vacuum and purified by column chromatography (1:12, ethyl acetate:hexane) to afford 2-(benzyloxy)-1,3-dimethoxybenzene **(2.53)** (22.6 g, 0.093 moles, 95%) as a light-yellow oil.

^{1}H NMR (400 MHz, CHLOROFORM-*d*) δ ppm: 3.88 (6 H, s, OCH_3), 5.10 (2 H, s, OCH_2Ph), 6.64 (2 H, d, Ar-H, J = 8.0 Hz), 7.06 (1 H, t, Ar-H, J= 2 x 8.5 Hz), 7.39 (3 H, m, Ar-H), 7.59 (2 H, d, Ar-H, *J* = 7.5 Hz);

^{13}C NMR (100 MHz, CHLOROFORM-*d*) δ ppm: 56.2 (2 x OCH_3), 75.1 (CH_2), 105.4 (2 x ArCH), 123.9 (ArCH), 127.9 (2 x ArCH), 128.2 (2 x ArCH), 128.5 (ArCH), 137.2 (ArC), 138.1 (ArC) 153.9 (2 x ArC);

V_{max} cm^{-1}: 3060, 2935, 1725, 1565, 1412, 1260, 730;

HRMS: Calculated 244.1099, found 267.1101 [$M + Na^+$];

Synthesis of intermediate 3-(benzyloxy)-2,4-dimethoxybenzaldehyde (2.54) Protected intermediate **(2.53)** (22 g, 0.090 moles) was dissolved in anhydrous DMF (19.7 g, 0.270 moles, 21 mL) under the atmosphere of nitrogen and cooled to -10 °C. To

this was added phosphorus (V) oxychloride (27.8 g, 0.181 moles, 17 mL) dropwise. The solution was stirred at the same temperature for 10 minutes, then allowed to reach room temperature and heated to 80 °C in an oil bath under anhydrous conditions. After 7 hours of reaction time, the mixture was brought to room temperature, cooled to -10 °C with salted ice and poured on to crushed ice and then quenched slowly with 100 mL of cooled aqueous solution of sodium acetate (10%). The resultant aqueous solution was extracted with diethyl ether (3 x 100 mL), dried with $MgSO_4$ and concentrated under vacuum. Finally the product was purified using column chromatography (1:10, ethyl acetate:hexane) affording 3-(benzyloxy)-2,4-dimethoxybenzaldehyde **(2.54)** (16 g, 0.059 moles, 65%) as yellow oil.

^{1}H NMR (400 MHz, CHLOROFORM-*d*) δ ppm : 3.93 (3 H, s, OCH_3), 4.04 (3 H, s, OCH_3), 5.06 (2 H, s, O$\underline{C}H_2$Ph), 6.78 (1 H, d, Ar-H, J= 8.8 Hz), 7.40 (3 H, m, Ar-H), 7.51 (2 H, dd, Ar-H, J= 2 x 2 Hz), 7.65 (1 H, d, Ar-H, J= 8.8 Hz), 10.28 (1 H, s, CHO);

^{13}C NMR (101 MHz, CHLOROFORM-*d*) δ ppm: 56.3 (OCH_3), 62.6 (OCH_3), 75.4 (CH_2), 107.5 (ArCH), 123.4 (ArCH), 124.5 (2 x ArCH), 128.2 (ArCH), 128.4 (ArC-CH_2), 128.4 (2 x ArCH), 137.1 (2 x $\underline{\text{ArC}}$-OCH3), 140.5 ($\underline{\text{ArC}}$-CHO), 157.4 ($\underline{\text{ArC}}$-OCH2) 188.9 (CHO);

V_{max} cm^{-1}: 2945, 2840, 1675, 1590, 1460, 1290, 1090, 695;
MS: Calculated 272.1049, found 295.1680 [M + Na^+].

Synthesis of intermediate 3-(benzyloxy)-2,4-dimethoxyphenyl formate (2.55)

3-(benzyloxy)-2,4-dimethoxybenzaldehyde **(2.54)** (15.64 g, 0.057 moles) was dissolved in dry DCM (100 mL) and cooled to 0 °C. To this was added *m*CPBA (15.32 g, 77% purity, 0.068 moles) by dissolving in dry DCM (100 mL) and allowed to stir at 0 °C for 90 minutes. The DCM was evaporated under vacuum and the resultant fraction was dissolved in 200 mL of diethyl ether and vigorously washed with an aqueous $NaHCO_3$ solution (3 x 200 mL, 5%) followed by a water wash (200 mL) and a saturated aqueous solution of NaCl (200 mL). The ether layer was then dried with $MgSO_4$ and concentrated under vacuum and purified by column chromatography (1:9, ethyl acetate:hexane) to afford 3-(benzyloxy)-2,4-dimethoxyphenyl formate **(2.55)** (12.8 g, 0.044 moles, 77%) as a dark yellow oil.

^{1}H NMR (400 MHz, CHLOROFORM-*d*) δ ppm: 3.87 (3 H, s, OCH_3), 3.90 (3 H, s, OCH_3), 5.10 (2 H, s, CH_2), 6.68 (1 H, d, ArH, J = 9.3 Hz), 6.85 (1 H, d, ArH, J = 8.8 Hz), 7.40 (3 H, m, ArH), 7.52 (2 H, m, ArH), 8.29 (1 H, s, CHO);

^{13}C NMR (101 MHz, CHLOROFORM-*d*) δ ppm: 56.3 (OCH_3), 61.4 (OCH_3), 75.4 (CH_2), 106.7 (2 x ArCH), 107.8 (ArCH), 116.7 (2 x ArCH), 128.1 (ArC), 128.3 (2 x ArCH), 128.4 (2 x ArC), 128.4 (ArC), 128.4 (ArC) 159.7 (CHO);

V_{max} cm^{-1}: 3430, 2940, 1740, 1485, 1085, 735;

HRMS: Calculated 288.0998, found 311.3817 [M + Na^+].

Synthesis of intermediate 3-(benzyloxy)-2,4-dimethoxyphenol (2.56)

3-(benzyloxy)-2,4-dimethoxyphenyl formate **(2.55)** (12.00 g, 0.042 moles) was dissolved in MeOH (60 mL) and THF (40 mL) and cooled to 0 °C before an aqueous NaOH solution (60 mL, 2 M) was added. After 1 hour the solvents were removed under vacuum and the reaction was acidified with aqueous HCl solution (75 mL, 2 M) and it was extracted with diethyl ether (3 x 100 mL). All diethyl ether fractions were combined and washed once with 5% $NaHCO_3$ (200 mL), dried with $MgSO_4$ and once again concentrated in vacuum and purified by column chromatography (1:9 ethyl acetate:hexane) to afford 3-(benzyloxy)-2,4-dimethoxyphenol **(2.56)** (8.2 g, 0.031 moles, 76%) as a yellow oil.

^{1}H NMR (400 MHz, CHLOROFORM-*d*) δ ppm: 3.82 (3 H, s, OCH_3), 3.96 (3 H, s, OCH_3), 5.08 (2 H, s, CH_2), 5.48 (1 H, br.s, OH) 6.60 (1H, d, ArH, J = 9.3 Hz), 6.68 (1H, d, ArH, J = 8.8 Hz), 7.40 (3H, m, ArH), 7.51 (2H, m, ArH);

^{13}C NMR (101 MHz, CHLOROFORM-*d*) δ ppm: 56.7 (OCH_3), 61.5 (OCH_3), 75.3 (CH_2), 107.8 (ArCH), 108.8 (ArCH), 128.0 (ArCH), 128.3 (2 x ArCH), 128.4 (2 x ArCH), 137.6 (ArC), 140.8 (ArC), 141.2 (ArC), 144.0 (ArC), 147.2 (ArC);

V_{max} cm^{-1}: 3430, 2940, 1490, 1090, 730;

HRMS: Calculated 260.1049, found 283.1735 [M + Na^+].

Formylation of (2.56) to give 4-(benzyloxy)-2-hydroxy-3,5-dimethoxybenzaldehyde (2.57)

Anhydrous magnesium dichloride (900 mg, 9.453 mmoles) and solid paraformaldehyde (312 mg, 10.390 mmoles) were added to a dry two necked round bottom flask under the atmosphere of nitrogen. This was followed by the addition of dry tetrahydrofuran (25 mL) and triethylamine (964 µL, 6.916 mmoles, freshly dried and distilled over CaH_2) dropwise and the mixture was stirred for 10 minutes. 3-(benzyloxy)-2,4-dimethoxyphenol **(2.56)** (900

mg, 3.458 mmoles) was added dropwise by dissolving in dry THF (2 mL) and the mixture was immersed in an oil bath at 75 °C. After 5 hours, the reaction was allowed to reach room temperature, filtered and solvent evaporated using rotary evaporator. The reaction mixture was re-dissolved in diethyl ether (100 mL), washed with 1 M HCl (3 x 50 mL) and water (3 x 50 mL), dried with $MgSO_4$ and concentrated *in vacuo*. Finally the mixture was purified by column chromatography (1:9, ethyl acetate:hexane) to afford 4-(benzyloxy)-2-hydroxy-3,5-dimethoxybenzaldehyde **(2.57)** (590 mg, 2.046 mmoles, 59%) as yellow oil.

^{1}H NMR (400 MHz, CHLOROFORM-*d*) δ ppm: 3.87 (3 H, s, OCH_3), 3.92 (3 H, s, OCH_3), 5.26 (2 H, s, CH_2), 6.80 (1 H, s, ArH), 7.39 (3 H, m, ArH), 7.49 (2 H, m, ArH), 9.80 (1 H, s, CHO), 10.96 (1 H, s, OH);

^{13}C NMR (101 MHz, CHLOROFORM-*d*) δ ppm: 56.6 (OCH_3), 61.1 (OCH_3), 75.5 (CH_2), 109.5 (ArCH), 115.7 (ArC), 128.2 (2 x ArCH), 128.4 (3 x ArCH), 137.0 (ArC), 141.7 (ArC), 146.9 (ArC), 149.3 (ArC), 151.6 (ArC), 194.9 (CHO);

V_{max} cm^{-1}: 3341, 2928, 1520, 1436, 1289;

HRMS: Calculated 288.0998, found 311.1684 ($M + Na^+$).

Protection of the phenol to give 4-(benzyloxy)-2-((*tert*-butyldimethylsilyl)oxy)-3,5-dimethoxybenzaldehyde (2.58)

4-(benzyloxy)-2-hydroxy-3,5-dimethoxybenzaldehyde **(2.57)** (17.64 g, 0.061 moles) was dissolved in 100 mL of anhydrous DMF under nitrogen atmosphere , then imidazole (6.66 g, 0.098 moles) and *tert*-butyl(chloro)dimethylsilane (13.8 g, 0.092 moles) were added and stirred for 90 minutes at room temperature. The reaction was quenched with 200 mL of saturated NaCl solution and extracted with diethyl ether (3 x 200 mL), dried with Na_2SO_4 and concentrated under vacuum. Finally the crude product was purified by column chromatography (1:25, ethyl acetate:hexane) affording 4-(benzyloxy)-2-((*tert*-butyldimethylsilyl)oxy)-3,5-dimethoxybenzaldehyde **(2.58)** (13.50 g, 0.033 moles, 55%) as clear oil that solidified on further vacuum drying.

^{1}H NMR (400 MHz, CHLOROFORM-*d*) δ ppm: 0.20 (6 H, s, 2 x $SiCH_3$), 1.03 (9 H, s, Si-C-$(CH_3)_3$), 3.81 (3 H, s, OCH_3), 3.86 (3 H, s, OCH_3), 5.19 (2 H, s, CH_2), 7.10 (1 H, s, ArH), 7.33 (3 H, m, ArH), 7.47 (2 H, m, ArH), 10.36 (1 H, s, CHO);

^{13}C NMR (101 MHz, CHLOROFORM-*d*) δ ppm: -4.6 (2 x $SiCH_3$), 18.6 ((Si-$\underline{C}$-$CH_3)_3$), 25.8 ((Si-C-$\underline{CH_3})_3$), 56.8 (OCH_3), 61.0 (OCH_3), 75.3 (CH_2), 107.7 (ArCH), 114.7 (ArC), 128.1 (ArCH), 128.2 (2 x ArCH), 128.4 (2 x ArCH), 137.2 (ArC), 142.1 (ArC), 145.6 (ArC), 148.9 (ArC), 153.0 (ArC), 203.2 (CHO);

V_{max} cm^{-1}: 2935, 1650, 1465, 1260, 1140, 840;

HRMS: Calculated 402.1863, found 403.2761 [M + H^+],

MP: 66-68 °C.

Synthesis of intermediate 1-(4-(benzyloxy)-2-((*tert*-butyldimethylsilyl)oxy)-3,5-dimethoxyphenyl)ethan-1-ol (2.59)

4-(benzyloxy)-2-((*tert*-butyldimethylsilyl)oxy)-3,5-dimethoxybenzaldehyde **(2.58)** (10.64 g, 0.026 moles) was stirred with anhydrous THF (30 mL) and methyl magnesium bromide (6.2 g, 0.052 moles, 17.30 mL, 3.0 M) at 0 °C for 1 hour under nitrogen atmosphere. Upon completion the reaction mixture was diluted with diethyl ether (150 mL), cooled to 0 °C and than quenched by slowly adding cooled 1 M HCl (100 mL) with stirring. Finally the crude product was purified by column chromatography (1:10, ethyl acetate:hexane) to afford 1-(4-(benzyloxy)-2-((*tert*-butyldimethylsilyl)oxy)-3,5-dimethoxyphenyl)ethan-1-ol **(2.59)** (8.6 g, 0.020 moles, 78%).

^{1}H NMR (400 MHz, CHLOROFORM-*d*) δ ppm: 0.21 (6 H, d, 2 x Si$\underline{C}H_3$, *J* = 5.7 Hz), 1.03 (9 H, s, Si-C-$(CH_3)_3$), 1.47 (3 H, d, $COHCH_3$, *J* = 6.4 Hz), 3.82 (3 H, s, OCH_3), 3.85 (3 H, s, OCH_3), 5.06 (2 H, s, CH_2), 5.29 (1 H, m, $\underline{CH}$), 6.78 (1H, s, ArH), 7.32 (3 H, m, ArH), 7.50 (2 AH, m, ArH);

^{13}C NMR (101 MHz, CHLOROFORM-*d*) δ ppm: -4.2 (2 x Si$\underline{C}H_3$), 18.8 ((Si-$\underline{C}$-$CH_3)_3$), 23.4 (CH-$\underline{C}H_3$), 26.1 ((Si-C-$\underline{CH_3})_3$,), 56.3 (OCH_3), 60.7 (OCH_3), 64.4 (CH), 75.2 (CH_2), 103.8 (ArCH), 127.9 (ArC), 128.3 (2 x ArCH), 128.3 (2 x ArCH), 131.6 (ArCH), 137.7 (ArC), 139.5 (ArC), 140.7 (ArC), 144.6 (ArC), 148.0 (ArC);

V_{max} cm^{-1}: 2930, 1465, 1060, 825;

HRMS: Calculated 418.2176, found 441.3124 [M + Na^+].

Synthesis of intermediate 1-(4-(benzyloxy)-2-((*tert*-butyldimethylsilyl)oxy)-3,5-dimethoxyphenyl)ethan-1-one (2.60)

1-(4-(benzyloxy)-2-((*tert*-butyldimethylsilyl)oxy)-3,5-dimethoxyphenyl)ethan-1-ol **(2.59)** (1.30 g, 3.11 mmoles) was stirred with Dess-Martin Periodinane (1.45 g, 3.42 mmoles) in dry DCM (20 mL) at 0 °C for 15 minutes. The reaction was quenched with aqueous solution of sodium bicarbonate (5%), extracted with diethyl ether (3 x 100 mL) and purified by column chromatography (1:16, ethyl acetate:hexane) to afford the ketone **(2.60)** (0.96 g, 2.30 mmoles, 74%) as clear oil.

^{1}H NMR (400 MHz, CHLOROFORM-*d*) δ ppm: 0.13 (6 H, s, 2 x $SiCH_3$), 1.01 (9 H, s, Si-C-$(CH_3)_3$), 2.62 (3 H, s, $COC\underline{H}_3$), 3.82 (3 H, s, OCH_3), 3.84 (3 H, s, OCH_3), 5.13 (2 H, s,CH_2), 6.84 (1 H, s, ArH), 7.37 (3 H, m, ArH), 7.47 (2 H, m, ArH);

^{13}C NMR (101 MHz, CHLOROFORM-*d*) δ ppm: -4.3 (2 x $Si\underline{C}H_3$), 18.5 ((Si-$\underline{C}$-$CH_3)_3$), 25.9 ((Si-C-$\underline{C}H_3)_3$,), 30.9 (CO-$\underline{C}H_3$), 56.1 (OCH_3), 61.0 (OCH_3), 75.1 (CH_2), 106.5 (ArCH), 127.7 (ArC), 128.1 (2 x ArCH), 128.3 (2 x ArCH), 128.4 (ArCH), 137.3 (ArC), 143.0 (ArC), 145.2 (ArC), 145.8 (ArC), 147.9 (ArC) , 201.0 (C=O);

V_{max} cm^{-1}: 2945, 1675, 1585, 1460, 1285, 1090, 730;

HRMS: Calculated 416.2019, found 417.3811 [M + H^+]

Synthesis of 1-(4-(benzyloxy)-2-hydroxy-3,5-dimethoxyphenyl)ethan-1-one (2.61)

1-(4-(benzyloxy)-2-((*tert*-butyldimethylsilyl)oxy)-3,5-dimethoxyphenyl)ethan-1-one **(2.60)** (6.4 g, 0.015 moles) was dissolved in anhydrous THF (20 mL) under an atmosphere of nitrogen and cooled to 0 °C. To this was added TBAF (1.0 M in THF) (4.97 g, 0.019 mole, 19 mL) dropwise at the same temperature. The reaction was quenched after 10 minutes with saturated aqueous sodium chloride solution and extracted with diethyl ether. Upon drying the organic layer with sodium sulphate and evaporating the organic solvent, the crude product obtained was further purified by column chromatography (9:1, hexane:ethyl acetate) to afford 1-(4-(benzyloxy)-2-hydroxy-3,5-dimethoxyphenyl)ethan-1-one **(2.61)** (3.9 g, 0.013 moles, 85%).

^{1}H NMR (400 MHz, CHLOROFORM-*d*) δ ppm: 2.60 (3 H, s, $COCH_3$), 3.85 (3 H, s, OCH_3), 3.90 (3 H, s, OCH_3), 5.24 (2 H, s, CH_2), 6.95 (1 H, s, Ar-H), 7.33 (3 H, m, Ar-H), 7.50 (2 H, m, Ar-H), 12.42 (1 H, s, OH);

^{13}C NMR (101 MHz, CHLOROFORM-*d*) δ ppm: 26.8 ($COCH_3$), 56.8 (OCH_3), 61.0 (OCH_3), 75.4 (CH_2), 107.7 (ArCH), 114.7 (ArC), 128.2 (2 x ArCH), 128.2 (ArCH), 128.4 (2 x ArCH), 134.2 (ArC), 142.1 (ArC), 145.6 (ArC), 148.9 (ArC), 153.0 (ArC), 203.2 (C=O);

V_{max} cm^{-1}: 2940, 1650, 1270, 1090, 735;

HRMS: Calculated 302.1154, found 325.1978 [M + Na^+].

Synthesis of ethyl 3-(4-(benzyloxy)-2-hydroxy-3,5-dimethoxyphenyl)-3-oxopropanoate (2.62)

1-(4-(benzyloxy)-2-hydroxy-3,5-dimethoxyphenyl)ethan-1-one **(2.61)** (2.5 g, 0.008 moles) was dissolved in diethyl carbonate (30 mL). To this was added sodium hydride (1.9 g, 0.080 moles) very slowly and the reaction mixture was heated at 75 °C for 30 min. After completion the reaction was quenched with minimum amount of methanol, acidified with cooled aq. HCl, extracted with diethyl ether (3×100 mL) and purified by column chromatography (4:1, hexane:ethyl acetate) to afford ethyl 3-(4-(benzyloxy)-2-hydroxy-3,5-dimethoxyphenyl)-3-oxopropanoate **(2.62)** (2.8 g, 0.0075 moles, 90%).

^{1}H NMR (400 MHz, CHLOROFORM-*d*) δ ppm: 1.30 (3 H, t, *J* = 2 x 7 Hz, OCH_2- $\underline{CH_3}$), 3.84 (3 H, s, OCH_3), 3.90 (3 H, s, OCH_3), 3.96 (2 H, s, CO-$\underline{CH_2}$- CO), 4.24 (2 H, q, *J* = 7.09 Hz), 5.26 (2 H, s, O-CH_2-Ph), 6.92 (1 H, s, Ar-H), 7.34 (3 H, m, Ar-H), 7.49 (2 H, m, Ar-H), 11.90 (1 H, s, OH);

V_{max} cm^{-1}: 2940, 1740, 1680.82, 1596.33, 1530.21, 1453.55, 1280, 740;

HRMS: Calculated 374.1366, found 397.2333 [M + Na^+].

Synthesis of 7-(benzyloxy)-4-hydroxy-6,8-dimethoxy-2H-chromen-2-one (2.63)

Ethyl 3-(4-(benzyloxy)-2-hydroxy-3,5-dimethoxyphenyl)-3-oxopropanoate **(2.62)** (0.58 g, 1.55 mmoles) was stirred with toluene (20 mL) at 120 °C. After 16 hours, the toluene was evaporated off under vacuum and the solid obtained was washed few times with diethyl

ether, affording the 4-hydroxycoumarin **(2.63)** (0.42 g, 1.27 mmoles, 82%) as off white solid

^{1}H NMR (400 MHz, CHLOROFORM-*d*) δ ppm: 3.87 (3 H, s, OCH_3), 3.95 (3 H, s, OCH_3), 5.17 (2 H, s, O-CH_2-Ph), 5.92 (1 H, s, C=C<u>H</u>), 7.06 (1 H, s, Ar-H), 7.33 (3 H, m, Ar-H), 7.48 (2 H, m, Ar-H);

^{13}C NMR (101 MHz, CHLOROFORM-*d*) δ ppm: 56.1 (OCH_3), 61.9 (OCH_3), 75.6 (O-<u>C</u>H_2-Ph), 90.5 (C=<u>C</u>H), 99.0 (ArCH), 111.8 (ArC), 128.2 (ArCH), 128.3 (2 x ArCH), 128.4 (2 x ArCH), 137.0 (ArC), 141.4 (ArC), 142.7 (ArC), 145.3 (ArC), 150.5 (ArC), 166.2 (<u>C</u>=CH) 166.4 (C=O);

V_{max} cm^{-1}: 2946, 1655, 1541, 1512, 1370, 1295, 1267, 1252, 1193, 1133, 1070, 822;

HRMS: calculated 328.0947, found [M + H^+] 329.2081,

MP: 185-188 °C.

Synthesis of 7-(benzyloxy)-6,8-dimethoxy-2-oxo-2H-chromen-4-yl trifluoromethanesulfonate (2.64)

4-hydroxycoumarin **(2.63)** (500 mg, 1.523 mmoles) was stirred with triethylamine (231 mg, 2.284 mmoles, 318 µL) in anhydrous DCM (10 mL) at 0 °C for 5 minutes under the atmosphere of nitrogen. To this trifluoromethanesulphonic anhydride (559 mg, 1.982 mmoles, 333 µL) was added dropwise slowly via syringe. After stirring for 15 minutes, the reaction was concentrated *in vacuo* at a low temperature and purified by column chromatography (1:7, ethyl acetate:hexane) to afford 7-(benzyloxy)-6,8-dimethoxy-2-oxo-2H-chromen-4-yl trifluoromethanesulfonate **(2.64)** (650 mg, 1.412 mmoles, 93%) as a light yellow solid.

Synthesis of *tert*-butyl (5-(7-(benzyloxy)-6,8-dimethoxy-2-oxo-2H-chromen-4-yl)-2-methoxyphenyl)carbamate (2.65)

Triflate **(2.64)** (650 mg, 1.412 mmoles), aryl boronic ester **(2.14)** (592 mg, 1.694 mmoles) and potassium carbonate (488 mg, 3.530 mmoles) were dissolved in toluene:ethanol:water mixture (3:1:1, 20 mL). To this tetrakis (triphenylphosphine) palladium (0) (85 mg, 0.074 mmoles) was added and the reaction was refluxed for 30 minutes. Upon completion the reaction mixture cooled to room temperature, diluted with ethyl acetate (200 mL) and dried with Na_2SO_4. Solvent was evaporated using rotary evaporator and product was purified by

column chromatography (1:3, ethyl acetate:hexane) to afford the Boc-protected aniline **(2.65)** (550 mg, 1.031 mmoles, 73%) as off-white solid.

^{1}H NMR (400 MHz, CHLOROFORM-*d*) δ ppm: 1.53 (9 H, s, $(CH_3)_3$), 3.81 (3 H, s, OCH_3), 3.99 (3 H, s, OCH_3), 4.02 (3 H, s, OCH_3), 5.21 (2 H, s, CH_2), 6.34 (1 H,s, C=CH), 6.96 (1 H, s, ArH), 7.01 (1 H, d, ArH, *J*=8.31 Hz), 7.12 (1 H, dd, ArH, *J*=8.31, 1.96 Hz), 7.16 (1 H, br.s, NH), 7.38 (3 H, m, ArH), 7.53 (2 H, m, ArH), 8.34 (1 H, s, ArH);

^{13}C NMR (101 MHz, CHLOROFORM-*d*) δ ppm: 28.3 (C-($\underline{C}H_3)_3$), 55.9 (OCH_3), 56.2 (OCH_3), 61.9 (OCH_3), 75.6 (CH_2), 80.8 ($\underline{C}$-$(CH_3)_3$), 103.7 (ArCH), 110.3 (ArCH), 113.4 (C=CH), 114.8 (ArC), 118.6 (ArCH), 122.6 (ArCH), 128.2 (ArCH), 128.2 (ArC), 128.3 (2×ArCH), 128.4 (2×ArCH), 137.2 (ArC), 141.8 (ArC), 143.3 (ArC), 144.7 (ArC), 148.7 (ArC), 150.0 (ArC), 152.6 (ArC), 155.3 ($\underline{C}$=CH), 160.8 (C=O);

V_{max} cm^{-1}: 3432, 2976, 2938, 1718, 1528, 1480, 1453, 1417, 1390, 1248, 1153, 1131, 1029, 751;

HRMS: Calculated 533.2050, found 534.2123 ($M + H^+$).

Synthesis of 4-(3-amino-4-methoxyphenyl)-7-(benzyloxy)-6,8-dimethoxy-2H-chromen-2-one (2.66)

N-Boc aniline **(2.65)** (46 mg, 0.086 mmoles) was dissolved in dry DCM (3 mL) under atmosphere of nitrogen and cooled to -10 °C. To this was added dry cooled trifluoroacetic acid (1 mL) and stirred for 90 minutes at 0 °C. Following this step the reaction mixture was diluted with cold water (10 mL), quenched with 5% $NaHCO_3$ (20 mL) and extracted with diethyl ether (3×30 mL). After drying the organic layer with sodium sulphate, solvent was evaporated using rotary evaporator and the oil left behind was further purified by column chromatography (1:2, ethyl acetate:hexane) to afford the aniline **(2.66)** (25 mg, 0.058 mmoles, 67%) as yellow solid.

^{1}H NMR (400 MHz, CHLOROFORM-*d*) δ ppm: 3.71 (2 H, br.overlapping signal, NH_2), 3.76 (3 H, s, OCH_3), 3.96 (3 H, s, OCH_3), 4.02 (3 H, s, OCH_3), 5.19 (2 H, s, CH_2), 6.27 (1 H, s, C=C$\underline{H}$), 6.83 (3 H, m, ArH), 6.92 (1 H, d, ArH, *J*=8 Hz), 7.39 (3 H, m, ArH), 7.53 (2 H, m, ArH);

^{13}C NMR (101 MHz, CHLOROFORM-*d*) δ ppm: 55.6 (OCH_3), 56.4 (OCH_3), 61.9 (OCH_3), 75.6 (CH_2), 103.8 (ArCH), 110.3 (ArCH), 113.3 (C=CH), 114.5 (ArCH), 115.0 (ArC), 118.7 (ArCH), 128.2 (ArCH), 128.3 (ArC), 128.4 (2×ArCH), 128.4 (2×ArCH), 136.6 (ArC), 137.1 (ArC), 141.8 (ArC), 143.4 (ArC), 144.7 (ArC), 148.3 (ArC), 149.9 (ArC), 155.9 (C=CH), 160.9 (C=O);

V_{max} cm^{-1}: 2975, 2936, 1745, 1527, 1480, 1445, 1413, 1385, 1024, 752;

HRMS: Calculated 433.1525, found 434.1598 ($M + H^+$).

Synthesis of *tert*-butyl (5-(7-hydroxy-6,8-dimethoxy-2-oxo-2H-chromen-4-yl)-2-methoxyphenyl)carbamate (2.67)

N-Boc aniline **(2.65)** (236 mg, 0.442 mmoles) was dissolved in MeOH:DCM (2:1, 25 mL). To this was added Pd/C (23 mg, 10% by weight) and allowed to stir for 90 minutes under the atmosphere of hydrogen using balloon at room temperature. Upon completion the reaction was filtered through a cotton plug and evaporated using rotary evaporator. Finally the crude product was further purified by column chromatography (1:1, ethyl acetate:hexane) to afford the phenol **(2.67)** (165 mg, 0.372 mmoles, 84%) as very light yellow solid.

^{1}H NMR (400 MHz, CHLOROFORM-*d*) δ ppm: 1.53 (9 H, s, $(CH_3)_3$), 3.87 (3 H, s, OCH_3), 3.98 (3 H, s, OCH_3), 4.12 (3 H, s, OCH_3), 6.14 (1 H, s, C=CH), 6.27 (1 H, s, ArH), 6.96 (1 H, s, ArH), 7.00 (1 H, d, ArH, *J*= 8.56 Hz), 7.12 (1 H, dd, ArH, *J*=8.31, 2.20 Hz), 7.15 (1 H, br.s, NH), 8.32 (1 H, s, OH);

^{13}C NMR (101 MHz, CHLOROFORM-*d*) δ ppm: 28.3 (C-(CH_3)$_3$), 55.9 (OCH_3), 56.4 (OCH_3), 61.7 (OCH_3), 80.8 (C-$(CH_3)_3$), 103.1 (ArCH), 110.3 (ArCH), 111.3 (C=CH), 111.8 (ArC), 118.8 (ArCH), 122.6 (ArCH), 128.2 (ArC), 128.3 (ArC), 134.7 (ArC), 142.2 (ArC), 143.4 (ArC), 144.2 (ArC), 148.7 (ArC), 152.7 (ArC), 155.7 (C=CH), 160.9 (C=O);

V_{max} cm^{-1}: 3423, 3358, 2934, 1721, 1710, 1571, 1529, 1482, 1449, 1440, 1389, 1249, 1215, 1158, 1124, 1028;

HRMS: Calculated 443.1580, found 444.1677 ($M + H^+$).

Synthesis of 4-(3-amino-4-methoxyphenyl)-7-hydroxy-6,8-dimethoxy-2H-chromen-2-one (2.68)

Phenol **(2.67)** (50 mg, 0.113 mmoles) was dissolved in dry DCM (3 mL) under atmosphere of nitrogen and cooled to -10 °C with salted ice. To this was added dry cooled trifluoroacetic acid (1 mL) and stirred for 90 minutes at 0 °C. Following this step the reaction mixture was diluted with DCM (50 mL) and solvent was evaporated at low temperature using rotary evaporator. The oil left behind was redissolved in DCM (10 mL) and stirred with 5% $NaHCO_3$ (3 mL) for 2 minutes. Aqueous layer was removed with the help of Pasteur pipette and the organic layer was dried with Na_2SO_4. Upon evaporation of organic solvent, the crude residue obtained was further purified by column chromatography (2:1, ethyl acetate:hexane) to afford the aniline **(2.68)** (36 mg, 0.105 mmoles, 93%) as off-white solid.

^{1}H NMR (400 MHz, DMSO-d_6) δ ppm: 3.72 (3 H, s, OCH_3), 3.85 (3 H, s, OCH_3), 3.86 (3 H, s, OCH_3), 5.00 (2 H, br.s, NH_2), 6.07 (1 H, s, C=C<u>H</u>), 6.74 (1 H, dd, ArH, *J*=8.07, 2.20 Hz), 6.84 (1 H, d, ArH, *J*= 1.96 Hz), 6.85 (1 H, s, ArH), 6.96 (1 H, d, ArH, *J*= 8.31 Hz), 10.00 (1 H, br.s, OH);

^{13}C NMR (101 MHz, DMSO-d_6) δ ppm: 55.9 (OCH_3), 56.5 (OCH_3), 61.2 (OCH_3), 103.8 (ArCH), 110.1 (ArC), 110.3 (C=<u>C</u>H), 111.0 (ArCH), 113.8 (ArCH), 116.9 (ArCH), 128.2 (ArC), 135.7 (ArC), 138.5 (ArC), 143.9 (ArC), 144.5 (ArC), 145.6 (ArC), 148.0 (ArC), 156.7 (<u>C</u>=CH), 160.6 (C=O);

V_{max} cm^{-1}: 3415, 3322, 2940, 1715, 1561, 1497, 1393, 1243, 1076, 1035, 815, 744;

HRMS: Calculated 343.1056, found 344.1126 ($M + H^+$),

MP: 203-205 °C.

Synthesis of benzyl 2-((4-(3-((*tert*-butoxycarbonyl)amino)-4-methoxyphenyl)-6,8-dimethoxy-2-oxo-2H-chromen-7-yl)oxy)acetate (2.69)

Phenol **(2.67)** (70 mg, 0.158 mmoles) was dissolve in acetone (20 mL). To this was added benzyl bromoacetate (0.316 mmoles, 72 mg, 50 µL) and potassium carbonate (65 mg, 0.473 mmoles). The resultant mixture was refluxed for 3 hours. Upon completion the

reaction was concentrated and purified by column chromatography (1:2, ethyl acetate:hexane) to afford the product **(2.69)** (84 mg, 0.142 mmole, 90%) as white solid.

^{1}H NMR (400 MHz, CHLOROFORM-*d*) d ppm: 1.53 (9 H, s, $(CH_3)_3$), 3.75 (3 H, s, OCH_3), 3.98 (3 H, s, OCH_3), 4.02 (3 H, s, OCH_3), 4.89 (2 H, s, CH_2), 5.26 (2 H, s, CH_2), 6.33 (1 H, s, C=C<u>H</u>), 6.95 (1 H, s, ArH), 7.00 (1 H, d, ArH, *J*= 8.56 Hz), 7.11 (1 H, dd, ArH, *J*=8.44, 2.08 Hz), 7.15 (1 H, br.s, NH), 7.38 (5 H, m, ArH), 8.32 (1 H, s, ArH);

^{13}C NMR (101 MHz, CHLOROFORM-*d*) d ppm: 28.3 (C-(<u>C</u>H_3)$_3$), 55.9 (OCH_3), 56.2 (OCH_3), 62.1 (OCH_3), 66.8 (CH_2), 69.7 (CH_2), 80.8 (<u>C</u>-$(CH_3)_3$), 103.7 (ArCH), 110.3 (ArCH), 113.4 (C=<u>C</u>H), 114.6 (ArC), 118.6 (ArCH), 122.6 (ArCH), 128.1 (ArC), 128.3 (ArC), 128.5 (ArCH), 128.6 (2×ArCH), 128.6 (2×ArCH), 135.3 (ArC), 140.5 (ArC), 143.3 (ArC), 143.7 (ArC), 148.7 (ArC), 148.8 (ArC), 152.6 (NH-<u>C</u>=O), 155.3 (<u>C</u>=CH), 160.7 (C=O) 168.8 (C=O);

V_{max} cm^{-1}: 2933, 2852, 1680, 1610, 1553, 1523, 1470, 1336, 1235;

HRMS: Calculated 591.2104, found 592.2168 ($M + H^+$);

MP: 98-100 °C.

Synthesis of 2-((4-(3-((*tert*-butoxycarbonyl)amino)-4-methoxyphenyl)-6,8-dimethoxy-2-oxo-2H-chromen-7-yl)oxy)acetic acid (2.70)

Benzyl ester **(2.69)** (76 mg, 0.128 mmoles) was dissolved in MeOH:DCM (2:1, 10 mL). To this was added Pd/C (7.6 mg, 10% by weight) and allowed to stir for 2 hours under the atmosphere of hydrogen using balloon at room temperature. Upon completion the reaction was filtered through a cotton plug and evaporated using rotary evaporator. The product was redissolved in ethyl acetate (100 mL) and washed with 2 M HCl (2×20 mL). After evaporating the organic solvent, the crude product obtained was further purified by column chromatography (1:1:0.02, ethyl acetate:hexane:formic acid) to afford the acid **(2.70)** (62 mg, 0.124 mmoles, 96%) as off-white solid.

^{1}H NMR (400 MHz, CHLOROFORM-*d*) δ ppm: 1.53 (9 H, s, $(CH_3)_3$), 3.88 (3 H, s, OCH_3), 3.99 (3 H, s, OCH_3), 4.15 (3 H, s, OCH_3), 4.79 (2 H, s, CH_2), 6.39 (1 H, s, C=<u>CH</u>), 7.02 (1 H, d, ArH, *J*= 8.31 Hz), 7.07 (1 H, s, ArH), 7.13 (1 H, dd, ArH, *J*=8.31, 2.20 Hz), 7.17 (1 H, br.s, NH), 8.32 (1 H, s, ArH);

^{13}C NMR (101 MHz, CHLOROFORM-*d*) δ ppm: 28.3 (C-(<u>C</u>H$_3$)$_3$), 55.9 (OCH$_3$), 56.4 (OCH$_3$), 62.4 (OCH$_3$), 71.1 (CH$_2$), 80.9 (<u>C</u>-(CH$_3$)$_3$), 104.0 (ArCH), 110.4 (ArCH), 114.1 (C=<u>C</u>H), 115.8 (ArC), 118.7 (ArCH), 122.6 (ArCH), 127.6 (ArC), 128.3 (ArC), 140.4 (ArC), 143.0 (ArC), 143.2 (ArC), 148.1 (ArC), 148.9 (ArC), 152.7 (NH-<u>C</u>=O), 155.1 (<u>C</u>=CH), 160.2 (C=O), 170.0 (OH-<u>C</u>=O);

V_{max} cm^{-1}: 3432, 2976, 2938, 1722, 1559, 1530, 1482, 1454, 1420, 1391, 1250, 1228, 1156, 1138, 1098;

HRMS: Calculated 501.1635, found 502.1690 (M+H$^+$);

MP: 88-90 °C.

Synthesis of 2-((4-(3-amino-4-methoxyphenyl)-6,8-dimethoxy-2-oxo-2H-chromen-7-yl)oxy)acetic acid (2.71)

Acid **(2.70)** (43 mg, 0.086 mmoles) was dissolved in dry DCM (3 mL) under atmosphere of nitrogen and cooled to -10 °C with salted ice. To this was added dry cooled trifluoroacetic acid (1 mL) and stirred for 2 hours at 0 °C. Following this step the reaction mixture was diluted with DCM (50 mL) and solvent was evaporated at 35 °C using rotary evaporator. The remainder was redissolved in DCM:MeOH (9:1, 10 mL) and stirred with 5% $NaHCO_3$ (1 mL) for 2 minutes. Aqueous layer was carefully removed with the help of Pasteur pipette and the organic layer was dried with Na_2SO_4. Upon evaporation of organic solvent, the crude residue obtained was washed few times with diethyl ether to afford the aniline **(2.71)** (28 mg, 0.070 mmoles, 81%) as yellow solid.

^{1}H NMR (600 MHz, DMSO-d_6) δ ppm: 3.70 (3 H, s, OCH$_3$), 3.84 (3 H, s, OCH$_3$), 3.94 (3 H, s, OCH$_3$), 4.38 (2 H, s, CH$_2$), 5.02 (2 H, br.s, NH$_2$), 6.15 (1 H, s, C=<u>C</u>H), 6.73 (1 H, dd, ArH, *J*=8.44, 2.20 Hz), 6.84 (1 H, d, ArH, *J*= 2.20 Hz), 6.85 (1 H, s, ArH), 6.95 (1 H, d, ArH, *J*= 8.44 Hz);

^{13}C NMR (151 MHz, DMSO-d_6) δ ppm: 55.9 (OCH$_3$), 56.5 (OCH$_3$), 61.7 (OCH$_3$), 72.5 (CH$_2$), 103.9 (ArCH), 111.0 (ArCH), 111.9 (C=<u>C</u>H), 113.4 (ArC), 113.8 (ArCH), 116.9 (ArCH), 128.0 (ArC), 138.5 (ArC), 140.5 (ArC), 143.3 (ArC), 145.2 (ArC), 148.0 (ArC), 149.3 (ArC), 156.3 (<u>C</u>=CH), 160.3 (C=O), 171.8 (COOH);

V_{max} cm^{-1}: 3333, 2931, 2880, 1681, 1597, 1449, 1414, 1373, 1256, 1114;

HRMS: Calculated 401.1111, found 402.1175.

5.2 Experimental Chapter 3

Synthesis of (4-(benzyloxy)-2-((*tert*-butyldimethylsilyl)oxy)-3,5-dimethoxyphenyl)(3-((*tert*-butyldimethylsilyl)oxy)-4-methoxyphenyl)methanol (3.01)

(5-bromo-2-methoxyphenoxy)(*tert*-butyl)dimethylsilane **(2.09)** (952 mg, 3 mmoles) was dissolved in dry THF (10 ml) under the atmosphere of nitrogen and cooled to -80 °C over 30 minutes. To this was added *n*-butyl lithium (2 mL, 5 mmoles, 2.5 M solution in hexane) dropwise over 30 mins and allowed further to stir for 10 mins at the same temperature. Afterwards, benzaldehyde **(2.57)** (920 mg, 2.285 mmoles) was added as solid and allowed the reaction to gradually reach room temperature over the duration of two hours. The reaction was then diluted with diethyl ether (100 mL) and washed with 1 M aq.HCl (2 × 50 mL). Finally the product was dried with Na_2SO_4 and purified by column chromatography (1:10, ethyl acetate:hexane) to afford the product **(3.01)** (1260 mg, 1.966 mmoles, 86%) as light yellow oil.

^{1}H NMR (400 MHz, CHLOROFORM-*d*) δ ppm: 0.15 (6 H, s, 2 × Si-$\underline{CH_3}$), 0.21 (3 H, s, Si-$\underline{CH_3}$), 0.25 (3 H, s, Si-$\underline{CH_3}$), 1.00 (9 H, s, C$(CH_3)_3$), 1.00 (9 H, s, C$(CH_3)_3$), 3.71 (3 H, s, OCH_3), 3.82 (3 H, s, OCH_3), 3.82 (3 H, s, OCH_3), 5.05 (2 H, s, CH_2), 6.15 (1 H, s, CH), 6.48 (1 H, s, ArH) , 6.84 (1 H, d, ArH, *J* = 8.56 Hz), 6.88 (1 H, d, ArH, *J* = 1.96 Hz), 6.95 (1 H, dd, ArH, *J* = 8.40, 2.40 Hz), 7.38 (3 H, m, ArH), 7.50 (2 H, m, ArH);

^{13}C NMR (101 MHz, CHLOROFORM-*d*) δ ppm: -4.62 (2×Si-CH_3), -4.13 (Si-CH_3), -4.10 (Si-CH_3), 18.45 ($\underline{C}(CH_3)_3$), 18.75 ($\underline{C}(CH_3)_3$), 25.74 (C($\underline{C}H_3)_3$), 26.14 (C($\underline{C}H_3)_3$), 55.58 (OCH_3), 56.17 (OCH_3), 60.80 (OCH_3), 69.81 (CH), 75.17 (CH_2), 105.84 (ArCH), 111.78 (ArCH), 119.58 (ArCH), 119.80 (ArCH), 127.89 (ArCH), 128.26 (2×ArCH), 128.33 (2×ArCH), 129.92 (ArC), 135.66 (ArC), 137.69 (ArC), 140.44 (ArC), 141.07 (ArC), 144.72 (ArC), 144.81 (ArC), 147.87 (ArC), 150.23 (ArC);

V_{max} cm^{-1}: 3480, 2954, 2932, 2860, 1509, 1484, 1462, 1419, 1252, 1225, 1128, 1082, 979, 835;

HRMS: Calculated 640.3252, found 663.3154 ($M + Na^+$).

Synthesis of (4-(benzyloxy)-2-((*tert*-butyldimethylsilyl)oxy)-3,5-dimethoxyphenyl)(3-((*tert*-butyldimethylsilyl)oxy)-4-methoxyphenyl)methanone (3.02)

Diphenylmethanol **(3.01)** (1150 mg, 1.794 mmoles) was dissolved in dry DCM (20 ml) at 0 °C. To this was added Dess Martin Periodinane (840 mg, 1.980 mmoles). The reaction was allowed to stir at same temperature for 30 minutes before being quenched with 5% aqueous $NaHCO_3$ (50 ml) and extracted with DCM (2 × 50 ml). After drying the organic layer with Na_2SO_4, solvent was evaporated and the remainder was purified by column chromatography (1:14, ethyl acetate:hexane) to afford the benzophenone **(3.02)** (960 mg, 1.502 mmoles, 84%) as light yellow oil.

^{1}H NMR (400 MHz, CHLOROFORM-*d*) δ ppm: 0.00 (6 H, s, 2 × Si-$\underline{CH_3}$),0.17 (6 H, s, 2 × Si-$\underline{CH_3}$), 0.68 (9 H, s, $C(CH_3)_3$), 1.00 (9 H, s, $C(CH_3)_3$), 3.82 (3 H, s, OCH_3), 3.85 (3 H, s, OCH_3), 3.89 (3 H, s, OCH_3), 5.14 (2 H, s, CH_2), 6.67 (1 H, s, ArH), 6.88 (1 H, d, ArH, *J* = 8.56 Hz), 7.38 (4 H, m, ArH), 7.52 (3 H, m, ArH);

^{13}C NMR (101 MHz, CHLOROFORM-*d*) δ ppm: -4.7 (2×Si-CH_3), -4.7 (2×Si-CH_3), 18.2 ($\underline{C}(CH_3)_3$), 18.4 ($\underline{C}(CH_3)_3$), 25.5 ($C(\underline{C}H_3)_3$), 25.7 ($C(\underline{C}H_3)_3$), 55.5 (OCH_3), 56.1 (OCH_3), 60.9 (OCH_3), 75.2 (CH_2), 107.0 (ArCH), 110.7 (ArCH), 122.6 (ArCH), 125.7 (ArCH), 128.0 (ArCH), 128.3 (ArC), 128.3 (2×ArCH), 128.4 (2×ArCH), 135.7 (ArC), 130.8 (ArC), 137.5 (ArC), 140.9 (ArC), 143.7 (ArC), 145.5 (ArC), 148.2 (ArC), 155.5 (ArC), 195.0 (C=O);

V_{max} cm^{-1}: 2956, 2931, 2857, 1781, 1511, 1461, 1419, 1276, 1228, 1132. 835, 780;

HRMS: Calculated 638.3095, found 639.3178 ($M + H^+$).

Synthesis of (4-(benzyloxy)-2-hydroxy-3,5-dimethoxyphenyl)(3-hydroxy-4-methoxyphenyl)methanone (3.03)

(4-(benzyloxy)-2-((*tert*-butyldimethylsilyl)oxy)-3,5-dimethoxyphenyl)(3-((*tert*-butyldimethylsilyl)oxy)-4-methoxyphenyl)methanone **(3.02)** (200 mg, 0.313 mmoles) was dissolved in anhydrous THF (5 mL) under an atmosphere of nitrogen and cooled to 0 °C. To this was added TBAF (1.0 M in THF) (204.7 mg, 0.783 mmoles, 783 µL) dropwise at the same temperature. The reaction was quenched after 10 minutes with saturated aqueous

sodium chloride solution (30 mL) and extracted with DCM (2 × 30 mL). Upon drying the organic layer with sodium sulphate and evaporating the organic solvent, the crude product obtained was further purified by column chromatography (1:2, ethyl acetate:hexane) to afford (4-(benzyloxy)-2-hydroxy-3,5-dimethoxyphenyl)(3-hydroxy-4-methoxyphenyl)methanone **(3.03)** (72 mg, 0.175 mmoles, 56%) as yellow oil.

^{1}H NMR (400 MHz, CHLOROFORM-*d*) δ ppm: 3.74 (3 H, s, OCH_3), 3.95 (3 H, s, OCH_3), 4.01 (3 H, s, OCH_3), 5.27 (2 H, s, CH_2), 5.77 (1 H, s, OH), 6.95 (1 H, s, ArH), 6.97 (1 H, d, ArH, *J*= 8.31 Hz), 7.30 (1 H, overlapping-dd, ArH, *J*= 8.31, 2.01 Hz), 7.34 (1 H, d, ArH, *J*=1.96 Hz), 7.40 (3 H, m, ArH), 7.50 (2 H, m, ArH), 12.10 (1 H, s, OH);

^{13}C NMR (101 MHz, CHLOROFORM-*d*) δ ppm: 56.1 (OCH_3), 56.8 (OCH_3), 61.1 (OCH_3), 75.4 (CH_2), 109.9 (ArCH), 110.8 (ArCH), 114.2 (ArC), 115.6 (ArCH), 122.6 (ArCH), 128.1 (ArCH), 128.2 (2×ArCH), 128.4 (2×ArCH), 131.4 (ArC), 137.3 (ArC), 142.2 (ArC), 145.2 (ArC), 145.4 (ArC), 148.5 (ArC), 149.8 (ArC), 153.4 (ArC), 199.1 (C=O);

V_{max} cm^{-1}: 3320, 3210, 2981, 2826, 1577, 1530, 1438, 1322, 1237, 1132;

HRMS: Calculated 410.1366, found 411.1435 ($M + H^+$).

Synthesis of (2,4-dihydroxy-3,5-dimethoxyphenyl)(3-hydroxy-4-methoxyphenyl)methanone (3.04)

Benzyl protected compound **(3.03)** (33 mg, 0.080 mmoles) was dissolved in MeOH:DCM (2:1, 5 mL). To this was added Pd/C (3.3 mg, 10% by weight) and allowed to stir for 90 minutes under the atmosphere of hydrogen at room temperature. Upon completion the reaction was filtered through a cotton plug and evaporated using rotary evaporator. Finally the crude product was further purified by column chromatography (1:2, ethyl acetate:hexane) to afford the phenol **(3.04)** (22 mg, 0.069 mmoles, 85%) as yellow solid.

^{1}H NMR (600 MHz, DMSO-d_6) δ ppm: 3.69 (3 H, s, OCH_3), 3.76 (3 H, s, OCH_3), 3.86 (3 H, s, OCH_3), 6.85 (1 H, s, ArH), 7.06 (1 H, d, ArH, *J*= 8.44 Hz), 7.17 (1 H, d, ArH, *J*=2.20 Hz), 7.19 (1 H, dd, ArH, *J*= 8.07, 2.20 Hz), 9.47 (1 H, s, OH), 10.01 (1 H, s, OH), 11.90 (1 H, s, OH);

^{13}C NMR (151 MHz, DMSO-d_6) δ ppm: 56.1 (OCH_3), 56.7 (OCH_3), 60.5 (OCH_3), 110.3 (ArCH), 111.2 (ArC), 111.7 (ArCH), 116.4 (ArCH), 122.3 (ArCH), 130.8 (ArC), 136.1 (ArC), 141.2 (ArC), 146.7 (ArC), 147.8 (ArC), 151.7 (ArC), 152.2 (ArC), 197.8 (C=O);

V_{max} cm^{-1}: 3338, 2929, 1567, 1497, 1446, 1266, 1025, 912, 779;

HRMS: Calculated 320.0896, found 321.0963 (M + H),

MP: 186-188 °C.

Synthesis of *N*,*N*-dibenzyl-5-bromo-2-methoxyaniline (3.05)

Bromoaniline **(2.12)** (300 mg, 1.493 mmoles) was dissolved in ethanol (18 mL). To this was added K_2CO_3 (825 mg, 5.971 mmoles) by dissolving in water (6 mL) and benzyl bromide (766 mg, 4.478 mmoles, 533 µL). The resultant mixture was allowed to stir at 70 °C for 7 hours. Upon completion the reaction was concentrated by evaporating the volatile solvent and the remainder was redissolved in DCM (100 mL) and washed once with water (50 mL). After drying the organic layer with Na_2SO_4, solvent was evaporated and the residue obtained was further purified by column chromatography (1:25, ethyl acetate:hexane) to afford the product **(3.05)** (442, 1.156 mmoles, 77%) as clear oil that solidified on further vacuum drying.

^{1}H NMR (400 MHz, CHLOROFORM-*d*) δ ppm: 3.92 (3 H, s, OCH_3), 4.27 (4 H, s, 2×CH_2), 6.78 (1 H, d, ArH, *J*= 8.56 Hz), 6.93 (1 H, d, ArH, *J*= 2.45 Hz), 7.05 (1 H, dd, ArH, *J*= 8.56, 2.20 Hz), 7.31 (10 H, m, ArH);

^{13}C NMR (101 MHz, CHLOROFORM-*d*) δ ppm: 55.3 (2×CH_2), 55.8 (OCH_3), 113.0 (ArC), 113.2 (ArCH), 124.3 (ArCH), 124.7 (ArCH), 127.0 (2×ArCH), 128.2 (4×ArCH), 128.3 (ArC), 128.5 (4×ArCH), 138.5 (ArC), 141.4 (ArC), 152.2 (ArC);

HRMS: Calculated 381.0728, found 382.0789 ($M + H^+$),

MP: 60-62 °C.

Synthesis of (4-(benzyloxy)-2-((*tert*-butyldimethylsilyl)oxy)-3,5-dimethoxyphenyl)(3-(dibenzylamino)-4-methoxyphenyl)methanol (3.06)

N,*N*-dibenzyl-5-bromo-2-methoxyaniline **(3.05)** (123 mg, 0.322 mmoles) was dissolved in dry THF (5 ml) under the atmosphere of nitrogen and cooled to -80 °C over 30 minutes. To this was added *n*-butyl lithium (33 mg, 0.515 mmoles, 206 µL, 2.5 M solution in hexane) dropwise over 30 mins and allowed further to stir for 10 mins at the same temperature. Afterwards, benzaldehyde **(2.57)** (100 mg, 0.248 mmoles) was added as solid and allowed the reaction to gradually reach room temperature over the duration of two hours. The

reaction was then diluted with diethyl ether (100 mL) and washed with 1 M aq.HCl (2 × 50 mL). Finally the product was dried with Na_2SO_4 and purified by column chromatography (1:8, ethyl acetate:hexane) to afford the product **(3.06)** (122 mg, 0.099 mmoles, 70%) as light yellow oil.

^{1}H NMR (400 MHz, CHLOROFORM-*d*) δ ppm: 0.18 (3 H, s, Si-$\underline{CH_3}$), 0.24 (3 H, s, Si-$\underline{CH_3}$), 0.99 (9 H, s, C$(CH_3)_3$), 3.60 (3 H, s, OCH_3), 3.82 (3 H, s, OCH_3), 3.94 (3 H, s, OCH_3), 4.25 (4 H, s, 2×CH_2), 5.07 (2 H, s, CH_2), 6.09 (1 H, d, CH, *J*=2.93 Hz), 6.30 (1 H, s, ArH), 6.89 (1 H , overlapping-d, ArH, *J*=8.4 Hz), 6.90 (1 H , overlapping-d, ArH, *J*=2.4 Hz), 6.94 (1 H , dd, ArH, *J*= 8.4,1.83 Hz), 7.30 (13 H, m, ArH), 7.53 (2 H, m, ArH);

^{13}C NMR (101 MHz, CHLOROFORM-*d*) δ ppm: -4.13 (Si-CH_3), -4.08 (Si-CH_3), 18.75 ($\underline{C}(CH_3)_3$), 26.15 (C($\underline{C}H_3)_3$), 55.64 (2×CH_2), 55.73 (OCH_3), 56.18 (OCH_3), 60.78 (OCH_3), 69.86 (CH), 75.13 (CH_2), 105.93 (ArCH), 111.51 (ArCH), 119.92 (ArCH), 120.37 (ArCH), 126.72 (2×ArCH), 127.89 (ArCH), 128.06 (4×ArCH), 128.28 (2×ArCH), 128.32 (2×ArCH), 128.49 (4×ArCH), 129.90 (ArC), 135.15 (ArC), 137.77 (ArC), 139.11 (2×ArC), 139.67 (ArC), 140.41 (ArC), 141.02 (ArC), 144.62 (ArC), 147.82 (ArC), 152.38 (ArC);

V_{max} cm^{-1}: 2954.00, 2931.55, 2855.29, 1505.69, 1484.65, 1460.91, 1418.76, 1363.15, 1238.64, 1128.08, 1079.05, 1027.60, 833.07, 696.28;

HRMS: Calculated 705.3486, found 728.3387 (M +Na^+).

Synthesis of (4-(benzyloxy)-2-((*tert*-butyldimethylsilyl)oxy)-3,5-dimethoxyphenyl)(3-(dibenzylamino)-4-methoxyphenyl)methanone (3.07)

Diphenylmethanol **(3.06)** (105 mg, 0.149 mmoles) was dissolved in dry DCM (10 mL) at 0 °C. To this was added Dess Martin Periodinane (69 mg, 0.164 mmoles). The reaction was allowed to stir at same temperature for 30 minutes before being quenched with 5% $NaHCO_3$ (50 mL) and extracted with DCM (2 × 50 mL). After drying the organic layer with Na_2SO_4, solvent was evaporated and the remainder was purified by column chromatography (1:10, ethyl acetate:hexane) to afford the benzophenone **(3.07)** (83 mg, 0.118 mmoles, 79%) as light yellow oil.

^{1}H NMR (400 MHz, CHLOROFORM-*d*) δ ppm: -0.09 (6 H, s, Si-$(CH_3)_2$), 0.65 (9 H, s, C$(CH_3)_3$), 3.79 (3 H, s, OCH_3), 3.85 (3 H, s, OCH_3), 3.99 (3 H, s, OCH_3), 4.24 (4 H, s, 2×CH_2), 5.15 (2 H, s, CH_2), 6.60 (1 H, s, ArH), 6.90 (1 H , d, ArH, *J*=8.31 Hz), 7.28, (13 H , m, ArH), 7.45 (1 H, dd, ArH, *J*= 8.56, 2.20 Hz), 7.51 (3 H, m, ArH);

^{13}C NMR (101 MHz, CHLOROFORM-*d*) δ ppm: -4.7 (Si-($\underline{C}H_3)_2$)), 18.0 ($\underline{C}(CH_3)_3$), 25.4 (C($\underline{C}H_3)_3$), 26.2 ($\underline{C}(CH_3)_3$), 55.6 (2×CH_2), 55.8 (OCH_3), 56.2 (OCH_3), 60.9 (OCH_3), 75.2 (CH_2), 107.1 (ArCH), 110.5 (ArCH), 122.9 (ArCH), 126.9 (2 × ArCH), 127.0 (ArCH), 127.3 (ArC), 128.0 (ArCH), 128.1 (ArC), 128.2 (4×ArCH), 128.3 (2×ArCH), 128.4 (2×ArCH), 128.4 (4×ArCH), 130.2 (ArC), 138.9 (2×ArC), 139.7 (ArC), 140.9 (ArC), 143.7 (ArC), 145.6 (ArC), 148.1 (ArC), 157.4 (ArC), 194.9 (C=O);

V_{max} cm^{-1}: 2933, 2857, 1654, 1589, 1461, 1419, 1344, 1249, 1130, 1085, 1028, 837, 783;

HRMS: Calculated 703.3329, found 704.3399 ($M + H^+$)

Synthesis of (4-(benzyloxy)-2-hydroxy-3,5-dimethoxyphenyl)(3-(dibenzylamino)-4-methoxyphenyl)methanone (3.08)

(4-(benzyloxy)-2-((*tert*-butyldimethylsilyl)oxy)-3,5-dimethoxyphenyl)(3-(dibenzylamino)-4-methoxyphenyl)methanone **(3.07)** (80 mg, 0.114 mmoles) was dissolved in anhydrous THF (3 mL) under the atmosphere of nitrogen and cooled to 0 °C. To this was added TBAF (1.0 M in THF) (45 mg, 0.172 mmoles, 172 µL) dropwise at the same temperature. The reaction was quenched after 10 minutes with saturated aqueous sodium chloride solution (20 mL) and extracted with diethyl ether (3 × 30 mL). Upon drying the organic layer with sodium sulphate and evaporating the organic solvent, the crude product obtained was further purified by column chromatography (1:8, ethyl acetate:hexane) to afford (4-(benzyloxy)-2-hydroxy-3,5-dimethoxyphenyl)(3-(dibenzylamino)-4-methoxyphenyl)methanone **(3.08)** (55 mg, 0.093 mmoles, 82%) as yellow oil that solidified on further vacuum drying.

^{1}H NMR (400 MHz, CHLOROFORM-*d*) δ ppm: 3.58 (3 H, s, OCH_3), 3.94 (3 H, s, OCH_3), 4.03 (3 H, s, OCH_3), 4.30 (4 H, s, 2×CH_2), 5.25 (2 H, s, CH_2), 6.82 (1 H, s, ArH), 7.00 (1 H , d, ArH, *J*=8.80 Hz), 7.30 (15 H, m, ArH), 7.52 (2 H, m, ArH), 12.08 (1 H, s, OH);

^{13}C NMR (101 MHz, CHLOROFORM-*d*) δ ppm: 55.2 (2×CH_2), 55.8 (OCH_3), 56.8 (OCH_3), 61.1 (OCH_3), 75.4 (CH_2), 110.8 (ArCH), 110.9 (ArCH), 114.4 (ArC), 122.3 (ArCH), 124.8 (ArCH), 127.0 (2×ArCH), 128.1 (ArCH), 128.2 (2×ArCH), 128.3 (4×ArCH), 128.4 (2×ArCH), 128.5 (4×ArCH), 130.5 (ArC), 137.3 (ArC), 138.4 (2×ArC), 140.0 (ArC), 142.1 (ArC), 145.1 (ArC), 148.4 (ArC), 153.2 (ArC), 156.3 (ArC), 199.2 (C=O);

V_{max} cm^{-1}: 3340, 2931, 2833, 1507, 1456, 1419, 1331, 1128;

HRMS: Calculated 589.2464, found 590.2515 ($M + H^+$).

Synthesis of (3-amino-4-methoxyphenyl)(2,4-dihydroxy-3,5-dimethoxyphenyl)methanone (3.09)

(4-(benzyloxy)-2-hydroxy-3,5-dimethoxyphenyl)(3-(dibenzylamino)-4-methoxyphenyl)methanone **(3.08)** (50 mg, 0.085 mmoles) was dissolved in MeOH:DCM (2:1, 5 mL). To this was added $Pd(OH)_2/C$ (10 mg, 20% by weight) and allowed to stir for 90 minutes under the atmosphere of hydrogen at room temperature. Upon completion the reaction was filtered through a cotton plug and evaporated using rotary evaporator. Finally the crude product was further purified by column chromatography (1:1, ethyl acetate:hexane) to afford the benzophenone **(3.09)** (17 mg, 0.053 mmoles, 63%) as yellow solid.

^{1}H NMR (600 MHz, DMSO-d_6) δ ppm: 3.68 (3 H, s, OCH_3), 3.76 (3 H, s, OCH_3), 3.86 (3 H, s, OCH_3), 5.02 (2 H, s, NH_2), 6.88 (1 H, s, ArH), 6.92 (1 H, d, ArH, *J*= 7.80 Hz), 6.95 (1 H, dd, ArH, *J*=8.4, 1.83 Hz), 7.04 (1 H, d, ArH, *J*= 1.83 Hz), 10.01 (1 H,s, OH) 12.12 (1 H, s, OH);

^{13}C NMR (151 MHz, DMSO-d_6) δ ppm: 56.0 (OCH_3), 56.7 (OCH_3), 60.5 (OCH_3), 110.0 (ArCH), 110.6 (ArCH), 111.0 (ArC), 114.4 (ArCH), 119.2 (ArCH), 131.0 (ArC), 136.1 (ArC), 138.1 (ArC), 141.1 (ArC), 147.8 (ArC), 149.9 (ArC), 152.5 (ArC), 198.7 (C=O);

V_{max} cm^{-1}: 3404, 3313, 2935, 1593, 1491, 1421, 1293, 1079, 759;

HRMS: Calculated 319.1056, found 320.1130 ($M + H^+$);

MP: 187-189 °C.

Synthesis of 4-oxo-4-(2,3,4-trimethoxyphenyl)butanoic acid (3.13)

1,2,3-trimethoxybenzene **(3.12) (**3 g, 0.018 moles**)** was dissolved in dry DCM (30 mL) and cooled to -10 °C with salted ice. To this was added succinic anhydride (2.3 g, 0.023 moles) followed by the portion-wise addition of $AlCl_3$ (4.8 g, 0.036 moles). After 6 hours, the reaction mixture was quenched by the addition of cooled 2 M aqueous HCl (30 mL) and extracted with diethyl ether (3 × 30 mL). After drying the organic layer with Na_2SO_4 and evaporating the organic solvent, the remainder was purified by flash column chromatography (1:3:0.033, ethyl acetate:hexane:formic acid) to afford the acid **(3.13)** (2.8 g, 0.010 moles, 58%) as a white solid.

^{1}H NMR (400 MHz, CHLOROFORM-*d*) δ ppm: 2.78 (2 H, t, CH_2, *J*= 6.40 Hz), 3.33 (2 H, t, CH_2, *J*= 6.40 Hz), 3.89 (3 H, s, OCH_3), 3.93 (3 H, s, OCH_3), 4.01 (3 H, s, OCH_3), 6.74 (1 H, d, ArH, *J*= 9.05 Hz), 7.59 (1 H, d, ArH, *J*= 9.05 Hz);

^{13}C NMR (101 MHz, CHLOROFORM-*d*) δ ppm: 28.6 (CH_2), 37.6 (CH_2), 56.1 (OCH_3), 60.9 (OCH_3), 61.4 (OCH_3), 107.2 (ArCH), 124.9 (ArC), 125.8 (ArCH), 142.0 (ArC), 154.4 (ArC), 157.7 (ArC), 178.9 (COOH), 198.1 (C=O);
V_{max} cm^{-1}: 3384, 2942, 1723, 1711, 1292, 1102;

HRMS: 268.0947, found 291.0849 ($M + Na^+$).

Synthesis of 4-(2,3,4-trimethoxyphenyl)butanoic acid (3.14)

Compound **(3.13)** (2.00 g, 0.007 moles) was stirred with Pd/C (880 mg, 10% by weight) in acetic acid and ethanol (3:1, 30 mL) under atmosphere of hydrogen. After stirring for 12 hours at room temperature, the reaction mixture was filtered through a cotton plug, concentrated using rotary evaporator under reduced pressure and the oil left behind was purified by flash column chromatography using (1:3:0.033, ethyl acetate:hexane:formic acid) to afford the acid **(3.14)** (1.78 g, 0.007moles, 94%) as white solid.

^{1}H NMR (400 MHz, CHLOROFORM-*d*) δ ppm: 1.87 - 2.01 (2 H, m, CH_2), 2.41 (2 H, t, CH_2, *J*=7.34 Hz), 2.64 (2 H, t, CH_2, *J*=7.58 Hz), 3.86 (3 H, s, OCH_3), 3.89 (3 H, s, OCH_3), 3.90 (3 H, s, OCH_3), 6.62 (1 H, d, ArH, *J*= 8.80 Hz), 6.84 (1 H, d, ArH, *J*= 8.80 Hz);

^{13}C NMR (101 MHz, CHLOROFORM-*d*) δ ppm: 25.7 (CH_2), 29.0 (CH_2), 33.5 (CH_2), 56.0 (OCH_3), 60.7 (OCH_3), 60.9 (OCH_3), 107.2 (ArCH), 123.9 (ArCH), 127.2 (ArC), 142.3 (ArC), 151.9 (ArC), 152.2 (ArC), 179.8 (COOH);

V_{max} cm^{-1}: 3370, 2942, 1708, 1098;

HRMS: 254.1154, found 277.0752 ($M + Na^+$).

Synthesis of 5,6,7-trimethoxy-3,4-dihydronaphthalen-1(2H)-one (3.15)

Carboxylate compound **(3.14)** (90 mg, 0.354 mmoles) was stirred with polyphosphoric acid 115% (1.5 g,) at 75 °C for one hour. Afterwards the reaction was quenched by the addition of ice cooled water (20 mL) and extracted with DCM (3 × 20 mL). Upon drying and evaporating the organic layer, the remainder was purified by flash column chromatography

(1:4, ethyl acetate:hexane) to afford the compound **(3.15)** (77 mg, 0.326 mmoles, 92%) as white solid.

^{1}H NMR (400 MHz, CHLOROFORM-*d*) δ ppm: 2.07 - 2.14 (2 H, m, CH_2), 2.61 (2 H, t, CH_2, *J*= 6.4 Hz), 2.89 (2 H, t, CH_2, *J*= 6.11 Hz), 3.87 (3 H, s, OCH_3), 3.90 (3 H, s, OCH_3), 3.95 (3 H, s, OCH_3), 7.40 (1 H, s, ArH);

^{13}C NMR (101 MHz, CHLOROFORM-*d*) δ ppm: 22.9 (CH_2), 23.0 (CH_2), 38.8 (CH_2), 56.0 (OCH_3), 60.7 (OCH_3), 60.9 (OCH_3), 105.1 (ArCH), 128.1 (ArC), 132.1 (ArC), 147.1 (ArC), 150.4 (ArC), 152.0 (ArC), 197.6 (C=O);

MP: 75 °C.

Synthesis of 5,6,7-trimethoxy-3,4-dihydronaphthalen-1-yl trifluoromethanesulfonate (3.16)

Tetralone compound **(3.15)** (880 mg, 3.725 mmoles) was dissolved in dry DCM (15 mL) at 0 °C under the atmosphere of nitrogen. To this was added *N*,*N*-diisopropylethylamine (845 µL, 4.850 mmoles), followed by the dropwise addition of triflic anhydride (810 µL, 4.815 mmoles). The reaction was allowed to stir for one hour before solvent volume being reduced using rotary evaporator at 30 °C under reduced pressure. Upon concentration, the reaction mixture was purified by flash column chromatography (1:9, ethyl acetate:hexane) to afford the triflate **(3.16)** (1150 mg, 4.867 mmoles, 84%) as clear oil.

^{1}H NMR (400 MHz, CHLOROFORM-*d*) δ ppm 2.49 (2 H, td, CH_2, *J*= 8.31, 4.89 Hz), 2.84 (2 H, t, CH_2, *J*= 8.01 Hz), 3.87 (3 H, s, OCH_3), 3.88 (3 H, s, OCH_3), 3.91 (3 H, s, OCH_3), 5.98 (1 H, t, C=CH, *J*= 4.97 Hz), 6.75 (1 H, s, ArH);

^{13}C NMR (101 MHz, CHLOROFORM-*d*) δ ppm: 19.5 (CH_2), 22.1 (CH_2), 56.1 (OCH_3), 60.9 (OCH_3), 60.9 (OCH_3), 101.5 (ArCH), 117.1 (C=<u>C</u>H), 120.2 (CF_3), 122.4 (ArC), 124.2 (ArC), 143.2 (ArC), 145.9 (ArC), 150.8 (ArC), 152.0 (<u>C</u>=CH), 197.6 (C=O);

^{19}F NMR (377 MHz, CHLOROFORM-*d*) δ ppm: -73.78 (CF_3)

Synthesis of *tert*-butyl(2-methoxy-5-(5,6,7-trimethoxy-3,4-dihydronaphthalen-1-yl)phenoxy)dimethylsilane (3.17)

Triflate **(3.16)** (100 mg, 0.272 mmoles), boronic acid **(2.10)** (92 mg, 0.326 mmoles) and potassium carbonate (94 mg, 0.680 mmoles) were dissolved and stirred in a biphasic

toluene:ethanol:water mixture (3:1:1, 10 mL). To this tetrakis (triphenylphosphine) palladium (0) (16 mg, 0.014 mmoles) was added and the reaction mixture was heated for 2 hours at 70 °C. After 2 hours the reaction mixture was diluted with ethyl acetate (30 mL), dried with magnesium sulphate and concentrated *in vacuo*. Finally purified by flash column chromatography (1:9, ethyl acetate:hexane) to afford the silyl ether product **(3.17)** (94 mg, 0.206 mmoles, 76%) as colourless oil.

^{1}H NMR (400 MHz, CHLOROFORM-*d*) δ ppm: 0.20 (6 H, s, 2 × Si-CH_3), 1.02 (9 H, s, C(CH_3)$_3$), 2.35 (2 H, td, CH_2, *J*=8.07, 4.89 Hz), 2.82 (2 H, t, CH_2, *J*=8.07 Hz), 3.68 (3 H, s, OCH_3), 3.86 (3 H, s, OCH_3), 3.90 (3 H, s, OCH_3), 3.92 (3 H, s, OCH_3), 6.01 (1 H, t, C=CH, *J*= 4.65 Hz), 6.46 (1 H, s, ArH), 6.85-6.88 (2 H, m, ArH) , 6.91 (1 H, d, ArH, *J*= 1.96 Hz);

^{13}C NMR (101 MHz, CHLOROFORM-*d*) δ ppm: -4.6 (2 × Si-CH_3), 18.5 (C(CH_3)$_3$), 20.3 (CH_2), 23.1 (CH_2), 25.7 (C(CH_3)$_3$), 55.5 (OCH_3), 56.1 (OCH_3), 60.9 (OCH_3), 61.0 (OCH_3), 106.3 (ArCH), 111.7 (ArCH), 121.5 (ArCH), 122.1 (ArCH), 122.6 (ArC), 126.6 (C=CH), 131.1 (ArC), 133.7 (ArC), 139.0 (ArC), 141.4 (ArC), 144.6 (ArC), 150.2 (ArC), 150.4 (ArC), 151.1 (C=CH);

V_{max} cm^{-1}: 2941, 1553, 1480, 1146, 1094;

HRMS: Calculated 456.2332, found 457.2393 ($M + H^+$).

Synthesis of 2-methoxy-5-(5,6,7-trimethoxy-3,4-dihydronaphthalen-1-yl)phenol (3.18)

Silyl ether **(3.17)** (110 mg, 0.241 mmoles) was dissolved in anhydrous THF (2 mL) under the atmosphere of nitrogen and cooled to 0 °C. To this was added TBAF (1.0 M in THF) (126 mg, 0.482 mmoles, 482 µL) dropwise at the same temperature. The reaction was quenched after 10 minutes with saturated aqueous sodium chloride solution (20 mL) and extracted with diethyl ether (3 × 20 mL). Upon drying the organic layer with sodium sulphate and evaporating the organic solvent, the crude product obtained was further purified by flash column chromatography (1:3, ethyl acetate:hexane) to afford the phenol **(3.18)** (75 mg, 0.219 mmoles, 91%) as light yellow oil that solidified on further vacuum drying.

^{1}H NMR (600 MHz, CHLOROFORM-*d*) δ ppm: 2.35 (2 H, td, CH_2, *J*=7.95, 4.65 Hz), 2.80 (2 H, t, CH_2, *J*=8.07 Hz), 3.70 (3 H, s, OCH_3), 3.89 (3 H, s, OCH_3), 3.91 (3 H, s,

OCH_3), 3.94 (3 H, s, OCH_3), 5.67 (1 H, s, OH), 6.03 (1 H, t, C=CH, *J*= 4.77 Hz), 6.49 (1 H, s, ArH), 6.85 (1 H, dd, ArH, *J*= 8.4, 1.8 Hz) , 6.87 (1 H, d, ArH, *J*= 8.4 Hz), 6.96 (1 H, d, ArH, *J*= 1.8 Hz);

^{13}C NMR (151 MHz, CHLOROFORM-*d*) δ ppm: 20.4 (CH_2), 23.1 (CH_2), 56.0 (OCH_3), 56.2 (OCH_3), 60.9 (OCH_3), 61.0 (OCH_3), 106.4 (ArCH), 110.4 (C=<u>C</u>H), 115.1 (ArCH), 120.4 (ArCH), 122.8 (ArC), 126.8 (ArCH), 131.0 (ArC), 134.3 (ArC), 139.0 (<u>C</u>=CH), 141.5 (ArC), 145.3 (ArC), 145.8 (ArC), 150.3 (ArC), 151.0 (ArC);

V_{max} cm^{-1}: 2944, 2835, 1586, 1432, 1346;

HRMS: Calculated 342.1467, found 365.1066 ($M + Na^+$).

Synthesis of 3-(6-(3-((*tert*-butyldimethylsilyl)oxy)-4-methoxybenzoyl)-2,3,4-trimethoxyphenyl)propanal (3.19)

To a stirred solution of silyl ether **(3.17) (**290 mg, 0.635 mmoles**)** in acetic acid:acetic anhydride (2:1, 2 mL) was added $K_2Cr_2O_7$ (230 mg, 0.783 mmoles) portion-wise while heating the reaction mixture at 40 °C. After 3 hours, the reaction mixture was cooled to room temperature, quenched by the addition of ice cooled 5% $NaHCO_3$ (30 mL) and extracted with diethyl ether (3 × 30 mL). Upon drying the organic layer with Na_2SO_4, it was concentrated using rotary evaporator and finally purified by flash column chromatography (1:6, ethyl acetate:hexane) to afford the product **(3.19)** (102 mg, 0.209 mmoles, 40%) as yellow oil.

^{1}H NMR (400 MHz, CHLOROFORM-*d*) δ ppm: 0.18 (6 H, s, 2 × Si-CH_3), 1.00 (9 H, s, C(CH_3)$_3$), 2.69 (2 H, m, CH_2), 2.84 (2 H, m, CH_2), 3.81 (3 H, s, OCH_3), 3.90 (3 H, s, OCH_3), 3.93 (3 H, s, OCH_3), 3.94 (3 H, s, OCH_3), 6.61 (1 H, s, ArH), 6.87 (1 H, d, ArH, *J*= 8.80 Hz), 7.37 (1 H, overlapping-dd, ArH), 7.39 (1 H, overlapping-d, ArH), 9.73 (1 H, distorted-t, CHO);

^{13}C NMR (101 MHz, CHLOROFORM-*d*) δ ppm: -4.6 (2 × Si-CH_3), 18.4 (<u>C</u>(CH_3)$_3$), 20.3 (CH_2), 25.7 (C(<u>C</u>H_3)$_3$), 45.2 (CH_2), 55.6 (OCH_3), 56.1 (OCH_3), 60.8 (OCH_3), 61.0 (OCH_3), 107.4 (ArCH), 110.7 (ArCH), 121.9 (ArCH), 125.6 (ArC), 126.0 (ArCH), 130.5 (ArC), 134.7 (ArC), 143.5 (ArC), 145.0 (ArC), 151.4 (ArC), 152.3 (ArC), 155.8 (ArC), 196.2 (C=O), 202.1 (CHO);

V_{max} cm^{-1}: 2933, 2854, 1736, 1702, 1654, 1578, 1547;

HRMS: Calculated 488.2230, found 489.2291 ($M + H^+$)

Synthesis of 3-(6-(3-hydroxy-4-methoxybenzoyl)-2,3,4-trimethoxyphenyl)propanal (3.20)

Silyl ether **(3.19)** (100 mg, 0.205 mmoles) was dissolved in anhydrous THF (2 mL) under the atmosphere of nitrogen and cooled to 0 °C. To this was added TBAF (1.0 M in THF) (80 mg, 0.307 mmoles, 307 µL) dropwise at the same temperature. The reaction was quenched after 10 minutes with saturated aqueous sodium chloride solution (20 mL) and extracted with diethyl ether (3 × 20 mL). Upon drying the organic layer with sodium sulphate and evaporating the organic solvent, the crude product obtained was further purified by flash column chromatography (1:1, ethyl acetate:hexane) to afford the phenol **(3.20)** (47 mg, 0.126 mmoles, 61%) as light yellow oil that solidified on further vacuum drying.

^{1}H NMR (600 MHz, CHLOROFORM-*d*) δ ppm: 2.69 (2 H, m, CH_2), 2.83 (2 H, m, CH_2), 3.80 (3 H, s, OCH_3), 3.93 (3 H, s, OCH_3), 3.94 (3 H, s, OCH_3), 3.99 (3 H, s, OCH_3), 6.60 (1 H, s, ArH), 6.91 (1 H, d, ArH, *J*= 8.44 Hz), 7.39 (1 H, dd, ArH, *J*= 8.4, 2.20 Hz), 7.41 (1 H, d, ArH, *J*= 1.83 Hz), 9.72 (1 H, t, CHO, 1.47 Hz);

^{13}C NMR (151 MHz, CHLOROFORM-*d*) δ ppm: 20.2 (CH_2), 45.2 (CH_2), 56.1 (OCH_3), 56.2 (OCH_3), 60.8 (OCH_3), 61.0 (OCH_3), 107.5 (ArCH), 109.9 (ArCH), 116.1 (ArCH), 124.2 (ArCH), 125.6 (ArC), 131.0 (ArC), 134.6 (ArC), 143.6 (ArC), 145.5 (ArC), 151.1 (ArC), 151.4 (ArC), 152.3 (ArC), 196.4 (C=O), 202.2 (CHO);

V_{max} cm^{-1}: 2931, 2823, 1723, 1697, 1646, 1559, 1523;

HRMS: Calculated 374.1366, found 397.0964 ($M + Na^+$).

5.3 Experimental Chapter 4

Synthesis of ((2S,3R)-3-((*tert*-butoxycarbonyl)amino)-2-hydroxy-4-phenylbutanoyl)-L-leucine (4.01)

Bestatin **(1.44)** (500 mg, 1.621 mmoles) and potassium carbonate (282 mg, 2.040 mmoles) were dissolved together in THF:water (1:1, 20 mL) at 0 °C. This was followed by the addition of di-*tert*-butyl dicarbonate (422 mg, 1.934 mmoles) in THF (2 mL). Afterwards

the reaction was brought to room temperature and allowed to stir for 6 hours. Upon completion, the reaction was quenched with aqueous NaOH (2 M, 50 mL) and the aqueous layer was washed with diethyl ether (2×50 mL). Afterwards, the aqueous layer was acidified with aqueous HCl (2 M, 70 mL) and extracted with dichloromethane (3 × 50 mL). The combined organic layers were dried with $MgSO_4$, filtered and evaporated using rotary evaporator to afford the carbamate compound **(4.01)** (558 mg, 1.366 mmoles, 84%) as white crystalline solid.

^{1}H NMR (600 MHz, CHLOROFORM-*d*) δ ppm: 0.90 (3 H, d, Leu-CH3, *J* =6 Hz), 0.92 (3 H, d, Leu-CH3, *J*=6 Hz), 1.28 (9 H, s, $C(CH_3)_3$), 1.6 - 1.69 (2 H, m, Leu-CH_2), 1.65-1.67 (1 H, m, $CH(CH_3)_2$), 2.84 (1 H, d, Ar-CH_2, *J*=5.1 Hz), 4.05 (1 H, m , CHNH-Boc), 4.18 (1 H, m, CHOH), 4.61 (1 H, t, CHNH, *J*=6.7 Hz), 5.17 (1 H, d, NH, *J*=7.8 Hz), 6.35 (1 H, br. s, OH), 7.18-7.25 (5 H, m, 5 x ArH), 7.42 (1 H, m, NH);

^{13}C NMR (151 MHz, CHLOROFORM-*d*) δ ppm: 21.4 (Leu-CH_3), 23.1 (Leu-CH_3), 24.8 ($\underline{C}H$-$(CH_3)_2$), 28.2 ($C(\underline{C}H_3)_3$), 36.6 (Ar-CH_2), 40.7 (Leu-CH_2), 50.5 (CHNH-Boc), 55.3 (CHNH), 73.6 (CHOH), 80.4 ($\underline{C}(CH_3)_3$), 126.5 (ArCH), 128.5 (2 x ArCH), 129.3 (ArCH), 129.6 (ArCH), 138.1 (ArC), 157.4 (Boc-NH$\underline{C}$=O), 173.6 (COOH), 175.6 (HOCH-$\underline{C}$=O);

V_{max} cm^{-1}: 3440, 2961, 1750, 1689, 1527, 1508, 1456;

HRMS: Calculated 408.2260, found 431.2149 ($M + Na^+$);

MP: 99-100 °C.

In situ synthesis of pentafluorophenyl ((2S,3R)-3-((*tert*-butoxycarbonyl)amino)-2-hydroxy-4-phenylbutanoyl)-L-leucinate (4.02)

Boc bestatin **(4.01)** (200 mg, 0.490 mmoles) was dissolved in dry DCM (15 mL) with the aid of few drops of DMF, under the atmosphere of nitrogen at 0 °C. To this was added pentafluorophenol (99 mg, 0.539 mmoles) by dissolving in dry DCM (1 mL), followed by the addition of *N*-(3-dimethylaminopropyl)-*N′*-ethylcarbodiimide hydrochloride (122 mg, 0.637 mmoles). The reaction was gradually allowed to reach room temperature over the duration of 3 hours. Afterwards, the reaction was diluted with diethyl ether (100 mL), washed with water (2 × 50 mL) and quickly dried with $MgSO_4$. After evaporating the

organic layer, the compound (4.02) (233 mg, 0.406 mmoles, 83%) was afforded as clear oil that solidified on further vacuum drying.

Synthesis of 2-methoxy-5-(6,7,8-trimethoxy-2-oxo-2H-chromen-4-yl)phenyl ((benzyloxy)carbonyl)-L-leucinate (4.03)

Phenol (2.22) (60 mg, 0.167 mmoles) was dissolved in dry DCM (10 mL) under the atmosphere of nitrogen at 0 °C. To this was added *N*-Cbz leucine (58 mg, 0.218) followed by addition of *N*-(3-dimethylaminopropyl)-*N′*-ethylcarbodiimide hydrochloride (EDC.HCl) (42 mg, 0.218 mmoles) and 4-dimethylaminopyridine (DMAP) (2 mg, 0.016 mmoles). Reaction mixture was stirred and gradually allowed to reach room temperature over the duration of 3 hours. Upon completion the reaction mixture was diluted with DCM (50 mL) and washed once with water (30 mL). The organic layer was quickly dried with Na_2SO_4 and after concentrating under reduced pressure the remainder was purified by flash column chromatography (1:2, ethyl acetate:hexane) to afford carbamate compound (4.03) (90 mg, 0.149 mmoles, 89%) as clear oil that solidified on further vacuum drying.

^{1}H NMR (400 MHz, CHLOROFORM-*d*) δ ppm: 1.04 (6 H, overlapping doublets, Leu-CH_3), 1.72 (1 H, m, C<u>H</u>$(CH_3)_2$), 1.90 (2 H, m, Leu-CH_2), 3.77 (3 H, s, OCH_3), 3.91 (3 H, s, OCH_3), 4.03 (3 H, s, OCH_3), 4.08 (3 H, s, OCH_3) , 4.69 (1 H, m, C<u>H</u>-NH), 5.15 (2 H, s, C<u>H</u>$_2$-Ph), 5.21 (1 H, d, NH), 6.31 (1 H, s, C=CH), 6.76 (1 H, s, ArH), 7.13 (1 H, d, ArH, *J*=8.31 Hz), 7.22 (1 H, s, ArH), 7.36 (6 H, m, ArH);

^{13}C NMR (101 MHz, CHLOROFORM-*d*) δ ppm: 21.9 (Leu-CH_3), 22.9 (Leu-CH_3), 24.8 (<u>C</u>H$(CH_3)_2$), 41.7 (Leu-CH_2), 52.8 (<u>C</u>H-NH), 56.0 (OCH_3), 56.3 (CH-NH), 61.5 (OCH_3), 61.9 (OCH_3), 67.1 (Ar-CH_2), 103.0 (ArCH), 112.8 (C=<u>C</u>H), 113.6 (ArCH), 114.2 (ArC), 123.4 (ArCH), 127.2 (ArCH), 127.9 (ArC), 128.1 (2 × ArCH), 128.2 (ArCH), 128.6 (2 × ArCH), 136.2 (ArC), 139.3 (ArC), 141.4 (ArC), 143.4 (ArC), 146.0 (ArC), 149.7 (ArC), 152.2 (ArC), 154.1 (<u>C</u>=CH), 155.9 (HN-C=O), 160.6 (Lactone-O-<u>C</u>=O), 171.3 (Ar-O-<u>C</u>=O);

V_{max} cm^{-1}: 3351, 2956, 1710, 1513, 1453, 1387, 1270, 1217, 1130

HRMS: Calculated 605.2261, found 606.2313 ($M + H^+$)

Synthesis of 2-methoxy-5-(6,7,8-trimethoxy-2-oxo-2H-chromen-4-yl)phenyl ((2S,3R)-3-((*tert*-butoxycarbonyl)amino)-2-hydroxy-4-phenylbutanoyl)-L-leucyl-L-leucinate (4.04)

Compound **(4.03)** (85 mg, 0.140 mmoles) was stirred with PFP ester of bestatin **(4.02)** (110 mg, 0.191 mmoles) and Pd/C (8.5 mg, 10% by weight) in EtOAc:EtOH (1:1) under the atmosphere of hydrogen. After 90 minutes palladium species were filtered through a cotton plug and organic solvent was evaporated at 35 °C under reduced pressure before the remainder was purified by flash column chromatography (1:1, ethyl acetate:hexane) to afford the compound **(4.04)** (68 mg, 0.079 mmoles, 56%) as white solid.

^{1}H NMR (400 MHz, CHLOROFORM-*d*) d ppm: 0.90 (3 H, d, Leu-CH_3, *J*= 6.36 Hz), 0.94 (3 H, d, Leu-CH_3, *J*= 6.11 Hz), 1.01 (6 H, t, 2×Leu-CH_3, *J*= 5.87 Hz), 1.41 (9 H, s, $C(CH_3)_3$), 1.56-1.70 (4 H, m, 2 × CH_2), 1.70-1.77 (2 H, m, 2 × C<u>H</u>$(CH_3)_2$), 1.78-1.84 (1 H, m, C<u>H</u>$(CH_3)_2$), 3.05 (1 H, dd, CH_2-Ph), 3.22 (1 H, m, CH_2-Ph), 3.78 (3 H, s, OCH_3), 3.91 (3 H, s, OCH_3), 3.96-4.00 (1 H, m, CH-NH), 4.03 (3 H, s, OCH_3), 4.07 (3 H, s, OCH_3), 4.17 (1 H, dd, C<u>H</u>-OH, *J*= 7.34, 2.93 Hz), 4.52 (1 H, m, C<u>H</u>-NH-Boc), 4.83 (1 H, m, C<u>H</u>-NH), 4.99 (1 H, d, NH, *J*= 8.07 Hz), 5.79 (1 H, br.s, OH), 6.30 (1 H, s, C=CH), 6.68 (1 H, br. d, NH), 6.76 (1 H, s, ArH), 7.12 (1 H, d, ArH, *J* = 8.56 Hz), 7.22-7.27 (5 H, m, 4 × ArH, 1 × NH), 7.31 (2 H, m, 2 × ArH), 7.34 (1 H, dd, ArH, *J*= 8.00, 2.23 Hz);

^{13}C NMR (151 MHz, CHLOROFORM-*d*) δ ppm: 21.7 (Leu-CH_3), 21.9 (Leu-CH_3), 22.8 (Leu-CH_3), 23.1 (Leu-CH_3), 24.6 (<u>C</u>H$(CH_3)_2$), 24.9 (<u>C</u>H$(CH_3)_2$), 28.2 (C-(<u>C</u>$H_3)_3$), 36.0 (Ar-CH_2), 40.3 (Leu-CH_2), 41.2 (Leu-CH_2), 51.1 (CH-NH), 51.2 (CH-NH), 54.4 (CH-NH), 56.0 (CH-NH), 56.0 (OCH_3), 56.3 (OCH_3), 61.5 (OCH_3), 61.9 (OCH_3), 74.7 (CH-OH), 80.7 (<u>C</u>-$(CH_3)_3$), 103.0 (ArCH), 112.8 (ArCH), 113.6 (C=<u>C</u>H), 114.2 (ArC), 123.4 (ArCH), 126.8 (ArCH), 127.2 (ArCH), 127.9 (ArC), 128.6 (2 × ArCH), 129.3 (2 × ArCH), 137.9 (ArC), 139.4 (ArC), 141.4 (ArC), 143.4 (ArC), 146.0 (ArC), 149.7 (ArC), 152.2 (ArC), 154.2 (<u>C</u>=CH), 157.9 (Boc-C=O), 160.6 (Lactone-O-<u>C</u>=O), 170.8 (HN-C=O), 171.5 (Ar-O-<u>C</u>=O), 173.1 (HN-C=O);

V_{max} cm^{-1}: 3365, 3277, 2956, 1717, 1640, 1513, 1389, 1131, 752;

HRMS: Calculated 861.4048, found 862.4415 ($M + H^+$)

Synthesis of (2R,3S)-3-hydroxy-4-(((S)-1-(((S)-1-(2-methoxy-5-(6,7,8-trimethoxy-2-oxo-2H-chromen-4-yl)phenoxy)-4-methyl-1-oxopentan-2-yl)amino)-4-methyl-1-oxopentan-2-yl)amino)-4-oxo-1-phenylbutan-2-aminium 2,2,2-trifluoroacetate (4.05)

Carbamate compound **(4.04)** (29 mg, 0.034 mmoles) was dissolved in dry DCM (3 mL) under atmosphere of nitrogen and cooled to -10 °C with salted ice. To this was added dry cooled trifluoroacetic acid (1 mL) and stirred for 90 minutes at 0 °C. Following this step the reaction mixture was diluted with DCM (50 mL) and solvent was evaporated at 35 °C using rotary evaporator under reduced pressure. The product left after evaporation was redissolved in minimum amount of THF and precipitated from it by adding small quantity of hexane to afford the product **(4.05)** (29 mg, 0.033 mmoles, 98%) as white solid.

^{1}H NMR (600 MHz, DMSO-d_6) d ppm: 0.85 - 0.88 (9 H, m, 3 × Leu-CH_3), 0.94 (3 H, d, Leu-CH_3, *J*= 5.87 Hz), 1.51 (2 H, t, Leu-CH_2, *J* = 7.15 Hz), 1.61 - 1.67 (1 H, m, C<u>H</u>$(CH_3)_2$), 1.70 - 1.74 (2 H, m, Leu-CH_2) , 1.74 – 1.78 (1 H, m, C<u>H</u>$(CH_3)_2$), 2.78 (1 H, dd, Ar-C<u>H</u>$_2$, *J*= 13.94, 6.79 Hz), 2.92 (1 H, dd, Ar-C<u>H</u>$_2$, *J*= 13.94, 7.34 Hz), 3.51 (1 H, br.s, C<u>H</u>-NH_2), 3.70 (3 H, s, OCH_3), 3.85 (3 H, s, OCH_3), 3.89 (3 H, s, OCH_3), 3.94 (3 H, s, OCH_3), 3.98 (C<u>H</u>-OH), 4.40 (1 H, q, C<u>H</u>-NH, *J*= 7.20 Hz), 4.52 (1 H, q, C<u>H</u>-NH, *J*= 7.20 Hz), 6.35 (1 H, s, C=CH), 6.62 (1 H, d, OH, 3.85 Hz), 6.75 (1 H, s, ArH), 7.26 - 7.29 (4 H, m, ArH), 7.33 - 7.36 (3 H, m, ArH), 7.52 (1 H, dd, ArH, *J*= 8.44, 2.02 Hz), 7.88 (2 H, br.s, NH_2), 8.10 (1 H, d, NH, *J*= 8.07 Hz), 8.64 (1 H, d, NH, *J*= 7.34 Hz);

^{13}C NMR (151 MHz, DMSO-d_6) δ ppm: 21.3 (Leu-CH_3), 21.9 (Leu-CH_3), 22.7 (Leu-CH_3), 22.9 (Leu-CH_3), 24.1 (<u>C</u>H$(CH_3)_2$), 24.2 (<u>C</u>H$(CH_3)_2$), 34.7 (Ar-CH_2), 39.3 (Leu-CH_2), 40.9 (Leu-CH_2), 50.5 (CH-NH), 50.8 (CH-NH), 54.4 (CH-NH_2), 55.8 (OCH_3), 56.1 (OCH_3), 61.0 (OCH_3), 61.5 (OCH_3), 68.5 (CH-OH), 103.0 (ArCH), 113.1 (C=<u>C</u>H), 113.5 (ArCH), 113.7 (ArC), 123.2 (ArCH), 126.9 (ArC), 127.0 (ArCH), 127.6 (ArCH), 128.6 (2 × ArCH), 129.4 (2 × ArCH), 136.1 (ArC), 138.8 (ArC), 140.8 (ArC), 142.6 (ArC), 145.3 (ArC), 149.3 (ArC), 151.9 (ArC), 153.5 (<u>C</u>=CH), 159.5 (Lactone-O-<u>C</u>=O), 170.5 (HN-C=O), 170.7 (Ar-O-<u>C</u>=O), 172.1 (HN-C=O);

V_{max} cm^{-1}: 2958, 1514, 1388, 1272, 1199, 1031, 1051, 722;

HRMS: Calculated 761.3524, found 762.3601 ($M + H^+$),

MP: 146-149 °C.

Synthesis of 2-methoxy-5-(6,7,8-trimethoxy-2-oxo-2H-chromen-4-yl)phenyl ((benzyloxy)carbonyl)-L-valinate (4.06)

Phenol **(2.22)** (80 mg, 0.223 mmoles) was dissolved in dry DCM (10 mL) under the atmosphere of nitrogen at 0 °C. To this was added *N*-Cbz valine (73 mg, 0.290 mmoles) followed by addition of *N*-(3-dimethylaminopropyl)-*N′*-ethylcarbodiimide hydrochloride (EDC.HCl) (56 mg, 0.290 mmoles) and 4-dimethylaminopyridine (DMAP) (2 mg, 0.016 mmoles). Reaction mixture was stirred and gradually allowed to reach room temperature over the duration of 3 hours. Progress of the reaction was monitored by TLC using $KMnO_4$ as visualising reagent and upon completion the reaction mixture was diluted with DCM (50 mL) and washed once with water (30 mL). The organic layer was quickly dried with Na_2SO_4 and after concentrating under reduced pressure the remainder was purified by flash column chromatography (1:1, ethyl acetate:hexane) to afford carbamate compound **(4.06)** (125 mg, 0.211 mmoles, 95%) as white solid.

^{1}H NMR (400 MHz, CHLOROFORM-*d*) δ ppm: 1.07 (3 H, d, Val-CH_3, *J*=6.85 Hz), 1.13 (3 H, d, Val-CH_3, *J*=6.85 Hz), 2.44 (1 H, m, C<u>H</u>$(CH_3)_2$), 3.77 (3 H, s, OCH_3), 3.91 (3 H, s, OCH_3), 4.03 (3 H, s, OCH_3), 4.07 (3 H, s, OCH_3), 4.62 (1 H, dd, C<u>H</u>-NH, *J*= 8.80, 4.40 Hz), 5.15 (2 H, s, CH_2), 5.36 (1 H, d, NH, *J*= 8.80 Hz), 6.30 (1 H, s, C=CH), 6.76 (1 H, s, ArH), 7.13 (1 H, d, ArH, *J*= 8.56 Hz), 7.20 (1 H, s, ArH), 7.37 (6 H, m, ArH);

^{13}C NMR (101 MHz, CHLOROFORM-*d*) δ ppm: 17.3 (Val-CH_3), 19.1 (Val-CH_3), 31.3 (<u>C</u>H$(CH_3)_2$), 55.9 (OCH_3), 56.3 (OCH_3), 59.2 (CH-NH), 61.5 (OCH_3), 61.9 (OCH_3), 67.2 (CH_2), 103.0 (ArCH), 112.9 (C=<u>C</u>H), 113.6 (ArCH), 114.2 (ArC), 123.4 (ArCH), 127.3 (ArCH), 127.9 (ArC), 128.1 (2 × ArCH), 128.3 (ArCH), 128.6 (2 × ArCH), 136.2 (ArC), 139.2 (ArC), 141.4 (ArC), 143.4 (ArC), 146.0 (ArC), 149.7 (ArC), 152.2 (ArC), 154.1 (<u>C</u>=CH), 156.3 (HN-C=O), 160.6 (Lactone-O-<u>C</u>=O), 170.3 (Ar-O-<u>C</u>=O);

V_{max} cm^{-1}: 3336, 2963, 2940, 1716, 1513, 1388, 1272, 1131, 1090, 751;

HRMS: Calculated 591.2104, found 592.2164 ($M + H^+$).

Synthesis of 2-methoxy-5-(6,7,8-trimethoxy-2-oxo-2H-chromen-4-yl)phenyl ((2S,3R)-3-((*tert*-butoxycarbonyl)amino)-2-hydroxy-4-phenylbutanoyl)-L-leucyl-L-valinate (4.07)

Compound **(4.06)** (80 mg, 0.135 mmoles) was stirred with PFP ester of bestatin **(4.02)** (110 mg, 0.191 mmoles) and Pd/C (8 mg, 10% by weight) in EtOAc:EtOH (1:1) under the atmosphere of hydrogen. After 90 minutes palladium species were filtered through a cotton plug and organic solvent was evaporated at 35 °C under reduced pressure before the remainder was purified by flash column chromatography (1:1, ethyl acetate:hexane) to afford the compound **(4.07)** (64 mg, 0.075 mmoles, 56%) as white solid.

^{1}H NMR (600 MHz, CHLOROFORM-*d*) d ppm: 0.90 (3 H, d, Leu-CH_3, *J*= 6.24 Hz), 0.95 (3 H, d, Leu-CH_3, *J*= 5.87 Hz), 1.07 (6 H, d, Val-$(CH_3)_2$, *J*= 6.60 Hz), 1.41 (9 H, s, $C(CH_3)_3$), 1.62-1.65 (1 H, m, Leu-CH_2), 1.65-1.67 (1 H, m, Leu-C<u>H</u>$(CH_3)_2$), 1.70-1.74 (1 H, m, Leu-CH_2), 2.44 (1 H, m, Val-C<u>H</u>$(CH_3)_2$), 3.05 (1 H, dd, Ar-C<u>H</u>$_2$, *J*= 13.02, 5.32 Hz), 3.27 (1 H, br.m, Ar-C<u>H</u>$_2$), 3.78 (3 H, s, OCH_3), 3.91 (3 H, s, OCH_3), 3.97 (1 H, br.s, C<u>H</u>-OH), 4.03 (3 H, s, OCH_3), 4.07 (3 H, s, OCH_3), 4.19 (1 H, dd, C<u>H</u>-NH-Boc, *J*= 7.52, 2.75 Hz), 4.49 (1 H, m, Leu-C<u>H</u>-NH), 4.80 (1 H, dd, Val-C<u>H</u>-NH, *J*= 8.44, 4.40 Hz), 4.96 (1 H, d, NH, *J*= 7.70 Hz), 5.90 (1 H, br.s, NH), 6.31 (1 H, s, C=CH), 6.75 (2 H, overlapping-s, 1 × ArH, 1 × NH), 7.13 (1 H, d, ArH, *J*= 8.80), 7.21-7.27 (4 H, m, ArH), 7.30-7.33 (2 H, m, ArH), 7.35 (1 H, dd, ArH, *J*= 8.44, 1.47 Hz);

^{13}C NMR (151 MHz, CHLOROFORM-*d*) δ ppm: 17.5 (Val-CH_3), 19.1 (Val-CH_3), 21.7 (Leu-CH_3), 23.1 (Leu-CH_3), 24.6 (Leu-<u>C</u>H$(CH_3)_2$), 28.2 (C(<u>C</u>$H_3)_3$), 31.2 (Val-<u>C</u>H$(CH_3)_2$), 35.8 (Ar-CH_2), 40.1 (Leu-CH_2), 51.4 (Leu-<u>C</u>H-NH), 55.9 (OCH_3), 56.1 (<u>C</u>H-OH), 56.3 (OCH_3), 57.3 (Val-<u>C</u>H-NH), 61.5 (OCH_3), 61.9 (OCH_3), 75.1 (<u>C</u>H-NH-Boc), 80.9 (<u>C</u>$(CH_3)_3$), 102.9 (ArCH), 112.8 (ArCH), 113.7 (C=<u>C</u>H), 114.2 (ArC), 123.4 (ArCH), 126.8 (ArCH), 127.3 (ArCH), 127.9 (ArC), 128.6 (2 × ArCH), 129.3 (2 × ArCH), 138.0 (ArC), 139.3 (ArC), 141.4 (ArC), 143.4 (ArC), 146.0 (ArC), 149.7 (ArC), 152.2 (ArC), 154.1 (<u>C</u>=CH), 160.6 (Lactone-O-<u>C</u>=O), 169.8 (Ar-O-<u>C</u>=O), 171.6 (HN-C=O), 173.2 (HN-C=O), 173.4 (HN-C=O);

V_{max} cm^{-1}: 3313, 2961, 2934, 1720, 1649, 1514, 1389, 1273, 1133, 1049, 754;

HRMS: Calculated 847.3891, found 848.3969 ($M+H^+$).

Synthesis of (2R,3S)-3-hydroxy-4-(((S)-1-(((S)-1-(2-methoxy-5-(6,7,8-trimethoxy-2-oxo-2H-chromen-4-yl)phenoxy)-3-methyl-1-oxobutan-2-yl)amino)-4-methyl-1-oxopentan-2-yl)amino)-4-oxo-1-phenylbutan-2-aminium 2,2,2-trifluoroacetate (4.08)

Carbamate compound **(4.07)** (41 mg, 0.048 mmoles) was dissolved in dry DCM (3 mL) under atmosphere of nitrogen and cooled to -10 °C with salted ice. To this was added dry cooled trifluoroacetic acid (1 mL) and stirred for 90 minutes at 0 °C. Following this step the reaction mixture was diluted with DCM (50 mL) and solvent was evaporated at 35 °C using rotary evaporator under reduced pressure. The product left after evaporation was redissolved in minimum amount of THF and precipitated from it by adding small quantity of hexane to afford the product **(4.08)** (41 mg, 0.048 mmoles, 98%) as white solid.

^{1}H NMR (600 MHz, DMSO-d_6) δ ppm: 0.87 (6 H, t, 2 × Leu-CH_3, J= 7.15 Hz), 1.02 (3 H, d, Val-CH_3, J= 6.78 Hz), 1.04 (3 H, d, Val-CH_3, J= 6.78 Hz), 1.51 (2 H, m, Leu-CH_2), 1.65 (1 H, m, Leu-C<u>H</u>$(CH_3)_2$), 2.26 (1 H, m, Val-C<u>H</u>$(CH_3)_2$), 2.79 (1 H, dd, Ar-C<u>H</u>$_2$, J= 13.93, 6.78 Hz), 2.93 (1 H, dd, Ar-C<u>H</u>$_2$, J= 13.93, 7.53 Hz), 3.52 (1 H, br.s, C<u>H</u>-OH), 3.71 (3 H, s, OCH_3), 3.86 (3 H, s, OCH_3), 3.90 (3 H, s, OCH_3), 3.94 (3 H, s, OCH_3), 3.99 (1 H, br.s, C<u>H</u>-NH_2), 4.42 (1 H, m, Val-C<u>H</u>-NH), 4.50 (1 H, m, Leu-C<u>H</u>-NH), 6.35 (1 H, s, C=CH), 6.64 (1 H, br.s, OH), 6.76 (1 H, s, ArH), 7.27 (4 H, m, ArH), 7.35 (3 H, m, ArH), 7.53 (1 H, dd, ArH, J= 8.28, 1.88 Hz), 7.88 (2 H, br.s, NH_2), 8.08 (1 H, d, NH, J= 8.28 Hz), 8.56 (1 H, d, NH, J= 7.53 Hz);

^{13}C NMR (151 MHz, DMSO-d_6) δ ppm: 18.1 (Val-CH_3), 18.8 (Val-CH_3), 21.9 (Leu-CH_3), 22.9 (Leu-CH_3), 24.1 (Leu-<u>C</u>H$(CH_3)_2$), 29.7 (Val-<u>C</u>H$(CH_3)_2$), 34.7 (Ar-<u>C</u>H_2), 40.9 (Leu-<u>C</u>H_2), 50.8 (Leu-<u>C</u>H-NH), 54.3 (<u>C</u>H-OH), 55.8 (OCH_3), 56.0 (OCH_3), 57.7 (Val-<u>C</u>H-NH), 61.0 (OCH_3), 61.5 (OCH_3), 68.4 (<u>C</u>H-NH_2), 102.9 (ArCH), 113.2 (C=<u>C</u>H), 113.6 (ArCH), 113.7 (ArC), 123.2 (ArCH), 127.0 (ArC), 127.1 (ArCH), 127.7 (ArCH), 128.6 (2 × ArCH), 129.4 (2 × ArCH), 136.1 (ArC), 138.7 (ArC), 140.8 (ArC), 142.6 (ArC), 145.3 (ArC), 149.3 (ArC), 152.0 (ArC), 153.4 (<u>C</u>=CH), 159.5 (Lactone-O-<u>C</u>=O), 169.5 (Ar-O-<u>C</u>=O), 170.5 (HN-C=O), 172.4 (HN-C=O);

V_{max} cm^{-1}: 2963, 1669, 1513, 1388, 1130, 1090, 750;

HRMS: Calculated 747.3367, found 748.3423 ($M + H^+$),

MP: 122-124 °C.

Synthesis of 4-(3-((*tert*-butoxycarbonyl)amino)-4-methoxyphenyl)-6,8-dimethoxy-2-oxo-2H-chromen-7-yl ((benzyloxy)carbonyl)-L-valinate (4.09)

Phenol **(2.67)** (60 mg, 0.135 mmoles) was dissolved in dry DCM (10 mL) under the atmosphere of nitrogen at 0 °C. To this was added *N*-Cbz valine (44 mg, 0.176 mmoles) followed by addition of *N*-(3-dimethylaminopropyl)-*N*′-ethylcarbodiimide hydrochloride (EDC.HCl) (34 mg, 0.176 mmoles) and 4-dimethylaminopyridine (DMAP) (1.6 mg, 0.013 mmoles). Reaction mixture was stirred and gradually allowed to reach room temperature over the duration of 3 hours. Upon completion the reaction mixture was diluted with DCM (50 mL) and washed once with water (30 mL). The organic layer was quickly dried with Na_2SO_4 and after concentrating under reduced pressure the remainder was purified by flash column chromatography (1:2, ethyl acetate:hexane) to afford carbamate compound **(4.09)** (88 mg, 0.130 mmoles, 96%) as off white solid.

^{1}H NMR (400 MHz, CHLOROFORM-*d*) δ ppm: 1.09 (3 H, d, Val-CH_3, *J*= 6.85 Hz) 1.15 (3 H, d, Val-CH_3, *J*=6.85 Hz, 3 H), 1.52 (9 H, s, C(CH_3)$_3$), 2.50 Val-C<u>H</u>(CH_3)$_2$), 3.76 (3 H, s, OCH_3), 3.98 (3 H, s, OCH_3), 4.03 (3 H, s, OCH_3), 4.74 (1 H, dd, C<u>H</u>-NH, *J*= 9.29, 4.40 Hz), 5.18 (2 H, s, CH_2), 5.38 (1 H, d, NH, *J*= 9.29 Hz), 6.40 (1 H, s, C=CH), 7.01 (1 H, overlapping-d, ArH, *J*= 8.4 Hz), 7.02 (1 H, overlapping-s, ArH), 7.12 (1 H, overlapping-dd, ArH, *J*= 8.56, 2.20 Hz), 7.14 (1 H, overlapping-s, ArH), 7.37 (5 H, m, ArH), 8.32 (1 H, br.s, NH);

^{13}C NMR (101 MHz, CHLOROFORM-*d*) δ ppm: 17.0 (Val-CH_3), 19.1 (Val-CH_3), 28.3 (C(<u>C</u>H_3)$_3$), 31.4 (<u>C</u>H(CH_3)$_2$), 55.9 (OCH_3), 56.2 (OCH_3), 59.0 (CH-NH), 61.9 (OCH_3), 67.2 (CH_2), 80.8 (<u>C</u>(CH_3)$_3$), 103.5 (ArCH), 110.3 (C=<u>C</u>H), 114.6 (ArCH), 117.4 (ArC), 118.8 (ArCH), 122.7 (ArCH), 127.8 (ArC), 128.1 (ArCH), 128.2 (ArCH), 128.3 (ArCH), 128.6 (2 × ArCH), 136.2 (ArC), 141.0 (ArC), 142.6 (ArC), 148.3 (ArC), 148.8 (ArC), 152.6 (ArC), 155.2 (ArC), 156.2 (<u>C</u>=CH), 160.2 (Lactone-O-<u>C</u>=O), 169.7 (HN-C=O);

V_{max} cm^{-1}: 2958, 1720, 1529, 1390, 1249, 1227, 1159, 1089, 1036, 754;

HRMS: Calculated 676.2632, found 677.2703 (M + H^+).

MP: 111-113 °C.

Synthesis of 4-(3-((*tert*-butoxycarbonyl)amino)-4-methoxyphenyl)-6,8-dimethoxy-2-oxo-2H-chromen-7-yl ((2S,3R)-3-((*tert*-butoxycarbonyl)amino)-2-hydroxy-4-phenylbutanoyl)-L-leucyl-L-valinate (4.10)

Compound **(4.09)** (86 mg, 0.127 mmoles) was stirred with PFP ester of bestatin **(4.02)** (115 mg, 0.200 mmoles) and Pd/C (8.6 mg, 10% by weight) in EtOAc:EtOH (1:1, 10 mL) under the atmosphere of hydrogen. After 90 minutes palladium species were filtered through a cotton plug and organic solvent was evaporated at 35 °C under reduced pressure before the remainder was purified by flash column chromatography (1:1, ethyl acetate:hexane) to afford the compound **(4.10)** (58 mg, 0.062 mmoles, 49%) as white solid.

^{1}H NMR (600 MHz, CHLOROFORM-*d*) δ ppm: 0.92 (3 H, d, Leu-CH_3, *J*= 6.24 Hz), 0.95 (3 H, d, Leu-CH_3, *J*= 6.24 Hz), 1.08 (6 H, dd, valine-CH_3, *J*= 6.79, 1.65 Hz), 1.41 (9 H, s, $C(CH_3)_3$), 1.52 (9 H, s, $C(CH_3)_3$), 1.65-1.67 (1 H, m, Leu-CH_2) ,1.67-1.69 (1 H, m, Leu-C$\underline{H}(CH_3)_2$), 1.72-1.75 (1 H, m, Leu-CH_2), 2.48 (1 H, m, Val-C$\underline{H}(CH_3)_2$), 3.05 (1 H, dd, Ar-C$\underline{H}_2$, *J*= 13.94, 5.50 Hz), 3.25 (1 H, br.m, Ar-C$\underline{H}_2$), 3.76 (3 H, s, OCH_3), 3.98 (3 H, s, OCH_3), 4.04 (3 H, s, OCH_3), 4.20 (1 H, dd, C$\underline{H}$-NH-Boc, *J*= 7.52, 2.75 Hz), 4.51 (1 H, m, Leu-C$\underline{H}$-NH), 4.94 (1 H, dd, Val-C$\underline{H}$-NH, *J*= 8.80, 4.40 Hz), 4.99 (1 H, d, NH, *J*= 8.07 Hz), 5.83 (1 H, br.s, NH), 6.40 (1 H, s, C=CH), 6.76 (1 H, d, NH, *J*= 7.34 Hz), 7.00 (1 H, overlapping-d, ArH, *J*= 8.4 Hz), 7.01 (1 H, overlapping-s, ArH), 7.12 (1 H, dd, ArH, *J*= 8.4, 1.8 Hz), 7.14 (1 H, s, ArH), 7.24 (3 H, m, ArH), 7.31 (2 H, m, ArH), 8.32 (1 H, br.s, NH);

^{13}C NMR (151 MHz, CHLOROFORM-*d*) δ ppm: 17.3 (Val-CH_3), 19.1 (Val-CH_3), 21.8 (Leu-CH_3), 23.1 (Leu-CH_3), 24.6 (Leu-$\underline{C}H(CH_3)_2$), 28.2 ($C(\underline{C}H_3)_3$), 28.3 ($C(\underline{C}H_3)_3$), 31.4 (Val-$\underline{C}H(CH_3)_2$), 35.8 (Ar-CH_2), 40.3 (Leu-CH_2), 51.6 (Leu-$\underline{C}$H-NH), 55.9 (OCH_3), 56.1 ($\underline{C}$H-OH), 56.2 (OCH_3), 57.1 (Val-$\underline{C}$H-NH), 61.9 (OCH_3), 75.0 ($\underline{C}$H-NH-Boc), 80.8 ($\underline{C}(CH_3)_3$), 80.8 ($\underline{C}(CH_3)_3$), 103.5 (ArCH), 110.3 (ArCH), 114.6 (C=$\underline{C}$H), 117.4 (ArC), 118.8 (ArC), 122.7 (ArCH), 126.7 (ArCH), 127.8 (ArCH), 128.4 (ArC), 128.6 (2 × ArCH), 129.3 (2 × ArCH), 135.4 (ArC), 138.1 (ArC), 141.0 (ArC), 142.6 (ArC), 148.3 (ArC), 148.8 (ArC), 152.6 (HN-C=O), 155.2 ($\underline{C}$=CH), 158.0 (HN-C=O), 160.2 (Lactone-O-$\underline{C}$=O), 169.3 (Ar-O-C=O), 171.6 (HN-C=O), 173.1 (HN-C=O);

V_{max} cm^{-1}: 2961, 1720, 1529, 1391, 1249, 1155, 1131, 750;

HRMS: Calculated 932.4419, found 933.4458 ($M + H^+$).

Synthesis of 5-(7-((((2S,3R)-3-ammonio-2-hydroxy-4-phenylbutanoyl)-L-leucyl-L-valyl)oxy)-6,8-dimethoxy-2-oxo-2H-chromen-4-yl)-2-methoxybenzenaminium 2,2,2-trifluoroacetate (4.11)

Carbamate compound **(4.10)** (56 mg, 0.060 mmoles) was dissolved in dry DCM (3 mL) under atmosphere of nitrogen and cooled to -10 °C with salted ice. To this was added dry cooled trifluoroacetic acid (1 mL) and stirred for 90 minutes at 0 °C. Following this step the reaction mixture was diluted with DCM (50 mL) and solvent was evaporated at 35 °C using rotary evaporator under reduced pressure. The product left after evaporation was redissolved in minimum amount of THF and precipitated from it by adding small quantity of hexane to afford the TFA salt **(4.11)** (56 mg, 0.058 mmoles, 97%) as light yellow solid.

^{1}H NMR (600 MHz, DMSO-d_6) δ ppm: 0.89 (6 H, t, 2 × Leu-CH_3, *J*= 6.24 Hz), 1.04 (6 H, t, 2 × Val-CH_3, *J*= 5.40 Hz), 1.52-1.57 (2 H, m, Leu-CH_2), 1.65-1.69 (1 H, m, Leu-C<u>H</u>$(CH_3)_2$), 2.27-2.31 (1 H, m, Val-C<u>H</u>$(CH_3)_2$), 2.79 (1 H, dd, Ar-C<u>H</u>$_2$, *J*= 13.75, 6.79 Hz), 2.94 (1 H, dd, Ar-C<u>H</u>$_2$, *J*= 13.75, 7.52 Hz), 3.53 (1 H, br.s, C<u>H</u>-OH), 3.67 (3 H, s, OCH_3), 3.86 (3 H, s, OCH_3), 3.86 (3 H, s, OCH_3), 4.00 (1 H, m, C<u>H</u>-NH_2), 4.49-4.51 (1 H, m, Leu-C<u>H</u>-NH), 4.53-4.55 (1 H, m, Val-C<u>H</u>-NH), 6.33 (1 H, s, C=CH), 6.62 (1 H, br-d, OH, *J*= 4.77 Hz), 6.79 (1 H, dd, ArH, *J*=7.89, 1.65 Hz), 6.87 (1 H, d, ArH, *J*= 1.83 Hz), 6.97 (1 H, overlapping-s, ArH), 6.98 (1 H, overlapping-d, ArH, *J*= 8.44 Hz), 7.27 (3 H, m, ArH), 7.35 (2 H, m, ArH), 7.88 (2 H, br.s, NH_2), 8.12 (1 H, d, Leu-NH, *J*= 8.07 Hz), 8.56 (1 H, d, Val-NH, *J*= 8.07 Hz);

^{13}C NMR (151 MHz, DMSO-d_6) δ ppm: 18.4 (Val-CH_3), 19.3 (Val-CH_3), 22.4 (Leu-CH_3), 23.5 (Leu-CH_3), 24.6 (Leu-<u>C</u>H$(CH_3)_2$), 30.5 (Val-<u>C</u>H$(CH_3)_2$), 35.2 (Ar-CH_2), 41.3 (Leu-CH_2), 51.5 (Leu-<u>C</u>H-NH), 54.9 (<u>C</u>H-OH)), 55.9 (OCH_3), 56.5 (OCH_3), 57.8 (Val-<u>C</u>H-NH), 62.1 (OCH_3), 68.9 (<u>C</u>H-NH_2), 103.9 (ArCH), 111.1 (ArCH), 114.0 (ArCH), 114.1 (C=<u>C</u>H), 117.2 (ArCH), 117.3 (ArC), 127.5 (ArCH), 127.6 (ArC), 129.1 (2 × ArCH), 129.9 (2 × ArCH), 135.5 (ArC), 136.6 (ArC), 138.4 (ArC), 140.9 (ArC), 142.5 (ArC), 148.1 (ArC), 148.2 (ArC), 155.8 (<u>C</u>=CH), 159.7 (Lactone-O-<u>C</u>=O), 169.4 (Ar-O-C=O), 171.0 (Leu-HN-C=O), 172.8 (Val-HN-C=O);

V_{max} cm^{-1}: 2958, 1670, 1514, 1388, 1272, 1131, 1050, 722;

HRMS: Calculated 732.3370, found 733.3422 (M + H^+),

MP: 122-125 °C.

Synthesis of *tert*-butyl (S)-(1-((5-(7-(benzyloxy)-6,8-dimethoxy-2-oxo-2H-chromen-4-yl)-2-methoxyphenyl)amino)-4-methyl-1-oxopentan-2-yl)carbamate (4.12)

Aniline compound **(2.66)** (114 mg, 0.263 mmoles) was dissolved in dry DCM (15 mL) at 0 °C under the atmosphere of nitrogen. This was followed by the sequential addition of Boc-leucine (182 mg, 0.789 mmoles), PyBroP (368 mg, 0.789 mmoles) and diisopropylethylamine (102 mg, 0.789 mmoles, 137 µL) at 0 °C. Reaction was gradually allowed to reach room temperature and stirred for 4 hours. Afterwards the reaction was quenched with 1 M HCl (30 mL) and extracted with DCM (3×50 mL). Upon evaporating the organic solvent, the remainder was purified by flash column chromatography (1:2, ethyl acetate:hexane), to afford the product **(4.12)** (160 mg, 0.247 mmoles, 94%) as yellow oil that solidified on further vacuum drying.

^{1}H NMR (400 MHz, CHLOROFORM-*d*) δ ppm: 1.00 (6 H, m, 2 × Leu-CH_3), 1.50 (9 H, s, $C(CH_3)_3$), 1.56-1.61 (1 H, m, Leu-CH_2), 1.75-1.78 (1 H, m, Leu-C<u>H</u>$(CH_3)_2$), 1.78-1.82 (1 H, m, Leu-CH_2), 3.80 (3 H, s, OCH_3), 4.00 (3 H, s, OCH_3), 4.02 (3 H, s, OCH_3), 4.30 (1 H, m, Leu-C<u>H</u>-NH), 4.96 (1 H, d, NH, *J*=7.58 Hz), 5.20 (2 H, s, Ar-CH_2), 6.32 (1 H, s, C=CH), 6.93 (1 H, s, ArH), 7.04 (1 H, d, ArH, *J*= 8.31 Hz), 7.20 (1 H, dd, ArH, *J*= 8.44, 1.83 Hz), 7.35-7.42 (3 H, m, ArH), 7.53 (2 H, m, ArH), 8.55 (1 H, br.s, NH), 8.58 (1 H, d, ArH, *J*=1.96 Hz);

^{13}C NMR (101 MHz, CHLOROFORM-*d*) δ ppm: 21.8 (Leu-CH_3), 22.9 (Leu-CH_3), 24.9 (<u>C</u>H$(CH_3)_2$), 28.3 (C(<u>C</u>$H_3)_3$), 41.0 (Leu-CH_2), 56.0 (OCH_3), 56.3 (OCH_3), 61.9 (OCH_3), 75.7 (Ar-CH_2), 103.5 (ArCH), 110.4 (C=<u>C</u>H), 113.6 (ArCH), 114.7 (ArC), 120.3 (ArCH), 124.2 (ArCH), 124.9 (ArC), 128.2 (ArCH), 128.3 (2 × ArCH), 128.4 (2 × ArCH), 137.2 (ArC), 141.8 (ArC), 143.3 (ArC), 144.7 (ArC), 149.3 (ArC), 150.0 (ArC), 155.1 (<u>C</u>=CH), 160.8 (Lactone-O-<u>C</u>=O), 170.9 (Ar-HN-C=O);

V_{max} cm^{-1}: 3347, 2958, 1710, 1678, 1518, 1392, 1130, 1047, 752;

HRMS: Calculated 646.2890, found 647.2943 ($M + H^+$).

Synthesis of *tert*-butyl (S)-(1-((5-(7-hydroxy-6,8-dimethoxy-2-oxo-2H-chromen-4-yl)-2-methoxyphenyl)amino)-4-methyl-1-oxopentan-2-yl)carbamate (4.13)

Benzyl ether **(4.12)** (150 mg, 0.232 mmoles) was dissolved in MeOH:DCM (2:1, 10 mL). To this was added Pd/C (15 mg, 10% by weight) and allowed to stir for 90 minutes under the atmosphere of hydrogen at room temperature. After completion the reaction was filtered through a cotton plug and upon evaporating the organic solvent, the crude product obtained was further purified by column chromatography (1:1, ethyl acetate:hexane) to afford the phenol **(4.13)** (110 mg, 0.198 mmoles, 85%) as off-white solid.

^{1}H NMR (400 MHz, CHLOROFORM-*d*) δ ppm: 1.00 (6 H, dd, 2 × Leu-CH_3, *J*= 6.11, 4.90 Hz), 1.50 (9 H, s, $C(CH_3)_3$), 1.61 (1 H, m, Leu-CH_2), 1.72-1.77 (1 H, m, Leu-C<u>H</u>$(CH_3)_2$), 1.78-1.83 (1 H, m, Leu-CH_2), 3.86 (3 H, s, OCH_3), 3.99 (3 H, s, OCH_3), 4.12 (3 H, s, OCH_3), 4.30 (1 H, m, Leu-C<u>H</u>-NH), 4.93 (1 H, br.s, NH), 6.12 (1 H, br.s, OH), 6.26 (1 H, s, C=CH), 6.93 (1 H, s, ArH), 7.04 (1 H, d, ArH, *J*=8.56 Hz), 7.20 (1 H, dd, ArH, *J*=8.44, 2.08 Hz), 8.54 (1 H, br.s, NH), 8.55 (1 H, d, ArH, *J*=2.20 Hz);

^{13}C NMR (101 MHz, CHLOROFORM-*d*) δ ppm: 22.0 (Leu-CH_3), 22.9 (Leu-CH_3), 24.9 (<u>C</u>H$(CH_3)_2$), 28.3 (C(<u>C</u>$H_3)_3$), 41.0 (Leu-CH_2), 54.1 (Leu-<u>C</u>H-NH), 56.0 (OCH_3), 56.5 (OCH_3), 61.7 (OCH_3), 79.4 (<u>C</u>$(CH_3)_3$), 102.9 (ArCH), 110.4 (ArCH), 111.3 (ArC), 111.9 (C=<u>C</u>H), 120.5 (ArCH), 124.1 (ArCH), 128.3 (ArC), 131.5 (ArC), 134.7 (ArC), 142.3 (ArC), 143.4 (ArC), 144.2 (ArC), 149.3 (ArC), 155.5 (<u>C</u>=CH), 160.9 (Lactone-O-<u>C</u>=O), 170.9 (Ar-HN-C=O);

V_{max} cm^{-1}: 3315, 2859, 1697, 1534, 1506, 1396, 1254, 1088;

HRMS: Calculated 556.2421, found 557.2502 ($M+H^+$).

Synthesis of 4-(3-((S)-2-((*tert*-butoxycarbonyl)amino)-4-methylpentanamido)-4-methoxyphenyl)-6,8-dimethoxy-2-oxo-2H-chromen-7-yl ((benzyloxy)carbonyl)-L-valinate (4.14)

Phenol **(4.13)** (90 mg, 0.162 mmoles) was dissolved in dry DCM (10 mL) under the atmosphere of nitrogen at 0 °C. To this was added *N*-Cbz valine (53 mg, 0.210 mmoles) followed by addition of *N*-(3-dimethylaminopropyl)-*N*′-ethylcarbodiimide hydrochloride (EDC.HCl) (40 mg, 0.210 mmoles) and 4-dimethylaminopyridine (DMAP) (2 mg, 0.016

mmoles). Reaction mixture was stirred and gradually allowed to reach room temperature over the duration of 3 hours. Upon completion the reaction mixture was diluted with DCM (50 mL) and washed once with water (30 mL). The organic layer was quickly dried with Na_2SO_4 and after concentrating under reduced pressure the remainder was purified by flash column chromatography (1:2, ethyl acetate:hexane) to afford carbamate compound **(4.14)** (110 mg, 0.139 mmoles, 86%) as white solid.

^{1}H NMR (400 MHz, CHLOROFORM-*d*) δ ppm: 1.00 (6 H, t, 2 × Leu-CH_3, *J*= 5.62 Hz), 1.09 (3 H, d, Val-CH_3, *J*=6.85 Hz), 1.15 (3 H, d, Val-CH_3, *J*=6.85 Hz), 1.50 (9 H, s, $C(CH_3)_3$), 1.65-1.75 (1 H, m, Leu-C<u>H</u>$(CH_3)_2$), 1.74-1.83 (2 H, m, Leu-CH_2), 2.50 ((1 H, m, Val-C<u>H</u>$(CH_3)_2$)), 3.75 (3 H, s, OCH_3), 4.00 (3 H, s, OCH_3), 4.03 (3 H, s, OCH_3), 4.28 (1 H, m, Leu-C<u>H</u>-NH), 4.73 (1 H, dd, Val-C<u>H</u>-NH *J*=9.41, 4.03 Hz), 4.92 (1 H, br.s, NH), 5.18 (2 H, s, Ar-CH_2), 5.37 (1 H, d, NH, *J*=9.29 Hz), 6.39 (1 H, s, C=CH), 6.99 (1 H, s, ArH), 7.05 (1 H, d, ArH, *J*=8.31 Hz), 7.20 (1 H, dd, ArH, *J*=8.44, 2.08 Hz), 7.33-7.40 (5 H, m, ArH) 8.53 (1 H, br.s, NH), 8.55 (1 H, d, ArH, *J*=2.20 Hz);

^{13}C NMR (101 MHz, CHLOROFORM-*d*) δ ppm: 17.0 (Val-CH_3), 19.1 (Val-CH_3), 22.9 (Leu-CH_3), 24.9 (Leu-CH_3), 28.3 (C(<u>C</u>$H_3)_3$), 31.4 (Leu-<u>C</u>H$(CH_3)_2$), 31.6 (Val-<u>C</u>H$(CH_3)_2$), 40.9 (Leu-CH_2), 56.0 (OCH_3), 56.2 (OCH_3), 59.0 (Val-<u>C</u>H-NH), 61.9 (OCH_3), 67.2 (Ar-CH_2) 77.2 (<u>C</u>H-NH-Boc), 80.5 (<u>C</u>$(CH_3)_3$), 103.3 (ArCH), 110.5 (ArCH), 114.8 (C=<u>C</u>H), 117.3 (ArC), 120.4 (ArCH), 124.2 (ArCH), 127.5 (ArC), 127.8 (ArC), 128.1 (2 × ArCH), 128.2 (ArCH), 128.6 (2 × ArCH), 135.5 (ArC), 136.2 (ArC), 141.0 (ArC) , 142.6 (ArC), 148.3 (ArC), 149.5 (ArC), 155.0 (<u>C</u>=CH), 158.2 (HN-C=O), 160.1 (Lactone-O-<u>C</u>=O), 169.6 (Ar-O-<u>C</u>=O), 170.9 (HN-C=O);

V_{max} cm^{-1}: 3326, 2963, 1722, 1531, 1391, 1174, 1037, 755;

HRMS: Calculated 789.3473 found 790.3559 ($M + H^+$).

Synthesis of 4-(3-((S)-2-((*tert*-butoxycarbonyl)amino)-4-methylpentanamido)-4-methoxyphenyl)-6,8-dimethoxy-2-oxo-2H-chromen-7-yl ((2S,3R)-3-((*tert*-butoxycarbonyl)amino)-2-hydroxy-4-phenylbutanoyl)-L-leucyl-L-valinate (4.15)

Compound **(4.14)** (90 mg, 0.114 mmoles) and PFP ester of bestatin **(4.02)** (98 mg, 0.171 mmoles) were stirred together with Pd/C (9 mg, 10% by weight) in EtOAc:EtOH (1:1) under the atmosphere of hydrogen. After 90 minutes palladium species were filtered

through a cotton plug and organic solvent was evaporated at 35 °C under reduced pressure before the remainder was purified by flash column chromatography (1:1, ethyl acetate:hexane) to afford the compound **(4.15)** (62 mg, 0.059 mmoles, 52%) as white solid.

^{1}H NMR (400 MHz, CHLOROFORM-*d*) δ ppm: 0.91-0.93 (3 H, m, Leu-CH_3), 0.95 (3 H, d, Leu-CH_3, *J*= 6.11 Hz), 0.99 (6 H, dd, 2 × Leu-CH_3, *J*= 6.05, 5.07 Hz), 1.08 (6 H, d, 2 × Val-CH_3, *J*= 6.85), 1.41 (9 H, s, $C(CH_3)_3$), 1.49 (9 H, s, $C(CH_3)_3$), 1.53-1.61 (2 H, m, Leu-CH_2), 1.64-1.67 (2 H, m, Leu-CH_2), 1.70-1.75 (2 H, m, 2 × Leu-C<u>H</u>$(CH_3)_2$), 2.44-2.52 (1 H, m, Val-C<u>H</u>$(CH_3)_2$), 3.04 (1 H, dd, Ar-CH_2, *J*= 13.39, 5.93 Hz), 3.23 (1 H, m, Ar-CH_2), 3.74 (3 H, s, OCH_3), 3.99 (3 H, s, OCH_3), 4.03 (3 H, s, OCH_3), 4.20 (1 H, br.s, AHPA-C<u>H</u>-NH), 4.28 (1 H, br.s, C<u>H</u>-OH), 4.52 (1 H, m, Leu-C<u>H</u>-NH), 4.93 (1 H, dd, Val-C<u>H</u>-NH, *J*= 8.93, 4.52), 5.01 (1 H, d, NH, *J*= 7.95 Hz), 5.83 (1 H, br.s, OH), 6.38 (1 H, s, C=CH),6.77 (1 H, d, NH, *J*= 8.19 Hz), 6.98 (1 H, s, ArH), 7.04 (1 H, d, ArH, *J*= 8.56 Hz), 7.19 (1 H, dd, ArH, *J*=8.44, 2.08 Hz), 7.22-7.27 (3 H, m, ArH), 7.30-7.35 (2 H, m, ArH), 8.54 (1 H, br.s, NH), 8.56 (1 H, overlapping-d, ArH, *J*= 2.08 Hz);

^{13}C NMR (101 MHz, CHLOROFORM-*d*) δ ppm: 17.3 (Val-CH_3), 19.1 (Val-CH_3), 21.8 (Leu-CH_3), 22.0 (Leu-CH_3), 22.9 (Leu-CH_3), 23.1 (Leu-CH_3), 24.6 (Leu-<u>C</u>H$(CH_3)_2$), 24.9 (Leu-<u>C</u>H$(CH_3)_2$), 28.2 (C(<u>C</u>$H_3)_3$), 28.3 (C(<u>C</u>$H_3)_3$), 31.3 (Val-C<u>H</u>$(CH_3)_2$), 36.1 (ArCH_2), 40.4 (Leu-CH_2), 41.4 (Leu-CH_2), 51.6 (Leu-<u>C</u>H-NH), 56.0 (OCH_3), 56.2 (OCH_3), 57.1 (Val-<u>C</u>H-NH), 61.9 (OCH_3), 74.9 (AHPA-<u>C</u>H-NH), 80.4 (<u>C</u>$(CH_3)_3$), 80.7 (<u>C</u>$(CH_3)_3$), 103.3 (ArCH), 110.5 (ArCH), 114.7 (C=<u>C</u>H), 117.3 (ArC), 120.4 (ArCH), 124.2 (ArC), 126.7 (ArCH), 127.5 (ArC), 127.8 (ArCH), 128.6 (2 × ArCH), 129.3 (2 × ArCH), 135.4 (ArC), 138.1 (ArC), 141.0 (ArC), 142.5 (ArC), 148.3 (ArC), 149.5 (ArC), 154.9 (<u>C</u>=CH), 160.1 (Lactone-O-<u>C</u>=O), 169.2 (Ar-HN-<u>C</u>=O), 170.9 (Ar-O-<u>C</u>=O), 171.7 (Leu-HN-<u>C</u>=O), 173.0 (Val-HN-<u>C</u>=O);

V_{max} cm^{-1}: 3313, 2961, 1688, 1530, 1493, 1255, 1164, 1132, 754, 700;

HRMS: Calculated 1045.5260, found 1046.5319 ($M + H^+$);

MP: 140-142 °C.

Synthesis of (S)-1-((5-(7-((((2S,3R)-3-ammonio-2-hydroxy-4-phenylbutanoyl)-L-leucyl-L-valyl)oxy)-6,8-dimethoxy-2-oxo-2H-chromen-4-yl)-2-methoxyphenyl)amino)-4-methyl-1-oxopentan-2-aminium 2,2,2-trifluoroacetate (4.16)

Carbamate compound **(4.15)** (42 mg, 0.040 mmoles) was dissolved in dry DCM (3 mL) under atmosphere of nitrogen and cooled to -10 °C with salted ice. To this was added dry cooled trifluoroacetic acid (1 mL) and stirred for 90 minutes at 0 °C. Following this step the reaction mixture was diluted with DCM (50 mL) and solvent was evaporated at 35 °C using rotary evaporator under reduced pressure. The product left after evaporation was redissolved in the minimum of volume of THF and precipitated from it by adding small quantity of hexane to afford the TFA salt **(4.16)** (42 mg, 0.039 mmoles, 98%) as white solid.

^{1}H NMR (600 MHz, DMSO-d_6) δ ppm 0.89 (6 H, t, 2 × Leu-CH_3, *J*=6.42 Hz,), 0.92 (3 H, overlapping-d, Leu-CH_3, *J*= 6.24 Hz), 0.94 (3 H, overlapping-d, Leu-CH_3, *J*= 6.24 Hz), 1.04 (6 H, t, 2 × Val-CH_3, *J*=6.42 Hz), 1.49-1.59 (2 H, m, Leu-CH_2), 1.62-1.67 (2 H, m, Leu-CH_2), 1.67-1.72 (2 H, m, 2 × Leu-C<u>H</u>$(CH_3)_2$), 2.27-2.32 (1 H, m, Val-C<u>H</u>$(CH_3)_2$), 2.80 (1 H, dd, Ar-CH_2, *J*= 13.75 Hz), 2.94 (1 H, dd, Ar-CH_2, *J*= 13.75 Hz), 3.54 (1 H, br.s, AHPA-C<u>H</u>-NH_2), 3.72 (3 H, s, OCH_3), 3.87 (3 H, s, OCH_3), 3.97 (3 H, s, OCH_3), 4.00 (1 H, br.m, C<u>H</u>-OH), 4.21 (1 H, m, Leu-C<u>H</u>-NH_2), 4.49-4.55 (2 H, m, 1 × Leu-C<u>H</u>-NH, 1 × Val-C<u>H</u>-NH), 6.45 (1 H, s, C=CH), 6.68 (1 H, br.s, OH), 7.02 (1 H, s, ArH), 7.28 (3 H, m, ArH), 7.34 (3 H, m, ArH), 7.47 (1 H, dd, ArH, *J*=8.44, 1.47 Hz), 7.91 (2 H, br.s, NH_2), 8.08 (1 H, br.s, ArH), 8.12 (1 H, d, NH, *J*=8.07 Hz), 8.22 (2 H, br.s, NH_2), 8.56 (1 H, d, NH, *J*=8.07 Hz), 10.18 (1 H, s, Ar-NH);

^{13}C NMR (151 MHz, CHLOROFORM-*d*) δ ppm: 17.9 (Val-CH_3), 18.8 (Val-CH_3), 21.9 (Leu-CH_3), 22.0 (Leu-CH_3), 22.7 (Leu-CH_3), 23.0 (Leu-CH_3), 23.7 (Leu-<u>C</u>H$(CH_3)_2$), 24.1 (Leu-<u>C</u>H$(CH_3)_2$), 29.4 (Val-C<u>H</u>$(CH_3)_2$), 34.7 ($ArCH_2$), 40.4 (Leu-CH_2), 40.9 (Leu-CH_2), 50.9 (Leu-<u>C</u>H-NH), 51.4 (Leu-<u>C</u>H-NH_2), 54.4 (AHPA-<u>C</u>H-NH_2), 56.0 (OCH_3) , 56.1 (OCH_3), 57.4 (Val-<u>C</u>H-NH), 61.6 (OCH_3), 68.4 (<u>C</u>H-OH), 103.0 (ArCH), 112.3 (ArCH), 114.3 (C=<u>C</u>H), 116.6 (ArC), 123.4 (ArCH), 125.7 (ArC), 126.2 (ArCH), 126.3 (ArC), 126.9 (ArCH), 128.6 (2 × ArCH), 129.4 (2 × ArCH), 135.1 (ArC), 136.2 (ArC), 140.5 (ArC), 142.0 (ArC), 147.8 (ArC), 151.6 (ArC), 153.8 (<u>C</u>=CH), 159.0 (Lactone-O-<u>C</u>=O), 168.8 (Ar-HN-<u>C</u>=O), 168.9 (Ar-O-<u>C</u>=O), 170.5 (Leu-HN-<u>C</u>=O), 172.4 (Val-HN-<u>C</u>=O);

V_{max} cm^{-1}: 2963, 1670, 1535, 1456, 1392, 1179, 1130, 1036, 722;

HRMS: Calculated 845.4211, found 846.4283 ($M + H^+$),

MP: 149-153 °C.

Synthesis of 5-(4-(benzyloxy)-2-((((benzyloxy)carbonyl)-L-valyl)oxy)-3,5-dimethoxybenzoyl)-2-methoxyphenyl ((benzyloxy)carbonyl)-L-valinate (4.17)

Di-hydroxy-benzophenone **(3.04)** (35 mg, 0.085 mmoles) was dissolved in dry DCM (10 mL) under the atmosphere of nitrogen at 0 °C. To this was added *N*-Cbz valine (64 mg, 0.255 mmoles) followed by addition of *N*-(3-dimethylaminopropyl)-*N′*-ethylcarbodiimide hydrochloride (EDC) (49 mg, 0.255 mmoles) and 4-dimethylaminopyridine (DMAP) (1 mg, 0.0085 mmoles). Reaction mixture was stirred and gradually allowed to reach room temperature over the duration of 3 hours. Upon completion the reaction mixture was diluted with DCM (50 mL) and washed with water (2 × 20 mL). The organic layer was quickly dried with Na_2SO_4 and after concentrating under reduced pressure the remainder was purified by flash column chromatography (1:3, ethyl acetate:hexane) to afford carbamate compound **(4.17)** (70 mg, 0.080mmoles, 94%) as light yellow oil

^{1}H NMR (400 MHz, CHLOROFORM-*d*) δ ppm: 0.81 (3 H, d, Val-CH_3, *J*= 6.36 Hz), 0.95 (3 H, d, Val-CH_3, *J*= 6.85 Hz), 1.02 (3 H, d, Val-CH_3, *J*= 6.85 Hz), 1.10 (3 H, d, Val-CH_3, *J*= 6.36 Hz), 2.10 (1 H, m, Val-C<u>H</u>$(CH_3)_2$), 2.42 (1 H, m, Val-C<u>H</u>$(CH_3)_2$), 3.85 (6 H, s, OCH_3), 3.87 (3 H, s, OCH_3), 4.34 (1 H, dd, C<u>H</u>-NH, *J*= 9.29, 4.40 Hz), 4.65 (1 H, dd, C<u>H</u>-NH, *J*= 9.05, 3.67 Hz), 5.15 (6 H, m, 3 × CH_2), 5.29 (1 H, d, NH, *J*= 9.29 Hz), 5.35 (1 H, d, NH, *J*= 8.80 Hz), 6.78 (1 H, s, ArH), 6.96 (1 H, d, ArH, *J*= 8.80 Hz), 7.38 (13 H, m, ArH), 7.52 (3 H, m, ArH), 7.75 (1 H, d, ArH, *J*= 8.31 Hz);

^{13}C NMR (101 MHz, CHLOROFORM-*d*) δ ppm: 16.9 (Val-CH_3), 17.1 (Val-CH_3), 19.1 (Val-CH_3), 19.2 (Val-CH_3), 30.8 (Val-<u>C</u>H$(CH_3)_2$), 31.4 (Val-<u>C</u>H$(CH_3)_2$), 56.0 (OCH_3), 56.3 (OCH_3), 59.0 (2 × Val-<u>C</u>H-NH), 61.3 (OCH_3), 66.9 (CH_2), 67.2 (CH_2), 75.4 (CH_2), 107.1 (ArCH), 111.7 (ArCH), 124.8 (ArCH), 127.2 (ArCH), 128.0 (2 × ArCH), 128.1 (ArCH), 128.2 (ArCH), 128.2 (2 × ArCH), 128.3 (ArCH), 128.3 (2 × ArCH), 128.4 (2 × ArCH), 128.5 (2 × ArCH), 128.6 (2 × ArCH),130.1 (ArC), 130.2 (ArC), 135.7 (ArC), 136.2 (ArC), 136.4 (ArC), 137.1 (ArC), 139.0 (ArC), 144.2 (ArC), 146.3 (ArC), 151.7 (ArC). 155.4 (ArC), 156.1 (HN-C=O), 156.2 (HN-C=O), 169.8 (Ar-O-<u>C</u>=O), 170.2 (Ar-O-<u>C</u>=O), 191.4 (C=O);

V_{max} cm^{-1}: 3354, 2965, 1710, 1511, 1461, 1123, 748, 697;

HRMS: Calculated 876.3469, found 877.3520 ($M + H^+$).

Synthesis of 5-(2-((((2S,3R)-3-((*tert*-butoxycarbonyl)amino)-2-hydroxy-4-phenylbutanoyl)-L-leucyl-L-valyl)oxy)-4-hydroxy-3,5-dimethoxybenzoyl)-2-methoxyphenyl ((2S,3R)-3-((*tert*-butoxycarbonyl)amino)-2-hydroxy-4-phenylbutanoyl)-L-leucyl-L-valinate (4.18)

Compound **(4.17)** (49 mg, 0.056 mmoles) was stirred with PFP ester of bestatin **(4.02)** (100 mg, 0.174 mmoles) and Pd/C (10 mg, 20% by weight) in EtOAc:EtOH (1:1, 10 mL) under the atmosphere of hydrogen. After 90 minutes palladium species were filtered through a cotton plug and the organic solvent was evaporated at 35 °C under reduced pressure before the remainder was purified by flash column chromatography (1:1, ethyl acetate:hexane) to afford the compound **(4.18)** (38 mg, 0.029 mmoles, 52%) as white solid.

^{1}H NMR (600 MHz, DMSO-d_6) δ ppm: 0.76 - 0.85 (18 H, m, 2 × Val-CH_3, 4 × Leu-CH_3), 1.01 (6 H, t, 2 × Val-CH_3, *J*= 6.97 Hz), 1.28 (9 H,s, $C(CH_3)_3$), 1.29 (9 H,s, $C(CH_3)_3$), 1.42-1.50 (4 H, m, 2 × Leu-CH_2), 1.55-1.60 (2 H, m, 2 × Leu-C<u>H</u>$(CH_3)_2$), 1.94-1.97 (1 H, m, Val-C<u>H</u>$(CH_3)_2$), 2.22-2.25 (1 H, m, Val-C<u>H</u>$(CH_3)_2$), 2.62-2.68 (2 H, m, $ArCH_2$), 2.76-2.81 (2 H, m, $ArCH_2$), 3.70 (3 H, s, OCH_3), 3.77 (3 H, s, OCH_3), 3.80 (2 H, m, 2 × C<u>H</u>-NH-Boc), 3.85 (3 H, s, OCH_3), 3.92-3.96 (2 H, m, 2 × C<u>H</u>-OH), 4.36-4.41 (2 H, m, 2 × Val-C<u>H</u>-NH), 4.49-4.55 (2 H, m, 2 × Leu-C<u>H</u>-NH), 5.68 (1 H, br.d, CH-O<u>H</u>, *J*= 9.17 Hz), 5.72 (1 H, br.d, CH-O<u>H</u>, *J*=8.80 Hz), 6.06 (1 H, d, NH, *J*= 6.24 Hz), 6.11 (1 H, d, NH, *J*= 9.54 Hz), 6.17 (1 H, d, NH, *J*= 9.54 Hz), 6.78 (1 H, s, ArH), 7.18-7.28 (11 H, m , ArH), 7.37 (1 H, d, ArH, *J*= 1.47 Hz), 7.60 (2 H, m, 1 × ArH, 1 × NH), 8.24 (1 H, d, NH, *J*= 8.80 Hz), 8.51 (1 H, d, NH, *J*= 7.70 Hz), 9.76 (1 H, br.s, Ar-OH);

^{13}C NMR (151 MHz, DMSO-d_6) δ ppm: 17.8 (Val-CH_3), 18.6 (Val-CH_3), 19.3 (Val-CH_3), 19.5 (Val-CH_3), 22.2 (Leu-CH_3), 22.4 (Leu-CH_3), 23.6 (Leu-CH_3), 23.7 (Leu-CH_3), 24.3 (Leu-<u>C</u>H$(CH_3)_2$), 24.4 (Leu-<u>C</u>H$(CH_3)_2$), 28.6 (2×C(<u>C</u>$H_3)_3$)), 30.1 (Val-<u>C</u>H$(CH_3)_2$), 30.2 (Val-<u>C</u>H$(CH_3)_2$), 37.9 ($ArCH_2$), 38.0 ($ArCH_2$), 42.1 (Leu-CH_2), 42.2 (Leu-CH_2), 50.4 (Leu-<u>C</u>H-NH), 50.6 (Leu-<u>C</u>H-NH), 55.0 (2 × <u>C</u>H-OH), 56.7 (OCH_3), 56.7 (OCH_3), 57.0 (Val-<u>C</u>H-NH), 58.1 (Val-<u>C</u>H-NH), 60.4 (OCH_3), 71.8 (<u>C</u>H-NH-Boc), 71.9 (<u>C</u>H-NH-Boc), 78.0 (2 × <u>C</u>$(CH_3)_3$)), 107.8 (ArCH), 112.9 (ArCH), 121.2 (ArC), 124.0 (ArCH), 126.5 (2 × ArCH), 128.6 (4 × ArCH), 129.7 (4 × ArCH), 129.9 (ArC), 130.3 (ArC), 130.7 (ArCH), 136.6 (ArC), 139.2 (ArC), 139.2 (ArC), 139.2 (ArC), 140.6 (ArC), 146.4 (ArC), 155.3 (HN-C=O), 155.3 (HN-C=O), 155.4 (ArC), 169.6 (Ar-O-<u>C</u>=O), 169.8 (Ar-O-<u>C</u>=O), 171.9 (HN-C=O), 171.9 (HN-C=O), 172.6 (HN-C=O), 172.9 (HN-C=O), 190.9 (C=O);

V_{max} cm^{-1}: 3313, 2964, 1766, 1650, 1505, 1279, 1168, 1025, 756, 701;

HRMS: Calculated 1298.6574, found 1299.6625 ($M + H^+$).

Synthesis of (2S,3R)-4-(((S)-1-(((S)-1-(5-(2-((((2S,3R)-3-ammonio-2-hydroxy-4-phenylbutanoyl)-L-leucyl-L-valyl)oxy)-4-hydroxy-3,5-dimethoxybenzoyl)-2-methoxyphenoxy)-3-methyl-1-oxobutan-2-yl)amino)-4-methyl-1-oxopentan-2-yl)amino)-3-hydroxy-4-oxo-1-phenylbutan-2-aminium 2,2,2-trifluoroacetate (4.19)

Carbamate compound **(4.18)** (30 mg, 0.023 mmoles) was dissolved in dry DCM (3 mL) under atmosphere of nitrogen and cooled to -10 °C with salted ice. To this was added dry cooled trifluoroacetic acid (1 mL) and stirred for 90 minutes at 0 °C. Following this step the reaction mixture was diluted with DCM (50 mL) and solvent was evaporated at 35 °C using rotary evaporator under reduced pressure. The product left after evaporation was redissolved in minimum amount of THF and precipitated from it by adding small quantity of hexane to afford the TFA salt **(4.19)** (30 mg, 0.022 mmoles, 98%) as white solid.

^{1}H NMR (600 MHz, DMSO-d_6) δ ppm: 0.750 - 0.80 (6 H, m, 2 × Val-CH_3), 0.83-0.87 (12 H, m, 4 × Leu-CH_3), 1.01 (6 H, t, 2 × Val-CH_3, *J*= 7.70 Hz), 1.46-1.53 (4 H, m, 2 × Leu-CH_2), 1.60-1.66 (2 H, m, 2 × Leu-C<u>H</u>$(CH_3)_2$), 1.94-1.98 (1 H, m, Val-C<u>H</u>$(CH_3)_2$), 2.20-2.25 (1 H, m, Val-C<u>H</u>$(CH_3)_2$), 2.78 (2 H, td, $ArCH_2$, *J*= 14.86, 6.97 Hz), 2.93 (2 H, dd, $ArCH_2$, *J*= 13.75 Hz, 7.15 Hz), 3.51 (2 H, m, 2 × C<u>H</u>-NH_2), 3.69 (3 H, s, OCH_3), 3.77 (3 H, s, OCH_3), 3.84 (3 H, s, OCH_3), 3.99 (2 H, br.s, 2 × C<u>H</u>-OH), 4.37-4.41 (2 H, m, 2 × Val-C<u>H</u>-NH), 4.42-4.51 (2 H, m, 2 × Leu-C<u>H</u>-NH), 6.63 (2 H, br.d, 2× CH-O<u>H</u>), 6.77 (1 H, s, ArH), 7.24 (1 H, overlapping-d, ArH, *J*= 8.80) 7.25-7.30 (6 H, m, ArH) , 7.33-7.36 (4 H, m, ArH), 7.36 (1 H, overlapping-d, ArH, *J*= 2.20 Hz), 7.60 (1 H, dd, ArH, *J*=8.44, 1.83 Hz),7.88 (4 H, br.s, 2 × NH_2), 8.06 (2 H, dd, 2 × NH, *J*=7.70, 2.57 Hz), 8.31 (1 H, d, NH, *J*= 8.80 Hz), 8.57 (1 H, d, NH, *J*= 7.70 Hz), 9.79 (1 H, br.s, Ar-OH);

^{13}C NMR (151 MHz, DMSO-d_6) δ ppm: 17.3 (Val-CH_3), 18.1 (Val-CH_3), 18.8 (Val-CH_3), 19.0 (Val-CH_3), 21.8 (Leu-CH_3), 22.0 (Leu-CH_3), 22.8 (Leu-CH_3), 23.0 (Leu-CH_3), 24.1 (Leu-<u>C</u>H$(CH_3)_2$), 24.1 (Leu-<u>C</u>H$(CH_3)_2$), 29.7 (Val-<u>C</u>H$(CH_3)_2$), 29.8 (Val-<u>C</u>H$(CH_3)_2$), 34.6 ($ArCH_2$), 34.7 ($ArCH_2$), 40.7 (Leu-CH_2), 41.0 (Leu-CH_2), 50.8 (Leu-<u>C</u>H-NH), 51.0 (Leu-<u>C</u>H-NH), 54.3 (<u>C</u>H-NH_2), 54.4 (<u>C</u>H-OH), 56.2 (OCH_3), 56.2 (OCH_3), 56.5 (Val-<u>C</u>H-NH),

57.6 (Val-CH-NH), 60.1 (OCH_3), 68.4 (CH-NH_2), 68.4 (CH-OH), 107.3 (ArCH), 112.4 (ArCH), 121.2 (ArC), 123.5 (ArCH), 127.0 (ArCH), 127.1 (ArCH), 128.6 (2 × ArCH), 128.6 (2 × ArCH), 129.4 (2 × ArCH), 129.4 (2 × ArCH), 129.8 (ArC), 130.3 (ArCH), 136.1 (ArC), 136.1 (ArC), 138.7 (ArC), 140.1 (ArC), 143.2 (ArC), 145.9 (ArC), 154.9 (ArC), 169.1 (Ar-O-C=O), 169.4 (Ar-O-C=O), 170.4 (HN-C=O), 170.4 (HN-C=O), 172.0 (HN-C=O), 172.3 (HN-C=O), 190.4 (C=O);

V_{max} cm^{-1}: 3332, 2933, 1671, 1633, 1583, 1513, 1451, 1381, 1239, 1127, 1093, 954, 807, 761;

HRMS: Calculated 1098.5525, found 1099.5616 ($M + H^+$),

MP : 135-137 °C.

Synthesis of *tert*-butyl (S)-(1-((2-methoxy-5-(6,7,8-trimethoxy-2-oxo-2H-chromen-4-yl)phenyl)amino)-4-methyl-1-oxopentan-2-yl)carbamate (4.20)

Aniline compound **(2.16)** (100 mg, 0.280 mmoles) was dissolved in dry DCM (10 mL) at 0 °C under the atmosphere of nitrogen. This was followed by the sequential addition of Boc-leucine (130 mg, 0.562 mmoles), PyBroP (262 mg, 0.562 mmoles) and diisopropylethylamine (73 mg, 0.562 mmoles, 98 µL) at 0 °C. Reaction was gradually allowed to reach room temperature and stirred for 5 hours. Afterwards, the reaction was quenched with 1 M HCl (20 mL) and extracted with DCM (2×30 mL). Upon drying and evaporating the organic layer, the remainder was purified by flash column chromatography (1:3, ethyl acetate:hexane), to afford the product **(4.20)** (106 mg, 0.186 mmoles, 66%) as yellow oil that solidified on further vacuum drying.

^{1}H NMR (400 MHz, CHLOROFORM-*d*) δ ppm: 0.95 (3 H, d, Leu-CH_3, *J*= 6.11 Hz), 1.00 (3 H, d, Leu-CH_3, *J*= 6.11 Hz), 1.45 (9 H, s, C(CH_3)$_3$), 1.75-1.78 (1 H, m, Leu-CH(CH_3)$_2$), 1.68-1.92 (2 H, m, Leu-CH_2), 3.75 (3 H, s, OCH_3), 3.89 (3 H, s, OCH_3), 3.95 (3 H, s, OCH_3), 4.00 (3 H, s, OCH_3), 4.45 (1 H, m, Leu-CH-NH), 6.28 (1 H, s, C=CH), 6.81 (1 H, s, ArH), 7.05 (1 H, d, ArH, *J*=8.03 Hz), 7.18 (1 H, s, ArH), 7.43 (1 H, d, ArH, *J*=7.53 Hz), 8.51 (2 H, d, 2 ×NH-C=O, *J*=2.26 Hz);

^{13}C NMR (101 MHz, CHLOROFORM-*d*) δ ppm: 21.2 (Leu-CH_3), 22.2 (Leu-CH_3), 24.1 (CH(CH_3)$_2$), 28.2 (C(CH_3)$_3$), 39.7 (Leu-CH_2), 52.4 (Leu-CH-NH), 55.5 (OCH_3), 55.8 (OCH_3), 61.0 (OCH_3), 61.4 (OCH_3),79.5 (C(CH_3)$_3$), 102.6 (ArCH), 112.2 (C=CH), 113.4

(ArCH),113.9 (ArC), 122.7 (ArCH), 127.1 (ArCH), 127.5 (ArC), 137.9 (ArC), 141.1 (ArC), 142.8 (ArC), 144.7 (ArC), 149.4 (ArC), 152.2 (ArC), 154.9 (C=CH), 160.1 (Lactone-O-C=O), 171.4 (Ar-HN-C=O), 175.9 (HN-C=O);

V_{max} cm^{-1}: 3348, 2963, 2888, 1753, 1715, 1615, 1590, 1515, 1389;

HRMS: Calculated 570.2577, found 569.3926 ($M - H^+$).

Synthesis of (S)-2-amino-*N*-(2-methoxy-5-(6,7,8-trimethoxy-2-oxo-2H-chromen-4-yl)phenyl)-4-methylpentanamide (4.21)

Carbamate compound **(4.20)** (90 mg, 0.158 mmoles) was dissolved in dry DCM (3 mL) under atmosphere of nitrogen and cooled to -10 °C with salted ice. To this was added dry cooled trifluoroacetic acid (2 mL) and stirred for 90 minutes at 0 °C. Following this step the reaction mixture was diluted with DCM (30 mL) and solvent was evaporated at 35 °C using rotary evaporator under reduced pressure. The viscous oil obtained was redissolved in 10 mL DCM and stirred with 5% aq. sodium bicarbonate (2 mL) for 5 minutes before the aqueous layer was removed with the help of Pasteur pipette. The remaining organic layer was dried with $MgSO_4$ and solvent evaporated using rotary evaporator. The product left after evaporation was redissolved in small quantity DCM and gaseous HCl (from conc. HCl/H_2SO_4) was blown through it. Upon evaporating the DCM under reduced pressure, the solid left behind was washed with diethyl ether (3 × 5 mL) to afford the product **(4.21)** (57 mg, 0.112 mmoles, 71%) as white solid.

^{1}H NMR (600 MHz, DMSO-d_6) δ ppm: 0.97 (3 H, d, Leu-CH_3, J= 5.9 Hz), 0.99 (3 H, d, Leu-CH_3, J= 5.9 Hz), 1.73-1.87 (1 H, dm, Leu-CH_2), 1.78-1.80 (1 H, m, Leu-C$\underline{H}(CH_3)_2$), 3.71 (3 H, s, OCH_3), 3.85 (1 H, m, Leu-C$\underline{H}$-NH_2), 3.90 (3 H, s, OCH_3), 3.93 (3 H, s, OCH_3), 3.94 (3 H, s, OCH_3), 4.40 (2 H, br.s, NH_2) 6.20 (1 H, s, C=CH), 6.88 (1 H, s, ArH), 7.02 (1 H, d, ArH, J=8.28 Hz), 7.12 (1 H, dd, ArH, J=8.47, 2.07 Hz), 7.59 (1 H, s, ArH), 8.51 (1 H, d, N$\underline{H}$-C=O, J=2.26 Hz);

^{13}C NMR (151 MHz, DMSO-d_6) δ ppm: 21.2 (Leu-CH_3), 21.5 (Leu-CH_3), 23.9 ($\underline{C}H(CH_3)_2$), 39.8 (Leu-CH_2), 51.3 (Leu-$\underline{C}$H-NH), 55.9 (OCH_3), 56.0 (OCH_3), 61.2 (OCH_3), 61.6 (OCH_3), 103.5 (ArCH), 110.5 (ArCH), 112.8 (C=$\underline{C}$H), 114.2 (ArC), 119.5 (ArCH), 123.7 (ArCH), 127.4 (ArC), 127.6 (ArC), 140.9 (ArC), 142.9 (ArC), 145.5 (ArC), 149.4 (ArC), 149.7 (ArC), 155.4 ($\underline{C}$=CH), 160.5 (Lactone-O-$\underline{C}$=O), 174.4 (Ar-HN-C=O);

V_{max} cm^{-1}: 3382, 2947, 2874, 1771, 1706, 1514, 1289, 733;

HRMS: Calculated 470.2053, found 471.2133 ($M + H^+$).

Synthesis of (2S,3R)-3-((*tert*-butoxycarbonyl)amino)-2-hydroxy-4-phenylbutanoic acid (4.23)

(2S, 3R)-3-Amino-2-hydroxy-4-phenylbutyric acid **(4.22)** (250 mg, 1.281 mmoles) was dissolved in water:MeOH (3:1). To this was added potassium carbonate (195 mg, 1.409 mmoles) by dissolving in water (2 mL), followed by the addition of di-*tert*-butyl dicarbonate (280 mg, 1.281) in THF (2 mL). The reaction was allowed to stir a room temperature one hour before the organic solvents were removed *in vacuo*, and the remaining aqueous layer was acidified with aqueous HCl (30 mL, 1 M). After extracting the aqueous layer with diethyl ether (3 × 30 mL), the organic layer was dried with $MgSO_4$ and solvent evaporated using rotary evaporator to afford the carbamate **(4.23)** (265 mg, 0.897 mmoles, 70%) as white solid.

^{1}H NMR (400 MHz, DMSO-d_6) δ ppm: 1.31 (9 H, s, $C(CH_3)_3$), 2.68 (1 H, dd, CH_2, J= 13.20, 7.82 Hz), 2.81 (1 H, dd, CH_2, J= 13.45, 7.09 Hz), 3.85 (1 H, d, C<u>H</u>OH, J = 2.45 Hz), 3.96-4.03 (1 H, m, C<u>H</u>NH), 6.39 (1 H, d, NH, J= 9.54 Hz), 7.17-7.22 (3 H, m, ArCH), 7.27-7.30 (2 H, m, ArCH);

V_{max} cm^{-1}: 3397, 2974, 1698, 1507, 1166, 1088, 699;

HRMS: Calculated 295.1420, found 318.1328 ($M + Na^+$).

Synthesis of pentafluorophenyl (2S,3R)-3-((*tert*-butoxycarbonyl)amino)-2-hydroxy-4-phenylbutanoate (4.24)

Carboxylate compound **(4.23)** (206 mg, 0.698 mmoles) was dissolved in dry DCM (10 mL) with the aid of few drops of DMF under the atmosphere of nitrogen at 0 °C. To this was added pentafluorophenol (141 mg, 0.768 mmoles) by dissolving in dry DCM (1 mL) followed by the addition of EDC.HCl (161 mg, 0.838 mmoles). The reaction was stirred and gradually allowed to reach room temperature over the reaction duration of 3 hours. Afterwards, the reaction was diluted with diethyl ether (100 mL), washed with water (2 × 50 mL) and quickly dried with Na_2SO_4. Upon evaporating the organic layer, the pentafluorophenyl ester **(4.24)** (232 mg, 0.503 mmoles, 72%) was afforded as clear oil that solidified on further vacuum drying.

Synthesis of *tert*-butyl ((2S,3R)-3-hydroxy-4-(((S)-1-((2-methoxy-5-(6,7,8-trimethoxy-2-oxo-2H-chromen-4-yl)phenyl)amino)-4-methyl-1-oxopentan-2-yl)amino)-4-oxo-1-phenylbutan-2-yl)carbamate (4.25)

Amine **(4.21)** (110 mg, 0.234 mmoles) was dissolved in dry DCM (8 mL) at 0 °C under the atmosphere of nitrogen. To this was added pentafluorophenyl ester **(4.24)** (130 mg, 0.282 mmoles) in dry DCM (2 mL), followed by the addition of diisopropylethylamine (91 mg, 0.702 mmoles, 123 µL). After one hour, the reaction was concentrated using rotary evaporator at 35 °C and the remainder was directly purified by flash column chromatography (ethyl acetate:hexane, 1:1) to afford the Boc-bestatin compound **(4.25)** (105 mg, 0.140 mmoles, 60%) as clear oil that solidified on further vacuum drying.

^{1}H NMR (600 MHz, CHLOROFORM-*d*) δ ppm: 0.95 (3 H, d, Leu-CH_3, *J*= 5.87 Hz), 0.99 (3 H, d, Leu-CH_3, *J*= 5.87 Hz), 1.40 (9 H, s, $C(CH_3)_3$), 1.63-1.85 (2 H, dm, Leu-CH_2), 1.68-1.73 (1 H, m, Leu-C<u>H</u>$(CH_3)_2$), 3.04-3.30 (2 H, m, $ArCH_2$) 3.80 (3 H, s, OCH_3), 3.96 (3 H, s, OCH_3), 4.03 (3 H, s, OCH_3), 4.07 (3 H, s, OCH_3), 4.22 (1 H, m, C<u>H</u>OH), 4.59-4.66 (1 H, m, Leu-C<u>H</u>-NH), 5.01 (1 H, d, NH, *J*=7.34 Hz), 6.30 (1 H, s, C=CH), 6.90 (1 H, s, ArH), 7.02 (1 H, d, ArH, *J*=8.07 Hz), 7.19 (2 H, d, 2 × ArH, *J*=8.80 Hz), 7.25 (2 H, m, 2 × ArH, *J*=8.10 Hz), 7.32 (2 H, t, 2 × ArH, *J*=7.44 Hz), 7.39 (1 H, br.s, NH), 8.51 (3 H, s, 2 × NH, 1 × ArH);

^{13}C NMR (151 MHz, CHLOROFORM-*d*) δ ppm: 21.5 (Leu-CH_3), 22.9 (Leu-CH_3), 24.6 (<u>C</u>H$(CH_3)_2$), 28.0 (C(<u>C</u>$H_3)_3$), 38.9 ($ArCH_2$), 40.1 (Leu-CH_2), 52.2 (Leu-<u>C</u>H-NH), 55.8 (<u>C</u>H-NH-Boc) 55.9 (OCH_3), 56.1 (OCH_3), 61.3 (OCH_3), 61.7 (OCH_3), 74.7 (CHOH), 80.8 (<u>C</u>$(CH_3)_3$) 103.2 (ArCH), 110.4 (ArCH), 113.3 (C=<u>C</u>H), 114.2 (ArC), 120.4 (ArCH), 124.1 (ArCH), 126.6 (ArCH), 127.2 (ArC), 127.9 (ArC), 128.5 (2 × ArCH), 129.1 (2 × ArCH), 137.8 (ArC), 141.2 (ArC), 143.2 (ArC), 145.6 (ArC), 149.2 (ArC), 149.5 (ArC), 155.0 (<u>C</u>=CH), 160.6 (Lactone-O-<u>C</u>=O), 169.6 (2 × HN-C=O);

V_{max} cm^{-1}: 3301, 2858, 2871, 1706, 1657, 1538, 1390, 1170, 740;

HRMS: Calculated 747.3367, found 746.3337 (M - H^+).

Synthesis of (S)-2-((2S,3R)-3-amino-2-hydroxy-4-phenylbutanamido)-*N*-(2-methoxy-5-(6,7,8-trimethoxy-2-oxo-2H-chromen-4-yl)phenyl)-4-methylpentanamide (4.26)

Carbamate compound **(4.25)** (80 mg, 0.107 mmoles) was dissolved in dry DCM (3 mL) under atmosphere of nitrogen and cooled to -10 °C with salted ice. To this was added dry cooled trifluoroacetic acid (1 mL) and stirred for 90 minutes at 0 °C. Following this step the reaction mixture was diluted with DCM (50 mL) and solvent was evaporated at 35 °C using rotary evaporator under reduced pressure. The product left behind was redissolved in DCM (10 mL) and stirred with 5% $NaHCO_3$ (2 mL) for 3 minutes. Afterwards the aqueous layer was carefully removed with the help of Pasteur pipette while the organic layer was dried with $MgSO_4$ and solvent evaporated *in vacuo.* The crude residue obtained was further purified by flash column chromatography (DCM:MeOH, 9:1) to afford the final compound **(4.26)** (38 mg, 0.059 mmoles, 55%) as off-white solid.

^{1}H NMR (400 MHz, CHLOROFORM-*d*) δ ppm: 0.96 (3 H, d, Leu-CH_3, *J*= 6.36 Hz), 0.99 (3 H, d, Leu-CH_3, *J*= 6.11 Hz), 1.66-1.85 (2 H, m, Leu-CH_2), 1.68-1.75 (1 H, m, C<u>H</u>-$(CH_3)_2$), 2.57 (1 H, dd, $ArCH_2$, *J*= 13.45, 9.78 Hz), 2.99 (1 H, m, $ArCH_2$), 3.64 (1 H, br.m, CH-NH_2), 3.77 (3 H, s, OCH_3), 3.94 (3 H, s, OCH_3), 4.01 (4 H, s, OCH_3, 1 × OCH_3, 1 × C<u>H</u>-OH), 4.05 (3 H, s, OCH_3), 4.64 (1 H, m, CH-NH), 6.28 (1 H, s, C=CH), 6.89 (1 H, , s, ArH), 7.01 (1 H, d, ArH, *J*= 8.56 Hz), 7.17 (1 H, dd, ArH, *J*= 8.56, 2.20 Hz), 7.22 (3 H, m, ArH), 7.29 (2 H, m, ArH), 7.81 (1 H, d, NH, *J*=8.07 Hz), 8.51 (1 H, d, ArH, *J*= 2.20 Hz), 8.53 (1 H, s, NH);

^{13}C NMR (101 MHz, CHLOROFORM-*d*) δ ppm: 22.0 (Leu-CH_3), 22.9 (Leu-CH_3), 25.0 (<u>C</u>H$(CH_3)_2$), 38.8 ($ArCH_2$), 40.4 (Leu-CH_2), 52.6 (CH-NH), 54.1 (CH-NH_2), 56.1 (OCH_3), 56.2 (OCH_3), 61.5 (OCH_3), 61.9 (OCH_3), 72.6 (CHOH), 103.4 (ArCH), 110.5 (ArCH), 113.4 (C=<u>C</u>H), 114.4 (ArC), 120.5 (ArCH), 124.3 (ArCH), 126.8 (ArCH), 127.3 (ArC), 128.0 (ArC), 128.8 (2 × ArCH), 129.2 (2 × ArCH), 138.1 (ArC), 141.3 (ArC), 143.3 (ArC), 145.8 (ArC), 149.4 (ArC), 149.7 (ArC), 155.2 (<u>C</u>=CH), 160.8 (Lactone-O-<u>C</u>=O), 170.0 (Ar-HN-C=O), 173.8 (HN-C=O);

V_{max} cm^{-1}: 3299, 2954, 2923, 2853, 2477, 1723, 1654, 1451, 1386, 1093, 1050, 700;

HRMS: Calculated 647.2843, found 648.2888 ($M + H^+$).

Synthesis of (E)-2-(((4-(3-((*tert*-butoxycarbonyl)amino)-4-methoxyphenyl)-6,7,8-trimethoxy-2H-chromen-2-ylidene)amino)oxy)acetic acid (4.27)

N-Boc protected aniline **(2.17)** (110 mg, 0.233 mmoles) was dissolved in ethanol:water (4:1, 15 mL) with the aid of small amount of heat. To this was added o-carboxymethyl hydroxylamine hemihydrochloride (33 mg, 0.303 mmoles) and sodium acetate (38 mg, 0.466 mmoles). The reaction was refluxed for 7 hours at a gentle heat. Afterwards, the reaction was cooled to room temperature, quenched with aq.HCl (2 M, 20 mL) and extracted with DCM (3×50 mL). Upon evaporating the organic solvent, the crude product obtained was further purified by flash column chromatography using ethyl acetate:hexane:formic acid (1:1:0.02) to afford the carboxylic acid **(4.27)** (90 mg, 0.17 mmoles,73%) as yellow oil that solidified on further vacuum drying.

^{1}H NMR (400 MHz, CHLOROFORM-*d*) δ ppm: 1.51 (9 H, s, $(CH_3)_3$), 3.77 (3 H, s, OCH_3), 3.94 (3 H, s, OCH_3) , 3.96 (3 H, s, OCH_3), 4.09 (3 H, s, OCH_3), 4.68 (2 H, s, CH_2), 6.22 (1 H, s, C=CH), 6.78 (1 H, s, ArH), 6.94 (1 H, d, ArH, J= 8 Hz), 7.04 (1 H, d, ArH, J= 8 Hz), 7.16 (1 H, s, NH), 8.23 (1 H, s, ArH), 9.78 (1 H, br.s, COOH);

^{13}C NMR (101 MHz, CHLOROFORM-*d*) δ ppm: 28.3 (C($\underline{C}H_3)_3$), 55.9 (OCH_3), 56.2 (OCH_3), 61.4 (OCH_3), 61.7 (OCH_3), 70.7 (CH_2), 80.7 ($\underline{C}(CH_3)_3$), 103.7 (ArCH), 110.2 (ArCH), 112.8 (C=$\underline{C}$H), 115.4 (ArC), 118.5 (ArCH), 122.4 (ArCH), 128.1 (ArC), 128.6 ($\underline{C}$=CH), 141.0 (ArC), 141.5 (ArC), 143.2 (ArC), 143.8 (ArC), 148.1 (ArC), 149.0 (ArC), 152.0 ($\underline{C}$=N), 152.7 (Boc-$\underline{C}$=O), 174.3 ($\underline{C}$OOH);

V_{max} cm^{-1}: 3433, 3057, 2978, 2939, 1724, 1635, 1589, 1531, 1387, 1267, 1130, 1102, 736;

HRMS: Calculated 530.1900, found 553.1769 ($M + Na^+$).

In situ synthesis of pentafluorophenyl (E)-2-(((4-(3-((*tert*-butoxycarbonyl)amino)-4-methoxyphenyl)-6,7,8-trimethoxy-2H-chromen-2-ylidene)amino)oxy)acetate (4.28)

Carboxylic acid **(4.27)** (105 mg, 0.198 mmoles) was dissolved in dry DCM (8 mL) under the atmosphere of nitrogen and cooled to 0 °C. To this was added Pentaflourophenol (40 mg, 0.218 mmoles) in dry DCM and *N*-(3-dimethylaminopropyl)-*N′*-ethylcarbodiimide hydrochloride (EDC) (42 mg, 0.219 mmoles) in dry DCM (2 mL). The reaction was kept

stirring for 2 hours at 0 °C and then allowed to stir at room temperature for 1 hour. After completion the reaction was quenched with water (40 mL), extracted with Diethyl ether (3×50 mL) and dried quickly with $MgSO_4$. Solvent was evaporated using rotary and the resultant crude product was further purified using ethyl acetate:hexane (1:4) to afford the pentafluorophenyl ester **(4.28)** (100 mg, 0.144 mmoles, 72%) as light yellow oil.

Synthesis of *tert*-butyl (E)-(5-(2-((2-(hydroxyamino)-2-oxoethoxy)imino)-6,7,8-trimethoxy-2H-chromen-4-yl)-2-methoxyphenyl)carbamate (4.29)

Pentafluorophenyl ester **(4.28)** (140 mg, 0.201 mmoles) was stirred in dry DMF (2 mL) under the atmosphere of nitrogen at room temperature. To this was added hydroxylamine hydrochloride (18 mg, 0.261 mmoles) and diisopropylethylamine (45 µL, 0.261 mmoles). The reaction was kept stirring for 10 minutes before being quenched with water (30 mL) and extracted with diethyl ether (3×50 mL). After evaporating the solvent, the product was further purified by column chromatography using just ethyl acetate to afford the product **(4.29)** (90 mg, 0.165 mmoles, 82%) as yellow solid.

^{1}H NMR (400 MHz, CHLOROFORM-*d*) δ ppm: 1.51 (9 H, s, $(CH_3)_3$), 3.77 (3 H, s, OCH_3), 3.95 (3 H, s, OCH_3) , 3.97 (3 H, s, OCH_3), 4.06 (3 H, s, OCH_3), 4.67 (2 H, s, CH_2), 6.19 (1 H, s, C=CH), 6.79 (1 H, s, ArH), 6.94 (1 H, d, ArH, J= 8.80 Hz), 7.04 (1 H, dd, ArH, J= 8.3 Hz, 1.5 Hz), 7.15 (1 H, s, NH), 8.23 (1 H, s, ArH);

^{13}C NMR (101 MHz, CHLOROFORM-*d*) δ ppm: 28.3 (C($\underline{C}H_3)_3$), 55.8 (OCH_3), 56.2 (OCH_3), 61.5 (OCH_3), 61.7 (OCH_3), 80.7 (CH_2), 103.8 (ArCH), 110.2 (ArCH), 112.5 (C=$\underline{C}$H), 115.4 (ArC), 118.5 (ArCH), 122.4 (ArCH), 128.1 (ArC), 128.5 (ArC), 140.9 (ArC), 141.4 (ArC), 143.4 ($\underline{C}$=CH), 144.0 (ArC), 148.1 (ArC), 149.2 (ArC), 152.5 (C=N), 152.6 (Boc-$\underline{C}$=O);

V_{max} cm^{-1}: 3434, 3208, 3058, 2978, 2938, 1723, 1673, 1563, 1588, 1531, 1494, 1387, 1267, 1248, 1158, 736;

HRMS: Calculated 545.2009, found 568.1880 (M + Na^+).

Synthesis of (E)-2-(((4-(3-amino-4-methoxyphenyl)-6,7,8-trimethoxy-2H-chromen-2-ylidene)amino)oxy)-*N*-hydroxyacetamide (4.30)

N-Boc hydroxamic acid **(4.29)** (80 mg, 0.147 mmoles) was stirred in cooled anhydrous DCM: trifluoroacetic acid (1:1, 2 mL) under the atmosphere of nitrogen at 0 °C for 90

mins. After 90 mins the reaction mixture was concentrated and the remainder was redissolved in DCM (10 mL) and stirred with saturated aqueous sodium bicarbonate (3 mL) for 5 minutes. After 5 minutes the aqueous layer was removed with the help of pipette while the organic layer was evaporated and the residue obtained was purified by column chromatography using DCM and methanol (1:0.1) to afford the hydroxamic acid **(4.30)** (47 mg, 0.106 mmoles, 72%) as light yellow solid.

^{1}H NMR (400 MHz, DMSO-d_6) δ ppm : 3.68 (3 H, s, OCH_3), 3.83(6 H, s, 2×OCH_3), 3.97 (3 H, s, OCH_3), 4.38 (2 H, s, CH_2), 4.93 (2 H, s, NH_2), 6.07 (1 H, s, C=CH), 6.67 (1 H, dd, ArH, *J*=8.16, 2.13 Hz,), 6.72 (1 H, s, ArH), 6.77 (1 H, d, ArH, *J*=2.26 Hz,), 6.91 (1 H, d, ArH, *J*= 8.28 Hz), 8.89 (1 H, br.s, OH), 10.56 (1 H, br.s, NH);

^{13}C NMR (101 MHz, DMSO-d_6) δ ppm : 55.3 (OCH_3), 56.0 (OCH_3), 60.9 (OCH_3), 61.2 (OCH_3), 71.5 (CH_2), 103.7 (ArCH), 110.5 (ArCH), 112.2 (C=<u>C</u>H), 113.3 (ArCH), 115.2 (ArC), 116.1 (ArCH), 128.0 (ArC), 137.9 (ArC), 140.5 (ArC), 141.0 (ArC), 142.3 (<u>C</u>=CH), 143.4 (ArC), 146.9 (ArC), 148.5 (ArC), 149.9 (C=N), 165.4 (-CH_2-<u>C</u>=O);

V_{max} cm^{-1}: 3359, 3203, 2938, 2841, 1684, 1634, 1585, 1515, 1385, 1241, 1129, 1099, 734;

HRMS: Calculated 445.1485, found 446.1543.

Synthesis of (E)-2-(((4-(3-hydroxy-4-methoxyphenyl)-6,7,8-trimethoxy-2H-chromen-2-ylidene)amino)oxy)acetic acid (4.31)

Phenol **(2.24)** (370 mg, 0.989 mmoles) was dissolved in ethanol:water mixture (4:1, 20 mL) with the aid of small amount of heat. To this was added sodium acetate (162.3 mg, 1.978 mmoles) and *O*-carboxymethyl hydroxylamine hemihydrochloride (140 mg, 1.285 mmoles). The reaction was refluxed for 7 hours at a gentle heat. After 7 hours the reaction was cooled to room temperature and quenched with aq.HCl solution (2 M, 50 mL) and extracted with DCM (3×50 mL). After drying with $MgSO_4$, the solvent was evaporated and the product was further purified using ethyl acetate:hexane:formic acid (1:1:0.04) to afford the carboxylic acid **(4.31)** (290 mg, 0.673 mmoles, 68%) as light yellow solid.

^{1}H NMR (400 MHz, DMSO-d_6) δ ppm : 3.68 (3 H, s, OCH_3), 3.83 (6 H, s, 2×OCH_3), 3.97 (3 H, s, OCH_3), 4.55 (2 H, s, CH_2), 6.15 (1 H, s, C=CH), 6.66 (1 H, s, ArH), 6.90 (1 H, s, ArH), 6.91 (1 H, dd, ArH, J= 1.87 Hz, 8.01 Hz), 7.05 (1 H, d, ArH, J= 8.78 Hz), 9.34 (1 H, br.s, OH);

^{13}C NMR (101 MHz, DMSO-d_6) δ ppm: 56. (OCH_3), 56.4 (OCH_3), 61.4 (OCH_3), 61.6 (OCH_3), 71.1 (CH2), 104.0 (ArCH), 112.7 (ArCH), 113.1 (C=CH), 115.5 (ArC), 115.9 (ArCH), 119.9 (ArCH), 128.4 (ArC), 140.9 (ArC), 141.5 (C=CH), 142.1 (ArC), 143.9 (ArC), 147.0 (ArC), 148.8 (ArC), 149.1 (ArC), 150.0 (C=N), 171.6 (C=O);

V_{max} cm^{-1}: 3349, 2934, 2881, 1724, 1649, 1523, 1323, 1148;

HRMS: Calculated 431.1216, found 454.1117 ($M + Na^+$).

Synthesis of pentafluorophenyl (E)-2-(((4-(3-hydroxy-4-methoxyphenyl)-6,7,8-trimethoxy-2H-chromen-2-ylidene)amino)oxy)acetate (4.32)

Carboxylic acid **(4.31)** (200 mg, 0.464 mmoles) was dissolved in anhydrous DCM (10 mL) with the aid of small quantity of DMF (1 mL) under an atmosphere of nitrogen and cooled to 0 °C. To this was sequentially added pentaflourophenol (94 mg, 0.51 mmoles) in dry DCM and *N*-(3-dimethylaminopropyl)-*N′*-ethylcarbodiimide hydrochloride (EDC) (98 mg, 0.510 mmoles). The reaction was allowed to stir for 3 hours, after which quenched with water (30 mL) and extracted with diethyl ether (3×50 mL). The organic layer was dried with $MgSO_4$ and concentrated using rotary evaporation. The resultant crude product was further purified by column chromatography using ethyl acetate:hexane (1:2) to afford the pentafluorophenyl ester **(4.32)** (210 mg, 0.352 mmoles, 76%) as light yellow oil that solidified on further vacuum drying.

^{1}H NMR (400 MHz, CHLOROFORM-*d*) δ ppm : 3.75 (3 H, s, OCH_3), 3.98 (3 H, s, OCH_3), 3.99 (3 H, s, OCH_3), 4.12 (3 H, s, OCH_3), 5.01 (CH_2), 6.20 (1 H, s, C=CH), 6.64 (1 H, s, ArH), 6.93 (1 H, dd, ArH, J= 2.01 Hz, 8 Hz), 6.97 (1 H, d, ArH, J= 8 Hz), 7.02 (1 H, d, ArH, J= 2.01 Hz);

^{13}C NMR (101 MHz, CHLOROFORM-*d*) δ ppm : 56.0 (OCH_3), 56.4 (OCH_3), 61.5 (OCH_3), 61.7 (OCH_3), 70.3 (CH_2), 103.6 (ArCH), 110.7 (ArCH), 113.0 (C=CH), 114.6 (ArC), 115.5 (ArCH), 120.4 (ArCH), 129.3 (ArC), 141.1 (ArC), 141.6 (C=CH), 143.1 (ArC), 144.1 (ArC), 145.7 (ArC), 147.1 (ArC), 149.0 (ArC), 151.8 (C=N), 166.1 (C=O);

V_{max} cm^{-1}: 3449, 2941, 2845, 1811, 1567, 1586, 1456, 1387, 1196, 1132, 1054, 738;

HRMS: Calculated 597.1058, found 598.1159 ($M + H^+$).

Synthesis of (E)-*N*-hydroxy-2-(((4-(3-hydroxy-4-methoxyphenyl)-6,7,8-trimethoxy-2H-chromen-2-ylidene)amino)oxy)acetamide (4.33)

To a stirred solution of pentafluorophenyl ester **(4.32)** (180 mg, 0.302 mmoles) in dry DMF (3 mL) under an atmosphere of nitrogen and room temperature was added hydroxylamine hydrochloride (25 mg, 0.362 mmoles) and neat diisopropylethylamine (47 mg, 63 µL, 0.362 mmoles). The reaction was stirred for 10 minutes before being quenched with water (30 mL) and extracted with diethyl ether (5×50 mL) containing small volume of DCM. The aqueous layer was carefully removed and the organic layer containing some of precipitated solid product was evaporated without drying with $MgSO_4$. Finally the solid was washed several times with diethyl ether and dried under high vacuum to afford the hydroxamic acid **(4.33)** (98 mg, 0.220 mmoles, 73%) as off white solid.

^{1}H NMR (400 MHz, DMSO-d_6) δ ppm: 3.67 (3 H, s, OCH_3), 3.83 (6 H, s, 2 × OCH_3), 3.97 (3 H, s, OCH_3), 4.38 (2 H, s, CH_2), 6.11 (1 H, s, C=CH), 6.66 (1 H, s, ArH), 6.89 (1 H, s, ArH), 6.90 (1 H, br.d, ArH, J= 8.3 Hz), 7.05 (1 H, d, ArH, J= 7.8 Hz), 8.92 (1 H, s, O<u>H</u>-NH), 9.34 (1 H, s, Ar-O<u>H</u>), 10.58 (1 H, s, NH);

^{13}C NMR (151 MHz, DMSO-d_6) δ ppm: 55.6 (OCH_3), 56.0 (OCH_3), 60.9 (OCH_3), 61.2 (OCH_3), 71.5 (CH_2), 103.5 (ArCH), 112.3 (ArCH), 112.6 (C=<u>C</u>H), 115.0 (ArC), 115.4 (ArCH), 119.3 (ArCH), 128.0 (ArC), 140.5 (ArC), 141.1 (ArC), 141.7 (<u>C</u>=CH), 143.4 (ArC), 146.6 (ArC), 148.3 (ArC), 148.5 (ArC), 149.8 (<u>C</u>=N), 165.3 (C=O);

V_{max} cm^{-1}: 3420, 2941, 1727, 1655, 1510, 1497, 1465, 1444, 1384, 1301 1258, 1130, 1114, 1021, 931;

HRMS: Calculated 446.1325, found 447.1427 (M + H).

Synthesis of *tert*-butyl (S)-(1-((2-methoxy-5-(6,7,8-trimethoxy-2-thioxo-2H-chromen-4-yl)phenyl)amino)-1-oxopropan-2-yl)carbamate (4.34)

Aniline compound **(2.18)** (170 mg, 0.466 mmoles) was stirred in dry DCM (15 mL) at 0 °C under the atmosphere of nitrogen. To this was sequentially added Boc-alanine (344 mg, 1.82 mmoles), PyBrop (425 mg, 0.912 mmole) and diisopropylethylamine (0.3 mL, 1.82 mmoles) at 0 °C. Reaction was gradually allowed to reach to room temperature and stirred for 5 hours. After 5 hours the reaction was quenched with 2 M HCl (20 mL) and extracted with DCM (3×50 mL). After evaporating the solvent, the product was purified by column

chromatography using ethyl acetate:hexane (1:1), to afford the product **(4.34)** (170 mg, 0.312 mmoles, 69%) as yellow solid.

^{1}H NMR (400 MHz, CHLOROFORM-*d*) δ ppm: 1.48 (3 H, d, *J*=7.03 Hz, CH-C$\underline{H}_3$), 1.51 (9 H, s, C(C$\underline{H}_3$)$_3$), 3.82 (3H, s, OCH_3), 4.00 (3H, s, OCH_3), 4.04 (3H, s, OCH_3), 4.08 (3H, s, OCH_3), 7.01 (1 H, s, C=CH), 7.04 (1 H, d, ArH, *J*= 8.28 Hz), 7.21 (1 H , s, ArH,) 7.23 (1 H, dd, ArH, *J*=8.53 Hz, 1.8 Hz), 8.58 (1 H, d, ArH, *J*= 2.01 Hz), 8.61 (1 H, br.s, NH);

^{13}C NMR (101 MHz, CHLOROFORM-*d*) δ ppm: 17.9 (Ala-CH-$\underline{C}H_3$), 28.3 (C($\underline{C}H_3$)$_3$), 56.0 (OCH_3), 56.2 (OCH_3), 61.5 (OCH_3), 62.1 (OCH_3), 102.6 (ArCH), 110.6 (C=$\underline{C}$H), 116.0 (ArC), 120.6 (ArCH), 124.4 (ArCH), 127.3 (ArC), 127.4 (ArCH), 140.9 (ArC), 146.0 (ArC),146.5 (ArC), 146.8 (ArC). 149.6 (ArC), 150.7 (ArC), 155.7 ($\underline{C}$=CH), 171.1 ($\underline{C}$=O), 195.8 (C=S);

V_{max} cm^{-1}: 3409, 2939, 2968, 1690, 1607, 1519, 1327, 1120;

HRMS: Calculated 544.1879, found 545.2017 ($M + H^+$).

Synthesis of (S,E)-2-(((4-(3-(2-((*tert*-butoxycarbonyl)amino)propanamido)-4-methoxyphenyl)-6,7,8-trimethoxy-2H-chromen-2-ylidene)amino)oxy)acetic acid (4.35)

Thione **(4.34)** (150 mg, 0.28 mmoles) was dissolved in EtOH:water (4:1, 20 mL) with aid of small amount of heat. To this was added sodium acetate (46 mg, 0.56 mmoles) and o-carboxymethyl hydroxylamine hemihydrochloride (40 mg, 0.366 mmoles). The reaction was refluxed for 7 hours at a gentle heat. After 7 hours the reaction was quenched with 2 M HCl (20 mL) and extracted with DCM (3×50 mL). Finally the product was purified by column chromatography using ethyl acetate:hexane:formic acid (1:1:0.04) to afford the carboxylic acid **(4.35)** (110 mg, 0.183 mmoles, 66%) as light yellow solid.

^{1}H NMR (400 MHz, CHLOROFORM-*d*) δ ppm: 1.46 (3 H, d, *J*=7.03 Hz, CH-C$\underline{H}_3$), 1.49 (9 H, s, C(C$\underline{H}_3$)$_3$), 3.77 (3 H, s, OCH_3), 3.96 (3 H, s, OCH_3), 3.97 (3 H, s, OCH_3), 4.09 (3 H, s, OCH_3), 4.69 (2 H, s, CH_2), 6.23 (1 H, s, C=CH), 6.78 (1 H, s, ArH), 6.98 (1 H, d, ArH, *J*= 8.03 Hz), 7.13 (1 H, d, ArH, *J*= 8.03 Hz), 8.47 (1 H, s, ArH), 8.58 (1 H, br.s, NH);

^{13}C NMR (101 MHz, CHLOROFORM-*d*) δ ppm: 18.1 (Ala-CH-$\underline{C}H_3$), 28.3 (C($\underline{C}H_3$)$_3$), 55.9 (OCH_3), 56.2 (OCH_3), 61.4 (OCH_3), 61.7 (OCH_3), 71.0 (CH2), 103.5 (ArCH), 110.3 (ArCH), 113.0 (C=$\underline{C}$H), 115.3 ($\underline{C}$=CH), 120.4 (ArCH), 124.0 (ArCH), 128.5 (ArC), 140.9

(ArC), 141.4 (ArC), 142.6 (ArC), 142.7 (ArC), 143.8 (ArC), 148.8 (ArC), 149.0 (ArC), 151.6 (C=N), 155.8 (NH-C=O), 170.0 (CH_2-C=O);

V_{max} cm^{-1}: 3320, 2979, 2940, 1699, 1588, 1532, 1495, 1456, 1386, 1264, 1135, 1101, 905, 863, 735

HRMS: Calculated 601.2272, found 624.222 ($M + Na^+$)

Synthesis of pentafluorophenyl (S,E)-2-(((4-(3-(2-((*tert*-butoxycarbonyl)amino)propanamido)-4-methoxyphenyl)-6,7,8-trimethoxy-2H-chromen-2-ylidene)amino)oxy)acetate (4.36)

Carboxylic acid **(4.35)** (90 mg, 0.150 mmoles) was dissolved in dry DCM (8 mL) under the atmosphere of nitrogen and cooled to 0 °C. To this was added pentaflourophenol (30.32 mg, 0.165 mmoles) in dry DCM and *N*-(3-dimethylaminopropyl)-*N′*-ethylcarbodiimide hydrochloride (EDC) (31.6 mg, 0.165 mmoles) in dry DCM:DMF (2:1, 2 mL). The reaction was kept stirring for 2 hours at 0 °C and then allowed to stir at room temperature for 1 hour. After completion the reaction was quenched with water (40 mL), extracted with diethyl ether (3×50 mL) and dried with $MgSO_4$. Solvent was evaporated using rotary and the resultant crude product was further purified using ethyl acetate:hexane (1:2) to afford the pentafluorophenyl ester **(4.36)** (65 mg, 0.085 mmoles, 57%) as light yellow oil.

^{1}H NMR (400 MHz, CHLOROFORM-*d*) δ ppm: 1.47 (3 H , d, CH-CH_3, *J*=7.28 Hz), 1.50 (9 H, s, C(CH_3)$_3$), 3.76 (3 H, s, OCH_3), 3.96 (3 H, s, OCH_3), 3.97 (3 H, s, OCH_3), 4.10 (3 H, s, OCH_3), 5.00 (2 H, s, CH_2), 6.21 (1 H, s, C=CH), 6.75 (1 H, s, ArH), 6.99 (1 H, d, ArH, *J*= 8.53 Hz), 7.14 (1 H, d, ArH, *J*= 8.53 Hz), 8.48 (1 H, d, ArH, *J*= 1.76 Hz), 8.56 (1 H, br.s, NH);

^{13}C NMR (101 MHz, CHLOROFORM-*d*) δ ppm: 28.3 (C(CH_3)$_3$), 55.9 (OCH_3), 56.3 (OCH_3), 61.5 (OCH_3) , 61.7 (OCH_3), 70.3 (CH_2), 103.6 (ArCH), 110.3 (ArCH), 113.0 (C=CH), 115.4 (ArC), 120.3 (ArCH), 124.0 (ArCH), 128.7 (ArC), 141.0 (ArC), 141.5 (C=CH), 142.8 (ArC), 143,9 (ArC), 148.7 (ArC), 149.1 (ArC) , 151.9 (ArC) , 166.2 (NH-C=O);

^{19}F NMR (377 MHz, CHLOROFORM-*d*) δ ppm: -151.93 (d, 2 F), -157.71 (t, 1 F), -162.17 (m, 2 F);

$V_{max\ cm}^{-1}$: 3322, 2940, 1697, 1588, 1588, 1521, 1426, 1388, 1261, 1163, 1136, 1097, 996;

HRMS: Calculated 767.2113, found 768.223 ($M + H^+$).

Synthesis of *tert*-butyl (S,E)-(1-((5-(2-((2-(hydroxyamino)-2-oxoethoxy)imino)-6,7,8-trimethoxy-2H-chromen-4-yl)-2-methoxyphenyl)amino)-1-oxopropan-2-yl)carbamate (4.37)

Pentafluorophenyl ester **(4.36)** (48 mg, 0.063 mmoles) was stirred in dry DMF (2 mL) under the atmosphere of nitrogen at room temperature. To this was added hydroxylamine hydrochloride (4.8 mg, 0.069 mmoles) and diisopropylethylamine (12 µL, 0.069 mmoles). The reaction was kept stirring for 10 minutes before being quenched with water (30 mL) and extracted with diethyl ether (3×50 mL). After evaporating the solvent, the product was further purified by column chromatography using ethyl acetate:hexane:formic acid (1:1:0.02) to afford the product **(4.37)** (30 mg, 0.049 mmoles, 78%) as light yellow solid.

^{1}H NMR (400 MHz, CHLOROFORM-*d*) δ ppm: 1.47 (3 H, d, Ala-CH_3 J= 7.3 Hz), 1.50 (9 H, s, $C(CH_3)_3$), 2.91 (1 H, s, C<u>H</u>-NH), 2.99 (), 3.78 (3 H, s, OCH_3), 3.96 (3 H, s, OCH_3), 3.98 (3 H, s, OCH_3), 4.07 (3 H, s, OCH_3), 4.70 (2 H, s, CH_2), 6.22 (1 H, s, C=CH), 6.79 (1 H, s, ArH), 6.99 (1 H, d, ArH, J= 8.5 Hz), 7.13 (1 H, d, ArH, J= 8.03 Hz),8.46 (1 H, d, ArH, J= 1.53 Hz), 8.60 (1 H, br.s, NH);

^{13}C NMR (101 MHz, CHLOROFORM-*d*) δ ppm: 18.0 (Ala-CH-<u>C</u>H_3), 28.3 ($C(\underline{C}H_3)_3$), 55.9 (OCH_3), 56.3 (OCH_3) , 61.5 (OCH_3), 61.7 (OCH_3), 72.4 (CH_2), 103.7 (ArCH), 110.4 (ArCH), 112.3 (C=<u>C</u>H), 115.3 (ArC), 120.3 (ArCH), 124.0 (ArCH), 128.3 (ArC), 140.8 (ArC), 141.4 (<u>C</u>=CH), 144.2 (ArC), 148.4 (ArC), 148.9 (ArC), 149.4 (ArC), 153.8 (C=N), 167.4 (CH_2-<u>C</u>=O), 171.0 (NH-<u>C</u>=O);

$V_{max\ cm^{-1}}$: 3252, 2939, 2965, 1683, 1587, 1532, 1495, 1386, 1249, 1055, 1098, 734;

HRMS: Calculated 616.2381, found 639.2258 ($M + Na^+$).

Synthesis of (S,E)-2-amino-*N*-(5-(2-((2-(hydroxyamino)-2-oxoethoxy)imino)-6,7,8-trimethoxy-2H-chromen-4-yl)-2-methoxyphenyl)propanamide (4.38)

The carbamate compound **(4.37)** (100 mg, 0.162 mmoles) was dissolved in anhydrous DCM (2 mL) under the atmosphere of nitrogen at 0 °C. To this was added cooled trifluoroacetic acid (2 mL) and allowed to stir for 90 minutes. Afterwards, the solvent was

evaporated at 35 °C and the remainder was redissolved in DCM (10 mL) and stirred with aqueous sodium hydrogen carbonate (2 mL, 5%) for 5 minutes. After 5 minutes, the aqueous layer was carefully removed with Pasteur pipette and the organic layer was evaporated. The solid residue obtained was washed several times with diethyl ether to afford the product **(4.38)** (65 mg, 0.126 mmoles, 78%) as light yellow solid.

^{1}H NMR (400 MHz, DMSO-d_6) δ ppm: 1.379 (3 H, d, Ala-CH_3, J=6.85 Hz), 3.71(3 H, s, OCH_3), 3.83 (3 H, s, OCH_3), 3.94 (3 H, s, OCH_3), 3.97 (3 H, s, OCH_3), 4.38 (2 H, s, CH_2), 6.18 (1 H, s, C=CH), 6.76 (1 H, s, ArH), 7.23 (1 H, d, ArH, J= 8 Hz), 7.30 (1 H, dd, ArH, J= 8.8 Hz, 2 Hz), 8.14 (1 H, s, ArH),8.90 (1 H, s, NH-OH)10.05 (1 H, s, NH) 10.57 (1 H, s, OH);

^{13}C NMR (101 MHz, DMSO-d_6) δ ppm: 20.4 (Ala-CH_3), 50.5 (CH-NH_2) 55.8 (OCH_3), 56.0 (OCH_3), 60.9 (OCH_3), 61.3 (OCH_3), 71.5 (CH_2), 103.3 (ArCH), 111.4 (ArCH), 112.9 (C=CH), 114.8 (ArC), 119.6 (ArCH), 123.9 (ArCH), 126.9 (ArC), 127.4 (ArC), 140.5 (ArC), 141.1 (ArC), 141.3 (C=CH), 143.4 (ArC), 148.6 (ArC), 149.2 (ArC), 149.8 (C=N), ,165.3 (CH_2-C=O), 173.6 (NH-C=O);

V_{max}: 2935, 1672, 1586, 1532, 1494, 1385, 1200, 1128, 1097, 773;

HRMS: Calculated 516.1856, found 517.1942 ($M + H^+$).

Synthesis of pentafluorophenyl 2-((4-(3-((*tert*-butoxycarbonyl)amino)-4-methoxyphenyl)-6,8-dimethoxy-2-oxo-2H-chromen-7-yl)oxy)acetate (4.39)

Carboxylic acid **(2.70)** (55 mg, 0.110 mmoles) was dissolved in dry DCM (5 mL) under the atmosphere of nitrogen and cooled to 0 °C. To this was added pentaflourophenol (22 mg, 0.121 mmoles) in dry DCM (1 mL) followed by the addition of *N*-(3-dimethylaminopropyl)-*N′*-ethylcarbodiimide hydrochloride (EDC) (27 mg, 0.143 mmoles). The reaction was kept stirring for 2 hours at 0 °C and then allowed to stir at room temperature for 1 hour. After completion the reaction mixture was directly poured onto column loaded with silica and purified by flash column chromatography using ethyl acetate:hexane (1:3) to afford the pentafluorophenyl ester **(4.39)** (55 mg, 0.082 mmoles, 75%) as off-white solid .

Synthesis of *tert*-butyl (5-(7-(2-(hydroxyamino)-2-oxoethoxy)-6,8-dimethoxy-2-oxo-2H-chromen-4-yl)-2-methoxyphenyl)carbamate (4.40)

Pentafluorophenyl ester **(4.39)** (55 mg, 0.082 mmoles) was stirred in dry DMF (2 mL) under the atmosphere of nitrogen at room temperature. To this was added hydroxylamine hydrochloride (7 mg, 0.102 mmoles) and diisopropylethylamine (17 µL, 0.098 mmoles). The reaction was kept stirring for 10 minutes before being quenched with water (10 mL) and extracted with diethyl ether (3×20 mL). After evaporating the organic solvent, the product was further purified by column chromatography using ethyl acetate:hexane:formic acid (4:1:0.05) to afford the product **(4.40)** (36 mg, 0.070 mmoles, 85%) as white solid.

^{1}H NMR (400 MHz, CHLOROFORM-*d*) δ ppm: 1.52 (9 H, s, C(C<u>H</u>$_3$)$_3$), 3.87 (3 H, s, OCH_3), 3.99 (3 H, s, OCH_3), 4.11 (3 H, s, OCH_3), 4.81 (2 H, s, CH_2), 6.37 (1 H,s, C=CH), 7.01 (1 H, d, ArH, *J*=8.31 Hz), 7.04 (1 H, s, ArH), 7.12 (1 H, dd, ArH, *J*=8.56, 2.20 Hz), 7.16 (1 H, s, NH), 8.31 (1 H, d, ArH, *J*=1.47 Hz), 10.38 (1 H, br.s., OH);

^{13}C NMR (101 MHz, CHLOROFORM-*d*) δ ppm: 28.3 C(<u>C</u>H$_3$)$_3$), 55.9 (OCH_3), 56.3 (OCH_3) 62.3 (OCH_3), 80.9 (CH_2), 104.2 (ArCH), 110.4 (ArCH), 113.9 (C=<u>C</u>H), 115.5 (ArC), 118.7 (ArCH), 122.6 (ArCH), 127.7 (ArC), 128.3 (ArC), 140.4 (ArC), 143.1 (ArC), 143.5 (ArC), 148.3 (ArC), 148.9 (ArC), 152.7 (HN-C=O), 155.1 (<u>C</u>=CH), 160.3 (Lactone-C=O), 166.0 (CH_2-<u>C</u>=O);

HRMS: Calculated 516.1744, found 517.1830 ($M + H^+$);

MP: 131-133 °C.

Synthesis of 2-((4-(3-amino-4-methoxyphenyl)-6,8-dimethoxy-2-oxo-2H-chromen-7-yl)oxy)-*N*-hydroxyacetamide (4.41)

Carbamate compound **(4.40)** (25 mg, 0.048 mmoles) was dissolved in dry DCM (3 mL) under atmosphere of nitrogen and cooled to -10 °C with salted ice. To this was added dry cooled trifluoroacetic acid (1 mL) and stirred for 90 minutes at 0 °C. Following this step, the reaction mixture was diluted with DCM (20 mL) and solvent was evaporated at 35 °C using rotary evaporator under reduced pressure. The residue obtained was redissolved in DCM (10 mL) and stirred with 5% aqueous $NaHCO_3$ for 3 minutes. Afterwards, the lower organic layer was carefully removed while the aqueous layer containing some of the precipitated product was filtered through a cotton plug. The precipitated product obtained

was combined with the organic layer, few drops of methanol were added to dissolve it and the organic solvents were evaporated *in vacuo*. The solid afforded was washed few times with diethyl ether and passed through a small silica pencil column using DCM:MeOH (9:1) to afford the product **(4.41)** (16 mg, 0.038, 80%) as light yellow solid.

^{1}H NMR (600 MHz, DMSO-d_6) δ ppm: 3.74 (3 H, s, OCH_3), 3.85 (3 H, s, OCH_3), 3.96 (3 H, s, OCH_3), 4.52 (2 H, s, CH_2), 5.02 (2 H, s, NH_2), 6.22 (1 H, s, C=CH), 6.76 (1 H, dd, ArH, *J*=8.07, 1.83 Hz), 6.85 (1 H, d, ArH, *J*=2.20 Hz, 1 H), 6.92 (1 H, s, ArH), 6.97 (1 H, d, ArH, *J*=8.44 Hz), 9.00 (1 H, br. s., NH), 10.70 (1 H, br. s., OH);

^{13}C NMR (151 MHz, DMSO-d_6) δ ppm: 55.4 (OCH_3), 56.1 (OCH_3), 61.6 (OCH_3), 70.6 (CH_2) 103.7 (ArCH) 110.5 (ArCH), 112.3 (C=CH), 113.3 (ArCH), 114.2 (ArC), 116.5 (ArCH), 127.3 (ArC), 138.1 (ArC), 140.4 (ArC), 142.5 (ArC), 143.5 (ArC), 147.6 (ArC), 148.6 (ArC), 155.5 (C=CH), 159.6 (Lactone-C=O), 164.1 (CH_2-C=O);

HRMS: Calculated 416.1220, found 417.1306 ($M + H^+$).

5.4 Tubulin binding activity

5.4.1 Equipment

Absorbance measurement was carried out using FLUOstar Optima 96 well plate reader equipped with thermostate function.

5.4.2 Plates

Assays were performed using Corning™ 96-Well Half-Area Plates (Fisher Scientific Ireland)

5.4.3 Chemicals

2-(*N*-morpholino)ethanesulfonic acid (MES), ethylene glycol-bis(β-aminoethyl ether)-*N*,*N*,*N*′,*N*′-tetraacetic acid (EGTA), magnesium chloride hexahydrate ($MgCl_2.6H_2O$), guanosine 5′-triphosphate lithium salt (GTP, Li salt) and glycerol.

5.4.4 Buffers

Extraction Buffer (EB 2.5 M)

0.25 M MES
1.25 mM $MgCl_2.6H_2O$
2.5 mM EGTA
Deionised water
The pH of the solution was adjusted to pH 6.6 by the dropwise addition of 10 M aq. NaOH. The buffer was stored at 4°C prior to use.

5.4.5 Extraction Buffer (EB)

For the preparation of extraction buffer (EB), deionised water (300 mL) was added to EB 2.5 M (200 mL). The buffer was adjusted to pH 6.6 by the dropwise addition of aqueous NaOH (2.5 M) and stored at 4 °C for further usage.

5.4.6 Isolation and purification of tubulin

Isolation and purification of tubulin from porcine brain was kindly performed by Dr. Walsh, using the procedure proposed by shelanski and co workers [167], with slight modifications.

5.4.7 Assay procedure

5.4.7.1 Dilution of tubulin stock

Assembling of tubulin was determined by recording the increase in optical density of the tubulin solution at 350 nm wavelength and 37 °C. The tubulin stock solution (1 mL) was diluted with EB buffer (3 mL) and mixed gently.

5.4.7.2 Procedure

Once the optimal concentration had been obtained for the tubulin solution, the effect of the DMSO blank was established. DMSO (1 µL) was pipetted into three wells of a 96-well plate and diluted tubulin solution (99 µL) was added to each well. The plate was immediately incubated at 37 °C in the plate-reader and was subjected to orbital shaking for five seconds. The UV absorption was measured at 350 nm over 35 min. The maximum slope of the resulting curve was measured and this represents the maximum rate of tubulin polymerisation.

This procedure was repeated for all concentrations of the test solutions (0.5, 1.0, 2.5, 5.0, 7.5 10 and 25 µM) where the maximum slope in this case represents the maximum rate of tubulin polymerisation in the presence of the inhibitory compound. All the compounds were assayed in duplicate, on three separated occasions and the IC_{50} determined from the dose response analysis. Combretastatin was assayed alongside the test compounds under the same conditions, as an inhibitory control.

5.4.7.3 Results

The results were analysed using a non-linear regression model. Sigmoidal dose response curves of percentage inhibition of tubulin polymerisation versus log drug concentration (M) were plotted. The percentage tubulin polymerisation for each compound was calculated as follows:

% tubulin polymerisation = [100 - mX / mB] x 100

Where, mX = maximum slope of test compound with concentration X

mB = maximum slope of DMSO blank solution of tubulin

Deviation from normal behaviour were quoted as goodness to fit values (R^2), where 1.0 is a perfect fit to the model. The errors bars represent the standard error. The curves were used to determine the IC_{50} values for each compound tested.

5.5 Aminopeptidase N Inhibition Assay

5.5.1 Materials

Bestatin, aminopeptidase N enzyme (leucine aminopeptidase microsomal from porcine kidney), L-Leucine *p*-nitroanilide and 4-(2-Hydroxyethyl)piperazine-1-ethanesulfonic acid (HEPES) were obtained from Sigma Aldrich.

5.5.2 Equipment

A FLUOstar Optima 96 well plate reader equipped with thermostat function.

5.5.3 Buffers and Solutions

Buffer solution

HEPES buffer (50 mM HEPES, 154 mM NaCl)

For the preparing of buffer, HEPES and NaCl were dissolved in deionised water and pH of the solution was adjusted to 7.4 by the dropwise addition of NaOH (2.5 M). The buffer was stored at 4 °C prior to use.

Substrate solution

4 mM suspension of L-Leucine *p*-nitroanilide was prepared in HEPES buffer that gave the final concentration of 1 mM in the well.

Enzyme solution

100 mU stock solution of enzyme was prepared that gave the final concentration of 5 mU in the well.

5.5.4 Procedure

- 50 µL of L-Leucine *p*-nitroanilide was added in to each well of 96 well plate to give a final concentration of 1 mM
- Different concentrations of test compounds were made in HEPES buffer and 100 µL was added into each well.
- The volume of the each well was brought to 190 µL by the addition of 40 µL of HEPES buffer.
- Finally, 10 µL of enzyme was added into each well to give final concentration of 5 mUnits.
- The plate was incubated for 1 h at 37 °C.
- After one hour, the absorbance was measured at 405 nm using a FLUOstar OPTIMA 96 well microplate reader.
- The percent inhibition was determined using the formula;

$$\% \text{ APN inhibition} = [100 - mX / mB] \times 100$$

Where, mX = mean absorbance of test compound

mB = maximum absorbance of the control

References

1. Abdel-Rahman, O., *Targeting vascular endothelial growth factor (VEGF) pathway in gastric cancer: preclinical and clinical aspects.* Critical reviews in oncology/hematology, 2015. **93**(1): p. 18-27.
2. Fitzmaurice, C., et al., *The global burden of cancer 2013.* JAMA oncology, 2015. **1**(4): p. 505-527.
3. Siegel, R.L., K.D. Miller, and A. Jemal, *Cancer statistics, 2015.* CA: a cancer journal for clinicians, 2015. **65**(1): p. 5-29.
4. *Cancer in Ireland 1994-2014: Annual Report of the National Cancer Registry. NCR, Cork, Ireland.* (2016) [cited 2018 18 Sep]; Available from: https://www.ncri.ie/sites/ncri/files/pubs/NCRReport_2016.pdf.
5. Folkman, J. *Role of angiogenesis in tumor growth and metastasis*. in *Seminars in oncology*. 2002. Elsevier.
6. Folkman, J., *Tumor angiogenesis: therapeutic implications.* New england journal of medicine, 1971. **285**(21): p. 1182-1186.
7. Wang, Z., et al. *Broad targeting of angiogenesis for cancer prevention and therapy*. in *Seminars in cancer biology*. 2015. Elsevier.
8. Sanhueza, C., et al., *The twisted survivin connection to angiogenesis.* Molecular cancer, 2015. **14**(1): p. 198.
9. Zhao, C. and A.S. Popel, *Computational model of microRNA control of HIF-VEGF pathway: insights into the pathophysiology of ischemic vascular disease and cancer.* PLoS computational biology, 2015. **11**(11): p. e1004612.
10. Hoeben, A., et al., *Vascular endothelial growth factor and angiogenesis.* Pharmacological reviews, 2004. **56**(4): p. 549-580.
11. Claesson-Welsh, L. and M. Welsh, *VEGFA and tumour angiogenesis.* Journal of internal medicine, 2013. **273**(2): p. 114-127.
12. Sato, T., et al., *Vascular endothelial growth factor receptor 1 signaling facilitates gastric ulcer healing and angiogenesis through the upregulation of epidermal growth factor expression on VEGFR1+ CXCR4+ cells recruited from bone marrow.* Journal of gastroenterology, 2014. **49**(3): p. 455-469.
13. Rundhaug, J.E., *Matrix metalloproteinases and angiogenesis.* Journal of cellular and molecular medicine, 2005. **9**(2): p. 267-285.
14. Welti, J., et al., *Recent molecular discoveries in angiogenesis and antiangiogenic therapies in cancer.* The Journal of clinical investigation, 2013. **123**(8): p. 3190-3200.

15. Kristensen, T.B., et al., *Anti-vascular endothelial growth factor therapy in breast cancer.* International journal of molecular sciences, 2014. **15**(12): p. 23024-23041.
16. Zetter, B.R., *Angiogenesis and tumor metastasis.* Annual review of medicine, 1998. **49**(1): p. 407-424.
17. Herbert, S.P. and D.Y. Stainier, *Molecular control of endothelial cell behaviour during blood vessel morphogenesis.* Nature reviews Molecular cell biology, 2011. **12**(9): p. 551.
18. Hinnen, P. and F. Eskens, *Vascular disrupting agents in clinical development.* British Journal of Cancer, 2007. **96**(8): p. 1159.
19. Konerding, M., E. Fait, and A. Gaumann, *3D microvascular architecture of pre-cancerous lesions and invasive carcinomas of the colon.* British journal of cancer, 2001. **84**(10): p. 1354.
20. Fang, J., H. Nakamura, and H. Maeda, *The EPR effect: unique features of tumor blood vessels for drug delivery, factors involved, and limitations and augmentation of the effect.* Advanced drug delivery reviews, 2011. **63**(3): p. 136-151.
21. Maeda, H., et al., *Tumor vascular permeability and the EPR effect in macromolecular therapeutics: a review.* Journal of controlled release, 2000. **65**(1-2): p. 271-284.
22. Mohammadi, M. and P. Chen, *Effect of microvascular distribution and its density on interstitial fluid pressure in solid tumors: a computational model*. Microvascular research, 2015. **101**: p. 26-32.
23. Siemann, D.W., *The unique characteristics of tumor vasculature and preclinical evidence for its selective disruption by tumor-vascular disrupting agents.* Cancer treatment reviews, 2011. **37**(1): p. 63-74.
24. Jain, R.K., *Normalizing tumor vasculature with anti-angiogenic therapy: a new paradigm for combination therapy.* Nature medicine, 2001. **7**(9): p. 987.
25. Wu, X.-Y., et al., *Mechanisms of tumor resistance to small-molecule vascular disrupting agents: treatment and rationale of combination therapy.* Journal of the Formosan Medical Association, 2013. **112**(3): p. 115-124.
26. Bellou, S., et al., *Anti-angiogenesis in cancer therapy: Hercules and hydra.* Cancer letters, 2013. **338**(2): p. 219-228.
27. Robert, N.J., et al., *RIBBON-1: randomized, double-blind, placebo-controlled, phase III trial of chemotherapy with or without bevacizumab for first-line treatment of human epidermal growth factor receptor 2–negative, locally recurrent or metastatic breast cancer.* Journal of Clinical Oncology, 2011. **29**(10): p. 1252-1260.

28. Yang, J.C., et al., *A randomized trial of bevacizumab, an anti–vascular endothelial growth factor antibody, for metastatic renal cancer.* New England Journal of Medicine, 2003. **349**(5): p. 427-434.
29. Giantonio, B.J., et al., *Bevacizumab in combination with oxaliplatin, fluorouracil, and leucovorin (FOLFOX4) for previously treated metastatic colorectal cancer: results from the Eastern Cooperative Oncology Group Study E3200.* Journal of Clinical Oncology, 2007. **25**(12): p. 1539-1544.
30. Shojaei, F., *Anti-angiogenesis therapy in cancer: current challenges and future perspectives.* Cancer letters, 2012. **320**(2): p. 130-137.
31. Giuliano, S. and G. Pagès, *Mechanisms of resistance to anti-angiogenesis therapies.* Biochimie, 2013. **95**(6): p. 1110-1119.
32. Denekamp, J., *Vascular attack as a therapeutic strategy for cancer.* Cancer and Metastasis Reviews, 1990. **9**(3): p. 267-282.
33. Thorpe, P.E., *Vascular targeting agents as cancer therapeutics.* Clinical Cancer Research, 2004. **10**(2): p. 415-427.
34. Cai, S.X., *Small molecule vascular disrupting agents: potential new drugs for cancer treatment.* Recent patents on anti-cancer drug discovery, 2007. **2**(1): p. 79-101.
35. Gaya, A. and G. Rustin, *Vascular disrupting agents: a new class of drug in cancer therapy.* Clinical Oncology, 2005. **17**(4): p. 277-290.
36. Sarkar, T., *Microtubule Targeting Anti-mitotic Agents as Anti-Cancer Drugs: A Review.* International Journal of Multidisciplinary Approach & Studies, 2015. **2**(5).
37. Nogales, E., *A structural view of microtubule dynamics.* Cellular and Molecular Life Sciences CMLS, 1999. **56**(1-2): p. 133-142.
38. Stanton, R.A., et al., *Drugs that target dynamic microtubules: a new molecular perspective.* Medicinal research reviews, 2011. **31**(3): p. 443-481.
39. Waterman-Storer, C.M. and E. Salmon, *Microtubule dynamics: treadmilling comes around again.* Current Biology, 1997. **7**(6): p. R369-R372.
40. Cassimeris, L., et al., *Dynamic instability of microtubules.* Bioessays, 1987. **7**(4): p. 149-154.
41. Avila, J., *Microtubule functions.* Life sciences, 1992. **50**(5): p. 327-334.
42. Balabanian, L., C.L. Berger, and A.G. Hendricks, *The Role of the Microtubule Cytoskeleton in Regulating Intracellular Transport.* Biophysical Journal, 2016. **110**(3): p. 466a.

43. Field, J.J., A. Kanakkanthara, and J.H. Miller, *Microtubule-targeting agents are clinically successful due to both mitotic and interphase impairment of microtubule function.* Bioorganic & medicinal chemistry, 2014. **22**(18): p. 5050-5059.
44. Jordan, M.A. and L. Wilson, *Microtubules as a target for anticancer drugs.* Nature Reviews Cancer, 2004. **4**(4): p. 253.
45. Solary, E., *Tubulin-targeting agent combination therapies: dosing schedule could matter.* British journal of pharmacology, 2013. **168**(7): p. 1555-1557.
46. Khrapunovich-Baine, M., et al., *Distinct pose of discodermolide in taxol binding pocket drives a complementary mode of microtubule stabilization.* Biochemistry, 2009. **48**(49): p. 11664-11677.
47. Nettles, J.H., et al., *The binding mode of epothilone A on α, ß-tubulin by electron crystallography.* Science, 2004. **305**(5685): p. 866-869.
48. Prota, A.E., et al., *Structural basis of microtubule stabilization by laulimalide and peloruside A.* Angewandte Chemie International Edition, 2014. **53**(6): p. 1621-1625.
49. Schiff, P.B., J. Fant, and S.B. Horwitz, *Promotion of microtubule assembly in vitro by taxol.* Nature, 1979. **277**(5698): p. 665.
50. Ringel, I. and S.B. Horwitz, *Studies with RP 56976 (taxotere): a semisynthetic analogue of taxol.* JNCI: Journal of the National Cancer Institute, 1991. **83**(4): p. 288-291.
51. Bollag, D.M., et al., *Epothilones, a new class of microtubule-stabilizing agents with a taxol-like mechanism of action.* Cancer research, 1995. **55**(11): p. 2325-2333.
52. Rothermel, J., et al. *EPO906 (epothilone B): a promising novel microtubule stabilizer*. in *Seminars in oncology*. 2003. Elsevier.
53. Dorléans, A., et al., *Variations in the colchicine-binding domain provide insight into the structural switch of tubulin.* Proceedings of the National Academy of Sciences, 2009. **106**(33): p. 13775-13779.
54. Prota, A.E., et al., *A new tubulin-binding site and pharmacophore for microtubule-destabilizing anticancer drugs.* Proceedings of the National Academy of Sciences, 2014. **111**(38): p. 13817-13821.
55. Gigant, B., et al., *Structural basis for the regulation of tubulin by vinblastine.* Nature, 2005. **435**(7041): p. 519.
56. Noble, R.L., *The discovery of the vinca alkaloids—chemotherapeutic agents against cancer.* Biochemistry and cell biology, 1990. **68**(12): p. 1344-1351.

57. Moudi, M., et al., *Vinca alkaloids.* International journal of preventive medicine, 2013. **4**(11): p. 1231.
58. Charpentier, M.S., et al., *Curcumin targets breast cancer stem-like cells with microtentacles that persist in mammospheres and promote attachment.* Cancer research, 2013: p. canres. 1778.2013.
59. Ganguly, A., et al., *Microtubule dynamics control tail retraction in migrating vascular endothelial cells.* Molecular cancer therapeutics, 2013.
60. Slobodnick, A., et al., *Colchicine: old and new.* The American journal of medicine, 2015. **128**(5): p. 461-470.
61. Leung, Y.Y., L.L.Y. Hui, and V.B. Kraus. *Colchicine—Update on mechanisms of action and therapeutic uses*. in *Seminars in arthritis and rheumatism*. 2015. Elsevier.
62. Pettit, G., et al., *Isolation and structure of the strong cell growth and tubulin inhibitor combretastatin A-4.* Experientia, 1989. **45**(2): p. 209-211.
63. Rustin, G.J., et al., *Phase I clinical trial of weekly combretastatin A4 phosphate: clinical and pharmacokinetic results.* Journal of clinical oncology, 2003. **21**(15): p. 2815-2822.
64. Sackett, D.L., *Podophyllotoxin, steganacin and combretastatin: natural products that bind at the colchicine site of tubulin.* Pharmacology & therapeutics, 1993. **59**(2): p. 163-228.
65. Lin, C.M., et al., *Antimitotic natural products combretastatin A-4 and combretastatin A-2: studies on the mechanism of their inhibition of the binding of colchicine to tubulin.* Biochemistry, 1989. **28**(17): p. 6984-6991.
66. Dark, G.G., et al., *Combretastatin A-4, an agent that displays potent and selective toxicity toward tumor vasculature.* Cancer research, 1997. **57**(10): p. 1829-1834.
67. Lin, C.M., et al., *Interactions of tubulin with potent natural and synthetic analogs of the antimitotic agent combretastatin: a structure-activity study.* Molecular pharmacology, 1988. **34**(2): p. 200-208.
68. Dowlati, A., et al., *A phase I pharmacokinetic and translational study of the novel vascular targeting agent combretastatin a-4 phosphate on a single-dose intravenous schedule in patients with advanced cancer.* Cancer Research, 2002. **62**(12): p. 3408-3416.
69. Liu, P., et al., *A phase I clinical trial assessing the safety and tolerability of combretastatin A4 phosphate injections.* Anti-cancer drugs, 2014. **25**(4): p. 462-471.

70. Zweifel, M., et al., *Phase II trial of combretastatin A4 phosphate, carboplatin, and paclitaxel in patients with platinum-resistant ovarian cancer.* Annals of oncology, 2011. **22**(9): p. 2036-2041.
71. Bhattacharyya, B., et al., *Anti-mitotic activity of colchicine and the structural basis for its interaction with tubulin.* Medicinal research reviews, 2008. **28**(1): p. 155-183.
72. Krendel, M., F.T. Zenke, and G.M. Bokoch, *Nucleotide exchange factor GEF-H1 mediates cross-talk between microtubules and the actin cytoskeleton.* Nature cell biology, 2002. **4**(4): p. 294.
73. Madaule, P. and R. Axel, *A novel ras-related gene family.* Cell, 1985. **41**(1): p. 31-40.
74. Monk, K.A., et al., *Design, synthesis, and biological evaluation of combretastatin nitrogen-containing derivatives as inhibitors of tubulin assembly and vascular disrupting agents.* Bioorganic & medicinal chemistry, 2006. **14**(9): p. 3231-3244.
75. Kanthou, C. and G.M. Tozer, *The tumor vascular targeting agent combretastatin A–4-phosphate induces reorganization of the actin cytoskeleton and early membrane blebbing in human endothelial cells.* Blood, 2002. **99**(6): p. 2060-2069.
76. Hirsh, J., et al., *American Heart Association/American College of Cardiology foundation guide to warfarin therapy.* Journal of the American College of Cardiology, 2003. **41**(9): p. 1633-1652.
77. Gilani, A., et al., *Hypotensive action of coumarin glycosides from Daucus carota.* Phytomedicine, 2000. **7**(5): p. 423-426.
78. Amin, K.M., D.E.A. Rahman, and Y.A. Al-Eryani, *Synthesis and preliminary evaluation of some substituted coumarins as anticonvulsant agents.* Bioorganic & medicinal chemistry, 2008. **16**(10): p. 5377-5388.
79. Gómez-Calderón, C., et al., *Antiviral effect of compounds derived from the seeds of Mammea americana and Tabernaemontana cymosa on Dengue and Chikungunya virus infections.* BMC complementary and alternative medicine, 2017. **17**(1): p. 57.
80. Torres, R., et al., *Antioxidant activity of coumarins and flavonols from the resinous exudate of Haplopappus multifolius.* Phytochemistry, 2006. **67**(10): p. 984-987.
81. Kayser, O. and H. Kolodziej, *Antibacterial activity of simple coumarins: structural requirements for biological activity.* Zeitschrift für Naturforschung C, 1999. **54**(3-4): p. 169-174.
82. Hadjipavlou-Litina, D., K. Litinas, and C. Kontogiorgis, *The anti-inflammatory effect of coumarin and its derivatives.* Anti-Inflammatory & Anti-Allergy Agents in

Medicinal Chemistry (Formerly Current Medicinal Chemistry-Anti-Inflammatory and Anti-Allergy Agents), 2007. **6**(4): p. 293-306.

83. Xiao, C.F., et al., *Design, synthesis and antitumor activity of a series of novel coumarin–stilbenes hybrids, the 3-arylcoumarins.* Chinese Chemical Letters, 2010. **21**(11): p. 1295-1298.
84. Bailly, C., et al., *Synthesis and biological evaluation of 4-arylcoumarin analogues of combretastatins.* Journal of medicinal chemistry, 2003. **46**(25): p. 5437-5444.
85. Pettit, G.R., et al., *Antineoplastic agents. 379. Synthesis of phenstatin phosphate1a.* Journal of medicinal chemistry, 1998. **41**(10): p. 1688-1695.
86. Álvarez, C., et al., *Exploring the effect of 2, 3, 4-trimethoxy-phenyl moiety as a component of indolephenstatins.* European journal of medicinal chemistry, 2010. **45**(2): p. 588-597.
87. Liou, J.-P., et al., *Synthesis and structure− activity relationships of 3-aminobenzophenones as antimitotic agents.* Journal of medicinal chemistry, 2004. **47**(11): p. 2897-2905.
88. Alvarez, C., et al., *Diarylmethyloxime and hydrazone derivatives with 5-indolyl moieties as potent inhibitors of tubulin polymerization.* Bioorganic & medicinal chemistry, 2008. **16**(11): p. 5952-5961.
89. Romagnoli, R., et al., *Design, synthesis and structure–activity relationship of 2-(3', 4', 5'-trimethoxybenzoyl)-benzo [b] furan derivatives as a novel class of inhibitors of tubulin polymerization.* Bioorganic & medicinal chemistry, 2009. **17**(19): p. 6862-6871.
90. Romagnoli, R., et al., *Design, synthesis, and biological evaluation of thiophene analogues of chalcones.* Bioorganic & medicinal chemistry, 2008. **16**(10): p. 5367-5376.
91. Hu, L., et al., *Novel potent antimitotic heterocyclic ketones: synthesis, antiproliferative activity, and structure–activity relationships.* Bioorganic & medicinal chemistry letters, 2007. **17**(13): p. 3613-3617.
92. Duan, J.-X., et al., *Potent antitubulin tumor cell cytotoxins based on 3-aroyl indazoles.* Journal of medicinal chemistry, 2007. **50**(5): p. 1001-1006.
93. Assaraf, Y.G., C.P. Leamon, and J.A. Reddy, *The folate receptor as a rational therapeutic target for personalized cancer treatment.* Drug Resistance Updates, 2014. **17**(4-6): p. 89-95.
94. Witkop, B., *Paul Ehrlich and his magic bullets, revisited.* Proceedings of the American Philosophical Society, 1999. **143**(4): p. 540-557.

95. Widakowich, C., et al., *Side effects of approved molecular targeted therapies in solid cancers.* The oncologist, 2007. **12**(12): p. 1443-1455.
96. FREI, E., et al., *The effectiveness of combinations of antileukemic agents in inducing and maintaining remission in children with acute leukemia.* Blood, 1965. **26**(5): p. 642-656.
97. Albain, K.S., et al., *Gemcitabine plus paclitaxel versus paclitaxel monotherapy in patients with metastatic breast cancer and prior anthracycline treatment.* Journal of Clinical Oncology, 2008. **26**(24): p. 3950-3957.
98. Nathan, P., et al., *Phase I trial of combretastatin A4 phosphate (CA4P) in combination with bevacizumab in patients with advanced cancer.* Clinical cancer research, 2012.
99. Riechelmann, R. and D. Girardi, *Drug interactions in cancer patients: A hidden risk?* Journal of research in pharmacy practice, 2016. **5**(2): p. 77.
100. Fortin, S. and G. Bérubé, *Advances in the development of hybrid anticancer drugs.* Expert opinion on drug discovery, 2013. **8**(8): p. 1029-1047.
101. Lee, K.-W., et al., *Antitumor activity of SK-7041, a novel histone deacetylase inhibitor, in human lung and breast cancer cells.* Anticancer research, 2006. **26**(5A): p. 3429-3438.
102. Andres, C., et al., *"Combretatropones"—hybrids of combretastatin and colchicine. Synthesis and biochemical evaluation.* Bioorganic & Medicinal Chemistry Letters, 1993. **3**(4): p. 565-570.
103. Ojima, I., et al., *A common pharmacophore for cytotoxic natural products that stabilize microtubules.* Proceedings of the National Academy of Sciences, 1999. **96**(8): p. 4256-4261.
104. Xu, J., et al., *Apatinib plus icotinib in treating advanced non-small cell lung cancer after icotinib treatment failure: a retrospective study.* OncoTargets and therapy, 2017. **10**: p. 4989.
105. O'shaughnessy, J., et al., *Superior survival with capecitabine plus docetaxel combination therapy in anthracycline-pretreated patients with advanced breast cancer: phase III trial results.* Journal of Clinical Oncology, 2002. **20**(12): p. 2812-2823.
106. CHOBANIAN, N.H., et al., *Histone deacetylase inhibitors enhance paclitaxel-induced cell death in ovarian cancer cell lines independent of p53 status.* Anticancer research, 2004. **24**(2B): p. 539-546.

107. Zhang, X., et al., *The discovery of colchicine-SAHA hybrids as a new class of antitumor agents.* Bioorganic & medicinal chemistry, 2013. **21**(11): p. 3240-3244.
108. Zhang, X., et al., *The design and discovery of water soluble 4-substituted-2, 6-dimethylfuro [2, 3-d] pyrimidines as multitargeted receptor tyrosine kinase inhibitors and microtubule targeting antitumor agents.* Bioorganic & medicinal chemistry, 2014. **22**(14): p. 3753-3772.
109. Danieli, B., et al., *Synthesis and Biological Evaluation of Paclitaxel□ Thiocolchicine Hybrids.* Chemistry & biodiversity, 2004. **1**(2): p. 327-345.
110. Bombuwala, K., et al., *Colchitaxel, a coupled compound made from microtubule inhibitors colchicine and paclitaxel.* Beilstein journal of organic chemistry, 2006. **2**: p. 13.
111. Nogales, E., S.G. Wolf, and K.H. Downing, *Correction: Structure of the αβ tubulin dimer by electron crystallography.* Nature, 1998. **393**(6681): p. 191.
112. Sauerwald, A., et al., *Structure of active dimeric human telomerase.* Nature structural & molecular biology, 2013. **20**(4): p. 454.
113. Maruyama, I.N., *Mechanisms of activation of receptor tyrosine kinases: monomers or dimers.* Cells, 2014. **3**(2): p. 304-330.
114. Olson, M.W., et al., *Characterization of the monomeric and dimeric forms of latent and active matrix metalloproteinase-9 differential rates for activation by stromelysin 1.* Journal of Biological Chemistry, 2000. **275**(4): p. 2661-2668.
115. Monod, J., J. Wyman, and J.-P. Changeux, *On the nature of allosteric transitions: a plausible model*, in *Selected Papers in Molecular Biology by Jacques Monod*. 1978, Elsevier. p. 593-623.
116. Yamaguchi, Y., et al., *Evaluation of synthesized coumarin derivatives on aromatase inhibitory activity.* Bioorganic & medicinal chemistry letters, 2017. **27**(12): p. 2645-2649.
117. Smith, I.E. and M. Dowsett, *Aromatase inhibitors in breast cancer.* New England Journal of Medicine, 2003. **348**(24): p. 2431-2442.
118. Quigley, G.J., et al., *Molecular structure of an anticancer drug-DNA complex: daunomycin plus d (CpGpTpApCpG).* Proceedings of the National Academy of Sciences, 1980. **77**(12): p. 7204-7208.
119. Hu, G.G., et al., *Structure of a DNA− bisdaunomycin complex.* Biochemistry, 1997. **36**(20): p. 5940-5946.

120. Wittman, M.D., et al., *Synthesis and antitumor activity of novel paclitaxel–chlorambucil hybrids.* Bioorganic & medicinal chemistry letters, 2001. **11**(6): p. 811-814.
121. Di Antonio, M., K.I. McLuckie, and S. Balasubramanian, *Reprogramming the mechanism of action of chlorambucil by coupling to a G-quadruplex ligand.* Journal of the American Chemical Society, 2014. **136**(16): p. 5860-5863.
122. Xiao, Q., et al., *Cytotoxic Peptide Conjugates: Anticancer Therapeutic Strategies.*
123. Schwarze, S.R., et al., *In vivo protein transduction: delivery of a biologically active protein into the mouse.* Science, 1999. **285**(5433): p. 1569-1572.
124. Gu, G., D. Dustin, and S.A. Fuqua, *Targeted therapy for breast cancer and molecular mechanisms of resistance to treatment.* Current opinion in pharmacology, 2016. **31**: p. 97-103.
125. Kim, J.-W. and H.-S. Lee, *Tumor targeting by doxorubicin-RGD-4C peptide conjugate in an orthotopic mouse hepatoma model.* International journal of molecular medicine, 2004. **14**(4): p. 529-564.
126. Lambert, J.M. and A. Berkenblit, *Antibody–drug conjugates for cancer treatment.* Annual review of medicine, 2018. **69**: p. 191-207.
127. Drachman, J.G. and P.D. Senter, *Antibody-drug conjugates: the chemistry behind empowering antibodies to fight cancer.* ASH Education Program Book, 2013. **2013**(1): p. 306-310.
128. Klute, K., et al., *Microtubule inhibitor-based antibody–drug conjugates for cancer therapy.* OncoTargets and therapy, 2014. **7**: p. 2227.
129. Guillemard, V. and H.U. Saragovi, *Taxane-antibody conjugates afford potent cytotoxicity, enhanced solubility, and tumor target selectivity.* Cancer research, 2001. **61**(2): p. 694-699.
130. Lambert, J.M. and C.Q. Morris, *Antibody–drug conjugates (ADCs) for personalized treatment of solid tumors: A review.* Advances in therapy, 2017. **34**(5): p. 1015-1035.
131. Chari, R.V., M.L. Miller, and W.C. Widdison, *Antibody–drug conjugates: an emerging concept in cancer therapy.* Angewandte Chemie International Edition, 2014. **53**(15): p. 3796-3827.
132. Bross, P.F., et al., *Approval summary: gemtuzumab ozogamicin in relapsed acute myeloid leukemia.* Clinical Cancer Research, 2001. **7**(6): p. 1490-1496.
133. Genentech, I. *KADCYLA®.* [cited 2018 20 SEP]; Available from: https://www.gene.com/download/pdf/kadcyla_prescribing.pdf.

134. Schmitt, C., et al., *Selective aminopeptidase-N (CD13) inhibitors with relevance to cancer chemotherapy.* Bioorganic & medicinal chemistry, 2013. **21**(7): p. 2135-2144.
135. Bhagwat, S.V., et al., *CD13/APN is activated by angiogenic signals and is essential for capillary tube formation.* Blood, 2001. **97**(3): p. 652-659.
136. Tsukamoto, H., et al., *Aminopeptidase N (APN)/CD13 inhibitor, Ubenimex, enhances radiation sensitivity in human cervical cancer.* BMC cancer, 2008. **8**(1): p. 74.
137. Ikeda, N., et al., *Clinical significance of aminopeptidase N/CD13 expression in human pancreatic carcinoma.* Clinical Cancer Research, 2003. **9**(4): p. 1503-1508.
138. Hashida, H., et al., *Aminopeptidase N is involved in cell motility and angiogenesis: its clinical significance in human colon cancer.* Gastroenterology, 2002. **122**(2): p. 376-386.
139. Zhang, X., et al., *Novel aminopeptidase N (APN/CD13) inhibitors derived from 3-phenylalanyl-N'-substituted-2, 6-piperidinedione.* Bioorganic & medicinal chemistry, 2010. **18**(16): p. 5981-5987.
140. Fukasawa, K., et al., *Aminopeptidase N (APN/CD13) is selectively expressed in vascular endothelial cells and plays multiple roles in angiogenesis.* Cancer letters, 2006. **243**(1): p. 135-143.
141. Luan, Y. and W. Xu, *The structure and main functions of aminopeptidase N.* Current medicinal chemistry, 2007. **14**(6): p. 639-647.
142. Mina-Osorio, P., *The moonlighting enzyme CD13: old and new functions to target.* Trends in molecular medicine, 2008. **14**(8): p. 361-371.
143. Zhang, Q., et al., *Expression and clinical significance of aminopeptidase N/CD13 in non-small cell lung cancer.* Journal of cancer research and therapeutics, 2015. **11**(1): p. 223.
144. Yamashita, M., et al., *Involvement of aminopeptidase N in enhanced chemosensitivity to paclitaxel in ovarian carcinoma in vitro and in vivo.* International journal of cancer, 2007. **120**(10): p. 2243-2250.
145. Inagaki, Y., et al., *Novel aminopeptidase N (APN/CD13) inhibitor 24F can suppress invasion of hepatocellular carcinoma cells as well as angiogenesis.* Bioscience trends, 2010. **4**(2).
146. Grams, F., et al., *Structure determination and analysis of human neutrophil collagenase complexed with a hydroxamate inhibitor.* Biochemistry, 1995. **34**(43): p. 14012-14020.

147. Umezawa, H., et al., *Bestatin, an inhibitor of aminopeptidase B, produced by actinomycetes.* The Journal of antibiotics, 1976. **29**(1): p. 97-99.

148. Rao, M., et al., *A new aminopeptidase inhibitor from Streptomyces strain HCCB10043 found by UPLC–MS.* Analytical and bioanalytical chemistry, 2011. **401**(2): p. 699-706.

149. Sekine, K., H. Fujii, and F. Abe, *Induction of apoptosis by bestatin (ubenimex) in human leukemic cell lines.* Leukemia, 1999. **13**(5): p. 729.

150. Ichinose, Y., et al., *Randomized double-blind placebo-controlled trial of bestatin in patients with resected stage I squamous-cell lung carcinoma.* Journal of the National Cancer Institute, 2003. **95**(8): p. 605-610.

151. Nishizawa, R., et al., *Synthesis and structure-activity relations of bestatin analogs, inhibitors of aminopeptidase B.* Journal of Medicinal Chemistry, 1977. **20**(4): p. 510-515.

152. Hudson, G., *Design, synthesis and evaluation of novel tumour vasculature-targeting agents', [thesis], Trinity College (Dublin, Ireland). School of Pharmacy & Pharmaceutical Sciences, 2007, pp 322.*

153. Coogan, A., *Design and synthesis of tubulin-binding agents, and their incorporation into novel dual-acting hybrid molecules targeting the tumour vasculature', [thesis], Trinity College (Dublin, Ireland). School of Pharmacy & Pharmaceutical Sciences, 2013, pp 297.*

154. Ishiyama, T., M. Murata, and N. Miyaura, *Palladium (0)-catalyzed cross-coupling reaction of alkoxydiboron with haloarenes: a direct procedure for arylboronic esters.* The Journal of Organic Chemistry, 1995. **60**(23): p. 7508-7510.

155. Garazd, Y.L., et al., *Modified coumarins. 23. Synthesis and structure of cyclohexyldihydroxanthyletin derivatives.* Chemistry of natural compounds, 2006. **42**(6): p. 652-655.

156. Song, A., X. Wang, and K.S. Lam, *A convenient synthesis of coumarin-3-carboxylic acids via Knoevenagel condensation of Meldrum's acid with ortho-hydroxyaryl aldehydes or ketones.* Tetrahedron Letters, 2003. **44**(9): p. 1755-1758.

157. Sun, J., et al., *Highly efficient chemoselective deprotection of O, O-acetals and O, O-ketals catalyzed by molecular iodine in acetone.* The Journal of organic chemistry, 2004. **69**(25): p. 8932-8934.

158. Hansen, T.V. and L. Skattebøl, *ortho-Formylation of Phenols; Preparation of 3-Bromosalicylaldehyde.* Organic Syntheses, 2005: p. 64-68.

159. Shah, R., *The design and synthesis of novel inhibitors of tubulin polymerisation', [thesis], Trinity College (Dublin, Ireland). School of Pharmacy & Pharmaceutical Sciences.*

160. Apitz, C. and D. Schranz, *Sildenafil-Bosentan Drug-Drug Interaction: A Word of Caution Regarding the Most Common Combination Therapy in Children with Advanced Pulmonary Arterial Hypertension.* Respiration, 2018.

161. Tosi, D., et al., *Rational development of synergistic combinations of chemotherapy and molecular targeted agents for colorectal cancer treatment.* BMC cancer, 2018. **18**(1): p. 812.

162. Martínez, J.M., et al., *Aminopeptidase activities in breast cancer tissue.* Clinical chemistry, 1999. **45**(10): p. 1797-1802.

163. Mishima, Y., et al., *Continuous treatment of bestatin induces anti-angiogenic property in endothelial cells.* Cancer science, 2007. **98**(3): p. 364-372.

164. Bauvois, B. and D. Dauzonne, *Aminopeptidase-N/CD13 (EC 3.4. 11.2) inhibitors: Chemistry, biological evaluations, and therapeutic prospects.* Medicinal research reviews, 2006. **26**(1): p. 88-130.

165. Breen, E., *'The design, synthesis and preliminary evaluation of prodrugs and hybrid drugs with tubulin polymerisation inhibitory activity and anti-proliferative activity', [thesis], Trinity College (Dublin, Ireland). School of Pharmacy & Pharmaceutical Sciences, 2013, pp 346.*

166. Melzig, M.F. and H. Bormann, *Betulinic acid inhibits aminopeptidase N activity.* Planta medica, 1998. **64**(07): p. 655-657.

167. Shelanski, M.L., F. Gaskin, and C.R. Cantor, *Microtubule assembly in the absence of added nucleotides.* Proceedings of the National Academy of Sciences, 1973. **70**(3): p. 765-768.